

**A comparison of the hydrothermal alteration systems
around the Mo-hosting White Pine Intrusion, Utah,
and the Buckingham Porphyry, Nevada**

Emily Smyk

Submitted in partial fulfillment of the requirements for the degree of

Masters of Science – Geology

Supervisors: Dr. Peter Hollings (Lakehead University)
and Dr. David R. Cooke (CODES-University of Tasmania)

*Geology Department
Lakehead University
Thunder Bay, Ontario
2015*

ABSTRACT

The White Pine Fork Mo porphyry has an estimated resource of 16 Mt of Mo at 0.1% Mo. The host intrusions are K-feldspar- and quartz-porphyritic monzo- to syeno-granites characterised by LREE enrichment, fractionated HREEs and negative Nb, Ta, Sr and Ti anomalies, consistent with a subarc mantle melt source. The granites also have an adakitic geochemical signature. A U-Pb age for zircon from a clast in the mineralized breccia pipe at White Pine yielded an age of 26.52 ± 0.42 Ma, which falls within the error of the White Pine intrusion age of 26.61 ± 0.24 Ma. Re-Os ages for duplicate samples of the Mo-mineralised quartz breccia are 30.21 ± 0.14 and 29.84 ± 0.15 Ma, which correlate with the age of the Little Cottonwood stock rather than the host intrusion and may represent Re-Os inheritance. In contrast, Buckingham Mo (-Cu) porphyry has an estimated resource of 1,000 Mt of Mo at 0.1% Mo and is hosted in Cretaceous K-feldspar- and quartz-porphyritic granites. Four feldspar- and quartz-porphyritic granites in the area were dated using LA-ICP-MS U-Pb of zircon and yielded ages of 38.68 ± 0.53 , 39.28 ± 0.58 , 40.76 ± 0.41 , and 40.81 ± 0.51 Ma and therefore unrelated to the Buckingham deposit, and instead are correlated with Tertiary magmatism associated with Au skarns in the nearby Battle Mountain district. The Tertiary intrusions are feldspar- and quartz porphyritic granites. Primitive mantle-normalized geochemistry of both suites of intrusive rocks have LREE enrichment, fractionated HREE, negative Nb, Ta and Ti anomalies and a slight enrichment of Zr and Hf, consistent with a subarc mantle source for both suites.

The most prominent alteration in both systems is phyllic alteration comprising an assemblage of white micas, quartz and pyrite. Potassic alteration was also observed at the White Pine Fork Mo breccia pipe and kaolinite and chlorite observed in SWIR data suggest advanced argillic alteration around the Buckingham system. These petrographic observations are

substantiated by the whole rock geochemistry. The potassic, phyllic, and possible advanced argillic alteration were mapped out by the absolute values of trace elements. The trace element geochemistry of quartz and pyrite can be used to fingerprint deposit types and as vectors towards mineralisation in alteration systems around ore deposits. At White Pine Fork, the hydrothermal quartz is characterised by higher Ti and As than the igneous quartz. The Li content of hydrothermal quartz is greater near the centre of the White Pine Fork deposit than in its margins. At Buckingham, quartz in the breccia cement at the centre of the deposit shows the highest concentration of Al, Li, K, Ca, As, and Sb, and metals (i.e. Cu, Fe, Zn, and Pb), whereas the igneous and sedimentary quartz shows the highest Ti values. The high values indicate that the primary Ti contents were not subjected to recalibration during hydrothermal alteration. The Al and Sb contents of quartz decrease away from the centre of deposit at Buckingham. This trend was not observed at White Pine Fork.

At White Pine Fork, pyrite occurs in a domain extending more than 1.5 km from the breccia pipe and is partially weathered to Fe-oxides and Fe-hydroxides. LA-ICP-MS analyses showed Ni and Co compositional zoning within the pyrite grains. The Ni content in the pyrite increases away from the centre of the White Pine Fork deposit. At Buckingham, the pyrite was almost completely altered to Fe-oxides and Fe-hydroxides in most of the surface samples studied here. The trace element concentrations of Au, Cu, and Cd in pyrite decreases away from the centre of deposit. Ni, Co and Pb zonations were also seen in the cores of the pyrite grains at Buckingham. LA-ICP-MS element maps in most of the surface samples studied here showed that the pyrite at Buckingham is depleted in trace elements relative to the weathering rinds which are enriched in Au, Ag, Cu, As, Sb and Mo. The increased Au concentration in the weathering rind suggests either an overprinting mineralised rind similar to the proximal skarns or Carlin-

style sediment hosted Au. This rind was then weathered during supergene alteration. Another possibility is that the cores of the sulphides acted as traps for the precipitation of precious metals from the hydrothermal event associated with the proximal Eocene granite intrusions which were subsequently concentrated in the weathering rind during supergene alteration.

The comparison the White Pine Fork and Buckingham Mo porphyries has refined the processes associated with hydrothermal alteration around Mo porphyry deposits and the applicability of trace element chemistry of alteration minerals as exploration tools.

ACKNOWLEDGMENTS

I would like to thank Dr. Peter Hollings for his incredible and continued support, mentorship, and guidance throughout this project as well as my undergraduate and graduate education and thesis. I would also like to thank Dr. David Cooke for his insight and help with the project and extending his welcome and his guidance for my analytical work done at the University of Tasmania. I would also like to show my gratitude for the Society of Economic Geologists Graduate Fellowship for helping to fund my studies and Freeport McMoran Copper & Gold Inc. for helping to fund the research at the Buckingham study site. As well, thank you to Anne Hammond and Kristi Tavener for preparing the thin sections and mounts used for petrography and detailed LA-ICP-MS studies. I could not have completed the field work without the help of Wesley Lueck, Ken Krahulec and Taylor Boden (Utah Geological Survey) and Robert Lee and Jeff Lulu (Freeport McMoRan Copper & Gold Inc.). As well, Mike Baker, Sandrin Feig, Karsten Goemann, Sarah Gilbert, and Jay Thompson were incredibly helpful in guiding me with my trace element geochemical analyses at the facilities of the University of Tasmania. This project would not have been possible without the continuous support of the Geology departments, faculties and students at Lakehead University and CODES at the University of Tasmania. Lastly, I would like to give a special thank you to my friends and family for their support and patience throughout the past two years and to Nathan Steeves for his unconditional support and friendship through the last year of my degree.

Table of Contents

ABSTRACT	ii
ACKNOWLEDGMENTS	iv
Table of Contents	v
Figures and Tables	ix
Chapter 1: Introduction	1
1.1 Objectives of the study	1
1.2 Location	2
1.3 Porphyry deposits	4
1.4 Green rock vs. white rock environments	8
Chapter 2: Regional geology of the Wasatch Mountain Range	9
2.1 The Cottonwood and Park City area geology	9
2.1.1 Oligocene and Eocene intrusive and extrusive rocks	11
2.1.2 Little Cottonwood stock and the White Pine intrusion	13
2.2 Structural history of the Cottonwood and Park City area	15
2.3 Mineralization in the Cottonwood and Park City region	16
Chapter 3: Regional geology of the Battle Mountain mining district	18
3.1 The Paleozoic Geology of the Battle Mountain mining district	19
3.2 Cretaceous intrusive rocks of the Battle Mountain district	21
3.3 Eocene intrusive rocks of the Battle Mountain district	23
3.4 Tectonic history of the Copper Basin area	25
3.5 Mineralisation in the Copper Basin area	27
3.5.1 Buckingham Mo ± Cu system	27
3.5.2 Supergene/hypogene Cu mineralisation	28
3.5.3 Au ± Cu skarn mineralisation	28
3.5.4 Carlin-style Au mineralisation	28
Chapter 4: Methodology	30
4.1 Field mapping and sample collecting	30
4.2 Petrography	31
4.3 Whole rock geochemistry	32
4.4 Geochronology	32
4.4.1 U-Pb dating	32

4.4.2 <i>Re-Os dating</i>	34
4.5 <i>Mineral chemistry</i>	34
4.5.1 <i>Cathodoluminescence imaging of quartz</i>	36
4.5.2 <i>Quartz mineral chemistry</i>	36
4.5.3 <i>Pyrite mineral chemistry</i>	37
4.5.4 <i>Quality ranking</i>	37
4.6 <i>Short-wave infrared spectroscopy</i>	40
Chapter 5: <i>Field Observations and Petrography</i>	41
5.1 <i>White Pine Fork Mo porphyry lithologies</i>	41
5.1.1 <i>Little Cottonwood stock</i>	41
5.1.2 <i>White Pine intrusion</i>	43
5.1.3 <i>White Pine Fork Mo breccia pipe</i>	44
5.1.4 <i>Lamprophyric dykes</i>	46
5.1.5 <i>Alteration and the vein stockwork in the granites</i>	47
5.2 <i>SWIR data</i>	51
5.3 <i>Buckingham lithologies and alteration</i>	53
5.3.1 <i>Harmony Formation</i>	53
5.3.2 <i>Buckingham Intrusions</i>	55
5.3.3 <i>Tertiary granites</i>	55
5.3.4 <i>Hydrothermal breccias</i>	57
5.3.5 <i>Alteration and the vein stockwork in the granites</i>	61
5.3.6 <i>SWIR data</i>	64
Chapter 6: <i>Whole Rock Geochemistry and Geochronology</i>	66
6.1 <i>White Pine Fork Mo porphyry lithologies</i>	66
6.1.1 <i>Little Cottonwood Intrusion</i>	66
6.1.2 <i>White Pine Intrusion</i>	67
6.1.3 <i>Lamprophyric Dykes</i>	68
6.2 <i>Buckingham Mo (-Cu) porphyry lithologies</i>	70
6.2.1 <i>Buckingham porphyry</i>	70
6.2.2 <i>Tertiary granites</i>	70
6.2.3 <i>Hydrothermal breccias</i>	71
6.3 <i>U-Pb and Re-Os dating of the White Pine Fork breccia pipe</i>	73
6.4 <i>U-Pb and Re-Os dating of the Battle Mountain Eocene granites</i>	73
Chapter 7: <i>Mineral trace element geochemistry</i>	76

7.1 <i>Quartz trace element geochemistry from the Little Cottonwood and White Pine intrusions</i>	78
7.2 <i>Quartz trace element geochemistry from the Buckingham porphyry</i>	82
7.3 <i>Trace element geochemistry of pyrite at White Pine Fork Mo porphyry</i>	86
7.4 <i>Trace element geochemistry of pyrite at Buckingham Mo (-Cu) porphyry</i>	88
7.5 <i>Au-rich rims around pyrite grains at Buckingham</i>	90
Chapter 8: Discussion	92
8.1 <i>Petrography of the White Pine Fork Mo porphyry</i>	92
8.2 <i>Petrography of the Buckingham Mo (-Cu) porphyry</i>	95
8.3 <i>Geochemistry</i>	97
8.3.1 <i>White Pine Fork Mo porphyry area</i>	97
8.3.2 <i>Magma fertility at White Pine Fork</i>	101
8.3.3 <i>Whole rock geochemistry mapped alteration</i>	103
8.3.4 <i>Buckingham Mo (-Cu) porphyry area</i>	106
8.3.5 <i>Whole rock geochemistry mapped alteration</i>	106
8.4 <i>White Pine Geochronology</i>	109
8.5 <i>Eocene granite geochronology</i>	110
Chapter 9: Mineral Chemistry and Applications	112
9.1 <i>Quartz</i>	112
9.1.1 <i>Igneous and hydrothermal quartz at White Pine Fork Mo porphyry</i>	115
9.1.2 <i>Igneous, sedimentary and hydrothermal quartz at Buckingham porphyry</i>	118
9.1.3 <i>Trace element substitution in quartz and mineral chemistry vectors</i>	128
9.1.4 <i>Comparisons between White Pine Fork, Buckingham, MAX and Bingham Canyon</i>	129
9.2 <i>Pyrite</i>	136
9.2.1 <i>Pyrite trace element geochemical vectors at White Pine Fork</i>	139
9.2.2 <i>Possible trace element geochemical vectors at Buckingham</i>	141
9.2.3 <i>Au-rich rims around pyrite at Buckingham</i>	142
Chapter 10: Summary and Conclusions	143
References	149
Appendix 1: Petrology	169
<i>White Pine Fork Mo Porphyry</i>	169
<i>Buckingham Mo (-Cu) Porphyry</i>	196
Appendix 2: Sample lists	225
<i>White Pine Fork Mo Porphyry</i>	225

<i>Buckingham Mo (-Cu) Porphyry</i>	227
<i>Polished mounts for White Pine Fork and Buckingham study sites</i>	229
Appendix 3: Geochronology from the White Pine Fork and Buckingham study areas	231
Appendix 4: White Pine Fork whole rock geochemistry	236
Appendix 5: Buckingham whole rock geochemistry	242
Appendix 6: White Pine Fork quartz mineral chemistry	248
Appendix 7: Buckingham quartz mineral chemistry	271
Appendix 8: White Pine Fork pyrite mineral chemistry	295
Appendix 9: Buckingham pyrite mineral chemistry	316

Figures and Tables

Chapter 1	1.1	Location of the White Pine Fork and the Buckingham study area	3
	1.2	Alteration zoning and overprinting relationships in a porphyry system	6
Chapter 2	2.1	Map of the geology and structural features within the Wasatch Mountains.	10
	2.2	Cross section with the estimated paleodepths of emplacement in the Wasatch Range	11
	2.3	A compilation of the intrusive suites in the Wasatch Range and the new ages produced by the P1060 project	12
	2.4	Geological map of the White Pine intrusion	14
Chapter 3	3.1	Map of the state of Nevada showing the location of the Buckingham study site along the Battle Mountain-Eureka Au trend	18
	3.2	Geological map of the Buckingham study area	20
	3.3	Structural map of Copper Basin	26
Chapter 4	4.1	Map showing the sampling locations at the White Pine study area.	30
	4.2	Map showing the sampling locations at the Buckingham study area.	31
	4.3	The location of the sample sites for mounts created at White Pine Fork	35
	4.4	The location of the sample sites for mounts created at Buckingham	35
	4.5	Examples of spot analyses from quartz data	38
	4.6	Examples of spot analyses from pyrite data	39
Chapter 5	5.1	Textural variations seen in the Little Cottonwood stock	41
	5.2	Transmitted light microphotograph of the unaltered Little Cottonwood stock	42
	5.3	QAPF plot, of the Little Cottonwood stock and White Pine	42

	intrusion	
5.4	Transmitted light microphotograph of altered plagioclase and the overgrowth of muscovite	43
5.5	Phenocrysts in the White Pine intrusion	44
5.6	The White Pine Fork Mo breccia pipe	44
5.7	Geological map of the White Pine intrusion with the pyrite alteration halo	45
5.8	Microphotograph of a lamprophyric dyke	47
5.9	Quartz-sericite veins	48
5.1	Microphotograph of a quartz vein in an altered monzogranite from the Little Cottonwood stock	50
5.11	Microphotograph of the mineralisation at White Pine Fork	50
5.12	Mineralised vein cross-cutting relationships	50
5.13	Map showing SWIR results at White Pine Fork	52
5.14	Microphotograph of a quartzite hosting a sericite-rich vein	54
5.15	Microphotograph of an altered feldspar-porphyritic granite	54
5.16	Microphotograph of a porphyritic Tertiary granite.	54
5.17	Locations of hydrothermal breccias and leached cap at Buckingham	58
5.18	Microphotograph of an unmineralised hydrothermal breccia	59
5.19	Microphotograph of a Tertiary hydrothermal breccia	59
5.20	Microphotograph of a quartz-hematite vein in the Tertiary hydrothermal breccia	59
5.21	Microphotograph of a sulphide-rich breccia	60
5.22	Microphotograph of an intersection of two hematite veins in a quartzite	63
5.23	Microphotograph of a barren quartz vein in a grain-supported quartzite	63
5.24	Microphotograph of a hydrothermal breccia hosted in a quartzite	63
5.25	Map showing SWIR results at Buckingham	65
Chapter 6		
6.1	TAS diagram of the Little Cottonwood stock and White Pine intrusion	67
6.2	Primitive mantle normalized trace element plots for the igneous rocks at White Pine Fork	69
6.3	TAS diagram of the Buckingham intrusions and the Tertiary granites	71
6.4	Primitive mantle normalized trace element plots for the granitic suites at Buckingham	72

	6.5	U-Pb concordia plots for the zircon age dates for the White Pine Fork granite clasts	74
	6.6	U-Pb concordia plots for the zircon age dates for the Tertiary Buckingham granites	75
Chapter 7			
	7.1	Hydrothermal quartz in outcrop, polished mount, and cathodoluminescence imaging	76
	7.2	BSE-CL images of different quartz textures	77
	7.3	Map showing the sample locations of the quartz mounts prepared for mineral chemistry analysis at White Pine Fork	78
	7.4	BSE-CL image of an igneous quartz grain from the Little Cottonwood stock	79
	7.5	BSE-CL images of sedimentary and hydrothermal quartz	84
	7.6	Map showing the location of the samples collected for pyrite mineral chemistry analyses	86
	7.7	Microphotograph of hydrothermal alteration around pyrite at White Pine Fork	87
	7.8	LA-ICP-MS element maps of S34, Co59, Fe57 and Ni60 in pyrite (WP13ES63)	88
	7.9	LA-ICP-MS element maps of S34, Co59, Fe57 and Pb208 in pyrite (WP13ES46)	88
	7.1	LA-ICP-MS element maps of S34, Co59, Fe57 and Pb208 in pyrite (WP13ES03)	88
	7.11	Map showing the sample locations of the pyrite mounts prepared for mineral chemistry analysis at Buckingham	89
	7.12	LA-ICP-MS element maps of a pyrite grain (BK13ES028)	91
	7.13	LA-ICP-MS element maps of a pyrite grain (BK13ES102)	91
	7.14	LA-ICP-MS element maps of a pyrite grain (BK13ES059)	91
Chapter 8			
	8.1	Map showing the centres of greater hydrothermal alteration at White Pine Fork	94
	8.2	Map showing the division of the muscovite centre and phengite periphery surrounding the White Pine intrusion.	94
	8.3	Map showing the centres of proposed advanced argillic hydrothermal alteration	96
	8.4	TAS diagram of regional whole rock geochemistry from the intrusive suite in the Wasatch range.	99
	8.5	Compilation of the intrusive suites in the Wasatch Range and	100

	the new ages produced by the P1060 project	
8.6	$^{87}\text{Rb}/^{86}\text{Sr}$ ratios in the regional whole rock geochemistry	100
8.7	Sr/Y vs. SiO_2 and Sr/Y vs. Y plots for White Pine Fork	102
8.8	Whole rock geochemistry normal log plots of Mo, Cu, Pb, Zn, Au, and Te at White Pine Fork	103
8.9	Alteration zones highlighted by whole rock geochemistry at White Pine Fork	104
8.10	Whole rock geochemical contours at White Pine Fork	105
8.11	Whole rock geochemistry normal log plots of Mo, Cu, Au, Ag, Pb, Zn, As, Sb, and Li at Buckingham	107
8.12	Alteration zones highlighted by whole rock geochemistry at Buckingham	107
8.13	Whole rock geochemical contours at Buckingham	108
8.14	Whole rock geochemical contours at Buckingham	109
Chapter 9		
9.1	Tukey box-and-whisker plot of the element concentrations in igneous quartz at White Pine Fork.	115
9.2	Tukey box-and-whisker plot of the element concentrations in hydrothermal quartz at White Pine Fork	116
9.3	Tukey box-and-whisker plot of the element concentrations in breccia cement quartz at White Pine Fork.	116
9.4	Map showing the locations of samples containing quartz analyses at White Pine Fork and the centre of deposit	117
9.5	Tukey box-and-whisker plot of the element concentrations in the igneous quartz at Buckingham	120
9.6	Tukey box-and-whisker plot of the element concentrations in the sedimentary quartz at Buckingham	121
9.7	Tukey box-and-whisker plot of the element concentrations in the hydrothermal vein quartz at Buckingham	121
9.8	Tukey box-and-whisker plot of the element concentrations in the breccia cement quartz at Buckingham	122
9.9	Map showing the locations of samples containing quartz analyses at Buckingham and the centre of deposit	123
9.1	Scatterplot and box-and-whisker plot of Al as a vector in hydrothermal quartz at Buckingham	125
9.11	Scatterplot and box-and-whisker plot of Sb as a vector in hydrothermal quartz at Buckingham	126
9.12	Trends in Al and Sb with new centre of deposit	128

9.13	Comparison of Li in hydrothermal quartz at White Pine Fork and MAX	130
9.14	Comparison of Al in hydrothermal quartz at White Pine Fork and MAX	131
9.15	Comparison of Ti in hydrothermal quartz at White Pine Fork and MAX	132
9.16	Comparison of the geochemistry of White Pine Fork and Bingham Canyon hydrothermal quartz	134
9.17	Comparison of the geochemistry of Buckingham and Bingham Canyon hydrothermal quartz	135
9.18	Scatterplot and box-and-whisker plot of Ni as a vector in pyrite at White Pine Fork	140
9.19	Scatterplots of Au, As, Cd and Cu in pyrite at Buckingham	141

Tables

2.1	Summary of the compositions, ages, paleodepths and local mineralisation for the Tertiary intrusions in the Wasatch Range	12
5.1	Summary of SWIR data data from the White Pine Fork Mo porphyry study area	51
5.2	Summary of SWIR data data from the Buckingham Mo (-Cu) porphyry study area	64
7.1	Mean trace element concentrations in different quartz types at White Pine Fork	81
7.2	Mean trace element concentrations in different quartz types at Buckingham	85

Chapter 1: Introduction

1.1 Objectives

This study was undertaken as a part of the P1060 project funded by numerous mining and exploration companies through AMIRA International. The P1060 project is a continuation of the P765 and P765A programs which successfully developed mineral chemistry vectors within porphyry copper systems to expand the extent of the recognized alteration footprint of mineral deposits. After successful studies in the P765A project, it was expanded into the P1060 project which focused on refining the known mineral chemistry vectors, but also adding new minerals to the tool box and testing proven vectoring tools in different environments.

The purpose of this current study was to apply the theories and methods created by the P1060 project to two study sites: the White Pine Fork Mo porphyry and the Buckingham Mo (-Cu) porphyry. One objective of this study was to collect data on Mo-porphyry systems, a style of mineralisation that was poorly represented in the P765, P765A and P1060 databases due to lack of sampling. In addition to expanded research on Mo porphyry systems, this study tested the effectiveness of quartz and pyrite as mineral tools in environments other than lithocaps, as well as developing new mineral vectoring tools in white rock environments. White rock environments are classified as host rocks that are dominantly sedimentary. The Buckingham porphyry was emplaced in a Paleozoic metasedimentary package, dominated by quartzites (Theodore et al., 1992). The relatively homogenous, inert quartz and white micas in these systems result in different alteration minerals forming around the mineralising system than around a system hosted in green rock (volcanic hosted) and lithocap environments. The other objective of this study was to increase the database for new mineral chemistry data for quartz and pyrite. The P765A project

focused on propylitic minerals (i.e., chlorite and epidote) typically found distal to the deposit. This study focussed on quartz and pyrite as Both the White Pine Fork and Buckingham have well-developed quartz and pyrite alteration halos around the mineralized centre.

1.2 Location

White Pine Fork Mo porphyry

The White Pine Fork porphyry is located in the Wasatch Mountains, Utah, USA. The study site is located approximately 50 km southeast of Salt Lake City, near the Snowbird resort in Alta (Fig. 1.1). Access to the study site was obtained by public trails leading up to White Pine Lake, Red Pine Lake, Maybird Gulch, and along the seasonal ski trails in the area.

Buckingham Mo (-Cu) porphyry

The Buckingham porphyry is located west of the town of Battle Mountain, Nevada, USA and is currently owned by Freeport McMoran Copper & Gold (Fig. 1.1). Access to the property was granted and sample collection and mapping for this study was supported by their geologists. Access to the Battle Mountain mining camp is located about 30 km southwest along the Nevada Highway 305 S. The property is approximately 8 km².

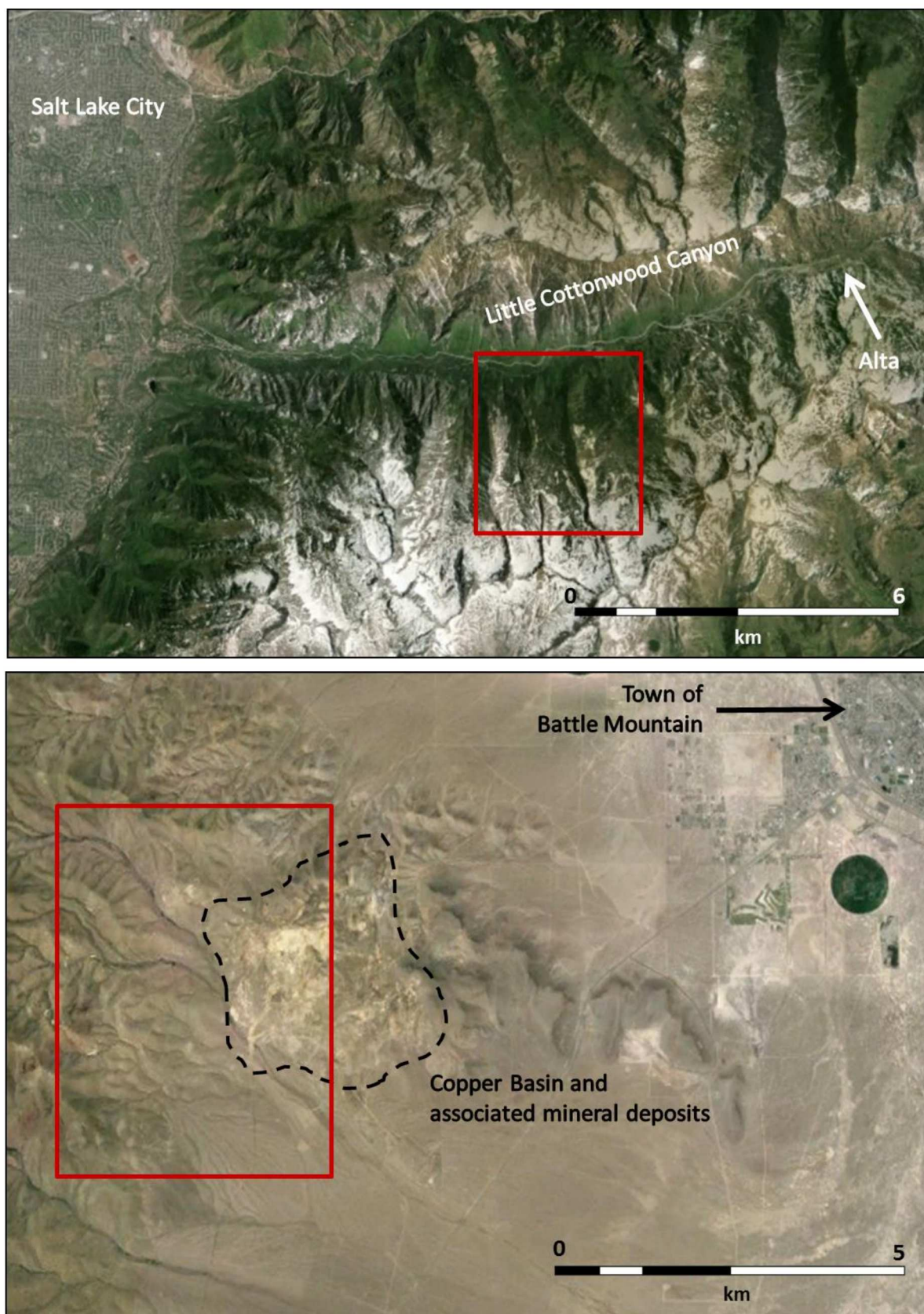


Figure 1.1: (Top) Location of the White Pine Fork study area outlined in the red box; and (bottom) the location of the Buckingham study area outlined in the red box.

1.3 Porphyry deposits

Porphyry deposits are low- to medium-grade, high tonnage, hypogene resources of numerous metals. The deposits can be subdivided by the main metal types found within them into Au, Cu, Mo, Sn and W, and Ag (Kirkham and Sinclair, 1996; Seedorff et al., 2005; Holliday and Cooke, 2007), although normally, more than one metal is present in a given deposit. Porphyry deposits are associated with hypogene mineralization and hydrothermal alteration mineral assemblages that occur in and around large porphyritic, epizonal and mesozonal complexes of felsic to intermediate compositions (Kirkham and Sinclair, 1996). The tectonic setting for these intrusions is typically related to large-scale subduction zones or rift settings such as oceanic island arcs, continental (Andean) arcs, accreted arc terranes, and in post-orogenic magmatic belts (Sillitoe, 1987). The metals present in the mineralized systems are related to the geochemistry of the host rocks and the degree of fractionation undergone in the associated igneous bodies. The less fractionated, calc-alkaline and alkaline intrusions are often associated with Au-Cu deposits, whereas the more fractionated intrusions are associated with Cu, Mo, and Sn-W deposits (Holliday and Cooke, 2007). The hypogene ore mineralization is dominantly structurally controlled and hosted within veins in the stockwork, fracture sets, and breccia pipes. In some deposits, the mining activity has focused on the supergene mineralization which results from the oxidation and leaching and precipitation of the ore metal into a tabular zone located stratigraphically above the intrusion and hypogene mineralization (Lowell and Guilbert, 1970; Corbett and Leach, 1998; Kirkham and Sinclair, 1996).

Holliday and Cooke (2007) outlined the characteristic hydrothermal alteration assemblages associated with the high-grade core of calc-alkalic porphyry deposits. A variation of these alteration zones can be observed in all porphyry deposits and the reoccurrence of the

common alteration minerals is the basis of the P1060 project. Holliday and Cooke (2007) outlined the following alteration mineral assemblages in the hydrothermal systems associated with the more common calc-alkaline intrusion complexes (Fig. 1.2):

1) *Potassic*: characterized by abundant secondary orthoclase ± biotite, and often an associated magnetite halo in the high-grade zone in the system. In alkaline systems, the core could have undergone calc-potassic alteration, characterized by the addition of garnet ± actinolite ± epidote

2) *Phyllic*: an overprinting alteration found near the core of the system characterized by abundant sericite + quartz + pyrite

3) *Advanced argillic*: an overprinting alteration characterized by quartz + alunite + kaolinite ± pyrophyllite. This hydrothermal alteration is potentially associated with high sulfidation state mineralisation

4) *Calc-silicate* (skarn mineral assemblages if carbonate wallrocks are present): characterized by garnet (andradite) + pyroxene (diopside) + epidote + calcite + chlorite + sulfides + quartz + anhydrite

5) *Propylitic* (often unmineralized, distal alteration halo): characterized by epidote + chlorite + carbonates ± pyrite ± actinolite. This alteration zone may extend several kilometers out from the centre of the mineralizing system (Norman et al., 1991; Garwin, 2002; Rae et al., 2003)

6) *Lithocaps* (a stratabound 'cap', rooted by intense phyllic and advanced argillic alteration, found in some porphyry deposits, located above the high-grade zone and below the magnetite-destructive clay and quartz-alunite alteration; Sillitoe, 1995): characterized by argillic and silicic alteration

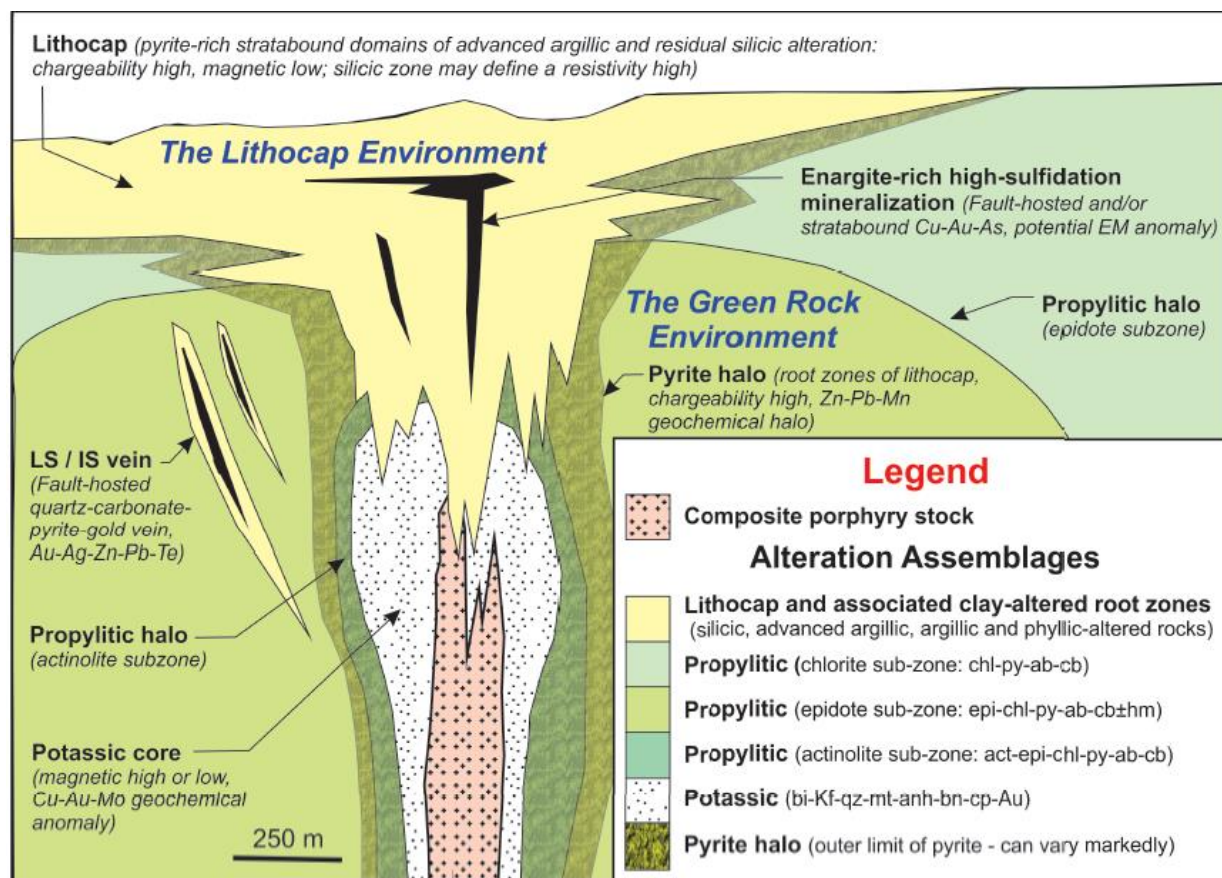


Figure 1.2: Alteration zoning and overprinting relationships in a porphyry system (modified after Holliday and Cooke, 2007; Cooke et al., 2014).

ab = albite, act = actinolite, anh = anhydrite, Au = gold, bi = biotite, bn = bornite, cb = carbonate, chl = chlorite, cp = chalcocopyrite, epi = epidote, hm = hematite, Kf = K-feldspar, mt = magnetite, py = pyrite, qz = quartz.

The hydrous fluids, which precipitate the metals in a porphyry system, also generate the hydrothermal alteration in the surrounding rocks. Several studies have suggested that the majority of the initial fluids involved in the transportation of metals are probably sourced from the magma with a smaller proportion coming from meteoric waters (e.g., Keith et al., 1995; Williams-Jones and Heinrich, 2005; Davidson et al., 2005). The mantle-sourced water and fluids are sourced from the volatile degassing of the cooling intrusion. For example, in the Questa Porphyry Mo Deposit in New Mexico, stable oxygen isotope analyses from the mineralized breccia pipe indicated that, in addition to the aplitic matrix, there was little to no meteoric water

component in the mineralizing fluid (Ross et al., 2002). There is evidence from other, F-poor deposits, that decreasing $\delta^{18}\text{O}$ values and geothermal gradients may indicate a higher meteoric water input (Ross et al., 2002). Meteoritic water is important in the formation of supergene mineralization and oxidation of the hypogene mineralization (Kirkham and Sinclair, 1996).

The classic alteration mineral zoning seen in porphyry deposits is the result of initial high temperatures and the subsequent cooling and influx of meteoric water (Kirkham and Sinclair, 1996). Gustafson and Hunt (1975) developed a model for the evolution of alteration mineral assemblages at the El Salvador porphyry Cu deposit in Chile. They suggested that the subsequent progressive changes from the higher temperature alteration assemblages (phyllic alteration) to lower temperature conditions (argillic alteration) resulted from a change from lithostatic to hydrostatic conditions. They also suggested that the initial emplacement of mineralizing porphyries occurred at depths of ~2 km, under lithostatic pressures. This significant depth helped to facilitate the development of potassic alteration and quartz stockwork veins under very hot (>400-500°C) and highly saline conditions. The evolution to the phyllic, argillic, and advanced argillic alteration zones was interpreted to have been either the result of the influx of deep circulating, connate fluids from the surrounding rocks or the cooling, laterally migrating magmatic-hydrothermal fluids moving away from the intrusion (Gustafson and Hunt, 1975; Dilles et al., 2000).

1.4 Green rock vs. white rock environments

One of the goals of the P1060 project was the creation of tools for mapping gradients of hydrothermal alteration in ‘green rock’, ‘white rock’, and lithocap environments. The previous P765, P765A and P1060 projects defined the green rock environment as being volcanic or intrusive hosted rocks; whereas, a white rock environment is hosted in clastic or chemical sedimentary rocks. In this study, the White Pine Fork Mo porphyry is hosted within the Little Cottonwood granitic stock, defining it as a green rock site whereas the Buckingham Mo(-Cu) porphyry is a white rock site due to it being hosted within a metasedimentary sequence. The wallrock composition influences the formation of alteration minerals. Cooke et al. (2014) suggested that the formation of a propylitic halo mineral assemblage requires a minor mass transfer of cations with the addition of H₂O, H₂S, CO₂, and [Ca]²⁺ to form hydrous minerals, pyrite, calcite, and hydrous Ca-aluminosilicate minerals, respectively. However, if ferromagnesian minerals are not already present in the rock (e.g., quartzites and limestones) then the characteristic chlorite, epidote, actinolite and hydrothermal alteration products will not form.

Chapter 2: Regional geology of the Wasatch Mountain Range

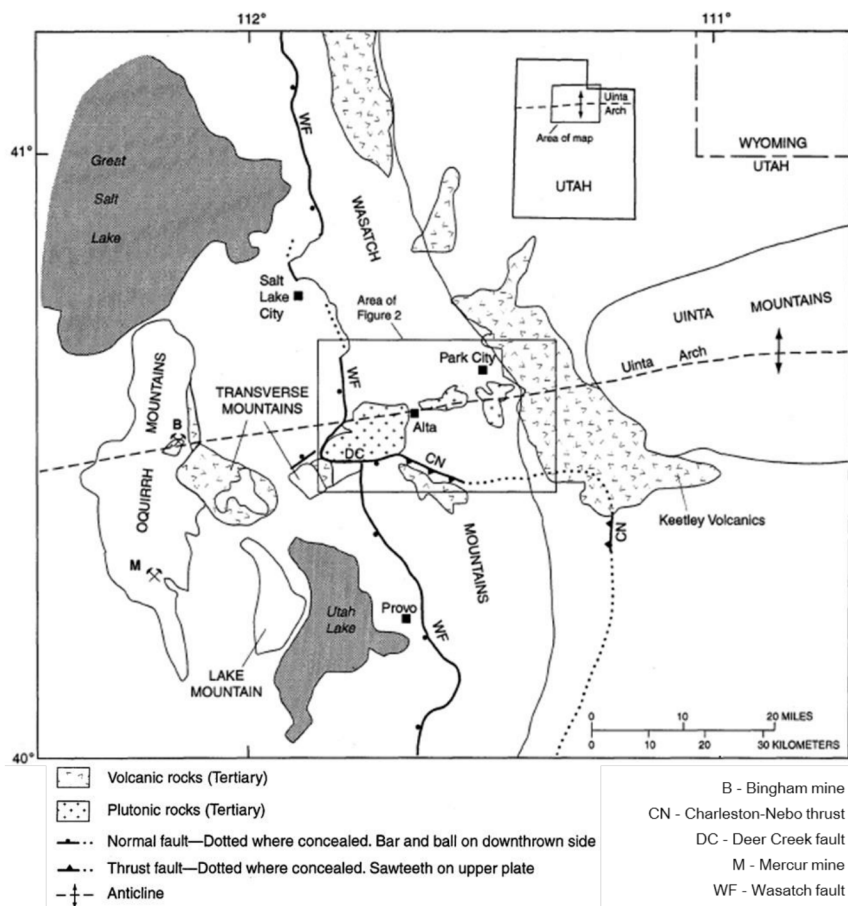
The north-trending Wasatch Mountain range lies at the intersection of the Basin and Range province and the Colorado Plateau, east of Salt Lake City, Utah (Fig. 2.1; John, 1997). The central Wasatch Mountains are composed of older Proterozoic and Mesozoic sedimentary and metamorphic rocks with younger Eocene to Oligocene igneous rocks (Crittenden, 1977; John, 1997). The study area has a complex geological history. The deformed and metamorphosed Paleoproterozoic basement (~1700-1800 Ma), which crops out east of the study area, near Park City is comprised of the cratonic rocks of Rodinia and is overlain by Neoproterozoic metamorphosed and unmetamorphosed clastic sedimentary rocks of the Little Willow and Big Cottonwood Formations (Spencer et al., 2012). These sedimentary formations represent some of the earliest clastic material shed into the Uinta rift basin during the earliest-known phases of the Rodinia supercontinent break-up (Spencer et al., 2012). The later clastic and chemical sedimentary rocks (late Proterozoic to Jurassic in age) have been interpreted to be sediment deposited along a passive continental margin (Crittenden et al., 1983; Spencer et al., 2012). This sequence is topped by the Keetley volcanic suite, which comprises intermediate lava flows and flow breccias as well as associated volcanoclastic and pyroclastic rocks. These rocks underwent periods of compression and extension, resulting in the emplacement of several granitic intrusions that are thought to be cogenetic with the Keetley volcanic rocks (John, 1997).

2.1 The Cottonwood and Park City area geology

The stratigraphic sequence in the Cottonwood and Park City area comprises rocks from the early Proterozoic to the Quaternary. The oldest rocks found in the area are the early Proterozoic metamorphic rocks including amphibolites, gneisses, schists, meta-conglomerates and sandstones. A nonconformity separates these rocks from the late Proterozoic quartzites,

shales, conglomerates and greywackes which contain evidence of glacial deposition (i.e., dropstones and glaciofluvial formations; Crittenden et al., 1983; John, 1997). The Proterozoic rocks eventually grade into Cambrian-aged dolostones, limestones, and finer grained sandstones and shales interpreted to represent shelf sedimentation (Crittenden et al., 1983; John, 1997). The youngest sedimentary rocks in the area are Jurassic in age and comprise sandstones, mudstones and conglomerates. These units can be distinguished from the older Cambrian sedimentary rocks by the lack of carbonate chemical sedimentary rocks (John, 1997).

The youngest rocks in the Wasatch range are Oligocene to Eocene in age. The Keetley volcanic rocks comprise intermediate lava flows and breccias with associated pyroclastic rocks. These volcanic rocks are thought to be surface, cogenetic expressions of the intrusive igneous rocks that were emplaced in the Paleoproterozoic basement and the Neoproterozoic- to Jurassic-aged sedimentary sequence (John, 1997).



2.1.1 Oligocene and Eocene intrusive and extrusive rocks

There are two generations of intrusive rocks exposed in the Central Wasatch Mountains which were emplaced from ~40 to 30 Ma. The Little Cottonwood, Alta and Clayton Peak stocks, are located in the western portion of the Wasatch range and have been interpreted to have deeper paleodepths of emplacement (~10 – 5 km; John, 1989). The Eastern Stocks include the Flagstaff, Valeo, Pine Creek, Mayflower and Park Premier stocks and have shallower calculated depths of emplacement (Figs. 2.2 and 2.3; Cooke et al., 2012). The Eastern Stocks have similar geochemical compositions to the Keetley Volcanics, which unconformably overlie the older sedimentary rocks (Vogel et al., 1997, 2001; John, 1997). The stocks cover a calc-alkaline series that range from a granite to diorite compositions; however, most of the rocks are granodiorites (John, 1989; Vogel et al., 1997). These units are high-K calc-alkaline rocks and are enriched in light rare earth and incompatible elements and show a Nb anomaly and no Eu anomaly (Vogel et al., 1997). Table 2.1 outlines the characteristic features of the intrusions from west of the Wasatch fault to Park Premier in the Central Wasatch Mountains (John et al., 1997). The ages were collected by the P1060 project.

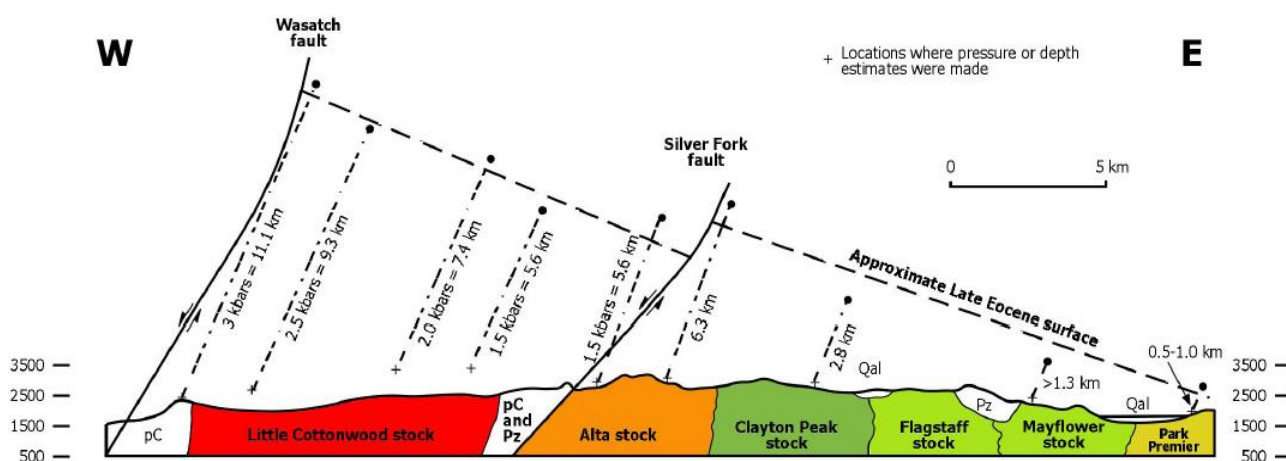


Figure 2.2: W – E cross section with the estimated paleodepths of emplacement and the erosional surface with the regional block tilting resulting from extensional tectonics (modified from John, 1989).

Table 2.1: Summary of the compositions, ages, paleodepths and local mineralisation for the major stocks formed during the Tertiary magmatism (modified from John et al., 1997; Vogel et al., 1997).

Unit	Composition	Age (U-Pb; Ma) (from P1060)	Emplacement Age (Ma)	Emplacement Depth (km)	Mineralisation
Little Cottonwood Stock	Granite to granodiorite	29.45 ± 0.31 29.63 ± 0.27 29.91 ± 0.34	30–31	9.3–5.6	White Pine Fork porphyry Mo (16 Mt at 0.1% Mo); Greisen alteration and possible Mo mineralisation
Alta Stock	Diorite to dacite/quartz diorite	32.82 ± 0.42	35–33	6.0–5.5	Big Cottonwood Mine; Mountain Lake Mine; Fe-Cu skarn deposits
Clayton Peak Stock	Granodiorite to quartz monzodiorite/monzonite	34.64 ± 0.51	36–35	2.8	Multiple polymetallic vein and replacement style deposits
Pine Creek Stock	Granodiorite porphyry	34.85 ± 0.39	38–41	2.8–1.3	Multiple polymetallic vein and replacement style deposits
Flagstaff Stock	Granodiorite to diorite/syenodiorite	35.09 ± 0.37	--	2.8–1.3	Polymetallic vein and replacement deposits including the Daly West and Judge mines
Park Premier Stock	Andesite to dacite/diorite porphyry	33.69 ± 0.6	35–32	0.5-1	Polymetallic vein and replacement deposits including: Mayflower Au-Ag-Pb-Zn-Cu vein mine; Park Premier composite porphyry Cu-Au, Cu skarn and polymetallic vein mine

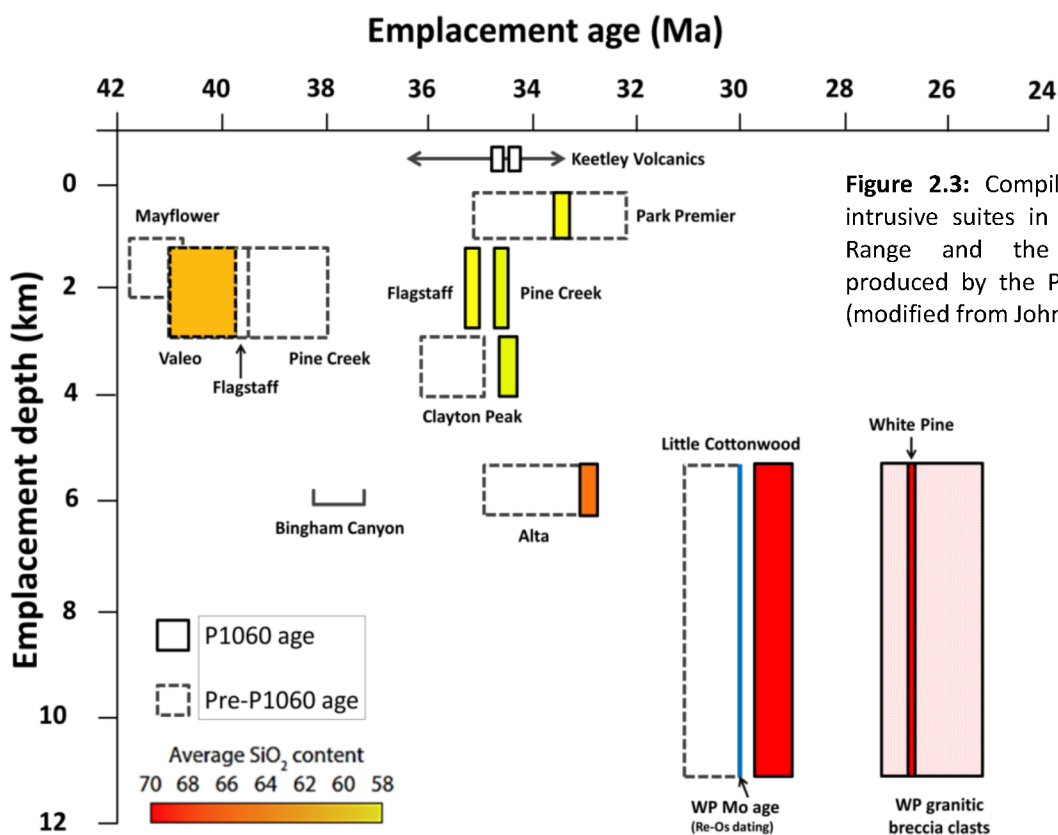


Figure 2.3: Compilation of the intrusive suites in the Wasatch Range and the new ages produced by the P1060 project (modified from John et al., 1997)

2.1.2 Little Cottonwood stock and the White Pine intrusion

The youngest igneous stock in the Wasatch Mountains is the Little Cottonwood stock. This igneous body contains a younger phase known as the White Pine intrusion. The Little Cottonwood stock is bound by two north-trending, normal faults: the Wasatch Fault to the west and the Silver Fork Fault to the east (Fig. 2.1). This intrusion was emplaced into older metasedimentary rocks, and possibly the Paleoproterozoic basement (John et al., 1997; Vogel et al., 1997). The majority of the unit is granodioritic to quartz monzonitic in composition with large (≤ 6 cm) K-feldspar phenocrysts. The mafic mineralogy is commonly biotite and hornblende with accessory titanite and magnetite. There are several aplitic and pegmatitic dykes throughout the intrusion. The unit also hosts xenoliths of the metamorphosed basement and later metasedimentary rocks. The White Pine Fork intrusion is a coarser grained, more leucocratic, K-feldspar- and quartz porphyritic phase of the Little Cottonwood Stock (John, 1989; Cooke et al., 2012). There are rare, younger, narrow (< 5 m wide), north-trending lamprophyric dykes which cross-cut both the Little Cottonwood and White Pine Fork intrusion (John, 1997).

The White Pine Fork Mo porphyry and mineralised breccia pipe is located in the eastern part of the Little Cottonwood intrusion (Fig. 2.4). The hydrothermal alteration around the mineralised zone is very similar to a porphyry-style alteration halo around known mineralised centres. The hydrothermal alteration has been described by John (1997) as occurring in in stockwork veins and vein selvages, fracture-controlled and disseminated pyrite with localised potassic and sericitic alteration. John (1997) also describes a green sericite + pyrite \pm fluorite \pm molybdenite alteration, similar to greisens. The porphyry hosts a quartz-cemented, rusty breccia pipe which includes the most intense hydrothermal alteration (sericitization and pyritization with significant potassic alteration and an extensive pyrite alteration halo; Fig. 2.4). Abundant, visible

molybdenite can be observed in veins, as well as pods within vein selvages and disseminated in the breccia clasts (John, 1997). Bromfield and Patten (1981) described the low-grade Mo (\pm W \pm Cu) mineralisation as being strongly associated with quartz stockwork veins that are commonly stained with secondary iron oxides. John (1983) noted seven different types of veins (Mo is associated with types 2, 3, and 4), suggesting multiple pulses of fluid:

1. Pyrite + sericite;
2. Vuggy quartz \pm pyrite with sericite vein selvages
3. Vuggy quartz \pm pyrite without sericite vein selvages
4. Granular quartz + pyrite
5. Sericite
6. K-feldspar
7. Anhydrite veins, partially altered to gypsum

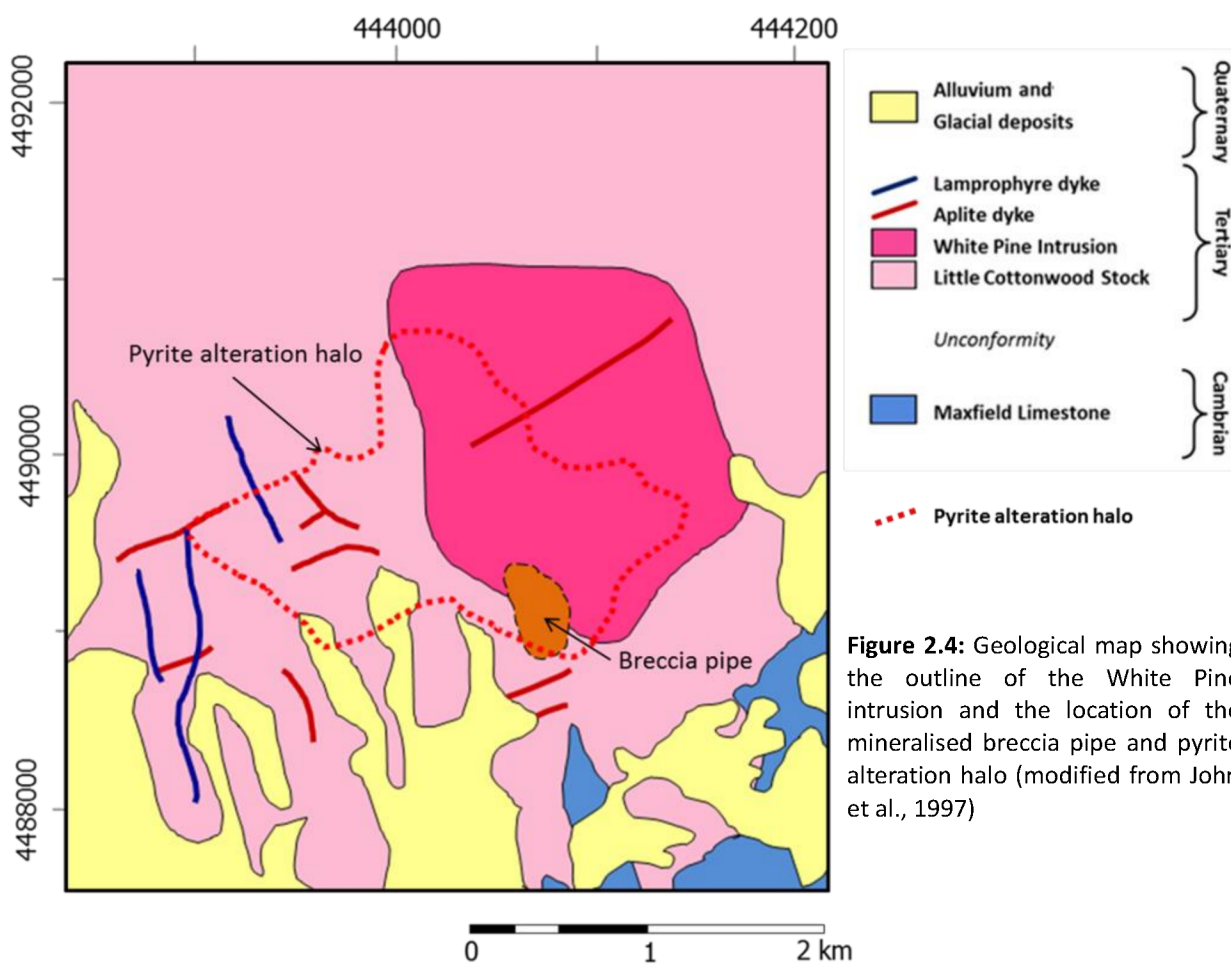


Figure 2.4: Geological map showing the outline of the White Pine intrusion and the location of the mineralised breccia pipe and pyrite alteration halo (modified from John et al., 1997)

2.2 Structural history of the Cottonwood and Park City area

The Cottonwood area has undergone multiple episodes of regional faulting and deformation. Early Tertiary structures in the Cottonwood area comprise east-striking thrust faults found in the Sevier orogenic belt (active from 130 – 40 Ma) and those related to the uplift along the west-plunging Neoproterozoic Uinta arch (a gently- to steeply-dipping regional-scale anticline; John, 1989). Three major thrust faults (the Alta, Mount Raymond, and Charleston-Nebo thrusts) and numerous minor faults propagated along weaker sedimentary strata during the collisional events. These faults have been proposed as the mechanism for emplacing a thicker allochthonous Paleozoic section over a thinner, equivalent autochthonous cratonic block (the Paleoproterozoic basement and earlier metasedimentary rocks; Crittenden, 1977; Willis, 1999). The Sevier orogeny and the Laramide orogeny (which temporally overlaps the Sevier mountain building event) lasted from 70 – 34 Ma (Sprinkel, 2014). The Laramide orogeny resulted in an uplift of basement rock (Willis, 1999). Both of these crustal shortening events resulted from the subduction of the Farallon Plate below the North American plate. After compression ceased, the resulting extensional stress regime allowed for the emplacement of the igneous intrusions in the Wasatch range (Willis, 1999). Most of the intrusions in the Wasatch Mountains were emplaced along the axis of the Uinta arch, with some porphyritic bodies intruding along minor folds formed off the main Uinta arch (Crittenden, 1977; John, 1989).

Crustal extension in the study area has been interpreted to be associated with Basin and Range tectonism. The Wasatch Mountains are along the eastern boundary of the Basin and Range province, with the western edge of the Cottonwood area bounded by the Wasatch fault (a north-striking, normal fault; Fig. 2.1; John, 1989). Another north-striking normal fault, the Silver Fork fault, bounds the other side of the Little Cottonwood stock and cuts and displaces the Alta

stock. The uplift (up to 11 km relative to the Salt Lake Basin) of the Little Cottonwood stock is interpreted to be the result of the formation of high-angle normal faults (John, 1997; Zoback, 1983; Parry and Bruhn, 1986, 1987). The uplift of the Wasatch Range has been proposed to have started at 17 Ma, but the majority of the uplift has been in the last 10 m.y. (Crittenden et al., 1973; Naeser et al., 1983; Parry and Bruhn, 1986). The uplift and tilting of the crustal block dipping approximately 20° to the west resulted in the exposure of deeper plutonic complexes in the western portion of the study area (i.e., the Little Cottonwood stock) and shallower and older plutons and coeval volcanic rock in the east (i.e., the Mayflower stock and Keetley volcanics; Fig. 2.2; John, 1989).

A second major orientation of faults that cut the Wasatch intrusions strike east-west. These faults may have been active during the emplacement of the igneous intrusions and it has been suggested that they were important for the transportation of mineralising fluids in local precious and base metal occurrences in the study area (John, 1989).

2.3 Mineralization in the Cottonwood and Park City region

The central Wasatch Mountains have been mined since 1868 (John, 1997). There are notable Ag-Pb-Zn±Cu±Au replacement and vein deposits, a low grade Cu-Au porphyry deposit, Cu skarn deposits and high-sulfidation (quartz-alunite) Au deposits (John, 1997). The Park City mining district produced >1.4 Moz of Au, 253 Moz of Ag, 2.7 billion lbs Pb, 1.5 billion lbs Zn, and 129 million lbs of Cu from 1872 to 1978 (John, 1997). There has also been mining of mostly Pb-Ag (±Cu±Au) replacement deposits along fissures in carbonate rocks in the Little and Big Cottonwood districts (John, 1997). The majority of the Ag-Pb-Zn mineralization in the Big and Little Cottonwood district is located along the Alta thrust. The ore bodies were formed as replacement of brecciated limestone and were later disrupted and displaced by the north-trending

normal faults (John, 1997). The main ore minerals are pyrite and galena with minor sphalerite, tetrahedrite, and W-minerals (John, 1997). At some localities, the ore mined was secondary metal oxides, sulphates, and hydroxides (Calkins and Buter, 1943). Carbonate-hosted polymetallic Cu-skarn deposits are also found in the Cottonwood district. Limestones of the Big Cottonwood formation were altered and replaced during metasomatism, resulting in local ore bodies of massive magnetite + bornite \pm chalcopyrite which also hosts some base metal and precious metal mineralization (John, 1997).

The White Pine Fork Mo occurrence is centralized around a rusty breccia pipe located near the southern portion of the White Pine intrusion (John, 1997). Three drill holes by Bear Creek Mining Co. intercepted a zone ~40 m thick containing ≤ 0.5 % MoS_2 starting at depths of 90 to 120 m. An estimate of 16 Mt at 0.1% Mo was obtained based on the drilling program (Bromfield and Patten, 1981). Bromfield and Patten (1981) describe this low-grade Mo (\pm W \pm Cu) mineralisation as being strongly associated with the, frequently Fe-stained, quartz stockwork veins. The majority of molybdenite occurs in veins, blebs, within vein selvages and disseminated in the breccia clasts (John, 1997).

Chapter 3: Regional geology of the Battle Mountain mining district

The Buckingham Mo (-Cu) porphyry is located in northern central Nevada, just north of the Carlin-style Battle Mountain-Eureka Au trend (Fig. 3.1) and is associated with supergene and hypogene Cu mineralization. The Battle Mountain mining district is a historically significant producer of copper, and more recently, gold and molybdenum (Theodore et al., 1992). The area hosts two generations of intrusive rocks which were emplaced into metasedimentary rocks. The oldest exposed rocks in the district belong to the Scott Canyon Formation, the Cambrian Harmony Formation and the upper Paleozoic rocks of the Antler sequence (Theodore et al., 1992). The Paleozoic metasedimentary sequence hosts the Late Cretaceous granitoid dykes and stocks associated with the Buckingham Mo and supergene Cu mineralisation. These metasedimentary rocks were also intruded by the later Eocene-aged granitic stocks which are associated with gold mineralisation and skarn alteration (Fig. 3.1; Theodore et al., 1992).

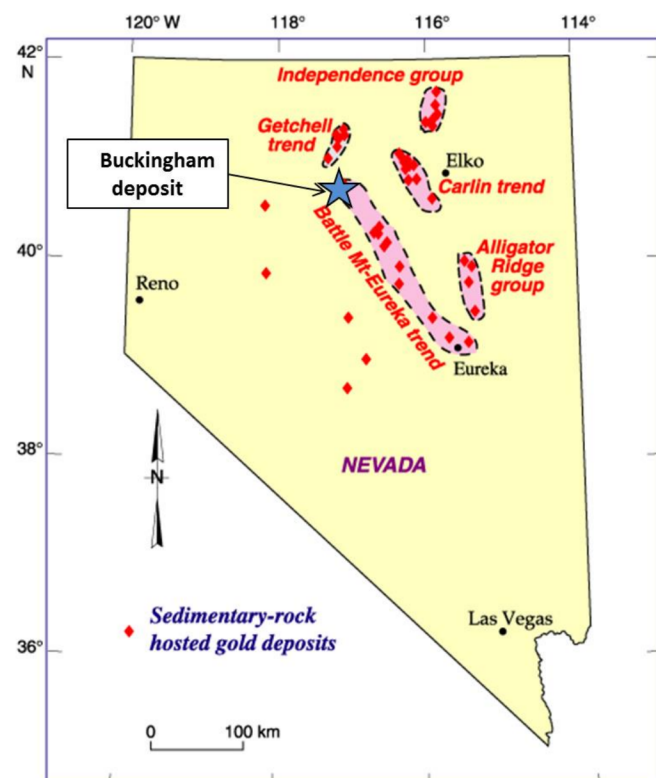


Figure 3.1: Map of the state of Nevada showing the location of the Buckingham study site along the Battle Mountain-Eureka Au trend (modified from the United States Geological Survey, 2012)

3.1 The Paleozoic Geology of the Battle Mountain mining district

The sedimentary sequences in the study area formed as the result of deposition during multiple tectonic episodes. The Devonian Scott Canyon sequence (>1500 m thick) comprises deep water sedimentary rocks such as chert, argillite, and intercalated volcanic rocks (greenstone) with minor carbonate rocks (Theodore et al., 1992). The argillitic and cherty units in the Scott Canyon formation are thinly laminated with some bedding. These beds and layers are deformed and fractured, frequently showing displacement along the faults (Roberts, 1964; Theodore et al., 1992). Andesitic to basaltic metavolcanic units make up a significant proportion of the formation. The rocks are predominantly pyroclastic (grainsize ranging from tuffs to coarse-grained breccias) with a minor component of the unit being massive flows. Syngenetic alteration of the rocks has been interpreted to suggest subaqueous eruptions (Roberts et al., 1964). Narrow fossiliferous, carbonate lenses and arkosic sandstones are found near the top of the sedimentary sequence (Roberts, 1964).

The Late Cambrian Harmony is considered to be a transitional formation from the Scott Canyon Formation. The Harmony formation (>1000 m thick) is composed of feldspathic sandstone (now quartzite), rock fragment-rich sandstone, shale, and limey shale and other carbonate-rich rocks. The formation is predominantly (<70%) sandstones and quartzites (Roberts, 1964). These rocks rarely show coarse-grained material and display consistent graded bedding and some evidence of turbiditic activity. This unit is considered to be autochthonous or parautochthonous. A thrusting event moved blocks of the Harmony formation eastward during the Paleozoic and westward during Mesozoic tectonism (Roberts et al., 1958). The sedimentary sequences overlying the Cambrian rocks is composed of three smaller units, in ascending order, the Battle Formation, Antler Peak Limestone, and the Edna Mountain Formation. This sequence

rests unconformably on the Harmony formation. These units contain carbonate rocks which grade into sedimentary rocks with a greater clastic proportion (conglomerates, sandstones, shales) and topped with fluvial deposits indicative of a near shore environment with marine and terrestrial clastic components. These rocks, including the intrusive suites, are covered by quaternary alluvium and young fluvial deposits (Fig. 3.2; Roberts, 1964; Theodore et al., 1992).

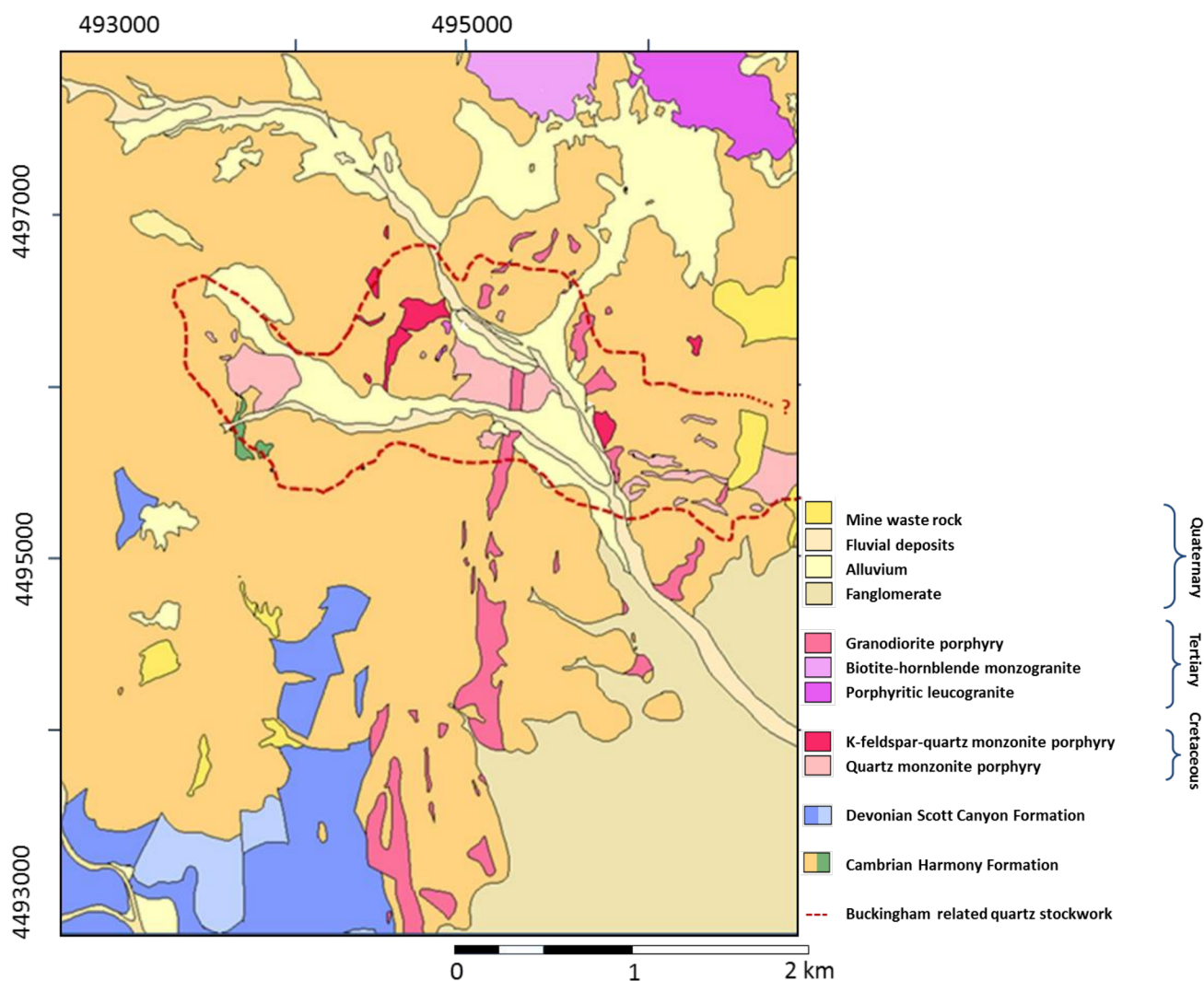


Figure 3.2: Geological map showing the Buckingham granites and the Eocene granites intruded into the Paleozoic metasedimentary rocks [modified after Keeler (2010) and Theodore et al. (1992)].

3.2 Cretaceous intrusive rocks of the Battle Mountain district

The dykes and stocks which host the Mo mineralisation in the Buckingham area are Cretaceous in age and consist of several approximately east-west-trending dikes and a smaller number of equant stocks (Theodore et al., 1992). The primary lithology is a homogenous monzogranite porphyry which intrudes the Upper Cambrian Harmony Formation (Fig. 3.2). This monzogranite has been dated by U-Pb in zircon from 92.2 ± 1.4 Ma to 98.8 ± 2.0 Ma (Keeler, 2010). Theodore et al (1992) describe the other key intrusive relationships and phases as follow. The Buckingham Camp's granitic complex including megacrystic monzogranite porphyry, aplite, and brecciated rocks. Locally, parts of the monzogranite are hydrothermally altered with most of the plagioclase feldspars reacting to white micas and clay minerals and the rock occasionally becoming silicified. The homogenous porphyritic monzogranite is texturally characterized by 10mm wide, bipyramidal and subrounded quartz phenocrysts, composing up to 20 to 25 volume percent of the rock. There are also pink K-feldspar phenocrysts (<15 mm) and hydrolosized plagioclase feldspar phenocrysts. Tabular sheets of biotite (<1.5mm wide) are dispersed irregularly in the monzogranite porphyry and are intensely altered to white mica and chlorite. The contacts of the megacrystic monzogranite with the very similar homogenous monzogranite are not well-developed but the megacrystic unit has been interpreted to crosscut the more homogenous monzogranite. Theodore et al. (1992) noted that there is also a highly altered monzogranite unit comprised large, pink or white, euhedral K-feldspar phenocrysts which are irregularly distributed in a medium-grained to microaplitic groundmass. This altered unit has a notable decrease in the overall abundance of quartz veins (but an increase in some places of weathered pyrite veins), and an increase in abundance of white mica and iron oxide minerals in comparison to the less altered monzogranites. There is often a well-developed quartz vein

stockwork and hydrolyzed alteration halo in the Paleozoic metasedimentary rocks adjacent to the highly altered unit.

The aplitic unit is the latest phase in the Buckingham monzogranite and composes a very minor component of the intrusive suite (Theodore et al., 1992). The rock is K-feldspar-rich (often >50 modal %) and has a component of quartz microphenocrysts. The unit crosscuts the megacrystic monzogranite porphyry. It also does not display the quartz stockwork veining often seen in the rest of the monzogranitic units (Theodore et al. 1992). Theodore et al. (1992) describe a very small (~20 m wide) circular area in the East stock of the Buckingham system that is made up of a probable breccia pipe. This unit has been interpreted to represent the last stages of the Buckingham molybdenum hydrothermal system. The pipe contains variable-sized fragments (10 to 15 mm in width) of different lithologies from the metasedimentary country rock (mostly intensely argillized shaly hornfels fragments derived from the Harmony Formation) and some partially rounded fragments of vein quartz (Theodore et al., 1992). The development of the breccia pipe is interpreted to be mostly post-Mo mineralization. However, some of the clasts and fragments have Cu-rich coatings on their weathered surfaces composed of secondary copper minerals: chrysocolla and/or malachite (Theodore et al., 1992; Blake, 1992). Blake (1992) suggested that the Cu may have migrated during the supergene alteration of nearby primary Cu minerals. A pebble dyke is found to the east of the system which cuts through all the same units which are cross-cut by the breccia dyke including some intensely-veined monzogranite porphyry. The dominant clast type are well-rounded, dark-gray pebbles and chert fragments, most likely derived from the Devonian Scott Canyon Formation at depth. The development of the pebble dyke has been suggested to be coeval with the breccia pipe (Theodore et al., 1992).

3.3 Eocene intrusive rocks of the Battle Mountain district

To the north of the Buckingham intrusion, there are several younger, Eocene intrusive bodies and a co-genetic rhyolite/rhyodacite (Fig. 3.2). Theodore et al (1992) describes three main intrusions: a biotite-hornblende monzogranite and younger leucogranite and granodiorite porphyries. The biotite-hornblende monzogranite is characterised by the occurrence of occasional plagioclase feldspar phenocrysts and hornblende \pm augite as the dominant mafic mineral phase. The largest body of the biotite-hornblende monzogranite is nearly circular in shape and measures about 800 m in diameter (Fig. 3.2). There are several much smaller equant bodies and dyke-like satellites to this larger intrusion. The extensive contact metamorphic aureoles around these smaller intrusions imply that at least some of these small outcrops of the biotite-hornblende monzogranite are underlain by more extensive intrusive rocks (Theodore et al., 1992). In places, the Harmony Formation metasedimentary rocks are recrystallized to a dense, black biotite hornfels. The fabric of quartz veins formed during the emplacement of the Eocene biotite-hornblende monzogranite is distinct from the veins associated with the emplacement of the Late Cretaceous Buckingham molybdenum system. Many of the quartz veins associated with the biotite-hornblende monzogranite show quartz-quartz banding, a texture not found in the Buckingham system (Theodore et al., 1992). The interfaces between the quartz bands are characterized by an increased concentration of microscopic solid inclusions of pyrite and fluid inclusions (which frequently host opaque minerals; Theodore et al., 1992). This monzogranite hosts an irregularly shaped hydrothermal breccia pipe about 500 m by 200 m. Similar to the breccia pipe hosted in the Buckingham system, this pipe boasts several different types of clasts, including brecciated quartz veins and fragments of the Paleozoic metasedimentary host rocks (Theodore et al., 1992).

A porphyritic leucogranite intrudes the Upper Cambrian Harmony Formation and contains xenoliths of the biotite-hornblende monzogranite but at the northwest end, the porphyritic leucogranite is intruded by Oligocene granodiorite porphyry and contains fragments of the younger granodiorite (Fig. 3.2; Theodore et al., 1992). There are biotite-rich baked zones (hornfels) found in the metasedimentary rocks which host both the leucogranite and granodiorite intrusion (Theodore et al., 1992). The leucogranite comprises Na-rich plagioclase, K-feldspar phenocrysts, and common bipyramidal quartz phenocrysts with clinopyroxene (Roberts, 1964). There are two different phases within the leucogranite, a smaller quartz dioritic phase near the northern end of the intrusion, and a much more common porphyritic leucotonalite phase in the eastern portion. The tonalitic body has been associated both spatially and possibly genetically with skarn mineralization and with well-developed quartz stockwork vein systems that formed extensively in rocks of the Harmony Formation north of the Copper Basin Mine (Theodore et al., 1992). The quartz veins often contain some pyrite (now weathered to Fe oxide minerals) and host rare quartz-epidote and quartz-K-feldspar veins (Theodore et al., 1992).

The granodiorite porphyry has a similar composition to the older monzogranite but with an increased modal abundance of quartz in the groundmass and hornblende and biotite phenocrysts. This intrusive body is unique in that it has undergone a moderate degree of propylitic alteration. Much of the hornblende and biotite has been altered to actinolite \pm titanite with rare secondary plagioclase and K-feldspar (Roberts, 1964; Theodore et al., 1992). The granodiorite is cross-cut by quartz-actinolite veins and is with associated skarn alteration along its contacts with adjacent Cambrian carbonate rocks (Theodore et al., 1992).

3.4 Tectonic history of the Copper Basin area

Continental rifting at the start of the Cambrian led to the formation of a new continental shelf and the deposition of a westward-thickening sequence of shelf sediments deposited from the end of the Proterozoic through the Cambrian (Roberts, 1964). The sedimentary rocks include shallow terrestrial material to shallow and deep marine sediments (Stewart and Poole, 1974). The sedimentation along this continental margin was disrupted by subsequent orogenic events including the Devonian-Mississippian Antler orogeny, which formed the Roberts Mountains allochthon, and the Permian-Triassic Sonoma orogeny, which resulted in the Golconda allochthon (Silberling and Roberts, 1962; Roberts, 1964). These periods of tectonism pre-date the later, unconformably over-lying Antler metasedimentary sequence. The subduction of the Farallon plate beneath North America, starting in the Jurassic, resulted in the magmatism in Copper Basin which continued until the mid-Tertiary (Barton, 1996). Arc magmatism ceased as the continental margin switched from a subduction zone to a transform margin (John, 2001). This termination of the convergent plate boundary in the late Eocene (~38-41 Ma) generated large-scale extensional forces that resulted in the formation of the Basin and Range province (Seedorff, 1991). The Battle Mountain mining district is structurally complex with the entire sequence of the metasedimentary rocks (composed of thrust plates of Paleozoic rocks that have been deformed into a broad anticline) cut by younger Tertiary low angle, normal brittle faults (Keeler, 2010). The notable faults in the area are the Contention, Buckingham, Second, and Long Canyon faults. The faults strike northwest and have shallow to steeper northeasterly dips (15° to $50-60^{\circ}$). The Elvira fault system strikes north-east and steeply dips to the northwest and has 335 m of displacement downdip. The fault systems have been suggested to be synchronous with the

emplacement of the Eocene igneous intrusions in the northern part of the study area (Keeler, 2010).

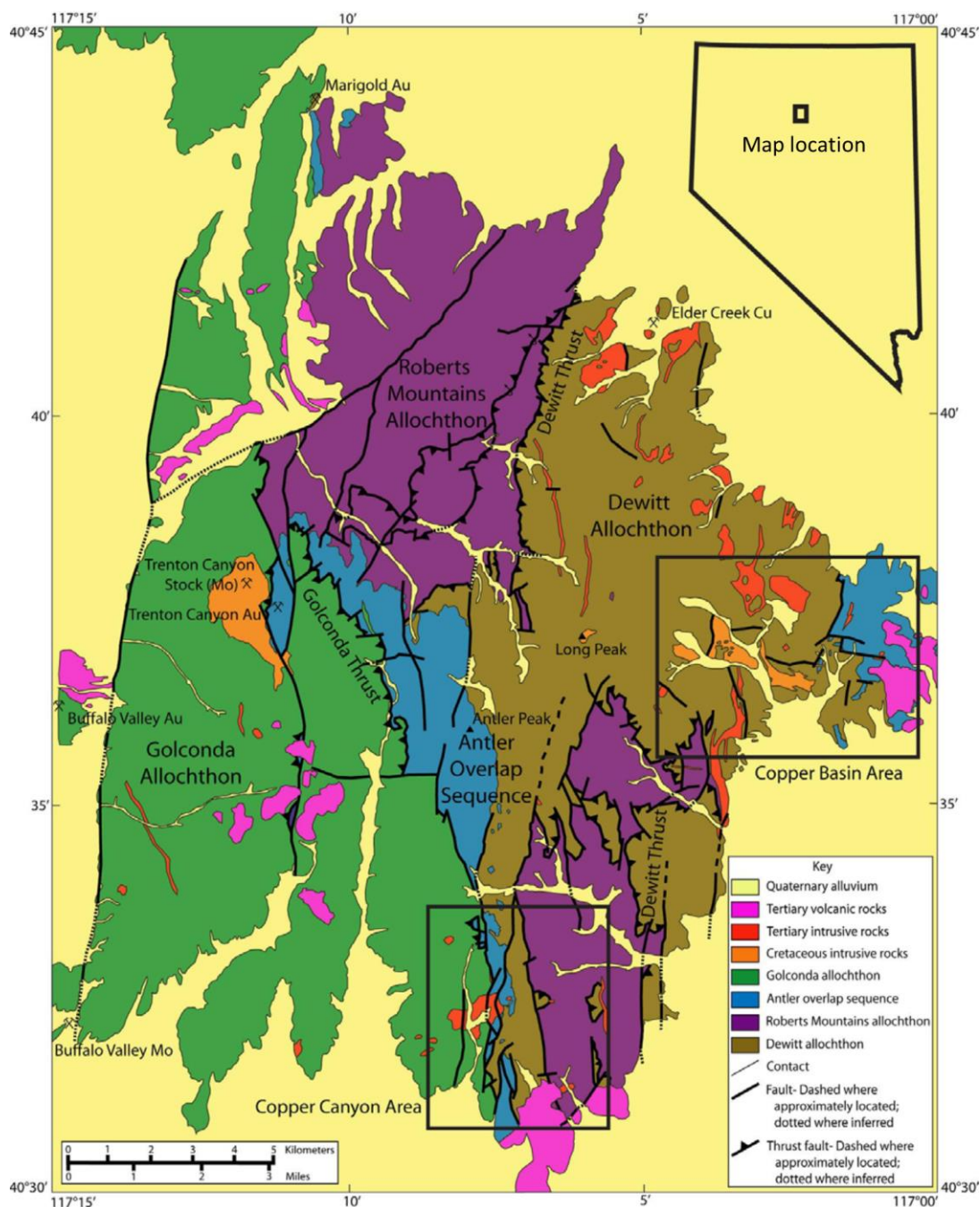


Figure 3.3: Structural map showing the major faults and tectonic blocks in the area surrounding the Copper Basin (modified from Keeler, 2010). The location of this map in the state of Nevada is outlined in the top right.

3.5 Mineralization in the Battle Mountain district

3.5.1 Buckingham Mo ± Cu system

The most recent resources of the Buckingham porphyry system have been estimated to be 1,000 Mt of Mo at 0.1% MoS₂ (Theodore et al., 1992). The stockwork vein-hosted molybdenum mineralisation has been interpreted to be associated with the emplacement of the Late Cretaceous composite porphyry system (Theodore et al., 1992). The molybdenite typically occurs as very fine-grained flakes, intergrown with white mica (probably sericite). In places the molybdenite is concentrated where white mica has completely replaced primary biotite and other mafic minerals or around the margins of quartz phenocrysts and radiating out into the groundmass (Theodore et al., 1992). However, the majority of the molybdenite is dispersed irregularly throughout the groundmass of the monzogranite porphyry (Theodore et al., 1992). The molybdenite often occurs as fine-grained blades concentrated in the granular groundmass. Locally, it occurs in quartz veins hosted within the Buckingham stock and adjacent metasedimentary rocks. Some small blades of molybdenite have narrow halos of ferrimolybdite and chrysocolla replacing molybdenite and chalcopyrite, respectively, formed as a result of weathering (Theodore et al., 1992). Fracture surfaces of the Buckingham porphyry show secondary copper minerals which either represent primary hypogene Cu minerals (i.e., chalcopyrite) which was weathered or Cu that has migrated from the adjacent Cu occurrences (Theodore et al., 1992; Blake, 1992). The dominant vein type, aside from the quartz stockwork, are quartz-white mica-pyrite veins (phyllic alteration mineral assemblage) with the majority of the pyrite altered to iron oxides (Theodore et al., 1992).

3.5.2 Supergene/hypogene Cu mineralisation

Secondary Cu mineralisation at Copper Basin is located in the Cretaceous monzogranite dykes and the stockwork quartz veins, to the west of the Buckingham system, and comprises

chrysocolla and turquoise, as well as malachite and azurite (Theodore et al., 1992). Blake (1992) notes that the principal hypogene sulphide minerals found beneath the leached cap and supergene blanket are pyrite, pyrrhotite, chalcopyrite, galena, sphalerite, molybdenite, marcasite, and rare arsenopyrite. The total sulphide abundance is generally low (~2 vol %) but can reach 5-10 vol % (Blake, 1992).

3.5.3 Au ± Cu skarn mineralisation

There are a number of Au and Au ± Cu skarn deposits in the Copper Basin area. The Au mineralisation in the northern part of the study area is hosted dominantly in the metasedimentary rocks in iron-oxide veins that are thought to have originally contained primary, high temperature, Fe-sulphides (Theodore et al., 1992). These veins were initially thought to have been associated with the Cretaceous magmatism. However, geochronology undertaken by Keeler (2010) and in this study show that the proximal intrusions are Eocene in age and that the Au mineralisation sits on the periphery of the larger porphyry deposit. The Au mineralisation has been suggested to represent a shallow extension of an Eocene porphyry Cu-(Au-Mo) system (Seedorff et al., 2005).

3.5.4 Carlin-style Au mineralisation

The Battle Mountain area is located west of the Roberts Mountains thrust, part of the larger Eureka mineral belt (Fig. 3.1). This mineral belt contains Eocene disseminated, sediment-hosted Carlin-style Au deposits (Theodore et al., 1992). The gold in these deposits is typically hosted as Au-rich rims on As-rich pyrite and marcasite or arsenopyrite and is also found disseminated in the sulphides that formed during mineralisation (Cline et al., 2005). One pulse of volcanism, associated with Carlin-style Au overprinting mineralisation, has been dated around ~40 – 36 Ma, making it similar in age to the granites responsible for the Au mineralisation at Copper Basin (Henry and Ressel, 2000). Although total contained Au and ore grades vary widely

across districts and within deposits, there are ten deposits in the Carlin, Getchell, and Battle Mountain Eureka trends which contain more than 5 million ounces of Au and four deposits which contain more than 10 million ounces (Fig. 3.1; Cline, 2005). The Nevada Bureau of Mines and Geology (2004) have listed the production of these deposits as exceeding 50 million ounces.

Chapter 4: Methodology

4.1 Field mapping and sample collecting

The field areas at White Pine and Buckingham were both accessible by foot. Sampling followed planned transects away from the centre of the mineralised system. The mapping coverage of the White Pine study area was completed in two weeks and extended from the base of the valley of the Little Cottonwood Canyon up to White Pine Lake (Fig. 4.1). At Buckingham, the sampling was completed in three days and the lack of tall vegetation and a lower topography made transects easier to follow (Fig. 4.2). The whole rock and petrography rock samples chosen were representative of the characteristic mineralogy and textures as well as hydrothermal alteration (i.e., veins and disseminated sulphides). Some samples of the least altered rock were collected for comparison to the altered rocks.

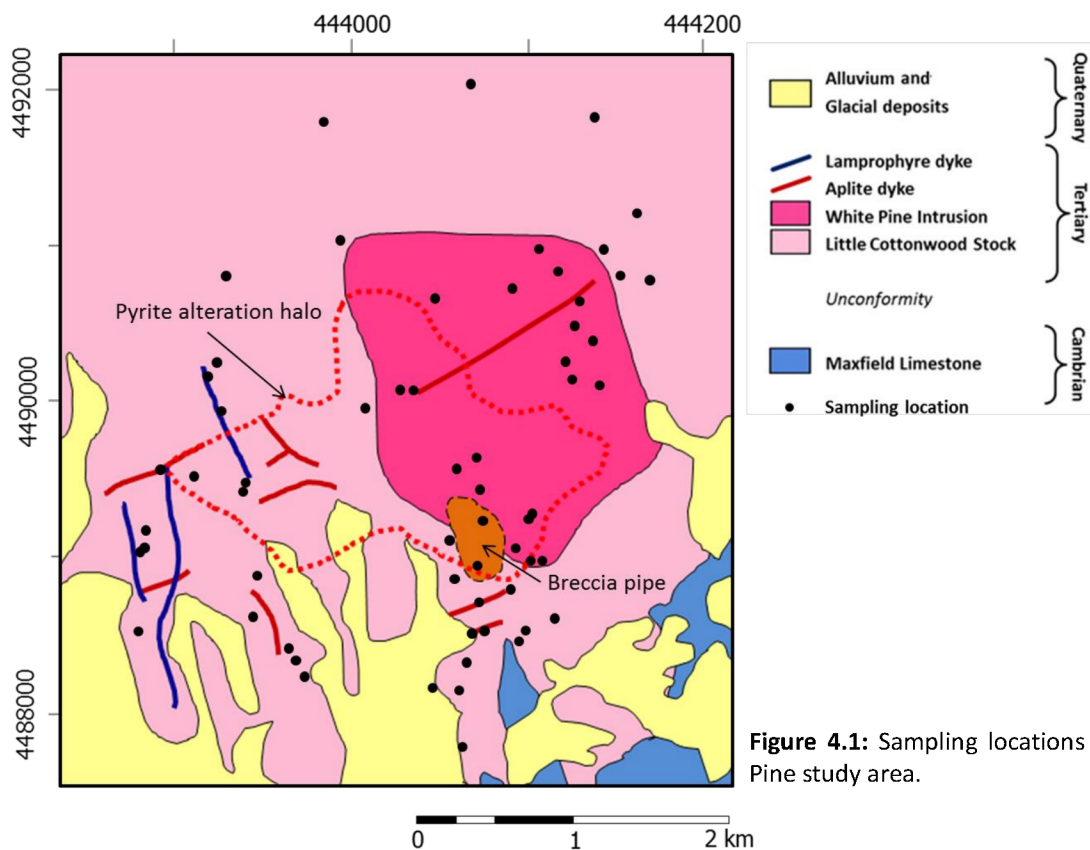
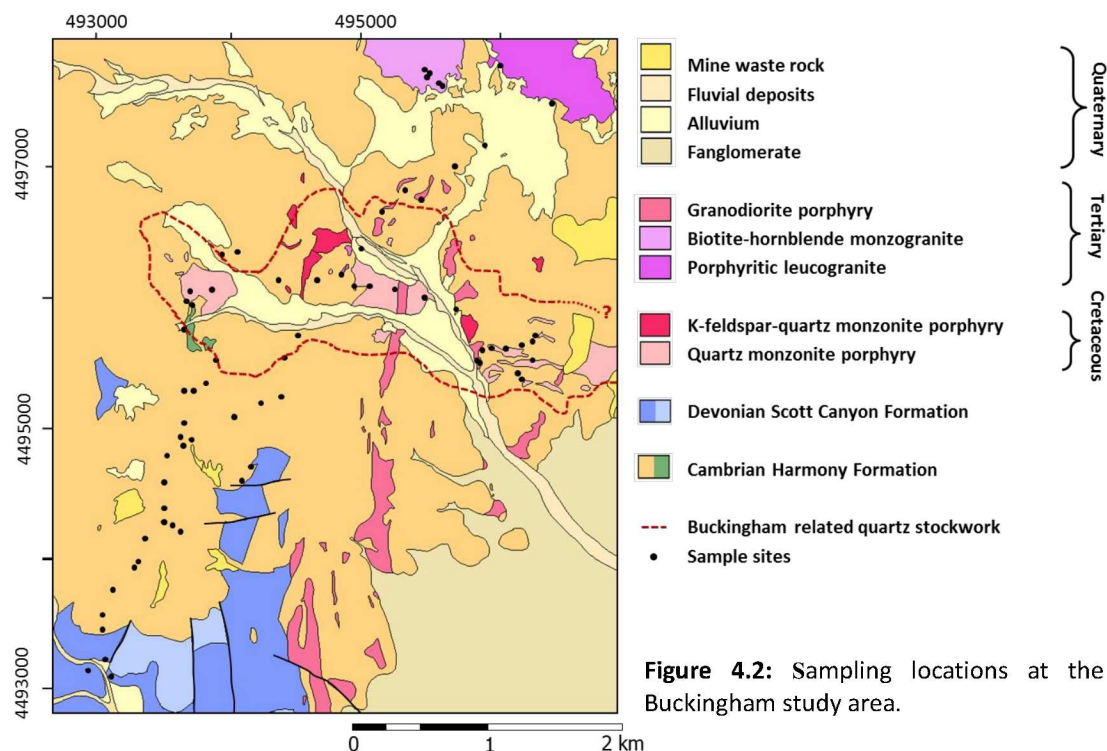


Figure 4.1: Sampling locations at the White Pine study area.



4.2 Petrography

Thirty nine polished thin sections (cut to $\sim 30\mu\text{m}$ thickness) and 58 polished mounts were prepared at Lakehead University, of which 40 were used for mineral chemistry analyses. These sections were used to characterise the lithologies and the alteration present at the two study sites. The samples were selected in the field in transects from the centre of deposit or the area of increased mineralisation moving out towards the periphery of the alteration halo. The samples collected were considered to be representative of the unit and any textures or variations and contain alteration or veining, where present. The rock samples used for creating thin sections were chosen to be representative samples of the lithologies and any variations within the units (i.e., different intrusive phases, alteration, or mineralisation) present within the study area. The granites were classified using a QAPF diagram, which plots the modal percentages of quartz, K-feldspar and plagioclase which have been normalized to 100%. Whole rock geochemistry and petrographic descriptions of the samples are presented in Appendices 1 and 4.

4.3 Whole rock geochemistry

Major and trace element data for a total of 67 samples from the White Pine Fork and 75 samples from the Buckingham study site were generated at ACME Analytical Laboratories Ltd. in Vancouver, Canada. The samples were submitted for analyses under the AA Lithochemical Package (acmelab.com, 2015). Samples were jaw crushed to 70% passing 10 mesh (2 mm), a 250 g aliquot was riffle split and pulverized to 95%, passing 150 mesh (100 μm) in a mild-steel ring-and-puck mill. 0.2 g of powdered sampler was fused in a graphite crucible with 1.5g of $\text{LiBO}_2/\text{LiB}_4\text{O}_7$ flux at 980°C for 30 minutes and then dissolved in 5% HNO_3 . Major elements were determined using a Jarrel Ash AtomComp Model 975/Spectro Ciros Vision inductively coupled plasmas emission spectrograph. Trace elements were analysed using a Perkin-Elmer Elan 6000 or 9000 inductively coupled plasma mass spectrometer. For both major and trace elements calibration standards, verification standards and reagent blanks were included in the sample sequence. Reported detection limits for the major elements are <0.04 wt% and <0.5 ppm for the majority of the trace elements but <0.05 ppm for the REE (acmelabs.com).

4.4 Geochronology

4.4.1 U-Pb dating

The granitic clasts from the White Pine Fork breccia pipe (sample WP13ES62) and the Tertiary granites from the Buckingham study site (samples BK13ES048, -50, -53, and -58) were dated by measuring U-Pb systematics in zircon by the laser ablation inductively coupled mass spectrometry (LA-ICP-MS) at CODES-University of Tasmania. LA-ICP-MS is now widely used for measuring U, Th and Pb isotopic data (e.g., Fryer et al., 1993; Compston, 1999; Black et al., 2003; Kosler and Sylvester, 2003; Black et al., 2004; Jackson et al., 2004; Chang et al., 2006; Harley and Kelly, 2007). The isotopes that were measured were ^{49}Ti , ^{56}Fe , ^{90}Zr , ^{178}Hf , ^{202}Hg ,

^{204}Pb , ^{206}Pb , ^{207}Pb , ^{208}Pb , ^{232}Th and ^{238}U . The element abundances in the zircons were calculated using Zr as the internal standard element and correcting for mass bias and drift (Kosler, 2001). The data reduction used for the results was based on the method outlined in Meffre et al. (2008) and Sack et al. (2011) and was similar to the methods in Black et al. (2004) and Paton et al. (2010).

At CODES, approximately 100 g of the sample was crushed in a Cr-steel ring mill to a <400 micron grain size. The non-magnetic heavy minerals were then separated from the crushed material and the zircons were hand-picked from the heavy mineral concentrate. The selected crystals were mounted, polished and washed using distilled water in an ultrasonic bath. The analyses were performed on an Agilent 7500cs quadrupole ICP-MS with a 193 nm Coherent Ar-F gas laser and the Resonetics S155 ablation cell. The downhole fractionation, instrument drift and mass bias correction factors for Pb/U ratios on the zircons were calculated using two analyses on the primary (91500 standard of Wiendenbeck et al. 1995) and one analysis on each of the secondary standard zircons (Temora standard of Black et al., 2003; JG1 of Jackson et al., 2004) analysed at the beginning of the session and every 15 unknown zircons. These quality assurance and control runs were completed using the same spot size and conditions as used on the samples. Additional secondary standards (Mud Tank Zircon of Black and Gulson, 1978; Penglai zircons of Li et al., 2010; Plesovice zircon of Slama et al., 2008) were also analysed. The correction factor for the $^{207}\text{Pb}/^{206}\text{Pb}$ ratio was calculated using large spots of NIST610. This standard was analysed after every 30 unknown measurements (corrections were done using the values recommended by Baker et al., 2004).

4.4.2 Re-Os dating

In addition to the granitic clasts from the White Pine breccia pipe, the molybdenite mineralisation was dated using Re-Os systematics at the University of Alberta Radiogenic Isotope Facility. Molybdenite is enriched in Re and contains insignificant common Os, meaning that essentially all ^{187}Os derives from ^{187}Re decay (Suzuki, 1996). After the molybdenite was isolated, the ^{187}Re and ^{187}Os concentrations were determined by isotope dilution mass spectrometry using Carius tube, solvent extraction, and chromatographic techniques as outlined by Selby and Creaser (2001). Rhenium and Os isotope ratios were measured using negative thermal ionization mass spectrometry on a Micromass Sector 54 mass spectrometer using Faraday collectors (Creaser et al., 1991; Volkening et al., 1991). The Chinese molybdenite powder HLP-5 (Markey et al., 1998) is routinely analyzed at the University of Alberta as a control sample. It has a determined average Re-Os date of 221.65 ± 0.45 Ma (1SD uncertainty, $n=11$). This Re-Os age date is identical to that reported by Markey et al. (1998) of 221.0 ± 1.0 Ma

4.5 Mineral chemistry

The mineral chemistry analyses for quartz and pyrite and any associated imaging were performed on polished circular mounts. These mounts were prepared at Lakehead University. Figures 4.3 and 4.4 below outline the location of the samples from which mounts were prepared from both study sites.

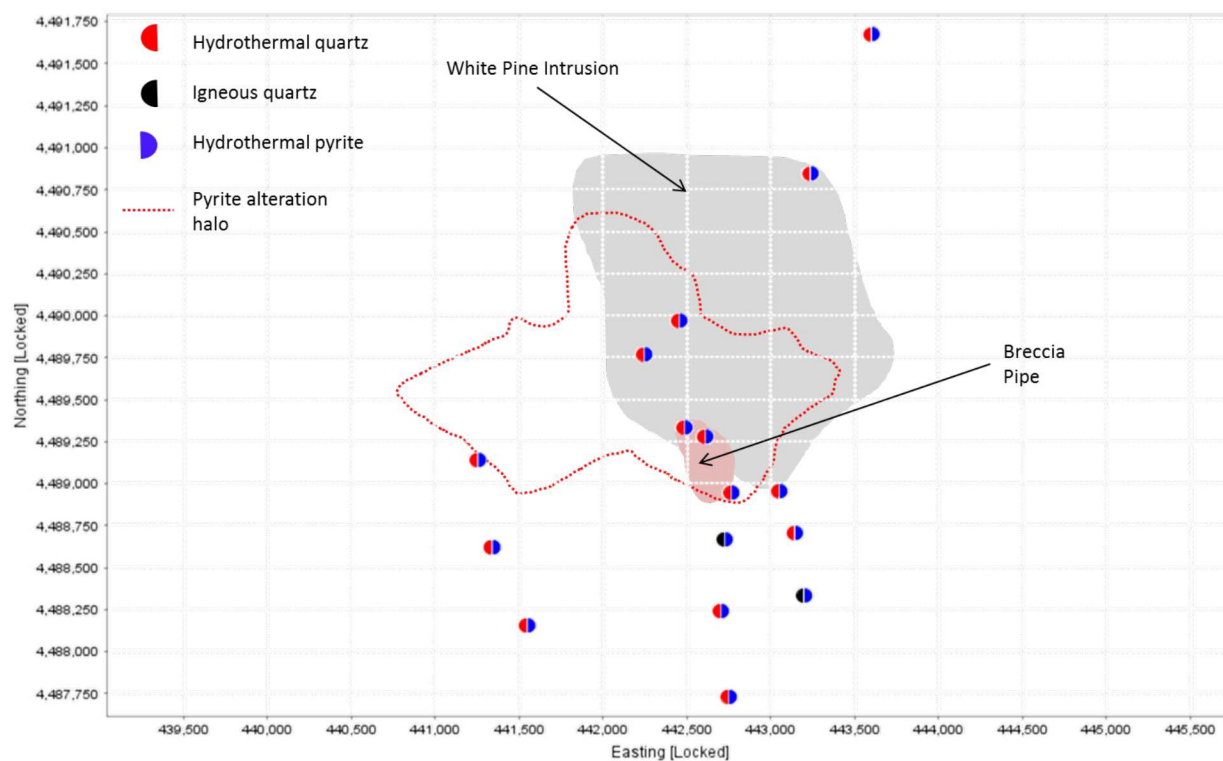


Figure 4.3: Locations of the mounts created at the White Pine study site for hydrothermal quartz, igneous quartz, and hydrothermal pyrite. Pyrite alteration halo from John et al. (1997).

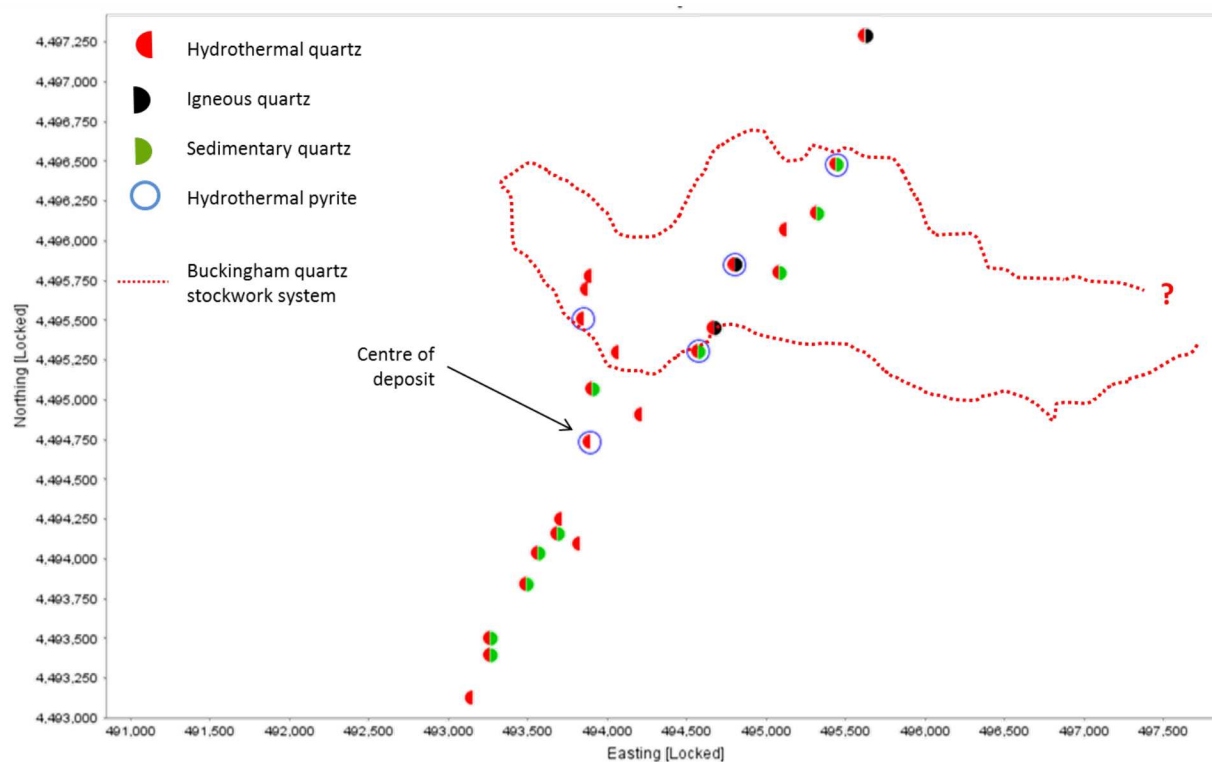


Figure 4.4: Locations of the mounts created at the Buckingham study site for hydrothermal quartz, igneous quartz, sedimentary quartz and hydrothermal pyrite. Quartz stockwork vein system boundary from Theodore et al. (1992).

4.5.1 Cathodoluminescence imaging of quartz

Prior to any analysis of the quartz samples, the igneous, sedimentary, cement, and hydrothermal quartz on the mounts underwent cathodoluminescence imaging. The imaging was completed at the University of Tasmania – Centre for Ore Deposits and Exploration Science (UTAS – CODES) Electron Microscopy and X-Ray Microanalytical Facility with the FEI Quanta 600 Environmental SEM. The cathodoluminescence (CL) imaging was completed with the GatanPanaCLF panchromatic CL detector. The imaging was used as a map to locate the spots for the laser ablation analyses to ensure measurements bracketed all compositional variations.

4.5.2 Quartz mineral chemistry

The quartz trace element geochemistry was collected by LA-ICP-MS at CODES at the University of Tasmania. The spots to be ablated on each quartz grain were mapped on scanned images of the mounts based on any available cathodoluminescence imaging. The ablation spot size was set to 47 μm , frequency 10 Hz, energy 85 mJ and fluence 14 J/cm^2 . The NIST612 standard was used as the primary external calibration standard and was run every 15 analyses, while a blank silica secondary standard was run under the same conditions as the quartz analyses every 30 spots. As well, GSD-1G, synthetic glass, standards were run at the beginning and end of every quartz session. Typically, four to six grains were sampled from one mount and up to six data points were selected for an average of 12 to 15 spots per grain. These data were collected, normalized to Si and run through an EXCEL spreadsheet which plotted the concentrations of the elements throughout the duration of the spot analysis. This spreadsheet was used to review each spot analysis and verify that it was a clean run and to eliminate any portion of the run containing obvious contaminations or mineral inclusions (Fig. 4.5). Detection limits for elements are found in Appendix 6.

4.5.3 Pyrite mineral chemistry

The pyrite trace element geochemistry was collected by LA-ICP-MS at CODES at the University of Tasmania. The spots to be ablated on each pyrite grain were mapped on scanned images of the pucks with spots located in the core, mantle and rim of the grain. The ablation spot size was set to 35 μm , frequency 5 Hz, energy 54 mJ and fluence 4 J/cm^2 . The GSD-1G standard was also used in the pyrite analyses in conjunction with the STDGL2b2 standard (a control sample with Fe as the internal standard element). These standards were run after each grain (approximately every 12 to 15 spot analyses per grain and three grains per mount) and at the start and end of each session. As well, the Peru Pyrite standard was used as the baseline for the Fe values. This data was collected and run through an Excel spreadsheet which plotted the concentrations of the elements throughout the duration of the spot analysis. This spread sheet was used to review each spot analysis and verify that it was a clean run and to eliminate any portion of the run containing obvious contaminations or mineral inclusions (Fig. 4.6). Detection limits for elements are found in Appendix 7.

4.5.4 Quality ranking

In addition to the reduction of the mineral chemistry data, each spot spectra collection was given a quality ranking of 1 to 4. The data collection for each spot ran for 60 seconds. After the data reduction, a run of which 10 to 19 seconds was kept and used was given a quality ranking of 1. A run which contains 20 to 29 seconds of data was given a ranking of 2. A run containing 30 to 39 seconds was designated a 3 and 40 to 60 seconds was given the highest quality ranking of 4 (Figs. 4.5 and 4.6).

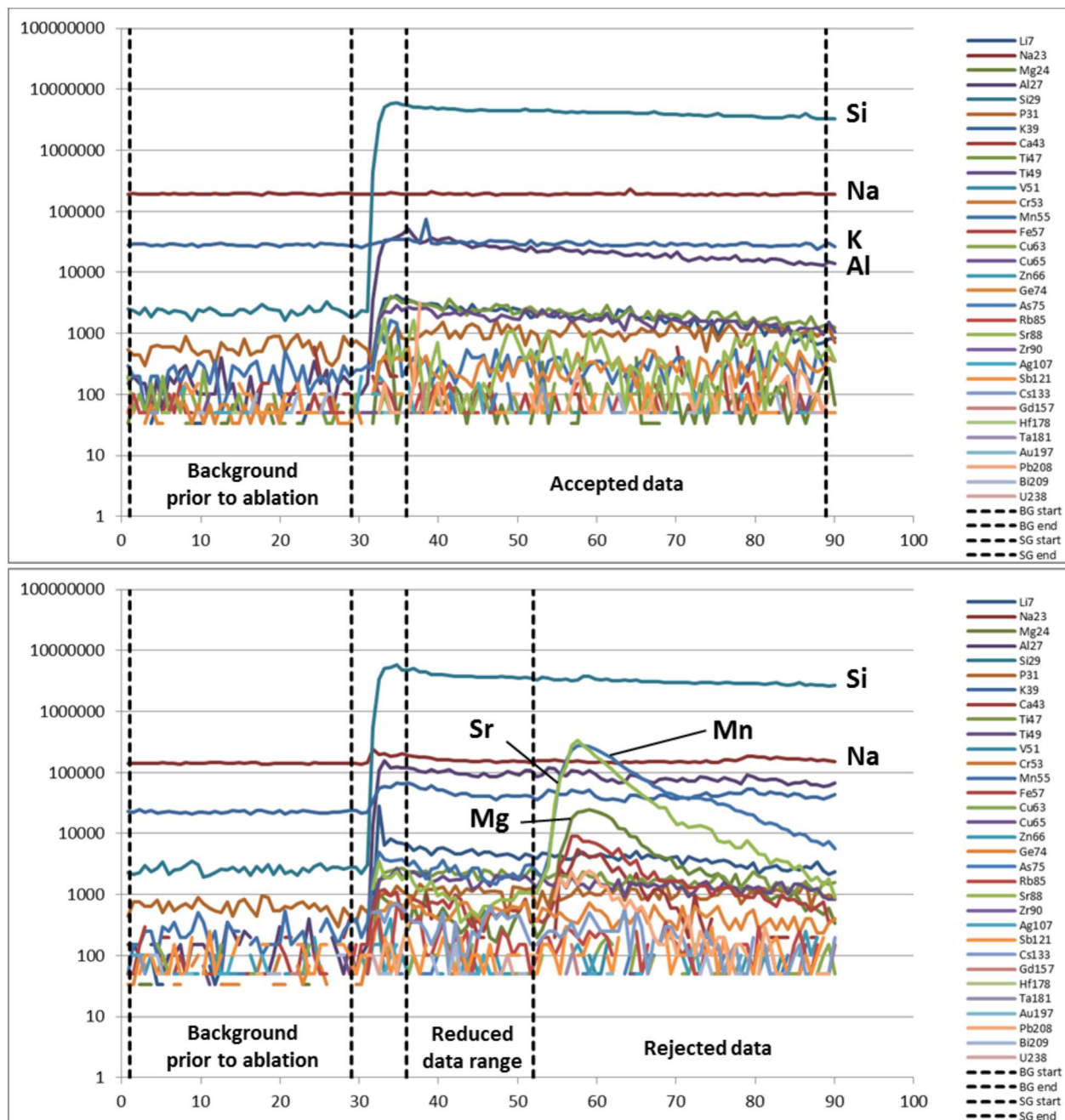


Figure 4.5: Two spot analyses from the quartz data. (top) an inclusion-free run from WP13ES06 - Circle 3, Spot 4 which has a quality ranking of 4; and (bottom) a run from BK13ES013 - Circle 1, Spot 2 in which the data has been reduced to remove a Sr-Mn-Mg-rich inclusion from the data set. This run has a quality ranking of 1.

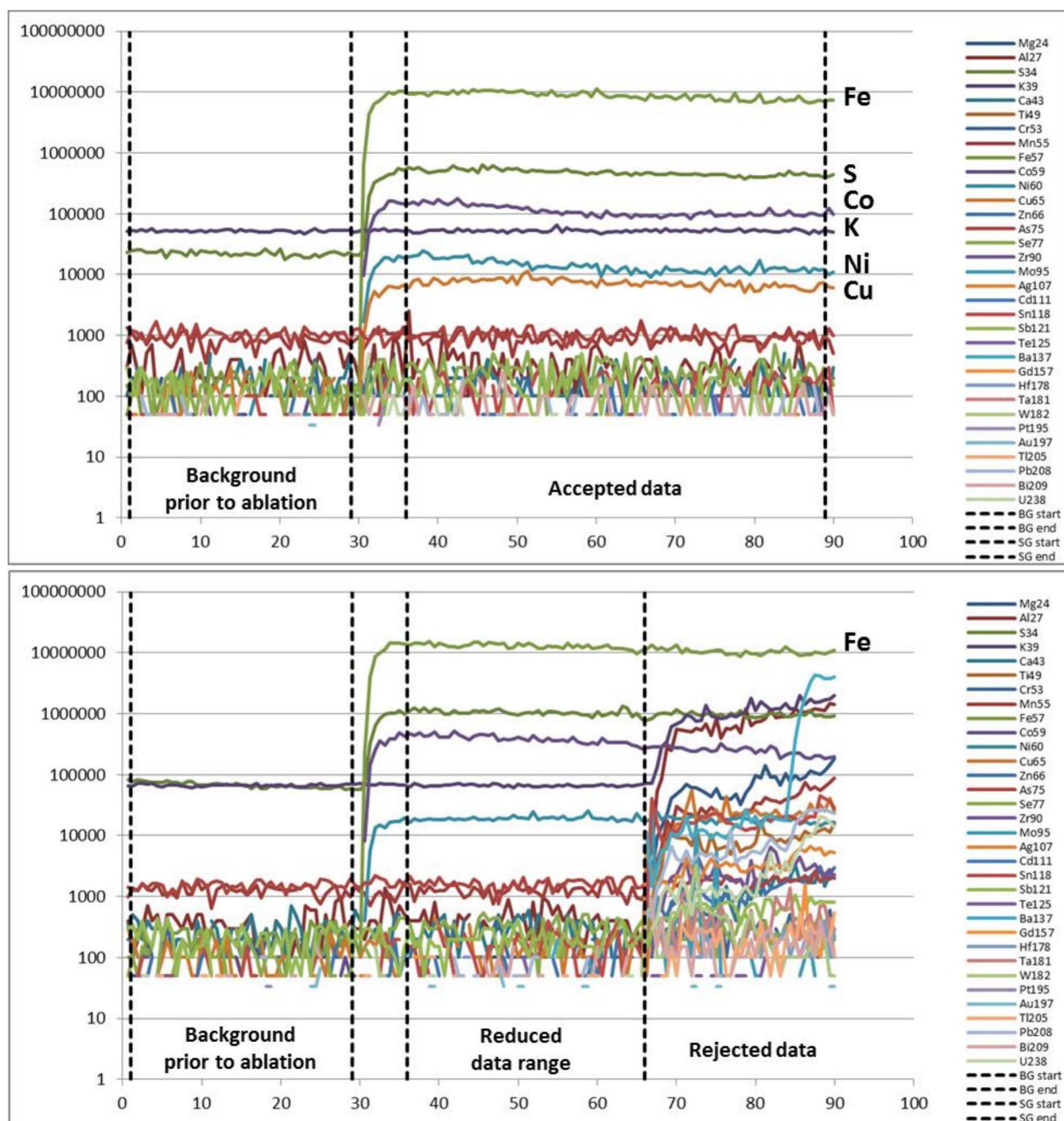


Figure 4.6: Two spot analyses from the pyrite data. (top) an inclusion-free run from WP13ES58 - Circle 1, Spot 2 which shows the homogenous incorporation of Ni, Co, and Cu into the pyrite. This run has a quality ranking of 4; and (bottom) a run from WP13ES07 – Circle 2, Spot 6 in which the data has been reduced to remove an inclusion from the data set. This run has a quality ranking of 3.

4.6 Short-wave infrared spectroscopy

Spectroscopic data were collected from the prepared mounts using a TerraSpec 4 Standard-Res mining analyzer. The sample spectra were measured in a darkened room on a ~1 cm diameter reading window with a run gathering data for 30 seconds. The light source was calibrated with a white plate standard after every sample. Raw spectra were imported into Indico® Pro acquisition software for the extraction of the peak parameters such as the wavelength, width and depth of specific absorption features. Spectra were interpreted by comparing the unknown spectra to reference spectra from The Spectral Geologist™ viewer software and the USGS spectral library.

Chapter 5: Field Observations and Petrography

5.1 White Pine Fork Mo porphyry lithologies

5.1.1 Little Cottonwood stock

The Little Cottonwood stock was sampled from the perimeter of the study area into the breccia pipe. Samples WP13ES67 and WP13ES68 were located on the periphery of the intrusion and are the least altered of the samples collected. The hand samples and thin sections showed a relatively unaltered, coarse-grained K-feldspar porphyritic granite with an equigranular groundmass and some rusty alteration along fracture planes (Fig. 5.1). The mafic mineral is dominantly biotite, with chlorite alteration; quartz content ranges from 24-39% of the rock, the K-feldspar comprises 33-51% of the unit, and the plagioclase feldspar ranges from 24-37% (Fig. 5.2). This rock plots as a monzogranite on the QAPF diagram (Fig. 5.3). The rusty surfaces were the result of the weathering of primary, magmatic magnetite. Some variations within the Little Cottonwood unit included aplitic dykes, mineral banding, and xenoliths sourced from the metasedimentary host rocks (Fig. 5.1).



Figure 5.1: Variations seen in the Little Cottonwood stock: (A) A typical, homogenous K-feldspar porphyritic monzogranite [WP13ES47]; (B) An aphanitic, aplitic dyke devoid of ferromagnesian minerals except for pyrite

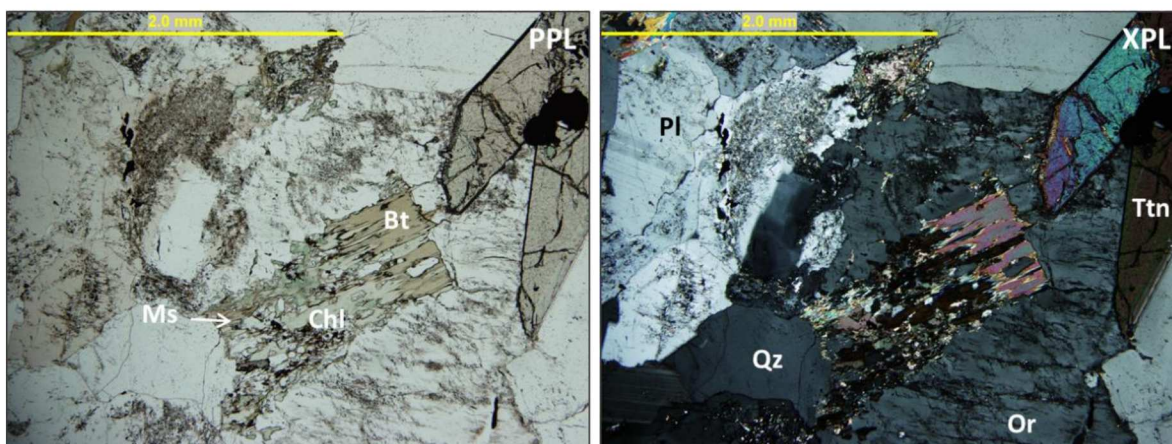


Figure 5.2: Transmitted light microphotograph of the unaltered Little Cottonwood stock (WP13ES68). Quartz [qz]; orthoclase [or]; plagioclase [pl]; biotite [bt]; muscovite [ms]; chlorite [chl]; and titanite [ttn]

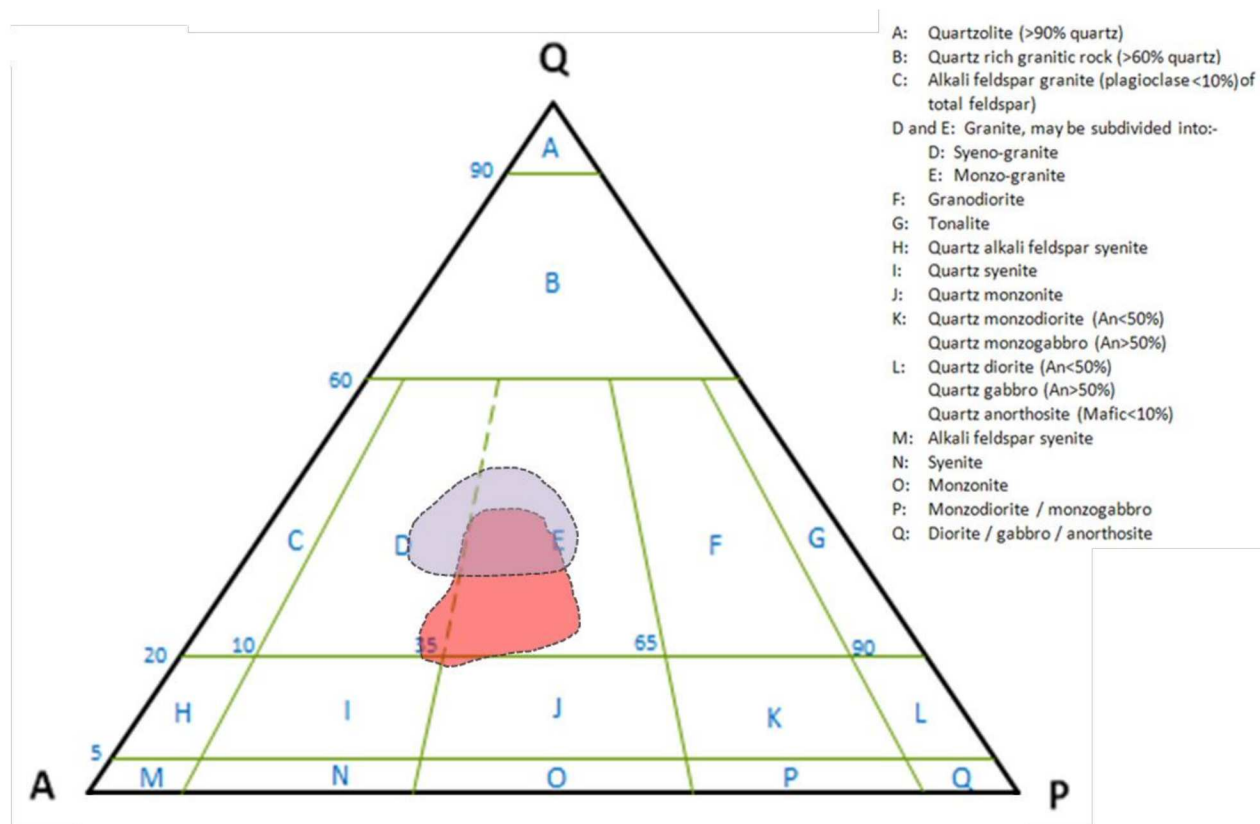


Figure 5.3: QAPF plot showing the Little Cottonwood stock (red) within the monzogranite field and the White Pine intrusion (blue) plotting closer to the quartz apex, but within the monzogranite-syenogranite field.

5.1.2 White Pine intrusion

The White Pine intrusion is a later phase of the Little Cottonwood stock and as such the major mineralogy of the two units is very similar. The differences lie in the textural characteristics and the degree of alteration. Some of the samples collected from the periphery of this igneous phase (e.g., WP13ES26) still show a substantial amount of alteration. The least altered samples were used to characterise the White Pine intrusion as a K-feldspar and quartz porphyritic syeno- to monzogranite with altered feldspar phenocrysts with an increased muscovite content relative to the Little Cottonwood stock (Fig. 5.4). The quartz content ranges from 35-46%, K-feldspar from 31-46%, and the plagioclase feldspar ranges from 18-30%. The samples from the White Pine intrusion plot as a monzogranite on the QAPF diagram (Fig. 5.3). Weakly altered biotite is present in the groundmass and frequent rusty spots (i.e. altering hydrothermal pyrite grains) and rusty quartz veins are present in all of the samples. Compared to the Little Cottonwood stock, there is a higher total quartz content and larger and more quartz eyes in the White Pine intrusion (Fig. 5.5).

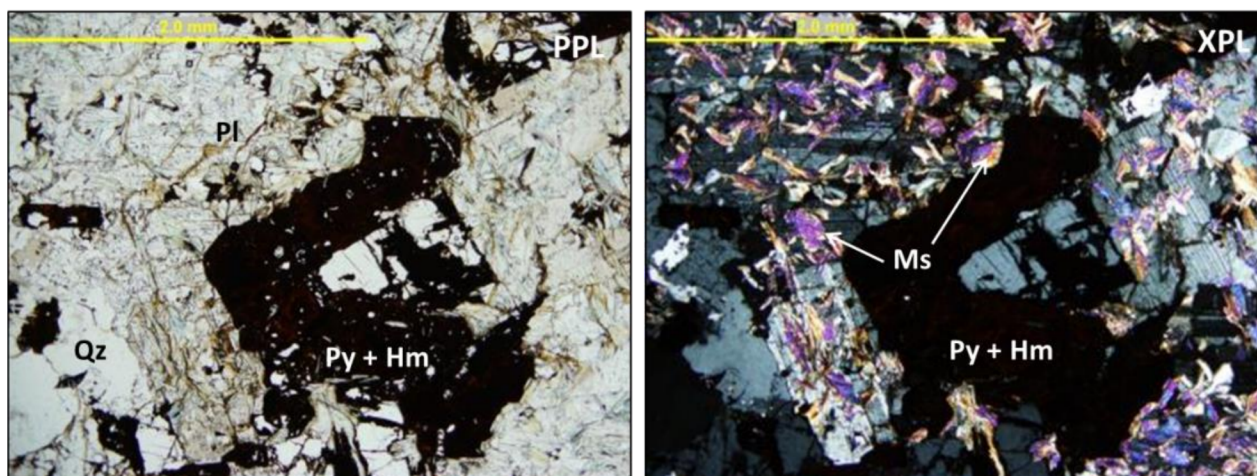


Figure 5.4: Transmitted light microphotograph of the altered plagioclase and the overgrowth of muscovite (WP13ES22). Quartz [qz]; plagioclase [pl]; muscovite [ms]; pyrite [py]; and hematite [hm].



Figure 5.5: Phenocrysts in the White Pine intrusion: (A) K-feldspar [Kfs]; and (B) Quartz [qz].

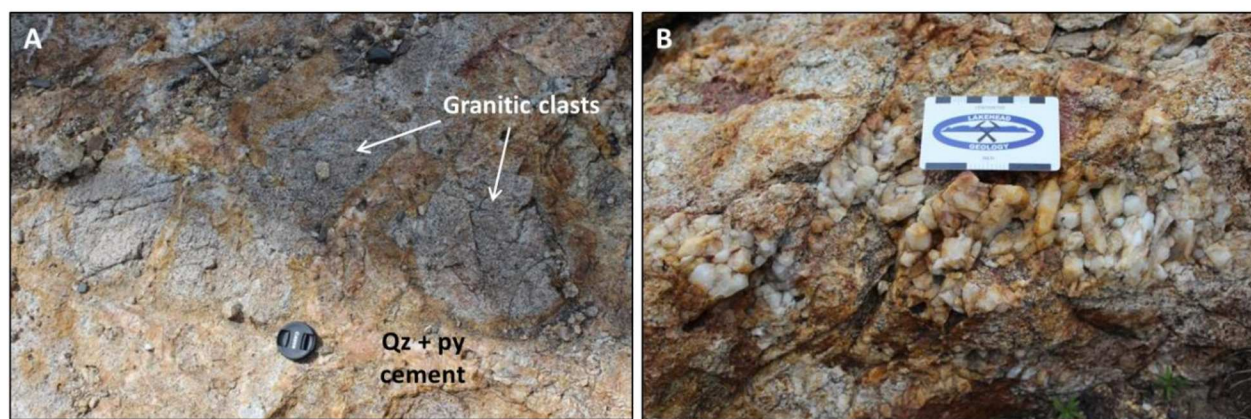


Figure 5.6: White Pine Fork Mo breccia pipe: (A) Granitic clasts; and (B) Vuggy quartz [qz] cement. The lens cap is 60 mm across.

5.1.3 White Pine Fork Mo breccia pipe

The breccia pipe is a portion of the White Pine intrusion shows significant hydrothermal alteration and brecciation. The breccia crops out as a rusty knoll of approximately 150 m by 200 m near the southern portion of the White Pine intrusion, at the contact with the Little Cottonwood stock (Fig. 4.1). The rock is a polymictic, chaotic breccia with fragments of strongly altered K-feldspar and quartz porphyritic granite and quartz hosted in a quartz (\pm K-feldspar) and primary pyrite vein stockwork. Euhedral pyrite and molybdenite are present throughout the cement. The granitic clasts have <10 mm sericite alteration rinds and range from <1 mm in size to >1 m and are irregular in shape (Fig. 5.6A). The presence of K-feldspar and quartz phenocrysts suggests that fragments belong to the younger White Pine intrusion, as opposed to

the Little Cottonwood stock which does not contain quartz phenocrysts. The alteration rinds of the clasts show the highest degree of hydrothermal alteration observed in the study area, with the complete replacement of feldspars to white mica and any ferromagnesian minerals to pyrite. The quartz clasts likely represent fragments of quartz veins or quartz breccia cement implying that brecciation occurred after the first stages of hydrothermal activity at White Pine. The cement is dominantly hematite-stained, vuggy, very coarse-grained (>15mm) quartz (Fig. 5.6B). Molybdenite was only observed in the breccia cement. Hydrothermal agnetite has been altered to pyrite and vein K-feldspar suggest that pervasive phyllic alteration overprinted earlier potassic alteration.

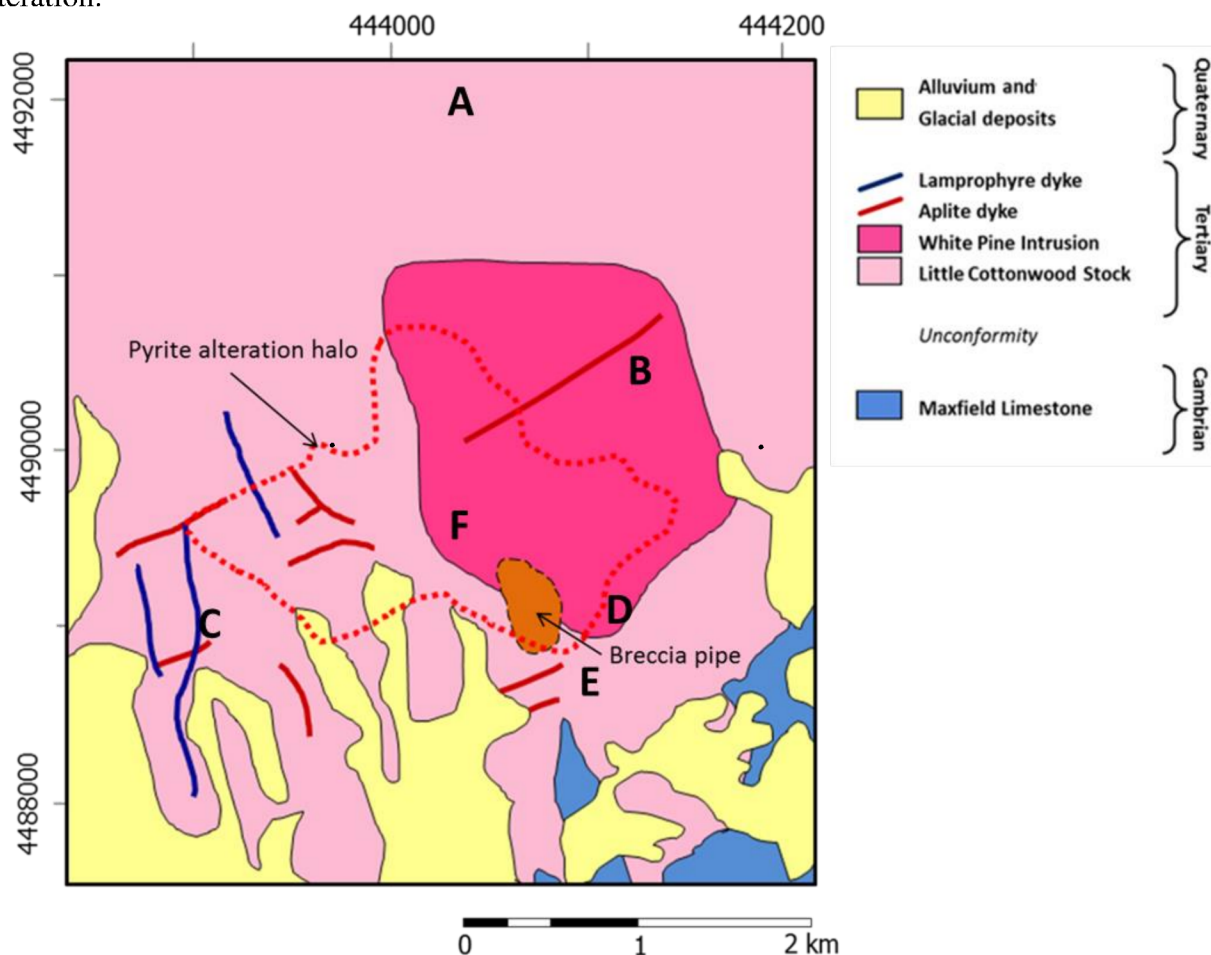


Figure 5.7: The mineralised breccia pipe is located along the southern contact of the White Pine intrusion and the Little Cottonwood stock. The lamprophyric dykes are north-trending and the aplitic dykes trend east-northeast. The pyrite alteration halo has been modified from John (1997). (A) WP13ES68; (B) WP13ES22; (C) WP13ES05; (D) WP13ES54; (E) WP13ES46; (F) WP13ES65

5.1.4 Lamprophyric dykes

The lamprophyric dykes were identified in the field as north-south trending, <5m wide, brown rocks which cross-cut the Little Cottonwood stock (Fig. 5.8A). They were mainly observed in the south eastern portion of the study area. The rocks were soft and contained visible biotite phenocrysts and trace sulphides. In thin section (WP13ES05), the groundmass was predominantly comprised altered feldspars (likely potassic, due to the lack of polysynthetic twins) and some anhedral quartz. The presence of quartz suggests the absence of feldspathoids. The fine-grained groundmass also contains patches of calcite, white micas and muscovite. The white micas are the result of almost complete sericite/white mica and other clay mineral alteration of the K-feldspar. Biotite is the dominant ferromagnesian mineral and it is randomly orientated and is altered to muscovite/phengite, magnetite and possibly chlorite. The dominant mineral assemblage is biotite (35%), orthoclase (35%), quartz (5-10%) and white micas (20%; Fig. 5.8B, C, D). There are small euhedral fluorite and red rutile grains throughout the groundmass. Minor amounts (<5%) of magnetite occur interstitially throughout the groundmass in needles and with hematite likely formed as a reaction product from the alteration of biotite. The sulphides observed in the hand samples are pyrite which occurs as isolated equant, subhedral crystals in the groundmass, frequently with a partial hematitic alteration rind.

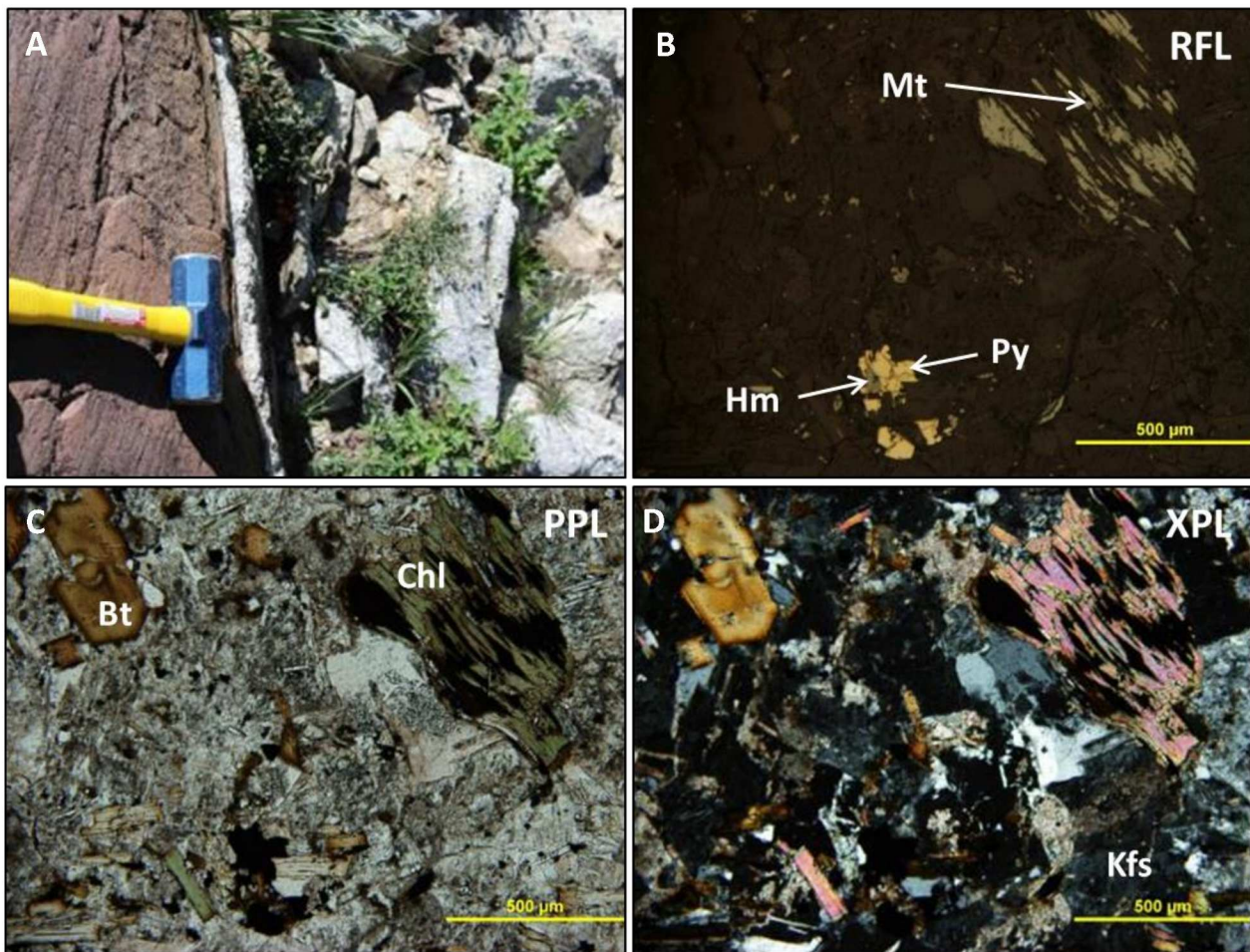


Figure 5.8: (A) Sharp contact of a lamprophyric dyke [left] and the Little Cottonwood stock [right]; (B) Reflected light photomicrograph of the oxides and sulphides: magnetite [mt], pyrite [py] and hematite [hm; WP13ES05]; (C) The mica minerals: biotite [bt], chlorite [chl] and muscovite in groundmass[WP13ES05]; (D) Altered orthoclase groundmass [K-feldspar – Kfs; WP13ES05].

5.1.5 Alteration and the vein stockwork in the granites

The Little Cottonwood stock and the White Pine intrusion have undergone hydrothermal alteration, notably phyllic alteration (quartz + pyrite + white mica mineral assemblage). The most common vein expression of this alteration is the occurrence of rusty quartz veins with sericitic or muscovite-rich selvages (Fig. 5.9). There is evidence of some primary potassic alteration in the breccia pipe, represented by the occurrence of adularia-quartz veins. However, the overprinting phyllic alteration is the most prominent.

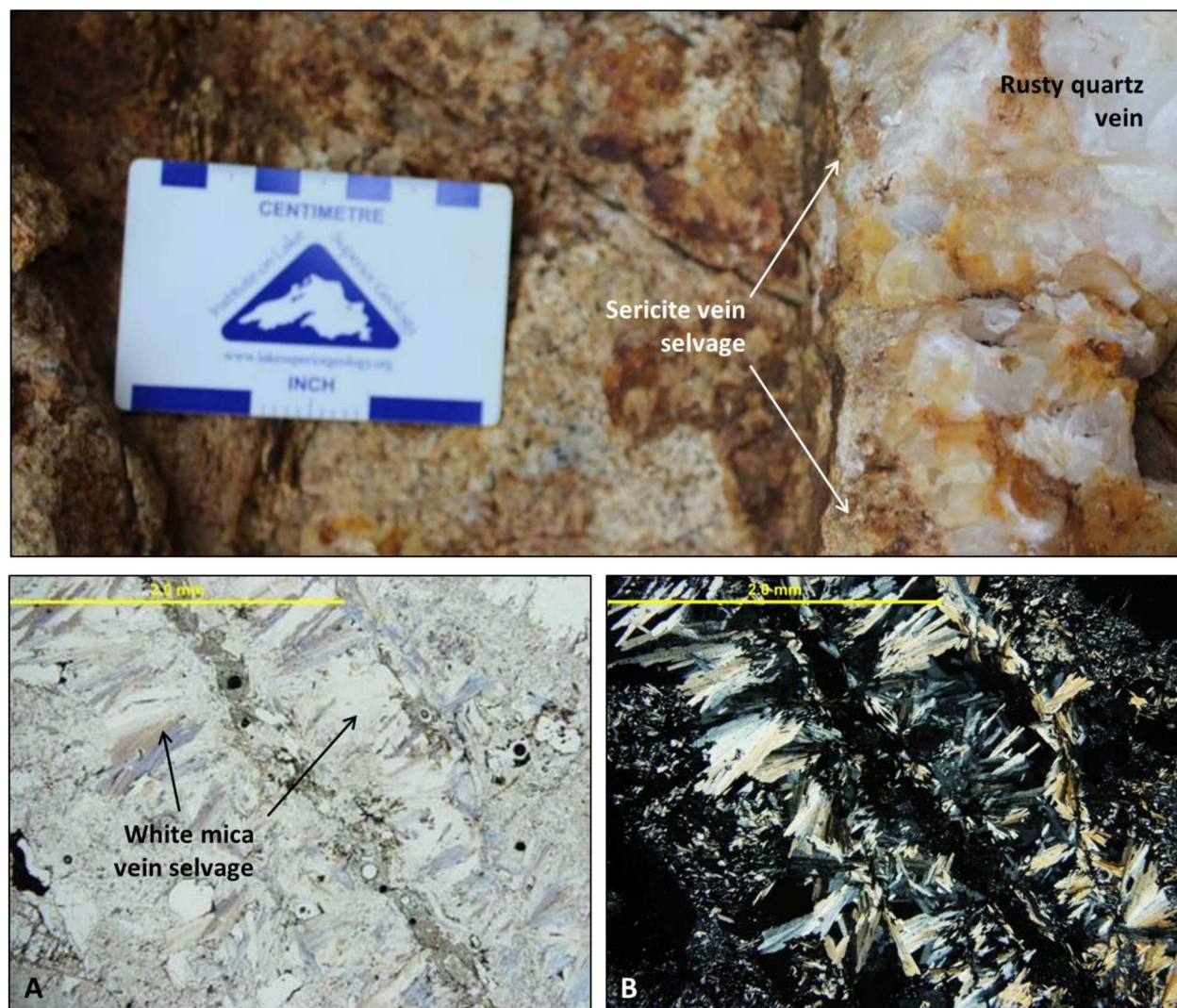


Figure 5.9: (Top) Quartz vein showing a sericite vein selvage; (Bottom; A + B) Transmitted light microphotograph of a white mica vein selvage (WP13ES54) in plane polarized light (left) and cross-polarized light (right)

The sericite alteration is commonly observed as the partial to complete alteration of the feldspars in the granites from orthoclase, microcline, and albite/oligoclase to muscovite/sericite, phengite, and other white micas. In the cases of partial alteration, the feldspars were affected differently. The coarser-grained, well-developed white micas were found within the plagioclase feldspars and, in grains where compositional zoning was evident, the micas preferentially altered the Ca-rich core. The K-feldspars (orthoclase, microcline, and perthite) has been affected by patchy, irregular alteration. As the proximity of the samples to the breccia pipe increased, so did the degree of hydrothermal alteration of the feldspars. The white mica alteration was also seen in

veinlets which cross-cut the samples (Fig. 5.9). These veinlets occasionally contained quartz and/or pyrite (Fig. 5.10)

The pyrite alteration seen at the White Pine Fork Mo porphyry was pervasive in the Little Cottonwood rocks surrounding the breccia pipe. The coarse-grained pyrite is typically euhedral and often seen as isolated grains throughout the groundmass of the rock. The precipitation of the minerals in the quartz-pyrite-sericite veins was observed to be cyclical. The first mineral to precipitate was white mica, followed by the quartz and then pyrite before the sequence was repeated (Fig. 5.10). In sample WP13ES46, a 20mm wide quartz vein showed a white mica-rich vein selvage around a coarse-grained, well annealed quartz vein with hematite as an alteration of primary pyrite that crystallized on the quartz vein in a cyclic pattern with sericite (Fig. 5.10). The pyrite found within veins outside of the ~700 m radius of the breccia pipe was typically very rusty (i.e., weathered to hematite) and anhedral to subhedral. The pyrite within the 700m radius of the breccia pipe is euhedral and less weathered (i.e., partial to absent hematitic mineral coronas). The pyrite grains within <500 m of the breccia pipe also exhibited higher mineral inclusion content (chalcopyrite, sphalerite, and galena; Fig. 5.11A). Sample WP13ES65 (located 609 m from the breccia pipe), contained two generations of veins. It was observed in the field that the older veins were mineralized with molybdenite flakes and lacked any other sulphides (Figs. 5.11B and 5.12). These veins were cut by pyrite-quartz veins which contained no molybdenite. This field relationship distinguished the mineralizing system from the later, overprinting alteration.

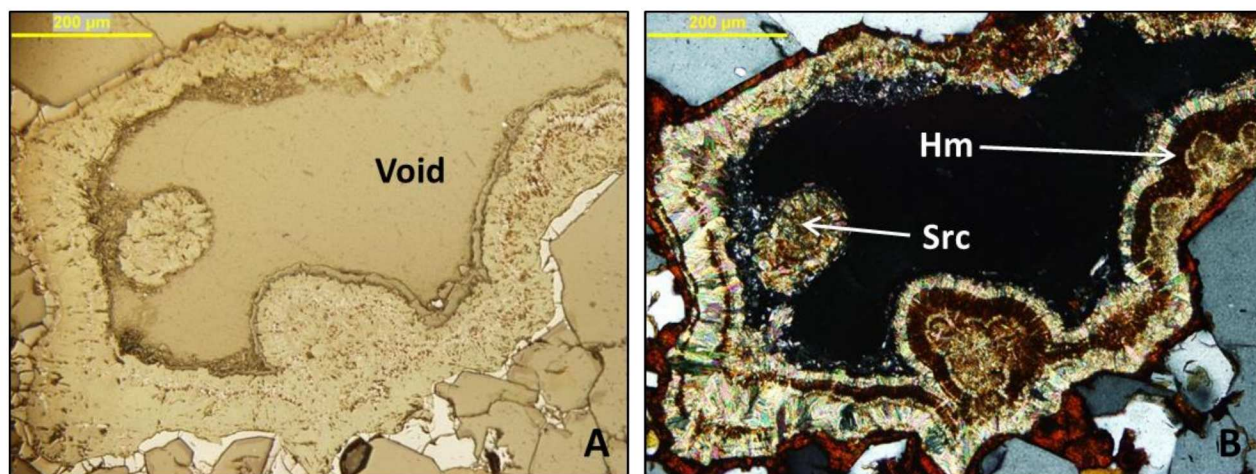


Figure 5.10: Quartz vein in an altered monzogranite from the Little Cottonwood stock showing hematite [hm] as an alteration of primary pyrite crystallised on the quartz vein in a repeating, cuniform pattern with sericite [src] (WP13ES46). Reflected light (left) and cross-polarised transmitted light (right)

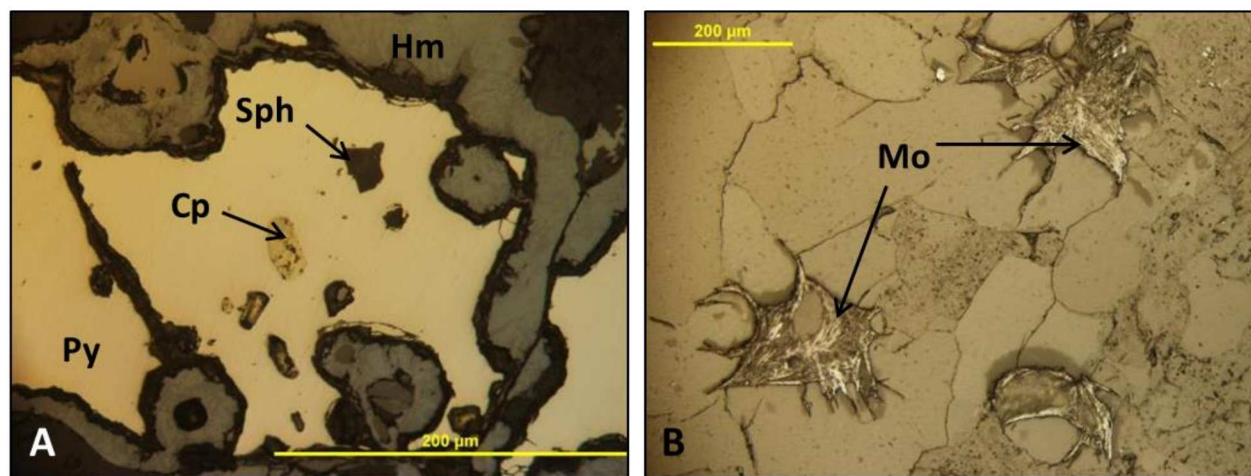


Figure 5.11: (A) Inclusion-rich pyrite [py] grain in a quartz vein with a well-developed hematite [hm] weathering rind. Chalcopyrite [cp] and sphalerite [sph; WP13ES28]; (B) Molybdenite needles [Mo; WP13ES65]. Reflected light.

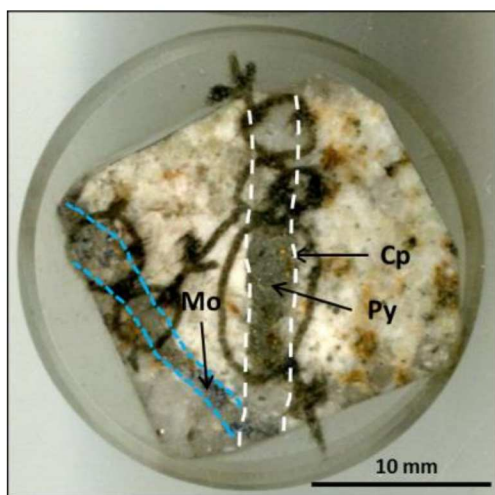


Figure 5.12: Scanned mount with the laser ablation tracks, targeting the quartz and pyrite. A younger quartz vein cross-cuts the quartz vein containing molybdenite.

5.2 SWIR data

The SWIR spectropy data collected on the pucks prepared for mineral chemistry analyses was used to characterise the alteration minerals present at the White Pine Fork Mo porphyry. The intense phyllic alteration observed during the mapping resulted in the formation of several white phyllosilicates including muscovite, sericite, phengite, and possible clay minerals. In the distal samples, the muscovite is euhedral and found as books in the groundmass and is interpreted to be magmatic in origin. The altered samples show muscovite replacing feldspars. The two most common minerals related to alteration were muscovite and phengite (found in all but two samples) with secondary siderite (found in 13 out of 41 samples; Fig. 5.13; Table 5.1).

Table 5.1: Summary of SWIR data data from the White Pine Fork Mo porphyry study area. *Mineral 1* is the most common and *Mineral 2* is the second most common mineral. Coordinates are NAD27.

Sample	Unit	Lithology	Easting	Northing	Elevation	Mineral 1	Mineral 2
WP13ES001	White Pine intrusion	Granite and quartz + pyrite vein	442630	4489434	2689	Phengite	
WP13ES002	Breccia pipe	Breccia clast and cement	442460	4489331	2680	Muscovite	Siderite
WP13ES002	Breccia pipe	Quartz cement and Mo	442460	4489331	2680	Muscovite	
WP13ES003	Little Cottonwood stock	Porphyritic granite	441521	4488155	2984	Phengite	
WP13ES006	Little Cottonwood stock	Porphyritic granite	441314	4488621	2881	Siderite	Muscovite
WP13ES006	Little Cottonwood stock	Quartz vein	441314	4488621	2881	Muscovite	
WP13ES007	Little Cottonwood stock	Altered granite	441229	4489140	2754	Phengite	
WP13ES013	Little Cottonwood stock	Porphyritic granite	442725	4487733	3093	Siderite	Muscovite
WP13ES014	Little Cottonwood stock	Aplitic pegmatite dyke	442725	4487733	3093	Muscovite	
WP13ES017	Little Cottonwood stock	Porphyritic granite	442844	4488617	2861	Phengite	Siderite
WP13ES018	Little Cottonwood stock	Porphyritic granite	442874	4488858	2811	Phengite	
WP13ES020	White Pine intrusion	Porphyritic granite	442578	4490390	2596	Muscovite	Siderite
WP13ES021	White Pine intrusion	Altered granite	441918	4490808	2491	Muscovite	Siderite
WP13ES022	White Pine intrusion	Porphyritic granite	443573	4491671	2463	Phengite	Siderite
WP13ES023	White Pine intrusion	Porphyritic granite	443213	4490846	2821	Muscovite	
WP13ES025	White Pine intrusion	Aplitic dyke	443156	4490596	2963	Paragonite	Montmorillonite
WP13ES026	White Pine intrusion	Porphyritic granite	443269	4490401	3036	Muscovite	
WP13ES027	White Pine intrusion	Porphyritic granite	443257	4490251	3026	Muscovite	Siderite
WP13ES028	White Pine intrusion	Porphyritic granite	443365	4490168	3039	Muscovite	
WP13ES030	Little Cottonwood stock	Porphyritic granite	440499	4488348	2984	Phengite	Siderite

WP13ES033	Little Cottonwood stock	Altered granite	440544	4488874	2919	Phengite	
WP13ES036	Little Cottonwood stock	Altered granite	441178	4489285	2747	Muscovite	
WP13ES040	Little Cottonwood stock	Porphyritic granite	442564	4488141	3043	Phengite	
WP13ES041	Little Cottonwood stock	Porphyritic granite	442676	4488242	2963	Phengite	Siderite
WP13ES043	Little Cottonwood stock	Aplitic dyke	442641	4488520	2858	Muscovite	
WP13ES044	Little Cottonwood stock	Porphyritic granite	442699	4488669	2819	Phengite	
WP13ES046	Little Cottonwood stock	Altered granite	442741	4488943	2804	Phengite	
WP13ES046	Little Cottonwood stock	Altered granite + quartz vein	442741	4488943	2804		Jarosite
WP13ES048	Little Cottonwood stock	Quartz-sericite vein	443156	4488003	3073	Phengite	
WP13ES049	Little Cottonwood stock	Porphyritic granite	443208	4488086	3103	Muscovite	Dolomite
WP13ES050	Little Cottonwood stock	Porphyritic granite	443175	4488331	3006	Phengite	Siderite
WP13ES052	Little Cottonwood stock	Porphyritic granite	443116	4488704	2954	Phengite	Siderite
WP13ES053	Little Cottonwood stock	Altered granite	443025	4488956	2885	Muscovite	
WP13ES054	White Pine intrusion	Porphyritic granite	442964	4489077	2869	Muscovite	
WP13ES058	Little Cottonwood stock	Altered granite	443727	4490549	2884	Muscovite	
WP13ES062	Breccia pipe	Breccia cement and clasts	442582	4489280	2741	Phengite	Siderite
WP13ES063	Breccia pipe	Breccia cement and clasts	442582	4489280	2741	Siderite	
WP13ES064	White Pine intrusion	Altered granite	442429	4489968	2703	Muscovite	
WP13ES065	White Pine intrusion	Altered granite	442221	4489771	2607	Phengite	Siderite
WP13ES066	White Pine intrusion	Altered granite	442084	4489641	2650	Muscovite	
WP13ES068	Little Cottonwood stock	Porphyritic granite	442823	4491905	2377	Muscovite	Siderite

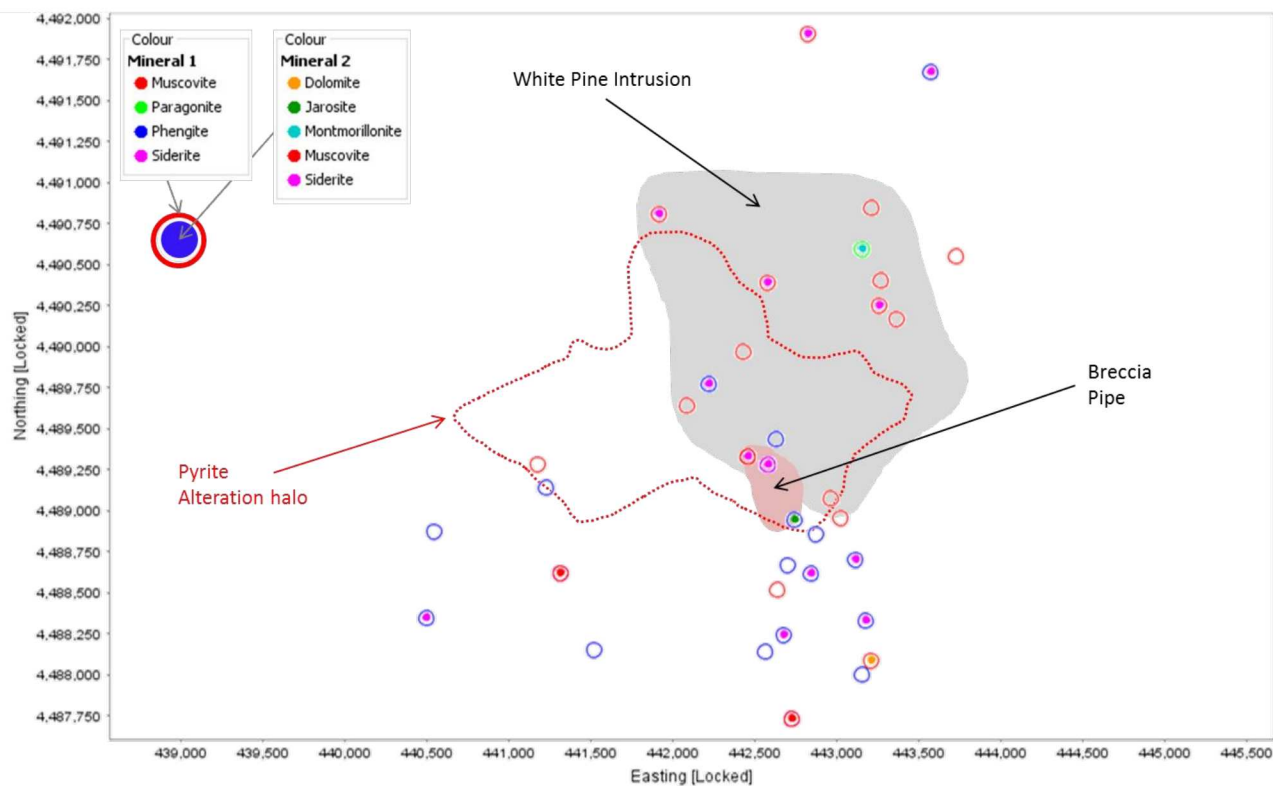


Figure 5.13: SWIR results in relation to the White Pine intrusion and the breccia pipe as well as the pyrite alteration halo (defined by John, 1997).

5.3 Buckingham lithologies and alteration

5.3.1 Harmony Formation

The Harmony Formation is a metasedimentary unit comprised predominantly of sandstones, arkosic sandstones, and pebble conglomerates (Theodore et al., 1992). The predominant lithology mapped and sampled was a quartzite which was composed of rounded, moderately sorted quartz grains up to ~2mm wide. There is no other clast type except for some minor (<1% total) feldspar grains. The rock is clast-supported and the interstitial material is white, soft and powdery micas and clay minerals. There were some variations in the unit where the metasandstone was more arkosic which is evidenced by white, opaque, altered grains. Transmitted light microscopy showed that the quartz clasts comprised up to 95% of the rock in some of the quartzite samples and in the rest. Some of the larger clasts (<1 mm) displayed subgrains. As not all the grains displayed subgrain boundaries it is likely that the subgrains formed pre-metamorphism, before erosion and deposition. The grains were typically well annealed with wavy grain boundaries interpreted to be the result of metamorphism. In the areas where the grain boundaries were not as annealed and the clasts have retained more of a rounded grain outline, the interstitial mineral is dominantly white micas, including muscovite (Fig. 5.14). The mica minerals occur as fine-grained laths and as aphanitic crystal aggregates of sub- to euhedral grains in the quartz matrix as an alteration product of the pelitic component of the sandstone protolith. The other minerals present in the rock were introduced as the result of hydrothermal alteration, weathering and veining. The most common vein types are quartz, quartz-pyrite and associated white micas.

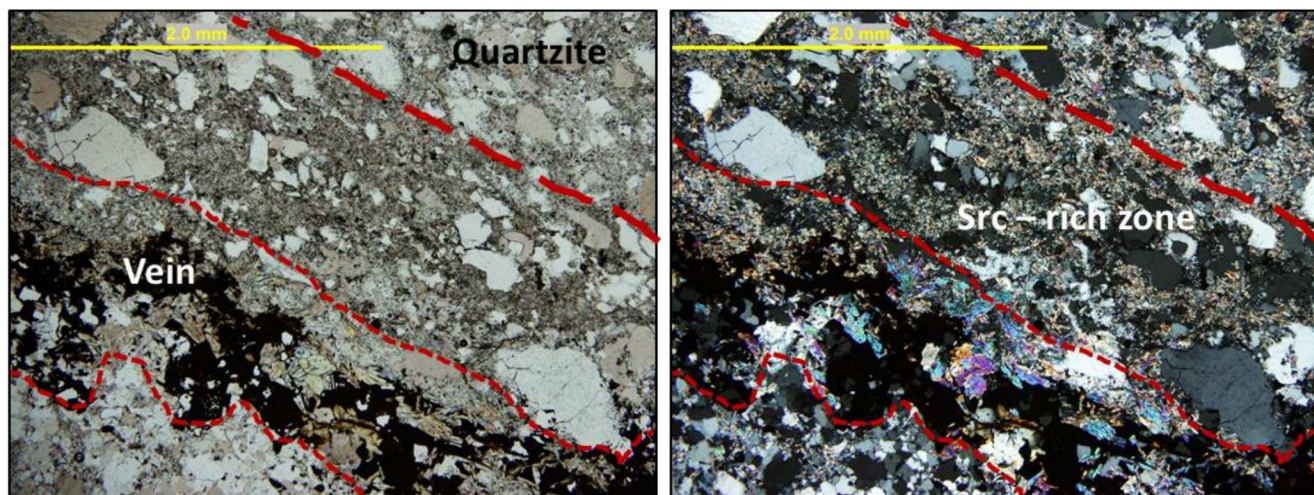


Figure 5.14: Quartzite hosting a sericite-rich vein [src]. The vein selvage contains a higher modal abundance of sericite than the quartzite groundmass (BK13ES003). Transmitted light plane polarized light (left) and cross-polarized light (right).

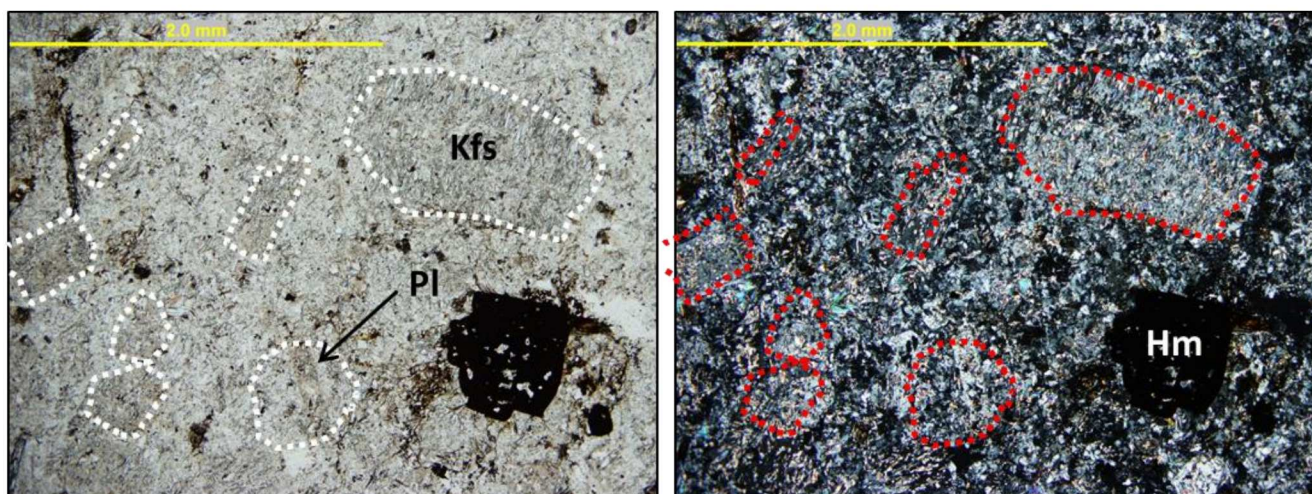


Figure 5.15: Altered feldspar-porphyrific granite (BK13ES011). The orthoclase? [Kfs] and plagioclase [pl] phenocrysts are outlined. They have been almost completely altered to white mica minerals. The hematite [hm] grain retains a relict pyrite cubic grain shape. Transmitted light plane polarized light (left) and cross-polarized light (right).

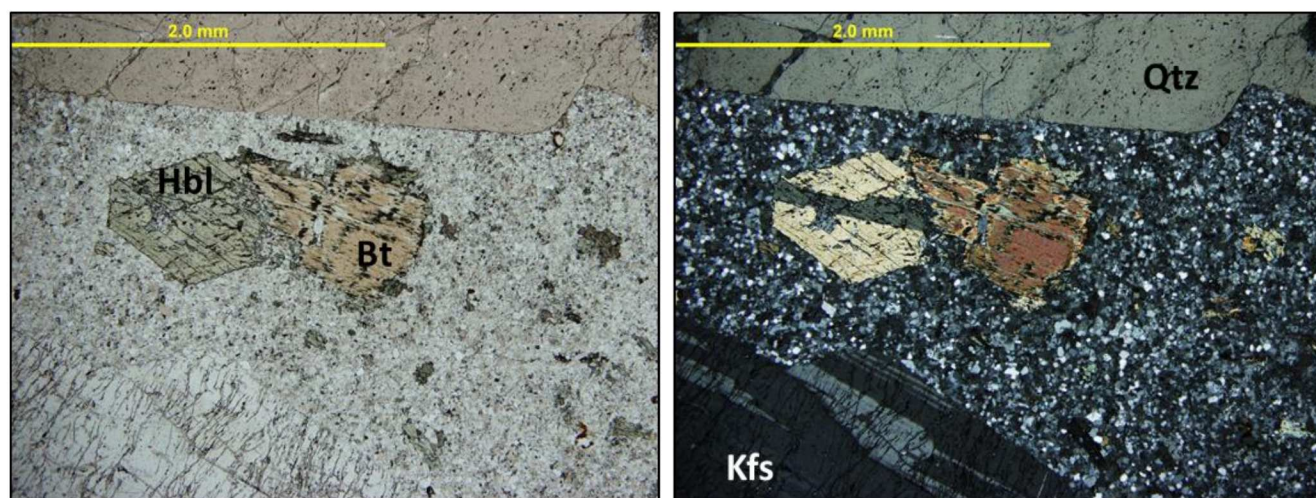


Figure 5.16: Hornblende- [hbl] bearing, orthoclase- [Kfs] and quartz- [qtz] porphyritic Tertiary granite. The primary ferromagnesian mineral has been altered to biotite [bt; BK13ES048]. Transmitted light plane polarized light (left) and cross-polarized light (right)

5.3.2 *Buckingham Intrusions*

The Buckingham granites are pervasively hydrothermally altered and comprise coarse-grained quartz and K-feldspar phenocrysts in a quartz–orthoclase–plagioclase groundmass that displays a granitic texture with annealed grain boundaries. The quartz phenocrysts are coarse-grained (up to 9mm wide), anhedral and rounded. These quartz eyes show some undulatory extinction and are unaltered. The K-feldspar phenocrysts in this sample are difficult to distinguish, other than by relict growth twins, from the plagioclase due to the extensive sericitic alteration. The larger relict grains of feldspar (which show some tartan twinning) are likely microcline, the grain shape and size closely resembles the phenocrysts seen in less altered samples. The plagioclase was determined to be oligoclase, is finer-grained than the K-feldspar and occurs as equant, euhedral, altered phenocrysts. They have been almost completely altered to white micas (the alteration replaces up to 95% of the plagioclase grain). Primary growth twins can be seen in some of the less altered grains. The groundmass has undergone sericite/white mica and other clay mineral alteration of the feldspars (Fig. 5.15). No magmatic ferromagnesian minerals were observed in the granites. Primary hydrothermal pyrite and its weathering reaction products of Fe-oxide occur throughout the groundmass, where altered, the hematite retains the relict outline of the pyrite.

5.3.3 *Tertiary granites*

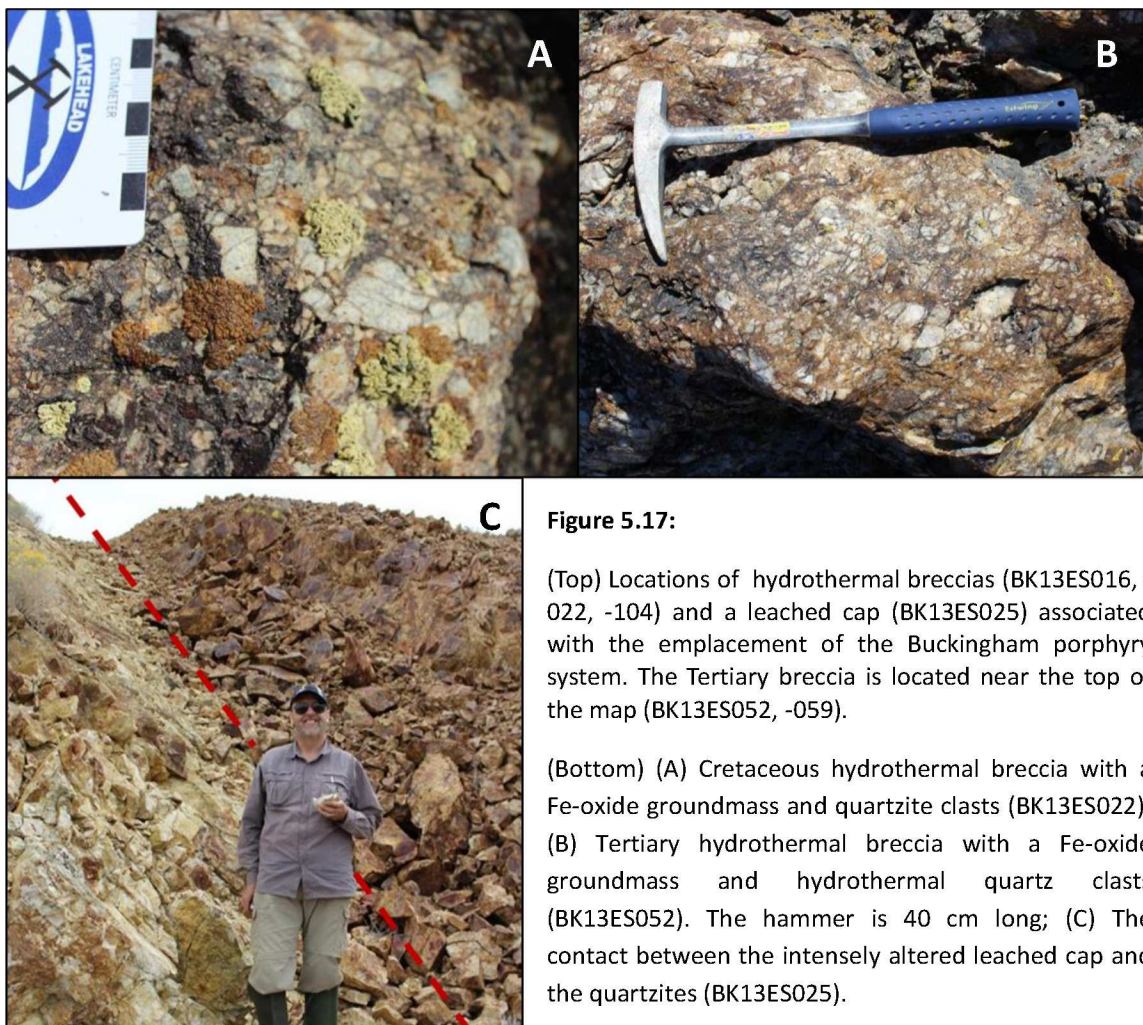
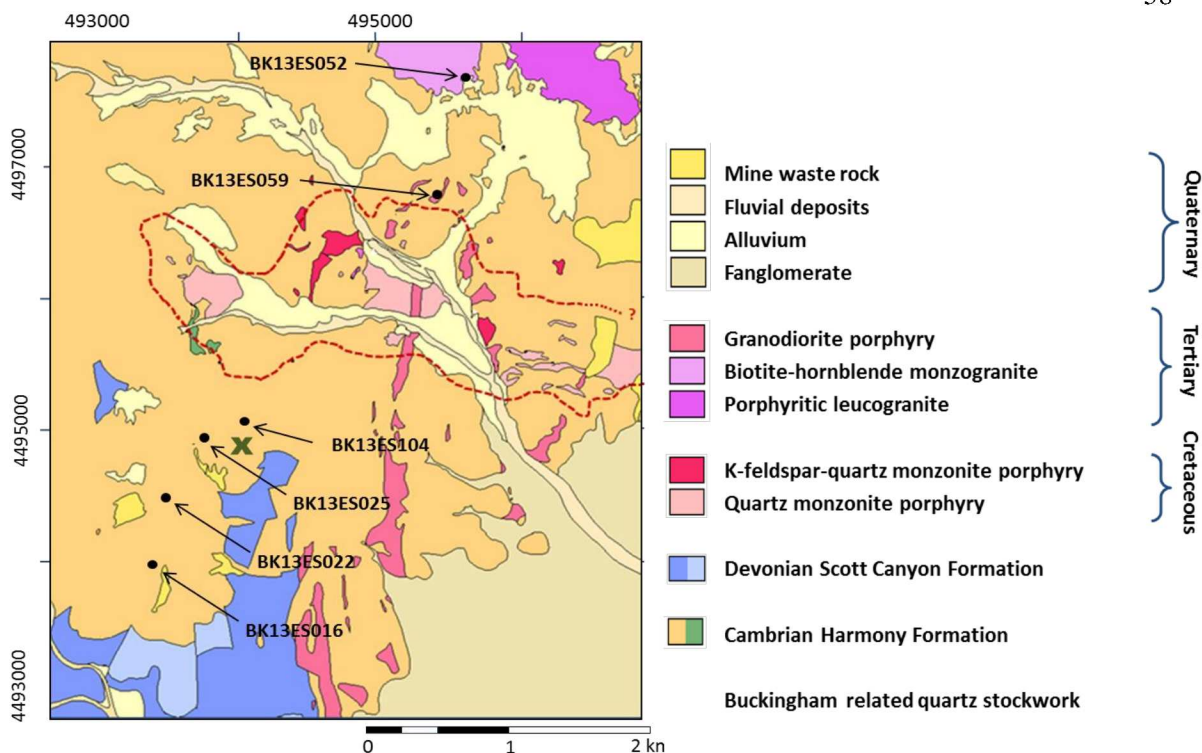
The younger, Tertiary granites are located in the northern part of the study area and are also hydrothermally altered. Two distinct lithologies have been recognised, a quartz feldspar-porphyrific hornblende monzogranite and a quartz K-feldspar-porphyrific granite. Samples BK13ES048 and BK13ES053 are monzogranites with quartz and feldspar phenocrysts in a quartz-microcline-oligoclase-hornblende groundmass. The quartz phenocrysts are very coarse-

grained with rounded quartz eyes that reach 9 mm in diameter. These grains show some undulatory extinction, no subgrain formation and are unaltered. There is also finer-grained, anhedral quartz in the altered groundmass. Feldspars in the very fine-grained groundmass have undergone some sericite/white mica and other clay mineral alteration. In some of the feldspar grains, white mica replaces up to 15% of the feldspar. The K-feldspar and plagioclase phenocrysts are euhedral and show some compositional zonation. The medium- to fine-grained K-feldspar phenocrysts (which show some tartan twinning) are microcline. Several, equant, euhedral altered phenocrysts are also found within the groundmass. They have been partially altered to white micas (~15% of the grain). The primary growth twins indicate that the plagioclase is oligoclase. The most common ferromagnesian mineral in these granites is hornblende which occurs as subhedral to euhedral, fragmented crystals throughout the groundmass (Fig. 5.16). The crystals range from being unaltered to weakly altered to biotite. Some trace epidote and titanite are also associated with the glomeritic ferromagnesian minerals.

Samples BK13ES050 and BK13ES51 have undergone more hydrothermal alteration than the granites which contained hornblende. These altered monzogranites are characterised by pervasive barren quartz stockwork veins in an altered fine-grained quartz and K-feldspar porphyritic quartz-orthoclase-plagioclase groundmass. The feldspars in the groundmass have undergone sericite/white mica and other clay mineral alteration, with white mica replacing up to 55-75% of some crystals. The primary, magmatic ferromagnesian minerals in these granites have been altered to opaque minerals (Fe-oxides), titanite and epidote. In sample BK13ES048, primary hydrothermal pyrite, often weathered to Fe-oxides, occur throughout the groundmass. Where present, the hematite often preserves the relict outline of the pyrite.

5.3.4 *Hydrothermal breccias*

Different generations of hydrothermal breccias were recognised at Buckingham that are interpreted to be associated with the emplacement of the Buckingham intrusion and with the Tertiary granites (Fig. 5.17). An unmineralized breccia, associated with the Cretaceous granites (BK13ES016), is characterised by hematite-jarosite-quartz veinlets cement. The breccia is chaotic and polymictic. The predominant clasts are quartzites composed of rounded, moderately sorted quartz grains of the Harmony Formation. Some of the larger grains (<1 mm) have subgrains of fragmented sedimentary grains (Fig. 5.18). The matrix of the quartzite is composed of very fine-grained quartz and white phyllosilicates as well as coarser crystals of either muscovite or phengite. There is a very minor (<1%) component of biotite-rich clasts that are likely sedimentary as the biotite suggests a more Al-rich or pelitic protolith. This breccia also contains wavy and anastomosing veinlets of very fine-grained hematite and aphanitic, greenish jarosite. The veins have the same mineralogy as the breccia cement and define a halo to the chaotic breccia. There are numerous, angular single quartz grains found within the hematitic cement which may be hydrothermal in origin or derived from disaggregation of the quartzite (Fig. 5.18). Some of defines a relict cubic shape, suggesting that pyrite was a primary breccia cement. Hematite is the main mineral in the matrix of the breccia veins. Local goethite (?) cement is associated with jarosite and occurs as patches around some of the quartzite clasts. Jarosite also occurs in patches around some of the quartzite clasts. No primary or secondary sulphides or granitic clasts were observed in the breccia.



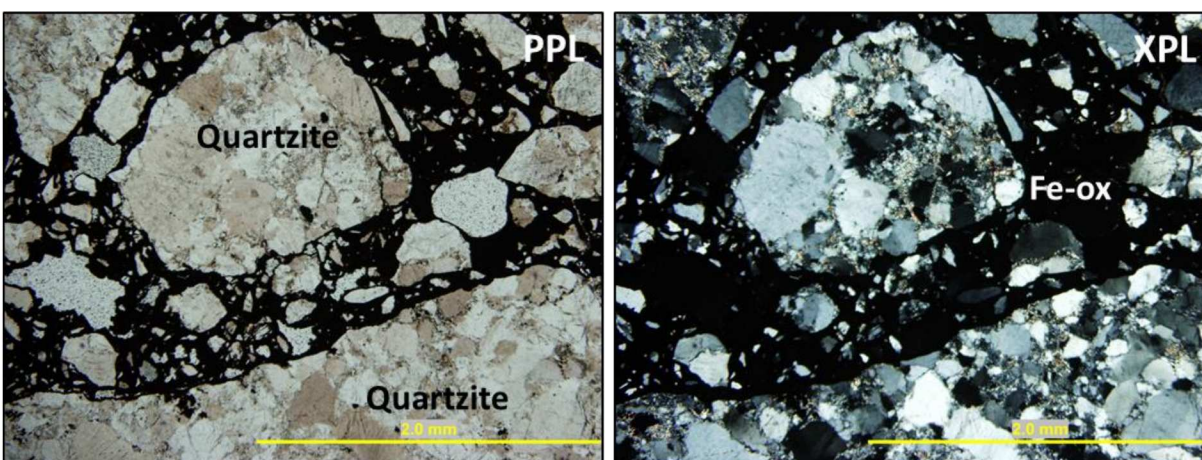


Figure 5.18: Unmineralised hydrothermal breccia (BK13ES016) characterised by hematite [Fe-ox]-jarosite-quartz cement and range of clast sizes.

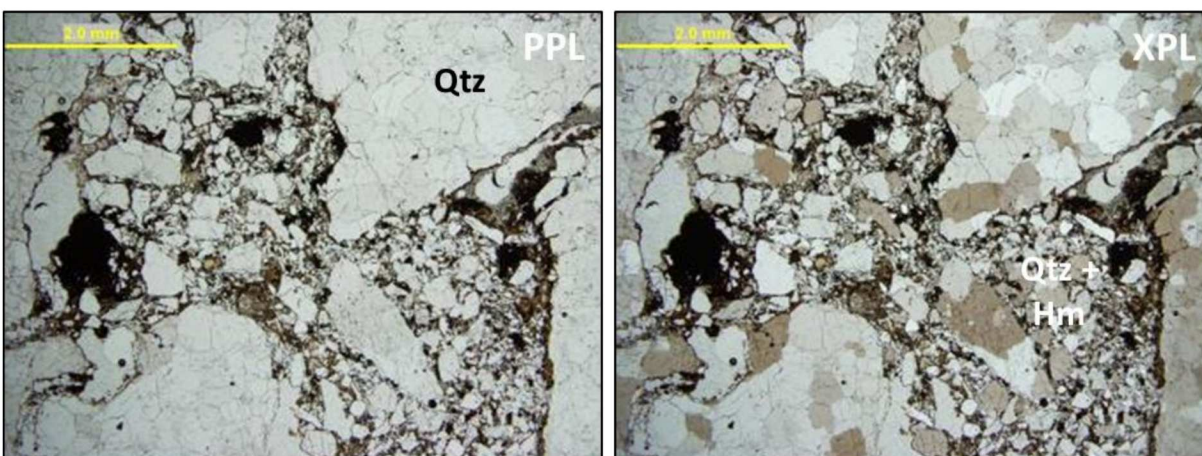


Figure 5.19: Tertiary hydrothermal breccia (BK13ES059) with a hematite [hm] and quartz [qtz] cement. The clasts are refragmented hydrothermal quartz that predates brecciation.



Figure 5.20: Quartz [qtz] and hematite [hm] vein in the Tertiary hydrothermal breccia (BK13ES052). The open space fill allowed for the growth of euhedral quartz and botryoidal hematite.

The breccia (sample BK13ES052) associated with the emplacement of the Tertiary

granites comprises hematite-jarosite-quartz cement around quartz vein clasts. The breccia is chaotic, monomictic and clast-supported. The clasts are hydrothermal, barren quartz with annealed grain boundaries. The clasts are variable in size, reaching up to >50 mm wide and very angular. The matrix of the breccia is composed of very fine-grained hematite, quartz and aphanitic yellow jarosite, which also occur in <1 mm veinlets. No quartz veins were observed cross-cutting the Fe-oxide veinlets or the annealed brecciated quartz matrix. Hematite is the main cement mineral, typically occurring with jarosite as patches around the clasts. The breccia likely had a sulphidic cement prior to weathering to Fe-oxides. Some relict cubic shapes are preserved, suggesting that hematite has replaced pyrite. In places, early hematite defines weathering rinds around specularite, which has pseudomorphed pyrite. The outer rind is weathered to a darker brown hematite, whereas the core of the altered grain is whiter, more reflective and non-magnetic. The Fe-oxides have grown in euhedral and botryoidal forms where open space was available (Fig. 5.20). No primary or secondary sulphides were observed.

A sample of a chaotic and polymictic mineralised breccia was collected near the Buckingham adit (Fig. 5.17). Sample BK13ES104 displays quartzite clasts and massive sulphide clasts cemented by quartz. The predominant clast types are massive sulphide clasts and older hydrothermal quartz clasts which are finer-grained than the groundmass quartz and very angular. The hydrothermal quartz clast size is variable and the clast size decreases towards the edges of the breccia. There is a minor (<10%) component of quartzite clasts in the breccia which are identified by rounder quartz grains which host interstitial white micas. The hydrothermal quartz cement contains pyrite and arsenopyrite. Pyrite occurs as euhedral grains in the quartz cement and is generally massive with cubic, inclusion-free cores, surrounded by very fine-grained grains of granular pyrite and arsenopyrite. This texture suggests that the older pyrite core acted as a

nucleation site for later sulphide precipitation. The arsenopyrite occurs as white rhombs in the quartz cement, or as euhedral rims on the pyrite (Fig. 5.21). Chalcopyrite and sphalerite occur as inclusions in the pyrite grains. Hematite only occurs as incomplete weathering rinds on some of the pyrite. No jarosite was observed.

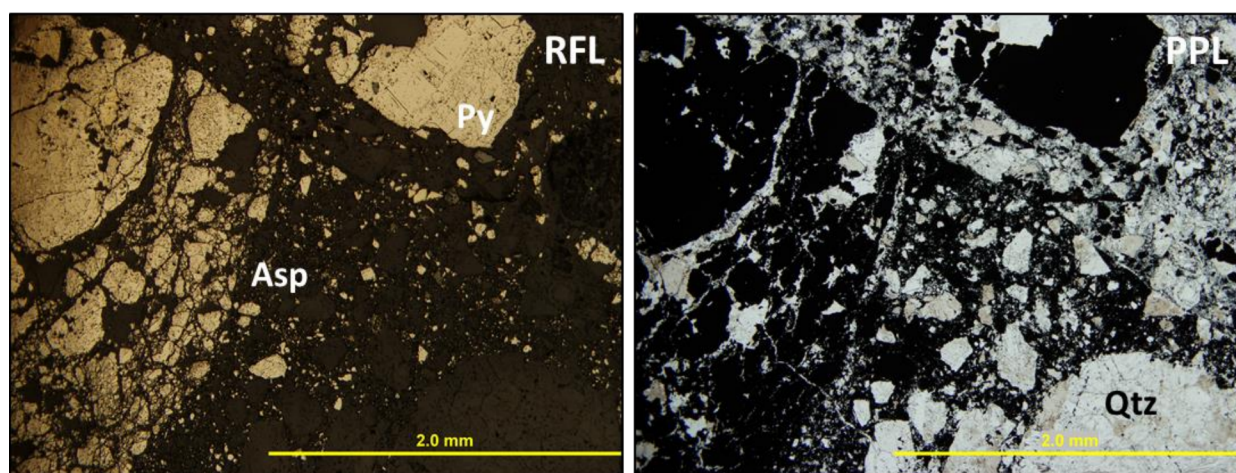


Figure 5.21: Sulphide-rich breccia with a very fine-grained sulphide and quartz [qtz] matrix and large pyrite [py], arsenopyrite [Asp], and quartzite clasts. The cubic cores of the pyrite can be seen near the top of the image.

5.3.5 Alteration and the vein stockwork in the granites

The two generations of granites have undergone hydrothermal alteration, notably phyllic alteration (quartz + pyrite + white mica mineral assemblage). The most common vein expression of this alteration is the occurrence of hematite-stained quartz veins with sericitic or muscovite-rich selvages (Fig. 5.22). There is also evidence of argillic alteration, as indicated by the formation of clay minerals, specifically the kaolinite, identified in the SWIR absorption data. The kaolinite is likely hypogene since it is concentrated around a leached cap and hydrothermal breccias, indicating areas of increased hydrothermal activity. The clay minerals were observed to replace the feldspars in the granites.

The phyllic alteration commonly occurs as the partial to complete replacement of feldspars in the granites from orthoclase, microcline, and albite/oligoclase to muscovite/sericite,

phengite, and other white micas. In the Cretaceous granites, the feldspars were typically completely altered whereas in the Tertiary granites, K-feldspar and plagioclase feldspar phenocrysts were less altered, generally retaining their primary growth twins. In the crystals where compositional zoning was evident, the micas preferentially altered the rim of the phenocrysts. This white mica alteration was also seen in the quartzites. Any feldspar clasts were altered and consequently could be distinguished from the unreactive quartz grains. Veinlets of white phyllosilicates occur in patches with coarser-grained, radiating muscovite in the quartzites. These veinlets are composed of ~85% very fine-grained white micas and some contain very fine-grained hematite (Fig. 5.14). The hematite is most likely a weathering product of primary pyrite in the veins. Barren quartz veins were also observed in the quartzites (Fig. 5.22).

The most intensively veined samples (BK13ES009 and BK13ES022) contained different generations of veins. Within the quartzite, there are localized breccias of very fine-grained hematite and aphanitic, greenish jarosite cement. The hematite and jarosite display some relict cubic shapes, suggesting they are after pyrite. The edges of the breccias tend to be composed of hematite with jarosite cores. In addition barren, fine-grained hydrothermal quartz veins which are cross-cut by the white mica veinlets were present. The jarosite in the veins occurs in patches and in veinlets with cross-cutting coarser-grained, radiating muscovite and possible phengite (Fig. 5.23)

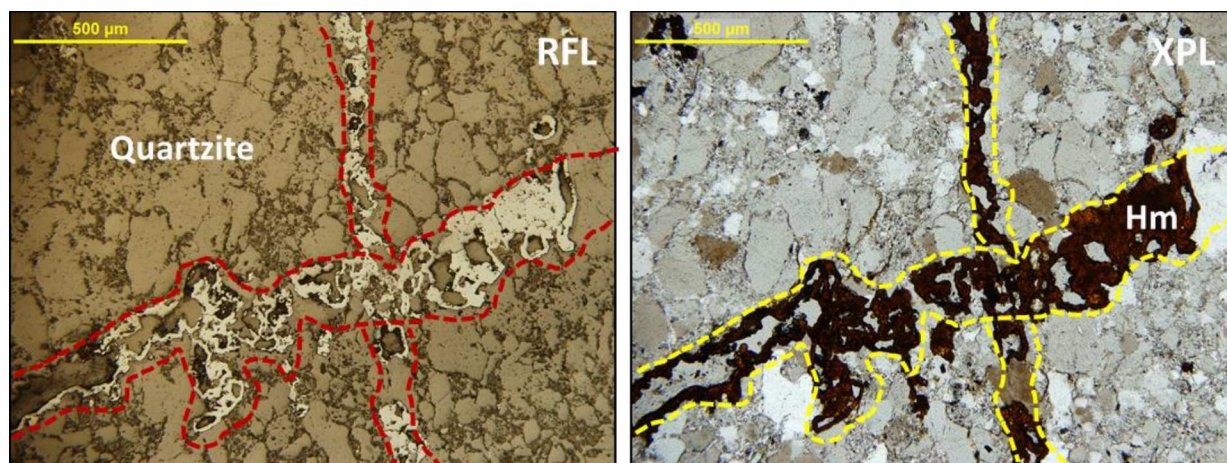


Figure 5.22: An intersection of two primary pyrite, now hematite [hm], veins in a quartzite (BK13ES021)

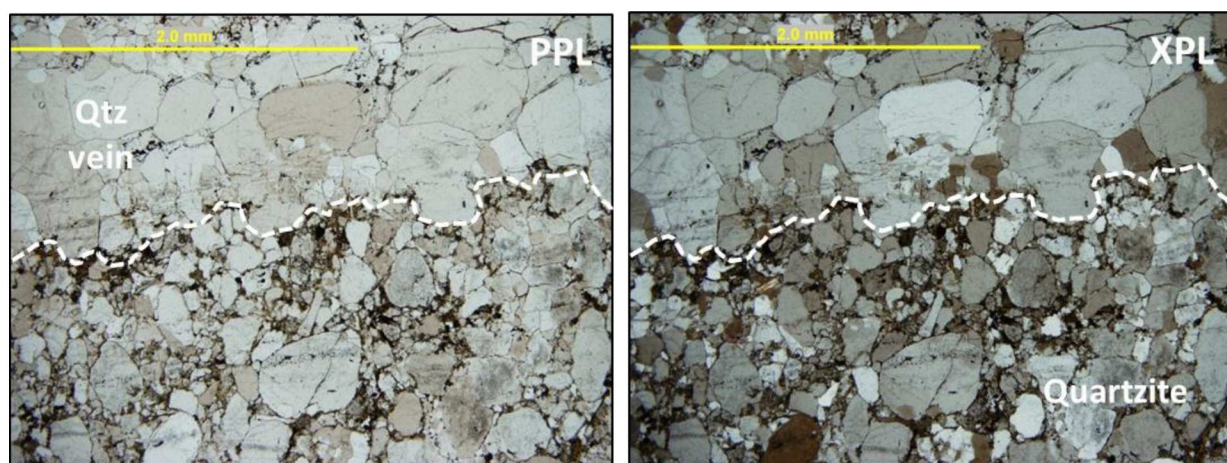


Figure 5.23: Barren quartz [qtz] vein in a grain-supported quartzite (BK13ES012)

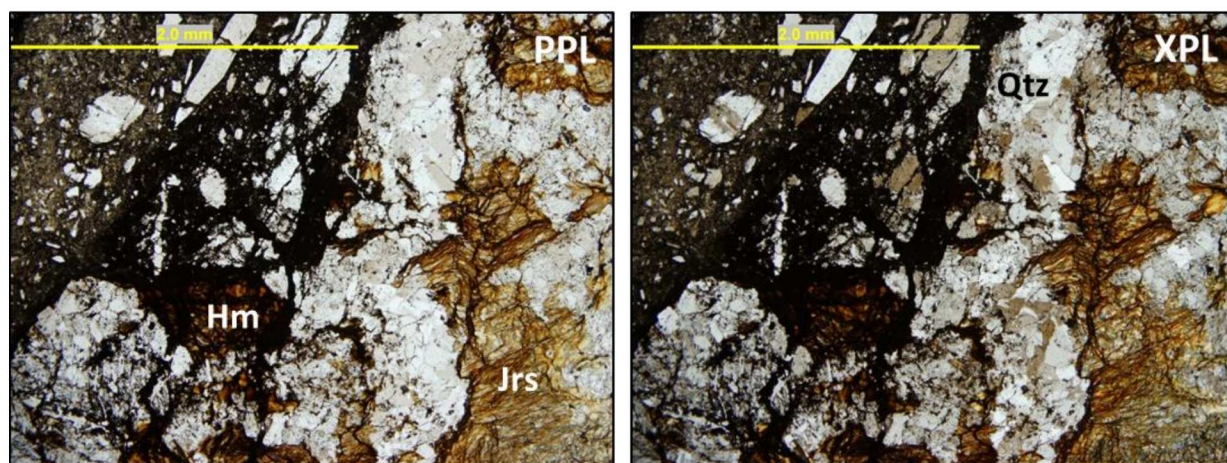


Figure 5.24: Hydrothermal breccia hosted in a quartzite (BK13ES009) with brecciating veinlets composed of very fine-grained hematite [hm] and aphanitic jarosite [jrs]

5.3.6 SWIR data

A Terraspec was used to analyse absorption features in the SWIR (short-wave infrared) region which are a function of the composition of the mineral in the mounts prepared for mineral chemistry analyses. This technique is particularly effective for distinguishing clay and mica minerals which may have similar appearance at the Buckingham study site. The intense phyllic and argillic alteration was observed in the altered Buckingham porphyry and the hosting metasedimentary rocks. The two most common minerals recorded were muscovite/phengite (found in 22 out of the 32 samples as the most common or second most common mineral) and kaolinite (found in 8 out of the 32 samples as the most common or second most common mineral; Table 5.2). Figure 5.25 shows a map of the minerals in Table 5.2 relative to the Buckingham quartz stockwork and system and the Copper Queen mineralisation (as defined by Theodore et al., 1992).

Table 5.2: Summary of SWIR data from the Buckingham porphyry study area. *Mineral 1* is the most common and *Mineral 2* is the second most common mineral. Coordinates are NAD27.

Sample	Unit	Lithology	Easting	Northing	Elevation	Mineral 1	Mineral 2
BK13ES001	Harmony Formation	Quartzite	494048	4495299	1940	Siderite	Muscovite
BK13ES003	Harmony Formation	Quartzite	493887	4495072	1960	Muscovite	
BK13ES005	Harmony Formation	Quartzite	493854	4495695	1862		
BK13ES006	Harmony Formation	Quartzite	493869	4495675	1835	Epidote	
BK13ES009	Harmony Formation	Quartzite	493872	4495778	1890	Phengite	Jarosite
BK13ES011	Buckingham intrusion	Porphyritic granite	493264	4493194	1774	Phengite	
BK13ES012	Harmony Formation	Quartzite	493242	4493400	1815	Muscovite	Chlorite
BK13ES013	Harmony Formation	Quartzite	493242	4493505	1851	Muscovite	Siderite
BK13ES014	Harmony Formation	Quartzite	493309	4493679	1902	Chlorite	Muscovite
BK13ES015	Harmony Formation	Quartzite	493467	4493840	1974	Muscovite	Gypsum
BK13ES017	Harmony Formation	Quartzite	493543	4494037	2023	Muscovite	
BK13ES018	Harmony Formation	Quartzite	493667	4494161	2038	Muscovite	Kaolinite
BK13ES020	Harmony Formation	Quartzite	493803	4494098	2055	Chlorite	
BK13ES021	Harmony Formation	Quartzite	493689	4494250	2005	Muscovite	
BK13ES023	Harmony Formation	Altered quartzite	493704	4494629	2023	Muscovite	Kaolinite
BK13ES025	Harmony Formation	Altered quartzite	493870	4494735	2034		

Chapter 6: Whole Rock Geochemistry and Geochronology

Whole rock geochemistry was completed on all of the samples collected in the field. The whole rock geochemistry of the igneous lithologies from both study areas was used to determine the progression from the initial crystallization and later hydrothermal alteration during the mineralisation event. The trace element geochemistry of the porphyries, granites and associated igneous bodies was used to provide insight into the evolution of the igneous rocks.

6.1 White Pine Fork Mo porphyry lithologies

6.1.1 Little Cottonwood Intrusion

This unit is characterized by anhydrous SiO_2 values of 66 – 75 wt.%, Fe_2O_3 values of 2 – 5 wt.%, MgO values of 0.4 – 1.6 wt.% and a Mg# of 20 – 47. The whole rock contents of Mo ranged from <1 to 302 ppm, with an average of 12 ppm. When the Little Cottonwood stock and the White Pine intrusion were plotted on a TAS (total alkali-silica) diagram, they fell within the granite, granodiorite and quartz monzonite fields (Fig. 6.1). The Little Cottonwood plotted slightly more in the granodiorite and quartz monzonite fields, reflecting a lower SiO_2 content than the White Pine intrusion. The Little Cottonwood is characterised by negative Nb and Ti anomalies ($\text{Nb}/\text{Nb}^* = 0.11 - 0.63$; $\text{Ti}/\text{Ti}^* = 0.20 - 0.54$), as well as generally positive Hf anomalies ($\text{Hf}/\text{Hf}^* = 0.74 - 2.02$; Appendix 4). Normalized to primitive mantle values, there is a Nb-Ta and Sr depletion (Fig. 6.2). The granite displays LREE enrichment, with a $\text{La}/\text{Sm}_{\text{cn}}$ values of 5.5 - 13.4; and well fractionated HREEs (denoted by the $\text{Gd}/\text{Yb}_{\text{cn}}$ values ranging from 2.9 – 7.0; Fig. 6.2).

6.1.2 White Pine Intrusion

The White Pine intrusion has anhydrous SiO_2 values of 69 – 77 wt.%, Fe_2O_3 values of 1 – 4 wt.%, MgO values of 0.5 – 1.0 wt.% and a Mg# of 28 – 54. The whole rock contents of Mo ranged from <1 to 1096 ppm, with an average of 133 ppm. Similarly to the Little Cottonwood stock, the White Pine intrusion is characterised by negative Nb and Ti anomalies ($\text{Nb}/\text{Nb}^* = 0.16 - 0.35$; $\text{Ti}/\text{Ti}^* = 0.21 - 0.56$), as well as positive Hf anomalies ($\text{Hf}/\text{Hf}^* = 0.71 - 2.49$; Appendix 4; Fig. 6.2). When these values are normalized to primitive mantle values, there is a depletion of Nb – Ta and Sr. The granite displays LREE enrichment, with $\text{La}/\text{Sm}_{\text{cn}}$ values of 5.5 -10.3 and well fractionated HREEs (denoted by the $\text{Gd}/\text{Yb}_{\text{cn}}$ values ranging from 3.0 – 7.2; Fig. 6.3).

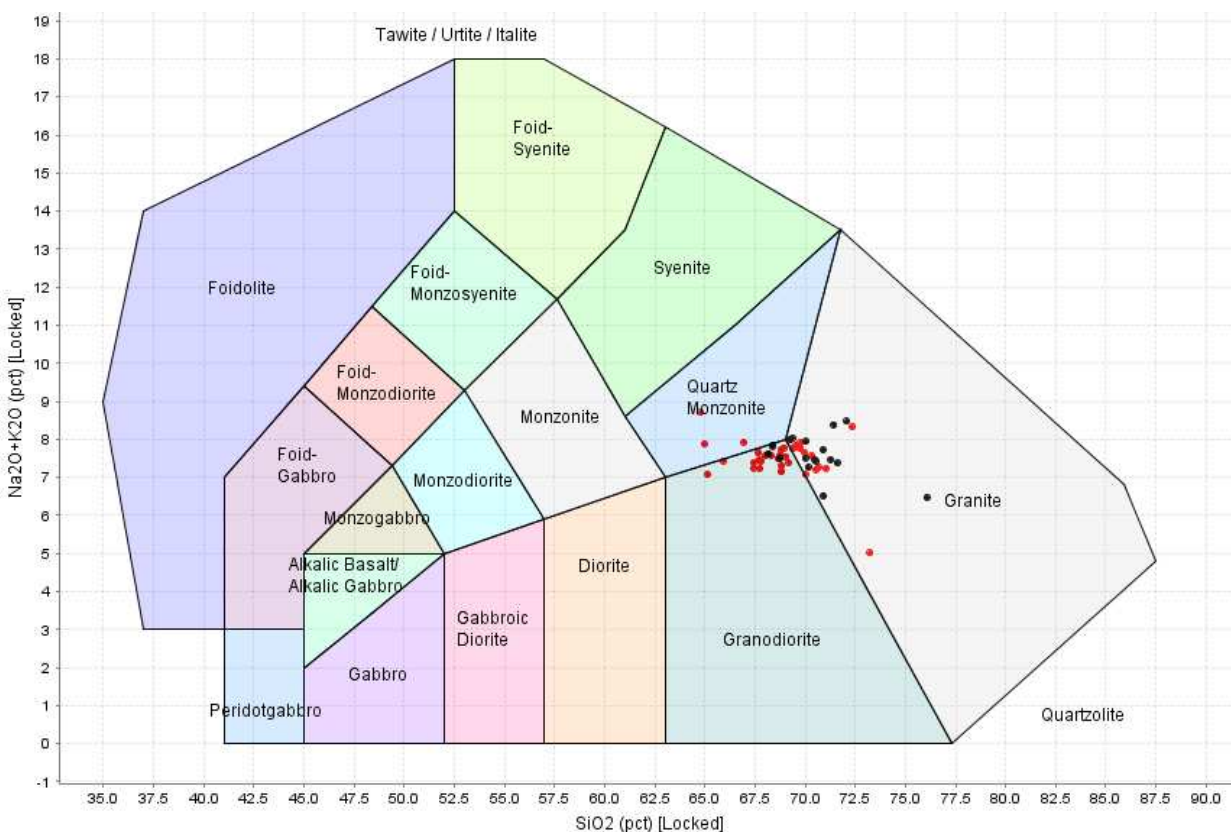


Figure 6.1: TAS diagram for the Little Cottonwood granitic rocks (red) and the White Pine intrusion (black). After Middlemost (1994).

6.1.3 Lamprophyric Dykes

The other igneous rocks sampled in this study were the four lamprophyric dykes. These dark-coloured dykes were narrow (<5 m) and cross-cut the Little Cottonwood stock. They are characterized by anhydrous SiO₂ values of 55 –61 wt.%, Fe₂O₃ values of 5 – 7 wt.%, MgO values of 2.8 – 5.0 wt.% and a Mg# of 55-62. The whole rock contents of Mo ranged from 0.06 to 0.86 ppm, with an average of 0.40 ppm. Similar to the Little Cottonwood stock and the White Pine intrusion, the dykes are characterised by negative Nb and Ti anomalies (Nb/Nb* = 0.10 – 0.14; Ti/Ti* = 0.21 – 0.33), as well as positive Hf anomalies (Hf/Hf* = 0.59 – 1.4; Appendix 4). Normalized to primitive mantle values, there is a depletion of Nb-Ta and Sr. As well, in two samples (WP13ES08 and WP13ES10) there is a slight enrichment in Sm and La. These dykes display a strong LREE enrichment, with a La/Sm_{cn} values of 6.9 – 7.1 and fractionated HREEs (Gd/Yb_{cn} values ranging from 5.5 – 8.8; Fig. 6.2).

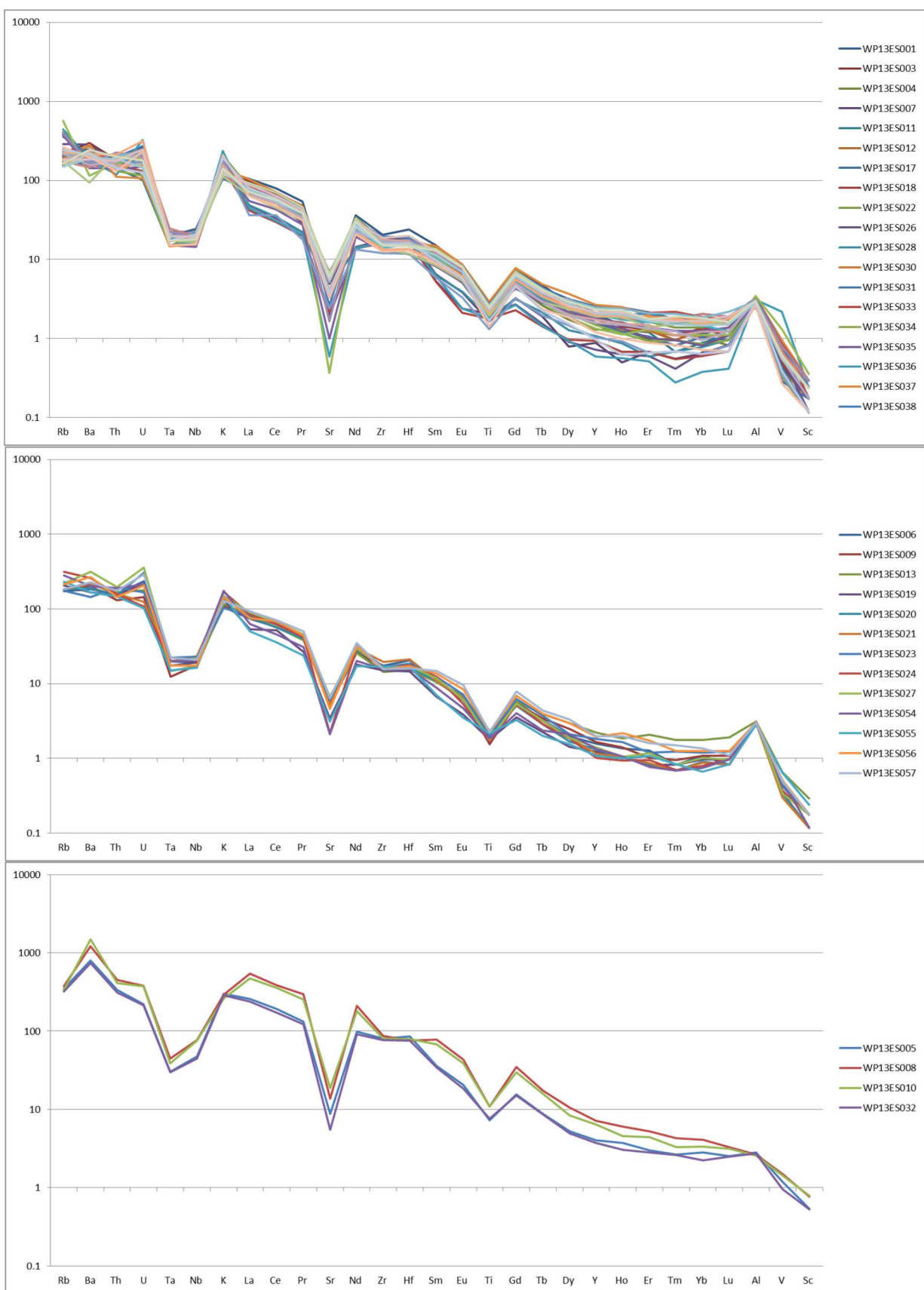


Figure 6.2: Primitive mantle normalized plots for the samples from the Little Cottonwood stock (top), White Pine intrusion (middle) and lamprophyric dykes (bottom). Normalizing values from Sun and McDonough (1989).

6.2 Buckingham Mo (-Cu) porphyry lithologies

6.2.1 Buckingham porphyry

This unit is characterized by anhydrous SiO₂ values of 70 – 85 wt.%, Fe₂O₃ values of 1 – 4 wt.%, MgO values of 0.3 – 1.6 wt.% and a Mg# of 24 – 54. As well, the whole rock geochemistry averaged 84 ppm of Mo, 212.0 ppm of Cu, and 1605 ppb of Ag. The Buckingham granites are characterised by negative Nb and Ti anomalies (Nb/Nb* = 0.21 – 0.45, with an outlier of 2.18; Ti/Ti* = 0.24 – 0.58), as well as positive Hf and Zr anomalies (Hf/Hf* = 0.86 – 2.46; Zr/Zr* = 0.96 – 2.37; Appendix 4; Fig. 6.4). The granite shows LREE enrichment, with La/Sm_{cn} values of 3.18 – 6.82; and moderately fractionated HREEs (denoted by the Gd/Yb_{cn} values ranging from 1.7 – 3.8; Fig. 6.4). When the Buckingham porphyry granites and the Tertiary granites were plotted on a TAS (total alkali-silica) diagram, the data points fell almost entirely in the granite field (Fig. 6.3). The outliers were all Tertiary granite samples.

6.2.2 Tertiary granites

The rock types vary from monzogranites to very Si-rich granites. As a whole, this unit is characterized by anhydrous SiO₂ values of 70 – 85 wt.%, Fe₂O₃ values of 1-3 wt.%, MgO values of 0.4 – 2.8 wt.% and a Mg# of 29 – 81. As well, the whole rock geochemistry averaged 4.2 ppm of Mo, 166 ppm of Cu, and 606 ppb of Ag. The Buckingham granites are characterised by negative Nb and Ti anomalies (Nb/Nb* = 0.29 – 0.97; Ti/Ti* = 0.25 – 0.53; Fig. 6.4), as well as positive Hf and Zr anomalies (Hf/Hf* = 1.06 – 4.28; Zr/Zr* = 0.77 – 4.28; Appendix 4). The granite shows LREE enrichment, with La/Sm_{cn} values of 2.1 – 5.9; and weakly fractionated HREEs (denoted by the Gd/Yb_{cn} values ranging from 1.5 – 2.5; Fig. 6.4).

6.2.3 Hydrothermal breccias

There are two generations of hydrothermal breccias in the study area. The older hydrothermal breccias are interpreted to have formed during the emplacement of the Buckingham system. The breccias are mineralized with average grades of 9.4 ppm of Mo, 232 ppm of Cu, and 3372ppb of Ag. In addition to the Buckingham hydrothermal breccias, one sample was collected from a hydrothermal breccia interpreted to have formed during the emplacement of the Eocene granites. This sample had whole rock grades of 3.0 ppm of Mo, 96 ppm of Cu, and 1496 ppm of Ag.

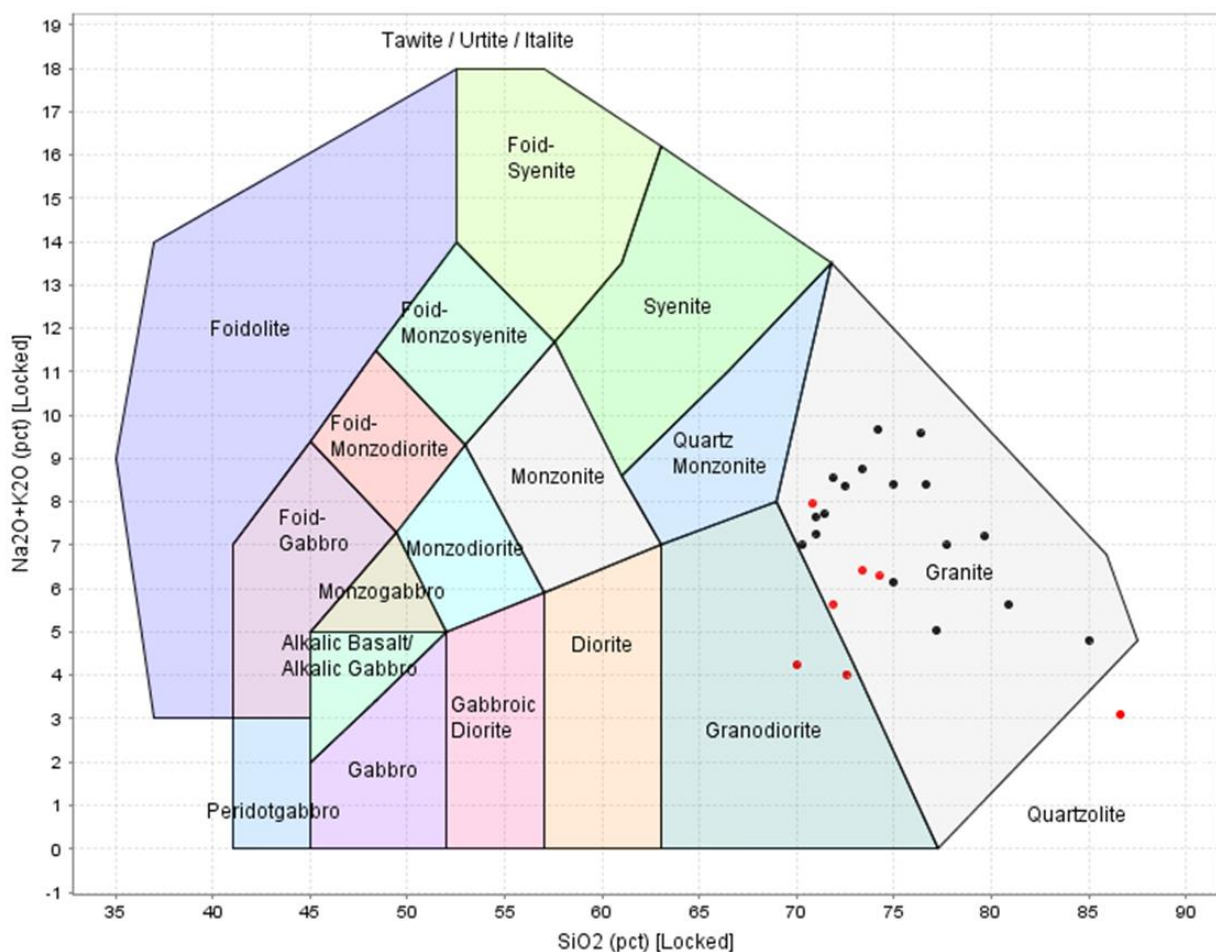


Figure 6.3: TAS diagram for the Buckingham granitic rocks (black) and the Tertiary granites (red). After Middlemost, (1994).

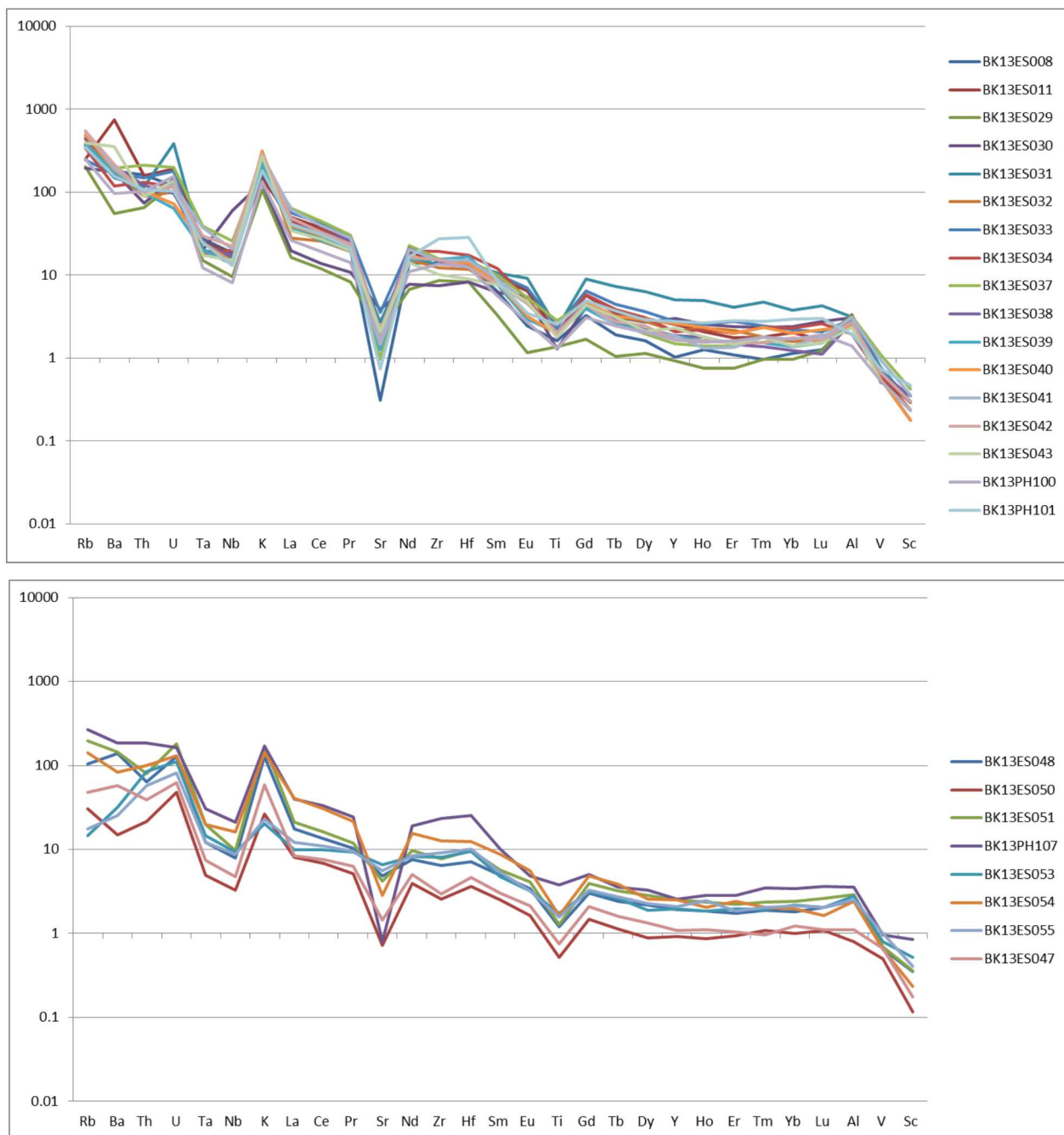


Figure 6.4: Primitive mantle normalized plots for the samples from the Buckingham porphyry (top) and the Tertiary granites (bottom). Normalizing values from Sun and McDonough (1989).

6.3 U-Pb and Re-Os dating of the White Pine Fork breccia pipe

The White Pine Fork Mo porphyry is most strongly mineralized at the breccia pipe near the southern end of the intrusion. The heterolithic breccia pipe is composed of fragments of a felsic intrusive rock thought to be the White Pine intrusion (a leucocratic, K-feldspar and quartz-porphyrific monzogranite) and hydrothermal quartz fragments. The cement is rusty (primary pyrite) Fe-oxides and vuggy quartz. The molybdenite from the hydrothermal cement to the breccia was collected in order to determine the age of mineralisation. At the White Pine Fork porphyry, two different minerals were dated. Fourteen zircons collected from the granitic clasts were dated using U-Pb systematics. As well, samples of the quartz cement and associated Mo mineralisation were dated using Re-Os systematics in the molybdenite. The average U-Pb age collected from the granitic clasts was 26.52 ± 0.42 Ma (Table 6.1). This age was determined by the plotting of $^{207}\text{Pb}/^{206}\text{Pb}$ against $^{236}\text{U}/^{206}\text{Pb}$ values of all 14 zircons (Fig. 6.5A). The concordia plot shows a mean squared weighted deviation (MSWD) value of 0.52, suggesting that the data fell within the statistical error of the analytical uncertainties. The Re-Os age of the molybdenite calculated as 30.21 ± 0.14 and 29.84 ± 0.15 Ma (Table 6.1). The 29.84 ± 0.15 Ma age is a duplicate age from the same sample which was reanalysed due to the unexpected age.

6.4 U-Pb and Re-Os dating of the Battle Mountain Eocene granites

The granites in the northern portion of the study area were suspected to be younger than the Cretaceous Buckingham-related intrusions. In order to test this, samples were submitted and the ages determined from these suspected Eocene granites were 38.68 ± 0.53 (from BK13ES048), 39.28 ± 0.58 (from BK13ES050), 40.76 ± 0.41 (from BK13ES058), and 40.81 ± 0.51 Ma (from BK13ES053; Table 6.1). Sample BK13ES048 was dated using 14 zircons which gave ages ranging from 37.0 ± 0.8 to 40.3 ± 0.7 Ma with one zircon giving an interpreted inherited age of

144.0±2 Ma. This zircon is shown on the Concordia diagram as a blue datum point (Fig. 6.5E). This concordia plot had a MSWD of 1.8, which infers that the data falls outside of the inherited analytical error. Sample BK13ES050 was dated using 14 zircons which gave ages ranging from 37.3±0.9 to 49.9 ±0.9 Ma with one zircon giving an interpreted inherited age of 132.0±2 Ma. This concordia plot had a MSWD of 1.9, which infers that the data falls outside of the inherited analytical error (Fig. 6.5 D). Sample BK13ES058 had an age of 40.76±0.41 which was collected from 12 zircons and had a range of 39.1±1.2 to 41.7±0.8 Ma. One zircon gave an age (of 48.6±1.1 Ma), which is suspected to mixing age domains and can be used with caution (Fig. 6.5B). There were two ages of 148 and 1282 Ma which were interpreted as Pb loss. The MSWD value is 0.51 which infers that this concordia age lies within statistical error of the inherent analytical error (Figs. 6.5B). Sample BK13ES053 had an age of 40.81±0.51 which was collected from 11 zircons and had a range of 40.0± 0.7 to 41.9±1.0 Ma. There were three ages which were interpreted as inherited, Proterozoic ages. The MSWD value is 0.46 which infers that this concordia age lies within statistical error of the inherent analytical error (Figs. 6.5C). These ages confirm the younger, Eocene age, as opposed to being related to the Cretaceous magmatism in the study area.

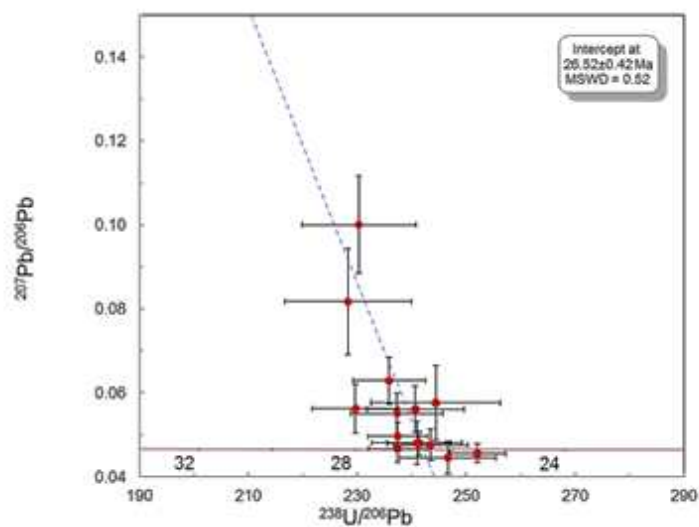


Figure 6.5: Concordia plot for the U-Pb ages collected for (A) the White Pine breccia pipe monzogranite clasts (WP13ES02)

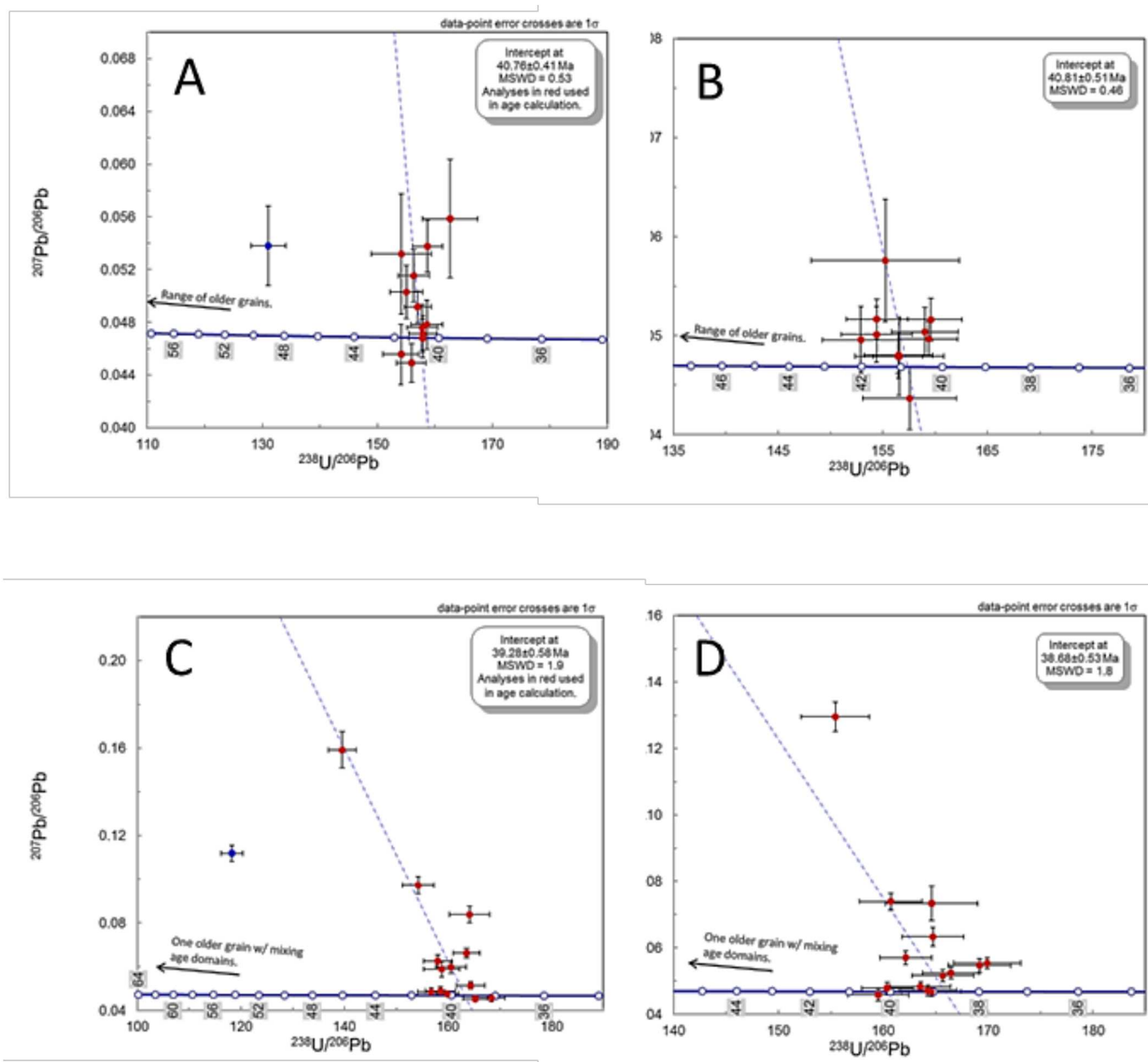


Figure 6.6: Concordia plots for the U-Pb ages collected for the Tertiary granites in the Battle Mountain area: (A) BK13ES058, (B) BK13ES053, (C) BK13ES050, and (D) BK13ES048.

Chapter 7: Mineral trace element geochemistry

The quartz and pyrite present at both study sites formed as the result of phyllic hydrothermal alteration, however they also occur as primary igneous and sedimentary minerals. These two alteration minerals were sampled and analysed to determine their effectiveness as mineral chemistry vectors to mineralisation. In addition to the development of vectoring tools, this study attempted to distinguish the different types of quartz (igneous, sedimentary and hydrothermal; Fig. 7.1) based on their mineral chemistry.

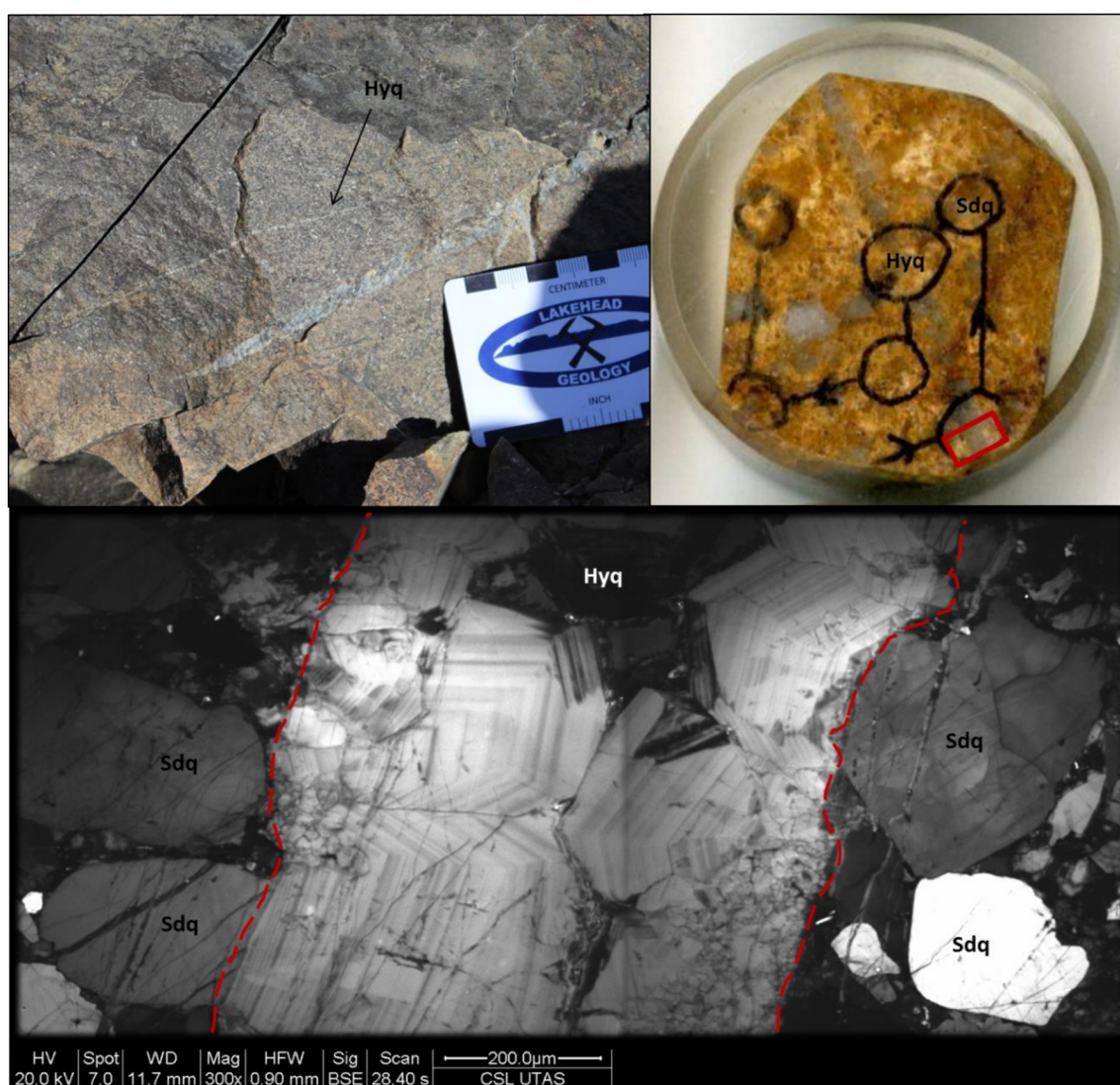


Figure 7.1: Sample BK13ES012; (top left) Outcrop-scale barren quartz vein [Hyq] cross-cutting a quartzite; (top right) a mount prepared and the quartz grains marked for LA-ICP-MS analyses; (bottom) a cathodoluminescence image of the zoned quartz vein, within the red rectangle superimposed on the polished mount, cross-cutting homogenous quartz clasts [Sdq].

The textural differences noted between the quartz types are easily recognized in cathodoluminescence (CL) imaging by lighting up at varying intensities. CL imaging highlights trace element variations in the compositions of the quartz. CL intensity variations are not specific to a single trace element and are not affected by fluid or mineral inclusions, only structurally bound elements. If the substituted elements increase the specific gravity of the quartz, the mineral specimen with that composition will be brighter than the quartz with an average lower specific gravity (Rusk et al., 2008). The sampled igneous quartz from White Pine Fork and Buckingham was coarse-grained phenocrysts with no to weak oscillatory zoning and no inclusions (Figs. 7.2B and 7.4). The composition is typically more homogenous than the hydrothermal quartz and sample spots were taken from the core to the rim of the crystals. The sedimentary quartz grains from the Buckingham study site were homogenous throughout and had various intensities (Fig. 7.2A). The hydrothermal quartz showed weak to very well-defined, alternating dark and light bands and euhedral, hexagonal grain shape outlines (Fig. 7.1). The breccia quartz has irregular patches and inconsistent zonation (Fig. 7.2D).

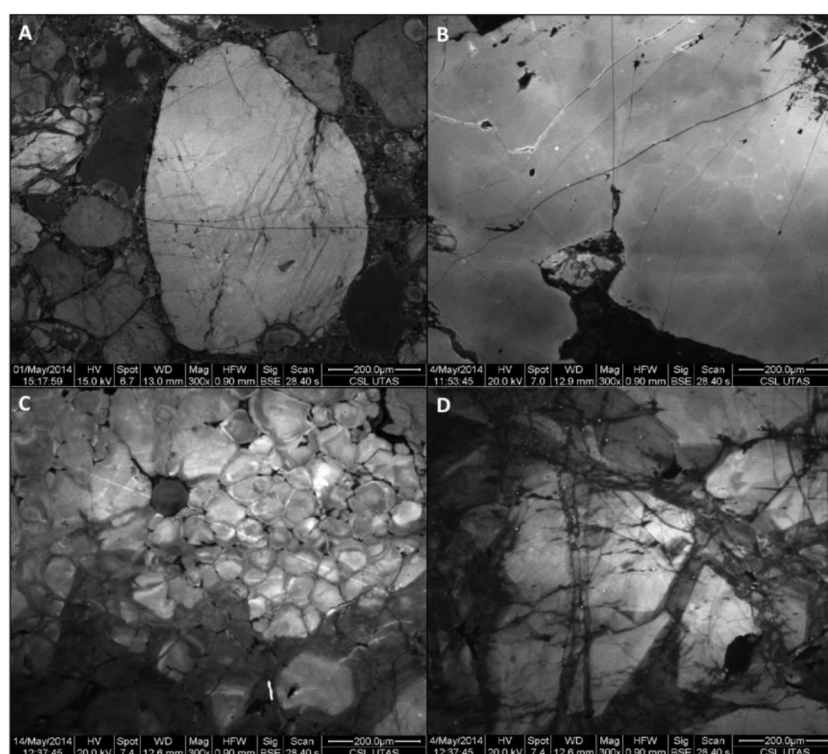


Figure 7.2

(A) Sedimentary quartz grains in a white mica groundmass [BK13ES003]

(B) Igneous quartz phenocryst [WP13ES022]

(C) Fine-grained zone within a quartz vein in a quartzite [BK13ES015]

(D) Breccia quartz [WP13ES63]

7.1 Quartz trace element geochemistry from the Little Cottonwood and White Pine intrusions

For the samples from the White Pine Fork Mo porphyry, a total of 229 quartz spot analyses, with 36 rejected runs (16%), were analysed. Of these analyses, 47 spots sampled background igneous quartz crystals from the Little Cottonwood and White Pine intrusions (Fig. 7.3). The igneous crystals were large and occasionally showed oscillatory compositional zoning during cathodoluminescence imaging (Fig. 7.2 and 7.3).

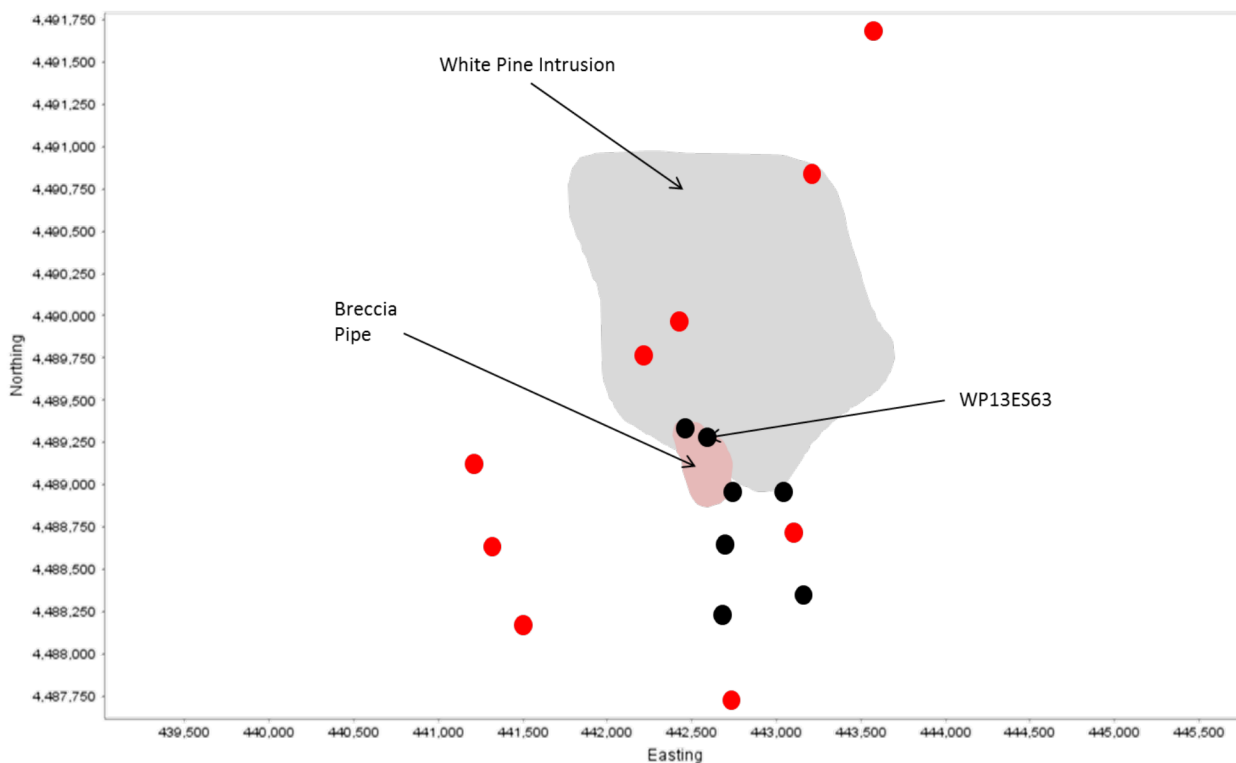


Figure 7.3: Sample locations of the quartz mounts prepared for mineral chemistry analysis at White Pine Fork. The red spots identify samples which included igneous quartz grains.

The White Pine and Little Cottonwood igneous quartz samples showed very little variation in the concentrations of trace elements. The more common Si-substituting elements, Ti (varied from <1 to 82 ppm, with a mean of 26.93 ppm) and Al content ranges (varied from 20 to 127 ppm with a mean of 57.12 ppm) were larger than the other elements. Bismuth (<0.3700 ppm) and Ge (<3.300 ppm) were also not very abundant in the igneous quartz. The highest values of Li (mean of 3.557 ppm), K (5.598 ppm), and Na (10.95 ppm) are associated with some of the highest concentrations of Al. Gold was at very low levels in the igneous quartz (below detection limits in 24 out of the 45 samples). The heavy metal content in the quartz spiked and these high values were not representative of the entire quartz grain. Fe had a mean of 28.69 ppm and a median of 2.100 ppm (two samples at 582 and 298 ppm) and Cu had a mean of 0.3273 ppm and a median value of 0.1480 (one sample spiked at 5.70 ppm). This spike was identified in the LA-ICP-MS data and they are interpreted here to represent mineral inclusions. In the igneous quartz at White Pine, the concentrations of As (<7.900 ppm, average of 2.151 ppm) and Sb (<0.2600 ppm, average of 0.0277 ppm) had more consistent values than other metals (Table 7.1).

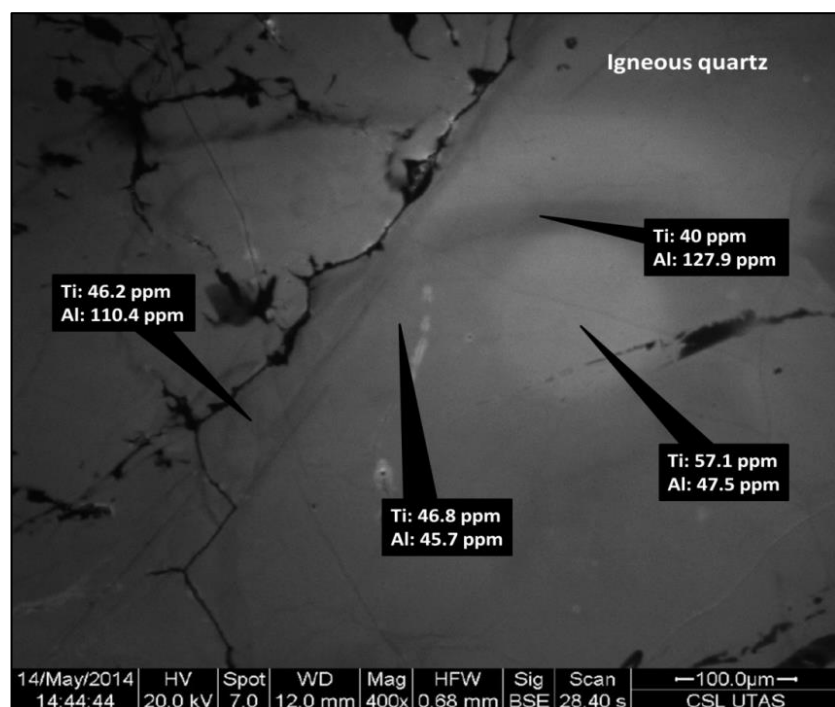


Figure 7.4: BSE-CL image of an igneous quartz grain from the Little Cottonwood stock (WP13ES13) showing a core with a slight increase in Ti

In addition to the igneous quartz samples, hydrothermal quartz, found in veins (132 spots) and as breccia cement (21 spots) which were associated with the emplacement of the intrusion, were also analysed. The selected vein quartz crystals from the Little Cottonwood and White Pine intrusions were large and sometimes showed oscillatory compositional zoning in cathodoluminescence images (Fig. 7.3). The breccia quartz cement was characterized by a marked increase in other mineral inclusions (i.e., sulphides and adularia) relative to the quartz veins in the rest of the samples. The breccia cement samples have similar Al values (mean of 75.27 ppm) to the vein quartz (mean of 147.0 ppm). Titanium varied from 1 to 79 ppm, with an average of 29.41 ppm in the vein quartz. The mean Ti value from the breccia cement samples is 37.60 ppm. Bismuth (mean is 0.0511 ppm in the vein quartz and 0.0032 in the breccia cement) and Ge (mean of 1.816 ppm in the vein quartz samples and 1.052 ppm in the breccia samples) were also not very abundant in the hydrothermal quartz. In the vein quartz, Li has a mean of 3.747 ppm, K, 19.32 ppm, and Na, 25.01 ppm. The breccia cement samples show that the Li (mean of 3.655 ppm), K (16.82 ppm), and Na (16.89ppm) values are similar to the vein quartz. Au was not recorded in significant amounts in the hydrothermal quartz or breccia cement. Iron (mean of 16.26 ppm in the vein quartz and 6.280 ppm in the breccia cement) and Cu (average of 0.4282 ppm in the vein quartz and 0.2912 ppm in the breccia cement) occur as inconsistent spikes and are not homogenous values. The concentrations of As (average of 3.526 ppm in the vein quartz and 6.756 ppm in the breccia cement) and Sb (average of 0.3257 ppm in the vein quartz and 0.0162 ppm in the breccia cement) were consistent throughout the crystals (Table 7.1).

Table 7.1: Trace element concentrations in different quartz types at White Pine Fork. All values are in ppm, except for Au, which is in ppb.

	Vein quartz (n_{max}=132)	Igneous quartz (n_{max}=47)	Breccia cement quartz (n_{max}=21)
Li7	3.747	3.557	3.655
Na23	25.01	10.95	16.89
Mg24	1.861	0.3823	0.8854
Al27	147.01	57.12	75.27
P31	17.12	16.46	13.42
K39	19.32	5.598	16.82
Ca43	31.40	35.40	39.34
Ti47	29.41	26.93	37.60
Ti49	29.34	27.15	37.65
V51	0.0207	0.0261	0.0295
Cr53	0.0819	0.1043	0.0673
Mn55	0.2092	0.1330	0.4179
Fe57	16.26	28.69	6.280
Cu63	0.4282	0.3273	0.2912
Cu65	0.4614	0.3257	0.4039
Zn66	0.1297	0.3098	0.1428
Ge74	1.816	1.220	1.0518
As75	3.526	2.151	6.756
Rb85	0.0715	0.0457	0.0975
Sr88	0.1979	0.1227	0.0815
Zr90	0.0139	0.0055	0.0056
Ag107	0.0268	0.0099	0.0207
Sb121	0.3257	0.0277	0.0162
Cs133	0.0164	0.0185	0.0539
Gd157	0.0060	0.0046	0.0082
Hf178	0.0031	0.0031	0.0037
Ta181	0.0011	0.0018	0.0010
Au197	0.0061	0.0045	0.0055
Pb208	0.1040	2.518	0.0814
Bi209	0.0511	0.0247	0.0032
U238	0.0067	0.0095	0.0022

7.2 Quartz trace element geochemistry from the Buckingham porphyry

At Buckingham, the quartz was categorised as sedimentary, igneous, vein or breccia quartz. The sedimentary quartz was collected from the Harmony Formation quartzites whereas the igneous grains were sourced from the Buckingham intrusions. In the field, quartz in veins that were cross-cutting the host rocks (identifiable as belonging to the Buckingham system by being mineralized or belonged to a quartz stockwork) was sampled. These quartz samples were classified as the hydrothermal quartz. The breccia quartz samples were BK13ES025 and BK13ES104, collected from areas of intense hydrothermal alteration and mineralisation. The breccia samples were separated from the hydrothermal vein quartz samples due to their increased sulphide content and mineral evidence of intense hydrothermal alteration.

From the samples collected at the Buckingham Mo (-Cu) porphyry, a total of 384 quartz spot analyses, with 75 rejected runs (19%), were collected. From these analyses, 77 spots sampled sedimentary quartz detrital grains from the quartzites of the Harmony Formation. The composition of these grains varied due to their multiple sources prior to erosion and deposition. The grains often appeared fragmented and compositionally homogeneous or irregular with cathodoluminescence imaging (Fig. 7.2 and 7.5).

In the sedimentary rocks, a wide range in values is expected due to the multiple sources of the detrital quartz. In the sedimentary quartz, Ti has a mean of 41.38 ppm and Al has a mean of 110.7 ppm in the sedimentary quartz. Bismuth (<0.040 ppm) and Ge (<3.600 ppm) had low contents in the sedimentary quartz. The highest Li (mean of 5.419 ppm), K (25.37 ppm), and Na (17.97 ppm) contents correlate with the highest Al contents. Iron (mean of 14.37 ppm), Cu (average of 0.3705 ppm), Pb (average of 0.115 ppm), and Zn (average of 0.2843 ppm) values show sporadic and inconsistent concentrations, often correlating with each other. Au was not

recorded in significant amounts in the sedimentary quartz (below detection limits in 38 out of the 78 samples). In the sedimentary quartz, the concentrations of As had a mean of 0.6987 ppm and Sb averaged 0.1151 ppm.

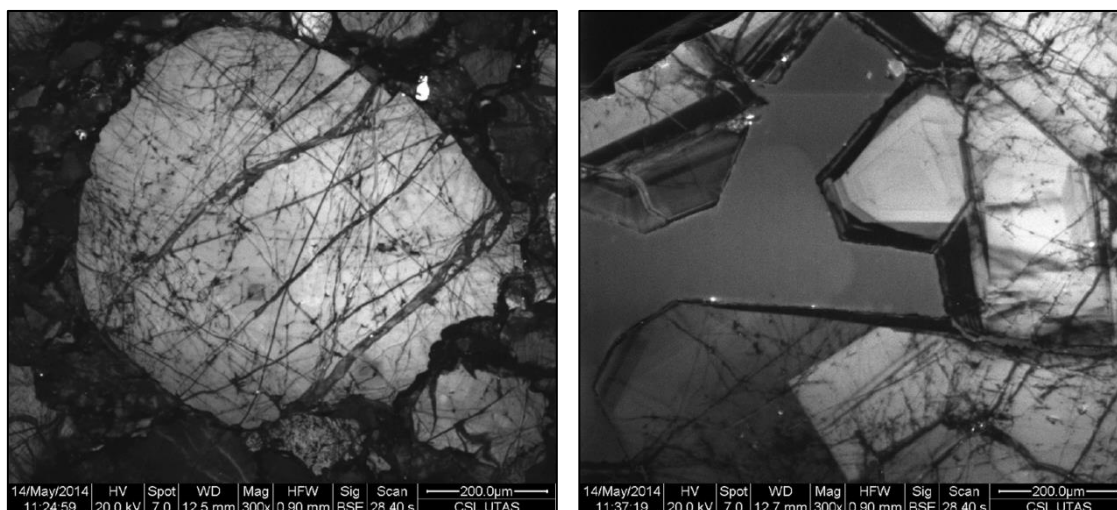


Figure 7.5: BSE-CL image of two quartz samples from BK13ES013. (Left) a detrital quartz grain with cross-cutting, clay-filled fractures and showing some slight, irregular compositional zoning; (Right) A hydrothermal vein quartz with euhedral crystals and compositional zoning.

In addition to the sedimentary quartz in the quartzites, there were 13 usable spots from the Buckingham intrusion. These samples, partially due to their smaller sample size, showed a narrower range in data. Titanium had a mean of 51.81 ppm, Al, 105.4 ppm and Bi and Ge were 0.0020 ppm and 1.531 ppm, respectively. Lithium (mean of 9.093 ppm), K (11.22 ppm), Ca (34.52 ppm) and Na (15.61 ppm) increase with higher concentrations of Al and Ti. The metal cations, Fe (mean of 4.397 ppm), Cu (average of 0.2666 ppm), Pb (mean of 0.0892 ppm), and Zn (mean of 0.2138 ppm) values show heterogeneous concentrations within a single quartz grain. As well, high concentrations of Pb and Zn often correlated. Gold was not present in significant amounts in the igneous quartz (below detection limits in 7 out of the 13 samples). The As values in the igneous quartz (mean of 2.741 ppm) and the Sb (mean of 0.0318 ppm) were homogenous throughout the crystal (Table 7.2)

The hydrothermal quartz at Buckingham was classified into two categories: vein quartz and breccia cement (Figs. 7.1 and 7.2). There were 218 usable spots collected from quartz veins (193 spots) and from hydrothermal breccias with a quartz and primary sulphide cement (25 samples). The vein quartz Ti and breccia cement Ti contents averaged 24.52 and 8.589 ppm, respectively. The Al content of the breccia quartz is higher than the vein quartz (average of 1067 ppm and 218.4 ppm, respectively). Vein quartz Bi (<0.050ppm) and Ge (<5.800 ppm) were similar to the breccia cement quartz Bi (<0.0300 ppm) and Ge (<5.500 ppm) values. The vein quartz has a mean of 10.48 ppm Li and the breccia cement has a mean of 90.59 ppm, with some values in the breccia cement reaching ~560.0 ppm. The K has a mean of 37.63 ppm in the vein quartz and 134.7 ppm in the breccia cement and the Ca values has a mean of 46.54 ppm in the vein quartz and 237.3 ppm in the breccia cement. The amount of Fe in the vein quartz (mean of 45.42 ppm) is lower than the breccia cement (mean of 68.10 ppm). The vein quartz shows Cu values averaging 3.743 ppm, Pb averaging 0.1559 ppm, and Zn averaging 0.3407 ppm. The breccia samples also contain higher amounts of Zn (mean of 5.457 ppm) with a similar amount of Cu (mean of 1.332 ppm) and Pb (0.4598 ppm) to the vein quartz. Au was not recorded in significant amounts in the hydrothermal quartz at Buckingham. The highest amount of As and Sb in the hydrothermal quartz was in the breccia cement quartz (mean of 28.41 ppm and 6.610 ppm, respectively). The vein quartz contained, for comparison, a mean of 2.197 ppm As and 0.1954 ppm Sb (Table 7.2).

Table 7.2: Trace element concentrations in different quartz types at White Pine Fork. All values are in ppm, except for Au, which is in ppb.

	Vein quartz (n_{max}=193)	Igneous (n_{max}=13)	Sedimentary (n_{max}=77)	Breccia cement (n_{max}=13)
Li7	10.48	9.0926	5.419	90.59
Na23	19.13	15.61	17.97	12.97
Mg24	2.101	0.9846	1.851	80.62
Al27	218.4	105.4	110.7	1067
P31	16.16	17.13	14.74	17.85
K39	37.63	11.22	25.37	134.7
Ca43	46.54	34.52	39.32	237.3
Ti47	24.52	51.81	41.38	8.589
Ti49	24.81	50.76	42.00	9.353
V51	0.2533	0.02112	0.02840	1.538
Cr53	0.2357	0.1037	0.1101	0.3379
Mn55	0.8203	0.3544	0.7972	5.767
Fe57	45.42	4.397	14.37	68.099
Cu63	3.743	0.3128	0.3705	1.332
Cu65	3.967	0.2666	0.4125	1.400
Zn66	0.3407	0.2138	0.2843	5.457
Ge74	1.829	1.531	0.9722	1.411
As75	2.197	2.741	0.6987	28.41
Rb85	0.1835	0.06183	0.1349	0.9150
Sr88	0.3425	0.09157	0.2374	0.6879
Zr90	0.03454	0.08375	0.02211	0.2821
Ag107	0.05397	0.03235	0.01747	0.05314
Sb121	0.1954	0.03184	0.1151	6.610
Cs133	0.05814	0.02867	0.03462	0.1591
Gd157	0.02162	0.005938	0.007606	0.01277
Hf178	0.003797	0.006097	0.003793	0.009742
Ta181	0.001571	0.001261	0.002028	0.004765
Au197	0.006364	0.004508	0.005183	0.003384
Pb208	0.1559	0.08924	0.1185	0.4598
Bi209	0.005130	0.002008	0.004814	0.006723
U238	0.008799	0.01489	0.003498	0.04030

7.3 Trace element geochemistry of pyrite at White Pine Fork Mo porphyry

The bulk of the pyrite from White Pine Fork Mo porphyry was predominantly found within the pyrite alteration halo (Fig. 7.6). The pyrite from the breccia pipe was euhedral and often found with chalcopyrite and molybdenite (Fig. 5.11). In some of the samples collected more distally from the deposit, the pyrite occurred as ‘disseminated’ crystals in the groundmass, and is interpreted to be altered from primary magnetite which was observed in least altered samples of the Little Cottonwood stock (Fig. 7.7). Chemical etching was performed on all of the pyrite samples to reveal any compositional zoning in reflected light microscopy, but none was observed. At White Pine Fork, three element maps were created from three pyrite samples (Fig. 7.6). Some compositional variation was seen in the element maps created by LA-ICP-MS. One sample was collected from the breccia pipe (WP13ES63; Fig. 7.8), one taken from one of the farthest samples (WP13ES03; Fig. 7.10), and one from a medial distance (WP13ES46; Fig. 7.9). The samples were homogenous in composition with the most noticeable variations seen in the breccia pyrite samples. In total, 290 spot analyses were collected from 23 samples containing hydrothermal pyrite.

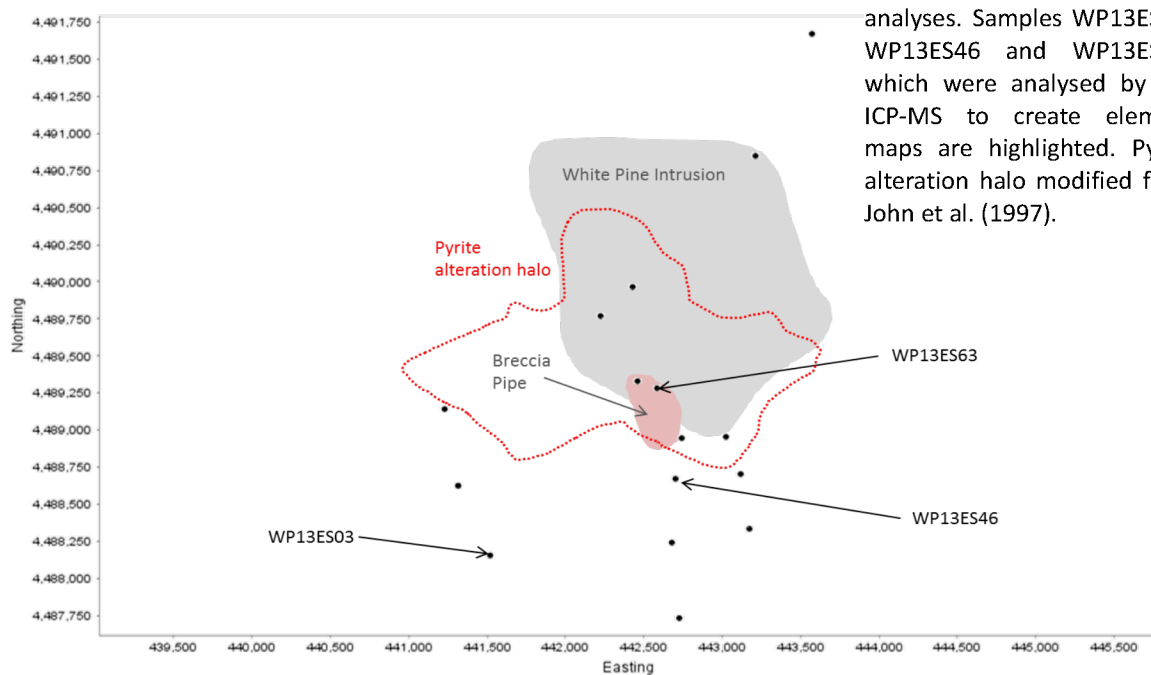


Figure 7.6: Sample locations for pyrite mineral chemistry analyses. Samples WP13ES63, WP13ES46 and WP13ES03, which were analysed by LA-ICP-MS to create element maps are highlighted. Pyrite alteration halo modified from John et al. (1997).

The pyrite did not contain significant amounts of precious metals with a mean of 0.0020 ppm of Au and 0.522 ppm of Ag. The pyrite also contained a mean value of 0.9630 ppm of Mo. Some of the metalloids, As (mean of 0.7390 ppm) and Sb (mean of 0.198 ppm), had homogenous values in pyrite. The metals Co (mean of 104.2 ppm), Ni (51.81 ppm), Cu (25.09 ppm), Zn (2.222 ppm), and Pb (2.300 ppm) showed compositional zonation in the element maps. Interruptions in the Co and Ni zonations, in the breccia pipe sample (WP13ES63), showed a brecciated grain edge with interrupted, repeating compositional zonation (Fig. 7.8). Another sample, taken 372 m from the breccia sample (WP13ES46) also shows compositional zonation with a Co-rich and a Pb-poor core (Fig. 7.9). Sample (WP13ES03), taken 1546 m from the breccia pipe, does show the same zonation with Pb-poor core; as well, the Co map shows a square outline which may indicate a relict grain shape (Fig. 7.10).

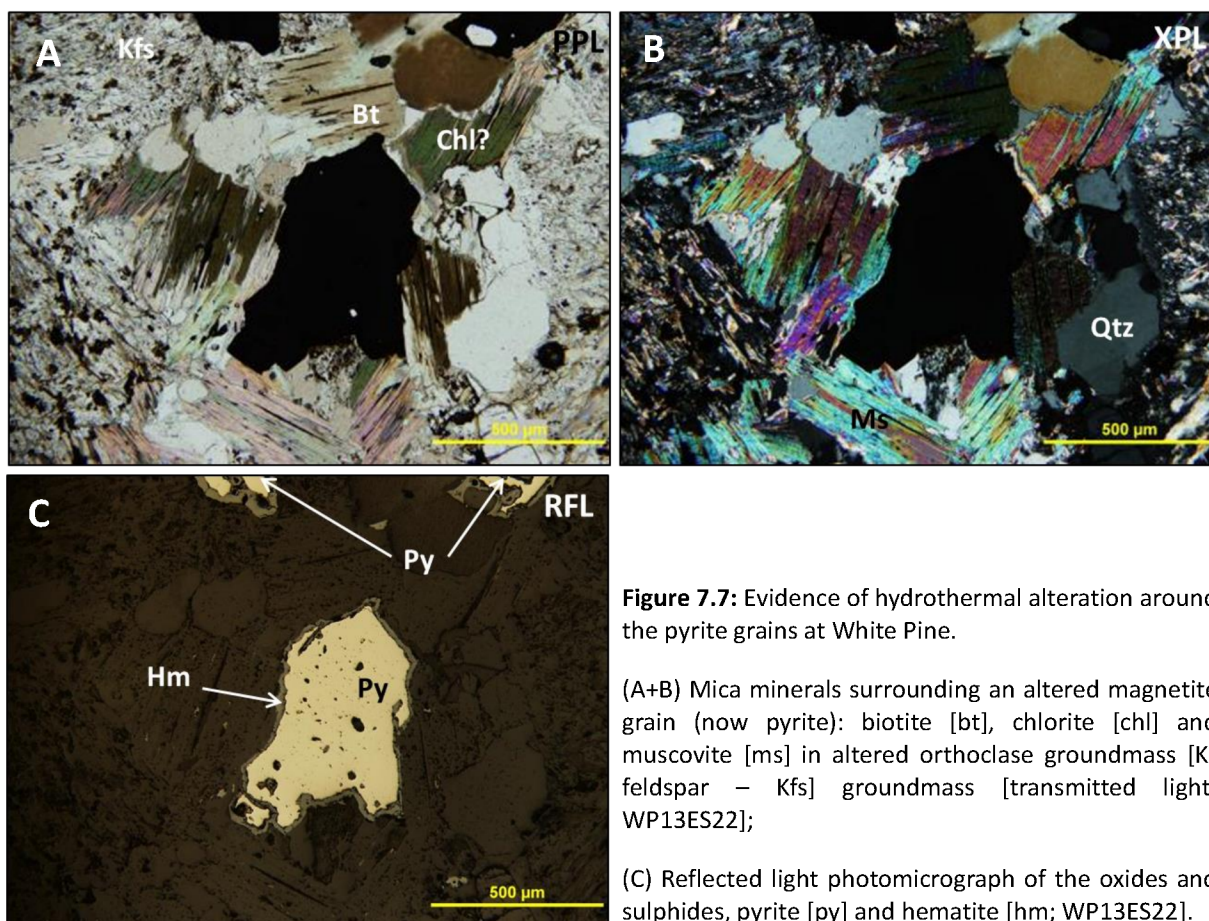


Figure 7.7: Evidence of hydrothermal alteration around the pyrite grains at White Pine.

(A+B) Mica minerals surrounding an altered magnetite grain (now pyrite): biotite [bt], chlorite [chl] and muscovite [ms] in altered orthoclase groundmass [K-feldspar – Kfs] groundmass [transmitted light; WP13ES22];

(C) Reflected light photomicrograph of the oxides and sulphides, pyrite [py] and hematite [hm; WP13ES22].

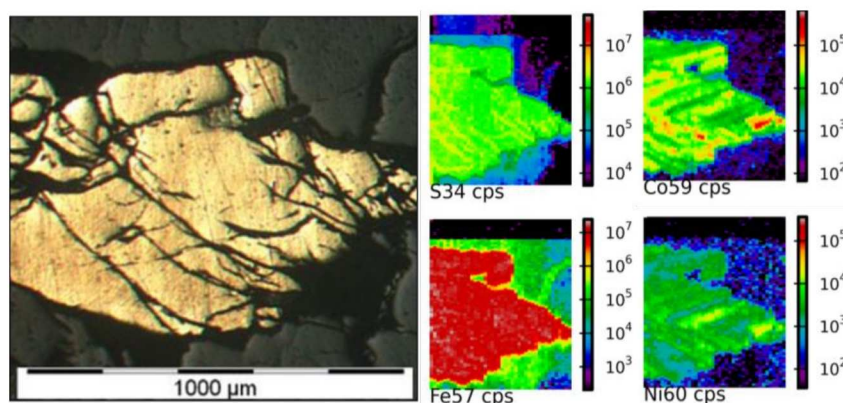


Figure 7.8: Element maps of S34, Co59, Fe57, and Ni60 collected by LA-ICP-MS of a pyrite grain (WP13ES63) collected from the breccia pipe. The Co and Ni maps show growth zones that are not continuous, indicating a fragmented pyrite grain.

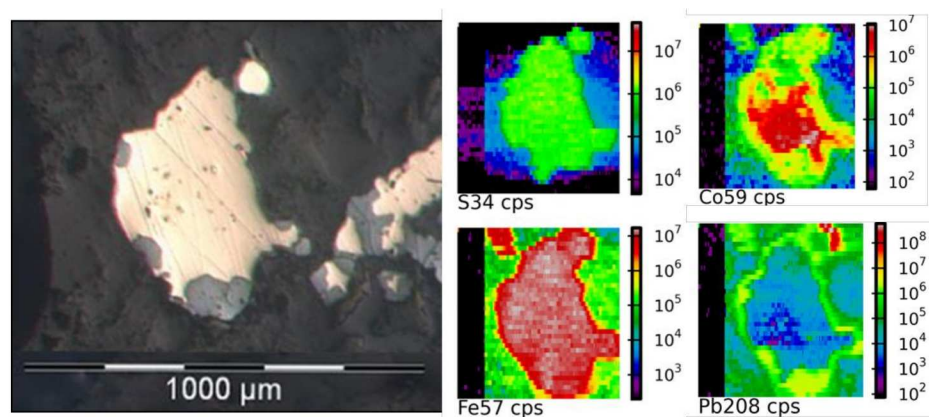


Figure 7.9 Element maps of S34, Co59, Fe57, and Pb208 collected by LA-ICP-MS of a pyrite grain (WP13ES46) collected 372 m from the breccia pipe. The element map shows the Co-rich and Pb-poor core of the grain grading into a more uniform composition. This grain also has iron oxide minerals along its perimeter (grey in reflected light).

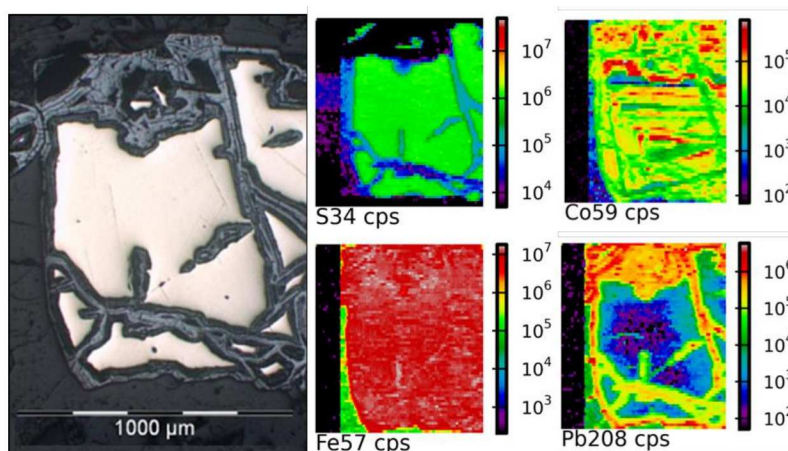


Figure 7.10: Element maps of S34, Co59, Fe57, and Pb208 collected by LA-ICP-MS of a distal pyrite grain (WP13ES03) collected 1546 m from the breccia pipe. The element map shows the Pb-poor core of the pyrite grain. This grain also has iron oxide minerals along its perimeter (grey in reflected light).

7.4 Trace element geochemistry of pyrite at Buckingham Mo(-Cu) porphyry

The pyrite at the Buckingham study site was difficult to analyse (Fig. 7.11). The majority of the Fe sulphides were partially or completely altered to Fe-oxides and hydroxides due to the extensive supergene alteration in the study area. The relict pyrite grains showed well-developed weathering rinds composed of Fe-oxides and Fe-hydroxides (Figs. 7.12, 7.13 and 7.14). Sulphides were analysed from three samples of pyrite and two samples of arsenian pyrite. Spot analyses of the sulphides do not include samples of the weathering rind. In total, 31 spots were collected from arsenian pyrite and 30 spots were collected from pyrite. As well, three maps were created of the three pyrite samples in order to investigate any compositional variations. Upon creating the maps, it was observed that all of the pyrite samples showed a weathering rind enriched in Au, Cu, and Mo.

The arsenian pyrite contained a mean of 27.57 ppm of Au and 50.56 ppm of Ag. The arsenian pyrite samples also contained 0.5688 ppm of Mo. The three samples of pyrite had a mean of 0.0023 ppm of Au, 0.1776 ppm of Ag and 0.1197 ppm of Mo. The arsenian pyrite contained much more As (mean of 121 778 [\sim 12.2 wt %] ppm vs 69.69 ppm [$<$ 0.01wt %] in the pyrite) and Sb (mean of 1360 ppm vs. 0.0738ppm in pyrite). The heavy metals means in the arsenian pyrite were Co (mean of 107.7 ppm), Ni (54.77 ppm), Cu (852.0 ppm), Zn (784.1 ppm), and Pb (1176 ppm). In the pyrite, the mean values of the heavy metal contents were lower for Cu (0.9671 ppm), Zn (0.2428 ppm), and Pb (4.490 ppm) and higher for Co (mean of 244.8 ppm) and Ni (177.4 ppm). The Co and Ni element maps from the pyrite samples show distinct compositional variations (Figs. 7.12, 7.13, and 7.14).

7.5 Au-rich rims around pyrite grains at Buckingham

The pyrite sampling included rocks from within the Buckingham porphyry, as well as the Harmony Formation and the younger Tertiary granites. The majority of the Fe sulphides were partially altered to Fe-oxides and hydroxides. Relict pyrite grains showed well-developed weathering rinds composed of Fe-oxides and Fe-hydroxides. The maps created using LA-ICP-MS (Figs. 7.12, 7.13, and 7.14) showed that the pyrite was depleted in trace elements relative to the weathering rind which was enriched in Au, Ag, Cu, As, Sb and Mo but not Fe and S.

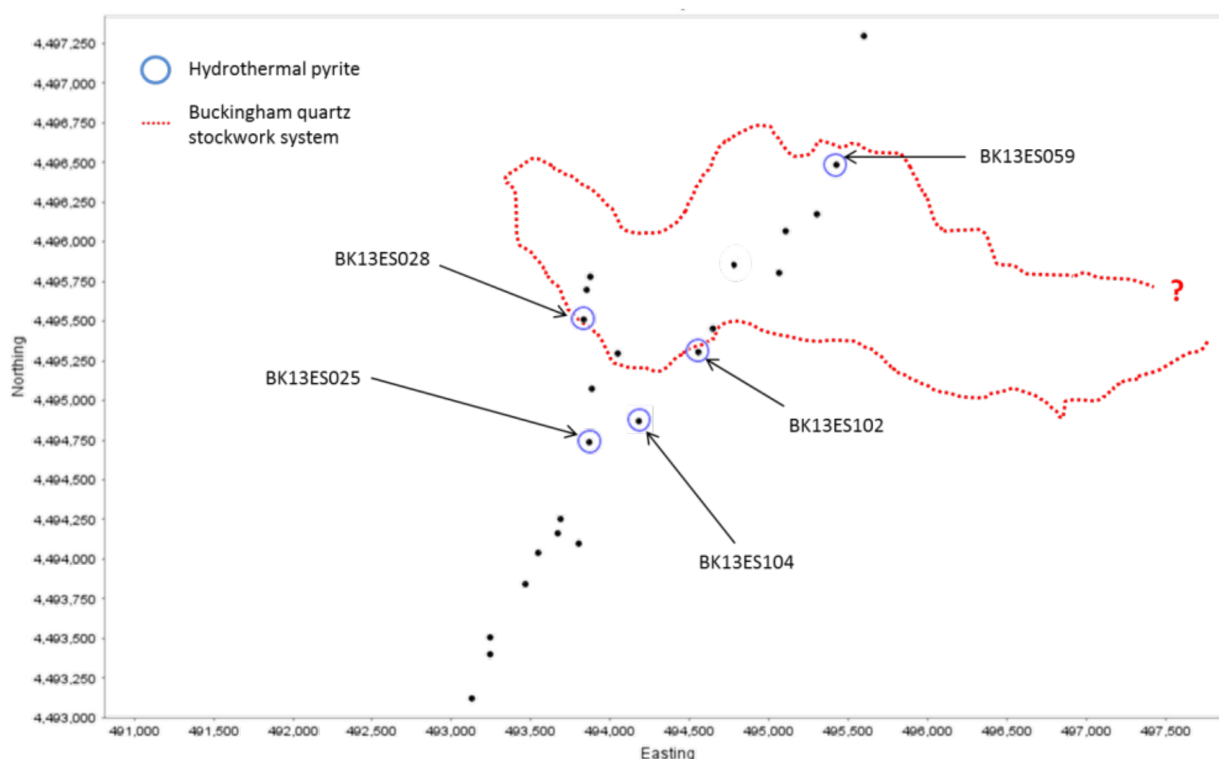


Figure 7.11: Location map for samples collected for pyrite mineral chemistry analyses. Samples BK13ES025 and BK13ES104 were arsenian pyrite. Samples BK13ES028, BK13ES059 and BK13ES102 were pyrite. Buckingham quartz stockwork outline modified from Theodore et al. (1992).

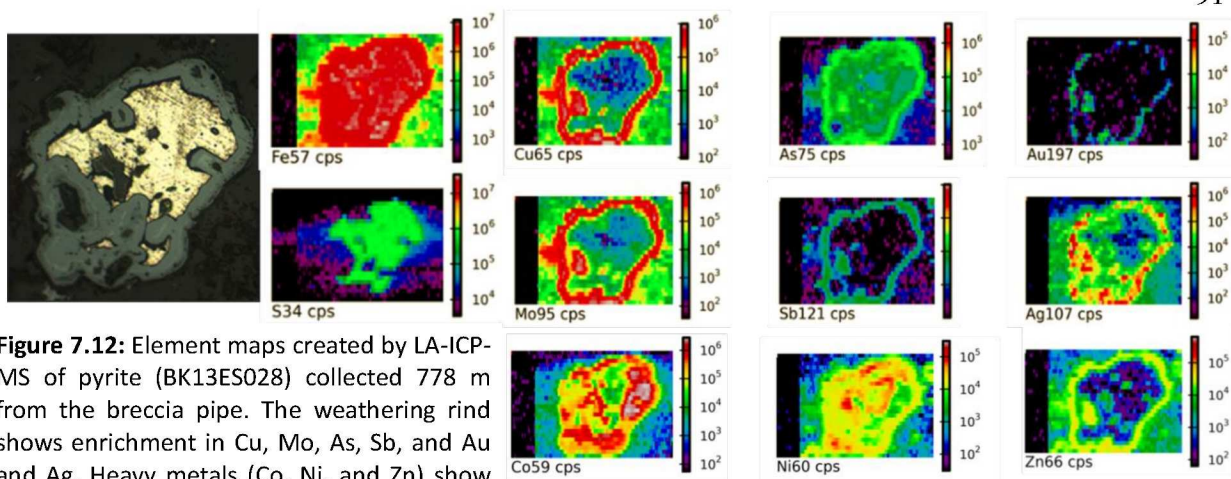


Figure 7.12: Element maps created by LA-ICP-MS of pyrite (BK13ES028) collected 778 m from the breccia pipe. The weathering rind shows enrichment in Cu, Mo, As, Sb, and Au and Ag. Heavy metals (Co, Ni, and Zn) show compositional zonation within the grain.

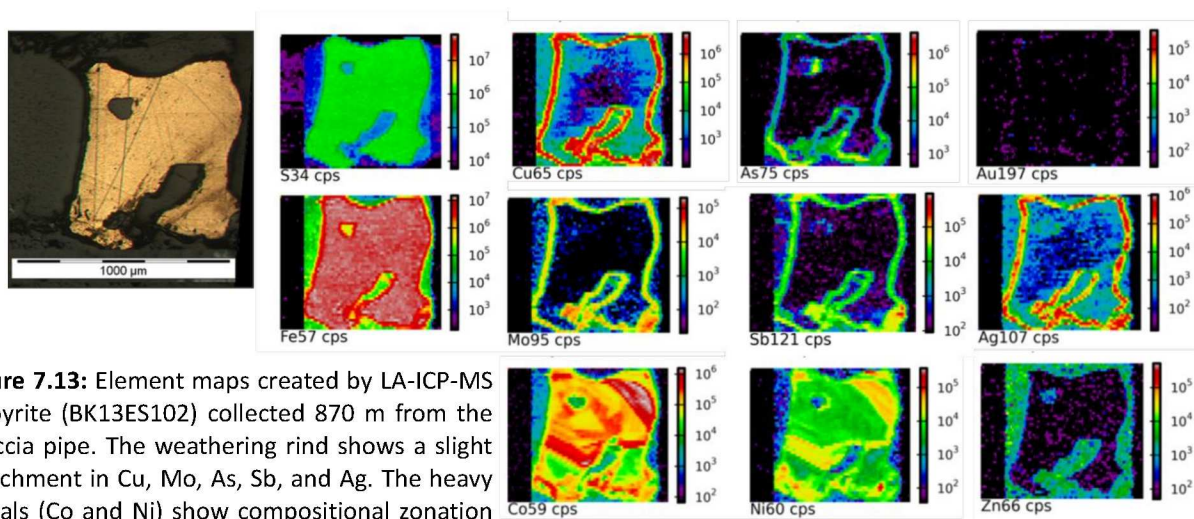


Figure 7.13: Element maps created by LA-ICP-MS of pyrite (BK13ES102) collected 870 m from the breccia pipe. The weathering rind shows a slight enrichment in Cu, Mo, As, Sb, and Ag. The heavy metals (Co and Ni) show compositional zonation within the grain.

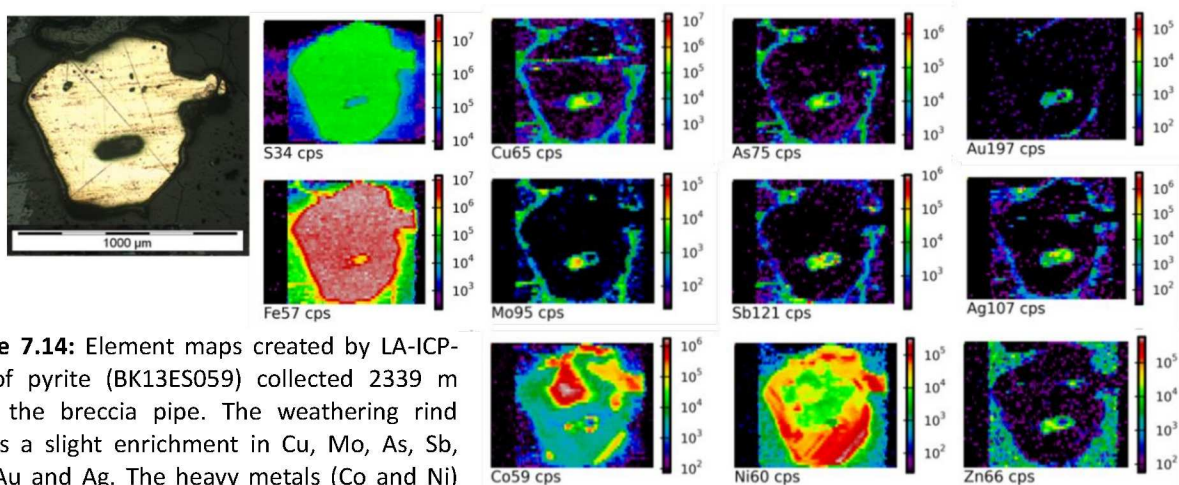


Figure 7.14: Element maps created by LA-ICP-MS of pyrite (BK13ES059) collected 2339 m from the breccia pipe. The weathering rind shows a slight enrichment in Cu, Mo, As, Sb, and Au and Ag. The heavy metals (Co and Ni) show compositional zonation within the grain.

Chapter 8: Discussion

8.1 Petrography of the White Pine Fork Mo porphyry

The two granites in the White Pine Fork Mo study area were both categorized as monzogranites and syenogranites using the QAPF diagram (Fig. 4.3). The younger White Pine intrusion is characterised by a higher SiO_2 consistent with the higher the modal percent of quartz and the formation of quartz phenocrysts compared to the Little Cottonwood stock. The rocks in or adjacent to the White Pine intrusion show a slightly higher degree of alteration, likely due to its proximity to the breccia pipe. The zone of intensely altered feldspars characterised by >80% replacement of the feldspar by sericite or other white micas, surrounds the breccia pipe and trends away from the White Pine Fork breccia (Fig.8.1).

The SWIR data from White Pine Fork were used to define muscovite and phengite domains as these were the two most common minerals found. In hydrothermal systems, phengite forms at 300°C during phyllic alteration and is often associated with coarse-grained, primary-growth quartz veins (Bongiolo et al., 2008). Meunier and Velde (1982) noted that the formation of phengite and muscovite in hydrothermally altered granites typically progresses from a Mg-rich fluid (formation of phengite) to the crystallisation of muscovite. The rough zonation of a muscovite>phengite core and the occurrence of phengite>muscovite primarily in the distal Little Cottonwood unit suggests a cooler, more Mg-rich fluid in the periphery of the system (Fig. 8.2). Petrographic characterisation of the distal muscovite suggests that it is igneous rather than hydrothermal suggesting that the alteration halo is limited to approximately 1500 m.

John (1997) described the alteration associated with the White Pine Fork Mo porphyry as consisting of stockwork veins and vein selvages, fracture-controlled and disseminated pyrite with localised potassic and sericitic alteration. John (1997) also describes a pervasive green sericite +

pyrite ± fluorite ± molybdenite alteration. The results of this study are broadly consistent with those observations except that molybdenite and calcite were not observed outside of the breccia pipe and sample WP13ES65, the other minerals, including fluorite were observed throughout the study area. However, the detailed work undertaken in this study makes it possible to better define the extent of the alteration halos. In addition to the intensity of the sericitization of the feldspars, the pyrite alteration halo was also mapped. The pyrite halo formed as the result of the alteration of primary magnetite and hydrothermal magnetite being altered to pyrite as well as the formation of the quartz-pyrite-sericite veins from the White Pine hydrothermal system. At White Pine Fork, the pyrite halo occurs within the muscovite zone (Fig. 8.2).

The mineralogy of the lamprophyres is consistent with minettes – a lamprophyric rock characterised by a dominant biotite and K-feldspar mineralogy. Tingey et al. (1991) discussed the wide-spread Tertiary lamprophyric magmatism related to the tectonics of Basin and Range province in the Wasatch Plateau in north-eastern Utah. They reported similar lithologies and occurrences as noted in this study with the rocks sharing similar mineral and geochemical characteristics.

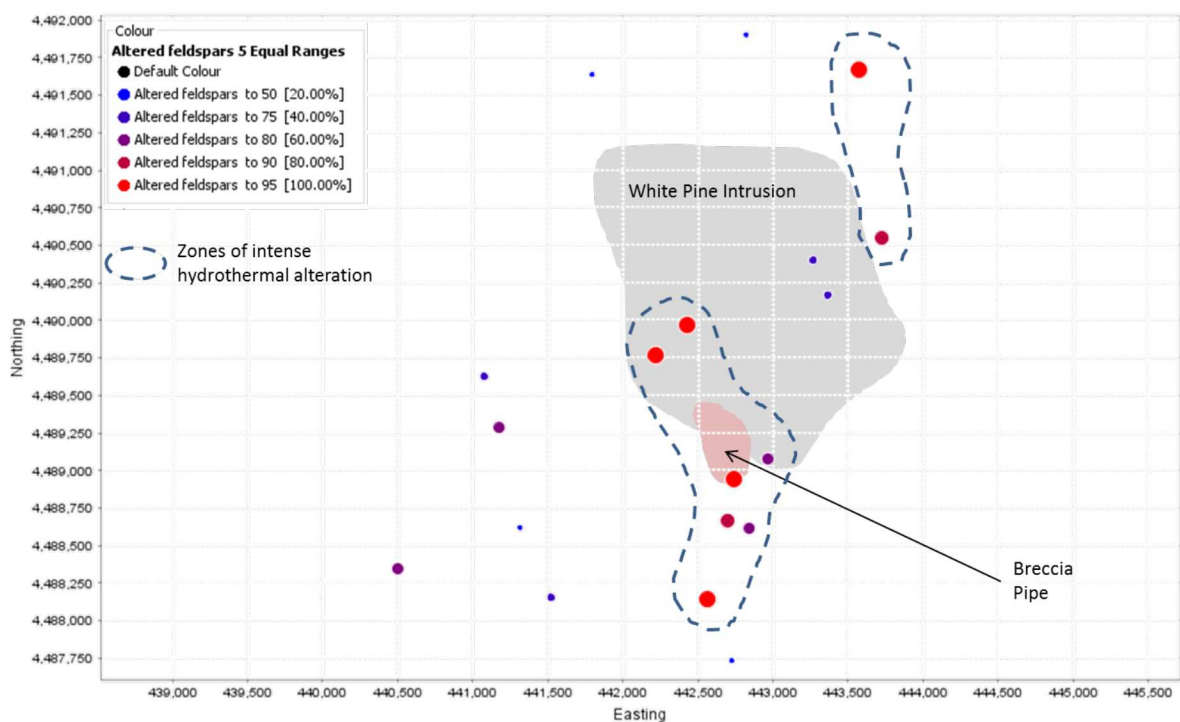


Figure 8.1: Centres of greater hydrothermal alteration as represented as >80% replacement of the feldspars by white micas at White Pine Fork

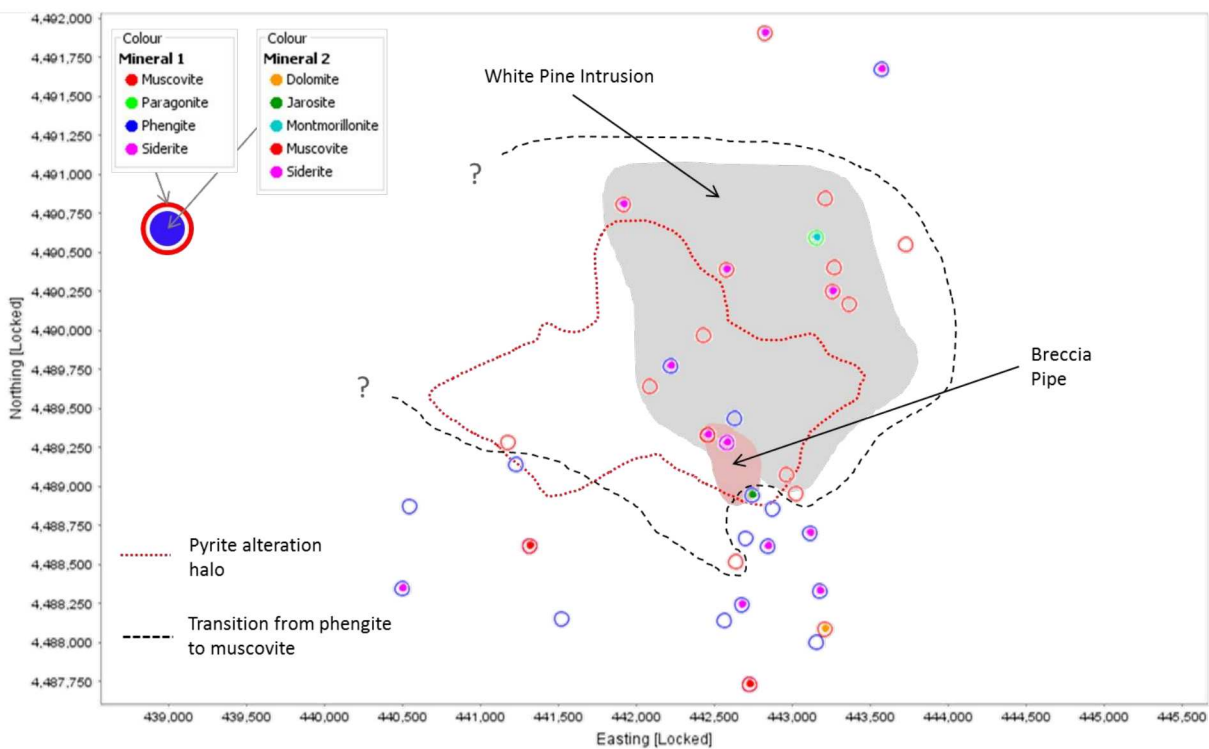


Figure 8.2: Mineral isograd with a muscovite centre and phengite periphery surrounding the White Pine intrusion. The pyrite halo is contained in the muscovite 'shell'.

8.2 Petrography of the Buckingham Mo (-Cu) porphyry

Both the Cretaceous and Eocene granites are coarse-grained quartz and K-feldspar porphyritic granites with a quartz–orthoclase–plagioclase groundmass that has undergone variable degrees of hydrothermal alteration. In the Cretaceous granites, any primary ferromagnesian minerals have been completely replaced, whereas in the Eocene granites, hornblende, biotite, and titanite were observed. Theodore et al. (1992) noted that clinopyroxene is observed in some portions of the Eocene intrusions.

Both suites of granites from this study are characterised by feldspars that are partially to completely replaced by white micas \pm clay minerals \pm sericite by possible, separate hydrothermal events occurring in different loci within the mapping area. The quartzites contained sericite-altered feldspar clasts as well as an altered micaceous, interstitial groundmass. Both the granites and quartzites contained relict minerals interpreted to have originally been hydrothermal pyrite that have undergone supergene weathering to form hematite, goethite and jarosite. In addition five samples collected contained pyrite. This is consistent with the observations of Theodore et al. (1992) who identified a phyllic alteration zone around Buckingham comprised of pyrite \pm white mica \pm quartz as veins and disseminated throughout the granites and quartzites. In addition Theodore et al. (1992) reported that localized portions of the Cretaceous monzogranites which had been hydrothermally altered were characterised by plagioclase feldspars altered to white micas and clay minerals and the rock occasionally becoming silicified. Similar silicification was observed in the hydrothermal breccias and well-veined rocks where quartz flooding resulted in very fine-grained, annealed grains in samples BK13ES104 and BK13ES016.

SWIR data collected in this study are consistent with an advanced argillic alteration mineral assemblage. Intense kaolinitization \pm clay minerals and chlorite accompanying white

mica \pm quartz \pm pyrite alteration of sedimentary rock and porphyry deposits is characteristic of hypogene intermediate argillic alteration (Chabert, 1997). Kaolinite was present in the SWIR data in samples in two locations, adjacent to the centre of deposit near an occurrence of a leached cap (BK13ES025) and near the Copper Queen deposit (Fig. 8.3). As well, chlorite, which was not identified in thin sections, was identified by the SWIR in samples proximal to the kaolinite occurrences. The presence of these two minerals strongly suggests the presence of advanced argillic alteration characteristic of intense hydrothermal activity. Kaolinite in quartz-rich rocks suggests a formation temperature of $\sim 200^{\circ}\text{C}$ which is at the lower end of temperatures estimated for phyllic alteration seen from fluid inclusion measurements from other porphyry copper deposits (Perry et al., 2002 and references therein).

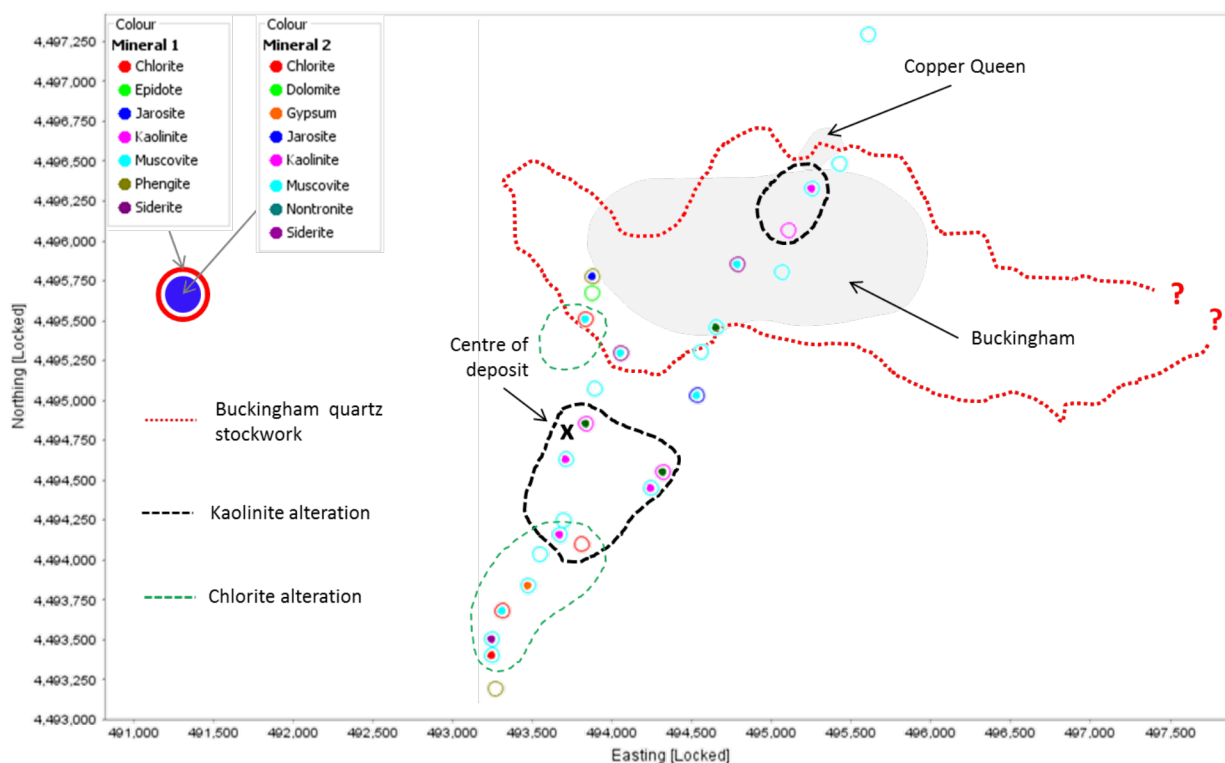


Figure 8.3: Proposed centres of advanced argillic hydrothermal alteration by the occurrence of kaolinite and chlorite. Buckingham deposit and associated quartz stockwork veining modified from Theodore et al. (1992).

8.3 Geochemistry

Molybdenum porphyry deposits are typically associated with granites and bimodal volcanism related to regional rifting and extensional tectonic activity in continental crust (Kirkham and Sinclair, 1996). Keith et al. (1995) suggested that the transition from compressional to extensional tectonics in a suprasubduction zone environment, in addition to emplacement in a thick continental crust, allows late-stage melts time to fractionate and become contaminated by subcontinental lithospheric mantle to the degree needed to concentrate Mo in the melt. The melt generated above the subducting slab would initially retain a MORB geochemical signature. However, dehydration of the downgoing slab will generate fluids that are enriched in large ion lithophile elements (K, Rb, Cs, Th, and LREEs) relative to the primitive mantle source melt.

8.3.1 White Pine Fork Mo porphyry area

The granites from the White Pink Fork area are geochemically similar. Both the Little Cottonwood stock and the White Pine intrusion, are characterised by LREE enrichment, depleted high field strength elements (HFSEs) and fractionated HREEs. This geochemistry is consistent with magmas derived from a subarc mantle melt (Kay and Mpodozis, 2002; Hollings et al., 2011a, b). The lamprophyres show similar geochemistry to the granites suggesting that they may have been derived from a broadly similar source region. Tingey et al. (1991) discussed the origin of lamprophyres cross-cutting the Little Cottonwood stock and suggested that they were generated by the fractionation of an ultrapotassic, ultramafic melt sourced from the asthenosphere. Prelević et al. (2004) argued that the isotopic signatures of minettes could be the result of mixing of ultramafic melts with a dacitic magma. Lamprophyric melts are associated with intra-continental tectonic settings, post-dating convergent tectonics and active margin

processes (Mitchell and Bergman, 1991). In active tectonic margins, lamproites may be associated with calc-alkaline lamprophyres and calc-alkaline silicic magmatism, so that the mixing of melts with a dacitic melt is possible in this tectonic environment (Prelević et al., 2004). At White Pine Fork, the geochemical signature of the granites is consistent with a tectonic environment of a convergent plate margin which could generate these late-stage, calc-alkaline lamprophyric melts.

Vogel et al. (1997; 2001) compiled the geochemistry of the intrusions of the Wasatch range. The Little Cottonwood and White Pine whole rock geochemistry from this study can be compared to geochemistry collected for regional data sets. When plotted on a TAS diagram, there is an evolution in the melt composition from a less silicic melt (Clayton Peak and Flagstaff/Mayflower intrusions) to an intermediate composition (Alta stock) to a granitic, more Si-rich rock with time (Little Cottonwood stock; Fig. 8.4). The estimated paleodepths by John (1989) and the ages calculated in this study and by the P1060 project further support an evolving melt in the Wasatch range (Figs. 8.5 and 8.6). The new ages of the project infer that the Mayflower, Flagstaff and Clayton Peak stocks are the oldest intrusions in the Wasatch range (emplacement ages of 41 – 34.5 My; John, 1989). The oldest intrusions would be the first to crystallize and would be the least fractionated, or evolved. These intrusions also crystallized at the shallowest depths (0.5 – 4 km). The Alta stock has an intermediate composition (diorite to granodiorite) between the predominantly monzonite and monzodiorite compositions of the Flagstaff, Mayflower, and Clayton Peak stocks and the granite composition of the Little Cottonwood stock. The Alta stock was emplaced ~35-33 Ma at depths of 5.5-6.5 km (John, 1989). The Little Cottonwood stock has an estimated emplacement depth of 6 – 12 km and is the youngest of the intrusions in the Wasatch range (Fig. 8.5). The progression of the Wasatch range

intrusions from intermediate to felsic compositions with age and emplacement depths indicates a progression of melts undergoing increased fractionation and assimilating more crustal material. Data from John (1999) show the evolution of the melts by the degree of crustal contamination. Rubidium is more compatible than Sr in melts and, therefore, during the formation of continental crust by fractionated melting of the upper mantle, Rb becomes enriched in the crust relative to Sr. Consequently, $^{87}\text{Rb}/^{86}\text{Sr}$ ratios can be used to investigate the amount of crustal contamination or melt fractionation from an upper mantle $^{87}\text{Rb}/^{86}\text{Sr}$ value of ~ 0.7000 (Faure, 1986). The $^{87}\text{Rb}/^{86}\text{Sr}$ values for the intrusive suites from the Wasatch range results in a trend of increased $^{87}\text{Rb}/^{86}\text{Sr}$ ratios in the more evolved granites (Little Cottonwood, ranges from 0.70765 to 0.70845) which steadily decreases with the less evolved suites of the Clayton Peak and Pine Creek stock (0.70665 to 0.70708). The Mayflower stock has an anomalously high value (0.70812; Fig. 8.6).

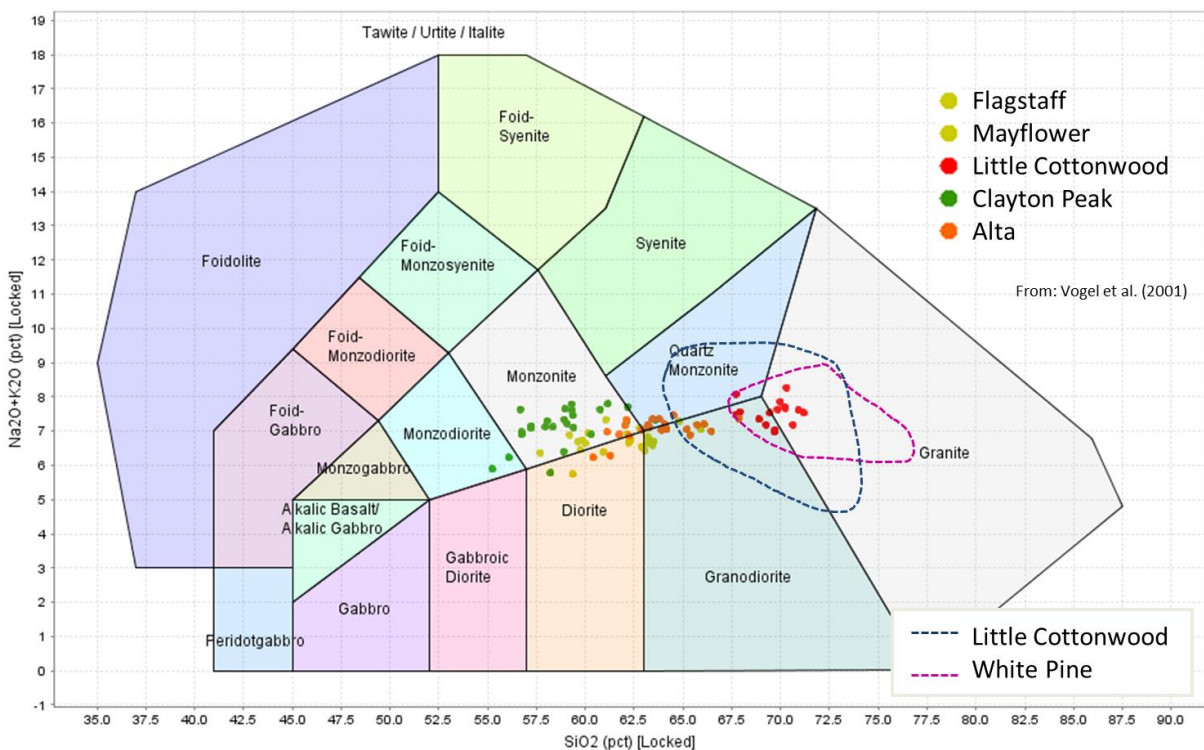


Figure 8.4: TAS diagram of the Vogel et al. (2001) whole rock geochemistry from the intrusive suite in the Wasatch Range. Data range from the Little Cottonwood and White Pine intrusions in this study is outlined. Diagram from Middlemost (1994)



Figure 8.5: Compilation of the intrusive suites in the Wasatch Range and the new ages produced by the P1060 project (modified from John, 1989).

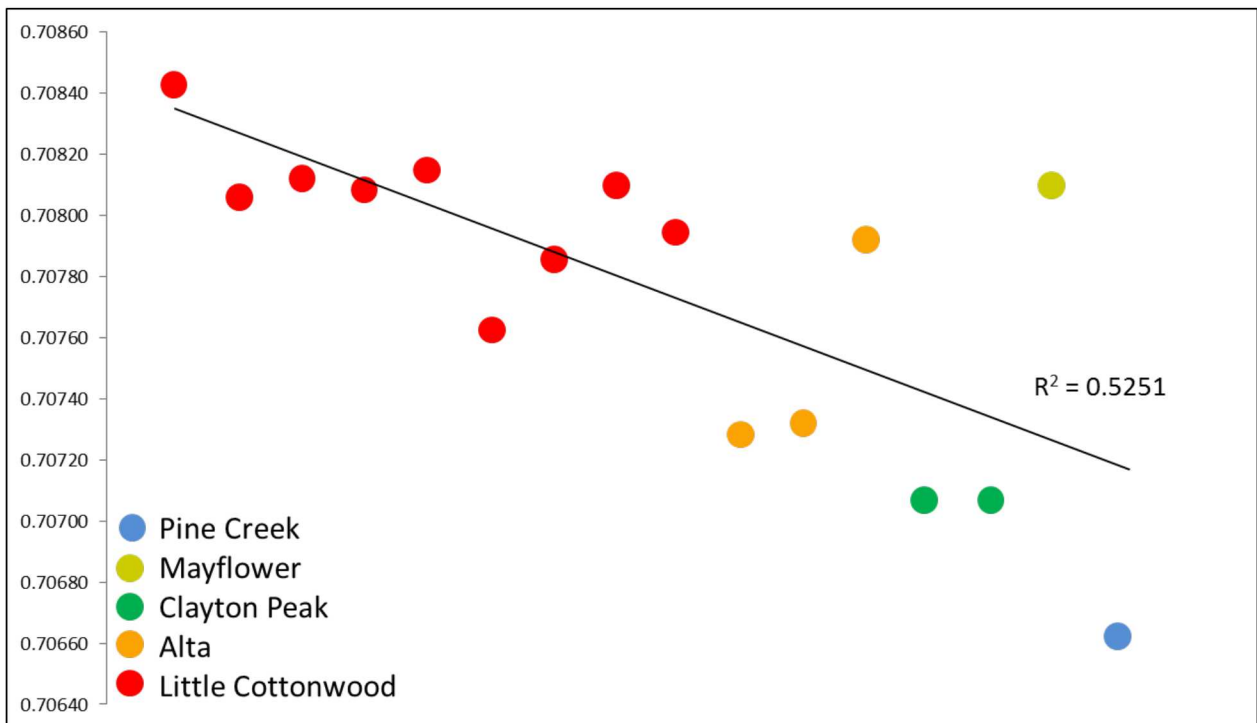


Figure 8.6: Scatterplot showing the $^{87}\text{Rb}/^{86}\text{Sr}$ ratios in the whole rock geochemistry decreasing with the less evolved suites (decreasing depth of emplacement and SiO_2 contents; data from John, 1999)

8.3.2 *Magma fertility at White Pine Fork*

The whole rock trace element geochemistry of the granites at White Pine Fork shows similarities to adakitic rocks often associated with volcanic arc rocks, notably those which host porphyry deposits and have been suggested to be linked to the mineralisation process (Defant and Drummond, 1990; Defant and Kepezhinskis, 2001; Chiaradia et al., 2009, 2012; Schütte et al., 2010). Adakitic (fertile) magmas are thought to form melts of subducted oceanic slabs that interact with mantle-wedge peridotite rocks during ascent (Defant and Drummond, 1990). The geochemical signature of adakites is a low Y (<18 ppm), Yb (<1.9 ppm) and other HREE with a high Sr content (>400 ppm; Defant and Drummond, 1990). A result of high pressure melting of garnet-bearing mantle rocks under hydrous conditions where the plagioclase (containing Sr) is assimilated into the magma and garnet and amphiboles (which contain the Y, Yb and HREEs) remains in the residue. At White Pine Fork, the Little Cottonwood and the White Pine intrusions (after being screened for LOI values greater than 1% to minimize the effect of alteration) fall within the fertile adakite fields on Sr/Y vs. SiO₂ and Sr/Y vs. Y plots (Figs. Xx and xx, respectively). In Figure xx, the data fall mostly within and near the Si-rich portion of the ore-forming rock field, as defined by Rohrlach and Loucks (2005) using modern day Pacific arc rock suites. The fields were defined using the modern day rocks in mineralised and barren deposits.

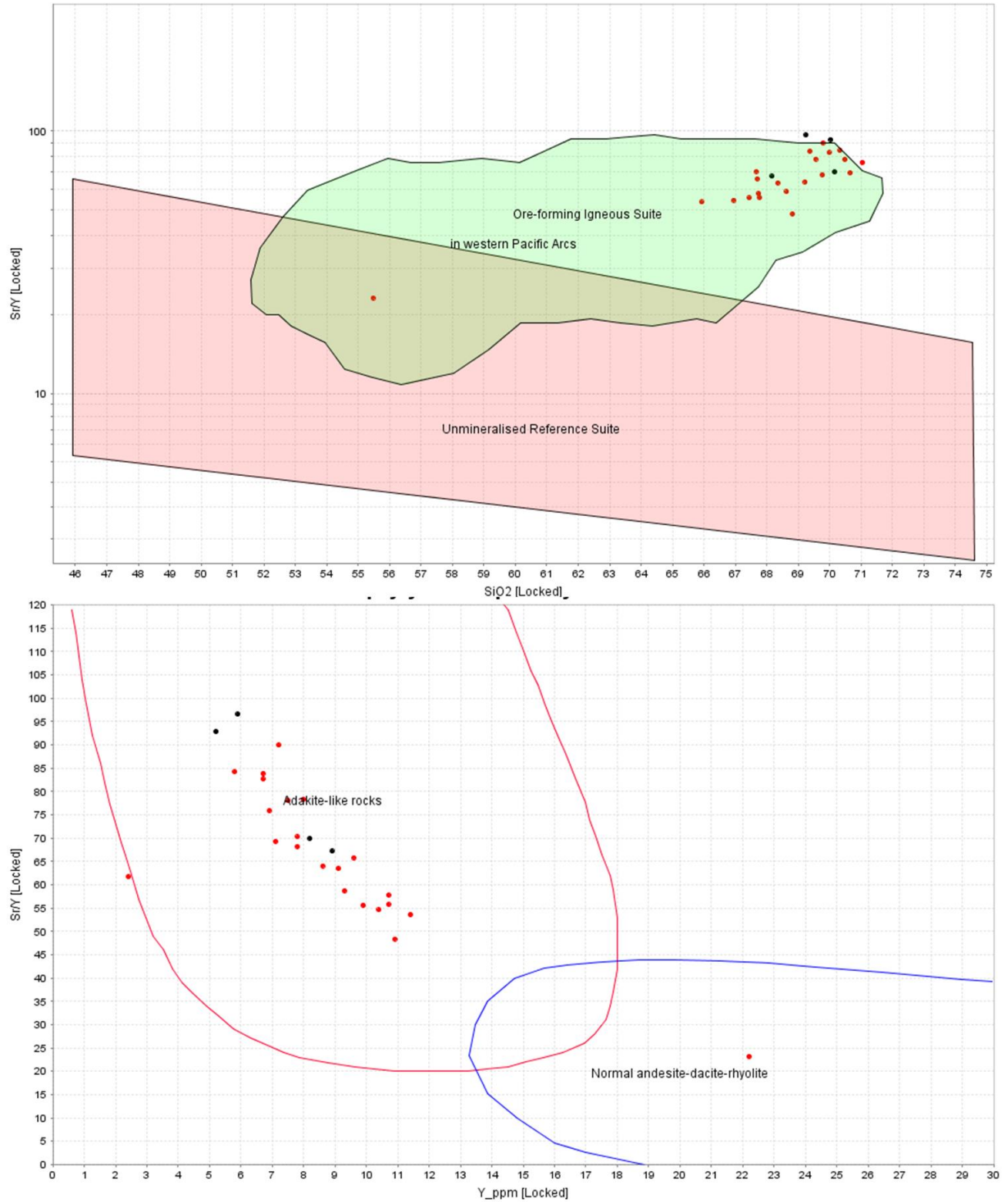


Figure 8.7: (Top) Sr/Y vs. SiO₂ and (bottom) Sr/Y vs. Y diagrams for the White Pine Fork study area. The Little Cottonwood granite (red) and the White Pine intrusion (black) plot within the fertile adakite fields.

8.3.3 Whole rock geochemistry mapped hydrothermal alteration

At White Pine Fork, the whole rock geochemistry of the granites can be used to further define the alteration around the mineralised centre. When the absolute whole rock trace element contents are plotted on a normal log distribution plot, normal, or background, concentrations of the elements will fall in a straight line, whereas any deviations from this line indicate a statistically anomalous value. On the plots in Figure Xx, anomalously high values plot above the linear trend whereas depleted values of the element will plot below the trend. The upper and lower limits of the linear trend are interpreted as the upper and lower limits of the background concentrations.

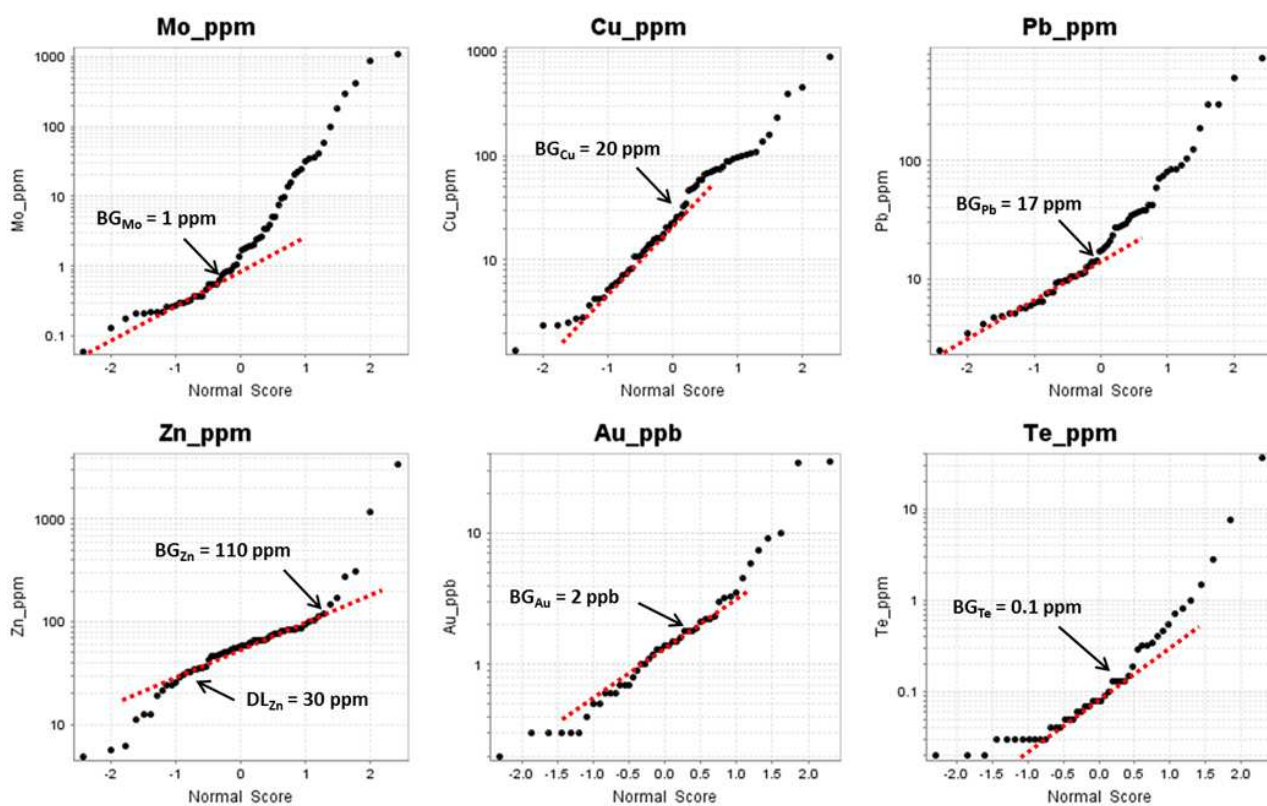


Figure 8.8: Normal log plots of Mo, Cu, Pb, Zn, Au and Te whole rock contents in the Little Cottonwood and White Pine granites. BG – upper background values; DL – upper depleted values

Once the background values of six key elements for the White Pine Fork granites were calculated, the data were plotted on a simplified geologic map and ranked as being depleted, background, anomalous or strongly anomalous (the upper quartile of the data set). Contours were added to the maps, highlighting areas of anomalously high or low concentrations of the six elements (Fig. xx). Molybdenum, Cu and Au were selected to highlight the areas of mineralisation and suggests potassic alteration which is intimately associated with mineralisation. High Zn and Pb values indicate phyllic and propylitic alteration whereas their depletion indicates potassic alteration (Halley et al., 2015). Tellurium was also selected as an element that identifies phyllic alteration since it concentrates in sheet silicates (Micko, 2010). The White Pine intrusion has strongly anomalous Mo, Cu, and Au concentrations above background levels extending into the surrounding Little Cottonwood stock (Fig. xx). The phyllic alteration zone (defined by Pb, Zn and Te) encompasses both the pyrite alteration halo (as defined by John et al., 1997) and the two corridors of intense phyllic alteration defined by the almost complete replacement of feldspar by white mica. The whole rock geochemistry successfully identified areas of mineralisation and associated potassic alteration and overprinting phyllic alteration identified through mapping and petrography .

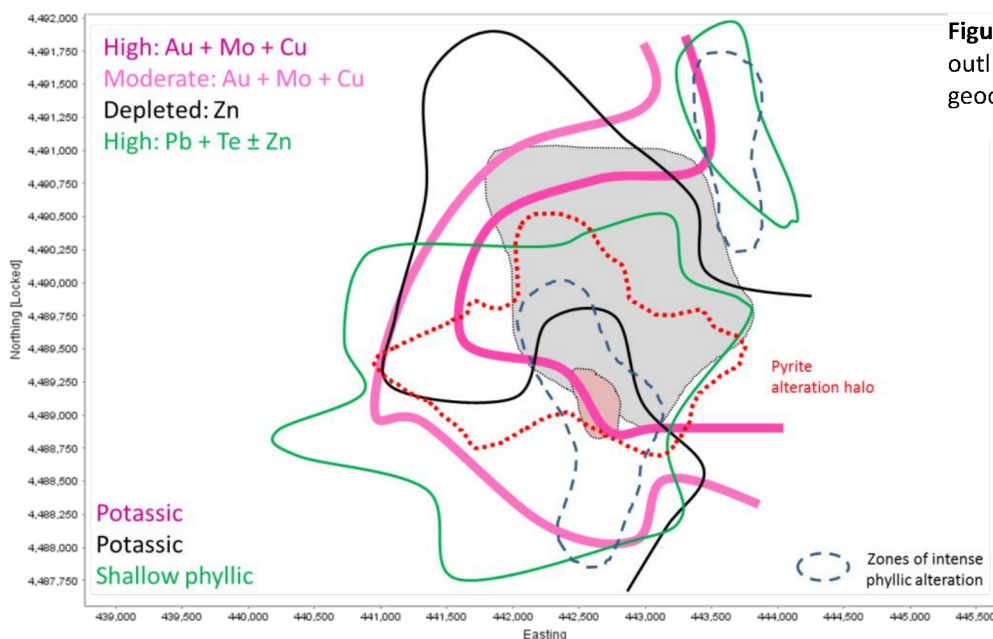


Figure 8.9: Alteration zones outlined by whole rock geochemistry and petrography

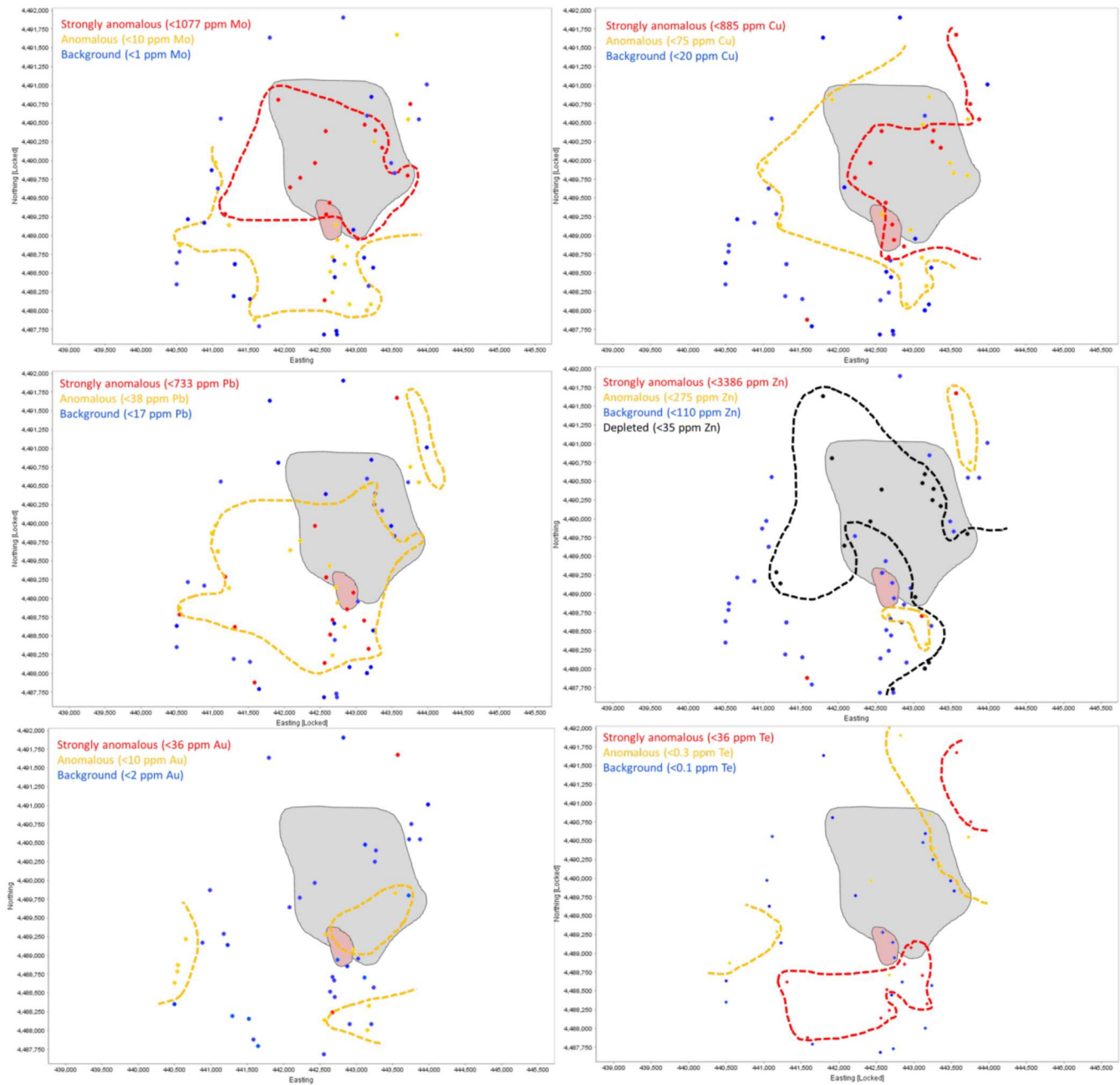


Figure 8.10: Contours outlining anomalous whole rock geochemical values for Mo, Cu, Pb, Zn, Au, and Te. White Pine intrusion and the breccia pipe are outlined on the map.

8.3.4 Buckingham Mo (-Cu) porphyry area

The two suites of granites from the Buckingham area are characterised by similar geochemical signatures with LREE enrichment, fractionated HREE and negative Nb, Ta and Ti anomalies characteristic of a subarc mantle melt source (Kay and Mpodozis, 2002; Hollings et al., 2011a, b). The whole rock average concentrations of 83.5 ppm of Mo in the Cretaceous granites are much higher than background crustal levels (Newsom and Palme, 1984; Newsom et al., 1986). The trace element geochemistry supports the subduction zone model for the formation of a porphyry deposit.

8.3.5 Whole rock geochemistry mapped hydrothermal alteration

At Buckingham, the whole rock geochemistry was also used to interpret different types of hydrothermal alteration in the homogenous quartzites. Using the same methodology as at White Pine Fork, maps for Mo, Cu, Au, Ag, Pb, Li, As, and Sb around the Buckingham intrusions were created (Figs. Xx and xx). Once the contours for anomalous values were plotted, the maps were consolidated into a single map (Fig xx). Above background levels of Mo, Cu, Au and Ag identified areas of increased mineralisation and potassic alteration (Halley et al., 2015). Adjacent to this inferred potassic alteration, there was a corridor of depleted Pb and As which is indicative of an extension of this potassic alteration. South of this alteration zone, increased Li and Sb suggest an over-printing phyllic alteration (Fig. Xx). There is a second corridor of increased Au and Ag contents to the south of the Buckingham intrusions but the absence of elevated Mo and Cu, suggests that this mineralisation is not related to the deeper porphyry mineralisation, but rather to mineralisation and alteration similar to that found in a lithocap (Cooke et al., 2014; Halley et al., 2015). The advanced argillic alteration interpreted from SWIR overlaps with this

field and is consistent with the existence of a lithocap. The sample selected to be the centre of deposit falls within the zone of the overprinting phyllic alteration (Fig. XX).

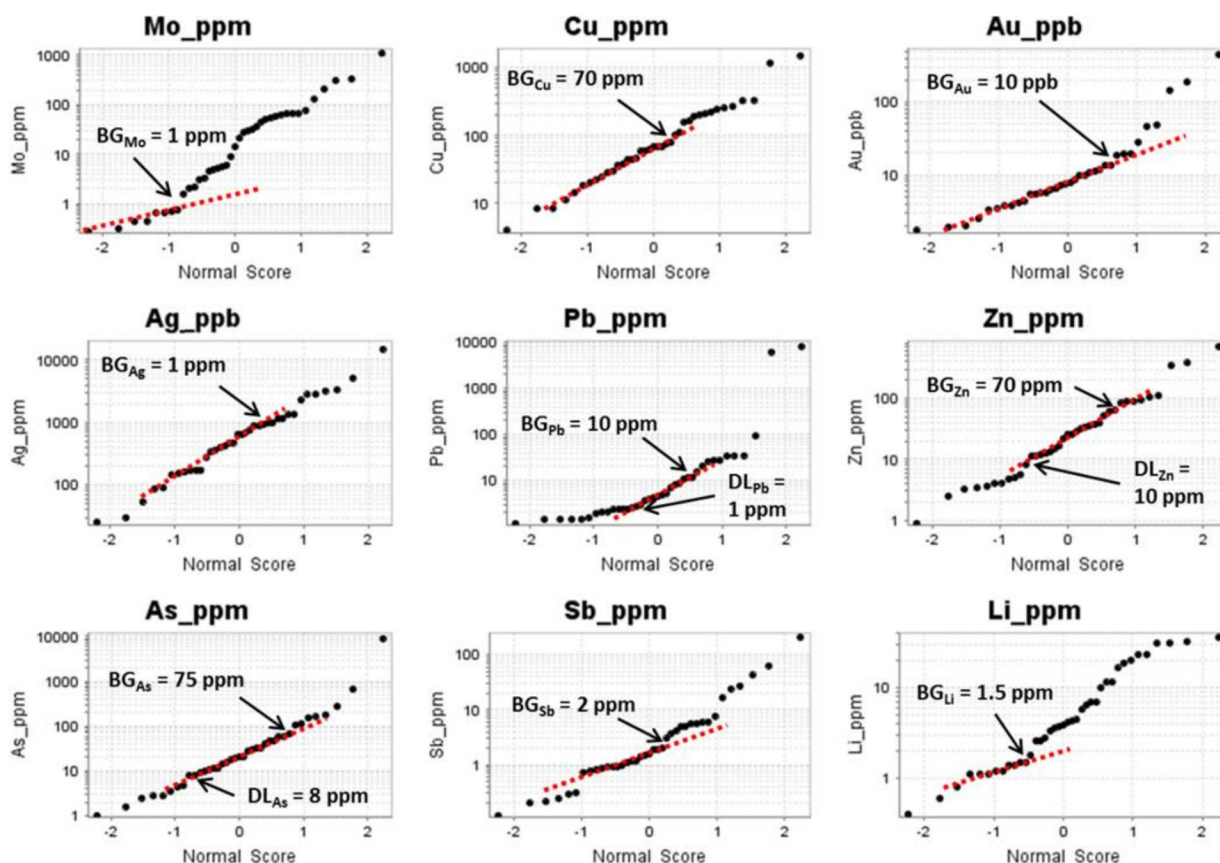


Figure 8.11: Normal log plots of Mo, Cu, Au, Ag, Pb, Zn, As, Sb and Li whole rock contents in the Harmony Formation quartzites. BG – upper background values; DL – upper depleted values

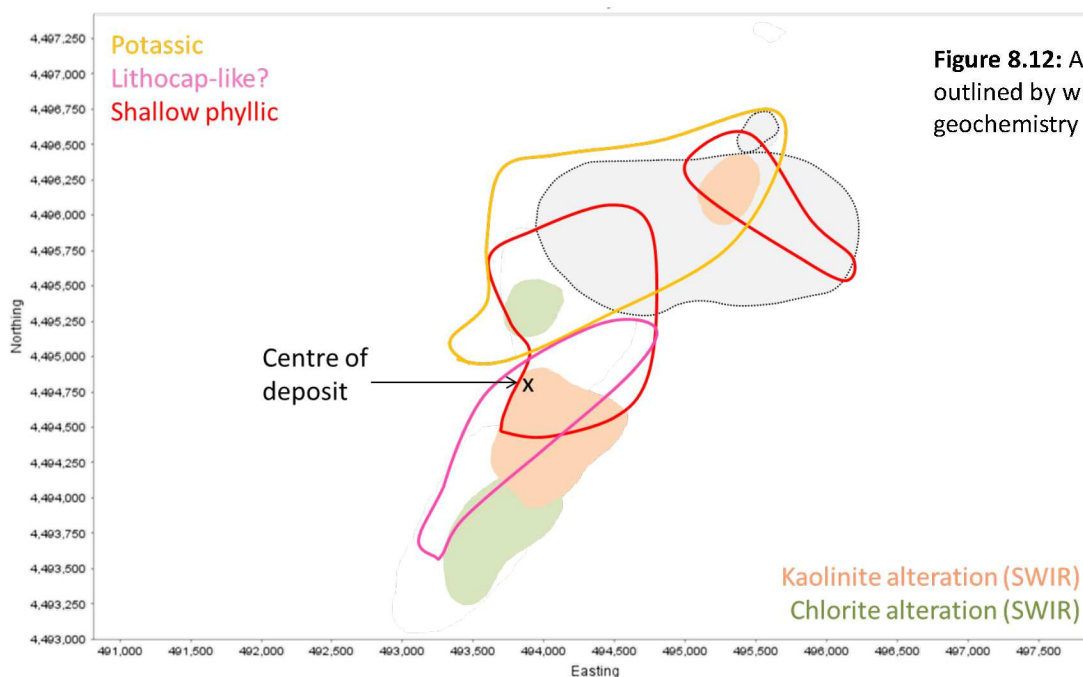


Figure 8.12: Alteration zones outlined by whole rock geochemistry and SWIR data

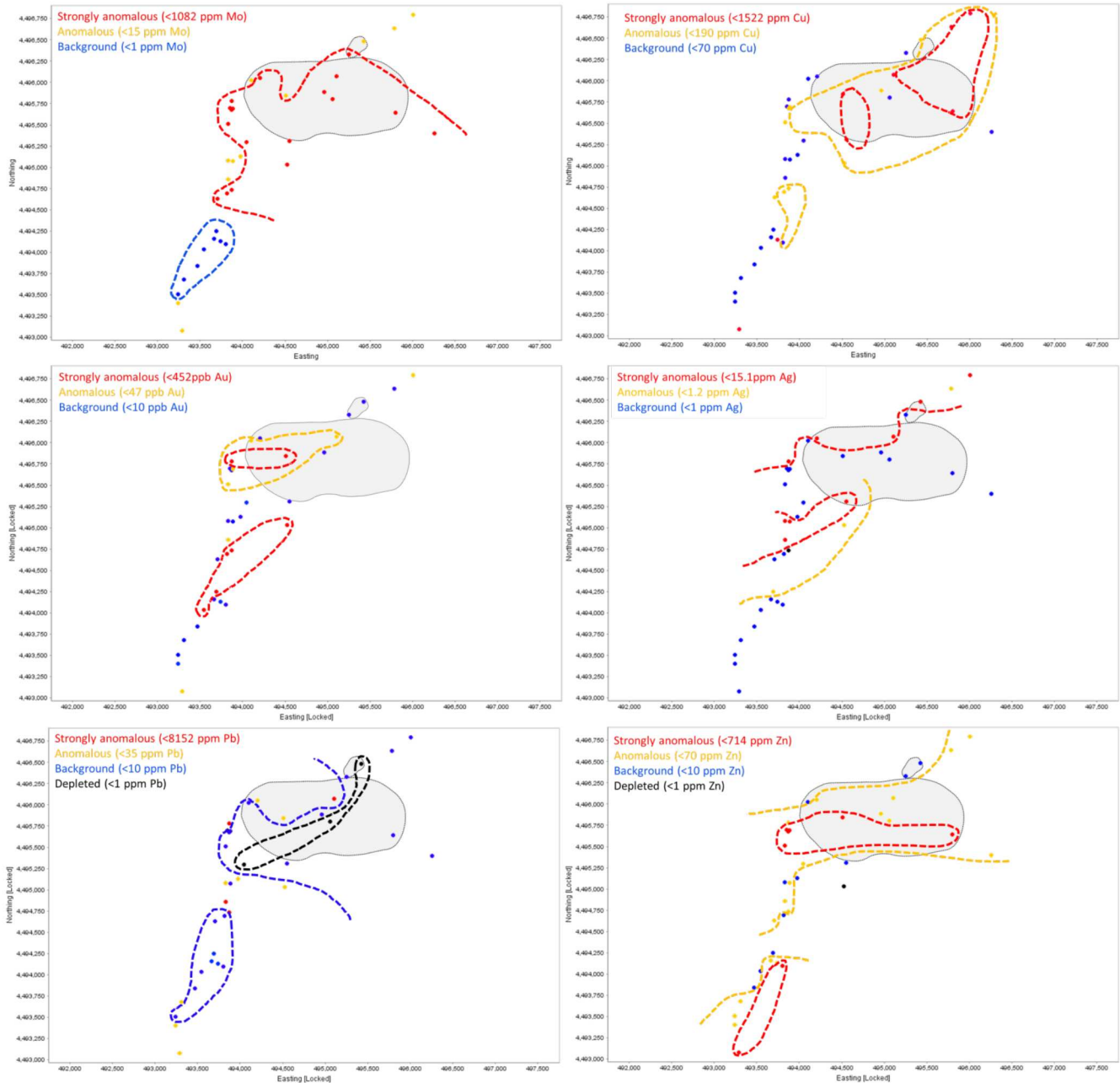


Figure 8.13: Contours outlining anomalous whole rock geochemical values for Mo, Cu, Au, Ag, Pb and Zn. The Buckingham intrusion and Copper Queen are outlined on the map (modified from Theodore et al., 1992).

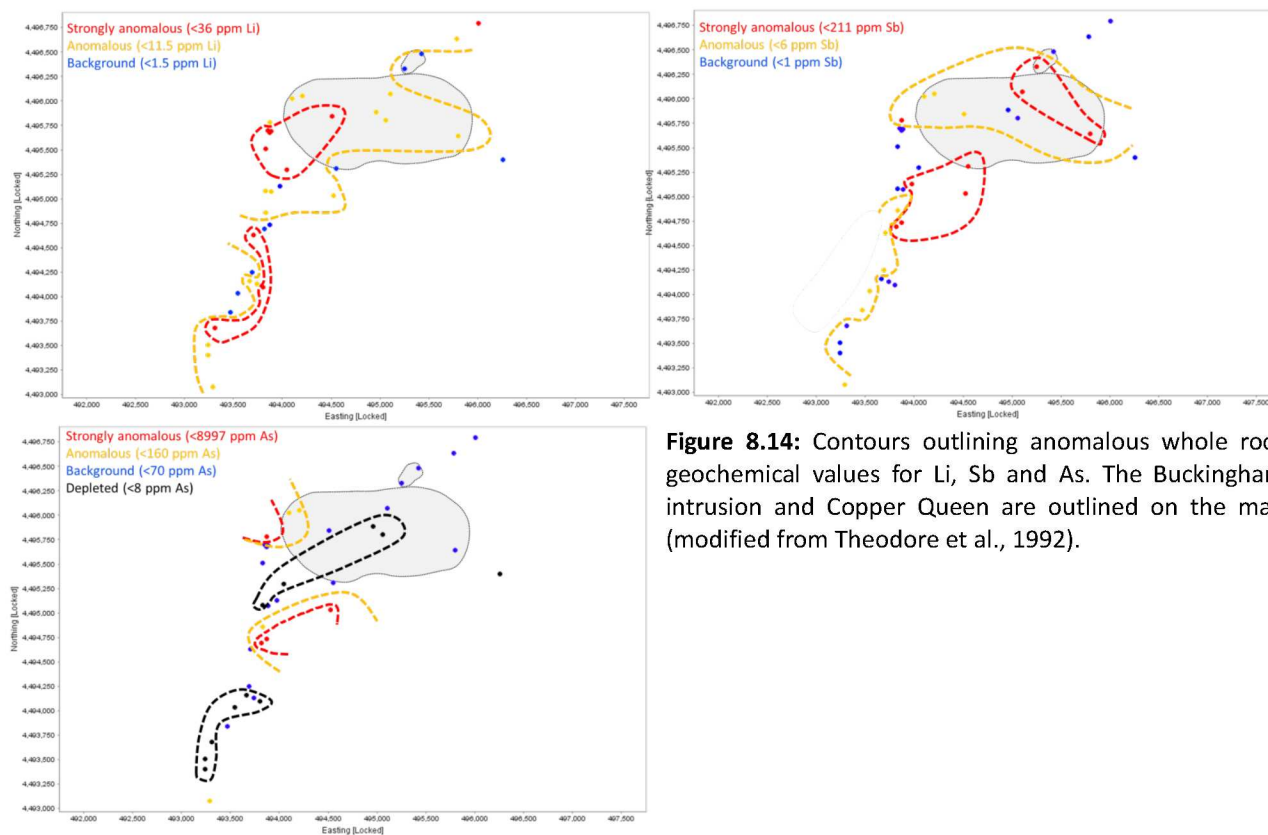


Figure 8.14: Contours outlining anomalous whole rock geochemical values for Li, Sb and As. The Buckingham intrusion and Copper Queen are outlined on the map (modified from Theodore et al., 1992).

8.4 White Pine Geochronology

The U-Pb age for the White Pine intrusion of 26.61 ± 0.24 Ma is younger than the ages for the Little Cottonwood stock of (29.45 ± 0.31 Ma, 29.63 ± 0.27 Ma, and 29.91 ± 0.34 Ma; Baker et al., 2014: pers. comm.). The younger age is consistent with the field observations that the White Pine intrusion is a younger, more leucocratic and felsic late phase than the Little Cottonwood. The new age for the granitic clasts from the White Pine breccia was 26.52 ± 0.42 Ma which falls within the error of previous age collected from the younger White Pine intrusion rather than the Little Cottonwood stock and makes it one of the youngest intrusive phases in the Wasatch Mountains (John et al., 1997; Baker, 2014: pers. comm.)

Molybdenum from the White Pine breccia dated in this study yielded a Re-Os age of 30.21 ± 0.14 Ma. As this age was older than the granite clasts within the breccia a replicate

analyses was undertaken which yielded a similar age of 29.84 ± 0.15 Ma. Given that the Mo samples came from the quartz cement breccia and not granitic clasts in the intrusion the apparent age discrepancy is hard to explain. The ~ 30 Ma age of the Mo mineralisation falls within the error of the Little Cottonwood intrusion which is difficult to reconcile given that it is hosted in and associated with younger clasts of the White Pine intrusion. One possibility is that the Mo mineralisation is inherited from the older intrusion and was remobilised during hydrothermal alteration, however there is no evidence for inherited Re-Os ages in Mo associated with porphyry systems (R. Creaser, 2014: pers. comm.). Further study is needed to resolve this issue.

8.5 Eocene granite geochronology

The new U-Pb ages determined for the Eocene granites for this study are 38.68 ± 0.53 , 39.28 ± 0.58 , 40.76 ± 0.41 , and 40.81 ± 0.51 Ma and they clearly postdate formation of the Buckingham system, which has been dated at 92.2 ± 1.4 Ma to 98.8 ± 2.0 Ma (Keeler, 2010). Previous studies of the granitoid bodies found in the northern part of the study area by Keeler (2010) and McKee (1992) obtained several dates which ranged from 38.7 ± 0.6 Ma to 39.9 ± 0.7 Ma. The U-Pb ages were calculated from LA-ICP-MS data collected from zircons in the granitic rocks (Keeler, 2010). There were other K-Ar and Ar-Ar ages from muscovite/sericite, hornblende, biotite, and chlorite collected from other igneous rocks in the area in the two studies. However, these ages are younger than the U-Pb ages created from the same samples. And have been interpreted as the result of resetting ages.

The Battle Mountain area is located west of the Roberts Mountains thrust, part of the larger Eureka mineral belt (Fig. 3.1). Cline et al. (2005) proposed a genetic model for all of the Carlin-style sedimentary-hosted Au deposits in Nevada, linking them to the emplacement of K-rich, calc-alkaline intrusions in calcareous sedimentary rocks from 42-36 Ma. The new ages

reported in this study suggest that the intrusions are coeval with the Tertiary volcanism and granitic intrusions associated with Carlin-style Au mineralisation (Henry and Ressel, 2000). Other features that support this interpretation include the gold-rich rims seen around pyrite grains (Figs. 7.12, 7.13, 7.14) as the gold in Carlin deposits is typically hosted in Au-rich rims on As-rich pyrite and marcasite or arsenopyrite (Cline et al., 2005). The majority of the Carlin deposits are also associated with skarn alteration similar to that seen in Copper Basin (Seedorff et al., 2005). The presence of the Tertiary granites in Copper Basin, which can be genetically linked to other intrusions in the region which host Au mineralisation, suggests the hydrothermal fluids could create the initial hypogene Au mineralisation seen surrounding the pyrite grains and other sulphides in the study area.

Chapter 9: Mineral Chemistry and Applications

The trace element geochemistry of quartz and pyrite was investigated for two purposes. The first was to investigate possible geochemical vectors to the centre of the deposit which could aid in exploration for other porphyry systems. The second was as a fingerprinting tool to help distinguish between hydrothermal, detrital, igneous, and breccia cement quartz.

9.1 Quartz

Quartz is a very common mineral in porphyry and epithermal systems. It is also a very common rock-forming mineral, and occurs as a major constituent in host rocks and related porphyry intrusions. In epithermal to mesothermal environments (<300°-350°C), quartz will precipitate with a decrease in temperature, with its maximum solubility in the fluid phase occurring around 350°C (Corbett and Leach, 1998). At higher temperatures >350°C, increases in temperature and pressure significantly increase the solubility of quartz. The silica-rich zone often present in the roof of porphyry systems is the result of a rapid temperature, pressure, and salinity decrease of the ascending fluids possibly associated with the change from a lithostatic to a hydrostatic regime and result in the formation of quartz stockwork systems (Corbett and Leach, 1998). Between 300°-350°C, these physical (i.e. pressure) and chemical variations (i.e., mixing with meteoric water and salinity) have a moderate influence on quartz deposition (Corbett and Leach, 1998; Rimstidt et al., 1998).

Quartz (SiO₂) is an exceptionally stable and unreactive framework silicate mineral with strong Si-O bonds that do not allow for a lot of elemental substitution, interstitial elements or microinclusions. Muller et al. (2003) showed that trace elements may replace Si in the crystal structure or that interstitial elements can enter in between the Si-O bonds. Some common cation substitutions for Si⁴⁺ include Al³⁺, Ti⁴⁺, Fe³⁺, Ge⁴⁺, and P⁵⁺ (Götze et al., 2001). Whereas, Li⁺,

H^+ , K^+ , and Na^+ , OH^- , and H_2O are common interstitial elements and compounds which serve the purpose of charge balancing, typically Al^{3+} (Dennen, 1966; 1967; Dennen et al., 1970; Lehmann, 1975; Weil, 1984, Breiter et al., 2013). In addition to the structural impurities, quartz frequently contains solid and fluid inclusions which may be difficult to distinguish from true element substitution or interstitial trace elements during LA-ICP-MS analysis. Finally, Al, Fe, and alkali metals (i.e., Li and K) form atomic couplings and substitute for Si, especially in low-temperature quartz (Muller et al., 2003 and references therein).

The substitution of elements into the quartz crystal structure is largely controlled by the physical and chemical characteristics of the hydrothermal fluids or the magmatic melt. In igneous rocks, the enrichment of Al, Li, Ge, and Be in magmatic quartz is observed in highly fractionated facies of both S- and A-type plutons (Breiter et al., 2013). The increased concentration of these elements in the minerals reflects their increased occurrence in the evolved melt. Breiter et al. (2013) noted that, in addition to the decreasing partitioning of Ti into quartz, a decrease in temperature and pressure facilitates the substitution of Al in the crystal lattice. However, the more important variable is the fluid chemistry, for example Rusk et al. (2008) stated that a high Al concentration in hydrothermal quartz does not entirely reflect temperature of quartz precipitation (except for it being $<350^\circ C$). Rather, it most likely reflects the aqueous Al concentration. A lower fluid pH greatly increases the solubility of Al and may be indicated by the presence of kaolinite which is indicative of acidic fluids (Rusk et al., 2008). Li^+ acts as a charge balancing cation for another cation – usually Al^{3+} (Muller et al., 2003). The increased incorporation of Al in the quartz crystal structure may account for the increase of Li to stabilize the lattice bonds. As well as Li and Al, the occurrence of Sb is common in quartz crystallizing in acidic conditions. Rusk et al. (2014) and Rusk (2010) noted that Sb is common in epithermal

deposits up to tens of ppms in quartz (which forms at ~200-300 °C). However, Sb is not often detectable in Mississippi valley deposits, Carlin, or porphyry-Cu quartz and its occurrence is not correlative to other elements in quartz (unlike Al and Li).

Breiter et al. (2013) showed that, in addition to the increased occurrence of Al, Li, Ge, and Be, an evolved melt is typically characterised by a strong depletion of Ti, and that the composition of the quartz phenocrysts will likely reflect the melt evolution. The ability for Ti to substitute for Si in quartz increases with the temperature of formation (Rusk et al., 2008; Rusk, 2010). This relationship between Ti and temperature allowed Wark and Watson (2006) to construct a titanium-in-quartz (TitaniQ) geothermometer. The geothermometer is based on the concept is that the Ti concentration in quartz is dependent on the temperature of formation as higher temperatures will result in more Ti directly substituting for Si in the quartz lattice. The geothermometer is most accurate when the activity of Ti is controlled by a pure TiO₂ mineral phase, typically rutile, or sphene (Wark and Watson, 2006; Thomas and Watson, 2011). However, the accuracy of the equation can be improved by considering additional geologic constraints such as pressure during formation and the Ti isotope used. In a study of granites and coeval felsic volcanic rocks, Breiter et al. (2011) showed that large variations between the Ti-rich core and Ti-depleted rims of quartz grains were the result of crystallization during a sudden decrease in pressure accompanied by a moderate temperature reduction. In addition to their relative concentrations in a melt, the temperature and pressure conditions of the crystallizing fluid will control the fractionation of Ti into the quartz structure with the increased Ti in quartz indicating higher temperatures of formation. Consequently, the presence of Ti-rich quartz should indicate a closer proximity to the heat source of the porphyry system and, therefore, the mineralisation.

9.1.1 Igneous and hydrothermal quartz at White Pine Fork Mo porphyry

Quartz trace element geochemical footprint

One of the goals of the P1060 project was to distinguish igneous, sedimentary and metamorphic quartz from hydrothermal quartz. At White Pine Fork, the geochemistry of the igneous quartz is within the range of other similar plutonic quartz samples noted in other studies (Breiter et al., 2013; Muller et al., 2003). The trace element compositions in the vein (i.e. hydrothermal) quartz were very similar to the igneous quartz with the Li (3.4 ppm), K (8.4 ppm), and Na (10.6 ppm) similar to the igneous quartz values (Li - 3.6 ppm, K - 4.8 ppm, and Na - 7.0 ppm). The increase of K in the breccia cement may be the result of potassic alteration. When the average concentration of Ti, Al, Bi, Li, Ge and metal elements are plotted as box and whisker plots, the geochemistry of the different types of quartz can be easily compared. The most noticeable variations between different types of quartz were seen in the Ti and the As. The hydrothermal (vein and breccia cement quartz) samples have higher mean Ti and As contents than the igneous quartz (Fig 9.2 and 9.3, respectively).

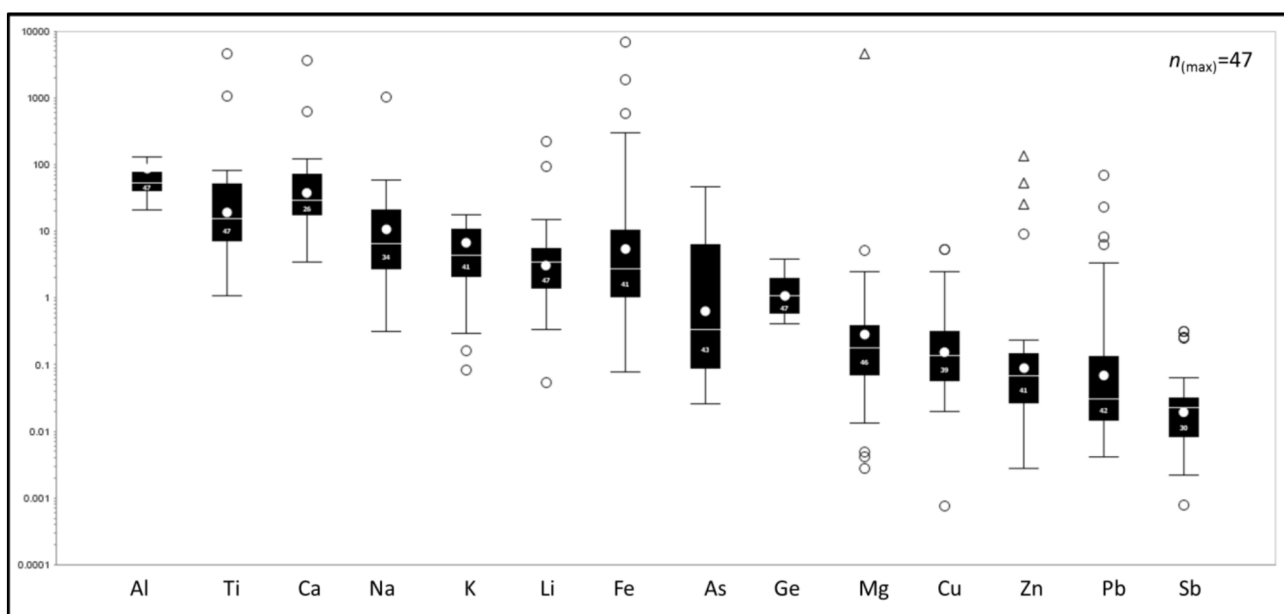


Figure 9.1: Tukey box-and-whisker plot of the element concentrations in igneous quartz at White Pine Fork. Element means are in ppm.

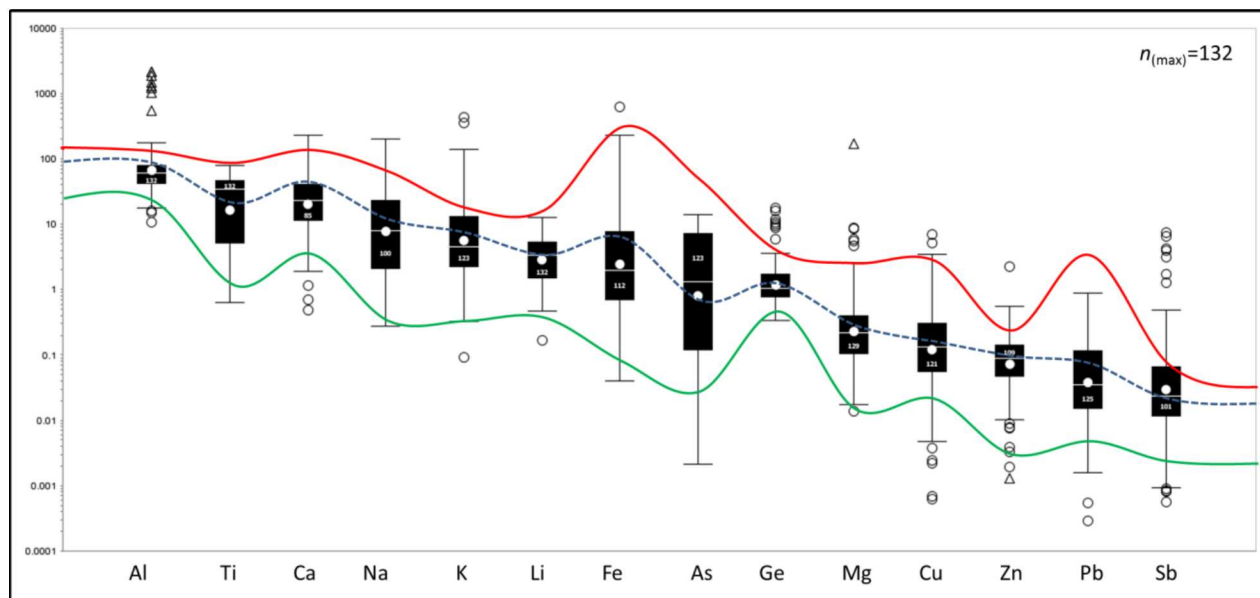


Figure 9.2: Tukey box-and-whisker plot of the element concentrations in hydrothermal quartz at White Pine Fork (excluding breccia samples). The upper and lower whisker value of the igneous quartz for each element is outlined in red and green, respectively. The mean value in igneous quartz is outlined by the blue dashed line.

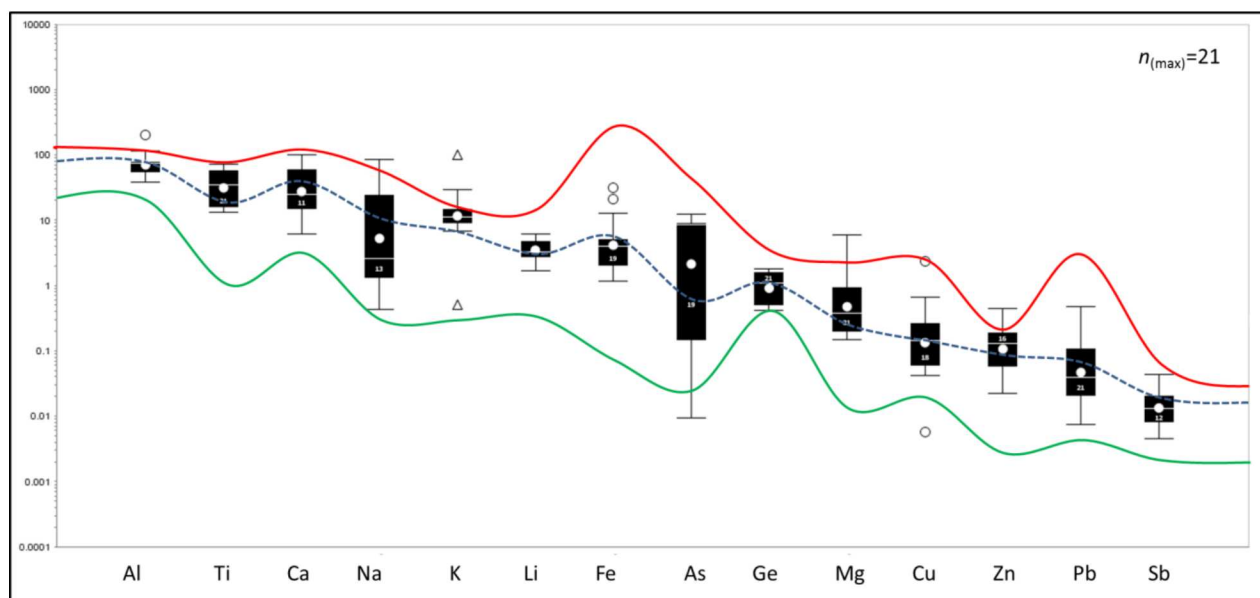


Figure 9.3: Tukey box-and-whisker plot of the element concentrations in the breccia cement quartz at White Pine Fork. The upper and lower whisker value of the igneous quartz for each element is outlined in red and green, respectively. The mean value in igneous quartz is outlined by the blue dashed line.

Trace element geochemical vectors

The P1060 project has successfully documented trace element geochemical vectors to the centre of porphyry deposits in the green rock environment using epidote and chlorite (Cooke et al., 2014; Wilkinson et al., 2015). For this study the absence of greenrock alteration meant that quartz and pyrite were investigated as possible vectors. Vectors were tested by plotting the spot data for each element measured in the hydrothermal quartz against the distance to the centre of the deposit determined by mineral chemistry and the alteration maps. The presence of potassic alteration and increased Mo and Cu support this centre of deposit selection. The distance to the centre was calculated by considering the location and elevation variations for each sample relative to a sample chosen to represent the centre of the deposit. For White Pine Fork sample WP13ES063, which was collected from the southern end of the breccia pipe and contained the most Mo mineralization, was chosen as the centre of deposit (Fig. 9.4).

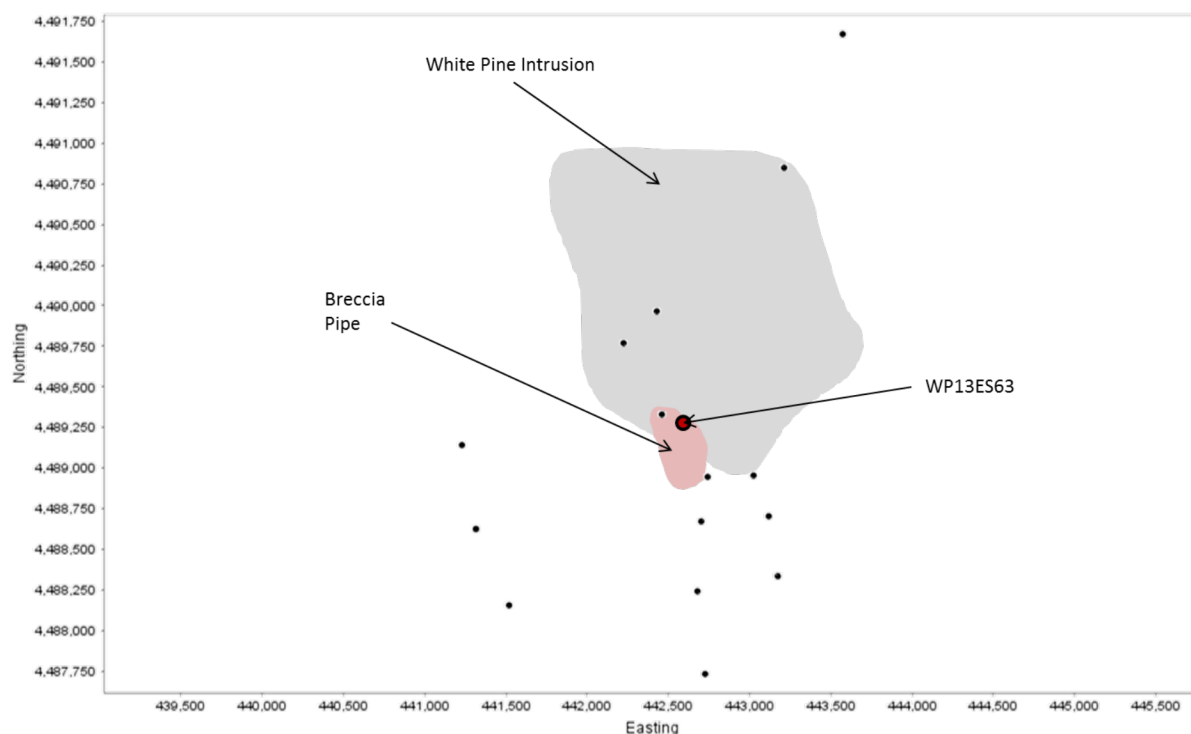


Figure 9. 4: Sample locations of quartz analyses at White Pine Fork. Sample WP13ES63 was chosen as the centre of deposit

The concentrations of all the elements in the hydrothermal quartz collected by LA-ICP-MS were plotted against their distance from the centre of the deposit. Lithium shows the most promising trend, with the data showing a slight increase away from the centre of the deposit (Fig. 9.6). The increase of Li peaks at ~1000 m and then decreases until the edge of the data study area, generating a geochemical ‘shoulder’ as has been noted in other mineral chemistry vectoring studies (e.g. Cooke et al., 2014; Wilkinson et al., 2015). The past studies explained geochemical shoulders as representing the limit of the hydrothermal system. Some of the element data becomes more erratic past 1300 m distance from the centre of the deposit. Titanium, Al, and Li in quartz have been used as geochemical vectors in other Mo-porphyry studies (Baig, 2015).

9.1.2 Igneous, sedimentary and hydrothermal quartz at Buckingham porphyry

Quartz trace element geochemical footprint

Four types of quartz were identified at Buckingham: vein quartz, breccia cement, igneous quartz and the sedimentary detrital quartz grains. The sedimentary quartz was collected from the Harmony Formation quartzites, whereas the igneous crystals were sourced from the Cretaceous Buckingham intrusions. The vein quartz included quartz occurring in veins cross-cutting the host rocks and the breccia samples that were collected from areas of intense hydrothermal alteration and increased mineralisation. In the samples which recorded values above the detection limit, the sedimentary quartz trace element geochemical values were different and often distinguishable from the hydrothermal and breccia cement samples with low concentrations of As and Sb. The primary difference between the breccia cement quartz and the other three quartz types was the higher trace element abundances and mineral inclusions in the breccia quartz. The breccia cement at the centre of the deposit showed the highest concentration of Al, Li, K, Ca, As, Sb and the metals Cu, Fe, Zn, Pb. The igneous and sedimentary units had the highest concentration of Ti

in quartz. The sedimentary quartz is interpreted to have multiple sources (including high temperature magmatic sources that yielded the high Ti quartz grains) and modes of generation prior to its erosion and deposition.

In the igneous samples, Ti (mean of 52 ppm), Al (mean of 105 ppm), Bi (<0.001 ppm) and Ge (<2.5 ppm) were within normal ranges for similar igneous quartz samples (e.g., Breiter et al., 2013; Muller et al., 2003). The vein quartz and breccia cement Ti (mean of 24.4 and 8.6 ppm, respectively) are lower than the average igneous and sedimentary quartz values (52 and 41 ppm, respectively; Figs. 9.5, 9.6, 9.7, 9.8). Lithium (mean of 9.1 ppm), K (11.2 ppm), Ca (12.5 ppm) and Na (11.7 ppm) also fall within normal ranges for igneous quartz and some of the higher concentrations of the charge balancing cations show a correlation with increased Al and Ti. All four types of quartz show similar Na, Li, K, and Ca values.

There is an increase in the Li content of the breccia quartz relative to the background igneous quartz. The igneous quartz had a mean of 9.1 ppm Li, the vein quartz has a mean of 10.5 ppm and the breccia cement 90.6 ppm, with some values reaching ~560 ppm. The Al content of the breccia quartz is higher than the vein quartz (mean of 1067 ppm and 218 ppm, respectively). Both values are higher than the background igneous Al values (a mean of 105 ppm).

The As values in the igneous quartz (mean of 2.5 ppm) are slightly higher than the concentrations of As in the sedimentary quartz grains (mean of 0.65 ppm) although these values are lower than the samples of hydrothermal quartz (Figs. 9.6 and 9.7). Arsenic and Sb are important elements in the Buckingham hydrothermal system. The centre of deposit contains a significant amount of arsenopyrite and As-rich pyrite. Antimony is geochemically very similar to As and occurs in a higher concentration in the breccia cement (mean of 6.6 ppm). The vein

quartz contained, for comparison, a mean of 2.1 ppm As and 0.17 ppm Sb (Fig. 9.8). These low values are within error of each other.

The increased amount of Fe in the hydrothermal vein and breccia quartz may represent more direct substitution for Si in the crystal lattice, or an increase in sulphide (i.e. pyrite and arsenopyrite) microinclusions, which are observed during petrographic analyses. Sudden spikes of Fe and As seen in the LA-ICP-MS analyses of the quartz samples were interpreted as sulphide microinclusions. Rusk et al. (2006) showed that the Fe content in quartz increases during phyllic alteration in porphyry and epithermal systems during the precipitation of pyrite. There is extensive phyllic alteration observed and recorded at Buckingham with petrographic studies. The presence of this hydrothermal alteration suggests that the fluids at Buckingham allow for this increased Fe content in quartz.

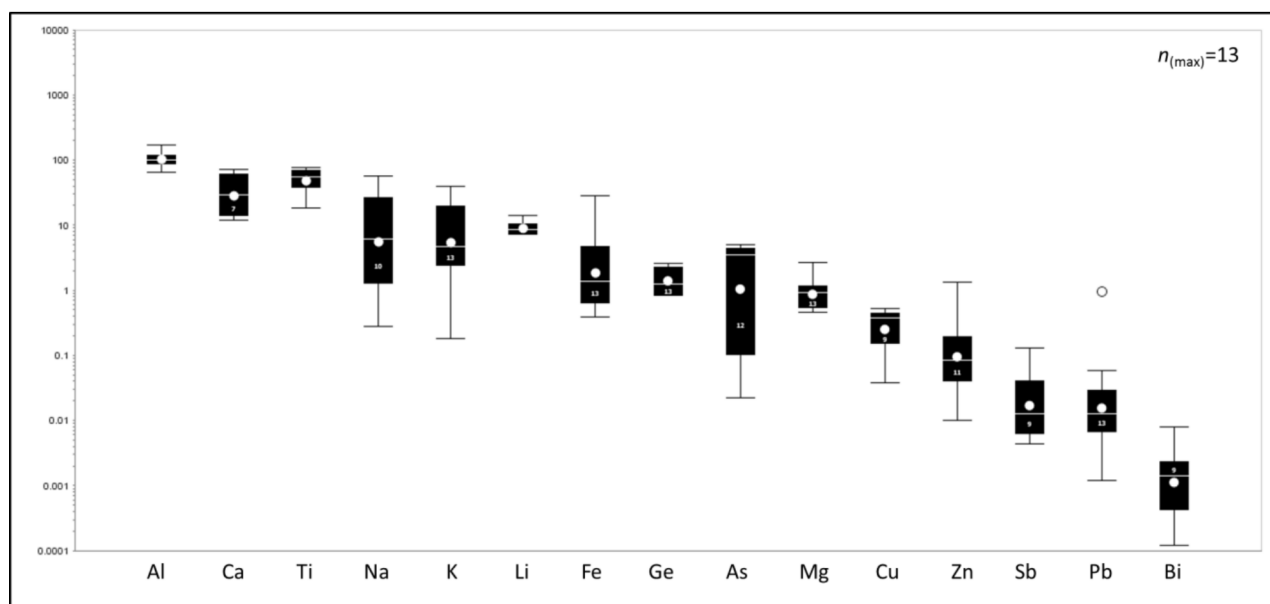


Figure 9.5: Tukey box-and-whisker plot of the element concentrations in the igneous quartz at Buckingham. All values are in ppm.

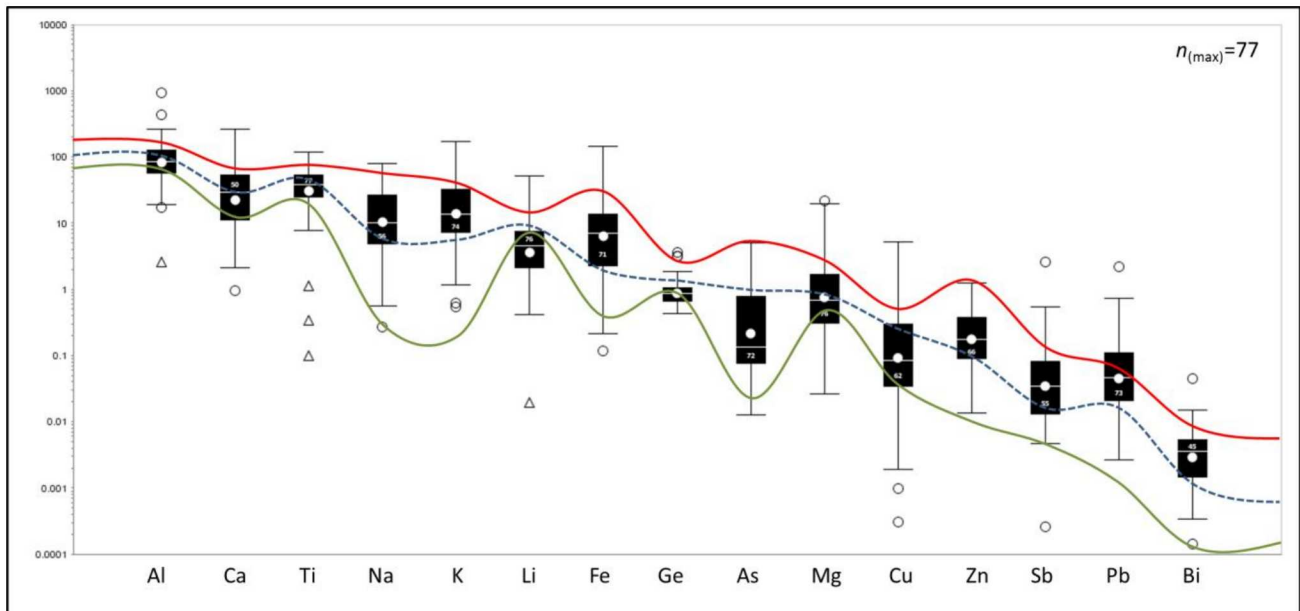


Figure 9.6: Tukey box-and-whisker plot of the element concentrations in the sedimentary quartz at Buckingham. The upper and lower whisker value of the igneous quartz for each element is outlined in red and green, respectively. The mean value in igneous quartz is outlined by the blue dashed line.

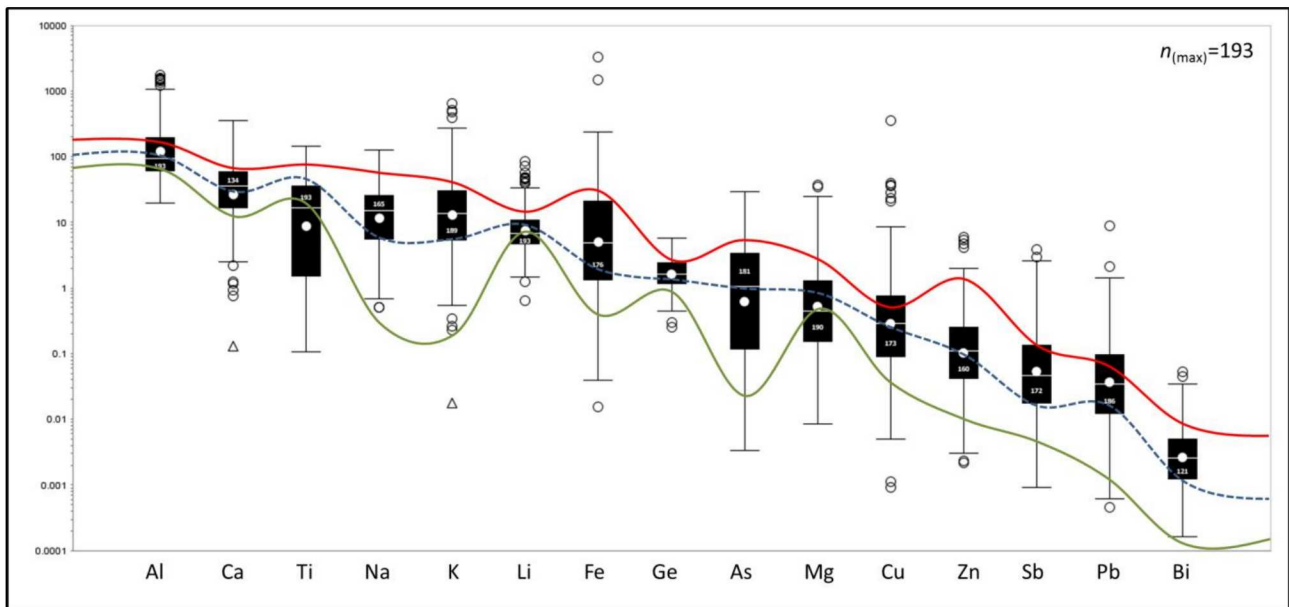


Figure 9.7 Tukey box-and-whisker plot of the element concentrations in the hydrothermal vein quartz at Buckingham. The upper and lower whisker value of the hydrothermal vein quartz for each element is outlined in red and green, respectively. The mean value in igneous quartz is outlined by the blue dashed line.

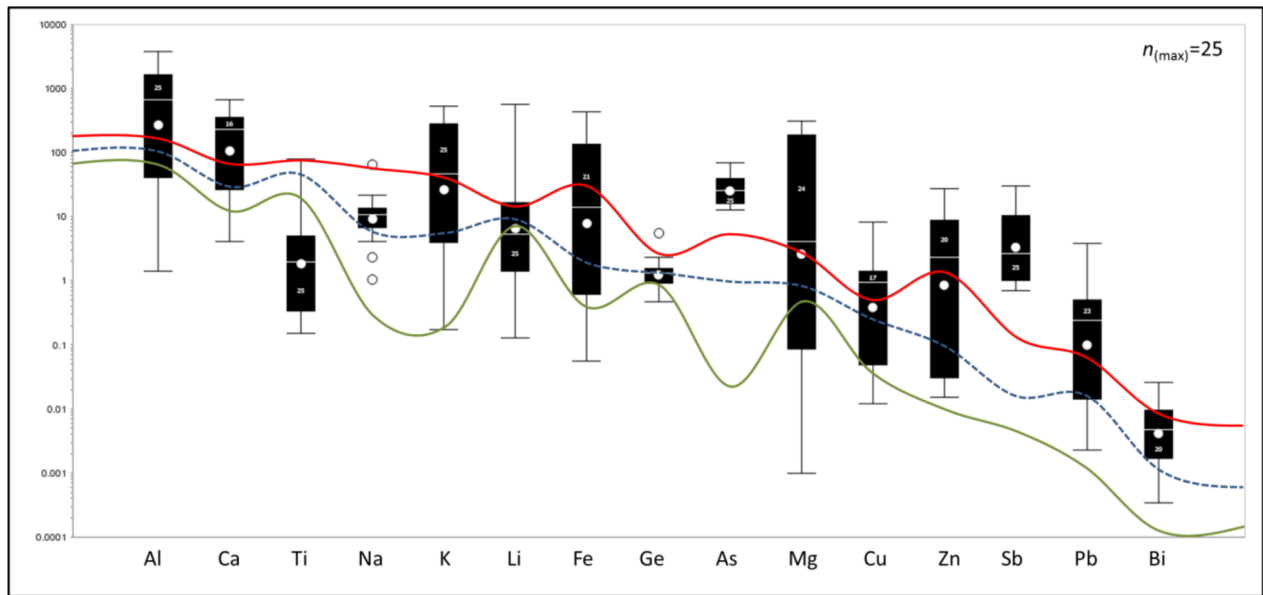


Figure 9.8: Tukey box-and-whisker plot of the element concentrations in the breccia quartz at Buckingham. The upper and lower whisker value of the hydrothermal vein quartz for each element is outlined in red and green, respectively. The mean value in hydrothermal vein quartz is outlined by the blue dashed line.

Possible quartz trace element geochemical vectors

The centre of deposit was less obvious for the Buckingham porphyry in comparison to the White Pine Fork porphyry; although the hydrothermal alteration surrounding the Buckingham intrusions was outlined in Theodore et al. (1992) sampling across the area showed extensive quartz stockwork which suggests that the deposit may be larger than currently shown (Fig. 9.9). Rather than select the centre of the Buckingham intrusion as outlined by Theodore et al. (1992; Fig. 9.9), sample BK13ES025 was selected as the centre of mineralisation as this contained the highest trace element abundance in quartz and although it falls outside the mapped zone of the Buckingham intrusion and associated stockwork, it is proximal to a historic mining adit. The whole rock geochemistry successfully mapped out potassic and phyllic alteration zones which support this centre of deposit. This sample is also richly mineralised with sulphides (dominantly arsenopyrite and pyrite) and contains breccia cement and fragmented quartz clasts (not analysed). The P1060 project has used similar methods to determine mineralized centres for blind test sites where the location of the mineralization was not initially revealed and have been correct the majority of the time.

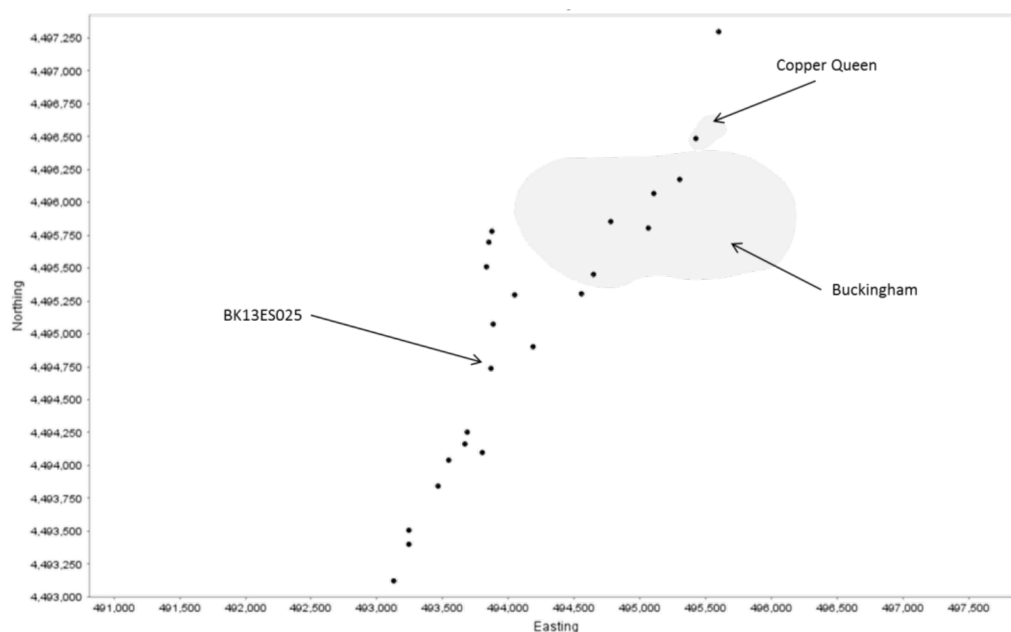


Figure 9.9: Sample locations for the quartz analyses at Buckingham. The north-east transect passes through sample BK13ES025, which was chosen as the centre of deposit. Buckingham system defined by Theodore et al. (1992).

There are two possible vectoring tools in quartz at Buckingham, Al and Sb. The concentration of Al in the hydrothermal quartz had the largest range closest to and at the centre of deposit. Moving away from the centre the spread of data and maximum value at each point decreases with a small spike at ~1500 m (9.9). The elevated sample at ~1500 m is associated with an atypical shale host rock which may have affected the results. The other promising mineral chemistry vector is Sb, which decreases away from the centre of the deposit (Fig. 9.11). Antimony in quartz at Buckingham at detectable levels appears to be restricted to hydrothermal quartz within 1800 m of the centre, with the highest concentration found in the samples adjacent to the centre. Box and whisker plots were used to ascertain whether the mean content of the element decreased, rather than just range of the element. The box-and-whisker plots show that the trend in Al is weak and that the trend seen in Sb is much stronger. The geochemical conditions under which certain elements partition into quartz are similar to the formation of the mineralisation shell in porphyry deposits. Seo et al. (2012) showed at Bingham Canyon that the precipitation of Mo was strongly linked to a lowering pH. There is mineralogical (i.e. kaolinite) and mineral chemistry (increased Al and Sb in quartz) evidence of acidic fluids at the mineralised centres at Buckingham. Although this centre of deposit was selected based on trace element chemistry of quartz and pyrite, another centre could have been selected closer to the Buckingham intrusions. This new centre would affect the current results. The chosen centre (sample BK13ES025) is the geochemical peak for many elements in quartz (e.g., Al, Li, K, Ca, As, Sb, Cu, Fe, Zn, and Pb). By choosing another centre, the data for BK13ES025 would cause geochemical shoulders by being a peak in those elements when plotting element concentrations against the distance to the centre of the deposit. Figure 9.12 shows an alternative centre of deposit. The peaks in the Al and Sb suggest likely mineralised centres.

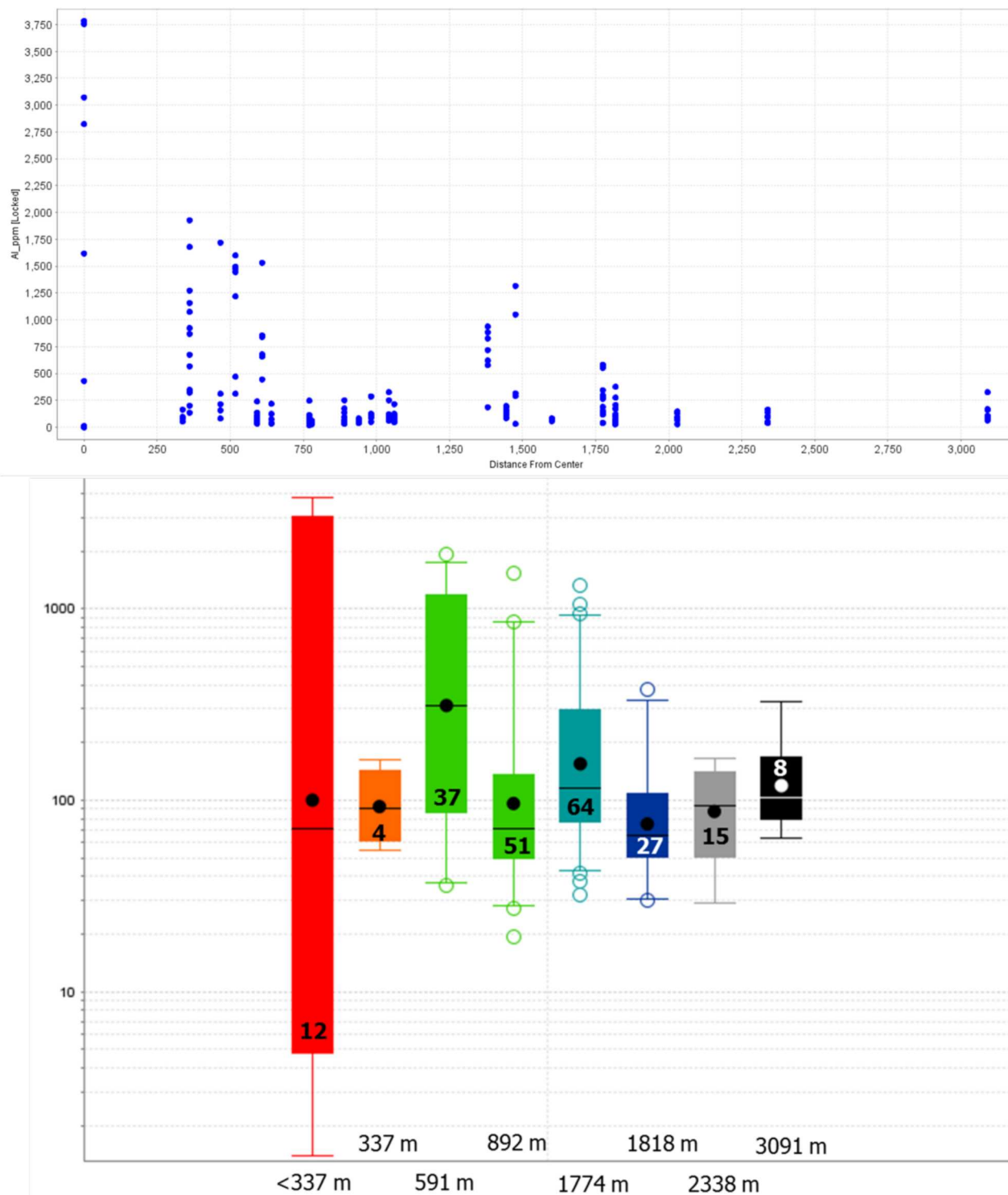


Figure 9.10: Scatterplot (top) and a box-and-whisker plot with the same data (bottom) showing the decreasing concentration of Al in the hydrothermal quartz at Buckingham. The box-and-whisker plot shows a weaker trend with inconsistent means. $n=218$

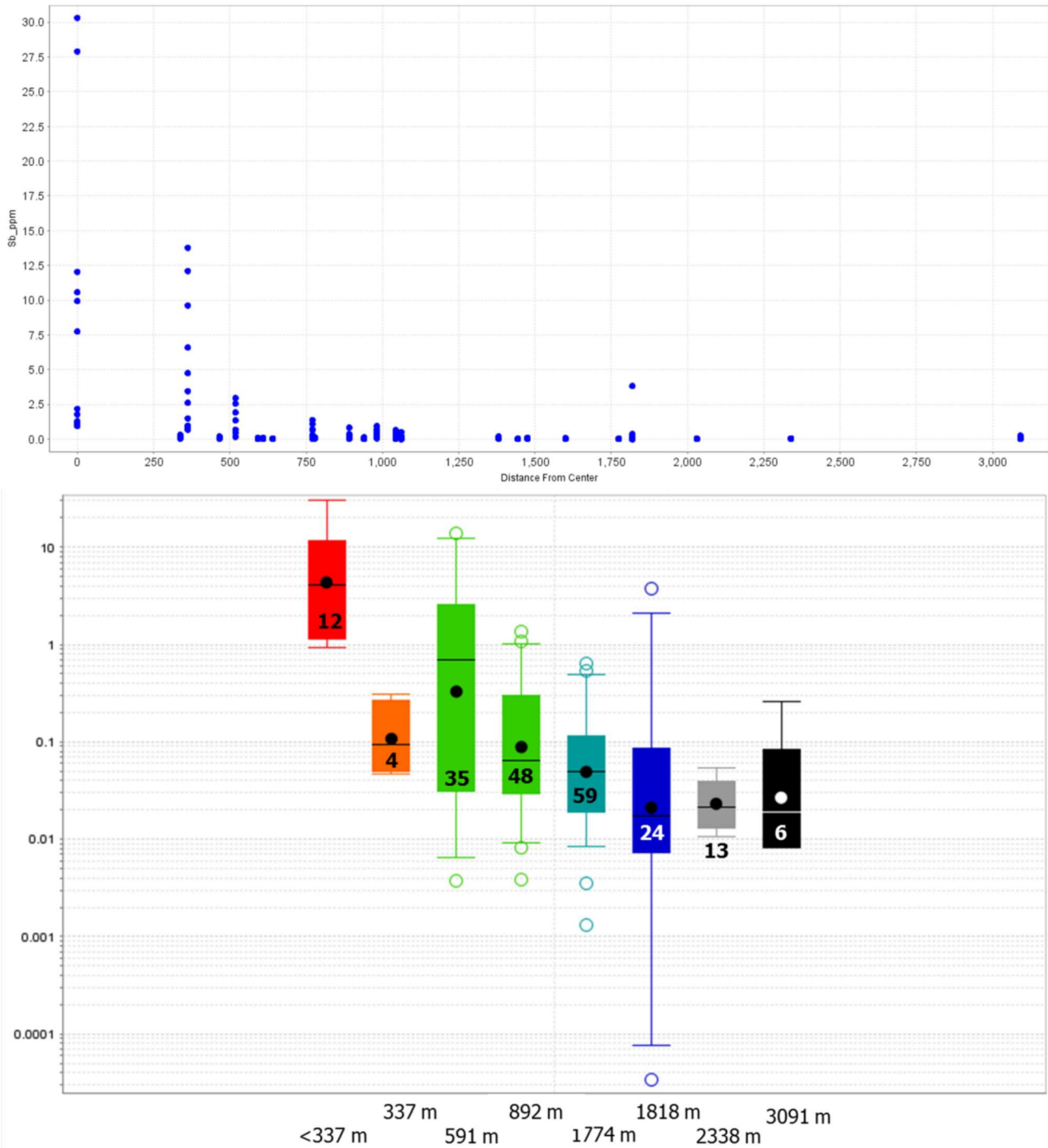


Figure 9.11: Scatterplot (above) and a box-and-whisker plot with the same data (right) showing the decreasing concentration of Sb in the hydrothermal quartz at Buckingham. The box-and-whisker plot shows a strong decreasing trend away from the proposed centre of deposit. $n=218$

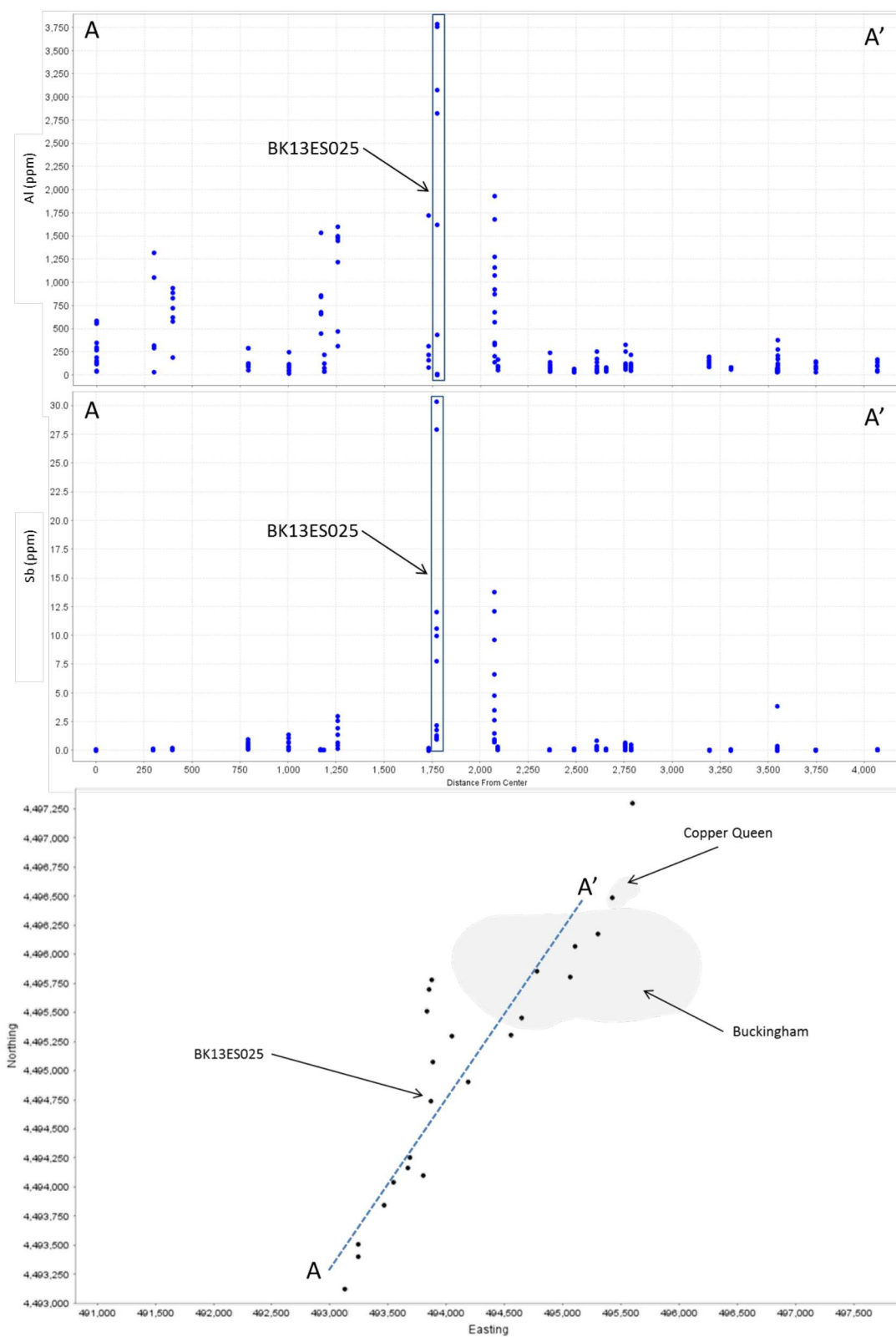


Figure 9.12: Sample BK13ES046 (A) was selected as the new arbitrary centre of deposit. Scatterplots (top and middle of Al and Sb in the hydrothermal quartz plotted against new distances to centre. The current centre of deposit (BK13ES025) is shown as the peak in both elements. $n=218$. Buckingham and Copper Queen occurrence from Theodore et al. (1992).

9.1.3 Trace element substitution in quartz and mineral chemistry vectors

At White Pine Fork, the only quartz chemistry vector was Li, which increased away from the centre of the deposit. Lithium acts as a charge balancing cation and its occurrence is often correlated with Al. At Buckingham, the highest concentration of Li was at the breccia pipe. Although these are opposing trends, the increase of Li correlates to an increase of Al at both study sites (Fig. 9.17). The substitution of Al into quartz is dependent on its availability in the hydrothermal fluids. The dissolution of Al is related to the acidity of the fluid (Breiter et al., 2013). A mineral indicator of an acidic fluid is the presence of kaolinite (Rusk et al., 2008). At Buckingham, several of the SWIR data proximal to the centre of deposit showed kaolinite as a prominent mineral suggesting an acidic fluid. This alteration was absent at White Pine Fork and calcite was present, implying that the fluids are less acidic at White Pine Fork. The neutral pH of the fluid, relative to Buckingham, may be why a peak of Al in quartz at the breccia pipe was absent at White Pine Fork.

The concentration of Ti in quartz is reliant on temperature; an increase in temperature results in an increase in Ti substituting for Si (Breiter et al., 2011). At White Pine, the igneous quartz does have lower concentrations of Ti than the breccia cement and vein quartz. However, at Buckingham, the hydrothermal quartz has lower Ti abundances than the igneous and sedimentary quartz (Figs. 9.2 and 9.3). The presence of Ti-rich hydrothermal quartz should indicate a closer proximity to the heat source of the porphyry system and, therefore, the mineralisation. This result was not seen in either deposit. White Pine Fork is a smaller deposit with a weaker alteration halo. The smaller size of the deposit might have resulted in a less well-developed alteration halo. Buckingham is a much larger deposit with multiple centres of intense hydrothermal alteration (i.e., several observed breccia pipes). Although the other mineral

chemistry suggests BK13ES025 as the centre of the deposit, it is not the only source of fluids in the area (i.e. samples BK13ES016, 017 and 104 were also brecciated rocks). The occurrence of increased Sb concentration in hydrothermal quartz towards the centre of the deposit is often seen in epithermal or low-temperature mineral deposits (Rusk, 2010; Rusk et al., 2014). The presence of kaolinite and the other clay minerals may indicate a transition in some of the stratigraphically higher parts of the system to an advanced argillic or epithermal-type mineralisation (Valencia et al., 2008). This alteration mineral assemblage characterises the formation fluids as being acidic and high-temperature, suggesting reasons for the increase of Al and Sb at the centre of the deposit.

9.1.4 Comparisons between White Pine Fork, Buckingham, MAX and Bingham Canyon

Baig (2015) investigated at the MAX Mo deposit in British Columbia, a Mo porphyry deposit with an estimated 1,380,000 tonnes at 0.5% MoS₂ and a measured and indicated resource estimate of 11,350,000 tonnes at a cutoff grade of 0.2% MoS₂ (Roca Mines, 2005). At MAX, Baig (2015) documented there was an increase in Ti, Al, and Li in quartz towards the centre of the deposit. These geochemical vectors were applied to the data from White Pine Fork. At White Pine Fork, the concentration of these elements showed no obvious trends towards the centre of the system (Figs. 9.13, 9.14, 9.15). The lack of any strong correlation at White Pine likely reflects the small size of the deposit and possibly defines a lower limit for the size of deposit to which vectoring models can be applied. It should be noted that at 1000 m from the centre of deposit at MAX, there is a sample with increased Ti and Al which indicates that the sample is paragenetically distinct and different.

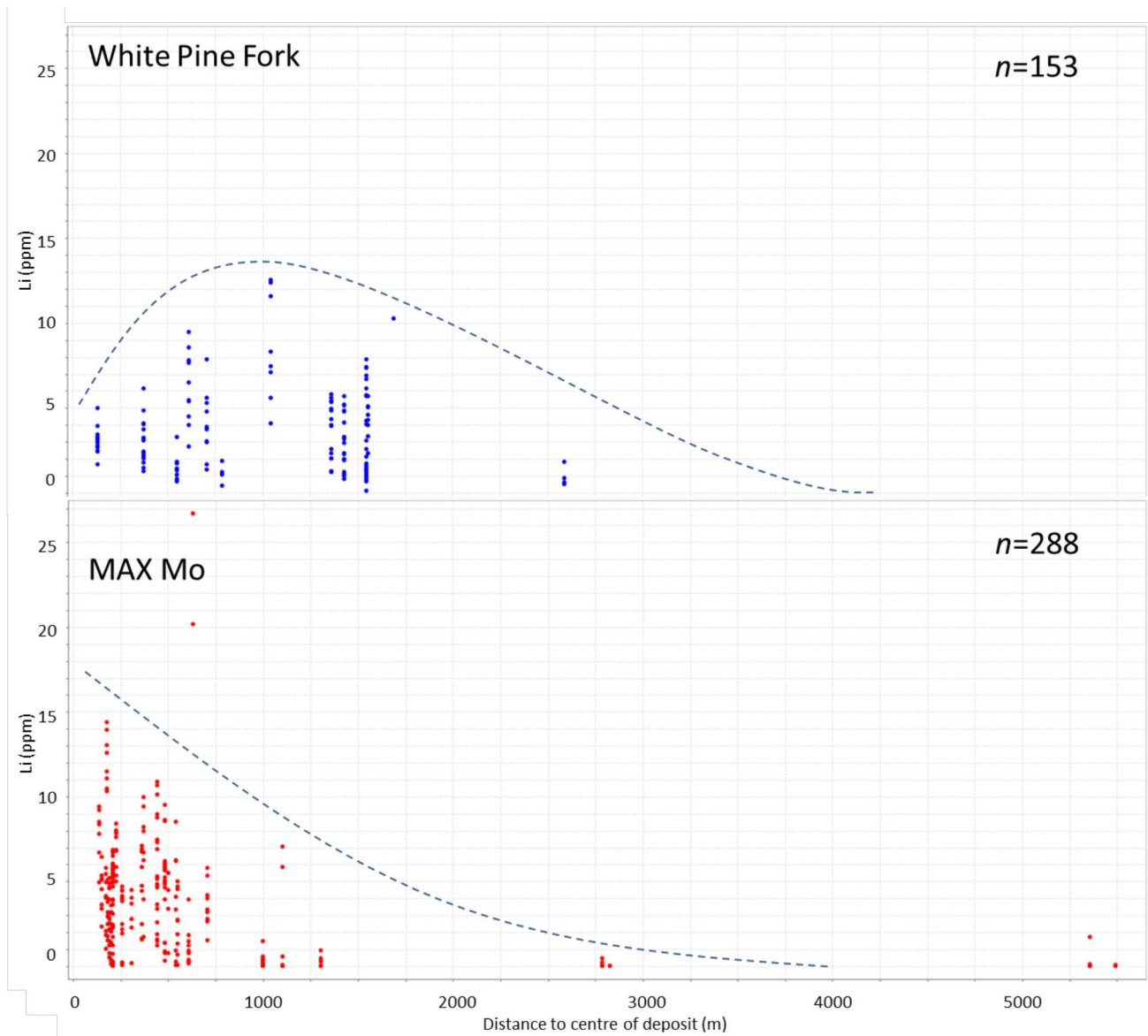


Figure 9.13: Scatterplots of the Li content in quartz from White Pine Fork (top) and MAX Mo (bottom) porphyries.

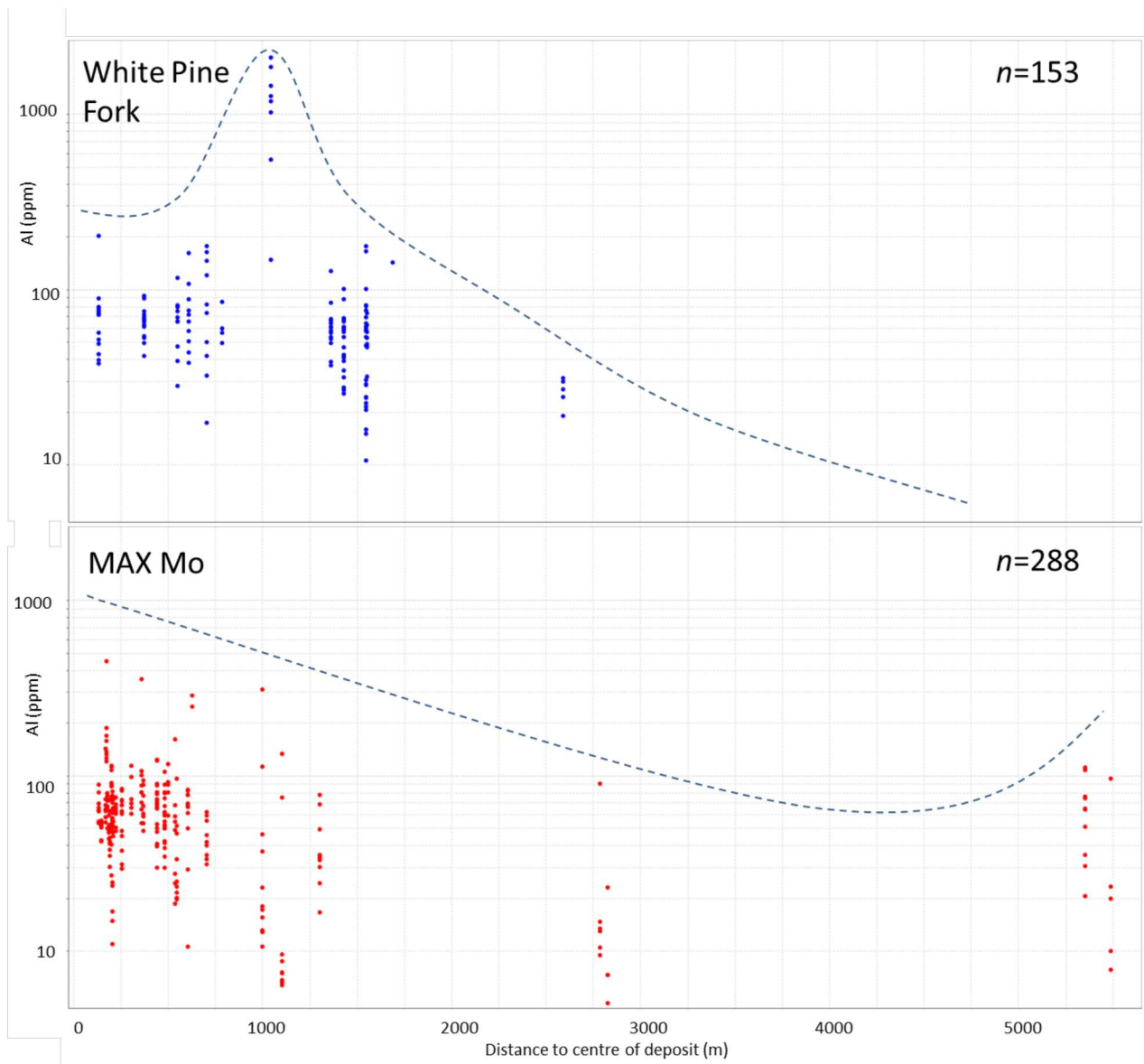


Figure 9.14: Scatterplots of the Al content in quartz from White Pine Fork (top) and MAX Mo (bottom) porphyries

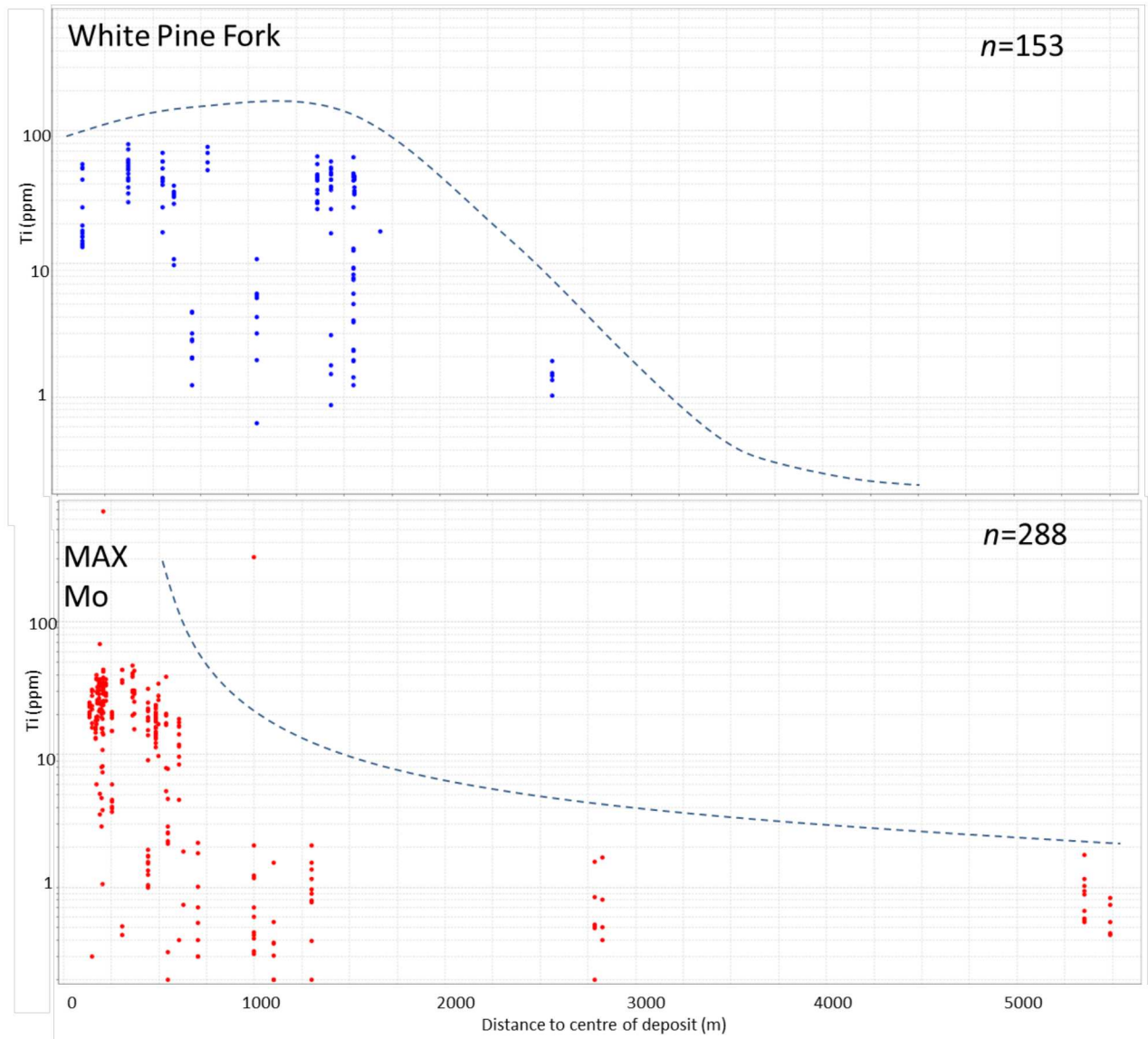


Figure 9.15: Scatterplots of the Ti content in quartz from White Pine Fork (top) and MAX Mo (bottom) porphyries

White Pine Fork, Buckingham and Bingham Canyon are all Mo-bearing porphyry deposits. Bingham Canyon is a porphyry Cu-Mo-Au deposit in north-central Utah. The mine produces about 300,000 tons of Cu, 400,000 ounces of Au; 4 million ounces of Ag, and 30 million pounds of Mo (Austin and Ballantyne, 2010). The Cu and later Mo mineralisation is hosted in separate shells around a barren core and is spatially associated with the Bingham Stock, a 2.1 km by 1.8 km equigranular monzonite intrusion, which is in turn intruded by a quartz monzonite porphyry dyke (QMP; Austin and Ballantyne, 2010). The stock intrudes Paleozoic quartzites, limestones and siltstones. Latite porphyry, quartz latite porphyry, and minette dykes intrude the QMP and extend beyond it for up to 7 km (Austin and Ballantyne, 2010). The Bingham stock has a U-Pb zircon age of 38.55 ± 0.19 Ma (Parry et al., 2001).

Bingham Canyon is located in the same district as the White Pine Fork porphyry. The lithologies and the zircon ages of the two deposits are very similar, making it a good comparative study. Quartz data from Bingham Canyon are part of the larger P1060 database. These data, when plotted with the White Pine Fork and Buckingham show some similarities and differences. The hydrothermal quartz data for Bingham Canyon was plotted on a similar Tukey plot as the White Pine Fork and Buckingham deposits. This data were then overlain on the hydrothermal quartz White Pine Fork plot (Fig. 9.16) and the hydrothermal quartz Buckingham plot (Fig. 9.17). The quartz from Bingham Canyon is geochemically similar to both of the deposits in this study. The biggest difference is the high amount of Mg and other metals (i.e. Cu, Zn and Pb) in the quartz at Bingham Canyon. In Fig. 9.16, the Bingham Canyon hydrothermal quartz data plot much higher than the metal content in hydrothermal quartz at White Pine Fork. At Buckingham, the metal content in hydrothermal quartz is greater than White Pine Fork, but less than Bingham Canyon. This increased concentration of metals might be the result of overall increased metal

tenor in the largest deposit (i.e., Bingham Canyon). For Al and Sb, the highest average content in quartz is at Bingham Canyon. White Pine has the highest Ti concentration with very similar values seen at Bingham Canyon. The Li concentrations in hydrothermal quartz were very similar for all three deposits. The highest content of Al and Sb in quartz at Bingham suggests similar acidic, high temperature alteration fluids as what was described at Buckingham in this study. Parry et al. (1998) note low-temperature illite-smectite alteration mineral assemblages as well as other clay mineral alteration near the mineralised shell at Bingham Canyon.

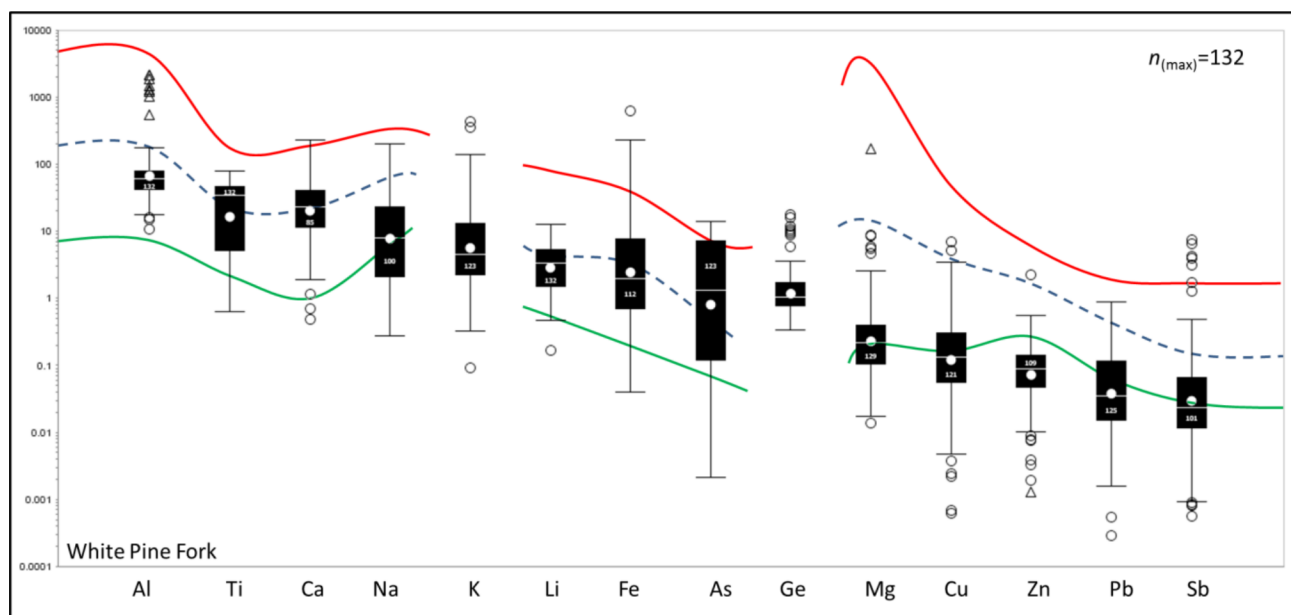


Figure 9.16: Tukey box-and-whisker plot of the element concentrations in the White Pine Fork hydrothermal quartz. The upper and lower whisker value of the hydrothermal quartz from Bingham Canyon for each element is outlined in red and green, respectively. The mean value in hydrothermal quartz is outlined by the blue dashed line. Data for K and Ge was below detection limits at Bingham Canyon.

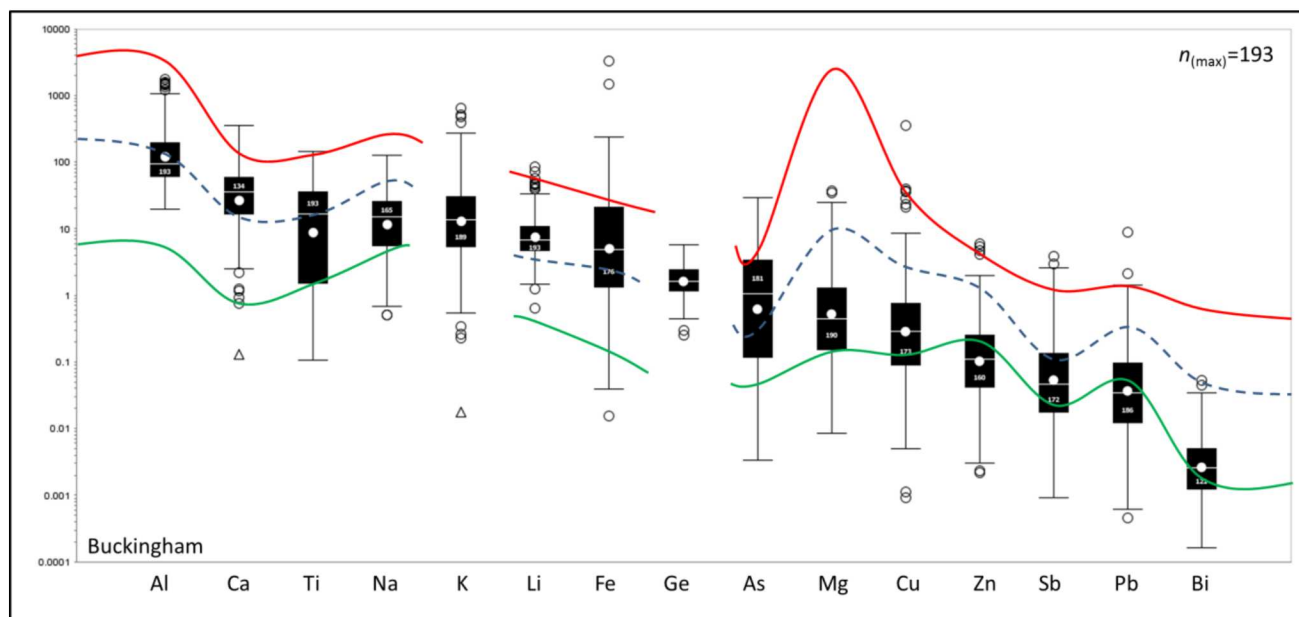


Figure 9.17: Tukey box-and-whisker plot of the element concentrations in the Buckingham hydrothermal quartz. The upper and lower whisker value of the hydrothermal quartz from Bingham Canyon for each element is outlined in red and green, respectively. The mean value in hydrothermal quartz is outlined by the blue dashed line. Data for K and Ge was below detection limits at Bingham Canyon.

9.2 Pyrite

Pyrite (FeS_2) is a very common mineral in almost all mineral deposits and is the most common sulphide mineral on Earth (Reich et al., 2013). It can also be formed as a result of diagenesis, metamorphism and hydrothermal activity (Reich et al., 2013). Its precipitation can control the partitioning of a wide array of trace elements (e.g., Au, Ag, As and heavy metals) and can affect the metal distribution in a porphyry deposit (Large et al., 2009). Pyrite, in porphyry systems, is typically concentrated in a 'pyritic shell' which usually envelope the core of the porphyry system and the mineralisation. This shell is the result of phyllic alteration which overprints the earlier potassic and propylitic alteration; although, pyrite can also be formed during potassic alteration (Lowell and Guilbert, 1970; Gustafson and Hunt, 1975; Seedorff et al., 2005; Reich et al., 2013; Cooke et al., 2014). In copper porphyry deposits, the pyrite + quartz + sericite veins are usually observed to cross-cut quartz veins that host the Cu mineralization and potassic alteration minerals (Reich et al., 2013).

Using transmission electron microscopy (TEM), secondary-ion mass spectrometry (SIMS) and electron microprobe analysis (EMPA), Deditius et al. (2011) have shown that Carlin-type and epithermal gold deposits host pyrite with a variety of trace metals (e.g., Cu, Co, Pb, Sb, As, Ag, Ni, Zn, Se, Te, and Hg) that occur in solid solution and/or cluster into metal nanoparticles or nano-inclusions (<100 nm size). Deditius et al. (2014) showed that the nanoparticles of metals can display varying degrees of compositional complexity (i.e. native metals, sulphides and sulfosalts, and Fe-bearing sulphides; Palenik et al., 2004, Deditius et al., 2011; Hough et al., 2012). Deditius et al. (2011) proposed that nanoparticles can form by syngenetic precipitation with the pyrite or by exsolving by post-depositional processes.

Pyrite-forming fluids are high-temperature (~600–700 °C) fluids, however, Reich et al. (2013) suggested that the majority of the trace element substitution happens at lower temperatures. Arsenic (and other trace elements)-rich vapors are introduced to Cu porphyry hydrothermal systems repeatedly and intermittently with lower-temperature (~300 °C), Cu-rich vapors. The supersaturation of these fluids at or near the pyrite grain surface in Cu and native Au (or Au tellurides) results in the precipitation/deposition of the chalcopyrite and Au nanoparticles and micrometer-scale aggregates on the pyrite grain (Deditius et al., 2011). Solid solution element substitution relies on the presence of the substituting ion being present in abundance, and is often a function of the chemistry of the ore-precipitating fluids (Deditius et al., 2011).

Arsenic can occur as the result of direct element substitution or as As-bearing inclusions or nanoparticles (Reich et al., 2013). It can also substitute for S in the pyrite structure as anionic As in reducing environments, whereas in more oxidized, shallower hydrothermal systems (e.g., epithermal Au deposits), As can occur as As^{3+} in pyrite (Reich et al., 2013). Reich et al. (2013) also noted that in porphyry system, there is a trend toward a decoupled behavior of Cu and As which strongly suggests that selective partitioning of metals into pyrite is most likely the result of changes in fluid composition. These changes are suspected to be the result of mixing with meteoric water and repeat intermittent pulses of magmatic/hydrothermal Cu and As-bearing fluids (Audétat et al., 1998, Heinrich et al., 1999 and 2004). Therefore, the samples collected proximal to the breccia pipe would have increased As and Cu available in the hydrothermal fluids to partition into the pyrite.

Bayliss (1989) proposed that most of the structurally-bound Cu in pyrite replaces Fe in the octahedral sites. The increased amount of elemental substitution in a sample may be due to increased distortion of the pyrite lattice by the presence of the other elements like As, Sb and Co

in solid solution (Reich et al., 2013). In addition, Cu frequently occurs as mineral inclusions. These inclusions have been suggested to occur when Cu's solubility limit is surpassed during pyrite growth from a hydrothermal fluid (Reich et al., 2013). Once the fluid is supersaturated, Cu-bearing sulphides (i.e. chalcopyrite) nanoparticles nucleate in the Cu-rich fluid at or close to the pyrite–fluid interface. These single nanoparticles then cluster to form larger, micrometer-sized Cu-bearing inclusions (Reich et al., 2013). The presence of nanoparticles is the most likely source of Cu in the pyrite since the solid solution of CuS_2 in FeS_2 (pyrite) is thermodynamically unstable unless temperature and pressure exceed the conditions typical of hydrothermal alteration and pyrite formation in porphyry systems (Shimazaki and Clark, 1970; Schmidt-Beurmann and Bente, 1995). Experimental studies have shown increased As content results in elevated Cu in the pyrite (Heinrich et al., 1999 and 2004).

Gold occurs in two mineralogical forms in pyrite: structurally bound ions (Au^+) and as free particles of native Au and/or Au-tellurides. Reich et al. (2013) noted that abundances of <10 ppm Au indicates that the Au is more likely structurally bound; whereas higher concentrations (100–1000 ppm) of Au are exclusively the result of micro- to nano-sized particles or clusters. According to Reich et al. (2005), the empirical solubility limit of Au is a function of As in pyrite. They suggested that as the concentration of As increases, so does the ability of the pyrite to allow more Au into its crystal lattice. As the Au is also sourced from the magmatic fluids, it will be available to partition or occur as inclusions in the pyrite closer to the centre of deposit/core of the hydrothermal system.

Nickel occurs in solid solution in pyrite, with Ni substituting for Fe in the octahedral sites (Reich et al., 2013). The evidence for the solid solution Ni (as opposed to the inclusions) can be seen in some element maps where the Ni maps are continuous, homogenous bands (e.g. Fig. 7.8).

Nickel contents in pyrite for hydrothermal ore deposits have been reported between 100 and 3000 ppm (Campbell and Ethier, 1984; Kaneda et al., 1986; Raymond, 1996; Hanley et al., 2010). Ni-rich pyrite coincides with Co enrichment in pyrite. Trace amounts of Co and Ni in sulfide deposits reflects the availability of the two elements in the ore-forming system (Reich et al., 2013).

9.2.1 Pyrite trace element geochemical vectors at White Pine Fork

The concentrations of all the elements in the hydrothermal pyrite from White Pine Fork were plotted against their distance from the centre of the deposit. The Ni content in pyrite showed the most promising trend, with the data showing an increase away from the centre of the deposit until ~1400 m and then decreasing again as a geochemical shoulder (Fig. 9.18). This trend could be formed by Ni depletion near the breccia pipe.

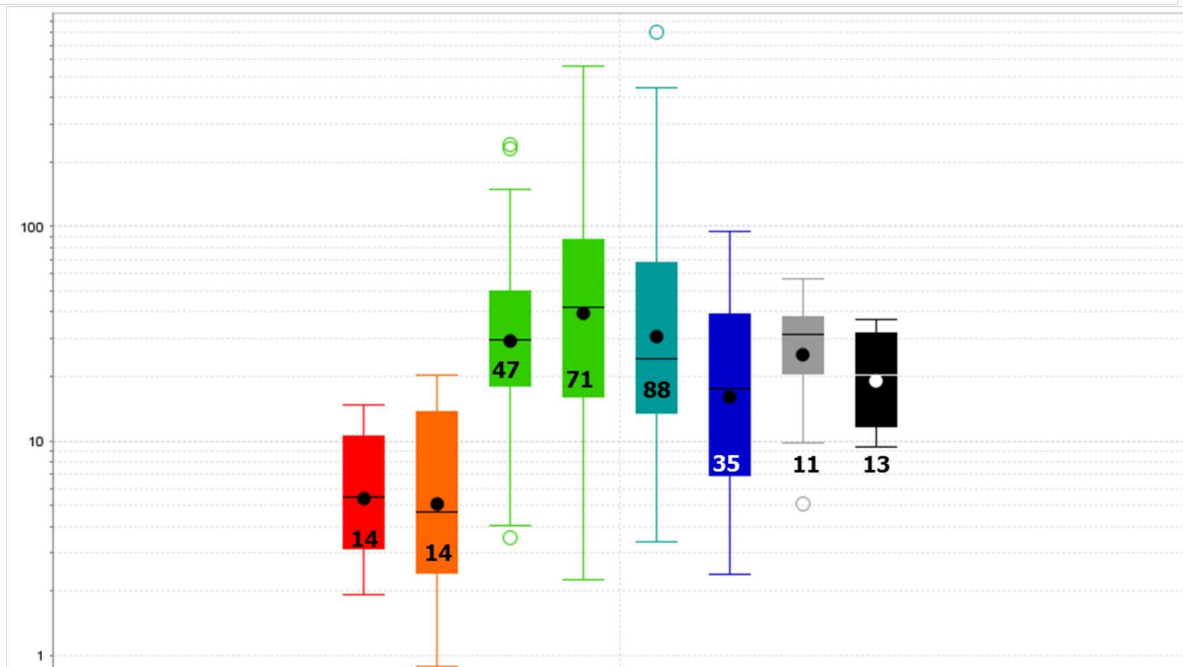
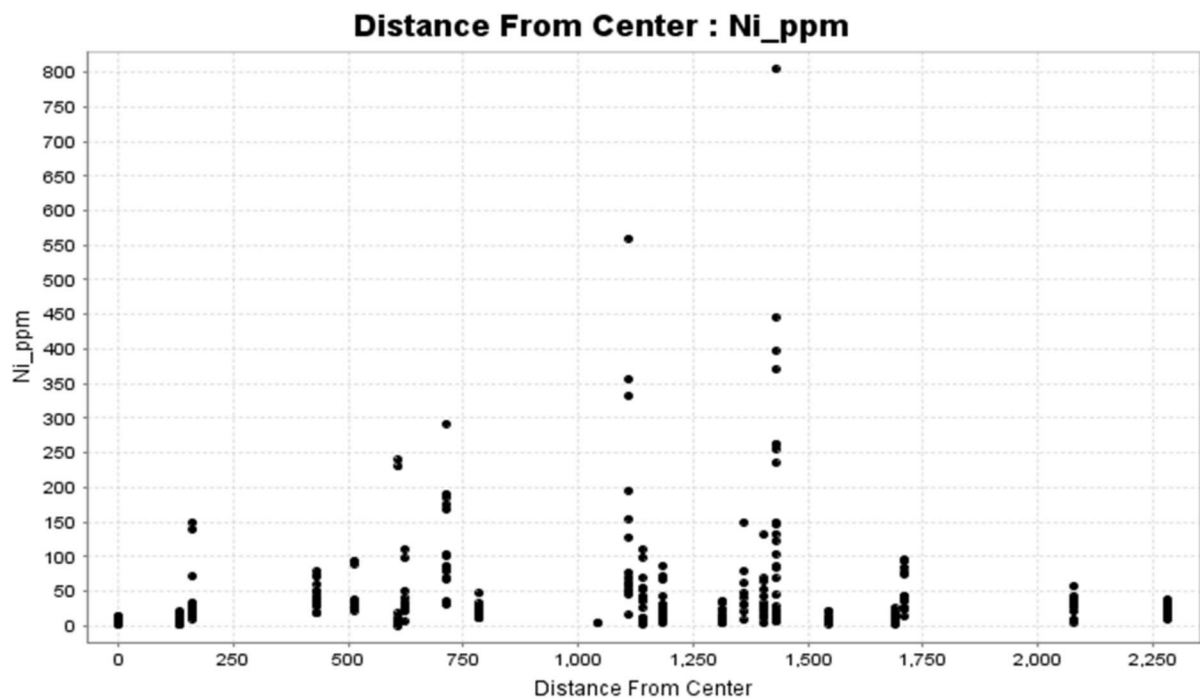


Figure 9.18: (Top) scatterplot showing the spot data values of Ni (ppm) plotted against the samples' distance from the centre of the deposit at White Pine Fork; (bottom) an 8 equal tail quartile box and whisker plot showing the increasing trend away from the centre of deposit as a geochemical 'shoulder'.

9.2.2 Possible trace element geochemical vectors at Buckingham

There were not enough pyrite samples to create useful and statistically valid mineral chemistry vectors. The trace element concentrations of the elements in arsenian pyrite and pyrite, notably Au, did decrease away from the centre of deposit (Fig. 9.19). A magmatic component of the mineralising fluid sourced from intrusions is enriched in As relative to meteoric fluids in the host rocks (Audétat et al., 1998, Heinrich et al., 1999 and 2004). The presence of arsenian pyrite at the breccia pipe may explain the increased Au content. Deditius et al. (2011) showed experimentally that Au will partition into arsenian pyrite more easily than pyrite. This may explain the increased Au content in the breccia pipe arsenian pyrite samples at Buckingham. Other elements (which have been determined as vectoring tools in other studies), such as As, Cu, and Cd, showed similar high concentrations in pyrite at the centre of deposit (Fig. 9.19).

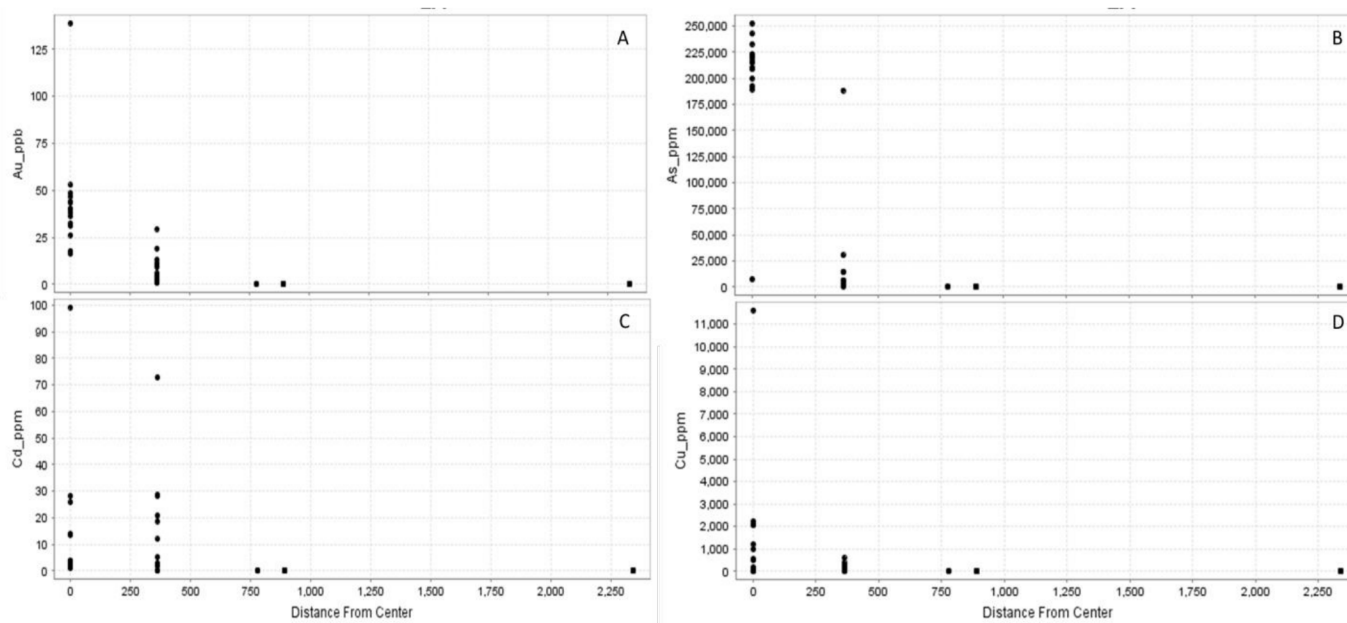


Figure 9.19: (below) Scatterplots showing the concentration of (A) Au, (B) As, (C) Cd, and (D) Cu in the pyrite and arsenian pyrite in relation to the distance from the centre of deposit. These elements, which have been used in past studies as vectoring tools.

9.2.3 *Au-rich rims around pyrite at Buckingham*

Arsenian pyrite containing large amounts of minor and trace elements is present in low- and high-temperature hydrothermal systems and sedimentary environments (Reich et al., 2005). The element maps created by LA-ICP-MS of the As-rich pyrite grains (on average ~5.5 wt % As) from the Buckingham study site showed precious metal-rich weathering rinds (Figs. 7.12, 7.13, and 7.14). The rinds are enriched in Au, Ag, As, Sb, Cu, and Mo but not Fe and S. If the rims of the pyrite grains were initially enriched in these elements, the resulting weathering rind would be as well. The increased Au concentration in the weathering rind may suggest an overprinting mineralisation similar to the proximal skarns or Carlin-style sediment hosted Au (Cline et al., 2005).

There are Au and Au ± Cu skarn deposits in the Copper Basin area, near these Eocene granites in the northern part of the study area. The Au is hosted dominantly in the metasedimentary rocks in iron-oxide veins that are thought to have originally been primary, high temperature, Fe-sulphides (Blake et al., 1992; Theodore et al., 1992). The Au mineralisation is thought to sit on the periphery of the larger porphyry deposit and represents shallow extensions of Eocene porphyries Cu-(Au-Mo) system (Seedorff et al., 2005). The presence of these Au-rich fluids in the area support the alternative explanation for the Au-rich rim, namely that the cores of the sulphides acted as traps for the precipitation of precious metals from the hydrothermal event associated with the proximal Eocene granite intrusions. These precious metals were later concentrated in the weathering rind during supergene alteration. Another possibility is that the high metal content in the oxide rims is a function of adsorption of ions from the system during weathering.

Chapter 10: Summary and Conclusions

This study characterised igneous and hydrothermal systems at two Mo-porphyry systems. The White Pine Fork Mo porphyry is the smaller of the two deposits, with an estimated resource of 16 Mt of Mo at 0.1% Mo (Bromfield and Patten, 1981). The mineralisation is associated with the White Pine intrusion, a K-feldspar- and quartz- porphyritic monzo- to syenogranite. U-Pb geochronology shows that the White Pine intrusion is younger than the larger Little Cottonwood stock (a K-feldspar-porphyritic monzogranite). The two intrusions are characterised by broadly similar geochemistry, however, the increased depletion in incompatible elements and the increased Si content in the White Pine intrusion show it is more evolved than the Little Cottonwood stock. The intrusions are characterised by an adakitic, LREE enrichment, HFSE depletions and fractionated HREE characteristic of a supra-subduction zone melt. The progressive depletion in incompatible elements from the Little Cottonwood to the White Pine intrusion implies a progressive melt evolution and is consistent with a broader evolution of the magma source in the Wasatch Mountains over time. The Mo mineralisation found in the White Pine Fork Mo breccia pipe was formed during the crystallisation of the White Pine intrusion which is characterised by average Mo abundances almost ten times greater than in the Little Cottonwood stock. The igneous clasts in the breccia pipe displayed large quartz phenocrysts similar to those observed in the White Pine intrusion, but not found in the Little Cottonwood stock. A clast within the breccia yielded a U-Pb age of 26.52 ± 0.42 Ma, which falls within the error of White Pine intrusion 26.61 ± 0.24 Ma (M. Baker: pers. comm., 2014) and indicates that the breccia must post date the White Pine intrusion. However, duplicate Re-Os ages of the Mo-mineralised quartz breccia cement (30.21 ± 0.14 and 29.84 ± 0.15 Ma) are older than the age of the White Pine intrusion, and instead correlate with the Little Cottonwood stock (U-Pb ages of

29.45±0.31 Ma, 29.63±0.27 Ma, and 29.91±0.34 Ma; M. Baker: pers. comm., 2014). This apparent contradiction is not supported by the cross-cutting relationships between the igneous intrusions in the field and may suggest that the Re-Os age is inherited from the older intrusion, however, Re-Os inheritance is not reported in the literature (R. Creaser, pers. comm., 2014).

The Buckingham Mo (-Cu) porphyry has an estimated resource of 1,000 Mt of Mo at 0.1% Mo (Theodore et al., 1992). Field mapping and petrology identified two different generations of intrusions in the study area. The Cretaceous suite was though pervasively and intensely hydrothermally altered, were determined to be K-feldspar- and quartz-porphyritic granites and no magmatic ferromagnesian minerals are preserved. The suite is characterised by LREE enrichment and fractionated HREEs and depleted incompatible elements. Theodore et al. (1992) interpreted this suite to belong to the Buckingham porphyry system. The younger, Eocene-aged intrusive rocks were feldspar- and quartz-porphyritic with a variation in the content of hornblende, biotite and titanite. The whole rock geochemistry of the Eocene granites is characterised by LREE enrichment and fractionated HREE signature. The Eocene granites were dated using U-Pb zircon and yielded Tertiary ages of 38.68±0.53, 39.28±0.58, 40.76±0.41, and 40.81±0.51 Ma, are consistent with the regional Tertiary magmatism in the Battle Mountain mining district (Theodore et al., 1992 and references therein). Both the Cretaceous and Eocene rocks are characterised by negative Nb, Ta and Ti anomalies and a slight enrichment of Zr and Hf consistent with a subarc mantle source. The trace element geochemistry and whole rock geochemistry of the Buckingham granites show a depletion of incompatible elements, suggesting that they formed from an evolved melt source.

The mineral chemistry of the alteration halos around the White Pine Fork Mo porphyry and the Buckingham Mo (-Cu), were investigated. The most prominent alteration style at both

sites was phyllic alteration characterised by an overprinting alteration found near the core of the system composed of abundant sericite + quartz + pyrite. The absence of greenrock minerals that have been investigated elsewhere (e.g., Cooke et al., 2014; Baig, 2015; Wilkinson et al., 2015) meant that this study focused on the mineral chemistry of quartz and pyrite. Other types of hydrothermal alteration observed included potassic (orthoclase \pm biotite \pm magnetite) at the White Pine Fork Mo breccia pipe and advanced argillic alteration (quartz + alunite + kaolinite \pm pyrophyllite) surrounding the Buckingham system (Fig. 7.2). At both study sites, the phyllic alteration was expressed as a partial to complete replacement of the feldspars (found in the groundmass of the granite and as phenocrysts or as the interstitial material to the quartz clasts in the quartzites at Buckingham) to white micas (i.e., sericite, muscovite, phengite, paragonite, and kaolinite). The phyllic alteration also formed quartz + sericite + pyrite veins. The pyrite also occurred sporadically throughout the groundmass as isolated grains which occasionally contained other sulphide mineral inclusions at both deposits. The hydrothermal alteration at White Pine Fork was successfully mapped out by whole rock geochemistry using the element zonation outlined by Halley et al. (2015). The increase of the ore elements and a depletion of Zn suggest potassic alteration which has been almost completely replaced by the phyllic alteration. The whole rock geochemistry also substantiates the domains of intense phyllic alteration. At Buckingham, the whole rock geochemistry can be used to identify zones of early potassic alteration (increased Au, Cu, and Mo and decreased Pb and Zn) as well as the overprinting phyllic alteration (increased Li and Sb; Halley et al., 2015).

The quartz trace element geochemistry for the two study sites was collected and analysed for two purposes: to investigate possible geochemical vectors to the centre of the deposit which could aid in exploration for other porphyry systems and as a fingerprinting tool to help

distinguish between hydrothermal, detrital, igneous, and breccia cement quartz. At White Pine, the only potential vectoring tool was the increasing Li content towards the centre of the system in the hydrothermal quartz. However, the trace element geochemistry was more useful for fingerprinting the different types of quartz as the hydrothermal (vein and breccia cement quartz) samples have higher Ti and As than the igneous quartz (Fig. 9.2). At Buckingham, the quartz data was collected from igneous, sedimentary, vein and breccia (hydrothermal) samples. The abundance of Al in the hydrothermal quartz varied the most closely to and at the centre of deposit with an apparent decrease away from the centre although this may also reflect a smaller data set. The other promising vector is Sb, which decreases away from the centre of the deposit. Antimony in quartz, at detectable levels, appears to be restricted to hydrothermal quartz within 1800 m of the centre of the system, with the highest concentration found in the samples proximal to the centre. The breccia cement at the centre of the deposit showed the highest concentration of Al, Li, K, Ca, As, and Sb, and the metals (i.e., Cu, Fe, Zn, and Pb). Whereas the igneous and sedimentary quartz showed the highest Ti values which contrasts with the White Pine results. The substitution of Al and Ti into quartz is a function of the chemistry and temperature of the precipitating fluid (Corbett and Leach, 1998). The decreased partitioning of Ti into quartz is the result of a decrease in temperature and pressure (Corbett and Leach, 1998). This decrease in Ti facilitates the substitution of Al in the crystal lattice which, in turn, reflects the aqueous Al concentration as a lower fluid pH greatly increases the solubility of Al. The As and Sb concentrations are not direct element substitutions, but rather located interstitially to the Si and O in the crystal lattice of the quartz. In comparison to other studied Mo porphyries, Bingham Canyon showed some similarities and differences to the White Pine Fork and Buckingham. The hydrothermal quartz chemistry showed that Bingham Canyon had the highest Sb, Al and metal

content in quartz. These element substitutions in the vein quartz suggest an argillic or late-stage clay mineral alteration and possible epithermal-like mineralisation at Bingham Canyon. As well, the increased metal tenor might be the result of a large, well-mineralised hydrothermal system.

The inability to apply other geochemical vectors from the P1060 that have worked at other study sites (e.g., MAX Mo and Bingham Canyon) will help constrain the applicability, the restrictions and complications of these exploration tools. The small size of the White Pine deposit may explain why the tools did not work well, as the hydrothermal system may have been too small to generate significant changes in the mineral chemistry; however the small MAX Mo porphyry did show some promising mineral chemistry vectors. This may indicate the minimum size required to generate effective vectors or alternatively differences in the host rock compositions (monzogranites at White Pine Fork and granodiorites at MAX Mo; Baig, 2015). At the Buckingham site, it is possible that the unexpectedly large size of the system or overlapping hydrothermal systems as suggested by Theodore et al. (1992) have complicated the results. Further study might help resolve this.

The pyrite from both study sites was interpreted to be completely hydrothermal in origin based on its occurrence predominantly in quartz veins and the fact that the least altered lithologies did not contain pyrite as a magmatic mineral. At both study sites, the pyrite had been weathered to produce Fe-oxide and -hydroxide weathering rinds and partial to complete grain replacement, making the sampling of large enough pyrite grains for analytical work difficult. At White Pine Fork, the pyrite was concentrated within a halo around the breccia pipe in the Little Cottonwood stock (Fig. 4.1). The best mineral geochemical vector at the White Pine Fork Mo porphyry was the Ni content in the pyrite which increased away from the centre of the deposit to ~1400 m before decreasing. The pyrite at the Buckingham study site was difficult to analyse, due

to the extensive supergene alteration in the study area. The surviving grains contained a core of pyrite and well-developed weathering rinds. The small pyrite sample population at Buckingham meant that statistically sound geochemical vectors could not be created, but the trace element concentrations of Au, Cu, and Cd in pyrite did decrease away from the centre of deposit. The weathering rinds of the pyrite at Buckingham were enriched in everything except Fe and S. Notably, the weathering rinds are enriched in Au, Ag, Cu, As, Sb and Mo. The increased Au concentration in the weathering rind may suggest an overprinting mineralisation similar to the proximal skarns or Carlin-style sediment hosted Au which has been reported in the Battle Mountain district, which lies along the Eureka Au trend (Cline et al., 2005). The ages generated from the Tertiary granites, as well, as the reported Au and Au \pm Cu skarn deposits in the Copper Basin area, suggest Carlin-style Au mineralisation.

The different behaviours of the trace element geochemistry in quartz and pyrite at different deposits are likely related to the hydrothermal system. At White Pine Fork, a small, single intrusion is present, creating a localized and weaker hydrothermal system. At Buckingham, the larger system and the presence of several areas of intense hydrothermal alteration (as shown by the numerous breccia pipes) may have resulted in less exact, or overlapping geochemical signatures.

The comparison of a smaller (White Pine Fork) and larger (Buckingham) Mo porphyry has helped to refine the processes associated with hydrothermal alteration around Mo porphyry deposits and the applicability of trace element chemistry of alteration minerals as exploration tools. The granites share similar mineralogy, geochemistry and hydrothermal alteration, which is predominantly phyllic at both sites. However, despite the similarities there are differences in the mineral chemistry which may reflect the small size or complex nature of the deposits.

References

- Audétat A., Günther D. and Heinrich C. A., 1998. Formation of a magmatic–hydrothermal ore deposit: insights with LA-ICP-MS analysis of fluid inclusions. *Science*, 279, pp. 2091–2094
- Austin, K. and Ballentyne, G., 2010. Geology and Geochemistry of Deep Molybdenum Mineralization at the Bingham Canyon Mine, Utah, USA. In: Krahulec, K. and Schroeder, K (Eds.), *Tops and Bottoms of Porphyry Copper Deposits: The Bingham and Southwest Tintic Districts, Utah*. Society of Economic Geologists, Inc. Guidebook Series, 41, pp. 35-49
- Baig, A., 2015. Geology and mineral chemistry of the MAX Mo-porphyry system, British Columbia. Unpublished M.Sc. Thesis, Thunder Bay, ON, Lakehead University, 174 p.
- Baker, J., Peate, D., Waight, T. and Meyzen, C., 2004. Pb isotopic analysis of standards and samples using a Pb-207-Pb-204 double spike and thallium to correct for mass bias with a double-focusing MC-ICP-MS. *Chemical Geology*, 211, pp. 275-303
- Barton, M. D., 1996. Granitic magmatism and metallogeny of southwestern North America. *Earth Sciences*, 87, pp. 261-280
- Bayliss, P., 1989. Crystal chemistry and crystallography of some minerals within the pyrite group. *American Mineralogy*, 74, pp. 1168–1176
- Black L. P., Gulson B. L. 1978. The age of the Mud tank Carbonatite, Strangways Range, Northern Territory. *BMR Journal of Australian Geology and Geophysics*, 3, pp. 227-232

- Black, L. P., Kamos, L., Allen, C.M., Aleinikoff, J.N., Davis, D.W., Korsch, R.J., Foudoulis, C., 2003. TEMORA 1: a new zircon standard for Phanerozoic U–Pb geochronology. *Chemical Geology*, 200, pp. 155– 170
- Black, L.P., Kamo, S.L., Allen, C.M., Davis, D.W., Aleninikoff, J.N., Valley, J.W., Mundil, R., Campbell, I.H., Korsch, R.J., Williams, I.S., Foudoulis, C., 2004. Improved $^{206}\text{Pb}/^{238}\text{U}$ microprobe geochronology by the monitoring of a trace-element related matrix effect; SHRIMP, ID-TIMS, ELA-ICP-MS, and oxygen isotope documentation for a series of zircon standards. *Chemical Geology*, 205, pp. 115-140
- Blake, D. W., 1992. Supergene copper deposits at Copper Basin. In: Theodore, T. G., Blake, D. W., Loucks, T. A., and Johnson, C. A. (Eds.), *Geology of the Buckingham stockwork molybdenum deposit and surrounding area, Lander County, Nevada*. U. S. Geological Survey Professional Paper 798-D, pp. 154-167
- Bongiolo E., Patrier-Mas, P., Mexias, A., Beaufort, D. and Laquintinie, M., 2008. Spatial And Temporal Evolution Of Hydrothermal Alteration At Lavras Do Sul, Brazil: Evidence From Dioctahedral Clay Minerals. *Geoscience World*, 56, 2, pp. 222-243
- Breiter, K., Ackerman, L., Svojtka, M., and Müller, A., 2013. Behavior of trace elements in quartz from plutons of different geochemical signatures: A case study from the Bohemian Massif, Czech Republic. *Lithos*, 175-176, pp. 54–67
- Bromfield, C.S. and Patten, L.L., 1981. Mineral resources of the Lone Peak Wilderness Study Area, Utah and Salt Lake Counties, Utah. In: *U.S. Geological Survey Bulletin 1491*, 117 p.

- Campbell F. A. and Ethier V. G., 1984. Nickel and cobalt in pyrrhotite and pyrite from the Faro and Sullivan orebodies. *Canadian Mineralogist*, 22, pp. 503–506
- Carten, R. B., White, W. H., and Stein, H. J., 1993. High-grade granite-related molybdenum systems: Classification and origin. In: Kirkham, R. V., Sinclair, W. D., Thorpe, R. I., and Duke, J. M. (Eds.), *Mineral deposit modeling: Geological Association of Canada Special Paper 40*, pp. 521-554
- Chabert, M., 1997. Campana Mahuida porphyry copper project, Neuquén, Argentina. Preliminary report. *Biblioteca de la Dirección de Minería de Neuquén*, 1, 40 p.
- Chang, Z., Vervoort, J. D., McClelland, W. C., and Knaack, C., 2006. U-Pb dating of zircon by LA-ICP-MS: *Geochemistry, Geophysics, Geosystems*, 7
- Chiaradia, M., 2009. Adakite-like rocks from fractional crystallization and assimilation of mafic lower crust: Eocene Macuchi arc (Western Cordillera, Ecuador). *Chemical Geology*, 265, pp. 468–487
- Chiaradia, M., Ulianov, A., Kouzmanov, K., Beate, B., 2012. Why large porphyry Cu deposits like high Sr/Y magmas? *Sci. Rep.*, 2, 685, 7 p.
- Cline, J. S., Hofstra, A. H., Muntean, J. L., Tosdal, R. D., and Hickey, K. A., 2005. Carlin-Type Gold Deposits in Nevada: Critical Geologic Characteristics and Viable Models. *Economic Geology 100th Anniversary Volume*, pp. 451–484
- Compston, W., 1999. Geological age by instrumental analysis: the 29th Hallimond Lecture. *Mineralogical Magazine*, 63, pp. 297-311

- Cooke, D.R., Hollings, P., Wilkinson, J.J., Tosdal, R.M., 2014. Geochemistry of porphyry deposits. In: H.D. Holland, K.K. Turekian (Eds.), *Treatise on Geochemistry* (Second edition), Elsevier, Oxford, pp. 357–381
- Corbett, G.J. and Leach, T.M., 1998. Controls on Hydrothermal Alteration and Mineralization. *Society of Economic Geologists Special Publication, No. 6*, pp. 69-82
- Creaser, R.A., Papanastassiou, D.A., and Wasserburg, G.J., 1991. Negative thermal ion mass spectrometry of osmium, rhenium and iridium: *Geochimica et Cosmochimica Acta*, 55, pp. 397–404
- Crittenden, M. D., 1965. Geology of the Dromedary Peak quadrangle, Utah. *USGS Geologic Quadrangle: 378*
- Crittenden, M. D., Christie-Blick, N., and Link, P. K., 1983. Evidence for two pulses of glaciation during the late Proterozoic in northern Utah and southeastern Idaho. *Geological Society of America Bulletin*, 94, 4, pp. 437-450
- Crittenden, M.D., Jr., 1977. Stratigraphic and structural setting of the Cottonwood area, Utah. In: Hill, J. D. (Ed.), *Geology of the Cordilleran hingeline*. Denver, Rocky Mountain Associated Geologists, pp. 363-379
- Davidson, P., Kamenetsky, V.S., Cooke, D.R., Frikkien, P., Hollings, P., Ryan, C, Van Achterbergh, E., Mernagh, T., Skarmeta, J., Serrano, L., and Vargas, R, 2005. Magmatic precursors of hydrothermal fluids at the Río Blanco Cu-Mo deposit, Chile: Links to silicate magmas and metal transport. *Economic Geology*, 100, pp. 963–978

- Deditius, A. P., Reich, M., Kesler, S. E., Utsunomiya, S., Chryssoulis, S. L., Walshe, J., and Ewing, R. C., 2014. The coupled geochemistry of Au and As in pyrite from hydrothermal ore deposits. *Geochimica et Cosmochimica Acta*, 140, pp. 644–670
- Deditius, A.P., Utsunomiya, S., Kesler, S.E., Reich, M., and Ewing, R.C., 2011. Trace elements nanoparticles in pyrite. *Ore Geology Review*, 42, pp. 32–46
- Defant M. and Kepezhinskas, P., 2001. Evidence suggests slab melting in arc magmas. *EOS*, 82, pp. 65–69
- Defant, M. and Drummond, M., 1990. Derivation of some modern arc magmas by melting of young subducted lithosphere. *Nature*, 347, pp. 662-665
- Dennen, W.H., 1966. Stoichiometric substitution in natural quartz. *Geochimica et Cosmochimica Acta*, 30, pp. 1235-1241. In: (1967) Trace elements in quartz as indicators of provenance. *Geological Society of America Bulletin*, 78, pp. 125-130
- Dennen, W.H., Blackburn, W.H., and Quesada, A., 1970. Aluminium in quartz as a geothermometer. *Contributing Mineralogy and Petrology*, 27, pp. 332-342
- Dilles, J.H., Einaudi, M.T., Proffett, J., and Barton, M.D., 2000. Overview of the Yerington porphyry copper district: Magmatic to nonmagmatic sources of hydrothermal fluids: Their flow paths and alteration effects on rocks and Cu-Mo-Fe-Au ores. *Society of Economic Geologists Guidebook Series*, 32, pp.55–66
- Faure, G., 1986. The Rb-Sr method of dating. In: *Principles of Isotope Geology*, Second Edition. John Wiley and Sons, New York, pp. 117-140

- Fryer, B.J., Jackson, S.E., Longerich, H.P., 1993. The Application of Laser Ablation Microprobe-Inductively Coupled Plasma-Mass Spectrometry (LA-ICP-MS) to in situ (U)-Pb Geochronology. *Chemical Geology*, 109, 1-8
- Garwin, S., 2002. The geological setting of intrusion-related hydrothermal systems near the Batu Hijau porphyry copper-gold deposit, Sumbawa, Indonesia. *Society of Economic Geologists, Special Publication, No. 9*, pp. 333-366
- Gettings, M., 2005. Magnetic mineralogy and models of magnetic susceptibility for altered rocks of the Stinking water porphyry, Wyoming, USA. Accessed at: <http://www.cosis.net/abstracts/IAGA2005/00691/IAGA2005-A-00691.pdf>
- Götze, J., Krbetschek, M.R., Habermann, D. and Wolf, D., 2001. High-resolution cathodoluminescence studies of feldspar minerals. In: Pagel, M., Barbin, V., Blanc, P. and Ohnenstetter, D. (Eds.), *Cathodoluminescence in Geosciences*, pp. 245-270
- Gustafson, L.B., and Hunt, J.P., 1975. The porphyry copper deposit at El Salvador, Chile. *Economic Geology*, 70, pp. 857-912
- Halley, S., Dilles, J., and Tosdal, R., 2015. Footprints: Hydrothermal Alteration and Geochemical Dispersion Around Porphyry Copper Deposits. *Society of Economic Geologists Newsletter*, January, 100, pp. 11-17
- Hanley J. J., MacKenzie M. K., Warren M. R., and Guillong M., 2010. Distribution and origin of platinum-group elements in alkalic porphyry Cu-Au and low sulfidation epithermal Au deposits in the Canadian Cordillera. In: 11th International Platinum Symposium, June 21-24

- Harley, S.L. and Kelly, N.M., 2007. Zircon: Tiny but timely. *Elements*, 3, 1, pp. 13-18
- Heinrich C. A., Driesner T., Stefánsson A. and Seward T. M., 2004. Magmatic vapour contraction and the transport of gold from porphyry environment to epithermal ore deposits. *Geology*, 32, pp. 761–764
- Heinrich C. A., Gunther D., Audétat A., Ulrich T. and Frischknecht R., 1999. Metal fractionation between magmatic brine and vapour, determined by microanalysis of fluid inclusions. *Geology*, 27, pp. 755–758
- Henry, C.D., and Ressel, M.W., 2000. Eocene magmatism of northeastern Nevada: the smoking gun for Carlin-type gold deposits. In: Cluer, J.K., Price, J.G., Struhsacker, E.M., Hardyman, R.F., and Morris, C.L. (Eds.), *Geology and Ore Deposits 2000: The Great Basin and Beyond*. Geological Society of Nevada, pp. 365–388
- Holliday, J.R., and Cooke, D.R., 2007. Advances in geological models and exploration methods for copper ± gold porphyry deposits. Decennial International Conference on Mineral Exploration 5, Toronto, Canada, Conference Proceedings, pp. 791–809
- Hollings, P., Cooke, D.R., Waters, P., and Cousens, B., 2011a. Igneous geochemistry of mineralized rocks of the Baguio district, Philippines: Implications for tectonic evolution and the genesis of porphyry-style mineralisation. *Economic Geology*, 106, pp. 1317–1333
- Hollings, P., Wolfe, R., Cooke, D.R., and Waters, P., 2011b. Geochemistry of Tertiary igneous rocks of Northern Luzon, Philippines: Evidence for a back-arc setting for alkalic porphyry copper-gold deposits slab roll-back?. *Economic Geology*, 106, pp. 1257–1277

- Hough R., Reich M. and Noble R., 2012. Noble Metal Nanoparticles in Ore Systems. In: Barnard, A. S. and Guo, H (Eds.), Nature's Nanostructures. Pan Stanford Publishing Pte. Ltd., pp. 978–981
- Howard, K.A. (Eds.), Tectonics and Stratigraphy of the Eastern Great Basin: Geological
- Jackson, S.E., Pearson, N.J., Griffin, W.L., Belousova, E.A., 2004. The application of laser ablation-inductively coupled plasma-mass spectrometry to in situ U–Pb zircon geochronology. *Chemical Geology*, 211, pp. 47-69
- John, D. A., 1997. Geologic setting and characteristics of mineral deposits in the central Wasatch Mountains, Utah. In: John, D.A., and Ballantyne, G.H. (Eds.), *Geology and ore deposits of the Oquirrh and Wasatch Mountains*. Society of Economic Geologists Guidebook no. 29, pp. 11-33
- John, D. A., 2001. Miocene and early Pliocene epithermal gold-silver deposits in the northern Great Basin, western United States: Characteristics, distribution, and relationship to magmatism. *Economic Geology*, 96, pp. 1827-1853
- John, D. A., Turrin, B.D., and Miller, R. J., 1997. New K-Ar and $^{40}\text{Ar}/^{39}\text{Ar}$ Ages of Plutonism, Hydrothermal Alteration, and Mineralization in the Central Wasatch Mountains, Utah. *Society of Economic Geologists, Inc. Guidebook Series*, 29, pp. 47-57
- John, D.A., 1989. Geologic setting, depth of emplacement and regional distribution of fluid inclusions in middle Tertiary intrusions of the central Wasatch Mountains, Utah. *Economic Geology*, 84, pp. 386-409

- Kaneda H., Shimazaki H. and Lee M. S., 1986. Mineralogy and geochemistry of the Au–Ag ore deposits of the South Korean Peninsula. *Mineralium Deposita*, 21, pp. 234–243
- Kay, S.M., and Mpodozis, C., 2002. Magmatism as a probe to the Neogene shallowing of the Nazca of the Nazca plate beneath the modern Chilean flat-slab. *Journal of South American Earth Sciences*, 15, pp. 39–57
- Keeler, D. A., 2010. Structural reconstruction of the copper basin area, battle mountain district, Nevada. Department of Earth Sciences: The University Of Arizona. 92 p.
- Keith, J., Christiansen, E., and Carten, R., 1995. The genesis of giant porphyry molybdenum deposits. Society of Economic Geologists. Special Publications, No. 2, pp. 285-315
- Kirkham, R. and Sinclair, W., 1996. Porphyry copper, gold, molybdenum, tungsten, tin, silver. In: Eckstrand, O. R., Sinclair, W. D., and Thrope, R. I. (Eds.), *Geology of Canadian Mineral Deposit Types*. GSC, Geology of Canada, No. 8, pp. 421-446
- Kosler J. and Sylvester P.J., 2003. Present trends and the future of zircon in geochronology; laser ablation ICP-MS. *Reviews in Mineralogy and Geochemistry*, 53, pp. 243-275
- Kosler, J., 2001. Laser-ablation ICP-MS study of metamorphic minerals and processes. In: Sylvester P. J. (Ed.), *LA-ICP-MS in the earth sciences; principles and applications*. Mineralogical Association of Canada Short Course Handbook, 29, pp. 185-202
- Kotlyar, B.B., Theodore, T.G., Singer, D.A., Moss, Ken, Campo, A.M., and Johnson, S.D., 1998. Geochemistry of the gold skarn environment at Copper Canyon, Nevada. *Economic Geology*, pp. 209-242

- Large R. R., Danyushevsky L. V., Hollit C., Maslennikov V., Meffre S., Gilbert S. E., Bull S., Scott R. J., Emsbo P., Thomas H., Singh B. and Foster J., 2009. Gold and trace element zonation in pyrite using a laser imaging technique: implications for the timing of gold in orogenic and Carlin-style sediment-hosted deposits. *Economic Geology*, 104, pp. 635–668
- Large, R.R., Danyushevsky, L.V., Hollit, C., Maslennikov, V., Meffre, S., Gilbert, S., Bull, S., Scott, R., Emsbo, P., Thomas, H., and Foster, J., 2009. Gold and trace element zonation in pyrite using a laser imaging technique: Implications for the timing of gold in orogenic and Carlin-style sediment-hosted deposits. *Economic Geology*, 104, pp. 635–668
- Lehmann, G., 1975. On the colour centres of iron in amethyst and synthetic quartz: a discussion. *American Mineralogist*, 60, pp. 335-337
- Li, X., Long, W.G., Li, Q.L., Liu, Y., Zheng, Y.F., Yang, Y.H., Chamberlain, K.R., Wan, D.F., Guo, C.H., Wang, X.C., Tao, H., 2010. Penglai Zircon Megacrysts: A Potential New Working Reference Material for Microbeam Determination of Hf-O Isotopes and U-Pb Age. *Geostandards and Geoanalytical Research*, 34, pp. 117-134
- Lowell, J.D. and Guilbert, J.M., 1970. Lateral and vertical alteration–mineralization zoning in porphyry ore deposits. *Economic Geology*, 65, pp. 373–408
- Meffre, S., Large, R. R., Scott, R., Woodhead, J., Chang, Z., Gilbert, S. E., Danyushevsky, L. V., Maslennikov, V., and Hergt, J. M., 2008. Age and pyrite Pb-isotopic composition of the giant Sukhoi Log sediment-hosted gold deposit, Russia. *Geochimica et Cosmochimica Acta*, 72, pp. 2377-2391

- Meunier, A. and Velde, B., 1982. Phengitization, Sericitization and potassium-beidellite in a hydrothermally-altered granite. *Clay Minerals*, 17, pp. 285-299
- Micko, J., 2010. The geology and genesis of the Central zone alkalic copper-gold porphyry deposit, Galore Creek district, northwestern British Columbia, Canada: Ph.D. thesis, Vancouver, University of British Columbia, 359 pp.
- Middlemost, A.K.: 1994. Naming materials in the magma/igneous rock system. *Earth-Science Reviews*, 37, pp. 215–224
- Mitchell, R. H. and Bergman, S. C., 1991. *Petrology of Lamproites*. New York: Plenum, 447 p.
- Müller, A., Wiedenbeck, M., Van Den Kerkhof, A. M., Kronz, A. and Simon, K., 2003. Trace elements in quartz – a combined electron microprobe, secondary ion mass spectrometry, laser-ablation ICP-MS, and cathodoluminescence study. *European Journal of Mineralogy*, 15, pp. 747–763
- Naeser, C.W., Bryant, B., Crittenden, M.D.J. and Sorensen, M.L., 1983. Fission-track ages of Nevada Bureau of Mines and Geology, 2004. *The Nevada mineral industry 2003*: Nevada Bureau of Mines and Geology Special Publication MI-2003, 78 p.
- Newsom, H.E., and Palme, H., 1984. The depletion of siderophile elements in the Earth's mantle: new evidence from molybdenum and tungsten. *Earth Planetary Science Letters*, 69, pp. 354-364

- Newsom, H.E., White, W. M., Jochum, K.P., and Hofman, A.W., 1986. Siderophile and chalcophile element abundances in oceanic basalts, Pb isotope evolution and growth of the Earth's core. *Earth Planetary Science Letters*, 80, pp. 299-313
- Norman, D.K., Parry, W.T., Bowman, J.R., 1991. Petrology and geochemistry of propylitic alteration at Southwest Tintic, Utah. *Economic Geology*, 86, pp. 13–28
- Palenik, C.S., Ustunomiya, S., Reich, M., Kesler, S.E., Wang, L., Ewing, R.C., 2004. “Invisible” gold revealed: direct imaging of gold nanoparticles in a Carlin-type deposit. *American Mineralogist*, 89, pp. 1359–1366
- Palenik, C.S., Utsunomiya, S., Reich, M., Kesler, S.E., Wang, L. and Ewing, R.C., 2004. Invisible gold revealed: direct imaging of gold nanoparticles in a Carlin-type deposit. *American Mineralogist*, 89, pp. 1359-1366
- Parry, W. T. and Bruhn, R. L., 1987. Fluid inclusion evidence for minimum 11 km vertical offset on the Wasatch Fault, Utah. *Geology*, 15, pp. 67–70
- Parry, W. T., Wilson, P.N., and Jasumback, M.D., 1998. Clay mineralogy and $^{40}\text{Ar}/^{39}\text{Ar}$ dating of phyllic and argillic alteration at Bingham Canyon, Utah. In: John, D.A. and Ballantyne, G.H., (Eds.), *Geology and Ore Deposits of the Oquirrh and central Wasatch Mountains, Utah*. Society of Economic Geologists Guidebook, 29 (second edition), pp. 171–188
- Parry, W. T., Wilson, P.N., Moser, D, and Heizler, M. T., 2001. U-Pb dating of zircon and $^{40}\text{Ar}/^{39}\text{Ar}$ dating of biotite at Bingham, Utah. *Economic Geology*, 96, pp. 1671–1683
- Parry, W.T. and Bruhn, R.L., 1986. Pore fluid and seismogenic characteristics of fault rock at depth on the Wasatch Fault, Utah. *Journal of Geophysical Research* 91, pp. 730-744.

- Paton, C., Woodhead, J. D., Hellstrom, J. C., Hergt, J. M., Greig, A., and Maas, R., 2010. Improved laser ablation U-Pb zircon geochronology through robust down-hole fractionation correction. *Geochemistry, Geophysics, Geosystems*, 11, pp. 1525-2027
- Prelević D, Foley, S., Cvetković V., and Romer, R., 2004. Origin of Minette by Mixing of Lamproite and Dacite Magmas in Veliki Majdan, Serbia. *Journal of Petrology*, 45, 4, pp. 759-792
- Rae, A.J., Cooke, D.R., Phillips, D., Yeats, C., Ryan, C., Hermoso, D., 2003. Spatial and temporal relationships between hydrothermal alteration assemblages at the Palinpinon geothermal field, Philippines: implications for porphyry and epithermal ore deposits. In: (Eds.) S.F. Simmons, I. Graham; *Volcanic, Geothermal, and Ore-forming Fluids: Rulers and Witnesses of Processes within the Earth*, Society of Economic Geologists, Special Publication, No. 10, pp. 223–246
- Raymond O. L., 1996. Pyrite composition and ore genesis in the Prince Lyell copper deposit, Mt Lyell mineral field, western Tasmania, Australia. *Ore Geology Reviews*, 10, pp. 231–250
- Reich M., Deditius A., Chryssoulis S., Li J. W., Ma C. Q., Parada M. A., Barra F. and Mittermayr F., 2013. Pyrite as a record of hydrothermal fluid evolution in a porphyry copper system: a SIMS/EMPA trace element study. *Geochimica et Cosmochimica Acta*, 104, pp. 42–62
- Reich, M., Kesler, S. E., Utsunomiya, S., Palenik, C. S., Chryssoulis, S. L. and Ewing, R. C., 2005. Solubility of gold in arsenian pyrite. *Geochimica et Cosmochimica Acta*, 69, pp. 2781–2796

- Richards, J. and Kerrich, R., 2007. Adakite-like rocks: Their diverse origins and questionable role in metallogenesis. *Economic Geology*, 102, Special Paper, pp. 537-576
- Roberts, R.J., 1964. Stratigraphy and structure of the Antler Peak quadrangle, Humboldt and Lander Counties, Nevada. U.S. Geological Survey Professional Paper 459-A, 93 p.
- Roberts, R.J., Hotz, P.E., Gilluly, J. and Ferguson, H.G., 1958. Paleozoic rocks in north-central Nevada. *American Association Petroleum Geologists Bulletin*, 42, 12, pp. 2813-2857
- Roca Mines, Inc., 2005. Preliminary Assessment, ROCA Mines Inc. MAX Molybdenum Project. Prepared by: Leong, K. In: MAX Molybdenum Project Scoping Study – May 2005
- Rohrlach, B. and Loucks, R., 2005. Multi-million-year cycling ramp-up of volatiles in a lower crustal magma chamber reservoir trapped below the Tampakan copper–gold deposit by Mio-Pliocene crustal compression in the southern Philippines. In: Porter, T. (Ed), *Super Porphyry Copper and Gold Deposits: A Global Perspective*. Adelaide:PGC Publishing; 270 p.
- Rollinson, H., 1993. *Using geochemical data: evaluation, presentation, interpretation*. Pearson Education Limited. Harlow, England. 352 p.
- Ross, P-S., Jébrak, M., and Walker, B., 2002. Discharge of hydrothermal fluids from a magma chamber and concomitant formation of a stratified breccia zone at the Questa Porphyry molybdenum deposit, New Mexico. *Economic Geology*, 97, pp. 1679-1699
- Rusk, B. G., Maydagan, L., Franchini, M., Mao, W. and Li, X., 2014. Cathodoluminescence and trace elements in quartz from porphyry-type ore deposits. GSA Annual Meeting in Vancouver, British Columbia (19–22 October 2014), Paper No. 293-1

- Rusk, B., 2010. Insights into hydrothermal processes from cathodoluminescence and trace elements in quartz. Proceedings of the 10th Biennial Meeting of the SGA, No. 2, pp. 749-751
- Rusk, B., Koenig, A., and Lowers, H., 2011. Visualizing trace element distribution in quartz using cathodoluminescence, electron microprobe, and laser ablation-inductively coupled plasma-mass spectrometry. *American Mineralogist*, 96, No. 5-6, pp. 703-708
- Rusk, B., Lowers, H., and Reed, M., 2008. Trace elements in hydrothermal quartz: Relationships to cathodoluminescent textures and insights into vein formation. *Geology*, 47, pp. 547-550
- Rusk, B., Reed, M., Dilles, J., and Kent, A., 2006. Intensity of quartz cathodoluminescence and trace element content of quartz from the porphyry copper deposit in Butte, Montana. *American Mineralogist*, 91, pp. 1300–1312
- Sack, P.J., Berry, R.F., Meffre, S., Falloon, T.J., Gemmell, J.B., Friedman, R.M., 2011. In situ location and U-Pb dating of small zircon grains in igneous rocks using laser ablation-inductively coupled plasma-quadrupole mass spectrometry. *Geochemistry, Geophysics, Geosystems*, 12
- Schmid-Beurmann P. and Bente K., 1995. Stability properties of $\text{CuS}_2\text{-FeS}_2$ solid solution series pyrite type. *Mineralogy and Petrology*, 53, pp. 333–341
- Schütte, P., Chiaradia, M., Beate, B., 2010. Petrogenetic Evolution of Arc Magmatism Associated with Late Oligocene to Late Miocene Porphyry-Related Ore Deposits in Ecuador. *Economic Geology*, 105, pp. 1243-1270

- Seedorff, E., 1991. Magmatism, extension, and ore deposits of Eocene to Holocene age in the Great Basin--Mutual effects and preliminary proposed genetic relationships. In: Raines, G. L., Lisle, R. E., Schafer, R. W. and Wilkinson, W. H. (Eds.), *Geology and ore deposits of the Great Basin*. Geological Society of Nevada, Symposium, Reno/Sparks, April 1990, Proceedings, 1, pp. 133-178
- Seedorff, E., Dilles, J. H., Proffett, J. M., Jr., Einaudi, M. T., Zurcher, L., Stavast, W. J. A., Johnson, D. A., and Barton, M. D., 2005. Porphyry deposits: Characteristics and origin of hypogene features. In: Hedenquist, J. W., Thompson, J. F. H., Goldfarb, R. J., and Richards, J. P. (Eds.), *Economic Geology 100th Anniversary Volume*, pp. 251-298
- Selby, D., and Creaser, R.A., 2001. Late and mid-Cretaceous mineralization in the Northern Cordillera: Constraints from Re-Os molybdenite dates. *Economic Geology*, 96, pp. 1461–1467
- Seo, J.H., Guillong, M., and Heinrich, C.A., 2012. Separation of molybdenum and copper in porphyry deposits: The roles of sulfur, redox and pH in ore mineral deposition at Bingham Canyon. *Economic Geology*, 107, pp. 333–356
- Shimazaki H. and Clark L. A., 1970. Synthetic FeS_2 – CuFe_2 solid solution and fukuchilite-like minerals. *Canadian Mineralogym* 10, pp. 648–664
- Silberling, N.J. and Roberts, R.J., 1962. Pre-Tertiary stratigraphy and structure of northwestern Nevada. Geological Society of America, Special Paper 72, 58 p.

- Sillitoe, R. H., 1987. Copper, gold and subduction: a trans-Pacific perspective. Pacific Rim Congress 87, Australasian Institute of Mining and Metallurgy Conference Proceedings, pp. 399-403
- Sillitoe, R., Hough, R., Reich, M., Noble, R., 2012. Noble Metal Nanoparticles in Ore Systems. In: Barnard, A. S. and Guo, H. (Eds.), Nature's Nanostructures, Pan Stanford Publishing Pte. Ltd., pp. 978–981
- Sillitoe, R.H., 1995. Exploration of porphyry copper lithocaps. In: Pacific Rim Congress 95, 19-22 November 1995, Auckland, New Zealand, proceedings: Carlton South, The Australasian Institute of Mining and Metallurgy, pp. 527-532
- Slama, J., Kosler, J., Condon, D.J., Crowley, J.L., Gerdes, A., Hanchar, J.M., Horstwood, M.S.A., Morris, G.A., Nasdala, L., Norberg, N., Schaltegger, U., Schoene, B., Tubrett, M.N. Shervais, J. W., 2001. Birth, death, and resurrection: The life cycle of suprasubduction zone ophiolites, *Geochemistry, Geophysics, Geosystems*, 2, 2000GC000080. Published January 31, 2001. Society of America Memoir 157, pp. 29–36
- Spencer, C. J., Hoiland, C. W., Harris, R. A., Link, P. K., Balgord, E. A., 2012. Constraining the timing and provenance of the Neoproterozoic Little Willow and Big Cottonwood Formations, Utah: Expanding the sedimentary record for early rifting of Rodinia. *Precambrian Research*, 204–205, pp. 57–65
- Sprinkel, D. A., 2014. The Uinta Mountains: A Tale of Two Geographies and More. Utah Geological Survey: Survey Notes, 46, 3, 3 p.

- Stewart, J.H., and Poole, F.G., 1974. Lower Paleozoic and uppermost Precambrian Cordilleran miogeocline, Great Basin, Western United States. In: Dickinson, W.R. (Ed.), Tectonics and sedimentation. Society of Economic Paleontologists and Mineralogists Special Publication 22, pp. 28-57
- Sun, S. S. and McDonough, W.F., 1989. Chemical and isotopic systematics of oceanic basalts: implications for mantle composition and processes. In: Magmatism in the ocean basins. Geological Society, Special Publication, 42, pp. 313–345
- Suzuki, K., 1996. Re-Os dating of molybdenites from ore deposits in Japan: Implications for the closure temperature of the Re-Os system for molybdenite and the cooling history of molybdenum ore deposits. *Geochimica et Cosmochimica Acta*, 64, pp. 223–232
- Tacker, R.C., and Candela, P.A., 1987. Partitioning of molybdenum between magnetite and melt: A preliminary experimental study of partitioning of ore metals between silicic magmas and crystalline phases. *Economic Geology*, 82, pp. 1827-1838
- Theodore, T. G., Blake, D. W., Loucks, T. A., and Johnson, C. A., 1992. Geology of the Buckingham stockwork molybdenum deposit and surrounding area, Lander County, Nevada. USGS Professional Paper: 798-D
- Theodore, T., 2012. Framework of Carlin-Type Gold Deposits. U.S. Geological Survey; Minerals.usgs.gov. N.p., 2012. Web. 20 July 2015
- Thomas, J. B. and Watson, E. B., 2011. Application of Ti-in-quartz solubility as a thermobarometer in rutile-free rocks. American Geophysical Union, Fall Meeting 2011, abstract #V11A-2489

- Tingey, D. G., Christiansen, E. H., Best, M. G., Ruiz, J., and Lux, D. R., 1991. Tertiary Minette and Melanephelinite Dikes, Wasatch Plateau, Utah - Records of Mantle Heterogeneities and Changing Tectonics. Earth Science Faculty Scholarship. Paper 97
- Valencia, V.A., Eastoe, C., Ruiz, J., Ochoa-Landin, L., Gehrels, G., Gonzalez-Leon, C., Barra, F., and Espinoza, E., 2008. Hydrothermal evolution of the porphyry copper deposit at La Caridad, Sonora, Mexico, and the relationship with a neighbouring high sulfidation epithermal deposit. *Economic Geology*, 103, pp. 473–491
- Vogel, T.A., Cambray, F.W., Constenius, K.N., 2001. Origin and emplacement of igneous rocks in the central Wasatch Mountains, Utah. *Rocky Mountain Geology*, 36, pp. 119-162
- Vogel, T.A., Cambray, F.W., Feher, L., Constenius, KN. and the WIB Research Team, 1997. Petrochemistry and emplacement history of the Wasatch igneous belt. *Society of Economic Geologists Guidebook*, No. 29, pp. 47-63
- Volkening, J., Walczyk, T., and Heumann, K.G., 1991. Osmium isotope ratio determinations by negative thermal ion mass spectrometry. *International Journal of Mass Spectrometry Ion Processes*, 105, pp. 147–159
- Wark, D. A. and Watson, E. B., 2006. TitanQ: a titanium-in-quartz geothermometer. *Contributions to Mineralogy and Petrology*, 152, pp. 743-754
- Weil, J.A., 1984. A review of electron spin spectroscopy and its application to the study of paramagnetic defects in crystalline quartz. *Physics and Chemistry of Minerals*, 10, pp. 149-165

- Whitehouse, M.J., 2008. Plesovice zircon - A new natural reference material for U-Pb and Hf isotopic microanalysis. *Chemical Geology*, 249, pp. 1-35
- Wiedenbeck, M., Alle, P., Corfu, F., Griffin W.L., Meier, M., Oberli, F., Vonquadt A., Roddick, J.C., Spiegel W., 1995. 3 Natural Zircon Standards for U-Th-Pb, Lu-Hf, Trace-Element and REE Analyses. *Geostandards Newsletter*, 19, pp. 1-23
- Wilkinson, J. J., Chang, Z., Cooke, D. R., Baker, M. J., Wilkinson, C. C., Inglis, S., Chen, H., Gemmell, J. B., 2015. The chlorite proximator: A new tool for detecting porphyry ore deposits. *Journal of Geochemical Exploration*, 152, May 2015, pp. 10–26
- William-Jones, A. E. and Heinrich, C. A., 2005. Vapor Transport of Metals and the Formation of Magmatic-Hydrothermal Ore Deposit. 100th Anniversary Special Paper: *Economic Geology*, 100, 7, pp. 1287-1312
- Willis, G.C., 1999. The Utah Thrust System – An Overview. In: Spangler, L.W., and Allen, C.J. (Eds.), *Geology of northern Utah and vicinity*. Utah Geological Association Publication, 27, pp. 1-9
- Zoback, M., 1983. Structure and Cenozoic tectonism along the Wasatch fault zone, Utah. *Geological Society of America Memoirs*, 157, pp. 3-28

APPENDICES

Appendix 1: Petrology

White Pine Fork Mo Porphyry

WP13ES03: Little Cottonwood stock

Mineral Modal Percentage:

Quartz – 25%

Plagioclase – 25%

K-feldspar – 35%

Muscovite and white mica – 10%

Chlorite – 2%

Biotite – 1%

Pyrite – 1%

Hematite – 1%

Titanite – <1%

Fluorite – <1%

This monzogranite has a coarse-grained quartz + orthoclase + albite groundmass showing a granitic texture with annealed grain boundaries. This sample has undergone sericite/white mica and other clay mineral(?) alteration. This alteration is restricted to the feldspars, with well-defined white muscovite laths occurring along the cleavage planes of the feldspars. In some of the albite grains, white mica replaces up to 70% of the grain. The primary biotite in the rock has been mostly altered to chlorite, intergrown muscovite and trace epidote. The grains show some Fe staining along the grain boundaries (hematite). The pyrite in the sample retained much of the cubic shape, but with pronounced Fe-oxide alteration rims.

Quartz – coarse-grained, anhedral and rounded grain shapes (quartz eyes). These grains show some undulatory extinction and are unaltered.

K-feldspar – the K feldspar in this sample occurs as mostly orthoclase and as anhedral-subhedral phenocrysts. Many of the smaller grains show perthitic exsolution. The grains are altered to sericite and white micas. The majority of the orthoclase grain show well developed very fine-grained sericitic alteration patches.

Plagioclase – determined to be albitic to oligoclase in composition using the Michel-Lévy method. The grains are medium- to coarse-grained and subhedral to euhedral. The plagioclase grains show well-developed white mica grains that grow preferentially along the cleavage planes of the host plagioclase grain, as the result of the sericitic alteration. The primary growth twins have been retained.

Chlorite – occurs as subhedral crystals in aggregates, fans and as laths. The chlorite is an alteration product of primary biotite with muscovite, epidote and hematite as the main reaction products.

Biotite – occurs as euhedral relict crystals that have been almost completely replaced by chlorite and other reaction products.

White mica – occurs as sub- to euhedral grains in the quartz-feldspar groundmass as an alteration product of the plagioclase (fine-grained laths) and the orthoclase (aphanitic crystal aggregates). Muscovite also occurs as a reaction product of the alteration of biotite.

Pyrite – The pyrite is hydrothermal and the euhedral grains are seen over-printing the quartz-feldspar groundmass. These grains have undergone some (<50% of the grains) alteration to Fe-oxides (hematite?).

Titanite – Occurs as mostly isolated, euhedral rhombs over printing the quartz-feldspar groundmass.

Fluorite – Occurs as mostly isolated, euhedral, hexagonal crystals occurring as inclusions and associated with the altered biotite

Hematite – Occurs as a reaction product of the alteration of biotite to chlorite and pyrite to Fe-oxides

*WP13ES05: Lamprophyre dyke***Mineral Modal Percentage:**

Biotite – 35%
 Orthoclase – 35%
 Quartz – 5-10%
 White mica – 20%
 Muscovite – 3%
 Chlorite – <1%
 Magnetite – 5%
 Pyrite – 1%
 Hematite – 1%
 Calcite – <1%
 Fluorite – <1%
 Rutile – <1%

This hydrothermally altered lamprophyric dyke shows a fine-grained biotite-orthoclase-quartz-white phyllosilicate groundmass with interstitial very fine-grained interstitial quartz and calcite and patches of white micas and muscovite. The sample has undergone almost complete sericite/white mica and other clay mineral(?) alteration of the K-feldspar. The biotite is randomly orientated and appears to be reacting to muscovite and magnetite and possibly chlorite. There are small euhedral fluorite and red rutile grains throughout the groundmass.

Biotite – occurs as euhedral, porphyritic crystals that have been partially replaced by muscovite and possibly chlorite and magnetite along the cleavage planes. The biotite appears to be magmatic, with some grains showing compositional zonation.

Quartz – this interstitial mineral occurs as very-fine grained anhedral crystals in between the orthoclase. It is distinguished from the feldspar by the lack of white mica alteration and its uniaxial, positive optic sign.

K-feldspar – the K feldspar in this sample is difficult to identify due to the extensive sericitic alteration. The relict larger grains appear to have retained some twinning.

White mica – occurs as mostly aphanitic crystal aggregates occurring as patches with irregular boundaries in the quartz-feldspar groundmass as an alteration product of the orthoclase.

Muscovite – occurs occasionally replacing the altered biotite and occurring with magnetite. Found mostly throughout the groundmass in fine-grained, euhedral sheets.

Magnetite – occurs as a reaction product of the alteration of biotite. Occurs interstitially throughout the groundmass in needles and with hematite.

Pyrite – occurs as isolated equant, subhedral crystals in the groundmass, frequently with a partial hematitic alteration rind

Hematite – occurs as a reaction product of the alteration of magnetite and biotite. Occurs interstitially throughout the groundmass in needles and with magnetite and pyrite.

Calcite – this interstitial mineral occurs as very-fine grained anhedral crystals in between the orthoclase in patches.

Fluorite – occurs throughout the groundmass as equant, euhedral hexagonal crystals. Some of the grains contain fluid inclusions.

Rutile – small, red needles often adjacent to the hematite-rich patches of the sample.

*WP13ES06: Little Cottonwood stock***Mineral Modal Percentage:**

Quartz – 20%
 Plagioclase – 25%
 K-feldspar – 40%
 Muscovite and white mica – 10%
 Biotite – 2%
 Magnetite – 2%
 Titanite – 1%
 Hematite – <1%
 Fluorite – <1%
 Chlorite – <1%

This monzogranite has a very coarse-grained quartz + orthoclase + albite groundmass showing a granitic texture with annealed grain boundaries. This sample has undergone sericite/white mica and other clay mineral(?) alteration that is restricted to the feldspars, with well-defined white muscovite laths occurring along the cleavage planes and within compositionally homogenous zones of the feldspars. In some of the albite grains, white mica replaces up to 50% of the grain. Some (~50%) of the primary biotite in the rock has been partially altered to chlorite, intergrown muscovite and trace epidote. The grains show some Fe staining along the grain boundaries (hematite). The pyrite in the sample retained much of the cubic shape, but formed Fe-oxide alteration rims. Titanite is associated with this pyrite.

Quartz – coarse-grained, anhedral and rounded grain shapes. These grains show some undulatory extinction and are unaltered. Some finer-grained quartz occurs in the K-spar phenocrysts.

K-feldspar – the K feldspar in this sample occurs as mostly orthoclase with some minor microcline and as anhedral-subhedral phenocrysts. The largest grains show perthitic exsolution. The grains without the exsolution show well-developed compositional zonation. A few large (10 mm wide) perthitic grains contain smaller orthoclase and quartz grains as inclusions. The grains are altered to sericite and white micas. The majority of the orthoclase grain show well developed very fine-grained sericitic alteration patches. The plagioclase grains show better-developed mica crystals. The alteration is often restricted to circular, compositionally homogenous zones within the phenocrysts.

Plagioclase – determined to be albitic to oligoclase in composition using the Michel-Lévy method. The grains are fine- to medium-grained and subhedral to euhedral. The plagioclase grains show well-developed white mica grains that grow preferentially along the cleavage planes of the host plagioclase grain as the result of the sericitic alteration. The primary growth twins have been retained

Biotite – occurs as euhedral relict crystals that have been partially to completely replaced by chlorite and other reaction products.

Chlorite – occurs as an alteration product of primary biotite with associated muscovite, epidote and hematite.

White mica – occurs as sub- to euhedral grains in the quartz-feldspar groundmass as an alteration product of the plagioclase (fine-grained laths) and the orthoclase (aphanitic crystal

aggregates). Muscovite also occurs as a reaction product of the alteration of biotite and occasionally occurs in the groundmass of the rock.

Pyrite – the pyrite is hydrothermal and the euhedral grains are seen over-printing the quartz-feldspar groundmass. These grains have undergone some (<50% of the grains) alteration to Fe-oxides (hematite?).

Titanite – occurs as mostly isolated, euhedral rhombs over printing the quartz-feldspar groundmass. Associated with the pyrite and relict magnetite(?)

Fluorite – occurs as mostly isolated, euhedral, hexagonal crystals occurring as inclusions and associated with the altered biotite

Hematite – occurs as a reaction product of the alteration of biotite to chlorite and pyrite to Fe-oxides

*WP13ES09: Little Cottonwood stock***Mineral Modal Percentage:**

Quartz – 30%

Plagioclase – 20%

K-feldspar – 30%

Muscovite and white mica – 13%

Biotite – 3%

Chlorite – 2%

Pyrite – 2%

Hematite – <1%

Titanite – <1%

This monzogranite has a coarse-grained quartz + orthoclase + albite groundmass showing a granitic texture with annealed grain boundaries. This sample has undergone significant sericite/white mica and other clay mineral(?) alteration. This alteration is restricted to the feldspars, with well-defined white muscovite laths occurring along the cleavage planes. In some of the albite grains, white mica replaces up to 75% of the grain. Much of the primary biotite in the rock has been partially altered to chlorite, intergrown with muscovite and trace epidote. The grains show some Fe staining along the grain boundaries (hematite). The pyrite in the sample retained much of the cubic shape, but formed Fe-oxide alteration rims.

Quartz – fine- to medium-grained, anhedral and rounded grain shapes. These grains show some undulatory extinction and are unaltered. Some finer-grained quartz occurs in the K-spar phenocrysts.

K-feldspar – the K feldspar in this sample occurs as mostly orthoclase as anhedral-subhedral phenocrysts. The largest grains show perthitic exsolution. The grains without the exsolution show well-developed compositional zonation. The grains are altered to sericite and white micas. The majority of the orthoclase grain show well developed very fine-grained (<0.01 mm) sericitic alteration patches. The plagioclase grains show better-developed mica crystals.

Plagioclase – determined to be albitic to oligoclase in composition using the Michel-Lévy method. The grains are fine- to medium-grained and subhedral to euhedral. The plagioclase grains show well-developed white mica grains that grow preferentially along the cleavage planes of the host plagioclase grain as the result of the sericitic alteration. The primary growth twins and simple albite twins have been retained

Biotite – occurs as subhedral and euhedral relict crystals that have been partially to completely replaced by chlorite and other reaction products.

Chlorite – occurs as an alteration product of primary biotite with associated muscovite, epidote and hematite.

White mica – occurs as sub- to euhedral grains in the quartz-feldspar groundmass as an alteration product of the plagioclase (fine-grained laths) and the orthoclase (aphanitic crystal aggregates). Muscovite also occurs as a reaction product of the alteration of biotite and occasionally occurs in the groundmass of the rock.

Pyrite – the pyrite is hydrothermal and the euhedral grains are seen over-printing the quartz-feldspar groundmass. These grains have undergone (<20% of the pyrite grains) alteration to Fe-oxides (hematite?).

Titanite – occurs as mostly glomeritic subhedral mineral clusters associated with biotite.

Hematite – occurs as a reaction product of the alteration of biotite to chlorite and pyrite to Fe-oxides

*WP13ES13: Little Cottonwood stock***Mineral Modal Percentage:**

Quartz – 20%

Plagioclase – 25%

K-feldspar – 45%

Muscovite and white mica – 5%

Biotite – 1%

Chlorite – 1%

Magnetite – 2%

Titanite – 1%

Hematite – <1%

This syenogranite has a very coarse-grained quartz + orthoclase + albite groundmass showing a granitic texture with annealed grain boundaries. This sample has undergone sericite/white mica and other clay mineral(?) alteration. This alteration is restricted to the feldspars, with well-defined white mica laths occurring along the cleavage planes and within compositionally homogenous zones of the feldspars. In some of the albite grains, white mica replaces up to 50% of the grain. 60% of the primary biotite in the rock has been partially altered to chlorite and hematite. The grains show some Fe staining along the grain boundaries (hematite). The pyrite in the sample retained much of the cubic shape, but formed Fe-oxide alteration rims.

Quartz – coarse-grained, anhedral and rounded grain shapes. The igneous grains show some undulatory extinction and are unaltered. Some finer-grained quartz occurs in the K-spar phenocrysts. There are also two coarse-grained, barren quartz veins (~1mm width) cross-cutting the sample.

K-feldspar – the K feldspar in this sample occurs as mostly orthoclase with some minor microcline and as anhedral-subhedral phenocrysts. The largest grains show perthitic exsolution. The grains without the exsolution show very well-developed compositional zonation. A few large (10 mm wide) perthitic grains contain smaller orthoclase and quartz grains as inclusions. The grains are altered to sericite and white micas. The majority of the orthoclase grain show well developed very fine-grained sericitic alteration patches. The alteration is often restricted to circular, compositionally homogenous zones within the phenocrysts.

Plagioclase – determined to be albitic to oligoclase in composition using the Michel-Lévy method. The grains are fine- to medium-grained and subhedral to euhedral. The plagioclase grains contain well-developed white mica grains that grow preferentially along the cleavage planes of the host plagioclase grain as the result of the sericitic alteration. The primary growth twins have been retained

Biotite – occurs as euhedral relict crystals that have been partially to completely replaced by chlorite and other reaction products.

Chlorite – occurs as an alteration product of primary biotite with associated muscovite, epidote and hematite.

White mica – occurs as sub- to euhedral grains in the quartz-feldspar groundmass as an alteration product of the plagioclase (fine-grained laths) and the orthoclase (aphanitic crystal

aggregates). Muscovite also occurs as a reaction product of the alteration of biotite and occasionally occurs in the groundmass of the rock.

Magnetite – the euhedral grains are seen over-printing the quartz-feldspar groundmass. These grains have undergone (<10% of the pyrite grains) alteration to Fe-oxides (hematite?).

Titanite – Occurs as mostly isolated, euhedral rhombs over printing the quartz-feldspar groundmass. Associated with the biotite and chlorite

Hematite – Occurs as a reaction product of the alteration of biotite to chlorite and magnetite to Fe-oxides

*WP13ES17: Little Cottonwood stock***Mineral Modal Percentage:**

Quartz – 15%

Hydrothermal quartz – 30%

Plagioclase – 20%

K-feldspar – 20%

Muscovite and white mica – 8%

Biotite – 5%

Pyrite – 2%

Titanite – <1%

Hornblende – <1%

Hematite – <1%

Chlorite – <1%

This sample contains numerous rusty quartz-pyrite veins. The host rock is a monzogranite. The sample has a very inequigranular quartz + orthoclase + albite groundmass with a granitic texture and annealed grain boundaries. This sample has undergone sericite/white mica and other clay mineral(?) alteration of plagioclase, with well-defined white mica laths occurring along the cleavage planes and within compositionally homogenous zones. In some of the albite grains, white mica replaces up to 80% of the grain. The primary biotite and hornblende in the rock has been slightly altered to chlorite (<10% of the mafic minerals). The pyrite in the sample retained much of the cubic shape, but formed Fe-oxide alteration rims and, in some cases, completely replaced the grain. Titanite is associated with this pyrite and hornblende.

Quartz – the igneous, anhedral and rounded quartz eyes are preserved and surrounded by very fine-grained hydrothermal quartz. These grains show some undulatory extinction and remain unaltered. Some finer-grained quartz occurs in the K-spar and pyrite phenocrysts.

K-feldspar – the K feldspar in this sample occurs as mostly orthoclase with some minor microcline and as unaltered, anhedral-subhedral phenocrysts. The largest grains show well-developed compositional zonation. Some possible orthoclase can be found in the groundmass, but is obscured by the sericite alteration.

Plagioclase – determined to be albitic using the Michel-Lévy method. The grains are fine- to medium-grained and subhedral to euhedral. The plagioclase grains show well-developed white mica grains that grow preferentially along the cleavage and fracture planes of the host plagioclase grain as the result of the sericitic alteration. The alteration is seen in the circular, compositionally homogenous zones within the phenocrysts and occurs in patches and irregularly throughout the crystal. The primary growth twins have been preserved.

Biotite – occurs as euhedral relict crystals that have been partially replaced by chlorite (<10%)

Chlorite – occurs as an alteration product of primary biotite with associated muscovite, epidote and hematite.

White mica – occurs as sub- to euhedral grains in the quartz-feldspar groundmass as an alteration product of the plagioclase (fine-grained laths and fine-grained mineral aggregates). Muscovite also occurs as a reaction product of the alteration of biotite and occasionally occurs in the groundmass of the rock.

Pyrite – the pyrite is hydrothermal and the euhedral grains are seen over-printing the quartz-feldspar groundmass. These grains have undergone some (<50% of the grains) to complete alteration to Fe-oxides (hematite?).

Titanite – occurs as mostly isolated, euhedral rhombs over printing the quartz-feldspar groundmass. Associated with the pyrite and relict magnetite(?)

Hornblende – occurs as mostly isolated, euhedral rhombs and rectangles over printing the quartz-feldspar groundmass. Associated with the pyrite and relict magnetite(?)

Hematite – occurs as a reaction product of the alteration of biotite to chlorite and pyrite to Fe-oxides

*WP13ES22: White Pine intrusion***Mineral Modal Percentage:**

Quartz – 20%

Hydrothermal quartz – 20%

Plagioclase – 10%

K-feldspar – 25%

Muscovite and white mica – 23%

Titanite – <1%

Pyrite – <1%

Hematite – 1%

This syenogranite has a coarse-grained quartz and K-feldspar porphyritic quartz-rich + orthoclase + albite groundmass with a granitic texture and annealed grain boundaries. The groundmass has undergone sericite/white mica and other clay mineral(?) alteration of the feldspars. There are well-defined white muscovite laths along the cleavage planes of the feldspars. In some of the plagioclase grains, white mica replaces up to 95% of the grain. The quartz vein has associated pyrite and coarser-grained muscovite. The pyrite in the sample retained much of the relict cubic shape, but formed Fe-oxide alteration rims or has been completely altered to Fe-oxides.

Quartz – coarse-grained, anhedral and rounded grain shapes (quartz eyes). These grains show some undulatory extinction and remain unaltered. There is also hydrothermal coarse-grained quartz hosted in a quartz-muscovite-pyrite vein (~8 mm wide). The quartz is bound by radiating muscovite and finer-grained white micas.

K-feldspar – the K-feldspar in this sample is difficult to distinguish from the plagioclase due to the extensive sericitic alteration. The relict larger grains (which show some possible perthitic exsolution) are more likely to be the K-feldspar, the grain shape and size closely resembles the phenocrysts seen in less altered samples.

Plagioclase – several, equant, euhedral altered phenocrysts are found within the groundmass. They have been almost completely altered to white micas. Primary growth twins can be seen in some of the less altered grain rims.

Muscovite – occurs occasionally replacing the altered feldspar, but is most common in the vein selvage, bordering both side of the quartz and pyrite vein. The crystals are euhedral and radiating.

White mica – occurs as sub- to euhedral grains in the quartz-feldspar groundmass as an alteration product of the plagioclase (fine-grained laths and aphanitic crystal aggregates) and the orthoclase as larger, parallel crystals.

Titanite – occurs as mostly isolated, euhedral or fragmented rhombs overprinting the quartz-feldspar groundmass. Frequently associated with altered K-feldspar grains.

Pyrite – the pyrite is hydrothermal and the euhedral grains are seen overprinting the quartz-feldspar groundmass. These grains have undergone some (70% to >95% of the feldspar grains) alteration to Fe-oxides (hematite). These grains are strongly associated with the quartz vein, with more isolated grains occurring in the granite groundmass.

Hematite – occurs as a reaction product of the pyrite weathering to Fe-oxide. The hematite retains the relict outline of the pyrite in many cases and is strongly associated with the quartz vein.

*WP13ES26: White Pine intrusion***Mineral Modal Percentage:**

Quartz – 40%

Plagioclase – 20%

K-feldspar – 28%

Muscovite and white mica – 10%

Pyrite – 1%

Hematite – 1%

This monzogranite shows a medium- to coarse-grained quartz and K-feldspar porphyritic quartz + orthoclase + albite groundmass with a granitic texture with annealed grain boundaries. The sample has undergone sericite/white mica and other clay mineral (?) alteration. This alteration is restricted to the feldspars, with well-defined white muscovite laths occurring along the cleavage planes. In some of the plagioclase and microcline grains, white mica and muscovite replaces up to 60% of the grain. The primary biotite in the rock has been altered to intergrown muscovite and some white micas (?) with opaque minerals. The grains show some Fe staining along the grain boundaries (hematite). The pyrite in the sample retained much of the cubic shape, but formed Fe-oxide alteration rims. The pyrite occurs mostly as isolated grains throughout the groundmass.

Quartz – the larger (<10 mm), euhedral phenocrysts show some undulatory extinction and remain unaltered. The groundmass contains finer-grained, anhedral and rounded grains that occur interstitially to the feldspars and quartz eyes.

K-feldspar – the K-feldspar in this sample occurs mostly as finer-grained anhedral orthoclase in the groundmass of the rock with some microcline as subhedral to euhedral and occasionally zoned phenocrysts. There is one large perthitic grain. The grains are altered to sericite and white micas. The majority of the orthoclase grain show well-developed, very fine-grained, irregular sericitic alteration patches.

Plagioclase – determined to be oligoclase in composition using the Michel-Lévy method. The grains are fine- to medium-grained and occur as subhedral to euhedral laths. The plagioclase grains show well-developed white mica grains that preferentially alter the core of the grains. The finer grained white mica replacement minerals occur in aggregates and are patchy. The primary growth twins and simple albite twins have been preserved in some grains.

White mica – occurs as sub- to euhedral grains in the quartz-feldspar groundmass as an alteration product of the plagioclase (fine-grained laths and aphanitic crystal aggregates) and the orthoclase (mostly aphanitic crystal aggregates). Muscovite also occurs as a reaction product of the alteration of biotite and in the groundmass of the rock as radiating fans of crystals. This muscovite is most likely hydrothermal.

Pyrite – the euhedral grains overprint the quartz-feldspar groundmass. The pyrite occurs mostly as isolated grains throughout the groundmass. These grains have undergone (<45% of the pyrite grains) alteration to Fe-oxides (hematite?).

Hematite – occurs as a reaction product of the alteration of biotite to muscovite and pyrite to Fe-oxides. Found throughout the groundmass and as weathering rinds around the pyrite and along cleavage planes in the biotite.

*WP13ES28: White Pine intrusion***Mineral Modal Percentage:**

Quartz – 30%

Plagioclase – 26%

K-feldspar – 30%

Muscovite and white mica – 10%

Biotite – 3%

Chlorite – <1%

Pyrite – 1%

Hematite – <1%

This monzogranite shows a medium- to coarse-grained quartz and K-feldspar porphyritic quartz-rich + orthoclase + albite groundmass with a granitic texture and annealed grain boundaries. The groundmass has undergone sericite/white mica and other clay mineral(?) alteration of the feldspars. This alteration is restricted to the feldspars, with well-defined white muscovite laths occurring along the cleavage planes. In some of the plagioclase grains, white mica and muscovite replaces up to 60% of the grain. Some of the primary biotite in the rock has been partially altered to intergrown muscovite and some

white micas (?). The grains show some Fe staining along the grain boundaries (hematite). The pyrite in the sample retained much of the cubic shape, but formed Fe-oxide alteration rims. The pyrite occurs mostly as isolated grains throughout the groundmass. A few pyrite grains are surrounded by muscovite sheets.

Quartz – fine- to medium-grained, anhedral and rounded grain shapes. These larger (<10 mm), euhedral phenocrysts show some undulatory extinction and are unaltered. The quartz eyes contain some feldspar phenocrysts.

K-feldspar – the K feldspar in this sample occurs mostly as orthoclase with some microcline as subhedral, and euhedral phenocrysts. There is also finer-grained, anhedral orthoclase in the groundmass of the rock. The grains are altered to sericite and white micas. The majority of the orthoclase grain show well-developed very fine-grained sericitic alteration patches.

Plagioclase – determined to oligoclase in composition using the Michel-Lévy method. The grains are fine- to medium-grained and subhedral to euhedral laths. The plagioclase grains show well-developed white mica grains that preferentially alter the core of the grains. The finer grained white mica replacement minerals occur in aggregates and are patchy. The primary growth twins and simple albite twins have been retained in some grains.

White mica – occurs as sub- to euhedral grains in the quartz-feldspar groundmass as an alteration product of the plagioclase (fine-grained laths and aphanitic crystal aggregates) and the orthoclase (mostly aphanitic crystal aggregates). Muscovite also occurs as a reaction product of the alteration of biotite and occasionally occurs in the groundmass of the rock.

Biotite – occurs as subhedral crystals that have been partially replaced by muscovite and possible chlorite and hematite.

Chlorite – occurs as a trace alteration product of primary biotite with muscovite and hematite as the main reaction products.

Pyrite – the pyrite is hydrothermal and the euhedral grains overprint the quartz-feldspar groundmass. The pyrite occurs mostly as isolated grains throughout the groundmass. These grains have undergone (<90% of the grains) alteration to Fe-oxides (hematite?).

Hematite – occurs as a reaction product of the alteration of biotite to chlorite and pyrite to Fe-oxides. Found throughout the groundmass.

*WP13ES30: Little Cottonwood stock***Mineral Modal Percentage:**

Quartz – 27%

Plagioclase – 23%

K-feldspar – 33%

White mica – 10%

Muscovite – 3%

Biotite – 1%

Chlorite – 1%

Pyrite – 1%

Titanite – 1%

Hematite – <1%

This monzogranite has a very coarse-grained quartz + orthoclase + albite groundmass showing a granitic texture with annealed grain boundaries. This sample has undergone sericite/white mica and other clay mineral(?) alteration. This alteration is restricted to the plagioclase, with well-defined white mica laths occurring along the cleavage planes and within compositionally homogenous zones. In the albite grains, white mica replaces up to 80% of the grain. The white mica laths compose a minor portion of the groundmass (~10%). The primary biotite has been slightly to completely altered to chlorite. The pyrite in the sample retained much of the cubic shape, but formed Fe-oxide alteration rims and, in some cases, completely replaced the grain. Titanite is

associated with pyrite and biotite.

Quartz – coarse-grained, anhedral and rounded grain shapes. The igneous grains show some undulatory extinction and are unaltered. Some finer-grained quartz occurs in K-spar phenocrysts. There are also two coarse-grained, barren quartz veins (~1mm width) cross-cutting the sample.

K-feldspar – the K feldspar in this sample occurs as mostly orthoclase with some possible trace microcline and as anhedral-subhedral phenocrysts. The largest grains show some perthitic exsolution. The grains without the exsolution show very well-developed compositional zonation. A few large (10 mm wide) perthitic grains contain smaller orthoclase and quartz grains as inclusions. The grains are altered to sericite and white micas. The majority of the orthoclase grains show well developed very fine-grained sericitic alteration patches. The plagioclase grains show better-developed mica crystals. The alteration is often restricted to circular, compositionally homogenous zones within the phenocrysts.

Plagioclase – determined to be albitic to oligoclase in composition using the Michel-Lévy method. The grains are fine- to medium-grained and subhedral to euhedral. The plagioclase grains show well-developed white mica grains that grow preferentially along the cleavage planes of the host plagioclase grain as the result of the sericitic alteration. The primary growth twins have been retained

Biotite – occurs as euhedral relict crystals that have been partially to completely replaced by chlorite and other reaction products.

Chlorite – occurs as an alteration product of primary biotite with muscovite, epidote and hematite as the main reaction products.

White mica – occurs as sub- to euhedral grains in the quartz-feldspar groundmass as an alteration product of the plagioclase (fine-grained laths) and the orthoclase (aphanitic crystal

aggregates). Muscovite also occurs as a reaction product of the alteration of biotite and frequently occurs in the groundmass of the rock, often intergrown in larger feldspar grains,

Muscovite – occurs as larger euhedral, laths in the groundmass

Pyrite – the euhedral grains are seen over-printing the quartz-feldspar groundmass. These grains have undergone some (<10% of the grains) alteration to Fe-oxides (hematite?).

Titanite – occurs as mostly isolated, euhedral rhombs over-printing the quartz-feldspar groundmass. Associated with the biotite and chlorite

Hematite – occurs as a reaction product of the alteration of biotite to chlorite and magnetite/pyrite to Fe-oxides

WP13ES36: Little Cottonwood stock

Mineral Modal Percentage:

Quartz – 25%

Plagioclase – 18%

K-feldspar – 25%

White mica – 15%

Muscovite – 7%

Pyrite – 3%

Hematite – 7%

This monzogranite was collected from a rusty, altered sample. It has a very coarse-grained quartz + orthoclase + albite groundmass showing a granitic texture with annealed grain boundaries. This sample has undergone sericite/white mica and pyrite alteration. The sericite alteration is restricted to the feldspars, with well-defined white mica laths occurring throughout all of the grains. In the albite grains, white mica and hematite replace up to 80% of the grain. The white mica laths comprise a major portion of the groundmass (~20%). The primary biotite has been slightly to completely altered to white micas. The pyrite in the sample retained much of the cubic shape, but formed Fe-oxide alteration rims and, in some cases, completely replaced the grain. There are no mafic minerals in this sample.

Quartz – coarse-grained, anhedral and rounded grain shapes. The grains show some undulatory extinction and are unaltered. Some finer-grained quartz occurs in the K-feldspar phenocrysts.

K-feldspar – the K-feldspar in this sample occurs as mostly orthoclase with some possible trace microcline and as anhedral-subhedral phenocrysts. The grains, along with the plagioclase, are altered to sericite and white micas. The majority of the orthoclase grain show well-developed very fine-grained sericitic alteration patches throughout the entire grain.

Plagioclase – determined to be oligoclase in composition using the Michel-Lévy method. The grains are fine- to medium-grained and subhedral to euhedral. The plagioclase grains show well-developed white mica grains that have grown throughout the crystal as the result of the sericitic alteration. The primary growth twins have been retained

White mica – occurs as sub- to euhedral grains in the quartz-feldspar groundmass as an alteration product of the plagioclase (fine-grained laths) and the orthoclase (aphanitic crystal aggregates). Muscovite also occurs as a reaction product of the alteration of biotite and frequently occurs in the groundmass of the rock, often intergrown with larger feldspar grains,

Muscovite – occurs as larger euhedral, laths in the groundmass. Often associated with the other white micas

Pyrite – the euhedral grains are seen over-printing the quartz-feldspar groundmass. These grains have undergone some (<10% of the altered pyrite grains) alteration to Fe-oxides (hematite?) and have Fe-oxide coronas

Hematite – Occurs as a reaction product of the alteration of biotite to chlorite and magnetite/pyrite to Fe-oxides. Found throughout the groundmass.

*WP13ES40: Little Cottonwood stock***Mineral Modal Percentage:**

Quartz – 25%

Plagioclase – 18%

K-feldspar – 25%

White mica – 15%

Titanite – 1%

Muscovite – 7%

Pyrite – 3%

Hematite – 7%

This monzogranite has a very coarse-grained quartz + orthoclase + albite groundmass with a granitic texture and annealed grain boundaries. This sample has undergone sericite/white mica and pyrite alteration. The sericite alteration is restricted to the feldspars, with well-defined white mica laths occurring throughout all of the grains and in the groundmass – overprinting the feldspars. Some of the albite grains, white mica and hematite replace >95% of the grain. The white mica laths compose a major portion of the groundmass (~20%). The primary biotite has been slightly to completely altered to white micas and muscovite. The

pyrite in the sample retained much of the cubic shape, but formed Fe-oxide alteration rims or, in some cases, completely replaced the grain. There are not any mafic minerals aside from the pyrite and hematite in this sample and trace titanite

Quartz – coarse-grained, anhedral and rounded grain shapes. The grains show some undulatory extinction and remain unaltered. Some finer-grained quartz occurs in the K-spar phenocrysts.

K-feldspar – the K-feldspar in this sample occurs mostly as anhedral to subhedral phenocrysts of orthoclase. The grains, along with the plagioclase, are altered to sericite, white micas and quartz. The majority of the orthoclase grains show well developed very fine-grained sericitic alteration patches throughout the entire grain as well coarser-grained muscovite and other white micas overprinting the grain.

Plagioclase – determined to be oligoclase in composition using the Michel-Lévy method. The grains are fine- to medium-grained and subhedral to euhedral. The plagioclase grains show well-developed white mica grains that have grown throughout and overprint the crystal as the result of the sericitic alteration. The primary growth twins have been retained.

White mica – occurs as sub- to euhedral grains in the quartz-feldspar groundmass as an alteration product of the plagioclase (fine-grained laths) and the orthoclase (aphanitic crystal aggregates). Muscovite also occurs as a reaction product of the alteration of biotite and frequently occurs in the groundmass of the rock, often intergrown with larger feldspar grains.

Muscovite – occurs as larger euhedral, radiating or fan-like laths in the groundmass. Often associated with the other white micas.

Pyrite – the euhedral grains are seen overprinting the quartz-feldspar groundmass. These grains have undergone some (<10% of the pyrite grains) alteration to Fe-oxides (hematite?) and have Fe-oxide coronas

Hematite – occurs as a reaction product of the alteration of biotite to chlorite and magnetite/pyrite to Fe-oxides. Found throughout the groundmass as a stain.

*WP13ES44: Little Cottonwood stock***Mineral Modal Percentage:**

Quartz – 35%
 Plagioclase – 25%
 K-feldspar – 30%
 White Mica – 10%
 Biotite – 1%
 Chlorite – <1%
 Pyrite – 3%
 Hematite – <1%

This monzogranite has a coarse-grained quartz + orthoclase + albite groundmass with a granitic texture and annealed grain boundaries. The sample has undergone significant sericite/white mica and other clay mineral(?) alteration. This alteration is restricted to the feldspars, with well-defined, very fine-grained white mica laths occurring along the cleavage planes and throughout the grains. In some of the feldspar grains, white mica replaces 40 - 90% of the grain. Some of the primary biotite in the rock has been partially altered to chlorite intergrown with muscovite. Many of the primary micas appear to have been completely altered to muscovite. The grains show some Fe staining along the grain boundaries (hematite). The pyrite in the sample retained much of the cubic shape, but formed Fe-oxide alteration rims.

Quartz – fine- to medium-grained, anhedral and rounded, elongate, irregular grain shapes. These grains show some undulatory extinction and remain unaltered. Some finer-grained quartz occurs in the K-feldspar phenocrysts.

K-feldspar – the K-feldspar in this sample occurs as mostly orthoclase as anhedral-subhedral phenocrysts. The grains are altered to sericite and white micas. The majority of the orthoclase grains show well-developed very fine-grained sericitic alteration patches. The plagioclase grains show better-developed mica crystals than the K-feldspar.

Plagioclase – determined to be albitic to mostly oligoclase in composition using the Michel-Lévy method. The grains are fine- to medium-grained and subhedral to euhedral. The plagioclase grains show well-developed white mica grains that grow throughout the host plagioclase grains as the result of the sericitic alteration. Primary growth twins and simple albite twins have been preserved.

Biotite – occurs as subhedral and euhedral relict, slightly bent crystals that have been partially completely replaced by white micas or muscovite and other reaction products.

Chlorite – occurs as an alteration product of primary biotite with muscovite, epidote and hematite as associated minerals.

White mica – occurs as sub- to euhedral grains in the quartz-feldspar groundmass as an alteration product of the plagioclase (fine-grained laths) and the orthoclase (aphanitic crystal aggregates). Muscovite also occurs as a reaction product of the alteration of biotite and occasionally occurs in the groundmass of the rock. It also occurs as a mineral corona around the altered sulphides.

Pyrite – the pyrite is hydrothermal and the euhedral grains are seen overprinting the quartz-feldspar groundmass. These grains have undergone alteration to Fe-oxides (hematite?).

Hematite – occurs as a reaction product of the alteration of biotite to chlorite and pyrite to Fe-oxide. Occurs as a mineral corona around the pyrite and rarely along the grain boundary edges of relict or altered biotite laths.

WP13ES46: Little Cottonwood stock - Alteration

Mineral Modal Percentage:

Quartz – 20%

White mica – 8%

Pyrite – 40%

Hematite – 1%

This sample was collected to examine a rusty quartz vein hosted within the Little Cottonwood stock. The quartz vein is 20 mm wide and a selvage is visible. There was no Mo mineralisation found in the vein in the field, or during petrographic analysis. The paragenesis of the vein is the crystallization of finer-grained quartz on the perimeter of the vein which grades into a coarser-grained quartz core. In the centre of the vein, uniform hematite (primary pyrite?) precipitated on the quartz and aphanitic, massive white micas precipitated on the hematite, forming bands.

Quartz – coarse-grained, anhedral, inequigranular and annealed grain outlines. The vein also contains interstitial hematite surrounding some of the quartz grains. There are also igneous quartz eyes left in the altered groundmass adjacent to the quartz-sericite-pyrite vein. These igneous quartz grains are anhedral, irregular and fine-grained. They occur interstitially to the relict subhedral feldspar grains.

Feldspars – the feldspars in this sample are almost completely altered to white micas. The relict phenocryst outlines and anhedral altered groundmass suggest the presence of both K-feldspar and plagioclase in the sample. The relict grain shape is preserved, however, any primary microcline, Carlsbad, or simple twins have been erased.

White mica – occurs as sub- to euhedral grains in the quartz-feldspar groundmass as an alteration product of the feldspars and it occurs as fine-grained laths and as aphanitic crystal aggregates. In the vein, the white micas are concentrated in the vein selvage and form bands with the hematite.

Hematite – Occurs as a primary mineral precipitate after the crystallization of the quartz vein – filling in voids. The hematite has subtle banding, suggesting it is primary as opposed to a reaction product.

*WP13ES54: White Pine intrusion***Mineral Modal Percentage:**

Quartz – 28%

Plagioclase – 25%

K-feldspar – 25%

Muscovite and white mica – 10%

Pyrite – 1%

Hematite – 1%

This monzogranite shows a medium- to coarse-grained quartz and K-feldspar porphyritic quartz + orthoclase + albite groundmass with a granitic texture with annealed grain boundaries. The sample has undergone sericite/white mica and other clay mineral(?) alteration. This alteration is restricted to the feldspars, with well-defined white muscovite laths occurring along the cleavage planes. In some of the plagioclase and microcline grains, white mica and muscovite replaces up to 80% of the grain. The primary biotite has been altered to

intergrown muscovite and white micas (?) with opaque minerals. The grains show some Fe staining along the grain boundaries (hematite). The pyrite in the sample retained much of the cubic shape, but formed Fe-oxide alteration rims. The pyrite occurs mostly as isolated grains throughout the groundmass.

Quartz – the larger (<10 mm), euhedral phenocrysts show some undulatory extinction and remain unaltered. The groundmass contains very fine-grained, anhedral and rounded grain shapes that occur interstitially to the feldspars. This quartz might be hydrothermally sourced or represent a finer-grained phase of the White Pine intrusion. The quartz groundmass is differentiated from the feldspars using its positive uniaxial optic sign and the lack of sericitic alteration.

K-feldspar – the K-feldspar in this sample occurs mostly as finer-grained anhedral orthoclase in the groundmass of the rock with some microcline as subhedral to euhedral phenocrysts. There is one large perthitic grain. The grains are altered to sericite and white micas. The majority of the orthoclase grain show well-developed, very fine-grained, irregular sericitic alteration patches.

Plagioclase – determined to be oligoclase in composition using the Michel-Lévy method. The grains are fine- to medium-grained and subhedral to euhedral laths. The plagioclase grains show well-developed white mica grains that preferentially alter the core of the grains. The finer grained white mica replacement minerals occur in aggregates and are patchy. The primary growth twins and simple albite twins have been preserved in some grains.

White mica – occurs as sub- to euhedral grains in the quartz-feldspar groundmass as an alteration product of the plagioclase (fine-grained laths and aphanitic crystal aggregates) and the orthoclase (mostly aphanitic crystal aggregates). Muscovite also occurs as a reaction product of the alteration of biotite and occasionally occurs in the groundmass of the rock as radiating fans of crystals.

Pyrite – the euhedral grains are seen over-printing the quartz-feldspar groundmass. The pyrite occurs mostly as isolated grains throughout the groundmass. These grains have undergone (45% of the pyrite grains) alteration to Fe-oxides (hematite?).

Hematite – occurs as a reaction product of the alteration of biotite to chlorite and pyrite to Fe-oxides. Found throughout the groundmass and as weathering rinds around the pyrite and along cleavage planes in the biotite.

*WP13ES58: Little Cottonwood stock***Mineral Modal Percentage:**

Quartz – 20%
 Plagioclase – 25%
 K-feldspar – 40%
 White mica – 8%
 Muscovite – 2%
 Biotite – 2%
 Magnetite – 2%
 Hematite – 1%

This monzogranite has a very coarse-grained quartz + orthoclase + albite groundmass with a granitic texture and annealed grain boundaries. The sample has undergone sericite/white mica and other clay mineral(?) alteration that is restricted to the feldspars. In the albite grains, white mica replaces up to 90% of the grain. Some of the primary biotite in the rock has been altered to muscovite and hematite/magnetite(?). The grains show some Fe staining along the grain boundaries (hematite). The pyrite in the sample retained its cubic shape, but formed Fe-oxide alteration rims.

Titanite is absent. Rhombohedral aggregates of alteration minerals suggest primary titanite prior to alteration?

Quartz – coarse-grained, anhedral and rounded grain shapes. These grains show some undulatory extinction and are unaltered. Some finer-grained quartz occurs in the K-feldspar phenocrysts.

K-feldspar – the K-feldspar in this sample occurs as mostly orthoclase with some minor microcline and as subhedral phenocrysts. Some grains show weak compositional zonation. A few large (10 mm wide) perthitic grains contain smaller orthoclase and quartz grains as inclusions. The almost the entire grain (90%) is altered to sericite and white micas. The orthoclase grains show well developed, very fine-grained sericitic alteration patches.

Plagioclase – determined to be oligoclase in composition using the Michel-Lévy method. The grains are fine- to medium-grained and subhedral to euhedral. The plagioclase grains show well-developed sericitic alteration. The primary growth twins have been preserved.

Biotite – occurs as euhedral relict crystals that have been partially to completely replaced by muscovite. No chlorite is present.

Muscovite – occurs as larger euhedral, radiating or fan-like laths in the groundmass. Often associated with the other white micas.

White mica – occurs as sub- to euhedral grains in the quartz-feldspar groundmass as an alteration product of the plagioclase (fine-grained laths) and the orthoclase (aphanitic crystal aggregates). They also occur in the groundmass of the rock and in cross-cutting veins as radiating crystals

Pyrite – the pyrite is hydrothermal and the euhedral grains are seen over-printing the quartz-feldspar groundmass. These grains have undergone some (<50% of the complete pyrite grains)

alteration to Fe-oxides (hematite?) which appear as mineral coronas. The largest pyrite grains in the sample are associated with fine-grained, bladed, radiating muscovite grains.

Hematite – occurs as a reaction product of the alteration of biotite to chlorite and pyrite to Fe-oxides. Occurs predominantly as alteration rims around the pyrite samples.

*WP13ES64: White Pine intrusion***Mineral Modal Percentage:**

Quartz – 30%

Hydrothermal quartz –35%

Muscovite and white mica – 34%

Hematite – 1%

Epidote – <1%

This altered granite shows a medium- to coarse-grained quartz porphyritic quartz + phyllosilicate groundmass with interstitial very fine-grained quartz and patches of white micas and muscovite. The sample has undergone almost complete sericite/white mica and other clay mineral(?) alteration. This alteration is restricted to the feldspars, with well-defined white muscovite laths occurring along the cleavage planes. In some of the plagioclase and microcline grains, white mica and

muscovite replaces the entire grain with only some possible relict grain outline remaining. No mafic minerals have been preserved, including titanite and pyrite. There is some hematitic staining and some possible trace epidote associated with coarse-grained muscovite.

Quartz – the larger (<10 mm), euhedral phenocrysts show some undulatory extinction and are unaltered. The groundmass contains very fine-grained, anhedral and rounded grains that occur interstitially to the feldspars. This quartz might be hydrothermally sourced and represent silicification of the groundmass. It may also represent a finer-grained phase of the White Pine intrusion.

White mica – occurs as sub- to euhedral grains in the quartz-feldspar groundmass as an alteration product of the plagioclase and the orthoclase (mostly aphanitic crystal aggregates occurring as patches with irregular boundaries). Some of the white micas outline veinlets (narrower than 1 mm) which may represent fluid pathways through the rock.

Hematite – occurs as a reaction product of the alteration of biotite and pyrite. Found throughout the groundmass and along some possible fluid pathways (white mica veinlets).

*WP13ES65: White Pine intrusion***Mineral Modal Percentage:**

Quartz – 20%

Hydrothermal quartz –50%

Muscovite and white mica – 15%

Altered biotite – 1%

Titanite – 1%

Pyrite – 1%

Chalcopyrite - <1%

Molybdenite - <1%

Hematite – <1%

This altered granite shows a medium- to coarse-grained quartz porphyritic quartz + orthoclase + albite groundmass with a granitic texture with annealed grain boundaries. The sample has undergone sericite/white mica alteration that is restricted to the feldspars. In some of the plagioclase and microcline (some twinning is still visible) grains, white mica and muscovite replaces up to 95% of the grain. No primary mafic silicate minerals are preserved in the sample other than trace altered biotite. The pyrite in the groundmass is significantly fresher than the pyrite reported in other samples from the White Pine intrusion and Fe-oxide alteration rims are rare in this section.

The pyrite occurs mostly as isolated grains throughout the groundmass. This sample contains numerous quartz veins, some of which contain molybdenite.

Quartz – the larger (<10 mm), euhedral phenocrysts show some undulatory extinction and are unaltered. The groundmass contains very fine-grained, anhedral and rounded grain shapes that occur interstitially to the feldspars. This quartz might be hydrothermally sourced and represent silicification of the groundmass. The sample also contains two generations of fine-grained quartz veins. One set, which run parallel to each other, contains radiating molybdenite crystal aggregates (1 mm wide). The larger cross-cutting vein (3 mm wide) is barren, aside from pyrite (observed in the field, not in the section). The veins do not have white mica or muscovite selvages. There is trace calcite intergrown in the larger vein.

White mica – occurs as sub- to euhedral grains in the quartz-feldspar groundmass as an alteration product of the plagioclase (fine-grained laths and aphanitic crystal aggregates) and the orthoclase (mostly aphanitic crystal aggregates). Muscovite also occurs as a reaction product of the alteration of biotite and occasionally occurs in the groundmass of the rock as radiating fans of crystals. The quartz veins do not contain white mica or muscovite.

Titanite – occurs as mostly isolated, euhedral or fragmented rhombs over-printing the quartz-feldspar groundmass. Frequently associated with altered biotite grains. The grain outlines appear to be fragmented.

Pyrite – the euhedral grains are seen over-printing the quartz-feldspar groundmass. The pyrite occurs mostly as isolated grains throughout the groundmass. These grains have undergone (45% of the grains) alteration to Fe-oxides (hematite?). In reflected light microscopy, inclusions of chalcopyrite are observed in the coarse pyrite grains.

Molybdenite – occurs in the core of the quartz veins. The needles occur as radiating, acicular crystals.

Hematite – occurs as a reaction product of the alteration of pyrite to Fe-oxides. Found throughout the groundmass and as rare, incomplete weathering rinds around the pyrite and along cleavage planes in the altered biotite.

WP13ES68: Little Cottonwood stock – Unaltered sample

Mineral Modal Percentage:

Quartz – 30%
 Plagioclase 30%
 K-feldspar – 30%
 Sericite – 5%
 Biotite – 4%
 Hornblende – 1%
 Chlorite – <1%
 Titanite – <1%
 Magnetite – <1%

This monzogranite has a coarse-grained, quartz and K-feldspar porphyritic quartz + orthoclase + albite groundmass with a granitic texture and annealed grain boundaries. In some of the feldspar grains, white mica replaces <10% of the grain. Some of the primary biotite in the rock has been partially altered to chlorite with intergrown muscovite. Titanite is present in long, euhedral rhombs (~1 mm). This sample represents the least altered Little Cottonwood stock granite to compare it to the phyllic alteration seen in the other samples.

Quartz – fine- to medium-grained, anhedral and rounded grain shapes. These grains show some undulatory extinction and remain unaltered.

K-feldspar – the K feldspar in this sample occurs as mostly orthoclase as anhedral-subhedral phenocrysts. There are some smaller grains showing microcline twinning. This sample is weakly altered to white phyllosilicate minerals.

Plagioclase – determined to be albitic to mostly oligoclase in composition using the Michel-Lévy method. The grains are fine- to medium-grained and subhedral to euhedral. The plagioclase grains show weak sericitic alteration. The primary growth twins and simple albite twins have been retained

White mica – occurs as sub- to euhedral grains in the quartz-feldspar groundmass as an alteration product of the plagioclase and the orthoclase as aphanitic crystal aggregates.

Biotite – occurs as subhedral and euhedral relict, slightly bent crystals that have been partially replaced by chlorite.

Hornblende – smaller (<0.8 mm), euhedral, slightly fragmented rhombohedral, green crystals. Found throughout the groundmass.

Chlorite – occurs as an alteration product of primary biotite and hornblende

Titanite – fine-grained, euhedral rhombs that are unaltered and associate with larger laths of biotite.

Magnetite – fine-grained, anhedral equant crystals that occur throughout the sample. Very minor (<5%) alteration to Fe-oxides.

*Buckingham Mo (-Cu) Porphyry**BK13ES003: Harmony Formation - Quartzite***Mineral Modal Percentage:**

Quartz – 80%

White mica – 18%

Muscovite – 1%

Hematite – 1%

Titanite <1%

This sample was collected to examine quartz veins in the quartzite. The quartzite is composed of rounded, moderately sorted quartz grains. There does not appear to be any other clast type. The matrix is composed of very fine-grained quartz and white phyllosilicates – either muscovite or phengite. The white phyllosilicates occur in patches and in veinlets with coarser-grained, radiating muscovite. These veinlets are composed of ~85% very fine-grained white micas and some contain very fine-grained hematite. There are some glomeritic titanite crystals which also trend along the veinlet.

Quartz – The quartz in the groundmass is rounded and moderately sorted. Some of the larger clasts (<1 mm) have subgrain formation. It is likely that the subgrains formed pre-metamorphism, before erosion and deposition as it is not present in all the grains.

White mica – occurs as sub- to euhedral grains in the quartz matrix as an alteration product of the pelitic component of the sandstone protolith. It occurs as fine-grained laths and as aphanitic crystal aggregates. In the vein, the white micas are aligned along their long axis and trend parallel to the veinlet.

Muscovite – Occurs as larger laths in the white mica-hematite veinlet. The sheets are radiating and intergrown with hematite.

Hematite – Occurs along the veinlet outlined by the increased concentration of white micas and lack of quartz clasts. The relict cubic shapes suggest it is after pyrite.

Titanite – Occurs along the veinlet outlined by the increased concentration of white micas and lack of quartz clasts. The grains are subhedral and glomeritic and the mineral clusters lie along the veinlet.

*BK13ES009: Harmony Formation - Quartzite***Mineral Modal Percentage:**

Quartz – 35%

Hydrothermal quartz – 10%

White mica – 20%

Muscovite – 5%

Hematite – 15%

Jarosite – 15%

This sample displays brecciating hematite + jarosite + quartz veinlets within the quartzite. The quartzite is composed of rounded, moderately sorted quartz grains. There is no other clast type. The quartz in the groundmass in this sample appears to be more annealed and retains less of the clastic appearance (result of metamorphism?) than in other samples. The matrix is composed of very fine-grained quartz and white phyllosilicates, as well as coarser either muscovite or phengite.

The sample contains veinlets composed of very fine-grained hematite and aphanitic greenish jarosite. The veining has brecciated the host rock, with fragmented clasts of the annealed quartzite in the vein. Barren hydrothermal quartz veins are cross-cut by the white mica veinlets. The jarosite in the veins occurs in patches and in veinlets with cross-cutting coarser-grained, radiating muscovite and possible phengite.

Quartz – The quartz in the groundmass is rounded and moderately sorted. It is the only clast type. Some of the larger clasts (<1 mm) have subgrain formation. It is likely that the subgrains formed pre-metamorphism, before erosion and deposition, as not all the grains show the subgrain boundaries. The grains are also well annealed with wavy grain boundaries (the result of metamorphism).

Hydrothermal quartz – The quartz in the veins is finer-grained than the groundmass quartz. In one portion of the section, there are quartz veinlets being cross-cut by the greenish white micas (sericite?).

White mica and sericite – Occurs as sub- to euhedral grains in the quartz matrix as an alteration product of the pelitic component of the sandstone protolith. It occurs as fine-grained laths and as aphanitic crystal aggregates. In the veining, there are two generations, the younger generation (phengite?) cross-cuts the sericite.

Muscovite – Occurs as larger laths in the white mica-hematite veinlet. The sheets are radiating and intergrown with the majority of the sericite and other white micas.

Hematite – Occurs along the veinlet and with jarosite. Some relict cubic shapes suggest it is after pyrite.

Jarosite – Occurs along the veinlet and with hematite. Some relict cubic shapes suggest it is after pyrite (intergrown with hematite).

*BK13ES011: Cretaceous granite***Mineral Modal Percentage:**

Quartz – 20%

K-feldspar – 10%

Plagioclase – 5%

Muscovite and white mica – 65%

Hematite – 1%

This granite comprises very altered coarse-grained quartz and K-spar phenocrysts in a quartz-rich + orthoclase + plagioclase groundmass showing a granitic texture with annealed grain boundaries. Feldspars in the groundmass have undergone sericite/white mica and other clay mineral alteration with white mica replacing up to 95% of some crystals. The pyrite in the sample retained much of the relict cubic shape, but formed

Fe-oxide alteration rims or has been completely altered to Fe-oxides.

Quartz – Coarse-grained, anhedral and rounded grain shapes (quartz eyes). These grains show some undulatory extinction and are unaltered. There is also finer-grained, anhedral quartz in the highly altered groundmass.

K-feldspar – The K-feldspar is difficult to distinguish from the plagioclase due to the extensive sericitic alteration. The larger relict grains (which show some tartan twinning) are more likely to be the microcline, the grain shape and size closely resembles the phenocrysts seen in less altered samples.

Plagioclase – Several, equant, euhedral altered phenocrysts are found within the groundmass. They have been almost completely altered to white mica. Primary growth twins can be seen in some of the less altered grain rims.

Muscovite – Occurs occasionally replacing the altered feldspar and in the groundmass. The best formed grains replace altered biotite. The altered sheets retain a brown, less altered core.

White mica – Occurs as sub- to euhedral grains in the quartz-feldspar groundmass as an alteration product of the plagioclase (fine-grained laths and aphanitic crystal aggregates) and the orthoclase as larger, parallel crystals.

Hematite – Occurs as a reaction product of the pyrite weathering to Fe-oxide. The primary pyrite was hydrothermal and the euhedral grains are seen over-printing the quartz-feldspar groundmass. The hematite retains the relict outline of the pyrite.

*BK13ES012: Harmony Formation - Quartzite***Mineral Modal Percentage:**

Quartz – 85%

White mica – 14%

Muscovite – 1%

Hematite – 1%

This sample was collected to examine quartz veins hosted within the quartzite. The quartzite is composed of rounded, moderately sorted quartz grains with <1% plagioclase and orthoclase clasts. The feldspars have retained their growth twins and are the same size as the smallest visible quartz grains. The matrix is composed of very fine-grained quartz and white phyllosilicates, either muscovite or phengite. There are narrow (<0.7 mm wide) quartz veins which are composed of very fine-grained quartz with wavy grain boundaries. The veins do not host white micas or primary pyrite.

Quartz – The quartz in the groundmass is rounded and moderately sorted. It is the dominant clast type, with some smaller feldspars. Some of the larger clasts (<1 mm) have subgrain formation. It is likely that the subgrains formed pre-metamorphism, before erosion and deposition, as not all the grains show the subgrain boundaries. The quartz in the vein is clean and much finer grained than the quartz clasts.

White mica – occurs as sub- to euhedral grains in the quartz matrix as an alteration product of the pelitic component of the sandstone protolith. It occurs as fine-grained laths and as aphanitic crystal aggregates.

Muscovite – Occurs as larger laths in the white mica-hematite veinlet. The sheets are radiating and intergrown with the majority of the hematite in the section.

Hematite – Occurs interstitially amongst the white mica groundmass

*BK13ES013: Harmony Formation - Quartzite***Mineral Modal Percentage:**

Quartz – 90%

White mica – 8%

Muscovite – 1%

Hematite – 1%

This sample was collected to examine quartz veins hosted within the quartzite. The quartzite is composed of rounded, moderately sorted quartz grains. The matrix is composed of very fine-grained quartz and white phyllosilicates, either muscovite or phengite. There are <7 mm wide quartz veins which are composed of medium-grained quartz with well-developed and annealed grain boundaries. These veins do not host white micas or primary pyrite.

Quartz – The quartz in the groundmass is rounded and moderately sorted. It is the dominant clast type. Some of the larger clasts (<1 mm) have subgrain formation. It is likely that the subgrains formed pre-metamorphism, before erosion and deposition, as not all grains show the subgrain boundaries. The quartz in the vein is clean and coarser-grained than the quartz clasts. The quartz vein shows no hematite or white mica in between the grain boundaries.

White mica – occurs as sub- to euhedral grains in the quartz matrix as an alteration product of the pelitic component of the sandstone protolith. It occurs as fine-grained laths and as aphanitic crystal aggregates.

Muscovite – Occurs as larger laths in the white mica-hematite veinlet. The sheets are radiating and intergrown with the majority of the hematite in the section.

Hematite – Occurs interstitially as a stain amongst the white mica groundmass

*BK13ES016: Harmony Formation – Hydrothermal breccia***Mineral Modal Percentage:**

Quartz – 50%

Hydrothermal quartz – 10%

White mica – 10%

Biotite – 5%

Hematite – 20%

Jarosite – 5%

This sample displays brecciating hematite + jarosite + quartz veinlets within the Harmony Formation quartzite. The breccia is chaotic and polymictic. The predominantly clast lithology is the Harmony Formation quartzite. The quartzite clasts are composed of rounded, moderately sorted quartz grains. The matrix of the quartzite is composed of very fine-grained quartz and white phyllosilicates as well as coarser muscovite or phengite. There is a very minor clast component of biotite-rich

clasts. These clasts may also be sedimentary in origin (from the Harmony formation) and the biotite suggests a more Al-rich or pelitic protolith. The sample contains veinlets composed of very fine-grained hematite and aphanitic greenish jarosite. The veining has brecciated the host rock, with fragmented clasts of the annealed quartzite in the vein. There are numerous, angular single quartz grains within the hematitic veins which may be hydrothermal in origin and were subsequently brecciated, or were the result of brecciation of the quartzite. The jarosite in the veins occurs in patches around some of the quartzite clasts. There are no primary or secondary sulphides.

Quartz – The quartz in the quartzite clasts is rounded and moderately sorted. Some of the larger clasts (<1 mm) show subgrain development. It is likely that the subgrains formed pre-metamorphism, before erosion and deposition as not all the grains show the subgrain boundaries. The grains are also well annealed with wavy grain boundaries (the result of metamorphism).

Hydrothermal quartz – The quartz in the breccia is finer-grained than the groundmass quartz and very angular. The numerous, angular single quartz grains found within the hematitic veins may be hydrothermal in origin and were subsequently brecciated; or were the result of brecciation of the quartzite into individual grains.

White mica and sericite – Occurs as sub- to euhedral grains in the quartz matrix as an alteration product of the pelitic component of the sandstone protolith in the quartzite clasts. It occurs as fine-grained laths and as aphanitic crystal aggregates.

Biotite – Occurs as sub- to euhedral grains in the quartz matrix as an alteration product of the pelitic component of the sandstone protolith in the quartzite clasts. It represents a secondary type of metasedimentary clast.

Hematite – Occurs as the main mineral matrix of the breccia veins. It was most likely a sulphidic breccia cement prior to its alteration to Fe-oxides. There may be a component of goethite in the cement. It occurs with jarosite. Some of the breccia vein outlines retained a relict cubic shape – suggesting the hematite is after pyrite.

Jarosite – Occurs along the veinlet and with hematite. Some relict cubic shapes suggest it is after pyrite (intergrown with hematite).

*BK13ES017: Harmony Formation - Quartzite***Mineral Modal Percentage:**

Quartz – 80%

White mica – 18%

Muscovite – 1%

Hematite – 1%

This sample was collected to examine quartz veins (<2mm) hosted within the quartzite. The quartzite is composed of rounded, moderately sorted quartz grains. There is no other clast type. The matrix is composed of very fine-grained quartz and white phyllosilicates, either muscovite or phengite. The white phyllosilicates occur in patches and in veinlets with coarser-grained, radiating muscovite. These veinlets are composed of very fine-grained quartz. There is a hematite-white mica vein running along the quartz vein.

Quartz – The quartz in the groundmass is rounded and moderately sorted. It is only clast type. Some of the larger clasts (<1 mm) have subgrain formation. It is likely that the subgrains formed pre-metamorphism, before erosion and deposition, as not all the grains show the subgrain boundaries. The quartz in the veins is finer-grained than the groundmass quartz.

White mica – occurs as sub- to euhedral grains in the quartz matrix as an alteration product of the pelitic component of the sandstone protolith. It occurs as fine-grained laths and as aphanitic crystal aggregates. In the hematitic vein, the white mica content is higher adjacent to the relict pyrite grains.

Muscovite – Occurs as larger laths in the quartzite matrix.

Hematite – Occurs along the quartz vein and is associated with the increased concentration of white micas. The relict cubic shapes suggest it is after pyrite.

*BK13ES018: Harmony Formation - Quartzite***Mineral Modal Percentage:**

Quartz – 87%

White mica – 12%

Muscovite – 1%

Hematite – 1%

This sample was collected to examine quartz veins (<1.5 mm wide) hosted within the quartzite. The quartzite is composed of rounded, moderately sorted quartz grains with <1% plagioclase and orthoclase clasts. The feldspars have retained their growth twins and are the same size as the smallest visible quartz grains. The matrix is composed of very fine-grained quartz and white phyllosilicates, either muscovite or phengite. There are narrow (<0.7 mm wide) quartz veins which are composed of very fine-grained quartz with wavy grain boundaries. These veins do not host white micas or primary pyrite.

Quartz – The quartz in the groundmass is rounded and moderately sorted. It is the dominant clast type, with some smaller feldspars. Some of the larger clasts (<1 mm) have subgrain formation. It is likely that the subgrains formed pre-metamorphism, before erosion and deposition, as not all the grains show the subgrain boundaries. The quartz in the vein is clean and much finer grained than the quartz clasts. There are some patches within the quartzite which show very fine-grained quartz that is possibly hydrothermal quartz.

White mica – occurs as sub- to euhedral grains in the quartz matrix as an alteration product of the pelitic component of the sandstone protolith. It occurs as fine-grained laths and as aphanitic crystal aggregates. There is a slight increase of white micas adjacent to the quartz veins.

Muscovite – Occurs as individual larger laths in the white mica, interstitial matrix.

Hematite – Occurs interstitially amongst the white mica groundmass

*BK13ES021: Harmony Formation - Quartzite***Mineral Modal Percentage:**

Quartz – 80%

White mica – 18%

Muscovite – 1%

Hematite – 1%

This sample was collected to examine rusty veins (<0.7 mm wide) hosted within the quartzite. The quartzite is composed of rounded, moderately sorted quartz grains. There is no other clast type. The matrix is composed of very fine-grained quartz and white phyllosilicates, either muscovite or phengite. These veinlets are composed of ~85% very fine-grained hematite and some contain very fine-grained white micas. There is some quartz in some of the veinlets.

Quartz – The quartz in the groundmass is rounded and moderately sorted. It is the only clast type. Some of the larger clasts (<1 mm) have subgrain formation. It is likely that the subgrains formed pre-metamorphism, before erosion and deposition, as not all the grains show the subgrain boundaries.

White mica – occurs as sub- to euhedral grains in the quartz matrix as an alteration product of the pelitic component of the sandstone protolith. It occurs as fine-grained laths and as aphanitic crystal aggregates. In the vein, the white micas make up a minor portion of the veinlets.

Muscovite – Occurs as larger laths in the white mica matrix

Hematite – The veinlet is outlined by the increased concentration of white micas and is dominantly defined by the presence of hematite. The relict cubic shapes suggest it is after pyrite.

*BK13ES022: Harmony Formation - Quartzite***Mineral Modal Percentage:**

Quartz – 35%

Hydrothermal quartz – 10%

White mica – 20%

Muscovite – 5%

Hematite – 12%

Jarosite – 18%

This sample displays brecciating hematite + jarosite + quartz + white mica veinlets within the quartzite. The quartzite is composed of rounded, moderately sorted quartz grains. There is no other clast type. The quartz in the groundmass in this sample appears to be more annealed and retains less of the clastic appearance (result of metamorphism?). The matrix is composed of very fine-grained quartz and white phyllosilicates as well as coarser either muscovite or phengite. This sample

shows fluid pathways through veinlets composed of very fine-grained hematite and aphanitic greenish jarosite. The veining has brecciated the host rock, with fragmented clasts of the annealed quartzite in the vein. Some of these clasts are quartzites with quartz veins hosted within the clast. The fluid pathways also show barren hydrothermal quartz veins which are cross-cut by the white mica veinlets. The jarosite in the veins occur in patches and tends to be in the centre of the veinlets with hematite selvages.

Quartz – The quartz in the groundmass is rounded and moderately sorted. Some of the larger grains (<1 mm) have subgrain formation. It is likely that the subgrains formed pre-metamorphism, before erosion and deposition, as not all the grains show the subgrain boundaries. The grains are also well annealed with wavy grain boundaries (the result of metamorphism).

Hydrothermal quartz – The quartz in the veins is finer-grained than the groundmass quartz. There are quartz veins in brecciated quartzite fragments in the vein.

White mica and sericite – Occurs as sub- to euhedral grains in the quartz matrix as an alteration product of the pelitic component of the sandstone protolith. It occurs as fine-grained laths and as aphanitic crystal aggregates.

Muscovite – Occurs as larger laths in the white mica-hematite veinlet. The sheets are radiating and intergrown with the majority of the sericite and other white micas.

Hematite – Occurs along the veinlet and occurs with jarosite. Some relict cubic shapes suggest it is after pyrite. The edges of the brecciating veins tend to be composed of hematite with jarosite cores.

Jarosite – Occurs along the veinlet and occurs with hematite. The core of the veins comprises relict cubic shapes suggesting it is after pyrite (intergrown with hematite).

*BK13ES028: Harmony Formation - Quartzite***Mineral Modal Percentage:**

Quartz – 35%

Hydrothermal quartz – 20%

White mica – 40%

Hematite – 5%

This sample was collected to examine quartz veins hosted within the quartzite. The quartzite is composed of rounded, well-sorted quartz grains. There is no other clast type. The matrix is composed of a much higher content of very fine-grained quartz and white phyllosilicates – either muscovite or phengite – than the other quartzite samples. There are <7 mm wide quartz veins which are composed of medium-grained quartz with well-developed and annealed grain boundaries. These quartz veins do not host white micas or primary pyrite. There is a single occurrence of altered pyrite and intergrown white micas in a vein.

Quartz – The quartz in the groundmass is rounded and moderately sorted. The groundmass is so fine-grained, that it suggests either recrystallization due to metamorphism or due to hydrothermal quartz replacement.

White mica – occurs as sub- to euhedral grains in the quartz matrix as an alteration product of the pelitic component of the sandstone protolith. It occurs as fine-grained laths and as aphanitic crystal aggregates. In the vein, the white micas are aligned along their long axis and trend parallel to the veinlet and are intergrown with the hematite.

Hematite – Occurs along the veinlet outlined by the increased concentration of white micas and lack of quartz clasts. The relict cubic shapes suggest it is after pyrite.

*BK13ES044: Harmony Formation - Quartzite***Mineral Modal Percentage:**

Quartz – 55%

Hydrothermal quartz – 40%

White mica – 3%

Muscovite – 1%

Hematite – 1%

Relict feldspars - <1%

This sample was collected to examine barren quartz veins hosted within the quartzite. The quartzite is composed of well annealed, medium- to coarse-grained quartz. The matrix is composed of fine-grained quartz and white phyllosilicates, either muscovite or phengite. As well, there are a few relict, clastic feldspar grains which have been partially altered to muscovite. There are <8 mm wide quartz veins which are randomly oriented and are composed of medium-grained

quartz with well-developed and annealed grain boundaries. These veins do not host white micas or primary pyrite. There are rusty, cubic outlines which suggest primary pyrite grains throughout the groundmass.

Quartz – The quartz in the groundmass is rounded and moderately sorted. Some of the larger clasts (<1 mm) have subgrain formation that likely formed pre-metamorphism, before erosion and deposition, as not all the grains show the subgrain boundaries.

Hydrothermal quartz – The quartz in the vein is clean and coarser-grained than the quartz clasts. The quartz vein shows no hematite or white mica in between the grain boundaries.

White mica – occurs as sub- to euhedral grains in the quartz matrix as an alteration product of the pelitic component of the sandstone protolith. It occurs as fine-grained laths and as aphanitic crystal aggregates. It also occurs as the alteration product of the feldspars.

Muscovite – Occurs as larger laths in the white mica-rich patches.

Hematite – Occurs interstitially as a stain amongst the white mica and clastic quartz groundmass.

*BK13ES048: Tertiary granite***Mineral Modal Percentage:**

Quartz – 27%

K-feldspar – 28%

Plagioclase – 22%

White mica – 12%

Hornblende – 10%

Biotite – <1%

Pyrite – <1%

Hematite – 1%

The monzogranite comprises quartz and feldspar phenocrysts in a quartz-rich + microcline + oligoclase + hornblende groundmass. Feldspars in the very fine-grained groundmass have been altered to sericite/white mica and other clay mineral with white mica replacing up to 15% of the crystals. The most common ferromagnesian mineral is hornblende which has been partially altered to biotite. The sample contains some quartz veins (<3mm wide) which cross-cut the phenocrysts and the groundmass and contain trace euhedral, altered pyrite.

Quartz – Very coarse-grained rounded phenocrysts which reach 9mm in diameter. These grains show some undulatory extinction, no subgrain formation and are unaltered. Fine-grained, anhedral quartz occurs in the altered groundmass. The largest quartz phenocrysts contain hornblende inclusions.

K-feldspar – The medium- to fine-grained K-feldspar crystals are euhedral and show some compositional zonation. They have undergone some sericitic alteration. The phenocrysts (which show some tartan twinning) are microcline.

Plagioclase – Several, equant, euhedral altered phenocrysts are found within the groundmass. They have been partially altered to white micas (~15% of the grain). Primary growth twins identify the composition as being oligoclase. The phenocrysts are euhedral and show some compositional zonation.

White mica – Occurs as sub- to euhedral grains in the quartz-feldspar groundmass as an alteration product of the plagioclase and the microcline. Dominantly occur as fine-grained laths and aphanitic crystal aggregates.

Hornblende – Occurs as subhedral to euhedral crystals throughout the groundmass. The crystals are not altered and are fragmented. Some crystals show simple twins and rarely occur as inclusions in quartz.

Biotite – Occurs as an alteration product of hornblende and with hematite.

Pyrite – Cubic crystals occur mostly as isolated grains in a quartz vein. Much of the pyrite has been altered to hematite.

Hematite – Occurs as a weathering product of pyrite and as an alteration product of the hornblende.

*BK13ES050: Tertiary granite***Mineral Modal Percentage:**

Quartz – 20%

Hydrothermal quartz – 35%

K-feldspar – 10%

Plagioclase – 5%

White mica – 28%

Hematite – 1%

Titanite – 1%

Epidote – <1%

Chlorite – <1%

This altered monzogranite with barren quartz stockwork veins comprises altered fine-grained quartz and K-spar phenocrysts in a quartz-rich + orthoclase + plagioclase groundmass. The feldspars in the groundmass have undergone sericite/white mica and other clay mineral alteration replacing up to 55% of some crystals. Primary, magmatic ferromagnesian minerals have been altered to opaque minerals (Fe-oxides), titanite and epidote. This sample contains quartz stockwork veins. There is trace chlorite associated with the vein selvages.

Quartz – Fine-grained, anhedral and rounded grain shapes (quartz eyes). These grains show some undulatory extinction and are unaltered. There is also finer-grained, anhedral quartz in the highly altered groundmass.

Hydrothermal quartz – The quartz in the veins is fine-grained and unmineralized with no associated pyrite/sericite alteration. There are rare fans of radiating chlorite.

K-feldspar – The K-feldspar is difficult to distinguish from the plagioclase due to the sericitic alteration but the larger relict grains (which show some tartan twinning) are more likely to be microcline. The K-feldspar have irregular and wavy grain boundaries.

Plagioclase – Several, equant, euhedral altered phenocrysts are found within the groundmass. They have been almost completely altered to white mica. Primary growth twins can be seen in some of the less altered grain rims. The plagioclase crystals have irregular and wavy grain boundaries.

White mica – Occurs as sub- to euhedral grains in the quartz-feldspar groundmass as an alteration product of the plagioclase and the microcline. Dominantly fine-grained laths and aphanitic crystal aggregates

Titanite – Occurs as mostly isolated, euhedral rhombs over-printing the quartz-feldspar groundmass. Its proximity to some ferromagnesian mineral clusters suggests that it may be the product of an alteration reaction

Chlorite – Occurs as subhedral crystals in aggregates along a quartz vein as fans and laths.

Epidote – Occurs as mostly isolated, subhedral, hexagonal crystals overprinting the quartz-feldspar groundmass and associated with the altered relict ferromagnesian minerals.

*BK13ES051: Tertiary granite***Mineral Modal Percentage:**

Quartz – 30%
 K-feldspar – 20%
 Plagioclase – 15%
 White mica – 12%
 Chlorite – 5%
 Hematite – <1%
 Titanite – <1%
 Clinozoisite – <1%

The monzogranite comprises quartz and feldspar phenocrysts in a quartz-rich + microcline + oligoclase groundmass. Feldspars in the very fine-grained groundmass have been altered to sericite/white mica and other clay minerals with white mica replacing up to 75% of the crystals. There are some suggestions of relict ferromagnesian minerals which have been altered to chlorite + muscovite? + hematite ± clinozoisite. There is no obvious mineralisation or pyrite present.

Quartz – Very coarse-grained rounded phenocrysts which reach 5mm in diameter. These grains show some undulatory extinction, no subgrain formation and are unaltered. There is also finer-grained, anhedral quartz in the altered groundmass.

K-feldspar – The medium- to fine-grained K-feldspar has undergone sericitic alteration. The phenocrysts (which show some tartan twinning) are microcline. The phenocrysts are euhedral and show some compositional zonation with the rims of the grains being preferentially altered.

Plagioclase – Several, equant, euhedral altered phenocrysts are found within the groundmass. They have been partially altered to white micas (~75% of the grain). Primary growth twins identify the composition as being oligoclase. The crystals are euhedral and show some compositional zonation with the rims of the grains being preferentially altered.

White mica – Occurs as sub- to euhedral grains in the quartz-feldspar groundmass as an alteration product of plagioclase and microcline. Dominantly occur as fine-grained laths and aphanitic crystal aggregates.

Chlorite – Occurs as complete replacement of subhedral to euhedral biotite sheets throughout the groundmass. Occurs with hematite and clinozoisite.

Titanite – Occurs as mostly isolated, euhedral rhombs over-printing the quartz-feldspar groundmass.

Clinozoisite – Occurs as acicular blue crystals forming glomeritic clusters in altered biotite sheets. They also occur sporadically throughout the quartz-feldspar groundmass.

BK13ES052: Tertiary Granites – Hydrothermal breccia

Mineral Modal Percentage:

Quartz – 85%

Hematite – 10%

Jarosite – 5%

Specularite – <1%

This sample displays brecciated hematite + jarosite + quartz veinlets. The breccia is chaotic, monomictic and clast-supported. The predominantly clast is older, crystallized hydrothermal quartz. The quartz is barren and contains annealed grain boundaries. The sample shows veinlets composed of very fine-grained hematite, quartz and aphanitic

yellow jarosite. The veining has brecciated previous quartz veins but there does not appear to be any quartz veins cross-cutting the Fe-oxide veinlets or the annealed brecciated quartz. The jarosite and hematite in the veins occurs in patches around the clasts. There are no primary or secondary sulphides. The hematite has formed some weathering rinds around specularite.

Quartz – The quartz clasts are hydrothermal in origin due to their annealed grain boundaries and lack of white mica or biotite (i.e., suggestions of a pelitic component). The clasts are variable in size, reaching up to >50 mm wide and are very angular.

Hematite – Occurs as the main matrix mineral of the breccia veins. It was most likely asulphidic breccia cement prior to its alteration to Fe-oxides. There may be a component of goethite in the cement. It occurs with jarosite. Some of the breccia veins outlines retained a relict cubic shape – suggesting the hematite is after pyrite. The Fe-oxides grow in euhedral and botryoidal forms in some locations.

Jarosite – Occurs along the veinlet and occurs with hematite. Some relict cubic shapes suggest it is after pyrite (intergrown with hematite).

Specularite – Occurs as isolated forms after pyrite. The outer rind is weathered to a darker brown hematite, while the core of the altered pyrite grain is whiter, more reflective and non-magnetic.

*BK13ES053: Tertiary granite***Mineral Modal Percentage:**

Quartz – 27%

K-feldspar – 33%

Plagioclase – 22%

White mica – 12%

Hornblende – 5%

Titanite – 1%

Epidote – <1%

The monzogranite comprises altered quartz and feldspar phenocrysts in a quartz-rich + microcline + oligoclase groundmass. Feldspars in the very fine-grained groundmass have been altered to sericite/white mica and other clay mineral which replaces up to 20% of some crystals. The most common ferromagnesian mineral is hornblende, which has not been altered, although it occurs with titanite and epidote. This sample contains some quartz and white mica veins and veinlets which cross-cut the phenocrysts and the groundmass.

Quartz – very coarse-grained rounded phenocrysts which reach 9mm in diameter. These grains show some undulatory extinction, no subgrain formation and are unaltered. There is also fine-grained, anhedral quartz in the altered groundmass.

K-feldspar – The medium- to fine-grained K-feldspar are euhedral and show some compositional zonation. They have undergone some sericitic alteration. The phenocrysts (which show some tartan twinning) are microcline.

Plagioclase – Several, equant, euhedral altered phenocrysts are found within the groundmass. They show compositional zoning and have been partially altered to white micas (~15% of the grain). Primary growth twins identify the composition as being oligoclase.

White mica – Occurs as sub- to euhedral crystals in the quartz-feldspar groundmass as an alteration product of the plagioclase and the microcline. Dominantly present as fine-grained laths and aphanitic crystal aggregates

Hornblende – occurs as subhedral to euhedral crystals throughout the groundmass. The crystals are not altered and are fragmented. Some grains some simple twins.

Titanite – Occurs as mostly isolated, euhedral rhombs over-printing the quartz-feldspar groundmass. Associated with hornblende and epidote.

Epidote – Occurs as mostly isolated, subhedral, hexagonal crystals over-printing the quartz-feldspar groundmass and associated with the altered relict ferromagnesian minerals.

*BK13ES061: Harmony Formation - Quartzite***Mineral Modal Percentage:**

Quartz – 80%

White mica – 12%

Muscovite – 5%

Biotite – 3%

Titanite – <1%

This sample was collected to examine cross-cutting quartz veins hosted within the quartzite. The quartzite is composed of rounded, moderately sorted quartz grains. There is no other clast type. The matrix is composed of very fine-grained quartz, biotite and white phyllosilicates, either muscovite or phengite. The white phyllosilicates and biotite occur in patches in the quartzite's matrix. There are <1 mm wide quartz veins which

are randomly oriented and are composed of medium-grained quartz with well-developed and annealed grain boundaries. These veins do not host white micas or primary pyrite

Quartz – The quartz in the groundmass is rounded and moderately sorted. Some of the larger clasts (<1 mm) have subgrains that likely formed pre-metamorphism, before erosion and deposition as not all the grains show the subgrain boundaries. The quartz in the veins is fine-grained and have well annealed grain boundaries. These veins do not host white micas or suggestions of primary pyrite

White mica – occurs as sub- to euhedral grains in the quartz matrix as an alteration product of the pelitic component of the sandstone protolith. It occurs as fine-grained laths and as aphanitic crystal aggregates. In the vein, the white micas are aligned along their long axis and trend parallel to the veinlet – defining it.

Muscovite – Occurs as larger laths in the white mica-biotite groundmass.

Biotite – Occurs as larger laths in the white mica-biotite groundmass.

Titanite – Grains are subhedral and glomeritic throughout the groundmass.

*BK13ES100: Cretaceous granite***Mineral Modal Percentage:**

Quartz – 40%

Hydrothermal quartz – 9%

K-feldspar – 10%

Plagioclase – 5%

Muscovite and white mica – 34%

Hematite – 1%

This altered granite comprises very altered coarse-grained quartz and K-feldspar phenocrysts in a quartz-rich + orthoclase + plagioclase groundmass that shows a granitic texture with annealed grain boundaries. Feldspars in the groundmass have been altered to sericite/white mica and other clay mineral alteration. In some of the plagioclase grains, white mica replaces up to 95% of the grain. The pyrite in the sample retains much of the relict cubic shape, but has Fe-oxide

alteration rims or has been completely altered to Fe-oxides.

Quartz – Coarse-grained, anhedral and rounded grain shapes (quartz eyes). These grains show some undulatory extinction and are unaltered. There is also finer-grained, anhedral quartz in the highly altered groundmass.

Hydrothermal quartz – The quartz in the veins is fine-grained and is associated with pyrite/sericite alteration.

K-feldspar – The K-feldspar is difficult to distinguish from the plagioclase due to the extensive sericitic alteration. The larger relict grains (which show some tartan twinning) are more likely microcline as the grain shape and size closely resembles the phenocrysts seen in less altered samples.

Plagioclase – Several, equant, euhedral altered phenocrysts are found within the groundmass. They have been almost completely altered to white micas. Primary growth twins can be seen in some of the less altered crystals rims.

Muscovite – Occurs occasionally replacing the altered feldspar and in the groundmass.

White mica – Occurs as sub- to euhedral grains in the quartz-feldspar groundmass as an alteration product of the plagioclase (fine-grained laths and aphanitic crystal aggregates) and the orthoclase as larger, parallel crystals.

Hematite – Occurs as a reaction product of the pyrite weathering to Fe-oxide. The primary pyrite was hydrothermal and the euhedral grains are seen over-printing the quartz-feldspar groundmass. The hematite retains the relict outline of the pyrite.

BK13ES104: Harmony Formation – Hydrothermal breccia

Mineral Modal Percentage:

Detrital quartz – 8%

Hydrothermal quartz – 52%

White mica – <1%

Pyrite – 25%

Arsenopyrite – 10%

Chalcopyrite – <1%

Sphalerite – <1%

Hematite – 5%

This sample displays brecciating quartz veinlets within the quartzite within a massive sulphide host. The breccia is chaotic and polymictic. The predominant ‘clast’ type is the brecciated massive sulphides and older quartz veins. There is a minor component of quartzite clasts in this unit. The quartz grains are round and show interstitial white micas. This sample shows fluid pathways marked by the precipitation of hydrothermal quartz cement and coeval precipitation of pyrite and arsenopyrite. The veining has brecciated the host rock, with some fragmented clasts of the annealed quartzite in the

vein. There are numerous, angular single quartz grains which are probably hydrothermal in origin that were subsequently brecciated. The sulphides present are pyrite and arsenopyrite with some chalcopyrite and sphalerite inclusions. There is no hematite, except for incomplete weathering rind on some of the pyrite, and no jarosite.

Quartz – The quartz in the probable quartzite clasts is rounded and moderately sorted. The suspected quartzite clasts appear to have clast-supported grain boundaries as opposed to annealed edges.

Hydrothermal quartz – The quartz in the breccia is finer-grained than the groundmass quartz and very angular. The grain size is variable.

White mica and sericite – Occurs as sub- to euhedral grains in the quartz matrix as an alteration product of the pelitic component of the sandstone protolith in the quartzite clasts. It occurs as fine-grained laths and as aphanitic crystal aggregates.

Pyrite – Occurs as euhedral grains in the quartz matrix. The pyrite is massive and shows cubic, inclusion-free cores, surrounded by very-fine grained granular pyrite and arsenopyrite. This texture suggests that the pyrite core acted as a nucleation site for later sulphide precipitation.

Arsenopyrite – Occurs as sub- to euhedral grains in the quartz matrix and is often associated with pyrite. It occurs as whiter, rhombs in the quartz cement, or as a mineral rind on the pyrite.

Chalcopyrite – Occurs as inclusions in the pyrite.

Sphalerite – Occurs as inclusions in the pyrite.

Hematite – Found on the pyrite grain boundaries as a weathering product.

Appendix 2: Sample lists

White Pine Fork Mo Porphyry

Sample descriptions and locations for the White Pine Fork Mo porphyry study area. UTM Coordinates are NAD27.

Sample	Unit	Lithology	Easting	Northing	Elevation	PTS	Mount
WP13ES001	White Pine intrusion	Granite and quartz-pyrite vein	442630	4489434	2689		
WP13ES002	Breccia pipe	Quartz cement and Mo	442460	4489331	2680		
WP13ES003	Little Cottonwood stock	Porphyritic granite	441521	4488155	2984	Yes	Yes
WP13ES004	Little Cottonwood stock	Porphyritic granite	441297	4488190	2925		
WP13ES005	Lamprophyre	Lamprophyric dyke	441314	4488621	2881	Yes	Yes
WP13ES006	Little Cottonwood stock	Porphyritic granite	441314	4488621	2881	Yes	Yes
WP13ES007	Little Cottonwood stock	Altered granite	441229	4489140	2754		
WP13ES008	Lamprophyre	Lamprophyric dyke	441077	4489629	2657		
WP13ES009	Little Cottonwood stock	Porphyritic granite	441077	4489629	2657	Yes	Yes
WP13ES010	Lamprophyres	Lamprophyric dyke	440987	4489867	2591		
WP13ES011	Little Cottonwood stock	Altered granite	441044	4489970	2572		
WP13ES012	Little Cottonwood stock	Porphyritic granite	441116	4490559	2508		
WP13ES013	Little Cottonwood stock	Porphyritic granite	442725	4487733	3093	Yes	Yes
WP13ES014	Little Cottonwood stock	Aplitic pegmatite dyke	442725	4487733	3093		
WP13ES015	Little Cottonwood stock	Xenolith in Little Cottonwood stock	442732	4487684	3090		
WP13ES016	Paleozoic metasedimentary rocks	Altered metasiltstone	442912	4488086	2987		
WP13ES017	Little Cottonwood stock	Porphyritic granite	442844	4488617	2861	Yes	Yes
WP13ES018	Little Cottonwood stock	Porphyritic granite	442874	4488858	2811		
WP13ES019	White Pine intrusion	Altered granite	442720	4489146	2769		
WP13ES020	White Pine intrusion	Porphyritic granite	442578	4490390	2596		
WP13ES021	White Pine intrusion	Altered granite	441918	4490808	2491		
WP13ES022	Little Cottonwood stock	Porphyritic granite	443573	4491671	2463	Yes	Yes
WP13ES023	White Pine intrusion	Porphyritic granite	443213	4490846	2821		
WP13ES024	White Pine intrusion	Porphyritic granite	443124	4490475	2949		
WP13ES025	White Pine intrusion	Aplitic dyke	443156	4490596	2963		
WP13ES026	White Pine intrusion	Porphyritic granite	443269	4490401	3036	Yes	Yes
WP13ES027	White Pine intrusion	Porphyritic granite	443257	4490251	3026		
WP13ES028	White Pine intrusion	Porphyritic granite	443365	4490168	3039	Yes	Yes
WP13ES030	Little Cottonwood stock	Porphyritic granite	440499	4488348	2984	Yes	Yes
WP13ES031	Little Cottonwood stock	Porphyritic granite	440503	4488632	2953		
WP13ES032	Little Cottonwood stock	Aplitic dyke	440542	4488788	2930		
WP13ES033	Little Cottonwood stock	Altered granite	440544	4488874	2919		
WP13ES034	Little Cottonwood stock	Altered granite	440653	4489218	2842		

Sample	Unit	Lithology	Easting	Northing	Elevation	PTS	PTS
WP13ES035	Little Cottonwood stock	Altered granite	440882	4489169	2808		
WP13ES036	Little Cottonwood stock	Altered granite	441178	4489285	2747	Yes	Yes
WP13ES037	Little Cottonwood stock	Altered granite	441648	4487790	3023		
WP13ES038	Little Cottonwood stock	Porphyritic granite	441587	4487880	2988		
WP13ES039	Little Cottonwood stock	Porphyritic granite	442554	4487684	3055		
WP13ES040	Little Cottonwood stock	Porphyritic granite	442564	4488141	3043	Yes	Yes
WP13ES041	Little Cottonwood stock	Porphyritic granite	442676	4488242	2963		
WP13ES042	Little Cottonwood stock	Porphyritic granite	442706	4488447	2890		
WP13ES043	Little Cottonwood stock	Aplitic dyke	442641	4488520	2858		
WP13ES044	Little Cottonwood stock	Porphyritic granite	442699	4488669	2819	Yes	Yes
WP13ES045	Little Cottonwood stock	Aplitic dyke	442675	4488713	2809		
WP13ES046	Little Cottonwood stock	Altered granite	442741	4488943	2804	Yes	Yes
WP13ES047	Little Cottonwood stock	Porphyritic granite	443156	4488003	3073		
WP13ES048	Little Cottonwood stock	Quartz-sericite vein	443156	4488003	3073		
WP13ES049	Little Cottonwood stock	Porphyritic granite	443208	4488086	3103		
WP13ES050	Little Cottonwood stock	Porphyritic granite	443175	4488331	3006		
WP13ES051	Little Cottonwood stock	Porphyritic granite	443241	4488575	2993		
WP13ES052	Little Cottonwood stock	Porphyritic granite	443116	4488704	2954		
WP13ES053	Little Cottonwood stock	Altered granite	443025	4488956	2885		
WP13ES054	White Pine intrusion	Porphyritic granite	442964	4489077	2869	Yes	Yes
WP13ES055	White Pine intrusion	Porphyritic granite	443722	4489798	3065		
WP13ES056	White Pine intrusion	Porphyritic granite	443536	4489832	3039		
WP13ES057	White Pine intrusion	Altered granite	443489	4489966	2987		
WP13ES058	Little Cottonwood stock	Altered granite	443727	4490549	2884	Yes	Yes
WP13ES059	Little Cottonwood stock	Porphyritic granite	443878	4490547	2844		
WP13ES060	Little Cottonwood stock	Porphyritic granite	443755	4490749	2805		
WP13ES061	Little Cottonwood stock	Porphyritic granite	443988	4491009	2749		
WP13ES062	Breccia pipe	Breccia cement and clasts	442582	4489280	2741		
WP13ES063	Breccia pipe	Breccia cement and clasts	442582	4489280	2741		
WP13ES064	White Pine intrusion	Altered granite	442429	4489968	2703	Yes	Yes
WP13ES065	White Pine intrusion	Altered granite	442221	4489771	2607	Yes	Yes
WP13ES066	White Pine intrusion	Altered granite	442084	4489641	2650		
WP13ES067	Little Cottonwood stock	Porphyritic granite	441797	4491637	2307		
WP13ES068	Little Cottonwood stock	Porphyritic granite	442823	4491905	2377	Yes	Yes

Buckingham Mo (-Cu) Porphyry

Sample descriptions and locations for the Buckingham Mo (-Cu) porphyry study area. UTM Coordinates are NAD27.

Sample	Unit	Lithology	Easting	Northing	Elevation	PTS
BK13ES001	Harmony Fm	Quartzite	494048	4495299	1940	
BK13ES002	Harmony Fm	Quartzite	493975	4495127	1955	
BK13ES003	Harmony Fm	Quartzite	493887	4495072	1960	Yes
BK13ES004	Harmony Fm	Quartzite	493828	4495078	1980	
BK13ES005	Harmony Fm	Quartzite	493854	4495695	1862	
BK13ES006	Harmony Fm	Quartzite	493869	4495675	1835	
BK13ES007	Harmony Fm	Quartzite	493884	4495688	1870	
BK13ES008	Buckingham porphyry	Porphyritic granite	494028	4495774	1853	
BK13ES009	Harmony Fm	Quartzite	493872	4495778	1890	Yes
BK13ES010	Harmony Fm	Slate	493290	4493079	1711	
BK13ES011	Buckingham porphyry	Porphyritic granite	493264	4493194	1774	Yes
BK13ES012	Harmony Fm	Quartzite	493242	4493400	1815	Yes
BK13ES013	Harmony Fm	Quartzite	493242	4493505	1851	Yes
BK13ES014	Harmony Fm	Quartzite	493309	4493679	1902	
BK13ES015	Harmony Fm	Quartzite	493467	4493840	1974	
BK13ES016	Hydrothermal Breccia	Polymictic breccia	493490	4493881	1984	Yes
BK13ES017	Harmony Fm	Quartzite	493543	4494037	2023	Yes
BK13ES018	Harmony Fm	Quartzite	493667	4494161	2038	Yes
BK13ES019	Harmony Fm	Quartzite	493740	4494130	2043	
BK13ES020	Harmony Fm	Quartzite	493803	4494098	2055	
BK13ES021	Harmony Fm	Quartzite	493689	4494250	2005	Yes
BK13ES022	Harmony Fm	Quartzite + breccia	493674	4494432	2021	Yes
BK13ES023	Harmony Fm	Altered quartzite	493704	4494629	2023	
BK13ES024	Harmony Fm	Altered quartzite	493819	4494693	2034	
BK13ES025	Harmony Fm	Altered quartzite	493870	4494735	2034	
BK13ES026	Harmony Fm	Leached cap	493796	4494753	2001	
BK13ES027	Harmony Fm	Quartzite	493834	4494857	1986	
BK13ES028	Harmony Fm	Quartzite	493830	4495512	1816	Yes
BK13ES029	Buckingham porphyry	Porphyritic granite	495943	4495282	1656	
BK13ES030	Buckingham porphyry	Porphyritic granite	495958	4495274	1660	
BK13ES031	Buckingham porphyry	Porphyritic granite	495986	4495359	1675	
BK13ES032	Buckingham porphyry	Porphyritic granite	496043	4495376	1690	
BK13ES033	Buckingham porphyry	Porphyritic granite	496157	4495370	1690	
BK13ES034	Buckingham porphyry	Porphyritic granite	496263	4495401	1720	
BK13ES035	Harmony Fm	Quartzite	496257	4495397	1711	
BK13ES036	Tertiary tectonism	Pebble dyke	496338	4495423	1748	

BK13ES037	Buckingham porphyry	Porphyritic granite	496359	4495459	1755	
BK13ES038	Buckingham porphyry	Porphyritic granite	496342	4495292	1765	
BK13ES039	Buckingham porphyry	Porphyritic granite	496262	4495161	1732	
BK13ES040	Buckingham porphyry	Porphyritic granite	496241	4495193	1732	
BK13ES041	Buckingham porphyry	Monzogranite	495555	4495735	1694	
BK13ES042	Buckingham porphyry	Porphyritic granite	495346	4495793	1736	
BK13ES043	Buckingham porphyry	Monzogranite	495158	4495801	1757	
BK13ES044	Harmony Fm	Quartzite	495061	4495804	1760	Yes
BK13ES045	Harmony Fm	Quartzite	495799	4495642	1675	
BK13ES046	Harmony Fm	Slate	493125	4493125	1740	
BK13ES047	Buckingham porphyry	Monzogranite	495575	4497315	1829	
BK13ES048	Tertiary granites	Granodiorite	495592	4497269	1821	Yes
BK13ES049	Tertiary granites	Granodiorite	495597	4497267	1818	
BK13ES050	Tertiary granites	Monzogranite	495602	4497295	1820	Yes
BK13ES051	Tertiary granites	Monzogranite	495704	4497207	1781	Yes
BK13ES052	Tertiary granites	Hydrothermal breccia	495681	4497212	1786	Yes
BK13ES053	Tertiary granites	Quartz granite	496126	4497348	1780	Yes
BK13ES054	Tertiary granites	Porphyritic granite	496496	4497072	1749	
BK13ES055	Tertiary granites	Granodiorite	496496	4497069	1748	
BK13ES056	Harmony Fm	Quartzite	496005	4496796	1731	
BK13ES057	Harmony Fm	Quartzite	495783	4496637	1727	
BK13ES058	Tertiary granites	Porphyritic granite	495531	4496420	1741	
BK13ES059	Harmony Fm	Cu-minzd quartzite	495423	4496484	1744	
BK13ES060	Harmony Fm	Quartzite	495288	4496112	1717	
BK13ES061	Harmony Fm	Quartzite	495300	4496176	1725	Yes
BK13ES062	Harmony Fm	Quartzite	495249	4496328	1764	
BK13ES063	Harmony Fm	Quartzite	495104	4496069	1731	
BK13ES100	Buckingham porphyry	Porphyritic granite	494781	4495855	1800	Yes
BK13ES101	Buckingham porphyry	Porphyritic granite	494649	4495456	1780	
BK13ES102	Harmony Fm	Quartzite	494552	4495308	1825	
BK13ES103	Harmony Fm	Quartzite	494527	4495031	1887	
BK13ES104	Buckingham porphyry	Breccia	494189	4494905	1943	Yes
BK13ES105	Harmony Fm	Hornfels	494314	4494553	1858	
BK13ES106	Tertiary granites	Quartz granite	494239	4494450	1866	
BK13ES107	Tertiary granites	Monzogranite	494379	4494988	1907	
BK13ES108	Harmony Fm	Quartzite	494101	4496025	1829	
BK13ES109	Harmony Fm	Quartzite	494207	4496050	1808	
BK13ES110	Harmony Fm	Quartzite	494507	4495843	1797	
BK13ES111	Harmony Fm	Quartzite	494959	4495888	1773	

Polished mounts for White Pine Fork and Buckingham study sites

Samples mounted and analysed for mineral chemistry at the White Pine Fork Mo porphyry and the Buckingham Mo (-Cu) porphyry study areas.

White Pine Fork Mo Porphyry							
Sample	Easting	Northing	Elevation	Hydrothermal Qz	Igneous Qz	Sedimentary Qz	Pyrite
WP13ES02	442460	4489331	2680	X			X
WP13ES03	441521	4488155	2984	X	X		X
WP13ES05	441314	4488621	2881	X			
WP13ES06	441314	4488621	2881	X	X		X
WP13ES07	441229	4489140	2754	X	X		X
WP13ES13	442725	4487733	3093	X	X		X
WP13ES22	443573	4491671	2463	X	X		X
WP13ES23	443213	4490846	2821	X	X		X
WP13ES41	442676	4488242	2963	X			X
WP13ES44	442699	4488669	2819				X
WP13ES46	442741	4488943	2804	X			X
WP13ES50	443175	4488331	3006				X
WP13ES52	443116	4488704	2954	X	X		X
WP13ES53	443025	4488956	2885	X			X
WP13ES63	442582	4489280	2741	X			X
WP13ES64	442429	4489968	2703	X	X		X
WP13ES65	442221	4489771	2607	X	X		X
Buckingham Mo (-Cu) Porphyry							
Sample	Easting	Northing	Elevation	Hydrothermal Qz	Igneous Qz	Sedimentary Qz	Pyrite
BK13ES001	494048	4495299	1940	X			
BK13ES003	493887	4495072	1960	X		X	
BK13ES006	493854	4495695	1862	X			
BK13ES009	493872	4495778	1890	X			
BK13ES012	493242	4493400	1815	X		X	
BK13ES013	493242	4493505	1851	X		X	
BK13ES015	493467	4493840	1974	X		X	
BK13ES017	493543	4494037	2023	X		X	
BK13ES018	493667	4494161	2038	X		X	
BK13ES020	493803	4494098	2055	X			
BK13ES021	493689	4494250	2005	X			
BK13ES025	493870	4494735	2034	X			X
BK13ES028	493830	4495512	1816	X			X
BK13ES044	495061	4495804	1760	X		X	
BK13ES046	493125	4493125	1740	X			
BK13ES050	495602	4497295	1820	X	X		
BK13ES059	495423	4496484	1744	X		X	X

BK13ES061	495300	4496176	1725	X		X	
BK13ES063	495104	4496069	1731	X			
BK13PH100	494781	4495855	1800	X	X		X
BK13PH101	494649	4495456	1780	X	X		
BK13PH102	494552	4495308	1825	X		X	X
BK13PH104	494189	4494905	1943	X			

Appendix 3: White Pine and Buckingham
geochronology data

Sample	WP13ES02													
Mthd	U-Pb													
Locality	WSR													
Min dated	Zr													
Unit	WP													
Rock type	Mzgpcc													
Age (Ma)	25.5	26	26	26.1	26.4	26.4	26.6	26.6	26.7	26.8	26.9	27	27.1	27.7
± 2 σ	0.5	1.3	1.2	0.9	0.8	1	0.7	0.9	0.8	1	1.4	0.6	0.6	1
206Pb/238U	0.004	0.0041	0.0043	0.0041	0.0041	0.0042	0.0041	0.0041	0.0042	0.0042	0.0044	0.0042	0.0042	0.0044
± 1 RSE	0.0205	0.0486	0.0453	0.0359	0.0281	0.0371	0.0243	0.0344	0.0282	0.0356	0.051	0.023	0.0226	0.0345
208Pb/232Th	0.0013	0.0019	0.0032	0.0014	0.0014	0.0016	0.0014	0.0014	0.0017	0.0014	0.0016	0.0013	0.0014	0.0016
± 1 RSE	0.0247	0.117	0.1152	0.0657	0.0509	0.0717	0.0449	0.0512	0.0612	0.0544	0.0789	0.0408	0.0447	0.0896
207Pb/206Pb	0.0455	0.0576	0.1	0.0445	0.0476	0.0561	0.048	0.0481	0.0629	0.0551	0.0817	0.0496	0.0467	0.0562
± 1 RSE	0.0488	0.1551	0.1159	0.087	0.0794	0.0979	0.0595	0.1073	0.0894	0.0884	0.1551	0.065	0.0697	0.1026
Pb204 (ppm)	0.0226	0.0129	0.043	0.024	0.0652	0.0155	0	0.0079	0.0367	0.0514	0	0.0287	0	0
Pb206 (ppm)	7.88	3.2178	5.2361	4.3453	4.2703	2.6703	5.1848	5.0986	3.8672	4.0331	2.0325	6.6883	4.5619	3.0932
Pb207 (ppm)	0.3596	0.1984	0.5637	0.1887	0.2029	0.1503	0.2457	0.2399	0.2439	0.2153	0.147	0.3186	0.2067	0.1599
Pb208 (ppm)	2.53	0.55	1.17	0.61	0.57	0.40	0.67	1.14	0.77	0.60	0.48	1.29	0.61	0.37
Th232 (ppm)	1913.67	330.83	360.11	458.96	401.74	273.54	494.41	865.88	444.71	445.17	308.73	1024.40	418.71	254.65
U238 (ppm)	1957.87	842.76	1319.31	1124.82	1060.67	653.61	1238.92	1286.24	929.36	1013.07	480.49	1655.36	1061.35	718.85
Tl49 (ppm)	5.95	5.75	0.03	0.49	3.18	0.73	3.24	4.74	2.10	5.36	9.46	3.62	1.24	1.40
Fe56 (ppm)	0.00	3.83	80.08	5.24	1.86	0.00	1.72	1.18	10.40	689.28	9.49	5.01	2.80	6.51
Hf178 (ppm)	11188.32	11925.37	12958.72	12926.68	13162.14	12155.74	13175.28	12185.12	12597.27	11870.56	11144.93	11717.39	12869.50	12157.71
238U/206Pb	252.046	244.4062	230.2822	246.6569	243.4809	240.6356	241.3749	240.9796	235.8695	237.2936	228.2954	237.408	237.4019	229.6701
± 1 Std Err	5.1747	11.8741	10.4431	8.8644	6.8371	8.9255	5.8571	8.292	6.6464	8.4551	11.6524	5.4496	5.3732	7.9344
207Pb/206Pb	0.0455	0.0576	0.1	0.0445	0.0476	0.0561	0.048	0.0481	0.0629	0.0551	0.0817	0.0496	0.0467	0.0562
± 1 Std Err	0.0022	0.0089	0.0116	0.0039	0.0038	0.0055	0.0029	0.0052	0.0056	0.0049	0.0127	0.0032	0.0033	0.0058
common Pb	0.8373	0.8373	0.8374	0.8373	0.8373	0.8373	0.8373	0.8373	0.8374	0.8374	0.8374	0.8374	0.8374	0.8374
206Pb/238U age	25.5257	26.322	27.9329	26.0823	26.4218	26.7336	26.6519	26.6955	27.2727	27.1093	28.1755	27.0963	27.097	28.0072
± 1 Std Err	0.5241	1.2788	1.2667	0.9374	0.7419	0.9916	0.6467	0.9186	0.7685	0.9659	1.4381	0.622	0.6133	0.9676
208Pb/232Th age	25.773	37.5787	65.415	27.6087	28.2685	31.3648	28.689	28.0799	34.6043	27.929	33.0537	26.5162	28.391	32.3548
± 1 Std Err	0.6364	4.3954	7.533	1.815	1.4388	2.2494	1.2884	1.4372	2.1184	1.5205	2.6072	1.0805	1.2687	2.9002
207Pb/206Pb age	-26.1445	515.023	1624.8777	-81.2985	78.3348	457.0902	97.2808	103.0792	705.684	415.8156	1239.091	178.1544	31.4316	460.8958
± 1 Std Err	59.1488	170.3279	107.7562	106.5218	94.2701	108.6197	70.3892	126.813	95.052	98.7931	151.9922	75.7683	83.4732	113.741
spot size (µm)	26	26	26	26	26	26	26	26	26	26	26	26	26	26
repetition (Hz)	5	5	5	5	5	5	5	5	5	5	5	5	5	5
fluence (Jcm²)	2.07	2.07	2.07	2.07	2.07	2.07	2.07	2.07	2.07	2.07	2.07	2.07	2.07	2.07
mode	spot													
Hg202	15.02	0.00	0.00	0.00	0.00	0.00	37.54	0.00	0.00	0.00	42.43	6.87	76.73	25.53
Pb204	8.94	6.14	21.24	11.02	28.33	6.92	0.00	3.60	16.67	23.32	0.00	12.92	0.00	0.00
Pb206	3186.42	1564.92	2637.33	2038.14	1894.72	1218.88	2042.86	2361.14	1793.70	1866.18	949.56	3077.16	1846.52	1300.43
Pb207	147.07	97.60	287.12	89.50	91.01	69.38	97.89	112.38	114.41	100.76	69.44	148.21	84.61	67.93
Pb208	1042.98	271.25	601.97	293.51	256.19	184.23	269.09	539.64	366.62	284.52	229.22	607.68	250.44	159.75
Th232	828803.53	172279.39	194128.18	230490.01	190726.70	133741.61	208605.79	429433.36	220782.87	220527.23	154360.81	504344.82	181427.83	114188.17
U238	938160.29	485537.42	786786.26	624942.18	557041.84	353575.38	578337.99	705771.96	510428.28	555197.45	265761.21	901552.27	508766.39	356373.91
Tl49	16.71	19.40	0.10	1.60	9.82	2.30	8.87	15.24	6.76	17.23	30.74	11.59	3.48	4.14
Fe56	0.10	253.61	5497.47	334.98	112.40	0.10	92.06	74.17	657.31	43456.59	604.59	314.17	154.60	374.57
Zr90	39173371	47118829	48806699	45445395	42998431	44218144	38172748	44864138	44943159	44833433	45272405	44584801	39220166	40789302
Hf178	1762609	2259339	2542227	2361908	2274395	2161772	2022354	2198370	2275834	2139607	2027940	2099582	2029095	1988194
Fe56BG	4653.60	4317.80	4407.07	4536.15	4660.07	5115.68	4423.71	4634.24	4516.04	4396.73	4526.63	4703.93	4563.26	4587.86

Notes: WSR – Wasatch Range; BTM – Battle Mountain; WP – White Pine intrusion; EG – Eocene granite; Zr – zircon, Mo – molybdenite; Qtz – quartz, Py – pyrite; Mzgp – monzogranite porphyry, Grd – granodiorite, Qgr – quartz granite

Appendix 3: White Pine and Buckingham
geochronology data

Sample	BK13ES048	BK13ES048	BK13ES048	BK13ES048	BK13ES048	BK13ES048	BK13ES048	BK13ES048	BK13ES048	BK13ES048	BK13ES048	BK13ES048	BK13ES048	BK13ES048	BK13ES048
Mthd	U-Pb	U-Pb	U-Pb	U-Pb	U-Pb	U-Pb	U-Pb	U-Pb	U-Pb	U-Pb	U-Pb	U-Pb	U-Pb	U-Pb	U-Pb
Locality	BTM	BTM	BTM	BTM	BTM	BTM	BTM	BTM	BTM	BTM	BTM	BTM	BTM	BTM	BTM
Min dated	Zr	Zr	Zr	Zr	Zr	Zr	Zr	Zr	Zr	Zr	Zr	Zr	Zr	Zr	Zr
Unit	EG	EG	EG	EG	EG	EG	EG	EG	EG	EG	EG	EG	EG	EG	EG
Rock type	Grd	Grd	Grd	Grd	Grd	Grd	Grd	Grd	Grd	Grd	Grd	Grd	Grd	Grd	Grd
Age (Ma)	37.4	37.6	37.7	38.2	38.3	38.6	38.6	39.1	39.1	39.1	39.2	40	40.3	38.7	144
± 2 σ	0.7	0.7	1	0.7	0.6	0.7	0.7	0.7	0.7	0.6	0.7	0.6	0.7	0.5	2.3
206Pb/238U	0.0064	0.0059	0.0059	0.0061	0.0061	0.006	0.006	0.0062	0.0061	0.0061	0.0062	0.0061	0.0062	0.0063	0.0228
± 1 RSE	0.0209	0.0188	0.0177	0.0267	0.0178	0.0162	0.0177	0.0185	0.0171	0.0166	0.0152	0.0174	0.0154	0.0183	0.016
208Pb/232Th	0.0071	0.0023	0.0025	0.0025	0.0031	0.002	0.0021	0.0046	0.0018	0.0022	0.0025	0.0022	0.0021	0.0022	0.0089
± 1 RSE	0.0431	0.0396	0.0444	0.0572	0.046	0.0305	0.032	0.0527	0.0457	0.0364	0.04	0.0328	0.0322	0.0431	0.0442
207Pb/206Pb	0.1296	0.0554	0.0547	0.0734	0.0633	0.0524	0.0516	0.074	0.0468	0.0472	0.057	0.0483	0.0478	0.0458	0.0558
± 1 RSE	0.0341	0.0303	0.0379	0.0711	0.0428	0.0332	0.033	0.0339	0.0313	0.0327	0.0345	0.029	0.0347	0.0409	0.0407
Pb204 (ppm)	0.0995	0	0	0.0296	0.0004	0.033	0.0241	0.0876	0.0001	0	0.0084	0.013	0.0114	0	0.0122
Pb206 (ppm)	6.6958	9.0216	6.3557	2.0926	8.031	9.5944	13.8195	10.6878	10.1994	10.9905	8.9741	7.2653	9.1312	6.7951	25.5829
Pb207 (ppm)	0.8797	0.4943	0.336	0.1495	0.4873	0.4938	0.7176	0.7899	0.4765	0.5138	0.5061	0.3519	0.4389	0.3133	1.4427
Pb208 (ppm)	1.84	0.75	0.46	0.31	0.62	1.00	1.19	1.07	0.42	1.06	0.89	0.62	0.76	0.40	1.12
Th232 (ppm)	252.18	344.29	195.79	128.26	218.54	516.77	599.46	231.18	226.90	495.75	357.25	281.12	359.68	190.90	123.66
U238 (ppm)	1065.21	1651.63	1101.40	356.18	1374.44	1651.38	2469.83	1736.86	1694.29	1836.90	1496.20	1215.70	1470.74	1118.73	1116.79
Ti49 (ppm)	7.33	9.37	4.49	5.44	2.83	2.38	4.21	3.56	0.99	4.32	2.84	3.87	2.67	2.18	9.69
Fe56 (ppm)	70.34	143.14	8.50	8.93	12.30	3.89	7.45	25.37	0.00	37.13	6.77	86.17	4.09	0.59	27.95
Hf178 (ppm)	10304.04	10746.19	10884.03	9959.84	11692.84	10840.50	10918.14	11694.29	11261.67	10408.96	10993.96	10879.30	10623.64	11004.26	11591.09
238U/206Pb	155.4255	169.9063	169.1774	164.6089	164.7376	166.4577	165.6775	160.7124	164.5675	164.2365	162.1306	163.5496	160.3786	159.5166	43.8987
± 1 Std Err	3.2516	3.1893	2.9884	4.397	2.9287	2.6921	2.9279	2.9749	2.8206	2.7209	2.4686	2.8537	2.4629	2.9157	0.7018
207Pb/206Pb	0.1296	0.0554	0.0547	0.0734	0.0633	0.0524	0.0516	0.074	0.0468	0.0472	0.057	0.0483	0.0478	0.0458	0.0558
± 1 Std Err	0.0044	0.0017	0.0021	0.0052	0.0027	0.0017	0.0017	0.0025	0.0015	0.0015	0.002	0.0014	0.0017	0.0019	0.0023
common Pb	0.8383	0.838	0.8381	0.8381	0.8381	0.8381	0.8381	0.8382	0.8381	0.8381	0.8382	0.8381	0.8382	0.8382	0.8451
206Pb/238U age	41.3431	37.8298	37.9923	39.0435	39.0131	38.6112	38.7925	39.9872	39.0533	39.1318	39.6385	39.2956	40.0702	40.286	145.1999
± 1 Std Err	0.8649	0.7101	0.6711	1.0429	0.6936	0.6245	0.6856	0.7402	0.6694	0.6483	0.6035	0.6857	0.6154	0.7364	2.3214
208Pb/232Th age	143.2272	46.2256	50.7467	49.663	63.3224	40.9534	42.1216	92.8884	37.0887	44.9196	49.6456	44.9902	41.8422	43.5642	178.9158
± 1 Std Err	6.1794	1.8288	2.2521	2.8405	2.9129	1.2486	1.3464	4.8995	1.6963	1.6351	1.986	1.4772	1.3481	1.8784	7.9089
207Pb/206Pb age	2092.4346	428.1607	399.5093	1024.098	718.7823	303.8976	269.2866	1040.7424	37.4761	57.0329	492.5369	113.2288	91.5071	-10.6273	444.0223
± 1 Std Err	29.9524	33.7756	42.4094	71.9177	45.4785	37.8474	37.8637	34.2493	37.4452	38.9724	38.002	34.228	41.1573	49.3588	45.2695
spot size (µm)	32	32	32	32	32	32	32	32	32	32	32	32	32	32	32
repetition (Hz)	5	5	5	5	5	5	5	5	5	5	5	5	5	5	5
fluence (Jcm²)	2.05	2.05	2.05	2.05	2.05	2.05	2.05	2.05	2.05	2.05	2.05	2.05	2.05	2.05	2.05
mode	Spot	Spot	Spot	Spot	Spot	Spot	Spot	Spot	Spot	Spot	Spot	Spot	Spot	Spot	Spot
Hg202	0.00	71.24	70.46	5.61	24.87	0.00	22.11	4.70	28.82	37.89	11.06	12.09	41.05	27.83	9.12
Pb204	34.62	0.00	0.00	14.84	0.13	15.75	9.48	37.62	0.04	0.00	3.84	6.36	5.26	0.00	5.48
Pb206	4140.37	7563.42	5214.07	1767.82	4623.18	7966.13	9592.70	7948.31	8316.43	7594.70	7299.11	5979.78	7121.96	5708.83	20121.65
Pb207	537.01	409.10	272.14	124.66	276.94	404.77	491.79	579.90	383.58	350.52	406.41	285.93	337.89	259.85	1120.24
Pb208	1128.43	619.45	372.01	260.10	353.77	818.05	818.37	784.97	336.46	727.89	714.09	502.66	584.65	336.46	869.84
Th232	150249.79	278095.91	154770.13	104367.73	121228.86	413355.62	400912.83	165621.52	178223.31	330008.81	279979.38	222853.45	270217.29	154490.48	93700.79
U238	678923.10	1427121.28	931406.40	310025.34	815636.82	1413034.65	1767037.54	1331106.86	1423569.93	1308035.32	1254398.18	1030899.61	1181948.36	968465.31	905272.03
Ti49	49.48	85.78	40.23	50.09	17.83	21.55	31.87	28.93	8.82	32.55	25.24	34.71	22.73	19.94	83.22
Fe56	10003.34	27592.67	1604.44	1731.68	1628.87	742.39	1188.92	4335.80	0.10	5896.11	1266.31	16285.11	732.05	114.79	5053.59
Zr90	115962949	157193398	153876932	158283065	107987840	155649373	130163312	139400512	152813125	129517633	152546716	154193614	146145923	157436571	147459296
Hf178	2608214	3687840	3655220	3443778	2755585	3684231	3102335	3559762	3758480	2944103	3660500	3664797	3391379	3784006	3731761
Fe56BG	19217.92	19264.33	19569.37	19411.63	19580.66	19227.05	19427.15	19706.16	19844.41	19593.78	19140.80	20048.06	19942.55	19848.50	19704.19

Appendix 3: White Pine and Buckingham
geochronology data

Sample	BK13ES050	BK13ES050	BK13ES050	BK13ES050	BK13ES050	BK13ES050	BK13ES050	BK13ES050	BK13ES050	BK13ES050	BK13ES050	BK13ES050	BK13ES050	BK13ES050	BK13ES050	BK13ES050
Mthd	U-Pb	U-Pb	U-Pb	U-Pb	U-Pb	U-Pb	U-Pb	U-Pb	U-Pb	U-Pb	U-Pb	U-Pb	U-Pb	U-Pb	U-Pb	U-Pb
Locality	BTM	BTM	BTM	BTM	BTM	BTM	BTM	BTM	BTM	BTM	BTM	BTM	BTM	BTM	BTM	BTM
Min dated	Zr	Zr	Zr	Zr	Zr	Zr	Zr	Zr	Zr	Zr	Zr	Zr	Zr	Zr	Zr	Zr
Unit	EG	EG	EG	EG	EG	EG	EG	EG	EG	EG	EG	EG	EG	EG	EG	EG
Rock type	Mzgp	Mzgp	Mzgp	Mzgp	Mzgp	Mzgp	Mzgp	Mzgp	Mzgp	Mzgp	Mzgp	Mzgp	Mzgp	Mzgp	Mzgp	Mzgp
Age (Ma)	37.3	38.2	38.3	38.9	38.9	39	39.4	39.5	39.9	39.9	40.2	40.4	40.9	49.9	131.7	
± 2 σ	0.9	0.6	0.6	0.6	0.5	0.8	0.7	0.9	0.9	0.7	0.6	0.7	0.7	0.9	2	
206Pb/238U	0.0061	0.0059	0.0061	0.0061	0.0061	0.0065	0.0062	0.0072	0.0063	0.0063	0.0063	0.0063	0.0064	0.0085	0.0211	
± 1 RSE	0.0236	0.0153	0.0157	0.0164	0.014	0.0193	0.0179	0.0188	0.0216	0.0173	0.0139	0.0182	0.0164	0.0176	0.0153	
208Pb/232Th	0.0037	0.0019	0.0026	0.0021	0.0019	0.0046	0.0026	0.0093	0.0023	0.0031	0.002	0.0025	0.0021	0.0047	0.0059	
± 1 RSE	0.0375	0.0326	0.0302	0.034	0.0254	0.0469	0.0338	0.0499	0.0512	0.0456	0.0213	0.0396	0.045	0.0282	0.0415	
207Pb/206Pb	0.0839	0.0456	0.0662	0.0514	0.0454	0.0973	0.0598	0.1591	0.0589	0.0625	0.0475	0.0489	0.0484	0.1119	0.0678	
± 1 RSE	0.0444	0.0346	0.0304	0.0319	0.0225	0.0391	0.0437	0.0522	0.0592	0.046	0.0212	0.0401	0.0382	0.0326	0.0203	
Pb204 (ppm)	0.0338	0.0187	0.0628	0.0068	0	0.0401	0	0.1316	0.0111	0	0	0.0204	0	0.0891	0.0444	
Pb206 (ppm)	8.5386	8.459	9.2446	7.7231	17.3415	11.1246	4.3935	12.7622	2.2485	6.3559	19.9777	7.9058	6.6296	8.0431	31.8675	
Pb207 (ppm)	0.703	0.3856	0.609	0.3949	0.7888	1.0912	0.2611	2.1396	0.1325	0.373	0.9431	0.3933	0.3186	0.8839	2.1554	
Pb208 (ppm)	1.36	0.61	1.12	0.52	1.43	2.01	0.52	4.83	0.31	0.52	3.68	0.55	0.35	2.41	0.89	
Th232 (ppm)	387.05	313.52	430.71	241.38	766.79	456.03	199.75	465.55	131.21	181.46	1869.44	226.82	165.64	523.18	163.85	
U238 (ppm)	1555.31	1476.49	1566.15	1311.76	2955.71	1784.41	717.57	1760.08	368.52	1049.80	3281.38	1261.65	1083.81	953.84	1663.09	
Ti49 (ppm)	4.56	3.14	2.60	2.79	3.26	11.33	5.96	6.99	10.28	2.66	6.08	0.75	3.00	8.67	5.33	
Fe56 (ppm)	333.10	14.27	118.82	9.18	1.83	557.68	173.92	574.52	61.87	93.73	62.47	52.78	1.85	2122.91	5.57	
Hf178 (ppm)	11186.71	10948.83	11227.69	11061.25	11260.94	11553.21	10089.77	11570.43	9938.16	10881.20	9814.19	10932.58	11062.65	10552.03	13771.70	
238U/206Pb	164.1588	168.3915	163.5751	164.3651	165.2564	154.2185	160.574	139.5836	158.7792	158.0146	159.8265	158.5343	156.7732	118.2461	47.2982	
± 1 Std Err	3.8807	2.568	2.5641	2.7029	2.3144	2.9834	2.881	2.6183	3.429	2.7273	2.2153	2.8894	2.5759	2.0806	0.7241	
207Pb/206Pb	0.0839	0.0456	0.0662	0.0514	0.0454	0.0973	0.0598	0.1591	0.0589	0.0625	0.0475	0.0489	0.0484	0.1119	0.0678	
± 1 Std Err	0.0037	0.0016	0.002	0.0016	0.001	0.0038	0.0026	0.0083	0.0035	0.0029	0.001	0.002	0.0019	0.0036	0.0014	
common Pb	0.8381	0.8381	0.8381	0.8381	0.8381	0.8383	0.8382	0.8386	0.8382	0.8382	0.8382	0.8382	0.8382	0.8391	0.8444	
206Pb/238U age	39.1503	38.1691	39.2895	39.1013	38.891	41.6656	40.0216	46.0185	40.4726	40.6678	40.2082	40.5349	40.9888	54.2877	134.8722	
± 1 Std Err	0.9255	0.5821	0.6159	0.643	0.5447	0.806	0.7181	0.8632	0.874	0.7019	0.5573	0.7388	0.6735	0.9552	2.0648	
208Pb/232Th age	75.6326	39.3718	51.9945	43.0155	37.5746	92.9453	52.5942	187.9618	47.0216	62.2314	39.695	49.6702	42.2265	94.1249	118.7033	
± 1 Std Err	2.8398	1.2839	1.5707	1.4646	0.9562	4.3596	1.78	9.3841	2.4061	2.8373	0.8454	1.9679	1.8991	2.6551	4.9234	
207Pb/206Pb age	1289.949	-20.8769	813.1315	257.3334	-36.021	1572.7996	596.4841	2446.2764	564.2128	692.1935	76.156	141.0262	119.2148	1829.8102	862.9542	
± 1 Std Err	43.2454	41.8093	31.802	36.6987	27.3372	36.6426	47.3822	44.138	64.5106	49.0374	25.1286	47.0566	45.0536	29.546	21.0343	
spot size (µm)	32	32	32	32	32	32	32	32	32	32	32	32	32	32	32	
repetition (Hz)	5	5	5	5	5	5	5	5	5	5	5	5	5	5	5	
fluence (Jcm ²)	2.05	2.05	2.05	2.05	2.05	2.05	2.05	2.05	2.05	2.05	2.05	2.05	2.05	2.05	2.05	
mode	Spot	Spot	Spot	Spot	Spot	Spot	Spot	Spot	Spot	Spot	Spot	Spot	Spot	Spot	Spot	
Hg202	0.00	9.46	0.00	0.00	0.00	26.98	12.99	112.38	6.98	19.51	47.88	24.09	32.11	40.00	0.00	
Pb204	12.63	8.16	27.24	2.88	0.00	13.69	0.00	41.95	4.83	0.00	0.00	8.65	0.00	33.16	21.54	
Pb206	5955.34	7200.31	7563.14	6392.25	14016.07	7055.84	3595.48	8134.43	1834.70	4834.25	16248.75	6181.44	5462.21	5817.00	29657.30	
Pb207	484.16	324.11	492.00	322.73	629.57	683.36	210.99	1346.78	106.79	280.13	757.47	303.66	259.26	631.24	1980.78	
Pb208	936.08	510.25	905.88	425.85	1141.50	1261.06	421.82	3045.32	248.50	394.81	2966.81	423.99	285.43	1723.87	821.61	
Th232	260180.26	257275.26	339633.23	192607.12	597394.64	278761.59	157579.66	286106.50	103189.30	133033.75	1465939.10	170916.12	131580.38	364764.93	146993.00	
U238	1118504.03	1296309.57	1321251.66	1119896.07	2463629.39	1166936.61	605648.54	1157303.84	310063.14	823411.46	2753022.10	1017077.20	921152.77	711504.61	1596212.12	
Ti49	34.77	29.27	23.28	25.27	28.82	78.55	53.39	48.78	91.70	22.14	54.18	6.45	27.05	68.60	54.31	
Fe56	53505.58	2801.61	22394.51	1752.58	340.43	81449.71	32808.08	84486.03	11627.69	16426.22	11719.73	9501.23	352.44	353969.79	1195.55	
Zr90	130907428	159884536	153582670	155480542	151757076	119034248	153687215	119767099	153165348	142797770	152801821	146727532	154802368	135834272	174756679	
Hf178	3194365	3816159	3760828	3748854	3726565	3000029	3380944	3019989	3320101	3388574	3268653	3499603	3732406	3124872	5247746	
Fe56BG	18781.39	18779.70	19273.81	19277.26	19325.08	18953.94	19343.99	19352.58	19290.18	19428.40	19464.55	19277.28	19316.01	19319.91	19308.27	

Appendix 3: White Pine and Buckingham
geochronology data

Sample	BK13ES053	BK13ES053	BK13ES053	BK13ES053	BK13ES053	BK13ES053	BK13ES053	BK13ES053	BK13ES053	BK13ES053	BK13ES053	BK13ES053	BK13ES053	BK13ES053	BK13ES053
Mthd	U-Pb	U-Pb	U-Pb	U-Pb	U-Pb	U-Pb	U-Pb	U-Pb	U-Pb	U-Pb	U-Pb	U-Pb	U-Pb	U-Pb	U-Pb
Locality	BTM	BTM	BTM	BTM	BTM	BTM	BTM	BTM	BTM	BTM	BTM	BTM	BTM	BTM	BTM
Min dated	Zr	Zr	Zr	Zr	Zr	Zr	Zr	Zr	Zr	Zr	Zr	Zr	Zr	Zr	Zr
Unit	EG	EG	EG	EG	EG	EG	EG	EG	EG	EG	EG	EG	EG	EG	EG
Rock type	Mzgp	Mzgp	Mzgp	Mzgp	Mzgp	Mzgp	Mzgp	Mzgp	Mzgp	Mzgp	Mzgp	Mzgp	Mzgp	Mzgp	Mzgp
Age (Ma)	40	40.2	40.2	40.8	40.8	41	41	41	41.4	41.4	41.9	240	591.1	1668.2	1748
± 2 σ	0.7	0.7	0.8	1.2	1.9	1.1	0.9	0.6	0.8	0.9	1	11.1	10	21.9	23.1
206Pb/238U	0.0063	0.0063	0.0063	0.0063	0.0064	0.0064	0.0064	0.0064	0.0065	0.0065	0.0065	0.0399	0.0978	0.3111	0.3122
± 1 RSE	0.0186	0.0174	0.0201	0.0284	0.0456	0.027	0.0209	0.0151	0.019	0.022	0.0241	0.0468	0.0172	0.0134	0.0134
208Pb/232Th	0.002	0.002	0.002	0.0021	0.0021	0.002	0.0023	0.0021	0.0023	0.0022	0.0021	0.0337	0.0463	0.0931	0.0904
± 1 RSE	0.0481	0.0364	0.0472	0.0629	0.0976	0.052	0.0504	0.0411	0.0384	0.0505	0.0484	0.0496	0.0196	0.0192	0.0226
207Pb/206Pb	0.0516	0.0497	0.0504	0.0437	0.0576	0.0479	0.048	0.0479	0.0517	0.0501	0.0496	0.091	0.0742	0.1466	0.1089
± 1 RSE	0.0415	0.0355	0.049	0.0726	0.1073	0.0821	0.0491	0.0356	0.0396	0.0556	0.0673	0.0138	0.0151	0.0091	0.0144
Pb204 (ppm)	0.0736	0.0285	0.0459	0.0176	0	0.0062	0.0672	0.0397	0	0	0.0163	0.0236	0.1099	0.0436	0.0362
Pb206 (ppm)	5.5542	7.0771	6.6388	1.6528	3.7912	1.8445	4.0759	8.3963	5.4106	3.3464	2.4855	28.9113	54.4349	96.8387	31.0261
Pb207 (ppm)	0.2832	0.3525	0.3346	0.0704	0.2053	0.0886	0.1897	0.3998	0.2756	0.1677	0.115	2.635	4.0566	14.223	3.3731
Pb208 (ppm)	0.29	0.47	0.53	0.13	0.29	0.23	0.21	0.37	0.52	0.28	0.21	1.98	12.07	16.10	3.35
Th232 (ppm)	150.61	236.87	281.96	64.01	159.94	114.35	98.27	175.98	236.18	131.21	99.13	75.39	250.35	166.40	36.51
U238 (ppm)	914.89	1164.49	1165.81	269.23	683.69	299.94	675.65	1354.96	883.02	546.93	406.84	851.07	549.72	308.65	99.83
Tl49 (ppm)	2.87	5.69	4.17	3.24	8.18	5.20	1.84	2.16	3.09	4.29	5.48	2.48	9.11	5.91	12.34
Fe56 (ppm)	2.64	1.81	0.00	0.00	1.51	0.83	0.05	0.00	3.60	0.00	0.00	8.75	7.67	8.57	2.52
Hf178 (ppm)	11417.30	11315.58	10407.01	10395.24	9471.76	9550.69	12157.17	11459.75	10739.67	10691.96	9626.23	11312.03	11335.43	11630.43	6777.75
238U/206Pb	159.5942	159.3773	159.0185	157.5675	155.2409	156.5702	156.4957	156.4563	154.4202	154.4029	152.9058	25.048	10.2284	3.2147	3.2034
± 1 Std Err	2.9622	2.781	3.1922	4.4806	7.0766	4.2346	3.2779	2.3636	2.9393	3.3893	3.6864	1.1725	0.1762	0.0431	0.043
207Pb/206Pb	0.0516	0.0497	0.0504	0.0437	0.0576	0.0479	0.048	0.0479	0.0517	0.0501	0.0496	0.091	0.0742	0.1466	0.1089
± 1 Std Err	0.0021	0.0018	0.0025	0.0032	0.0062	0.0039	0.0024	0.0017	0.002	0.0028	0.0033	0.0013	0.0011	0.0013	0.0016
common Pb	0.8382	0.8382	0.8382	0.8382	0.8383	0.8383	0.8383	0.8383	0.8383	0.8383	0.8383	0.8383	0.8523	0.8772	0.9765
206Pb/238U age	40.2665	40.3211	40.4118	40.7828	41.392	41.0418	41.0612	41.0715	41.6113	41.616	42.021	252.3577	601.3114	1745.9832	1751.3861
± 1 Std Err	0.7474	0.7036	0.8112	1.1597	1.8868	1.11	0.8601	0.6205	0.7921	0.9135	1.0131	11.8132	10.3614	23.3834	23.4924
208Pb/232Th age	39.5621	40.0934	41.045	42.0565	42.3512	40.2724	46.0076	42.218	45.559	44.0885	42.7355	669.1601	913.8996	1799.3841	1749.6427
± 1 Std Err	1.9018	1.4588	1.937	2.6473	4.1345	2.0951	2.3195	1.734	1.7478	2.2275	2.0701	33.1735	17.8737	34.4914	39.6196
207Pb/206Pb age	268.2692	178.7998	212.2471	-129.4661	513.9946	94.3084	100.2385	93.5019	270.2354	199.9678	174.7623	1446.9807	1048.232	2306.3968	1780.297
± 1 Std Err	47.6085	41.3973	56.7553	89.7482	117.9043	97.2553	58.1143	42.1785	45.3597	64.5982	78.5169	13.1066	15.2427	7.8383	13.0985
spot size (µm)	32	32	32	32	32	32	32	32	32	32	32	32	32	32	32
repetition (Hz)	5	5	5	5	5	5	5	5	5	5	5	5	5	5	5
fluence (Jcm²)	2.05	2.05	2.05	2.05	2.05	2.05	2.05	2.05	2.05	2.05	2.05	2.05	2.05	2.05	2.05
mode	Spot	Spot	Spot	Spot	Spot	Spot	Spot	Spot	Spot	Spot	Spot	Spot	Spot	Spot	Spot
Hg202	0.00	19.03	0.00	0.00	116.95	0.00	0.00	28.54	16.23	51.48	48.43	0.00	19.71	0.00	0.00
Pb204	27.72	11.08	20.19	6.42	0.00	2.27	27.57	14.74	0.00	0.00	6.41	9.33	37.44	14.41	13.81
Pb206	4506.17	5821.83	6126.55	1328.77	3570.33	1498.69	3448.98	6889.57	4519.53	2718.14	2037.44	23443.45	40227.82	69814.98	24104.71
Pb207	226.92	286.41	304.98	55.93	190.94	71.08	158.56	324.03	227.38	134.50	93.10	2110.21	2961.15	10128.58	2588.18
Pb208	230.51	379.75	488.71	103.33	273.73	182.78	178.67	300.76	429.66	226.76	171.66	1593.06	8832.08	11492.48	2575.45
Th232	117858.00	187935.69	250948.72	49642.10	145277.25	89638.65	80189.32	139303.47	190288.13	102779.38	78366.82	58950.41	178460.92	115719.97	27350.68
U238	766088.84	988574.97	1110212.65	223417.69	664470.65	251583.53	589913.10	1147677.62	761247.57	458400.58	344140.81	712037.20	419307.94	229676.46	80017.87
Tl49	25.52	51.36	42.21	28.55	84.46	46.43	17.09	19.48	28.31	38.20	49.27	22.04	73.89	46.80	105.10
Fe56	494.45	343.27	0.10	0.10	329.56	156.26	9.08	0.10	694.21	0.10	0.10	1638.85	1311.08	1427.79	452.63
Zr90	152619438	154705156	173534490	151273353	177122096	152920539	159076444	154414853	157120665	152713307	154134084	152423651	139031499	135645255	146026731
Hf178	3793966	3812418	3933365	3423077	3653332	3178738	4212994	3851685	3674319	3556758	3231778	3756460	3431135	3434430	2156435
Fe56BG	18396.28	18688.19	18420.79	18771.90	18508.66	18336.04	18723.63	18584.87	18641.67	18549.07	18755.38	18635.10	18522.10	18038.42	19139.01

Appendix 3: White Pine and Buckingham
geochronology data

Sample	BK13ES058	BK13ES058	BK13ES058	BK13ES058	BK13ES058	BK13ES058	BK13ES058	BK13ES058	BK13ES058	BK13ES058	BK13ES058	BK13ES058	BK13ES058	BK13ES058	BK13ES058
Mthd	U-Pb	U-Pb	U-Pb	U-Pb	U-Pb	U-Pb	U-Pb	U-Pb	U-Pb	U-Pb	U-Pb	U-Pb	U-Pb	U-Pb	U-Pb
Locality	BTM	BTM	BTM	BTM	BTM	BTM	BTM	BTM	BTM	BTM	BTM	BTM	BTM	BTM	BTM
Min dated	Zr	Zr	Zr	Zr	Zr	Zr	Zr	Zr	Zr	Zr	Zr	Zr	Zr	Zr	Zr
Unit	EG	EG	EG	EG	EG	EG	EG	EG	EG	EG	EG	EG	EG	EG	EG
Rock type	Qgr	Qgr	Qgr	Qgr	Qgr	Qgr	Qgr	Qgr	Qgr	Qgr	Qgr	Qgr	Qgr	Qgr	Qgr
Age (Ma)	39.1	40.1	40.5	40.7	40.7	40.7	40.8	40.9	41.2	41.3	41.3	41.7	48.6	147.9	1282.2
± 2 σ	1.2	0.7	0.7	0.6	0.7	0.6	0.6	0.7	0.8	0.8	1.4	0.8	1.1	2.7	40.6
206Pb/238U	0.0061	0.0063	0.0063	0.0063	0.0063	0.0063	0.0064	0.0064	0.0064	0.0064	0.0065	0.0065	0.0076	0.0239	0.227
± 1 RSE	0.0292	0.0162	0.0174	0.0156	0.0169	0.0154	0.0149	0.017	0.0163	0.0182	0.0336	0.0201	0.0227	0.0186	0.0329
208Pb/232Th	0.0021	0.0021	0.0019	0.002	0.0021	0.0019	0.0021	0.0023	0.0023	0.0021	0.0021	0.0018	0.0023	0.0146	0.0719
± 1 RSE	0.061	0.0446	0.0446	0.0384	0.0381	0.0452	0.0375	0.0436	0.0427	0.0575	0.0844	0.0621	0.0508	0.0337	0.0246
207Pb/206Pb	0.0559	0.0538	0.0478	0.0471	0.0476	0.0468	0.0492	0.0515	0.0449	0.0503	0.0532	0.0456	0.0538	0.0716	0.1097
± 1 RSE	0.0802	0.0368	0.0388	0.0292	0.0359	0.0311	0.0241	0.0388	0.0324	0.0396	0.0857	0.05	0.0557	0.0202	0.011
Pb204 (ppm)	0	0	0.0273	0	0.0251	0	0	0	0.0242	0	0.0273	0.0175	0	0.0289	0
Pb206 (ppm)	7.0626	8.8514	8.2907	11.1464	6.502	9.4225	13.1704	6.6231	8.3474	6.2902	3.6595	5.5222	9.972	37.7799	35.951
Pb207 (ppm)	0.3524	0.4776	0.388	0.5209	0.3089	0.4376	0.6504	0.3341	0.3716	0.3156	0.2012	0.2522	0.5058	2.6684	3.935
Pb208 (ppm)	1.01	0.35	0.38	0.44	0.39	0.30	0.52	0.31	0.41	0.22	0.26	0.21	0.51	2.46	3.51
Th232 (ppm)	550.99	162.90	198.38	224.53	181.94	156.14	247.00	130.91	177.04	108.52	139.69	122.01	238.23	162.44	48.55
U238 (ppm)	1289.14	1437.11	1355.49	1820.89	1066.38	1534.07	2146.36	1081.75	1364.21	1096.97	638.88	921.96	1520.75	1550.12	166.27
Ti49 (ppm)	13.50	2.26	2.26	1.90	4.30	2.41	2.96	2.16	1.21	2.37	1.27	2.71	4.77	4.44	4.10
Fe56 (ppm)	3.35	2.49	0.48	2.23	15.23	0.00	5.66	9.38	0.00	0.00	2.12	0.00	4.06	51.97	10.30
Hf178 (ppm)	9182.39	11693.26	10895.85	11217.21	11263.58	11753.02	11744.25	11994.89	12377.68	11902.79	10156.63	11162.29	11802.64	11603.20	10193.32
238U/206Pb	162.6522	158.7464	158.6075	157.9202	157.8207	157.8955	157.022	156.3406	155.9536	155.0598	154.1906	154.1282	131.0481	41.8663	4.405
± 1 Std Err	4.7504	2.5765	2.7588	2.463	2.6627	2.4388	2.3442	2.6514	2.5411	2.815	5.186	3.1007	2.9751	0.7774	0.1448
207Pb/206Pb	0.0559	0.0538	0.0478	0.0471	0.0476	0.0468	0.0492	0.0515	0.0449	0.0503	0.0532	0.0456	0.0538	0.0716	0.1097
± 1 Std Err	0.0045	0.002	0.0019	0.0014	0.0017	0.0015	0.0012	0.002	0.0015	0.002	0.0046	0.0023	0.003	0.0014	0.0012
common Pb	0.8382	0.8382	0.8382	0.8382	0.8382	0.8382	0.8382	0.8383	0.8383	0.8383	0.8383	0.8383	0.8383	0.8455	0.9362
206Pb/238U age	39.5118	40.4809	40.5162	40.692	40.7176	40.6984	40.924	41.1018	41.2035	41.4402	41.6731	41.6899	49.0045	152.1661	1318.8344
± 1 Std Err	1.154	0.657	0.7047	0.6347	0.687	0.6286	0.611	0.6971	0.6714	0.7523	1.4016	0.8387	1.1125	2.8256	43.3652
208Pb/232Th age	43.0216	42.0546	38.0019	39.7618	43.2798	38.3173	42.1747	46.9457	47.3706	41.8855	41.7487	35.9987	46.8761	292.6072	1403.6208
± 1 Std Err	2.6251	1.8772	1.6938	1.5283	1.6491	1.7314	1.58	2.0475	2.0206	2.4104	3.5255	2.2341	2.3815	9.86	34.556
207Pb/206Pb age	446.8219	361.0591	91.3142	56.2025	80.1479	38.4669	156.004	264.8097	-59.6513	209.3852	336.3077	-24.4655	362.8925	975.0184	1794.4345
± 1 Std Err	89.145	41.4631	45.9978	34.8061	42.656	37.2141	28.1926	44.5165	39.4834	45.9139	97.044	60.524	62.7569	20.5499	10.0266
spot size (µm)	32	32	32	32	32	32	32	32	32	32	32	32	32	32	32
repetition (Hz)	5	5	5	5	5	5	5	5	5	5	5	5	5	5	5
fluence (Jcm²)	2.05	2.05	2.05	2.05	2.05	2.05	2.05	2.05	2.05	2.05	2.05	2.05	2.05	2.05	2.05
mode	Spot	Spot	Spot	Spot	Spot	Spot	Spot	Spot	Spot	Spot	Spot	Spot	Spot	Spot	Spot
Hg202	33.01	4.27	0.00	77.20	24.29	0.00	100.78	24.51	31.61	31.92	0.00	37.89	31.82	0.00	9.89
Pb204	0.00	0.00	9.56	0.00	8.60	0.00	0.00	8.76	0.00	10.53	6.61	0.00	8.83	0.01	
Pb206	6834.66	7351.21	7094.65	9194.62	5343.49	7801.55	10972.22	5441.64	6913.72	5345.92	3547.08	4901.51	9265.08	26989.66	28586.83
Pb207	336.91	391.88	328.07	424.54	250.82	358.01	535.24	271.20	304.02	265.01	192.67	221.19	464.30	1883.28	3091.10
Pb208	969.82	284.93	318.27	356.72	319.20	242.54	425.12	249.83	338.08	183.74	250.51	182.23	470.40	1741.50	2765.37
Th232	514482.02	130580.34	163838.69	178731.92	144303.37	124782.88	198534.23	103806.60	141479.73	89023.27	130696.31	104503.14	213604.35	111980.64	37249.27
U238	1288100.97	1232793.74	1198043.94	1551140.16	905092.12	1312056.14	1846116.90	917938.88	1166598.95	962996.74	639696.57	845040.29	1459178.37	1143492.42	136513.60
Ti49	143.55	20.69	21.26	17.22	38.88	22.00	27.13	19.56	11.02	22.21	13.59	26.46	48.78	34.84	35.83
Fe56	749.64	478.37	94.39	426.13	2899.96	0.10	1091.94	1785.95	0.10	0.10	475.97	0.10	874.60	8597.23	1895.42
Zr90	182215466	156511189	161248765	155379515	154830087	156062072	156835808	154804842	155938033	160175921	182713314	167174487	175025287	134539425	149736418
Hf178	3640246	3978943	3820121	3790807	3792435	3987188	4007960	4037695	4199646	4144764	4033725	4058918	4492619	3395852	3320446
Fe56BG	19146.79	20273.70	20269.84	19407.74	19801.77	20549.39	19334.10	19902.53	19742.30	20384.42	20547.63	19256.59	19641.40	19211.38	19314.74

Appendix 4: White Pine
whole-rock geochemistry

Sample	SiO2	Al2O3	Fe2O3	MgO	CaO	Na2O	K2O	TiO2	P2O5	MnO	Cr2O3	Sum	Ba	Sc	Cs	Ga	Hf	Nb	Rb	Sn	Sr	Ta	Th	U	V	W	Zr
WP13ES001	68.71	16.10	3.08	0.57	1.06	3.64	3.87	0.47	0.19	0.03	<0.002	99.66	1688.00	3.00	2.40	22.20	7.30	17.10	141.70	5.00	366.00	0.80	13.20	5.40	49.00	18.80	226.70
WP13ES003	69.22	16.02	2.85	0.76	1.16	3.84	4.15	0.41	0.17	0.04	<0.002	99.64	2050.00	3.00	2.10	21.30	5.70	15.00	140.20	2.00	550.90	0.70	15.30	4.00	47.00	4.80	198.70
WP13ES004	70.33	15.52	2.71	0.66	1.41	3.88	3.68	0.40	0.16	0.04	<0.002	99.72	1522.00	3.00	1.90	21.40	5.80	14.70	125.00	<1	488.60	0.60	16.20	5.00	39.00	9.70	181.70
WP13ES005	58.10	13.91	4.85	2.65	3.96	1.14	8.62	1.51	0.89	0.07	0.02	99.04	5422.00	9.00	2.00	22.20	25.70	32.50	212.40	3.00	798.50	1.20	27.70	4.50	96.00	6.10	872.80
WP13ES006	70.66	15.22	2.78	0.67	1.68	4.09	3.17	0.38	0.16	0.04	<0.002	99.73	99.73	99.73	99.73	99.73	99.73	99.73	99.73	99.73	99.73	99.73	99.73	99.73	99.73	99.73	99.73
WP13ES007	70.54	13.94	3.50	0.41	1.03	3.53	3.68	0.35	0.14	0.02	<0.002	99.75	1344.00	2.00	1.50	21.70	5.60	14.70	129.80	1.00	456.40	0.70	14.90	2.30	47.00	7.50	181.90
WP13ES008	52.63	13.15	6.48	4.85	5.98	0.98	8.53	2.26	1.53	0.08	0.02	98.49	8274.00	13.00	1.00	21.80	22.90	53.70	233.10	2.00	1273.20	1.80	37.70	7.80	122.00	2.70	960.80
WP13ES009	70.48	15.38	2.47	0.59	2.12	4.13	3.35	0.33	0.14	0.05	<0.002	99.72	1415.00	2.00	1.70	20.90	4.90	12.60	113.10	<1	585.30	0.50	11.10	3.00	29.00	2.20	161.80
WP13ES010	51.30	12.26	6.12	4.61	6.44	1.12	7.33	2.19	1.47	0.07	0.02	98.34	9785.00	13.00	1.50	21.90	23.10	50.90	202.20	2.00	1678.80	1.50	33.10	7.40	113.00	19.70	855.10
WP13ES011	69.37	15.66	2.78	0.68	1.59	3.81	3.95	0.41	0.16	0.04	<0.002	99.70	1571.00	3.00	1.60	21.70	5.30	13.40	142.90	1.00	562.10	0.60	12.00	2.10	34.00	15.90	178.50
WP13ES012	69.77	15.58	2.87	0.75	1.71	3.94	3.84	0.41	0.16	0.05	0.00	99.67	1891.00	3.00	2.00	21.60	6.00	16.30	137.40	<1	531.90	0.80	13.50	4.80	34.00	8.40	185.70
WP13ES013	67.44	15.77	3.66	1.31	2.55	3.90	3.49	0.50	0.19	0.05	0.00	99.71	1501.00	5.00	2.40	19.60	4.70	12.10	113.80	<1	550.70	0.60	14.00	3.70	54.00	1.20	158.30
WP13ES014	76.85	13.19	0.93	0.15	0.29	3.13	4.77	0.09	0.03	0.01	0.00	99.94	425.00	1.00	1.60	16.70	4.30	9.10	143.30	<1	148.10	0.60	27.20	14.90	16.00	2.40	65.30
WP13ES015	55.47	16.83	7.00	4.60	4.99	4.07	3.33	1.19	0.65	0.18	0.01	99.60	1410.00	13.00	6.60	23.70	7.20	23.00	194.40	3.00	515.10	1.10	15.90	5.60	139.00	<0.5	227.10
WP13ES016	63.06	20.26	7.94	1.23	0.11	0.18	3.80	0.97	0.09	0.06	0.01	99.83	479.00	18.00	6.40	26.10	9.30	18.80	180.90	1.00	75.70	1.20	16.10	4.70	108.00	1.10	316.00
WP13ES017	65.92	16.28	4.25	1.58	2.37	3.84	3.60	0.60	0.27	0.06	0.00	99.67	1460.00	5.00	1.80	21.00	5.00	13.50	127.80	2.00	611.40	0.80	13.60	3.60	60.00	36.40	188.20
WP13ES018	69.19	15.53	3.46	0.90	1.03	3.79	3.60	0.50	0.22	0.06	0.01	99.73	1311.00	3.00	3.00	20.50	5.50	14.80	140.00	<1	347.50	0.90	16.10	4.40	41.00	32.60	192.50
WP13ES019	71.29	14.94	2.66	0.56	0.64	3.56	3.91	0.38	0.16	0.02	<0.002	99.77	1142.00	3.00	1.80	20.80	4.40	13.50	128.20	1.00	321.40	0.70	13.10	4.50	30.00	8.40	166.10
WP13ES020	69.25	15.61	2.98	0.70	1.83	3.75	4.24	0.42	0.18	0.02	0.00	99.61	1320.00	2.00	1.20	21.00	5.10	15.80	116.70	<1	570.00	0.90	13.00	6.40	28.00	6.60	186.20
WP13ES021	70.03	14.98	3.10	0.56	1.38	3.60	4.34	0.47	0.19	0.02	<0.002	99.72	1491.00	2.00	0.90	19.10	6.50	16.40	116.00	1.00	482.90	0.80	13.40	2.60	25.00	11.50	216.80
WP13ES022	68.81	14.67	4.03	0.87	0.35	1.15	6.01	0.53	0.24	0.13	0.00	99.20	1212.00	4.00	2.40	21.90	5.30	12.60	254.10	2.00	154.40	0.70	12.00	4.70	56.00	40.60	190.20
WP13ES023	70.15	15.31	2.94	0.75	2.16	4.21	3.05	0.42	0.19	0.04	0.00	99.76	993.00	3.00	1.60	21.50	5.70	16.30	110.40	<1	573.60	0.90	16.30	3.50	35.00	2.10	184.00
WP13ES024	70.55	15.54	2.35	0.61	0.09	2.45	4.99	0.35	0.12	<0.01	<0.002	99.72	1746.00	3.00	1.80	22.00	5.30	14.10	193.10	2.00	201.00	0.80	12.90	2.20	30.00	33.10	180.10
WP13ES025	78.16	13.86	0.61	0.13	0.02	0.09	4.83	0.05	0.02	0.06	<0.002	99.99	122.00	5.00	3.70	28.90	3.50	43.10	326.70	2.00	10.90	3.20	13.90	11.60	<8	3.60	37.60
WP13ES026	70.92	14.97	3.14	0.70	0.15	2.07	4.45	0.43	0.17	0.01	<0.002	99.70	1944.00	3.00	2.10	25.00	5.80	15.30	177.60	4.00	179.30	0.90	13.90	4.50	36.00	33.40	188.50
WP13ES027	69.35	15.44	2.72	0.61	1.30	3.61	4.42	0.38	0.17	0.02	<0.002	99.62	2165.00	3.00	1.20	21.10	5.20	15.40	136.80	2.00	624.50	0.80	16.30	7.40	28.00	21.50	179.50
WP13ES028	71.59	13.98	3.09	0.64	0.65	3.05	4.33	0.39	0.18	0.01	0.00	99.59	1229.00	2.00	2.30	19.50	5.00	15.00	155.10	2.00	390.60	0.90	16.10	4.80	35.00	45.60	176.20
WP13ES030	69.55	15.49	2.92	0.75	1.90	4.22	3.62	0.40	0.17	0.05	<0.002	99.68	1691.00	2.00	1.50	20.20	4.80	13.80	122.60	<1	626.30	0.60	12.90	4.10	27.00	2.40	160.90
WP13ES031	71.04	14.76	2.69	0.66	2.18	4.07	3.17	0.36	0.15	0.04	0.00	99.77	1085.00	3.00	1.90	21.50	4.80	13.50	116.70	<1	524.00	0.70	16.70	5.70	24.00	3.50	165.20
WP13ES032	58.72	13.72	4.89	3.43	4.08	1.55	8.49	1.61	0.96	0.08	0.02	99.11	5096.00	9.00	1.00	22.60	23.00	31.10	199.00	3.00	514.50	1.20	25.90	4.40	78.00	3.30	845.30
WP13ES033	68.80	16.53	2.46	0.73	1.05	3.45	4.29	0.38	0.17	0.03	<0.002	99.79	1055.00	3.00	2.40	30.10	5.20	11.80	241.50	2.00	203.40	0.60	12.90	2.70	78.00	89.50	177.50
WP13ES034	69.98	15.55	2.85	0.70	1.95	4.08	3.57	0.41	0.18	0.05	<0.002	99.71	1487.00	2.00	1.90	20.10	4.80	12.90	111.70	<1	553.80	0.60	11.10	2.40	28.00	10.50	179.80
WP13ES035	69.78	15.41	2.57	0.65	2.07	3.94	3.98	0.36	0.16	0.04	<0.002	99.62	1691.00	2.00	1.50	21.20	5.00	12.90	98.80	2.00	647.60	0.80	11.60	3.10	55.00	3.30	178.30
WP13ES036	67.98	15.41	4.08	0.96	0.10	0.72	6.84	0.38	0.14	0.03	<0.002	99.73	1249.00	4.00	1.80	47.60	5.20	11.40	272.20	9.00	54.60	0.60	9.80	6.60	177.00	23.30	179.80
WP13ES037	64.80	15.59	4.03	1.47	1.91	4.67	4.03	0.62	0.27	0.05	<0.002	99.59	1949.00	5.00	2.40	19.40	4.90	11.70	109.90	1.00	584.10	0.80	9.20	2.20	78.00	8.30	182.30
WP13ES038	64.96	16.07	3.88	1.23	1.80	3.21	4.67	0.57	0.27	0.08	<0.002	99.49	1424.00	4.00	3.80	21.20	5.60	13.50	221.30	2.00	243.20	0.90	13.50	4.60	70.00	82.70	215.40
WP13ES039	67.77	15.25	3.85	1.35	2.69	3.71	3.71	0.52	0.21	0.05	0.00	99.66	1410.00	5.00	2.40	19.10	4.70	13.30	106.20	<1	597.10	0.80	17.80	4.90	71.00	1.40	166.50
WP13ES040	65.13	17.05	4.54	1.49	0.27	1.24	5.83	0.55	0.23	0.04	0.00	99.74	772.00	6.00	4.30	27.00	4.50	12.80	349.80	2.00	33.80	0.90	13.60	3.10	106.00	74.00	184.90
WP13ES041	73.24	12.38	4.14	1.29	0.39	0.71	4.30	0.43	0.17	0.11	<0.002	99.77	975.00	4.00	4.00	16.40	3.50	10.10	230.00	1.00	92.20	0.60	11.90	4.30	54.00	36.10	142.50
WP13ES042	68.34	15.21	3.37	1.22	1.99	3.72	4.10	0.47	0.20	0.05	<0.002	99.68	1352.00	4.00	2.10	18.60	4.80	10.80	114.40	<1	577.80	0.80	14.80	3.50	53.00	4.00	155.40

All major oxides are in wt. %

All other elements in ppm except Au, Pt, Pd which are in ppb

Appendix 4: White Pine
whole-rock geochemistry

Sample	SiO2	Al2O3	Fe2O3	MgO	CaO	Na2O	K2O	TiO2	P2O5	MnO	Cr2O3	Sum	Ba	Sc	Cs	Ga	Hf	Nb	Rb	Sn	Sr	Ta	Th	U	V	W	Zr
WP13ES043	75.94	13.30	0.76	0.20	0.48	1.71	5.43	0.06	0.03	0.09	0.01	99.86	327.00	6.00	2.10	27.90	3.30	52.10	238.20	2.00	160.80	3.60	16.90	30.60	9.00	5.20	46.10
WP13ES044	67.69	15.26	3.67	1.34	2.72	3.74	3.71	0.49	0.21	0.05	<0.002	99.66	1421.00	4.00	1.90	18.70	4.70	11.00	100.70	1.00	632.10	0.60	11.20	3.80	58.00	3.40	177.90
WP13ES045	71.11	14.84	2.33	0.52	0.58	3.28	4.53	0.44	0.15	0.05	<0.002	99.60	1590.00	2.00	2.50	19.90	6.30	12.00	158.60	2.00	221.90	0.50	12.70	2.30	31.00	23.30	261.20
WP13ES046	72.35	14.37	2.16	0.42	0.24	3.02	5.30	0.28	0.13	0.02	<0.002	99.74	1170.00	2.00	2.30	19.40	3.60	15.80	145.40	1.00	223.90	0.80	12.40	3.60	29.00	50.00	132.20
WP13ES047	68.82	14.86	3.49	1.35	2.48	3.76	3.55	0.48	0.18	0.05	0.00	99.72	1022.00	5.00	2.10	18.20	5.00	13.90	110.00	1.00	527.30	1.00	16.10	5.20	56.00	9.60	176.70
WP13ES048	68.09	17.10	1.97	1.29	0.31	1.85	6.17	0.48	0.21	0.05	<0.002	99.79	828.00	4.00	4.20	25.10	4.40	15.70	301.40	2.00	93.00	1.20	16.10	4.10	64.00	26.30	163.70
WP13ES049	70.01	14.40	3.12	0.96	2.03	3.74	3.34	0.42	0.18	0.04	0.00	99.80	643.00	4.00	2.80	16.00	3.60	11.60	111.10	<1	374.00	0.70	17.70	4.00	45.00	2.30	152.40
WP13ES050	67.42	15.66	4.35	1.01	0.44	2.09	5.16	0.52	0.21	0.08	<0.002	99.71	1098.00	5.00	4.70	23.00	5.30	13.30	247.10	2.00	156.00	0.90	18.60	4.10	66.00	45.00	182.40
WP13ES051	69.03	14.90	3.40	1.09	1.63	3.36	4.19	0.46	0.20	0.05	<0.002	99.67	1497.00	4.00	3.60	19.60	5.20	12.50	133.80	<1	485.30	0.70	17.30	4.80	51.00	4.80	192.90
WP13ES052	68.92	14.73	3.25	1.07	1.38	3.15	4.63	0.45	0.21	0.05	<0.002	99.65	1478.00	4.00	3.70	19.50	4.10	12.80	140.20	1.00	389.90	0.80	17.80	6.50	49.00	18.90	148.20
WP13ES053	95.18	1.76	1.63	0.07	<0.01	0.05	0.79	0.03	0.03	<0.01	<0.002	99.94	118.00	<1	0.30	4.50	0.30	2.90	24.20	1.00	14.00	0.30	2.90	0.80	15.00	1.80	8.70
WP13ES054	70.89	14.55	2.94	0.56	0.38	2.57	5.15	0.39	0.16	0.03	<0.002	99.70	1383.00	2.00	2.10	19.90	4.80	14.60	175.10	2.00	195.80	0.80	15.90	4.40	41.00	69.10	171.30
WP13ES055	70.00	14.07	3.78	0.82	0.60	3.12	4.39	0.46	0.22	0.01	<0.002	99.71	1141.00	4.00	2.90	20.60	5.10	11.40	144.30	3.00	288.00	0.60	12.20	2.10	53.00	47.00	184.80
WP13ES056	68.37	15.04	3.32	0.84	1.24	3.62	4.22	0.48	0.20	0.04	<0.002	99.63	1835.00	3.00	3.10	18.50	5.20	12.20	132.80	<1	428.40	0.70	12.00	4.20	42.00	26.40	170.50
WP13ES057	68.16	15.32	3.39	0.97	2.20	3.82	3.81	0.48	0.21	0.05	<0.002	99.63	1575.00	3.00	2.60	19.90	4.90	14.70	114.80	1.00	598.00	0.90	14.70	6.00	41.00	3.10	172.90
WP13ES058	67.66	15.23	3.95	1.10	1.94	3.51	4.13	0.53	0.25	0.03	<0.002	99.64	1589.00	4.00	3.20	19.40	5.20	12.80	115.70	1.00	548.10	0.70	12.80	3.30	53.00	18.00	198.30
WP13ES059	67.74	15.09	3.85	1.21	2.69	3.66	3.58	0.55	0.25	0.05	<0.002	99.63	1532.00	4.00	1.80	18.30	4.80	13.90	93.40	1.00	618.20	0.80	12.20	2.60	48.00	1.70	170.80
WP13ES060	68.74	15.25	3.56	0.83	1.15	3.28	4.31	0.49	0.21	0.04	<0.002	99.64	1071.00	3.00	2.40	19.10	4.90	12.70	135.50	2.00	369.30	0.80	14.20	4.50	46.00	15.40	180.90
WP13ES061	68.63	14.66	3.57	1.12	2.60	3.53	3.96	0.49	0.20	0.05	<0.002	99.68	1313.00	4.00	1.40	18.70	4.50	13.60	93.70	<1	546.40	0.80	15.90	3.00	46.00	0.70	165.60
WP13ES062	78.83	10.43	2.00	0.69	0.03	0.12	4.61	0.32	0.09	0.02	<0.002	99.78	808.00	2.00	3.60	20.70	3.70	13.30	238.80	4.00	32.50	0.50	9.30	2.70	40.00	13.60	145.90
WP13ES063	73.02	13.00	2.49	0.45	0.14	1.71	6.26	0.37	0.14	0.01	<0.002	99.72	1184.00	2.00	2.40	16.20	4.20	19.70	220.10	2.00	116.90	0.80	9.80	1.40	27.00	16.40	181.00
WP13ES064	76.06	13.47	1.06	0.56	0.12	1.14	5.33	0.31	0.13	0.02	<0.002	99.72	1350.00	2.00	1.40	21.90	4.10	10.40	177.10	1.00	97.00	0.60	8.50	0.80	38.00	17.20	153.50
WP13ES065	71.43	13.20	2.00	0.48	1.17	2.31	6.08	0.30	0.12	0.02	<0.002	99.62	1335.00	2.00	1.60	17.70	3.90	10.90	162.20	1.00	301.90	0.60	11.00	4.80	22.00	9.30	137.80
WP13ES066	72.08	14.73	1.35	0.55	0.30	2.79	5.68	0.36	0.15	0.01	<0.002	99.69	1450.00	2.00	1.20	23.00	4.90	14.70	152.10	3.00	349.50	0.70	11.90	2.60	32.00	15.70	170.50
WP13ES067	68.30	14.96	3.54	1.02	2.14	3.72	3.84	0.51	0.22	0.04	0.00	99.68	1283.00	4.00	2.10	18.40	6.10	13.40	114.10	<1	525.40	0.80	14.90	5.10	49.00	3.30	205.70
WP13ES068	66.94	15.22	3.62	1.11	2.99	3.72	4.21	0.53	0.21	0.05	<0.002	99.65	1685.00	4.00	1.80	17.10	4.50	12.60	102.10	<1	567.90	0.70	16.70	3.70	51.00	0.80	167.30

All major oxides are in wt. %

All other elements in ppm except Au, Pt, Pd which are in ppb

Appendix 4: White Pine
whole-rock geochemistry

Sample	Y	La	Ce	Pr	Nd	Sm	Eu	Gd	Tb	Dy	Ho	Er	Tm	Yb	Lu	Ni	LOI	TOT/C	TOT/S	Mo	Cu	Pb	Zn	Ag	Ni	Co
WP13ES001	9.00	70.40	139.00	14.64	48.50	6.59	1.35	4.23	0.50	2.03	0.24	0.64	0.09	0.55	0.10	<10	1.90	0.08	0.80	35.56	232.26	29.00	59.50	488.00	3.00	4.50
WP13ES003	8.60	65.70	123.30	13.17	44.30	5.83	1.29	4.03	0.42	1.97	0.23	0.62	0.07	0.64	0.08	<10	1.00	0.02	0.02	0.37	20.55	12.43	57.40	152.00	3.80	3.90
WP13ES004	5.80	46.00	107.30	9.23	32.30	3.80	0.85	2.82	0.28	1.27	0.21	0.46	0.06	0.51	0.06	<10	0.90	0.03	0.05	0.13	10.67	10.38	55.20	88.00	2.50	4.10
WP13ES005	17.70	170.50	330.30	35.47	128.40	15.52	3.32	8.98	0.91	3.72	0.59	1.39	0.19	1.35	0.18	69.00	3.30	0.71	0.05	0.06	14.00	34.56	87.60	63.00	66.20	12.80
WP13ES006	99.73	99.73	99.73	99.73	99.73	99.73	99.73	99.73	99.73	99.73	99.73	99.73	99.73	99.73	99.73	99.73	99.73	99.73	99.73	99.73	99.73	99.73	99.73	99.73	99.73	99.73
WP13ES007	3.90	58.30	89.90	7.85	25.90	2.82	0.63	1.89	0.20	0.57	0.08	0.32	0.04	0.31	0.06	<10	2.60	0.01	0.62	9.27	22.98	23.51	24.20	446.00	1.10	0.80
WP13ES008	31.80	366.50	672.90	79.48	281.20	33.72	7.17	20.27	1.83	7.63	0.97	2.47	0.31	1.98	0.24	112.00	2.00	0.02	0.04	0.84	45.93	74.70	149.40	127.00	97.20	14.50
WP13ES009	7.50	51.70	100.60	10.81	36.00	4.62	1.06	3.22	0.37	1.80	0.23	0.48	0.07	0.53	0.08	<10	0.70	0.02	0.01	0.38	16.37	17.68	65.80	130.00	2.10	2.70
WP13ES010	27.50	304.90	595.60	66.04	229.60	28.29	6.12	16.73	1.62	5.86	0.71	2.00	0.23	1.57	0.22	110.00	5.40	0.96	0.27	0.28	27.57	36.80	113.70	135.00	111.20	19.90
WP13ES011	6.70	57.10	112.40	11.81	40.00	4.83	1.09	3.54	0.37	1.74	0.21	0.57	0.05	0.43	0.08	<10	1.20	0.03	0.10	9.64	25.53	27.53	75.90	622.00	1.90	2.60
WP13ES012	7.80	52.80	109.80	11.60	38.50	5.27	1.08	3.28	0.41	1.72	0.26	0.60	0.07	0.63	0.09	<10	0.60	0.02	0.04	0.55	14.28	9.44	67.00	44.00	3.10	4.50
WP13ES013	9.90	54.50	100.20	10.36	34.60	4.62	1.14	3.39	0.42	2.18	0.30	0.99	0.13	0.86	0.14	<10	0.80	0.07	0.02	0.22	2.76	5.12	42.90	16.00	9.00	7.30
WP13ES014	2.40	17.00	25.50	2.05	5.90	0.72	0.18	0.52	0.07	0.28	0.06	0.26	0.04	0.34	0.08	<10	0.50	0.01	<0.01	0.22	1.33	9.66	6.20	83.00	1.10	0.80
WP13ES015	22.20	97.20	209.10	23.21	84.10	10.96	2.65	7.51	0.88	3.93	0.69	1.80	0.26	1.73	0.26	55.00	1.30	0.08	<0.01	0.22	10.91	9.57	87.10	19.00	44.00	16.00
WP13ES016	39.40	47.70	108.00	12.84	49.00	8.41	1.53	7.09	1.17	6.76	1.39	4.35	0.57	4.12	0.55	29.00	2.10	<0.01	0.18	2.39	69.65	6.28	51.60	30.00	30.70	19.40
WP13ES017	11.40	59.00	111.50	12.04	43.40	5.65	1.26	4.09	0.47	2.32	0.40	1.03	0.13	1.00	0.14	<10	0.90	0.04	0.14	1.70	34.80	38.12	104.90	610.00	9.30	8.70
WP13ES018	9.10	62.30	119.40	12.33	42.70	6.09	1.28	4.07	0.45	2.00	0.30	0.68	0.08	0.66	0.09	<10	1.50	0.06	0.49	5.17	96.50	58.86	62.40	1828.00	4.00	5.90
WP13ES019	5.50	36.30	90.50	7.20	23.80	2.90	0.63	2.09	0.24	1.03	0.17	0.39	0.06	0.47	0.07	<10	1.60	0.03	0.29	1.89	98.33	27.18	84.40	249.00	2.10	3.50
WP13ES020	5.90	52.60	99.70	10.93	38.20	4.82	0.99	3.01	0.31	1.23	0.17	0.38	0.05	0.44	0.06	<10	0.60	0.04	0.08	850.53	88.94	7.64	26.00	117.00	1.50	1.60
WP13ES021	5.20	58.10	110.50	11.61	39.70	4.80	1.01	3.05	0.34	1.37	0.17	0.41	0.05	0.43	0.06	<10	1.00	0.03	0.06	22.18	49.45	6.35	24.20	217.00	1.10	1.30
WP13ES022	8.90	55.10	105.80	12.19	44.90	6.11	1.28	4.18	0.45	2.07	0.29	0.77	0.10	0.66	0.12	<10	2.40	0.10	0.53	1.80	885.86	733.62	3385.50	20387.00	4.20	8.10
WP13ES023	8.20	56.70	112.70	12.15	43.20	5.44	1.19	3.69	0.40	1.55	0.27	0.57	0.09	0.58	0.09	<10	0.60	0.02	0.01	0.31	26.10	7.73	46.00	61.00	3.00	3.80
WP13ES024	4.50	56.60	107.50	11.26	39.20	5.31	0.87	3.10	0.30	1.32	0.15	0.44	0.05	0.38	0.07	<10	2.70	0.09	0.28	20.68	32.53	18.67	19.30	268.00	0.60	0.40
WP13ES025	11.50	5.80	11.10	2.12	8.90	1.87	0.32	1.85	0.32	1.78	0.30	0.99	0.17	1.12	0.21	<10	2.20	0.02	<0.01	0.90	22.33	14.13	5.60	260.00	0.30	0.40
WP13ES026	3.20	32.00	57.00	5.95	19.10	2.29	0.39	1.56	0.16	0.65	0.10	0.28	0.03	0.32	0.05	<10	2.70	0.06	0.18	13.66	105.72	11.08	32.80	910.00	1.20	1.10
WP13ES027	6.30	61.20	118.10	12.33	39.40	5.11	1.02	3.19	0.34	1.37	0.17	0.55	0.06	0.49	0.07	<10	1.60	0.04	0.11	1.98	109.39	9.82	35.00	277.00	1.60	1.10
WP13ES028	4.80	32.60	60.90	6.06	18.90	2.75	0.65	1.86	0.23	0.92	0.14	0.28	0.05	0.38	0.07	<10	1.70	0.01	0.36	1076.92	89.45	14.01	30.80	610.00	1.30	2.20
WP13ES030	8.00	56.30	106.90	11.45	40.60	5.24	1.07	3.17	0.39	1.54	0.21	0.59	0.08	0.53	0.08	<10	0.60	0.04	<0.01	1.38	8.15	17.10	81.00	83.00	2.40	5.00
WP13ES031	6.90	49.10	91.20	9.94	35.70	4.37	0.88	3.06	0.33	1.58	0.20	0.51	0.06	0.51	0.07	<10	0.60	0.05	0.05	0.56	6.41	9.18	65.70	51.00	2.30	4.30
WP13ES032	16.80	161.60	300.90	33.44	121.10	15.08	3.05	8.90	0.91	3.55	0.49	1.34	0.19	1.09	0.18	72.00	1.60	0.07	0.05	0.38	10.75	41.67	85.20	66.00	66.40	11.80
WP13ES033	4.20	28.30	52.10	5.43	18.40	2.27	0.35	1.34	0.15	0.70	0.11	0.32	0.04	0.29	0.05	<10	1.90	0.02	0.03	1.93	17.87	37.85	36.30	594.00	1.20	1.00
WP13ES034	6.70	55.60	103.30	10.83	39.70	4.63	1.01	3.36	0.35	1.50	0.19	0.44	0.07	0.42	0.07	<10	0.40	0.03	0.01	0.21	7.91	11.30	58.60	59.00	2.20	4.10
WP13ES035	7.20	55.60	102.40	10.78	37.50	5.17	1.12	3.22	0.32	1.77	0.22	0.48	0.07	0.40	0.08	<10	0.70	0.03	0.03	0.21	12.96	13.00	66.60	120.00	2.30	3.40
WP13ES036	2.60	29.50	52.80	5.48	18.00	2.67	0.39	1.53	0.15	0.67	0.09	0.24	0.02	0.18	0.03	<10	3.10	0.04	0.39	35.20	11.95	91.78	12.40	1031.00	0.50	0.80
WP13ES037	11.80	68.80	123.50	12.77	42.60	6.46	1.43	4.52	0.51	2.66	0.40	0.92	0.13	0.82	0.11	<10	2.20	0.12	0.02	0.75	4.27	3.43	53.10	89.00	9.70	8.20
WP13ES038	10.50	57.50	110.50	11.80	39.90	5.61	1.35	4.08	0.46	2.13	0.32	0.98	0.11	0.86	0.12	<10	2.70	0.23	0.42	3.46	135.38	501.34	1160.90	7919.00	3.60	7.00
WP13ES039	10.70	56.00	104.00	10.98	39.10	5.53	1.22	3.67	0.41	2.18	0.39	1.01	0.16	0.92	0.13	<10	0.50	0.07	<0.01	0.18	2.38	4.16	35.60	145.00	9.00	7.60
WP13ES040	5.90	48.00	91.30	10.27	34.80	4.68	0.94	2.88	0.30	1.32	0.18	0.61	0.08	0.53	0.08	<10	3.40	0.03	0.26	24.81	15.78	298.37	75.10	9103.00	4.10	7.10
WP13ES041	8.10	37.00	73.80	7.39	25.40	3.55	0.85	2.49	0.30	1.56	0.25	0.64	0.09	0.60	0.10	<10	2.60	0.04	0.32	1.99	20.71	35.38	77.10	1435.00	5.50	6.90
WP13ES042	9.10	49.80	92.00	9.50	32.60	4.44	1.02	3.06	0.35	1.81	0.28	0.76	0.13	0.71	0.09	<10	1.00	0.01	0.04	0.30	4.27	10.47	46.90	152.00	7.70	7.10

All major oxides are in wt. %

All other elements in ppm except Au, Pt, Pd which are in ppb

Appendix 4: White Pine
whole-rock geochemistry

Sample	Y	La	Ce	Pr	Nd	Sm	Eu	Gd	Tb	Dy	Ho	Er	Tm	Yb	Lu	Ni	LOI	TOT/C	TOT/S	Mo	Cu	Pb	Zn	Ag	Ni	Co
WP13ES043	19.70	11.60	26.90	3.38	13.60	3.54	0.20	3.31	0.49	2.59	0.47	1.43	0.26	1.57	0.27	<10	1.90	0.08	0.01	2.66	3.69	104.67	51.30	812.00	0.30	0.20
WP13ES044	9.60	56.10	97.20	10.24	34.80	5.07	1.19	3.54	0.38	1.91	0.32	0.91	0.13	0.85	0.11	<10	0.80	<0.01	0.03	0.26	16.40	5.94	66.20	113.00	8.60	7.30
WP13ES045	4.10	76.70	143.40	14.86	50.20	6.40	1.34	3.15	0.26	1.05	0.12	0.22	0.03	0.20	0.03	<10	1.80	0.10	0.33	5.14	450.20	70.04	169.90	1135.00	1.00	2.40
WP13ES046	4.60	24.40	63.90	4.90	17.80	2.58	0.55	1.92	0.21	1.06	0.15	0.31	0.05	0.31	0.06	<10	1.50	0.02	0.25	3.49	94.66	27.30	55.30	341.00	1.50	3.50
WP13ES047	10.90	51.70	96.80	10.23	33.80	5.32	1.15	3.49	0.39	2.09	0.29	0.83	0.12	1.01	0.14	12.00	0.70	0.03	0.05	1.02	6.02	4.81	47.00	58.00	11.80	8.50
WP13ES048	6.00	51.30	93.80	9.80	32.30	4.24	0.86	2.63	0.27	1.25	0.18	0.61	0.06	0.50	0.09	<10	2.30	0.04	0.06	7.65	2.35	5.59	11.10	91.00	4.00	3.40
WP13ES049	8.50	43.20	78.20	8.47	29.20	3.67	0.89	2.76	0.31	1.72	0.30	0.66	0.11	0.77	0.11	<10	1.60	0.16	<0.01	2.52	2.75	7.54	32.30	33.00	9.90	6.30
WP13ES050	9.30	52.50	97.30	10.98	38.20	5.39	1.16	3.66	0.36	2.28	0.35	0.84	0.12	0.81	0.13	<10	2.80	0.07	0.54	0.86	47.80	187.33	119.20	16368.00	5.50	7.60
WP13ES051	11.00	50.70	99.60	10.34	37.10	4.85	1.14	3.61	0.40	2.22	0.39	0.99	0.15	0.89	0.16	<10	1.40	0.03	0.04	0.26	7.37	5.58	48.50	60.00	7.70	7.30
WP13ES052	8.70	43.20	89.20	9.04	29.60	4.26	1.02	3.27	0.36	1.78	0.31	0.81	0.13	0.74	0.13	<10	1.80	0.08	0.32	0.32	58.86	42.06	311.30	1114.00	6.80	6.40
WP13ES053	0.10	6.30	7.00	0.58	1.80	0.21	0.03	0.12	0.01	<0.05	<0.02	<0.03	<0.01	<0.05	<0.01	<10	0.40	0.01	0.28	15.85	5.14	13.84	4.80	147.00	0.30	0.20
WP13ES054	5.90	42.40	79.20	8.28	26.50	3.82	0.77	2.35	0.25	1.51	0.17	0.36	0.05	0.36	0.07	<10	2.10	0.03	0.35	0.37	68.29	83.70	93.60	505.00	1.40	3.30
WP13ES055	4.80	33.60	62.20	6.41	22.80	3.02	0.57	1.90	0.21	1.12	0.16	0.51	0.06	0.32	0.06	<10	2.30	0.03	0.22	99.53	72.34	31.66	21.30	1607.00	2.20	1.70
WP13ES056	8.60	50.80	117.90	11.77	42.20	5.97	1.37	4.04	0.42	2.15	0.35	0.81	0.09	0.60	0.09	<10	2.20	0.08	0.51	0.64	74.06	10.53	62.60	315.00	4.20	5.60
WP13ES057	8.90	63.20	123.90	13.63	46.80	6.48	1.58	4.60	0.47	2.41	0.32	0.76	0.11	0.66	0.08	<10	1.20	0.03	<0.01	1.06	66.09	4.69	71.60	70.00	4.20	6.50
WP13ES058	7.80	48.10	92.80	8.61	29.20	3.88	0.96	2.93	0.31	1.45	0.25	0.71	0.08	0.59	0.09	<10	1.30	0.02	0.44	3.90	51.96	10.96	67.50	264.00	4.60	5.40
WP13ES059	10.70	62.90	122.90	12.41	44.40	5.97	1.37	4.12	0.45	2.14	0.36	0.83	0.12	0.83	0.12	<10	1.00	0.02	<0.01	0.54	74.79	20.77	100.40	108.00	6.20	7.40
WP13ES060	7.10	44.90	91.70	8.89	30.20	4.15	0.95	2.79	0.31	1.40	0.24	0.63	0.09	0.46	0.09	<10	1.80	0.03	0.40	296.08	159.98	36.44	274.30	975.00	3.20	6.40
WP13ES061	9.30	50.30	95.90	10.39	34.20	5.07	1.15	3.61	0.40	2.02	0.33	0.79	0.11	0.72	0.11	<10	0.90	0.01	<0.01	0.46	5.58	2.47	85.10	15.00	5.10	6.20
WP13ES062	2.20	44.50	79.60	7.58	25.60	3.10	0.55	1.70	0.15	0.71	0.10	0.13	0.03	0.15	0.02	<10	2.60	0.03	0.22	57.83	102.14	125.21	35.20	1284.00	0.60	0.40
WP13ES063	3.20	36.10	66.90	6.54	20.60	2.68	0.47	1.67	0.15	0.90	0.10	0.22	0.03	0.27	0.04	<10	2.10	0.06	0.17	176.65	58.43	83.88	50.90	1092.00	0.90	0.40
WP13ES064	3.70	24.30	32.10	3.05	11.20	1.52	0.35	1.15	0.15	0.65	0.13	0.32	0.04	0.32	0.03	<10	1.50	0.02	0.04	31.74	79.08	293.35	34.30	4279.00	0.40	0.10
WP13ES065	5.30	42.10	81.80	8.47	27.70	3.91	0.95	2.64	0.25	1.32	0.16	0.41	0.06	0.35	0.05	<10	2.50	0.20	0.93	409.19	392.56	28.43	81.30	659.00	1.60	3.60
WP13ES066	4.30	53.90	104.00	10.49	35.50	4.30	0.95	2.70	0.24	1.12	0.10	0.31	0.05	0.31	0.05	<10	1.70	0.02	0.08	40.48	4.33	19.51	12.40	120.00	0.60	0.10
WP13ES067	9.60	59.50	111.60	11.59	40.70	5.62	1.30	3.89	0.42	1.88	0.35	0.85	0.12	0.82	0.14	<10	1.40	0.05	<0.01	0.81	2.52	6.49	29.10	44.00	4.60	6.90
WP13ES068	10.40	48.20	98.90	10.79	39.60	5.68	1.33	3.81	0.44	2.12	0.37	0.84	0.14	0.89	0.12	<10	1.00	0.08	0.12	0.54	7.09	5.07	48.70	150.00	6.40	7.30

All major oxides are in wt. %

All other elements in ppm except Au, Pt, Pd which are in ppb

Appendix 4: White Pine
whole-rock geochemistry

Sample	Mn	As	Au	Cd	Sb	Bi	Cr	B	Tl	Hg	Se	Te	Ge	In	Re	Be	Li	Pd	Pt
WP13ES001	213.00	0.40	<0.2	0.54	0.06	0.31	3.40	<1	0.17	<5	0.40	<0.02	<0.1	0.02	1.00	0.40	6.70	<10	<2
WP13ES003	336.00	0.80	0.60	0.11	0.06	0.12	5.00	<1	0.15	<5	<0.1	<0.02	<0.1	<0.02	<1	0.30	11.50	<10	<2
WP13ES004	294.00	0.10	0.40	0.10	0.08	0.23	2.90	<1	0.18	<5	<0.1	<0.02	<0.1	0.02	<1	0.30	9.20	<10	<2
WP13ES005	536.00	1.30	<0.2	0.10	0.10	0.16	102.10	<1	0.10	<5	<0.1	<0.02	0.30	0.04	<1	0.70	16.60	<10	<2
WP13ES006	99.73	99.73	99.73	99.73	99.73	99.73	99.73	99.73	99.73	99.73	99.73	99.73	99.73	99.73	99.73	99.73	99.73	99.73	99.73
WP13ES007	107.00	1.20	0.30	0.02	2.51	0.76	2.00	<1	0.13	<5	0.20	0.03	<0.1	0.03	<1	<0.1	4.10	<10	<2
WP13ES008	335.00	6.80	<0.2	0.37	0.34	0.36	127.80	<1	0.08	<5	0.20	<0.02	0.50	0.03	<1	1.30	9.00	<10	<2
WP13ES009	279.00	0.40	<0.2	0.17	0.03	0.19	3.20	<1	0.18	<5	<0.1	0.03	<0.1	<0.02	<1	0.20	10.60	<10	<2
WP13ES010	506.00	5.30	1.30	0.47	0.09	0.37	138.50	<1	0.11	<5	<0.1	<0.02	0.50	0.03	<1	1.20	55.20	<10	<2
WP13ES011	213.00	0.60	<0.2	0.30	0.04	1.12	2.60	<1	0.14	<5	<0.1	0.07	<0.1	0.05	<1	0.10	8.00	<10	<2
WP13ES012	316.00	0.70	<0.2	0.37	0.05	0.14	3.50	2.00	0.20	8.00	0.30	0.04	<0.1	<0.02	<1	0.50	9.60	<10	<2
WP13ES013	377.00	1.00	<0.2	0.03	0.04	0.04	12.60	<1	0.23	<5	<0.1	<0.02	0.10	<0.02	<1	0.20	11.00	<10	<2
WP13ES014	109.00	3.30	<0.2	0.04	0.07	0.04	1.70	<1	0.05	<5	<0.1	0.08	<0.1	<0.02	<1	<0.1	1.30	<10	<2
WP13ES015	778.00	1.10	<0.2	0.13	0.07	0.10	59.80	<1	0.64	<5	<0.1	<0.02	0.20	0.03	<1	0.50	53.20	<10	<2
WP13ES016	300.00	1.10	1.00	0.08	0.11	0.18	32.90	<1	0.80	<5	1.00	<0.02	<0.1	0.04	<1	1.00	45.40	<10	<2
WP13ES017	387.00	1.40	<0.2	0.39	0.06	1.76	11.20	<1	0.29	<5	<0.1	0.08	0.10	0.03	<1	0.30	11.80	<10	<2
WP13ES018	436.00	0.80	0.30	0.61	0.09	5.02	3.50	<1	0.19	<5	<0.1	0.81	<0.1	0.02	<1	0.30	5.90	<10	<2
WP13ES019	162.00	0.80	<0.2	0.58	0.04	0.32	2.40	<1	0.12	<5	0.20	0.06	<0.1	<0.02	<1	0.40	7.50	<10	<2
WP13ES020	101.00	1.50	<0.2	<0.01	0.05	0.10	3.00	<1	0.17	<5	0.40	<0.02	0.10	<0.02	50.00	0.10	9.50	*	<2
WP13ES021	100.00	0.80	<0.2	0.02	0.09	0.12	2.80	1.00	0.13	5.00	<0.1	0.03	<0.1	<0.02	<1	0.20	7.60	<10	<2
WP13ES022	919.00	5.10	34.40	8.84	0.18	96.18	2.80	2.00	0.26	53.00	<0.1	35.80	<0.1	1.33	<1	0.40	3.10	<10	<2
WP13ES023	193.00	0.70	<0.2	0.11	<0.02	0.15	3.40	<1	0.17	<5	<0.1	0.09	<0.1	<0.02	<1	0.20	11.20	<10	<2
WP13ES024	34.00	5.50	0.30	0.07	0.76	0.55	1.30	<1	0.14	9.00	<0.1	0.05	<0.1	0.03	<1	<0.1	1.10	<10	<2
WP13ES025	72.00	1.30	<0.2	0.01	0.98	0.66	0.60	2.00	0.15	16.00	<0.1	0.03	<0.1	<0.02	<1	<0.1	0.70	<10	2.00
WP13ES026	51.00	2.30	2.20	0.04	0.29	2.02	2.30	<1	0.11	<5	0.20	0.29	<0.1	0.07	<1	0.20	4.10	<10	<2
WP13ES027	125.00	1.30	0.70	0.06	0.06	0.32	3.40	<1	0.12	<5	0.40	0.04	<0.1	0.04	<1	0.30	6.80	<10	<2
WP13ES028	91.00	0.90	<0.2	<0.01	0.30	0.40	2.00	1.00	0.16	<5	0.20	0.13	<0.1	<0.02	30.00	<0.1	5.50	*	2.00
WP13ES030	289.00	0.50	0.30	0.16	0.04	0.17	4.50	<1	0.08	8.00	<0.1	0.06	<0.1	0.03	<1	0.50	15.50	<10	<2
WP13ES031	309.00	0.10	4.50	0.07	0.04	0.31	3.70	<1	0.21	12.00	<0.1	0.02	<0.1	0.04	<1	0.20	12.40	<10	<2
WP13ES032	428.00	2.20	3.50	0.24	0.20	0.32	102.30	<1	0.10	11.00	<0.1	<0.02	0.30	0.02	<1	1.30	11.50	17.00	<2
WP13ES033	110.00	0.70	3.00	0.14	0.04	1.50	2.40	<1	0.18	<5	<0.1	0.13	<0.1	<0.02	2.00	0.60	5.10	<10	3.00
WP13ES034	294.00	0.70	2.30	0.08	0.03	0.37	2.90	<1	0.17	11.00	<0.1	<0.02	<0.1	<0.02	<1	0.20	11.50	<10	<2
WP13ES035	279.00	0.30	1.80	0.10	<0.02	0.55	3.10	<1	0.16	7.00	0.20	<0.02	<0.1	<0.02	<1	0.30	12.60	<10	2.00
WP13ES036	39.00	1.60	1.80	0.12	0.35	3.51	1.30	<1	0.08	<5	0.20	0.19	<0.1	0.04	<1	0.10	2.90	<10	<2
WP13ES037	371.00	1.00	0.60	0.04	0.27	0.30	10.90	<1	0.04	8.00	<0.1	0.05	0.10	<0.02	1.00	0.50	20.90	<10	<2
WP13ES038	578.00	0.80	1.40	8.62	0.03	16.73	3.80	<1	0.18	12.00	<0.1	0.99	<0.1	0.41	<1	0.50	7.10	<10	<2
WP13ES039	380.00	1.60	1.40	0.03	0.04	<0.02	13.00	<1	0.21	7.00	<0.1	0.02	0.20	<0.02	<1	0.30	11.20	<10	2.00
WP13ES040	211.00	5.00	9.10	0.16	0.11	16.64	2.80	<1	0.20	16.00	<0.1	2.84	<0.1	0.07	<1	0.70	3.70	<10	<2
WP13ES041	811.00	74.00	35.20	0.71	0.27	1.09	3.90	<1	0.15	25.00	0.10	1.48	<0.1	<0.02	<1	1.00	4.70	<10	<2
WP13ES042	330.00	2.20	1.10	0.06	0.04	0.42	9.90	<1	0.12	7.00	<0.1	0.02	<0.1	<0.02	<1	0.30	8.50	<10	<2

All major oxides are in wt. %

All other elements in ppm except Au, Pt, Pd which are in ppb

Appendix 4: White Pine
whole-rock geochemistry

Sample	Mn	As	Au	Cd	Sb	Bi	Cr	B	Tl	Hg	Se	Te	Ge	In	Re	Be	Li	Pd	Pt
WP13ES043	438.00	0.70	1.50	0.46	0.09	1.25	1.10	<1	0.08	8.00	<0.1	0.41	<0.1	<0.02	<1	0.80	1.20	<10	2.00
WP13ES044	349.00	0.20	1.90	0.10	<0.02	0.32	11.70	1.00	0.19	<5	<0.1	<0.02	0.10	0.03	<1	0.20	11.30	<10	<2
WP13ES045	356.00	0.50	1.80	1.49	0.07	1.24	1.40	<1	0.15	6.00	0.30	0.32	<0.1	0.27	<1	0.30	2.10	<10	<2
WP13ES046	134.00	0.20	0.60	0.42	0.04	0.65	1.70	<1	0.09	<5	0.20	0.07	<0.1	0.04	<1	0.30	3.30	<10	<2
WP13ES047	402.00	0.70	<0.2	0.03	0.06	0.17	18.10	<1	0.28	<5	<0.1	<0.02	<0.1	<0.02	<1	0.30	12.50	<10	<2
WP13ES048	311.00	7.30	7.40	<0.01	0.05	0.11	2.60	1.00	0.27	<5	0.20	0.08	<0.1	<0.02	<1	0.80	2.40	<10	3.00
WP13ES049	332.00	1.70	1.20	0.05	0.11	0.05	12.40	1.00	0.14	<5	<0.1	<0.02	<0.1	0.02	<1	0.30	7.60	<10	<2
WP13ES050	559.00	5.90	9.90	0.88	0.15	46.02	3.00	<1	0.22	93.00	0.20	7.57	<0.1	0.07	<1	0.40	2.40	<10	<2
WP13ES051	408.00	1.00	0.70	0.09	0.10	1.68	10.70	<1	0.18	8.00	0.20	0.04	<0.1	<0.02	<1	0.30	8.70	<10	<2
WP13ES052	407.00	0.70	0.50	2.13	0.11	3.17	8.30	<1	0.22	7.00	<0.1	0.54	<0.1	0.13	<1	0.40	5.20	<10	<2
WP13ES053	31.00	0.20	1.50	<0.01	0.05	0.41	1.60	<1	<0.02	<5	0.40	<0.02	<0.1	<0.02	<1	<0.1	0.20	<10	<2
WP13ES054	202.00	3.40	3.20	0.95	0.07	1.33	1.70	<1	0.11	<5	<0.1	0.34	<0.1	0.04	<1	0.60	2.60	<10	<2
WP13ES055	109.00	1.00	0.50	<0.01	0.08	18.27	3.60	<1	0.17	<5	0.30	0.32	<0.1	0.09	<1	0.20	4.60	<10	<2
WP13ES056	329.00	4.80	3.30	0.46	0.07	1.27	3.20	<1	0.21	<5	<0.1	0.03	<0.1	<0.02	<1	0.80	5.80	<10	<2
WP13ES057	342.00	0.50	<0.2	0.19	0.11	0.51	4.90	<1	0.18	<5	<0.1	0.03	0.20	<0.02	<1	0.40	9.00	<10	<2
WP13ES058	275.00	0.20	0.80	0.31	0.19	0.99	5.80	<1	0.23	11.00	0.20	0.13	<0.1	0.03	<1	0.20	8.80	<10	<2
WP13ES059	382.00	0.40	2.10	0.23	0.05	0.28	6.50	<1	0.22	<5	0.10	<0.02	0.10	0.02	<1	0.20	9.20	<10	<2
WP13ES060	304.00	0.70	2.20	0.89	0.28	3.54	3.60	1.00	0.18	14.00	0.40	0.72	<0.1	0.44	1.00	0.30	4.70	*	<2
WP13ES061	347.00	0.20	0.20	0.11	0.03	<0.02	6.80	<1	0.21	<5	<0.1	<0.02	0.20	<0.02	1.00	0.20	6.70	<10	2.00
WP13ES062	55.00	0.90	1.60	0.42	0.17	87.45	1.60	<1	0.11	31.00	0.40	0.13	<0.1	0.46	<1	0.30	2.30	<10	<2
WP13ES063	59.00	1.20	5.90	0.54	0.12	24.17	2.10	<1	0.12	14.00	<0.1	0.05	<0.1	0.12	<1	0.30	2.40	28.00	<2
WP13ES064	32.00	2.90	0.90	0.17	0.10	17.95	1.00	<1	0.08	22.00	0.10	0.15	<0.1	0.06	<1	<0.1	1.20	<10	<2
WP13ES065	126.00	0.70	1.30	1.16	0.08	4.46	1.60	<1	0.08	11.00	<0.1	0.03	<0.1	0.04	14.00	0.60	3.50	*	<2
WP13ES066	74.00	0.10	1.00	<0.01	0.03	0.36	1.40	<1	0.10	<5	<0.1	<0.02	<0.1	<0.02	<1	0.30	5.70	<10	<2
WP13ES067	353.00	2.30	0.70	0.04	0.05	0.17	6.50	<1	0.18	5.00	<0.1	0.03	<0.1	<0.02	<1	0.20	7.00	<10	<2
WP13ES068	416.00	1.50	0.30	0.02	0.02	0.09	8.30	<1	0.25	<5	<0.1	0.10	0.10	<0.02	<1	0.30	9.50	<10	<2

All major oxides are in wt. %

All other elements in ppm except Au, Pt, Pd which are in ppb

Appendix 5: Buckingham
whole-rock geochemistry

Sample	SiO2	Al2O3	Fe2O3	MgO	CaO	Na2O	K2O	TiO2	P2O5	MnO	Cr2O3	Sum	Ba	Sc	Cs	Ga	Hf	Nb	Rb	Sn	Sr	Ta	Th	U	V	W	Zr
BK13ES001	66.53	14.14	5.53	1.18	0.42	1.93	7.59	1.09	0.12	0.06	0.01	99.71	941.00	16.00	5.40	17.30	4.90	21.00	216.00	2.00	147.60	1.50	11.70	3.00	109.00	18.30	173.90
BK13ES002	94.24	2.29	1.60	0.16	0.02	0.02	0.75	0.25	0.03	<0.01	0.00	99.88	168.00	1.00	1.10	2.80	5.60	4.50	42.80	2.00	2.90	0.40	2.20	0.80	24.00	8.80	216.80
BK13ES003	89.55	5.71	0.98	0.33	0.05	0.06	1.90	0.38	0.04	<0.01	0.00	99.82	536.00	4.00	4.60	7.70	6.40	5.90	90.00	<1	21.00	0.60	5.70	5.90	38.00	7.30	246.30
BK13ES004	73.19	14.27	1.71	0.17	1.00	2.60	4.66	0.24	0.04	<0.01	0.00	99.78	1032.00	4.00	3.30	14.70	2.70	11.10	155.90	2.00	240.20	1.50	7.00	5.00	30.00	11.70	84.90
BK13ES005	67.75	13.88	4.61	0.93	0.44	1.84	8.31	0.99	0.10	0.05	0.01	99.67	902.00	13.00	6.30	15.90	5.20	17.70	270.70	2.00	202.90	1.10	11.60	3.70	91.00	19.20	164.90
BK13ES006	61.39	16.38	5.61	1.50	0.69	2.68	8.84	1.25	0.15	0.06	0.01	99.62	831.00	19.00	8.20	20.90	5.70	23.30	295.60	3.00	220.60	1.50	13.10	4.70	133.00	8.30	191.20
BK13ES007	70.51	13.49	2.54	1.52	2.01	1.96	5.34	0.48	0.15	0.03	0.01	99.66	1506.00	6.00	7.30	17.00	4.70	13.40	204.60	2.00	405.50	0.90	9.70	2.30	77.00	2.60	171.80
BK13ES008	74.90	14.40	1.62	0.78	0.05	0.07	4.82	0.34	0.06	<0.01	0.00	99.76	1223.00	3.00	8.70	19.60	3.90	12.70	230.10	8.00	28.80	1.10	13.40	2.40	46.00	9.20	152.10
BK13ES009	73.76	12.57	2.74	0.72	0.12	0.12	5.19	0.38	0.30	<0.01	0.00	98.97	1145.00	4.00	8.30	21.60	4.30	12.10	241.00	42.00	151.90	1.00	8.60	6.10	55.00	23.70	154.20
BK13ES010	83.51	5.56	4.96	0.32	0.72	0.03	1.29	0.22	0.59	<0.01	0.01	99.76	891.00	5.00	3.40	7.80	1.90	4.80	37.80	<1	75.80	0.30	4.10	5.40	178.00	1.00	70.00
BK13ES011	69.06	16.50	2.68	0.70	0.32	3.31	4.14	0.42	0.19	0.01	<0.002	99.31	5084.00	4.00	5.80	21.40	4.10	12.90	154.00	2.00	199.00	1.00	13.10	3.90	50.00	5.60	164.40
BK13ES012	90.72	4.06	1.70	0.34	0.13	0.78	0.64	0.31	0.08	0.03	0.00	99.87	228.00	3.00	4.00	5.00	6.60	6.90	23.60	<1	20.60	0.40	6.30	1.50	23.00	1.10	263.40
BK13ES013	95.14	1.81	1.18	0.14	0.05	0.11	0.38	0.11	0.05	0.05	0.00	99.92	138.00	1.00	2.50	1.80	2.60	1.90	13.70	<1	8.70	0.10	1.80	0.60	11.00	<0.5	100.30
BK13ES014	83.45	5.69	5.68	1.23	0.25	0.73	0.54	0.29	0.06	0.04	0.00	99.88	225.00	3.00	3.50	6.80	6.00	4.60	20.10	<1	27.80	0.30	5.10	1.50	27.00	0.90	212.80
BK13ES015	91.25	3.22	2.33	0.14	0.23	0.31	0.51	0.18	0.03	0.01	0.00	99.91	109.00	2.00	1.70	3.60	4.20	3.10	22.80	<1	14.30	0.20	3.10	1.20	13.00	0.80	149.60
BK13ES016	74.87	3.17	16.41	0.24	0.20	0.03	0.77	0.19	0.17	0.10	0.00	99.86	155.00	3.00	4.90	4.00	4.20	2.90	50.00	<1	18.90	0.20	4.60	1.50	16.00	4.20	148.30
BK13ES017	90.74	4.56	1.24	0.25	0.18	0.03	1.36	0.34	0.03	<0.01	0.00	99.86	465.00	3.00	2.30	5.60	6.40	6.00	69.50	<1	16.00	0.50	4.20	1.70	22.00	3.30	259.60
BK13ES018	90.08	4.94	1.54	0.37	0.11	0.86	0.74	0.29	0.06	0.02	0.00	99.86	387.00	3.00	1.30	5.60	4.30	4.20	29.40	<1	19.20	0.40	5.50	1.50	24.00	0.50	210.80
BK13ES019	82.36	8.18	3.81	0.79	0.11	0.70	1.44	0.44	0.07	0.02	0.01	99.83	334.00	7.00	4.80	9.80	5.70	7.80	60.90	<1	32.80	0.60	7.10	2.40	41.00	0.70	220.50
BK13ES020	68.06	14.35	7.65	1.75	0.10	0.47	3.64	0.63	0.11	0.04	0.01	99.78	680.00	13.00	5.10	17.60	4.80	12.20	148.30	2.00	49.70	0.90	12.40	3.40	86.00	1.70	186.40
BK13ES021	85.45	6.81	3.05	0.27	0.16	0.05	2.20	0.39	0.03	<0.01	0.01	99.81	764.00	5.00	1.50	8.60	6.00	6.70	82.00	2.00	16.80	0.40	6.70	1.60	40.00	4.80	247.50
BK13ES022	83.38	5.00	5.26	0.29	0.10	0.08	2.07	0.25	0.13	<0.01	0.00	99.83	618.00	3.00	4.70	6.90	4.50	4.60	87.70	<1	42.60	0.40	8.40	1.80	30.00	7.60	175.40
BK13ES023	59.25	19.71	6.63	1.43	0.36	1.52	6.72	0.82	0.12	0.04	0.01	99.72	951.00	18.00	13.10	25.00	5.80	16.70	237.90	4.00	97.60	1.00	16.50	4.50	119.00	4.10	208.70
BK13ES024	84.18	4.00	7.38	0.19	0.05	0.05	1.57	0.31	0.14	0.01	0.00	99.84	490.00	3.00	4.10	5.80	6.40	5.10	85.20	1.00	25.20	0.30	5.50	1.50	26.00	8.70	233.50
BK13ES025	89.52	2.83	2.83	0.19	0.02	0.01	1.02	0.21	0.04	<0.01	0.00	99.04	152.00	3.00	1.20	5.50	4.00	4.20	67.80	25.00	4.20	0.30	2.10	1.10	21.00	13.40	156.00
BK13ES026	81.61	8.99	1.80	0.53	0.10	0.07	4.19	0.54	0.05	0.02	0.01	99.82	474.00	8.00	6.40	13.80	7.50	9.50	209.00	55.00	44.50	0.60	7.70	2.40	51.00	15.20	273.70
BK13ES027	90.03	4.56	1.42	0.28	0.10	0.40	1.43	0.32	0.03	<0.01	0.00	99.87	235.00	3.00	2.40	4.80	5.80	4.40	65.20	<1	43.30	0.30	4.50	1.30	24.00	13.60	223.30
BK13ES028	61.17	16.56	6.33	1.69	0.79	2.07	8.56	1.11	0.21	0.06	0.01	99.71	902.00	20.00	13.00	18.40	4.50	18.50	324.20	2.00	204.70	1.30	12.10	2.60	113.00	9.80	168.90
BK13ES029	72.99	15.64	1.65	0.52	0.25	2.86	3.13	0.29	0.05	<0.01	0.01	99.83	375.00	6.00	4.70	17.20	2.50	6.60	124.70	1.00	195.10	0.60	5.40	2.60	46.00	2.10	93.40
BK13ES030	68.99	15.24	3.00	1.58	0.51	3.23	3.83	0.27	0.11	0.40	0.01	99.61	1195.00	6.00	3.60	15.90	2.50	41.70	120.30	1.00	358.10	0.80	6.10	2.90	42.00	1.20	80.60
BK13ES031	69.62	15.46	1.95	0.86	0.18	1.33	6.95	0.48	0.05	<0.01	0.00	99.51	1018.00	5.00	5.60	15.50	4.20	11.40	224.30	2.00	249.80	0.80	9.60	7.80	63.00	187.50	148.70
BK13ES032	72.93	13.55	1.37	0.30	0.09	0.30	9.21	0.42	0.14	<0.01	<0.002	99.69	1243.00	4.00	5.20	13.80	3.60	9.70	270.70	2.00	188.60	0.80	7.50	2.10	44.00	93.20	134.60
BK13ES033	70.15	14.93	2.41	1.22	1.20	1.87	5.71	0.51	0.21	0.02	<0.002	99.66	1134.00	5.00	5.10	16.60	4.00	12.50	153.30	1.00	331.20	0.80	12.40	3.70	59.00	14.20	159.50
BK13ES034	78.33	9.84	2.19	0.32	0.05	0.17	6.91	0.42	0.09	<0.01	0.01	99.72	822.00	5.00	4.40	11.80	5.30	14.10	211.00	3.00	136.70	0.70	11.00	2.40	50.00	75.50	211.40
BK13ES035	91.25	3.93	1.10	0.17	0.04	0.06	2.57	0.15	0.02	<0.01	0.00	99.86	414.00	2.00	2.00	4.80	2.90	1.60	103.00	2.00	36.70	0.30	7.50	1.20	31.00	50.60	117.00
BK13ES036	65.21	8.18	9.06	0.64	1.08	0.10	4.52	0.35	0.32	<0.01	0.01	99.57	1071.00	11.00	10.50	11.80	2.40	7.30	139.20	3.00	427.40	0.50	17.10	2.30	107.00	45.80	84.90
BK13ES037	66.67	15.55	3.91	1.15	0.16	0.10	6.54	0.58	0.19	<0.01	<0.002	99.71	1297.00	7.00	10.50	21.30	4.40	17.40	285.10	8.00	87.30	1.50	17.20	4.00	88.00	73.90	166.90
BK13ES038	73.18	13.47	1.53	0.49	0.21	0.21	8.00	0.44	0.06	<0.01	0.00	99.70	1398.00	6.00	7.70	17.60	4.10	11.70	275.50	3.00	179.10	1.00	10.10	2.00	53.00	66.80	161.00
BK13ES039	75.61	12.61	1.31	0.37	0.09	0.20	6.61	0.43	0.06	<0.01	0.00	99.70	1199.00	5.00	6.70	14.60	5.00	9.50	235.90	2.00	117.20	0.80	8.10	1.30	54.00	85.00	167.50
BK13ES040	74.89	11.98	0.97	0.26	0.13	0.29	9.10	0.41	0.05	<0.01	0.00	99.71	1292.00	3.00	3.90	13.90	4.20	10.20	306.10	3.00	161.80	1.00	8.50	1.50	46.00	83.80	167.70

All major oxides are in wt. %

All other elements in ppm except Au, Pt, Pd which are in ppb

Appendix 5: Buckingham
whole-rock geochemistry

Sample	SiO2	Al2O3	Fe2O3	MgO	CaO	Na2O	K2O	TiO2	P2O5	MnO	Cr2O3	Sum	Ba	Sc	Cs	Ga	Hf	Nb	Rb	Sn	Sr	Ta	Th	U	V	W	Zr
BK13ES041	70.60	15.41	1.92	0.81	0.04	0.12	8.04	0.43	0.04	<0.01	<0.002	99.69	1326.00	6.00	7.10	19.60	4.50	14.20	341.70	6.00	149.30	1.50	8.30	2.50	78.00	33.20	164.30
BK13ES042	71.33	13.51	2.34	0.69	0.35	0.16	8.36	0.43	0.07	0.01	<0.002	99.67	1460.00	5.00	5.60	18.50	3.80	15.40	337.00	6.00	206.00	1.20	8.20	2.40	55.00	48.30	166.80
BK13ES043	74.85	11.72	1.54	0.40	0.50	0.19	8.02	0.38	0.07	<0.01	<0.002	99.59	2412.00	4.00	5.40	13.20	2.70	10.50	244.10	4.00	193.80	0.70	7.40	2.80	44.00	46.20	110.40
BK13ES044	90.44	4.24	0.75	0.21	0.05	0.07	3.00	0.10	0.04	<0.01	0.00	99.85	667.00	2.00	1.60	5.20	2.00	3.00	100.00	<1	54.50	0.20	3.20	1.20	21.00	22.10	60.30
BK13ES045	80.15	8.81	1.74	1.02	0.24	0.58	5.76	0.37	0.12	0.02	0.01	99.72	788.00	5.00	3.50	10.00	6.90	8.00	173.80	2.00	163.50	0.60	14.50	2.80	53.00	29.30	259.10
BK13ES046	96.96	0.92	1.10	0.18	0.04	<0.01	0.21	0.04	0.04	0.02	0.00	99.92	262.00	2.00	0.90	2.60	0.20	1.40	8.60	<1	7.20	<0.1	0.70	0.20	12.00	<0.5	10.80
BK13ES047	85.44	5.66	2.20	0.82	1.20	1.31	1.74	0.16	0.06	0.04	0.01	99.88	398.00	3.00	0.50	8.10	1.40	3.30	30.00	5.00	135.60	0.30	3.30	1.30	55.00	1.60	33.00
BK13ES048	72.87	12.56	2.74	1.55	2.83	2.56	3.81	0.26	0.09	0.04	0.01	99.75	968.00	6.00	0.70	14.80	2.20	5.60	65.80	3.00	459.70	0.50	5.40	2.70	54.00	1.50	72.40
BK13ES049	75.89	8.87	3.85	1.03	1.99	0.82	6.40	0.25	0.08	0.06	0.01	99.83	680.00	5.00	1.80	10.80	2.10	6.80	95.10	2.00	241.90	0.50	5.10	1.90	57.00	1.60	86.90
BK13ES050	89.61	4.08	2.18	0.40	0.42	1.10	0.79	0.11	0.06	0.04	0.01	99.92	102.00	2.00	1.60	7.20	1.10	2.30	19.20	4.00	67.00	0.20	1.80	1.00	41.00	2.40	28.40
BK13ES051	68.84	14.50	2.64	1.74	1.36	2.71	5.02	0.27	0.11	0.02	0.01	99.68	985.00	6.00	2.30	18.10	2.90	6.70	120.70	3.00	384.40	0.80	6.60	3.70	56.00	9.10	84.60
BK13ES052	96.99	0.35	1.25	0.07	0.42	<0.01	0.09	0.02	0.08	0.02	0.00	99.94	27.00	<1	0.30	1.60	<0.1	0.60	5.30	1.00	11.90	<0.1	0.30	2.20	17.00	1.50	2.30
BK13ES053	69.40	14.24	1.13	2.12	7.57	3.60	0.60	0.37	0.11	0.03	0.01	99.83	220.00	9.00	0.20	15.50	2.90	6.60	9.30	2.00	621.70	0.60	7.20	2.30	67.00	1.10	90.20
BK13ES054	73.33	12.15	2.14	0.81	3.51	1.96	4.25	0.35	0.21	0.05	0.00	99.80	576.00	4.00	0.80	14.60	3.80	11.40	88.30	2.00	268.60	0.80	8.50	2.70	54.00	3.90	139.50
BK13ES055	72.05	12.91	1.77	1.67	6.42	3.32	0.68	0.34	0.13	0.04	0.01	99.84	177.00	7.00	0.30	14.50	3.10	6.20	11.00	2.00	526.20	0.50	4.90	1.70	83.00	1.70	101.20
BK13ES056	53.02	25.69	3.72	1.75	0.20	0.49	10.16	0.67	0.14	<0.01	0.01	99.66	1404.00	18.00	5.60	35.10	2.50	16.50	355.70	5.00	121.60	1.20	25.50	8.20	110.00	22.60	79.50
BK13ES057	80.54	9.70	2.35	0.75	0.68	1.27	1.70	0.43	0.08	<0.01	0.01	99.80	291.00	6.00	2.70	12.70	7.10	9.20	85.80	3.00	190.60	0.70	15.90	3.50	46.00	10.00	274.30
BK13ES058	70.17	16.09	0.97	0.97	1.68	2.67	3.96	0.30	0.05	<0.01	0.02	99.55	971.00	8.00	4.10	17.90	2.80	6.80	118.80	5.00	450.30	0.70	8.60	11.50	49.00	3.00	95.50
BK13ES059	78.89	11.16	2.23	0.44	0.03	0.09	3.26	0.47	0.08	<0.01	0.01	99.83	438.00	7.00	3.20	15.10	6.40	10.00	130.00	5.00	36.40	0.70	12.00	3.20	47.00	18.70	209.60
BK13ES060	71.00	13.12	1.88	0.76	0.19	0.33	10.18	0.49	0.14	<0.01	0.01	99.62	1202.00	7.00	4.50	15.50	3.90	12.50	340.70	5.00	205.60	1.20	10.80	5.10	78.00	53.60	141.00
BK13ES061	80.56	9.17	1.28	0.69	0.33	0.86	5.36	0.39	0.08	<0.01	0.01	99.73	835.00	6.00	4.40	11.50	6.10	8.70	206.70	2.00	150.30	0.60	15.70	3.40	44.00	25.00	236.90
BK13ES062	83.57	8.56	1.14	0.21	0.05	0.13	4.26	0.30	0.06	<0.01	0.01	99.83	446.00	5.00	3.10	10.60	5.10	6.60	152.40	2.00	102.70	0.70	10.40	2.00	53.00	12.50	214.10
BK13ES063	83.80	7.57	1.36	0.29	0.10	0.15	4.90	0.28	0.05	<0.01	0.01	99.63	799.00	4.00	4.70	8.60	3.50	4.90	177.40	1.00	138.00	0.30	8.60	3.80	42.00	11.60	137.00
BK13PH100	83.86	7.12	1.70	0.49	0.38	0.76	3.99	0.28	0.06	0.01	0.01	99.78	661.00	4.00	2.30	8.20	3.80	5.70	154.90	1.00	138.00	0.50	8.60	3.20	44.00	30.90	150.90
BK13PH101	79.42	9.85	2.20	0.54	0.07	0.13	5.40	0.54	0.04	<0.01	0.01	99.74	1070.00	8.00	5.70	12.20	8.70	9.20	218.60	7.00	69.00	1.00	8.90	2.10	61.00	14.80	304.40
BK13PH102	83.25	7.58	2.65	0.32	0.04	0.11	3.68	0.28	0.06	<0.01	0.01	99.76	817.00	4.00	2.90	11.20	5.20	5.40	139.40	8.00	69.30	0.50	7.30	1.90	42.00	24.10	184.80
BK13PH103	55.41	16.13	9.34	0.95	0.15	0.14	6.30	1.05	0.06	<0.01	0.08	99.72	1143.00	25.00	16.90	29.90	3.30	13.00	323.60	5.00	68.10	1.10	11.80	2.80	170.00	60.50	130.20
BK13PH104	76.23	3.35	9.42	0.21	0.12	0.01	0.85	0.17	0.05	0.02	0.01	98.39	174.00	2.00	4.70	7.90	1.00	3.20	65.80	55.00	10.10	0.20	1.60	1.20	76.00	12.30	52.40
BK13PH105	72.96	10.96	5.85	1.96	0.35	0.08	4.09	1.45	0.28	0.06	0.02	99.76	957.00	13.00	5.10	15.70	5.60	40.10	157.10	1.00	23.70	2.20	10.40	1.30	97.00	3.80	245.90
BK13PH106	91.30	3.52	2.37	0.39	0.09	0.05	1.05	0.21	0.05	<0.01	0.00	99.84	498.00	3.00	1.30	5.70	5.30	4.80	47.30	<1	26.60	0.20	6.10	1.30	21.00	2.40	192.10
BK13PH107	68.90	17.35	2.32	0.92	0.11	0.49	4.92	0.79	0.06	<0.01	0.01	99.71	1246.00	14.00	6.10	23.80	7.50	14.40	162.80	4.00	72.50	1.20	15.00	3.30	78.00	22.80	254.40
BK13PH108	85.55	6.48	2.95	0.41	0.02	0.05	2.39	0.32	0.08	<0.01	0.01	99.87	292.00	4.00	2.50	8.40	6.70	6.90	133.70	3.00	30.00	0.60	11.30	1.80	31.00	13.30	241.20
BK13PH109	87.45	5.02	3.39	0.29	0.08	0.08	1.55	0.22	0.09	<0.01	0.00	99.89	144.00	3.00	1.70	4.90	4.20	4.10	72.20	2.00	16.70	0.40	7.60	1.60	31.00	15.40	158.60
BK13PH110	65.29	15.58	3.20	2.58	3.19	2.89	3.56	0.42	0.12	0.08	0.01	99.59	799.00	10.00	1.80	16.00	2.30	6.50	110.50	1.00	395.10	0.60	6.60	3.60	73.00	1.30	87.30
BK13PH111	87.89	5.36	1.07	0.65	0.12	0.24	3.11	0.22	0.05	0.01	0.00	99.83	496.00	4.00	1.80	7.20	3.40	4.30	107.80	<1	78.90	0.30	6.60	1.50	39.00	26.40	124.00

All major oxides are in wt. %

All other elements in ppm except Au, Pt, Pd which are in ppb

Appendix 5: Buckingham
whole-rock geochemistry

Sample	Y	La	Ce	Pr	Nd	Sm	Eu	Gd	Tb	Dy	Ho	Er	Tm	Yb	Lu	Ni	LOI	TOT/C	TOT/S	Mo	Cu	Pb	Zn	Ag	Ni	Co
BK13ES001	25.50	31.10	65.70	7.38	27.00	5.48	1.10	5.10	0.81	4.90	0.93	2.58	0.39	2.67	0.40	36.00	1.10	0.02	0.03	305.39	38.21	1.44	60.60	88.00	40.00	12.20
BK13ES002	7.90	9.30	18.30	2.09	7.70	1.53	0.16	1.48	0.21	1.47	0.25	0.82	0.13	0.87	0.14	<10	0.50	0.01	0.02	5.15	14.61	27.40	3.60	692.00	1.60	0.40
BK13ES003	18.70	16.20	35.00	4.16	16.80	3.39	0.75	3.64	0.55	3.65	0.73	2.16	0.30	1.99	0.29	<10	0.80	0.03	0.02	3.10	28.13	8.09	13.30	2782.00	3.40	2.50
BK13ES004	3.50	6.90	10.70	1.02	3.20	0.55	0.38	0.57	0.07	0.37	0.12	0.39	0.07	0.59	0.12	<10	1.90	0.03	0.05	2.14	57.85	34.39	4.90	2790.00	0.80	0.20
BK13ES005	23.70	33.40	71.30	8.35	30.50	5.96	1.33	5.33	0.78	5.31	0.96	2.70	0.39	2.29	0.39	17.00	0.80	0.03	0.04	334.17	36.10	1.44	105.30	167.00	20.80	7.00
BK13ES006	34.50	46.10	98.50	10.64	40.30	7.53	1.78	7.20	1.03	6.29	1.29	3.62	0.53	3.33	0.48	49.00	1.00	0.02	0.03	206.34	103.72	2.40	112.00	468.00	51.10	17.10
BK13ES007	14.80	26.10	54.40	6.41	23.70	4.37	1.23	3.88	0.49	2.68	0.47	1.46	0.20	1.47	0.20	27.00	1.60	0.02	0.02	26.95	162.62	5.27	87.80	358.00	29.70	5.40
BK13ES008	4.50	27.90	53.50	5.45	18.50	2.74	0.40	1.91	0.20	1.16	0.20	0.51	0.07	0.55	0.09	<10	2.70	0.03	0.10	43.91	19.23	49.68	3.10	2513.00	0.90	0.20
BK13ES009	9.40	23.00	43.90	4.57	16.60	3.35	0.83	3.53	0.48	2.58	0.37	0.98	0.14	0.81	0.12	<10	3.10	0.04	0.25	1081.10	61.92	6277.25	38.90	15108.00	1.30	0.40
BK13ES010	25.00	16.00	24.10	4.01	16.70	3.66	0.96	4.17	0.60	3.60	0.73	2.10	0.31	2.12	0.32	25.00	2.50	0.18	0.03	4.57	226.21	26.40	94.50	414.00	28.40	2.60
BK13ES011	11.40	33.80	64.40	6.98	25.20	4.04	1.06	3.32	0.37	2.15	0.33	0.83	0.13	0.99	0.12	<10	2.00	0.03	<0.01	0.80	4.47	6.49	9.40	374.00	1.30	2.40
BK13ES012	15.10	13.50	29.10	3.32	13.00	2.52	0.49	2.77	0.40	2.51	0.57	1.66	0.23	1.60	0.25	<10	1.10	0.03	0.02	2.09	8.21	11.99	16.90	54.00	7.50	3.00
BK13ES013	5.00	4.80	10.30	1.06	4.10	1.09	0.31	1.10	0.15	0.96	0.21	0.59	0.07	0.59	0.09	<10	0.90	0.04	0.02	0.76	3.93	2.50	11.60	25.00	4.80	1.60
BK13ES014	15.80	12.40	25.80	2.85	10.30	2.32	0.49	2.61	0.43	2.60	0.57	1.46	0.22	1.43	0.26	16.00	1.90	0.04	0.07	0.66	18.69	15.63	63.40	888.00	21.70	5.10
BK13ES015	9.30	7.80	15.80	1.80	6.10	1.33	0.22	1.42	0.22	1.47	0.33	0.97	0.15	1.05	0.16	<10	1.70	0.05	0.09	0.67	20.65	6.79	8.30	155.00	3.80	3.60
BK13ES016	28.10	10.20	22.70	2.90	12.80	3.61	1.21	5.93	0.97	6.08	1.22	3.06	0.43	2.52	0.34	52.00	3.70	0.17	0.05	0.60	17.57	19.26	290.60	641.00	55.70	23.70
BK13ES017	13.10	8.60	18.70	2.09	8.60	1.89	0.30	1.83	0.30	2.22	0.45	1.70	0.23	1.64	0.22	<10	1.10	0.05	0.07	0.45	11.15	4.24	5.70	403.00	1.30	0.40
BK13ES018	13.00	14.70	33.50	3.75	13.60	2.84	0.50	2.48	0.34	2.21	0.46	1.49	0.21	1.36	0.23	<10	0.80	0.02	0.02	0.28	8.51	1.59	11.10	172.00	3.30	1.00
BK13ES019	20.20	27.00	57.60	6.59	25.90	4.82	0.86	4.11	0.61	3.77	0.74	2.10	0.33	2.04	0.33	17.00	1.90	0.03	0.02	0.32	242.87	2.08	37.40	86.00	20.10	4.00
BK13ES020	39.90	42.40	94.20	12.49	54.40	10.21	1.97	9.30	1.32	7.39	1.30	3.82	0.58	3.41	0.50	24.00	3.00	0.03	0.04	0.71	45.16	2.76	82.50	30.00	25.20	5.80
BK13ES021	17.20	18.20	39.40	4.18	13.90	2.70	0.45	2.94	0.43	3.02	0.60	1.85	0.27	1.73	0.27	<10	1.40	0.03	0.08	0.43	21.83	1.95	3.40	1004.00	1.40	0.50
BK13ES022	11.80	13.70	29.00	3.02	11.40	2.16	0.39	2.24	0.33	2.25	0.47	1.29	0.18	1.31	0.23	<10	3.30	0.09	0.56	2.66	98.21	5.00	7.10	313.00	4.10	1.60
BK13ES023	41.50	57.80	115.90	13.23	51.70	9.68	1.65	8.75	1.27	8.09	1.48	4.27	0.65	4.25	0.62	17.00	3.10	0.03	0.05	65.74	77.84	3.01	26.00	143.00	19.10	4.30
BK13ES024	13.90	14.10	27.80	3.16	12.00	2.54	0.42	2.31	0.36	2.43	0.54	1.21	0.21	1.47	0.23	<10	2.00	0.09	0.06	20.76	68.88	2.38	4.70	741.00	1.70	0.70
BK13ES025	10.30	9.90	18.40	1.98	8.20	1.43	0.18	1.56	0.24	1.66	0.33	1.08	0.15	1.06	0.14	<10	2.40	0.01	0.42	36.41	155.16	8152.02	31.40	>100000	1.70	0.80
BK13ES026	18.40	21.50	44.20	5.03	19.30	4.36	0.57	3.93	0.56	3.53	0.76	2.15	0.30	2.29	0.33	<10	1.90	0.03	0.07	5.11	52.54	21.40	3.50	15566.00	1.60	0.70
BK13ES027	6.30	9.20	17.00	1.64	5.70	1.13	0.20	1.06	0.15	1.06	0.25	0.86	0.13	1.02	0.18	<10	1.30	0.02	0.09	5.74	44.05	93.21	15.20	3341.00	3.20	0.80
BK13ES028	34.30	42.30	88.20	10.55	38.70	7.98	1.51	7.12	1.02	6.45	1.21	3.37	0.49	3.23	0.47	39.00	1.10	0.02	0.02	131.53	69.47	4.72	89.60	639.00	44.00	12.50
BK13ES029	4.10	10.90	20.90	2.24	8.90	1.42	0.19	0.99	0.11	0.82	0.12	0.35	0.07	0.46	0.09	<10	2.40	0.05	0.03	32.78	2.83	20.91	250.50	100.00	11.80	0.30
BK13ES030	13.20	13.10	24.00	2.91	10.20	2.66	0.89	2.39	0.33	1.96	0.41	1.13	0.17	1.15	0.20	52.00	2.40	0.09	0.03	4.55	3.28	27.95	1202.10	92.00	60.50	10.60
BK13ES031	22.20	24.60	48.60	5.31	20.30	4.57	1.51	5.21	0.76	4.52	0.78	1.90	0.34	1.80	0.31	35.00	2.60	0.08	0.01	195.80	1721.54	2.58	30.40	112.00	34.40	7.30
BK13ES032	9.50	18.90	44.80	5.24	20.60	3.33	0.77	2.74	0.34	2.00	0.37	1.02	0.13	0.77	0.12	<10	1.40	0.04	0.05	61.22	365.72	28.37	8.40	347.00	2.20	0.60
BK13ES033	12.40	38.50	73.50	8.02	28.10	4.48	1.16	3.79	0.47	2.63	0.41	1.32	0.18	1.07	0.15	77.00	1.40	0.03	0.02	17.85	304.30	5.06	324.30	338.00	87.50	33.60
BK13ES034	9.20	29.60	61.10	6.92	26.50	5.20	0.84	3.39	0.41	2.22	0.36	0.95	0.17	1.12	0.19	<10	1.40	0.01	<0.01	201.08	92.31	246.71	36.70	7986.00	2.40	0.70
BK13ES035	7.40	13.60	24.40	2.90	12.50	1.78	0.32	1.46	0.18	1.17	0.24	0.50	0.11	0.62	0.11	<10	0.60	0.01	0.02	29.99	45.62	11.92	35.80	331.00	2.40	0.70
BK13ES036	6.90	59.20	117.20	16.45	79.80	9.25	1.58	3.58	0.39	1.92	0.29	0.80	0.14	0.69	0.11	<10	10.10	0.46	1.94	738.95	88.55	196.23	4.70	2411.00	1.30	0.30
BK13ES037	6.50	41.40	76.00	7.96	29.50	4.23	0.86	2.68	0.28	1.37	0.22	0.64	0.11	0.80	0.12	<10	4.90	0.04	0.62	9.56	94.56	45.24	2.10	1390.00	0.70	<0.1
BK13ES038	8.40	27.60	57.20	7.11	27.50	3.91	0.76	2.72	0.30	1.59	0.29	0.68	0.10	0.60	0.08	<10	2.10	0.04	0.11	64.12	78.60	14.41	4.60	1896.00	1.20	0.20
BK13ES039	8.10	24.50	45.50	5.28	20.40	3.30	0.48	2.28	0.27	1.54	0.26	0.74	0.11	0.66	0.11	<10	2.40	0.02	0.06	97.08	237.19	2.82	5.00	285.00	3.50	1.00
BK13ES040	11.60	26.70	52.90	6.07	22.20	3.52	0.53	2.74	0.34	2.13	0.38	0.93	0.17	0.97	0.16	<10	1.60	0.03	0.08	91.85	63.21	7.29	10.70	974.00	1.40	0.30

All major oxides are in wt. %

All other elements in ppm except Au, Pt, Pd which are in ppb

Appendix 5: Buckingham
whole-rock geochemistry

Sample	Y	La	Ce	Pr	Nd	Sm	Eu	Gd	Tb	Dy	Ho	Er	Tm	Yb	Lu	Ni	LOI	TOT/C	TOT/S	Mo	Cu	Pb	Zn	Ag	Ni	Co
BK13ES041	8.30	41.40	69.20	7.51	27.30	3.92	0.74	2.57	0.26	1.46	0.21	0.63	0.13	0.68	0.13	<10	2.30	0.02	0.04	98.22	8.35	243.30	47.90	753.00	3.20	0.80
BK13ES042	7.40	32.60	56.80	6.33	21.40	3.35	0.74	2.55	0.29	1.74	0.26	0.71	0.11	0.84	0.12	<10	2.40	0.10	0.04	150.89	115.06	29.83	12.80	3545.00	1.30	0.60
BK13ES043	10.30	23.20	47.20	5.35	18.90	3.29	0.79	2.52	0.33	1.53	0.29	0.69	0.13	0.67	0.11	<10	1.90	0.18	0.05	150.10	82.56	10.57	79.10	897.00	3.20	0.70
BK13ES044	4.50	9.20	17.60	1.94	8.00	1.24	0.28	1.06	0.15	0.74	0.13	0.48	0.06	0.40	0.07	<10	0.90	0.02	<0.01	57.87	29.79	1.41	28.10	157.00	7.60	0.60
BK13ES045	17.50	30.80	66.20	7.31	27.30	5.07	0.80	4.36	0.59	3.30	0.66	1.81	0.28	1.80	0.28	29.00	0.90	0.04	<0.01	14.19	264.82	3.86	339.90	173.00	33.50	2.70
BK13ES046	1.40	2.60	4.90	0.55	2.20	0.35	0.13	0.40	0.06	0.34	0.08	0.19	0.03	0.21	0.03	<10	0.40	0.13	<0.01	0.56	13.24	3.27	15.10	25.00	6.70	1.90
BK13ES047	4.90	5.70	13.30	1.70	6.70	1.31	0.35	1.22	0.17	0.96	0.18	0.49	0.07	0.60	0.08	<10	1.30	0.15	<0.01	1.43	41.78	10.53	15.60	134.00	7.80	2.10
BK13ES048	8.70	12.00	23.80	2.81	10.30	2.20	0.57	1.79	0.26	1.59	0.30	0.83	0.14	0.89	0.15	12.00	0.40	0.03	<0.01	3.77	255.61	6.23	20.90	644.00	11.30	3.10
BK13ES049	8.70	9.20	23.00	2.92	11.40	2.32	0.56	2.02	0.31	1.62	0.30	0.91	0.14	0.85	0.14	15.00	0.60	0.06	<0.01	0.49	15.76	9.40	16.00	56.00	13.00	1.80
BK13ES050	4.10	5.50	11.90	1.40	5.30	1.10	0.27	0.87	0.12	0.64	0.14	0.45	0.08	0.49	0.08	<10	1.10	0.05	0.02	2.17	60.91	6.36	14.80	196.00	6.10	1.80
BK13ES051	11.10	14.10	27.80	3.18	12.90	2.49	0.67	2.28	0.34	2.05	0.38	1.03	0.17	1.17	0.19	14.00	2.40	0.16	0.01	4.01	753.39	23.99	60.50	2058.00	17.00	7.00
BK13ES052	1.00	2.20	3.70	0.45	1.40	0.31	0.07	0.24	0.04	0.26	0.03	0.09	0.01	0.12	0.02	<10	0.60	0.08	0.05	2.98	95.32	24.45	23.80	1487.00	2.30	0.60
BK13ES053	8.90	6.70	17.60	2.57	11.10	2.07	0.54	1.87	0.28	1.38	0.30	0.93	0.14	1.06	0.15	<10	0.60	0.04	<0.01	0.79	14.10	4.31	4.80	72.00	2.00	0.30
BK13ES054	11.40	27.70	53.90	5.91	21.00	3.86	0.92	2.85	0.41	1.87	0.33	1.14	0.15	0.96	0.12	<10	1.00	0.03	0.01	3.41	115.65	8.66	32.10	289.00	3.40	1.90
BK13ES055	9.40	8.30	19.20	2.61	11.40	2.37	0.54	1.95	0.29	1.67	0.40	0.88	0.15	1.04	0.15	<10	0.50	0.03	<0.01	3.85	85.98	8.79	15.90	326.00	5.90	1.60
BK13ES056	32.70	109.10	200.80	23.04	78.80	13.50	2.23	10.05	1.38	6.80	1.20	3.52	0.49	2.96	0.43	23.00	3.80	0.02	0.02	8.94	325.73	4.43	11.70	1341.00	24.40	6.10
BK13ES057	29.50	36.40	75.20	8.15	32.60	5.50	0.93	4.90	0.75	4.37	0.90	2.66	0.40	2.48	0.35	<10	2.30	0.02	0.11	3.38	207.35	2.40	22.30	1136.00	10.90	2.80
BK13ES058	162.10	13.90	35.10	5.00	27.80	17.57	6.25	32.61	5.82	33.15	6.51	17.25	2.27	13.69	1.68	78.00	2.70	0.08	<0.01	0.42	1489.42	7.11	25.40	39.00	84.40	22.80
BK13ES059	15.10	28.00	57.00	6.16	23.40	3.90	0.62	2.91	0.42	2.67	0.55	1.50	0.26	1.65	0.25	<10	3.20	0.01	0.82	6.17	190.82	1.17	3.20	1316.00	8.40	7.40
BK13ES060	25.80	33.00	72.70	8.47	34.50	6.74	1.54	6.91	1.01	5.22	0.95	2.77	0.37	2.12	0.30	145.00	1.50	0.04	<0.01	67.24	204.30	3.78	713.60	989.00	148.60	24.60
BK13ES061	23.80	35.60	73.60	8.17	30.20	5.89	0.94	5.08	0.78	4.09	0.80	2.37	0.35	2.10	0.29	<10	1.00	0.03	<0.01	45.67	335.52	1.45	25.90	271.00	8.90	2.00
BK13ES062	11.50	27.30	52.30	5.73	22.10	3.98	0.74	3.23	0.40	2.19	0.43	1.16	0.19	1.14	0.17	<10	1.50	0.01	<0.01	50.73	67.60	2.30	4.00	925.00	2.50	0.60
BK13ES063	6.10	9.60	17.90	2.16	8.80	1.37	0.29	1.37	0.19	1.05	0.23	0.59	0.11	0.58	0.12	<10	1.10	0.02	<0.01	77.72	1522.14	35.32	34.20	2263.00	7.40	3.40
BK13PH100	7.50	18.00	33.80	3.86	14.70	2.43	0.45	1.81	0.26	1.50	0.25	0.77	0.13	0.82	0.14	11.00	1.10	0.04	<0.01	120.63	227.68	6.82	42.90	671.00	13.80	0.90
BK13PH101	12.40	27.70	54.30	5.84	22.00	3.58	0.58	2.90	0.39	2.11	0.43	1.34	0.20	1.44	0.22	<10	1.50	0.03	0.05	51.54	103.71	38.67	4.80	4466.00	1.80	0.50
BK13PH102	7.70	26.70	47.50	5.15	18.10	3.04	0.43	2.33	0.31	1.72	0.37	0.89	0.16	1.03	0.16	<10	1.80	0.01	0.14	66.99	253.79	10.68	2.50	5153.00	2.00	2.00
BK13PH103	17.60	37.80	66.70	7.11	27.30	4.49	1.06	3.77	0.55	3.29	0.65	1.99	0.29	1.81	0.28	<10	10.10	0.03	1.75	55.59	111.39	20.50	0.90	1160.00	0.80	0.10
BK13PH104	1.90	3.80	6.30	0.66	2.30	0.34	0.08	0.32	0.04	0.23	0.04	0.21	0.03	0.40	0.05	<10	7.90	0.02	5.90	1.04	759.62	7794.91	3116.00	>100000	4.30	5.10
BK13PH105	20.40	43.40	85.30	9.23	35.30	6.29	1.29	5.38	0.72	4.07	0.74	2.14	0.27	1.76	0.27	43.00	1.70	0.02	0.73	0.32	28.67	5.81	47.00	276.00	43.70	14.80
BK13PH106	4.50	11.60	21.50	2.38	7.60	1.27	0.16	1.10	0.15	0.90	0.13	0.45	0.08	0.59	0.10	<10	0.80	0.03	0.06	0.44	58.03	1.88	5.40	451.00	6.60	1.00
BK13PH107	11.20	26.20	56.40	6.46	25.00	4.35	0.78	2.86	0.37	2.32	0.45	1.31	0.25	1.61	0.26	<10	3.80	0.03	0.02	17.22	82.72	6.32	4.20	1167.00	1.60	0.40
BK13PH108	12.20	29.20	60.70	6.59	23.20	3.49	0.49	2.70	0.37	2.08	0.38	1.10	0.18	1.25	0.21	<10	1.60	0.02	0.11	5.06	24.80	8.88	4.10	650.00	1.40	0.30
BK13PH109	9.80	21.50	39.80	4.26	15.10	2.25	0.35	2.16	0.29	1.66	0.33	0.81	0.12	0.80	0.13	<10	1.70	0.04	0.13	31.97	59.48	33.93	12.40	3228.00	4.20	1.20
BK13PH110	13.90	16.50	31.90	3.92	14.90	2.93	0.91	2.85	0.41	2.33	0.46	1.27	0.20	1.18	0.19	12.00	2.70	0.02	0.01	1.58	1185.67	27.40	377.60	878.00	10.70	1.60
BK13PH111	8.10	17.70	33.30	3.76	13.90	2.39	0.54	2.10	0.28	1.44	0.30	0.80	0.12	0.83	0.11	12.00	1.10	0.02	<0.01	63.52	76.19	2.09	52.80	477.00	14.60	0.80

All major oxides are in wt. %

All other elements in ppm except Au, Pt, Pd which are in ppb

Appendix 5: Buckingham
whole-rock geochemistry

Sample	Mn	As	Au	Cd	Sb	Bi	Cr	B	Tl	Hg	Se	Te	Ge	In	Re	Be	Li	Pd	Pt
BK13ES001	263.00	3.50	3.40	0.22	0.20	0.22	81.60	1.00	0.39	<5	<0.1	0.15	0.30	0.06	<1	0.70	31.30	<10	<2
BK13ES002	55.00	28.90	7.10	0.02	42.12	0.21	12.00	1.00	0.08	18.00	0.10	0.11	<0.1	<0.02	<1	0.10	0.60	<10	<2
BK13ES003	38.00	11.10	2.00	0.45	1.43	0.15	9.20	2.00	0.22	11.00	0.40	0.07	<0.1	<0.02	23.00	0.20	3.90	<10	<2
BK13ES004	34.00	1.60	6.40	<0.01	0.12	0.06	7.40	1.00	0.05	<5	0.80	<0.02	<0.1	<0.02	2.00	0.10	1.50	<10	<2
BK13ES005	144.00	20.20	9.80	0.30	0.93	0.16	60.50	2.00	0.28	<5	<0.1	<0.02	0.20	0.03	<1	0.30	18.80	<10	<2
BK13ES006	196.00	15.50	6.30	0.74	0.94	0.26	84.90	<1	0.45	<5	<0.1	<0.02	0.20	0.04	<1	0.30	32.30	*	<2
BK13ES007	199.00	19.40	11.10	0.98	0.99	0.42	26.60	2.00	0.20	11.00	0.30	0.05	<0.1	<0.02	<1	0.50	23.00	<10	<2
BK13ES008	35.00	40.30	14.30	0.06	22.80	1.18	5.50	3.00	0.13	84.00	0.10	0.03	<0.1	0.10	<1	0.20	2.20	<10	<2
BK13ES009	32.00	273.80	49.30	0.72	27.47	4.66	6.40	4.00	0.11	153.00	2.30	0.45	<0.1	0.26	<1	0.30	2.60	*	<2
BK13ES010	52.00	105.40	18.60	0.10	4.87	0.10	20.40	5.00	0.04	43.00	3.90	0.11	<0.1	0.03	1.00	0.50	4.40	<10	3.00
BK13ES011	90.00	479.30	308.20	0.03	1.68	0.02	3.70	3.00	0.11	17.00	<0.1	<0.02	<0.1	<0.02	<1	0.40	5.80	<10	<2
BK13ES012	205.00	2.70	3.30	0.03	0.29	0.06	13.80	1.00	0.02	<5	<0.1	<0.02	<0.1	<0.02	<1	0.10	6.40	<10	<2
BK13ES013	377.00	2.50	1.70	0.03	0.21	0.03	12.50	1.00	<0.02	8.00	<0.1	<0.02	<0.1	<0.02	<1	<0.1	3.60	<10	<2
BK13ES014	258.00	2.70	2.50	0.09	0.90	0.07	18.00	2.00	0.06	10.00	0.40	<0.02	0.10	<0.02	<1	0.30	23.40	<10	<2
BK13ES015	101.00	67.90	1.90	0.05	3.72	0.11	9.70	2.00	0.03	13.00	0.20	0.05	<0.1	<0.02	<1	0.20	1.20	<10	<2
BK13ES016	758.00	186.50	25.60	0.40	12.30	0.21	8.40	6.00	0.07	11.00	0.20	0.18	<0.1	0.02	1.00	4.10	4.50	<10	<2
BK13ES017	35.00	9.90	28.20	0.11	5.50	0.58	7.40	2.00	0.09	7.00	0.10	0.16	<0.1	0.02	<1	0.10	1.10	<10	<2
BK13ES018	95.00	1.00	3.80	0.05	0.24	0.07	15.20	1.00	0.08	<5	<0.1	<0.02	<0.1	<0.02	<1	0.30	3.70	<10	<2
BK13ES019	78.00	47.50	3.70	0.50	1.45	0.07	28.30	2.00	0.63	8.00	<0.1	<0.02	<0.1	<0.02	<1	0.40	9.90	<10	<2
BK13ES020	168.00	7.90	5.70	0.16	1.56	0.18	30.00	2.00	0.53	<5	<0.1	0.08	<0.1	<0.02	1.00	1.80	20.30	<10	<2
BK13ES021	41.00	57.60	46.90	0.03	1.95	0.62	8.30	<1	0.06	<5	0.20	0.32	<0.1	<0.02	<1	0.10	1.20	<10	<2
BK13ES022	27.00	445.90	10.60	0.33	24.13	0.77	6.90	3.00	0.16	13.00	0.20	0.09	<0.1	<0.02	<1	<0.1	3.50	<10	<2
BK13ES023	160.00	11.70	5.40	0.03	2.97	0.09	40.80	3.00	0.36	7.00	0.10	0.04	<0.1	<0.02	10.00	1.30	30.80	<10	<2
BK13ES024	82.00	652.70	19.80	0.08	16.59	0.34	11.40	2.00	0.08	225.00	0.40	0.09	<0.1	<0.02	<1	0.50	1.10	<10	<2
BK13ES025	23.00	8996.80	451.50	0.43	210.18	0.19	8.30	1.00	0.13	331.00	2.10	0.11	<0.1	0.21	4.00	0.10	0.40	<10	<2
BK13ES026	36.00	4903.70	585.00	0.08	20.16	0.06	10.70	3.00	0.62	1725.00	0.80	0.08	<0.1	<0.02	3.00	0.30	1.50	<10	<2
BK13ES027	34.00	111.20	11.60	0.14	1.89	0.08	8.90	<1	0.05	94.00	0.40	<0.02	<0.1	0.04	2.00	0.20	3.30	<10	<2
BK13ES028	278.00	31.10	13.60	1.30	0.78	0.20	80.80	1.00	0.63	6.00	<0.1	0.15	0.20	0.04	<1	0.50	35.70	<10	<2
BK13ES029	24.00	72.50	17.60	0.80	17.02	0.02	8.00	2.00	0.07	20.00	<0.1	<0.02	<0.1	<0.02	39.00	0.40	0.90	<10	<2
BK13ES030	3136.00	27.70	3.60	0.17	0.81	0.08	44.60	2.00	0.06	24.00	<0.1	<0.02	<0.1	0.04	<1	0.80	18.10	<10	<2
BK13ES031	48.00	113.60	6.40	0.32	3.87	0.26	7.00	3.00	0.11	<5	0.10	<0.02	<0.1	<0.02	<1	0.30	9.50	<10	<2
BK13ES032	24.00	35.30	8.30	0.18	1.62	0.30	6.70	4.00	0.09	22.00	0.30	<0.02	<0.1	0.02	1.00	0.30	1.90	<10	<2
BK13ES033	115.00	79.50	5.50	9.21	3.07	0.21	4.70	4.00	0.29	20.00	<0.1	0.06	<0.1	<0.02	8.00	0.50	16.30	11.00	<2
BK13ES034	31.00	36.90	3.40	0.12	1.68	3.90	9.70	3.00	0.09	93.00	0.90	0.05	<0.1	0.04	<1	0.40	1.50	<10	<2
BK13ES035	37.00	8.00	<0.2	0.03	0.84	0.66	12.60	2.00	0.06	38.00	<0.1	0.03	<0.1	0.02	<1	<0.1	1.40	<10	<2
BK13ES036	21.00	1884.80	221.90	0.25	27.67	5.47	12.30	9.00	0.89	92.00	1.00	0.31	<0.1	0.20	<1	<0.1	25.80	<10	<2
BK13ES037	24.00	140.00	14.20	0.02	8.25	1.92	2.40	4.00	0.37	214.00	1.80	0.08	<0.1	0.18	<1	0.10	5.00	<10	<2
BK13ES038	27.00	14.50	2.00	<0.01	1.02	1.62	3.90	3.00	0.12	313.00	0.60	0.02	<0.1	0.03	<1	0.20	2.60	<10	<2
BK13ES039	26.00	15.60	2.10	0.07	1.36	0.50	5.10	3.00	0.08	51.00	0.40	<0.02	<0.1	<0.02	<1	<0.1	1.90	<10	<2
BK13ES040	18.00	11.50	2.20	0.04	0.60	0.50	4.00	2.00	0.05	7.00	0.30	<0.02	<0.1	0.02	<1	0.10	3.00	<10	<2

All major oxides are in wt. %

All other elements in ppm except Au, Pt, Pd which are in ppb

Appendix 5: Buckingham
whole-rock geochemistry

Sample	Mn	As	Au	Cd	Sb	Bi	Cr	B	Tl	Hg	Se	Te	Ge	In	Re	Be	Li	Pd	Pt
BK13ES041	26.00	69.90	24.70	0.90	7.96	1.35	2.20	3.00	0.09	15.00	0.60	0.10	<0.1	0.08	<1	0.30	1.60	<10	<2
BK13ES042	73.00	56.00	1.60	0.40	17.52	2.34	2.80	1.00	0.12	62.00	1.80	0.12	<0.1	0.09	<1	0.20	1.20	<10	<2
BK13ES043	56.00	12.20	15.70	0.43	1.42	0.48	3.40	3.00	0.06	36.00	0.20	0.03	<0.1	<0.02	<1	0.40	1.90	<10	<2
BK13ES044	65.00	4.30	<0.2	1.46	1.19	0.16	6.80	<1	0.04	5.00	<0.1	0.02	<0.1	<0.02	<1	0.30	2.60	<10	<2
BK13ES045	131.00	46.20	<0.2	2.14	7.69	1.10	24.30	2.00	0.14	10.00	<0.1	0.03	<0.1	0.03	<1	0.30	11.40	<10	<2
BK13ES046	136.00	3.10	<0.2	0.01	0.18	0.07	14.00	<1	<0.02	15.00	<0.1	0.04	<0.1	<0.02	<1	<0.1	3.10	<10	<2
BK13ES047	247.00	2.40	2.60	0.19	0.16	0.37	34.60	<1	<0.02	10.00	0.30	<0.02	0.30	0.03	<1	0.30	6.30	<10	<2
BK13ES048	142.00	1.20	24.40	0.15	0.12	0.07	37.80	1.00	0.05	<5	<0.1	<0.02	0.10	0.03	<1	0.20	6.30	<10	<2
BK13ES049	211.00	3.40	<0.2	0.17	0.16	0.04	50.00	<1	<0.02	6.00	<0.1	<0.02	0.20	<0.02	<1	0.30	2.20	<10	<2
BK13ES050	326.00	15.30	7.70	0.28	0.27	0.25	20.40	2.00	0.04	7.00	<0.1	0.03	0.20	0.03	<1	0.40	4.90	<10	<2
BK13ES051	159.00	29.80	26.90	1.43	0.12	1.33	66.70	1.00	<0.02	8.00	3.00	0.08	<0.1	0.09	57.00	0.60	14.00	<10	<2
BK13ES052	134.00	177.10	17.10	0.88	1.92	0.28	4.90	2.00	0.02	12.00	0.20	0.04	<0.1	0.03	<1	0.20	0.60	<10	<2
BK13ES053	48.00	0.70	2.60	0.07	0.06	0.06	11.20	<1	<0.02	<5	<0.1	<0.02	<0.1	<0.02	<1	0.10	2.00	<10	<2
BK13ES054	128.00	2.90	5.90	0.11	0.15	0.13	3.90	1.00	<0.02	<5	<0.1	0.02	0.10	<0.02	2.00	0.20	7.20	<10	<2
BK13ES055	114.00	2.20	3.40	0.13	0.23	0.13	19.10	1.00	<0.02	<5	<0.1	<0.02	0.10	<0.02	<1	<0.1	2.50	<10	<2
BK13ES056	53.00	14.10	13.60	0.15	1.09	0.93	23.50	1.00	0.51	8.00	0.30	0.24	<0.1	<0.02	<1	1.00	11.50	<10	<2
BK13ES057	36.00	27.10	7.70	0.16	0.80	0.41	21.90	2.00	0.34	7.00	1.00	0.10	<0.1	<0.02	10.00	0.20	4.30	<10	<2
BK13ES058	58.00	17.50	1.90	0.16	3.39	2.78	77.00	5.00	0.13	14.00	<0.1	0.21	<0.1	<0.02	3.00	0.20	8.00	<10	<2
BK13ES059	19.00	10.80	5.50	0.06	1.19	2.03	7.40	<1	0.11	<5	3.00	1.20	<0.1	<0.02	26.00	0.30	1.10	<10	<2
BK13ES060	61.00	41.20	4.40	4.93	6.07	2.62	21.60	2.00	0.23	<5	<0.1	0.38	<0.1	2.08	8.00	0.30	6.90	<10	<2
BK13ES061	67.00	4.80	7.30	0.15	0.31	2.33	37.20	2.00	0.27	<5	<0.1	0.03	0.10	0.07	<1	0.20	5.70	<10	<2
BK13ES062	27.00	17.20	4.10	0.07	5.59	0.53	7.20	2.00	0.05	<5	1.70	<0.02	<0.1	<0.02	<1	0.10	0.80	<10	<2
BK13ES063	49.00	33.10	19.20	1.78	5.81	0.22	23.00	2.00	0.07	<5	0.20	<0.02	<0.1	0.07	<1	0.10	4.10	<10	<2
BK13PH100	73.00	5.10	5.70	0.21	0.81	1.10	22.30	2.00	0.04	<5	0.30	0.10	<0.1	0.02	<1	0.20	7.30	13.00	<2
BK13PH101	35.00	67.90	27.50	0.14	38.21	1.53	9.80	3.00	0.11	27.00	0.90	0.16	<0.1	0.06	<1	<0.1	1.30	<10	<2
BK13PH102	24.00	20.40	8.60	0.08	63.76	0.58	5.90	2.00	0.11	<5	1.10	0.07	<0.1	0.03	<1	<0.1	1.40	<10	<2
BK13PH103	12.00	177.50	147.40	0.05	24.00	3.62	45.90	7.00	1.05	110.00	2.00	0.29	<0.1	0.04	<1	0.30	2.80	<10	<2
BK13PH104	99.00	>10000.0	3495.60	36.83	1520.58	11.79	3.70	2.00	1.81	2874.00	24.40	1.91	<0.1	0.64	<1	<0.1	1.10	<10	<2
BK13PH105	158.00	15.10	1.70	0.03	1.78	0.44	65.00	<1	1.15	10.00	<0.1	0.08	0.20	<0.02	<1	0.30	23.60	<10	<2
BK13PH106	42.00	7.30	10.70	0.02	1.61	0.36	11.80	2.00	0.07	<5	0.50	0.12	<0.1	<0.02	<1	0.20	4.50	<10	<2
BK13PH107	43.00	11.20	9.30	0.01	8.65	0.35	21.60	6.00	0.29	47.00	1.00	0.07	<0.1	<0.02	<1	0.40	15.60	<10	<2
BK13PH108	34.00	154.00	10.80	0.14	5.00	0.69	7.50	2.00	0.11	7.00	0.40	0.03	<0.1	<0.02	<1	<0.1	1.80	<10	<2
BK13PH109	26.00	159.90	9.90	0.23	4.23	0.81	5.90	<1	0.06	10.00	1.50	0.06	<0.1	<0.02	<1	0.20	1.50	<10	<2
BK13PH110	388.00	58.70	188.80	2.57	1.92	0.41	57.20	3.00	0.02	8.00	<0.1	0.47	<0.1	0.07	<1	0.80	16.40	<10	<2
BK13PH111	82.00	9.20	5.60	2.22	0.73	0.11	22.50	1.00	0.06	<5	<0.1	<0.02	<0.1	<0.02	<1	0.30	6.90	<10	<2

All major oxides are in wt. %

All other elements in ppm except Au, Pt, Pd which are in ppb

Appendix 6: White Pine
quartz mineral chemistry by LA-ICP-MS

Quartz sample		Distance*	Li7	Na23	Mg24	Al27	Si29	P31	K39	Ca43	Ti47	Ti49	V51	Cr53	Mn55	Fe57	Cu63	Cu65
Sample	type	(m)																
WP46-C1-S1	Vein Quartz	372.6	3.1154	2.0599	0.5250	72.0237	467500	18.5576	1.6842	-89.2127	57.1205	54.7686	0.0170	0.1784	0.1415	3.2537	0.0858	0.1271
WP46-C1-S2	Vein Quartz	372.6	4.8916	-0.9230	0.1792	65.9265	467500	17.3326	0.9393	37.6884	58.3216	57.6206	0.0045	0.1527	0.0629	1.6723	0.0667	-0.0181
WP46-C1-S3	Vein Quartz	372.6	2.2021	0.3262	0.1708	49.7118	467500	15.7042	-0.0494	13.5034	28.9256	28.6379	-0.0005	-0.0579	0.0688	-0.1732	0.0613	0.0314
WP46-C1-S4	Vein Quartz	372.6	3.7566	2.4629	0.2400	92.6102	467500	16.6633	50.5981	6.8702	50.8814	52.3266	0.0485	0.1018	0.0946	0.6884	0.0101	0.0235
WP46-C1-S5	Vein Quartz	372.6	1.8285	3.0382	0.1551	53.1463	467500	14.8722	14.6433	14.1790	79.2946	84.5310	0.0601	0.1696	0.0705	1.2121	0.0107	0.0548
WP46-C1-S6	Vein Quartz	372.6	6.1701	0.2956	0.2602	89.5185	467500	11.0229	9.8993	20.4426	60.5093	61.8367	-0.0011	0.0399	0.1010	1.2315	0.1556	0.1383
WP46-C1-S7	Vein Quartz	372.6	1.3048	1.3550	0.4967	54.1255	467500	16.2912	6.8941	-29.6221	42.6259	44.9027	-0.0030	-0.0554	0.1071	6.4405	0.1176	0.1795
WP46-C1-S8	Vein Quartz	372.6	2.0608	1.7384	0.3583	61.6718	467500	15.8140	29.3084	-5.9562	72.8498	71.5882	0.0697	0.0995	0.0708	9.3704	0.8023	1.0141
WP46-C1-S9	Vein Quartz	372.6	2.3646	16.2829	0.5572	63.1446	467500	18.6942	6.4829	-22.6365	52.1995	52.5474	0.0147	-0.0800	0.1083	10.2175	0.1114	0.1409
WP46-C1-S10	Vein Quartz	372.6	2.4556	5.7868	0.2535	75.2088	467500	15.1726	20.1004	6.5558	54.3998	54.9705	0.0107	0.0087	0.1299	1.2398	0.2646	0.1187
WP46-C1-S11	Vein Quartz	372.6	1.4860	0.9336	0.4081	41.6578	467500	19.1207	3.3980	49.5048	33.9851	34.2336	0.0130	0.0057	0.0480	3.2733	0.1604	0.2599
WP46-C1-S12	Vein Quartz	372.6	4.1229	2.4318	0.2358	66.0081	467500	17.6931	0.7698	1.1358	47.5030	47.2990	-0.0031	0.0547	0.0559	-0.0509	0.0529	-0.0346
WP46-C1-S13	Vein Quartz	372.6	4.0699	1.5251	0.2241	66.3019	467500	12.5427	-0.1867	13.6762	37.7418	39.3811	0.0079	-0.1411	0.0472	0.1776	0.0121	0.0460
WP46-C1-S14	Vein Quartz	372.6	3.2643	-2.2318	0.4567	69.3980	467500	18.6137	6.7299	65.2334	42.1768	42.9820	0.0154	0.0126	0.0796	1.9228	0.0861	0.1911
WP46-C1-S15	Vein Quartz	372.6	3.2805	-0.8833	0.2192	67.8385	467500	10.4731	2.2864	-1.8281	44.1960	45.2642	-0.0017	0.1340	0.0943	0.6599	0.0007	-0.0267
WP03-C1-S1	Vein Quartz	1546.4	0.6944	34.8881	0.0136	30.5462	467500	10.6962	5.1076	30.3747	4.9760	3.5033	-0.0085	0.0022	0.0459	0.2017	0.1735	0.0755
WP03-C1-S2	Vein Quartz	1546.4	5.7772	23.5194	0.1002	176.5891	467500	15.9110	22.6278	0.7037	12.5177	12.2742	0.0005	0.0287	0.3737	0.9958	0.7343	0.7336
WP03-C1-S3	Vein Quartz	1546.4	7.4317	12.8452	5.5103	165.8108	467500	16.4198	10.9945	-1.5076	13.0521	12.9839	0.0216	-0.0601	0.4835	21.9570	1.8341	1.8436
WP03-C1-S4	Vein Quartz	1546.4	1.5610	9.7036	0.2662	57.7846	467500	15.2574	5.9142	7.7863	7.6269	6.8088	0.0054	0.0561	0.0943	6.6007	0.3651	0.4366
WP03-C1-S5	Vein Quartz	1546.4	0.1652	11.9198	0.1520	10.5452	467500	15.6737	3.1240	23.4685	1.4101	1.2990	0.0141	0.0200	0.0404	4.5449	0.1579	0.1954
WP03-C2-S1	Vein Quartz	1546.4	4.0597	4.9918	-0.0210	101.0432	467500	14.8220	1.6242	23.1133	9.2369	8.6647	0.0119	0.0549	0.0842	2.2000	0.0289	-0.0001
WP03-C2-S2	Vein Quartz	1546.4	4.2720	3.5510	0.1344	76.2405	467500	15.6050	1.9228	-12.7003	7.8064	8.7164	0.0069	-0.0877	0.0869	0.1727	0.1908	0.2416
WP03-C2-S3	Vein Quartz	1546.4	1.4292	6.3474	0.0270	47.6902	467500	13.0912	1.6605	70.7622	5.9501	6.4924	-0.0014	-0.0771	-0.0007	0.8498	0.0024	0.0586
WP03-C2-S4	Vein Quartz	1546.4	1.7158	19.7295	0.1335	61.2656	467500	13.2488	2.2019	16.8435	8.3020	8.1437	-0.0097	-0.0926	0.1199	1.5480	0.1650	0.1472
WP03-C2-S5	Vein Quartz	1546.4	3.0882	10.7137	0.0567	81.4919	467500	18.2099	1.7617	3.7087	9.3486	7.8530	-0.0069	0.0627	0.1492	9.7919	0.1313	0.1119
WP13-C3-S1	Vein Quartz	1553.6	5.0971	-1.7373	0.0344	53.0136	467500	19.4536	0.0925	74.2631	35.4817	37.0070	-0.0121	0.1202	0.0373	-0.1924	0.0320	-0.0106
WP13-C3-S2	Vein Quartz	1553.6	5.7303	1.0240	0.0290	57.1169	467500	20.2493	-0.4549	23.1350	33.4397	33.5798	0.0078	0.0388	0.0351	-0.8015	-0.0100	0.0856
WP13-C3-S3	Vein Quartz	1553.6	4.3176	-0.1257	0.0674	47.9505	467500	23.1360	-0.4864	-47.5928	33.9522	34.8291	-0.0127	-0.0008	0.0347	0.3324	-0.0906	0.0324
WP13-C3-S4	Vein Quartz	1553.6	5.0482	6.9632	0.1275	62.8982	467500	18.9618	2.0194	-19.1965	37.6690	39.5704	0.0129	0.0492	0.0448	0.5272	0.0820	0.0266
WP13-C5-S1	Vein Quartz	1553.6	4.0169	2.0964	0.4885	48.7725	467500	18.7075	5.1195	-32.7563	42.9681	45.3654	-0.0116	-0.0592	0.0268	0.4709	0.0915	1.0454
WP13-C5-S2	Vein Quartz	1553.6	4.6028	4.4316	0.2672	73.1302	467500	17.1725	3.5310	-46.6123	44.8418	47.2264	0.0054	-0.0053	-0.0264	1.0174	0.0562	0.0278
WP13-C5-S3	Vein Quartz	1553.6	3.3443	1.4361	2.5555	47.0626	467500	21.2817	1.0352	28.7210	45.7615	46.3027	-0.0090	-0.0742	0.0633	0.6801	0.0755	0.0818
WP13-C5-S4	Vein Quartz	1553.6	2.3535	-2.8053	0.3458	31.8020	467500	18.7646	0.8515	17.0753	34.2770	34.4151	0.0017	-0.0412	0.0239	1.3162	0.0413	0.0842
WP22-C4-S1	Vein Quartz	2588.2	1.8600	-0.3018	0.0222	29.9000	467500	19.6446	-0.5035	43.7598	1.0178	0.8855	0.0052	-0.1119	0.0249	-1.8305	0.0079	-0.0162
WP22-C4-S2	Vein Quartz	2588.2	0.5366	0.2764	0.0310	19.0434	467500	17.4337	-0.7301	227.4427	1.5089	0.4858	0.0027	-0.0735	0.0486	5.0660	0.0651	0.2622
WP22-C4-S3	Vein Quartz	2588.2	0.5548	15.6521	0.0361	24.4276	467500	18.8429	5.3493	35.1612	1.3364	1.1277	0.0051	-0.0478	0.0912	7.6475	0.3301	0.3468
WP22-C4-S4	Vein Quartz	2588.2	0.8813	-0.5892	0.0509	26.8663	467500	16.6780	0.3945	27.0591	1.8591	1.3468	0.0143	-0.1994	0.0236	21.8891	0.2960	0.2778
WP22-C4-S5	Vein Quartz	2588.2	0.6348	31.9826	0.2016	31.3396	467500	14.8124	7.2340	43.4509	1.4480	1.3163	-0.0006	0.0175	0.4451	22.2118	0.7688	0.5572
WP06-C2-S1	Vein Quartz	1429.0	5.6995	1.0012	0.1680	67.9607	467500	15.5170	4.3078	45.5792	52.7383	54.5263	0.0045	-0.0281	0.0987	0.7276	0.0228	0.0752
WP06-C2-S2	Vein Quartz	1429.0	4.8636	-2.4774	0.0753	59.8479	467500	13.6432	3.1902	10.9984	48.7030	48.0002	0.0060	-0.0407	0.1144	0.9605	0.0236	0.0063
WP06-C2-S3	Vein Quartz	1429.0	5.1525	-0.1475	0.1070	61.0808	467500	12.1179	5.5343	-14.8315	46.9053	48.7270	-0.0001	0.0609	0.1073	-0.1165	0.0158	0.0110
WP06-C2-S4	Vein Quartz	1429.0	5.2315	-3.3171	0.0968	59.1548	467500	11.9592	3.8459	-12.1156	37.6854	39.5673	-0.0012	-0.0148	0.0838	0.5657	0.0203	-0.0564
WP06-C3-S2	Vein Quartz	1429.0	2.3771	115.3884	0.4570	101.1784	467500	17.1659	19.1558	111.9366	25.7669	26.6237	0.0470	0.1013	0.4509	2.7998	0.1104	0.0034
WP06-C3-S3	Vein Quartz	1429.0	4.1601	7.9020	0.1424	66.0651	467500	15.0226	6.5152	-37.4975	47.3408	48.8977	0.0115	0.1437	0.1205	7.2415	0.1898	0.1398
WP06-C3-S4	Vein Quartz	1429.0	3.2007	-1.0263	0.1547	40.9591	467500	14.7306	2.2523	14.1203	43.1050	43.0409	-0.0117	0.1131	0.0796	0.2779	-0.0095	0.0348
WP53-C1-S1	Vein Quartz	548.8	1.4462	36.4365	0.1465	69.1227	467500	16.2906	14.7438	45.5054	44.3565	45.0636	-0.0032	0.1542	0.1461	-0.4923	0.5633	0.4905
WP53-C1-S2	Vein Quartz	548.8	1.0868	130.2296	0.2918	79.4795	467500	17.8983	29.4434	-5.1816	43.8709	42.9721	0.0056	-0.0562	0.2335	1.9683	0.1035	0.0663

* distance from center of deposit

** All elements in ppm except Au which is in ppb

Appendix 6: White Pine
quartz mineral chemistry by LA-ICP-MS

Quartz sample		Distance*	Li7	Na23	Mg24	Al27	Si29	P31	K39	Ca43	Ti47	Ti49	V51	Cr53	Mn55	Fe57	Cu63	Cu65
Sample	type	(m)																
WP53-C1-S3	Vein Quartz	548.8	3.3134	1.5261	0.1832	81.0627	467500	19.0034	8.3064	-18.1628	58.9941	58.9889	-0.0008	0.0531	0.0948	0.4756	0.0631	0.0803
WP53-C1-S4	Vein Quartz	548.8	1.8404	17.2615	0.1469	75.5037	467500	15.1161	13.0535	-21.3665	58.9071	58.1485	-0.0003	0.1106	0.1197	-0.0368	0.2786	0.1597
WP53-C1-S5	Vein Quartz	548.8	0.8511	14.3561	0.1379	28.1060	467500	17.1006	1.5359	-17.5828	17.2993	15.9160	-0.0025	-0.0093	0.0366	0.3511	0.2335	0.2520
WP53-C2-S1	Vein Quartz	548.8	1.3715	10.8724	0.2559	47.2035	467500	15.8905	3.5202	-6.2358	41.3748	40.0242	0.0153	0.1553	1.8107	22.6406	1.5866	1.5474
WP53-C2-S2	Vein Quartz	548.8	1.4315	16.8159	0.1861	39.1862	467500	16.2515	3.8914	-32.5892	39.0673	37.3485	-0.0045	0.0051	0.1194	2.3408	0.0856	0.1747
WP53-C2-S3	Vein Quartz	548.8	0.6940	35.5912	0.3602	116.3973	467500	16.0448	32.0538	8.4027	68.3986	66.3955	-0.0051	0.0801	0.2893	2.2513	0.3183	0.3324
WP53-C2-S4	Vein Quartz	548.8	1.7610	8.0954	0.2666	66.0219	467500	14.8779	11.1226	-30.4262	51.9605	52.3848	0.0024	-0.1381	0.1608	1.3636	0.0786	0.0468
WP53-C2-S5	Vein Quartz	548.8	0.7916	38.9326	0.7956	65.7334	467500	17.0564	14.4717	31.7626	26.6561	28.2921	0.0056	-0.0071	1.4256	7.0287	1.8921	2.1374
WP05-C1-S1	Vein Quartz	1429.0	3.2996	-0.1922	0.0667	53.6164	467500	13.7199	1.2049	21.1752	51.3988	52.9019	0.0002	-0.0008	0.1239	2.8214	0.0129	0.0059
WP05-C1-S2	Vein Quartz	1429.0	1.2681	22.0080	0.0636	34.3777	467500	13.8926	2.4895	-40.0076	42.6062	41.9634	0.0034	0.0931	0.0097	0.1487	1.1760	1.3207
WP05-C1-S3	Vein Quartz	1429.0	2.0219	1.5768	0.2312	42.1338	467500	15.3694	2.6080	26.5853	47.8203	50.3390	-0.0014	-0.0472	0.0655	0.0397	0.0739	0.0444
WP05-C1-S4	Vein Quartz	1429.0	3.2939	-0.6730	0.1648	46.8234	467500	15.1169	0.4434	-23.7082	59.1196	58.9949	-0.0130	0.1381	0.0706	-0.3509	0.0397	0.0393
WP05-C2-S1	Vein Quartz	1429.0	1.0331	0.7886	0.3402	26.7528	467500	17.8465	2.0421	-17.3886	38.1949	36.2959	0.0109	0.0277	0.0752	-0.0489	0.7079	0.8559
WP05-C2-S2	Vein Quartz	1429.0	0.8433	8.1016	0.1222	27.6767	467500	14.4856	2.7493	-46.9154	16.9097	18.2047	-0.0024	-0.1702	0.1303	-0.0448	1.5730	1.9553
WP05-C2-S3	Vein Quartz	1429.0	1.1188	-0.4103	0.4570	25.4485	467500	16.7860	-0.1839	15.9288	43.2385	41.6062	-0.0012	-0.1389	0.0123	0.4700	0.4159	0.5087
WP05-C2-S4	Vein Quartz	1429.0	2.2858	-0.3917	0.3945	39.2062	467500	16.3038	1.4956	28.0849	36.1199	35.6120	0.0018	-0.0810	0.0518	0.7866	0.0273	0.0516
WP05-C2-S5	Vein Quartz	1429.0	2.0071	0.2918	0.2861	42.4110	467500	14.9449	2.8678	3.7018	47.0650	47.1100	0.0033	0.0830	0.0401	0.7656	0.0069	0.0320
WP05-C3-S1	Vein Quartz	1429.0	1.9632	78.5831	0.3046	57.3254	467500	13.0492	7.4141	10.9514	1.4771	1.3245	-0.0029	-0.0774	0.0921	3.0391	0.0872	0.1422
WP05-C3-S2	Vein Quartz	1429.0	4.8218	3.3991	0.0424	88.5064	467500	14.4805	7.5679	-2.9872	2.9069	2.0190	0.0070	-0.1343	0.0885	0.3029	0.3877	0.3686
WP05-C3-S3	Vein Quartz	1429.0	1.0542	1.6836	0.1265	31.5224	467500	16.2345	0.3270	23.0936	0.8640	3.2282	0.0189	-0.0212	0.2048	-1.3796	0.0664	0.0322
WP05-C3-S4	Vein Quartz	1429.0	2.9826	19.5620	0.3854	68.3526	467500	12.5348	6.6570	22.6605	1.7252	1.3061	-0.0056	0.0418	0.0990	-0.4323	3.1624	3.4634
WP64-C1-S1	Vein Quartz	704.8	1.3986	5.1148	0.3400	32.2196	467500	21.3326	1.1525	30.4308	1.2228	0.8229	0.0104	0.0403	0.0139	7.2658	0.2037	0.2310
WP64-C1-S2	Vein Quartz	704.8	3.0184	2.7728	0.4207	50.2778	467500	23.5357	5.5594	3.0119	1.9877	1.3247	-0.0049	0.0857	0.0543	6.9185	0.2175	0.2021
WP64-C1-S3	Vein Quartz	704.8	3.0668	9.1989	0.3489	41.7483	467500	19.6418	5.2134	-22.5627	1.9490	0.6303	0.0042	-0.2399	0.1155	8.3680	0.3117	0.3917
WP64-C1-S4	Vein Quartz	704.8	5.3096	0.5542	1.8790	81.9450	467500	19.0216	22.1821	16.8880	2.6419	1.8900	0.0277	-0.0826	0.2167	3.3595	0.0738	0.0945
WP64-C2-S1	Vein Quartz	704.8	3.8935	18.4186	5.8297	145.3918	467500	23.4404	67.8533	-89.5584	2.9816	2.0585	0.1553	-0.1051	0.5388	34.1013	3.4250	2.2101
WP64-C2-S2	Vein Quartz	704.8	3.7864	-2.4020	8.4681	163.6552	467500	23.0507	68.3221	35.4605	4.3679	4.5019	0.1715	-0.1277	0.5810	5.4413	0.1442	0.0967
WP64-C2-S4	Vein Quartz	704.8	7.8886	46.3944	2.2866	177.6044	467500	20.4313	49.4537	10.6126	2.6946	2.2319	0.0383	0.2008	0.7877	3.0408	1.6821	1.5037
WP64-C3-S1	Vein Quartz	704.8	1.6925	-0.1181	-0.0053	17.3653	467500	21.1652	-0.2176	-14.3117	4.2856	3.1302	0.0067	0.0556	0.0326	0.7621	0.1144	0.1037
WP64-C3-S2	Vein Quartz	704.8	5.6170	32.6204	1.7700	121.1922	467500	19.1163	28.6137	-49.5476	1.9488	1.8611	0.0260	-0.1208	0.3133	34.4749	6.9290	7.9028
WP64-C3-S3	Vein Quartz	704.8	4.7946	4.9304	0.8909	73.7293	467500	25.6488	7.9745	-65.2207	1.9736	1.3797	0.0132	-0.2510	0.4423	114.4430	5.0690	5.3157
WP52-C3-S1	Vein Quartz	785.5	1.9229	-3.8210	0.2225	85.1414	467500	14.8576	14.2923	1.8744	57.9681	58.7299	-0.0022	0.0594	0.2045	1.2761	0.0006	-0.0177
WP52-C3-S2	Vein Quartz	785.5	1.2298	-0.2208	0.1568	49.5862	467500	12.5845	1.9359	6.2361	50.8284	50.9632	-0.0039	-0.0399	0.0689	0.5794	0.0371	0.0040
WP52-C3-S3	Vein Quartz	785.5	0.4682	23.1602	0.0990	56.5414	467500	14.9681	1.9077	40.5997	67.9348	69.0671	0.0231	0.0430	0.0987	26.4904	0.1993	0.1536
WP52-C3-S4	Vein Quartz	785.5	1.0987	-2.2450	0.1825	60.0011	467500	11.5208	6.4669	33.0540	75.4399	71.1609	-0.0014	-0.1112	0.1942	5.8774	0.0108	0.0333
WP65-C2-S3	Vein Quartz	609.4	4.0334	68.5843	8.6486	161.3174	467500	15.3013	91.1028	82.5976	9.8075	10.7194	0.0644	0.1068	0.0890	53.8280	0.2698	0.2434
WP65-C2-S4	Vein Quartz	609.4	6.5126	0.9475	0.8971	65.8455	467500	13.5194	3.8082	38.2062	10.8249	11.3567	0.0043	0.1396	0.0649	166.4358	0.0969	0.0668
WP65-C3-S1	Vein Quartz	609.4	8.5866	-5.0080	0.3441	88.1919	467500	11.7650	2.9023	16.6396	38.7910	37.0481	-0.0035	0.0521	0.1149	1.1281	-0.0023	0.0378
WP65-C3-S2	Vein Quartz	609.4	7.6891	-2.3436	0.5447	71.9938	467500	13.2345	1.4935	18.7495	32.7829	32.8671	0.0043	0.0368	0.1340	2.9781	0.5019	0.4782
WP65-C3-S3	Vein Quartz	609.4	7.8231	2.2547	0.3204	75.7369	467500	14.4187	0.9135	-4.5555	33.6633	35.1075	0.0090	0.0938	0.0898	1.4042	0.2222	0.1813
WP65-C3-S4	Vein Quartz	609.4	9.5140	-2.0352	0.2550	107.8307	467500	13.3240	31.5642	25.6243	34.2012	34.9851	-0.0028	-0.0237	0.1069	0.9806	0.0047	0.0029
WP65-C4-S1	Vein Quartz	609.4	5.4951	-2.6274	0.9078	58.0634	467500	15.6591	5.4531	-6.4331	34.9436	34.9567	-0.0085	0.1118	0.1837	1.9735	0.7190	0.7385
WP65-C4-S2	Vein Quartz	609.4	5.4104	-2.1140	0.1675	50.8094	467500	12.3474	4.2616	-22.0446	33.2326	34.2354	0.0071	0.0006	0.0543	0.9066	0.1347	-0.0136
WP65-C4-S3	Vein Quartz	609.4	4.5398	-1.9293	0.0822	43.7618	467500	15.5716	-1.5463	10.8689	31.6008	31.3358	0.0186	-0.0497	0.0343	-0.0661	0.0211	0.0215
WP65-C4-S4	Vein Quartz	609.4	2.7467	5.4588	0.2945	38.0814	467500	15.6379	3.0674	-98.1023	28.4302	26.1470	0.0656	-0.0058	0.0118	12.0587	0.4867	0.4456
WP23-C5-S2	Vein Quartz	1688.3	10.2880	-1.5453	0.9349	142.4603	467500	13.1627	22.9073	51.2308	17.6323	16.9706	0.0088	0.0483	0.2953	12.7775	0.1376	0.1232
WP07-C1-S3	Vein Quartz	1360.2	2.0760	13.8607	1.2305	58.1231	467500	23.4329	3.5707	71.5755	28.6230	26.7927	0.0196	-0.0228	0.1438	8.1781	0.2898	0.3742

* distance from center of deposit

** All elements in ppm except Au which is in ppb

Appendix 6: White Pine
quartz mineral chemistry by LA-ICP-MS

Quartz sample		Distance*	Li7	Na23	Mg24	Al27	Si29	P31	K39	Ca43	Ti47	Ti49	V51	Cr53	Mn55	Fe57	Cu63	Cu65
Sample	type	(m)																
WP07-C1-S4	Vein Quartz	1360.2	1.2454	4.7447	0.2476	36.8561	467500	24.1052	1.9436	10.6374	25.7599	27.2127	0.0042	-0.1532	0.1097	10.7258	0.3793	0.3981
WP07-C2-S1	Vein Quartz	1360.2	5.4221	-0.8085	0.1480	60.5973	467500	19.8979	3.7076	9.1858	45.4163	43.7944	0.0017	0.1472	0.1284	0.3621	0.1455	0.1075
WP07-C2-S2	Vein Quartz	1360.2	5.4182	-0.1710	0.2047	66.3947	467500	19.5307	6.6395	-17.6477	45.6034	42.7737	-0.0004	-0.0169	0.0839	0.8538	0.0022	-0.0572
WP07-C2-S3	Vein Quartz	1360.2	4.0398	7.2271	0.4896	84.1581	467500	18.8521	19.9741	-63.2891	56.3828	54.1424	0.0049	-0.1523	0.2782	2.0316	0.3020	0.2391
WP07-C4-S1	Vein Quartz	1360.2	3.9592	1.1113	-0.0332	53.4597	467500	24.9876	6.3141	-46.9022	33.6519	35.2235	-0.0125	0.0460	0.1571	3.0844	0.0308	0.0899
WP07-C4-S2	Vein Quartz	1360.2	4.9892	6.3377	0.1488	56.8122	467500	17.2379	5.2514	26.2825	42.3702	42.3864	0.0109	-0.0248	0.1004	2.1431	0.1398	0.1136
WP07-C4-S3	Vein Quartz	1360.2	4.3613	1.5457	0.1097	49.4492	467500	18.1547	3.7701	19.5401	47.2628	47.6713	0.0029	-0.0230	0.0949	0.4794	0.1471	0.1364
WP07-C4-S4	Vein Quartz	1360.2	4.8850	1.2439	0.1393	52.1974	467500	16.6785	4.0033	-8.2769	42.7890	42.2632	0.0036	0.0969	0.1083	1.2002	0.0749	0.1206
WP07-C1-S1	Vein Quartz	1360.2	2.6066	54.6825	0.6480	127.0639	467500	125.1417	6.5624	58.5120	36.0545	36.2460	0.0169	0.1469	0.1091	621.9281	2.2551	2.5815
WP07-C1-S3	Vein Quartz	1360.2	2.0760	13.8607	1.2305	58.1231	467500	23.4329	3.5707	71.5755	28.6230	26.7927	0.0196	-0.0228	0.1438	8.1781	0.2898	0.3742
WP07-C1-S4	Vein Quartz	1360.2	1.3187	5.3732	1.4167	38.7572	467500	23.5831	2.2099	11.5052	29.4728	25.5740	0.0060	-0.0966	0.1197	55.8379	1.4076	1.3329
WP07-C2-S1	Vein Quartz	1360.2	5.6103	-0.6459	0.1779	61.4003	467500	19.9059	4.4382	7.7899	44.2056	43.9733	0.0113	0.1838	0.1613	0.8100	0.1584	0.2392
WP07-C2-S2	Vein Quartz	1360.2	5.3950	-0.3353	0.2430	67.8380	467500	20.5782	8.3568	-18.7710	45.5579	44.6150	0.0072	0.0045	0.0670	1.7840	-0.0046	-0.0299
WP07-C2-S3	Vein Quartz	1360.2	5.8433	13.5393	0.2166	63.9514	467500	17.6084	15.1978	-6.4977	63.8473	61.5007	0.0040	-0.0413	0.1340	2.3290	0.1531	0.0880
WP03-C1-S1	Vein Quartz	1546.4	2.5963	5.7344	0.2171	28.7581	467500	14.9228	1.2468	12.9630	26.7224	25.7979	-0.0208	0.1429	0.1199	3.7625	0.0985	0.2432
WP03-C1-S2	Vein Quartz	1546.4	6.1604	3.5063	0.0446	59.0540	467500	14.8293	2.8792	-22.7049	45.6057	45.5290	0.0025	-0.0224	0.1261	-0.1322	-0.0208	0.0415
WP03-C1-S3	Vein Quartz	1546.4	6.9361	0.7479	0.0557	64.0363	467500	11.5084	1.5348	86.2852	48.0082	47.5655	-0.0023	-0.0346	0.0515	-0.5329	-0.0614	-0.0062
WP03-C1-S4	Vein Quartz	1546.4	6.7095	0.8256	0.0788	58.8952	467500	8.9296	2.5289	0.4893	47.7689	47.9771	-0.0102	0.1418	0.0445	0.5569	-0.0377	0.0553
WP03-C2-S2	Vein Quartz	1546.4	5.7128	0.7342	0.0886	53.6716	467500	14.3021	4.5605	15.0510	42.2173	43.9869	-0.0185	-0.0121	0.0774	0.5252	0.0343	0.0148
WP03-C2-S3	Vein Quartz	1546.4	7.8814	9.6125	0.0671	80.6954	467500	12.4850	12.2802	27.4406	63.2428	62.6900	-0.0098	-0.0220	0.0948	0.2299	0.0037	0.0245
WP03-C2-S4	Vein Quartz	1546.4	7.4031	0.8722	0.0477	69.5578	467500	13.3792	1.4433	25.8912	44.9574	43.8049	-0.0067	-0.0350	0.0680	-0.3579	-0.0047	0.0144
WP03-C3-S1	Vein Quartz	1546.4	1.7556	6.9691	0.0219	24.2865	467500	12.0607	1.9600	18.9596	2.2123	2.1426	-0.0091	-0.2117	0.0731	0.5008	-0.0040	0.0097
WP03-C3-S2	Vein Quartz	1546.4	1.3611	30.4045	0.1524	24.2300	467500	12.7410	4.4349	10.2586	3.7534	3.3547	0.0002	-0.0857	0.1461	0.9373	0.8075	0.7613
WP03-C3-S3	Vein Quartz	1546.4	1.2526	13.3739	0.0584	15.9612	467500	11.9518	3.4611	-5.6981	2.2655	1.6593	-0.0091	0.0925	0.0036	-0.0023	0.0264	0.0126
WP03-C3-S4	Vein Quartz	1546.4	0.9683	23.1517	0.1449	20.6290	467500	11.5698	3.5691	41.5427	1.8746	1.7684	0.0124	0.0525	0.0720	1.5329	0.9953	1.1805
WP03-C4-S1	Vein Quartz	1546.4	1.1228	17.7295	0.0850	22.4516	467500	11.9320	6.0019	18.1425	2.2282	2.7008	0.0172	-0.0487	0.0388	-0.2221	0.1693	0.1112
WP03-C4-S2	Vein Quartz	1546.4	1.0082	58.2568	0.4345	21.4584	467500	13.1479	4.6898	54.1338	1.2255	1.5356	-0.0115	-0.2251	0.0945	24.0668	0.2991	-0.0207
WP03-C4-S3	Vein Quartz	1546.4	2.1491	21.8020	0.0726	28.5870	467500	13.1491	1.7852	-48.3022	3.6277	3.2901	0.0091	0.0266	0.0389	10.2612	0.1300	0.0239
WP03-C4-S4	Vein Quartz	1546.4	0.8230	5.7873	0.0174	15.0935	467500	13.6891	1.0598	82.8514	1.8483	1.9605	0.0102	0.0235	0.0632	-0.0672	0.8516	1.1003
WP63-C1-S1	Breccia Cemen	0.0	4.3374	0.9527	0.2291	74.2055	467500	14.1099	10.9168	-3.8036	67.6314	68.0997	0.0132	0.0099	0.1836	1.1583	0.0611	0.0247
WP63-C1-S2	Breccia Cemen	0.0	5.0135	-1.0429	0.1972	76.7069	467500	12.4159	12.4647	15.2549	66.7369	68.1309	0.0020	0.0303	0.2094	-0.8536	0.0509	-0.0316
WP63-C1-S3	Breccia Cemen	0.0	3.7472	2.5463	0.1550	65.8765	467500	12.6230	8.4162	6.1078	56.7902	51.3951	-0.0144	0.1389	0.1193	-0.1910	0.0809	0.0940
WP63-C2-S1	Breccia Cemen	0.0	6.0327	1.1883	0.1733	75.3246	467500	12.9670	9.1159	-11.6839	70.9289	73.7317	-0.0053	0.0126	0.2223	1.5039	-0.0510	0.0297
WP63-C2-S2	Breccia Cemen	0.0	5.9795	1.5243	0.3203	75.0022	467500	12.7185	20.6311	-23.7870	62.9241	67.2604	-0.0010	0.0567	0.2114	1.7836	-0.0145	0.0680
WP63-C2-S3	Breccia Cemen	0.0	5.8340	-1.4734	0.2050	76.2709	467500	10.1127	10.7069	19.7640	58.3729	61.0840	-0.0036	-0.0688	0.1613	4.7341	-0.0515	0.0170
WP63-C3-S1	Breccia Cemen	0.0	2.6864	83.9862	3.2950	115.5103	467500	13.4674	29.4357	24.4094	34.2358	34.4551	0.0640	-0.0163	0.2013	31.4575	2.3372	5.2157
WP02-C1-S1	Breccia Cemen	132.2	3.2812	-0.0960	1.4795	71.7704	467500	13.7154	14.7387	-0.9718	16.1006	16.7823	0.0298	0.1049	0.1257	2.4284	0.0058	0.0655
WP02-C1-S2	Breccia Cemen	132.2	3.4694	29.8061	5.9919	202.0161	467500	14.3515	101.1182	49.0328	26.4717	23.8282	0.1701	-0.0569	0.1389	20.6808	0.6558	0.4548
WP02-C1-S4	Breccia Cemen	132.2	3.1688	-3.9417	0.4843	49.2674	467500	14.1439	10.5877	101.4609	13.2841	13.8149	0.0099	0.0221	0.0635	4.0499	0.1829	0.1008
WP02-C1-S5	Breccia Cemen	132.2	2.7090	-5.3409	0.1979	38.0065	467500	16.1749	-0.9855	59.6333	13.8634	13.9844	0.0372	-0.0722	0.9819	4.9535	0.1520	0.1206
WP02-C1-S6	Breccia Cemen	132.2	2.9858	2.3314	0.5026	52.0271	467500	16.6806	6.7184	96.4206	15.8942	13.9133	-0.0020	-0.2121	3.1682	4.2837	0.1425	0.1060
WP02-C1-S7	Breccia Cemen	132.2	3.2866	0.4240	0.9283	78.8666	467500	14.8013	13.1420	-27.4218	16.8988	16.1904	0.0006	-0.0785	0.6045	4.3606	0.1819	0.3209
WP02-C1-S9	Breccia Cemen	132.2	3.9601	-1.2531	0.9019	56.6428	467500	12.5793	10.4038	7.2398	14.9523	13.6822	0.0109	0.0114	0.0679	3.9138	0.0727	0.0013
WP02-C1-S10	Breccia Cemen	132.2	5.0105	1.7457	1.4355	89.2403	467500	12.6199	19.2437	-1.8697	17.7107	16.3556	-0.0077	0.1605	0.0978	6.9133	0.1431	0.3560
WP02-C1-S11	Breccia Cemen	132.2	2.4487	-2.3392	0.3197	39.7972	467500	13.6789	0.5056	-22.0866	19.3029	20.0164	-0.0071	0.0322	0.2805	12.7327	0.2570	0.1720
WP02-C1-S12	Breccia Cemen	132.2	2.8253	-4.3039	0.1468	42.8222	467500	13.5512	9.1472	-25.3628	14.1310	15.4040	-0.0087	-0.0601	0.0816	3.9792	0.0603	0.0447
WP02-C2-S1	Breccia Cemen	132.2	3.0003	7.8171	0.5217	79.8329	467500	13.2827	14.6129	-44.8571	51.7848	52.7627	0.0004	-0.0490	0.1853	2.0712	0.0423	0.0566

* distance from center of deposit

** All elements in ppm except Au which is in ppb

Appendix 6: White Pine
quartz mineral chemistry by LA-ICP-MS

Quartz sample		Distance*	Li7	Na23	Mg24	Al27	Si29	P31	K39	Ca43	Ti47	Ti49	V51	Cr53	Mn55	Fe57	Cu63	Cu65
Sample	type	(m)																
WP02-C2-S2	Breccia Cemen	132.2	2.4948	18.8256	0.2212	75.8806	467500	15.4965	8.9527	31.3924	43.0697	42.1096	0.0099	-0.0527	0.3089	2.7294	0.2595	0.1367
WP02-C2-S3	Breccia Cemen	132.2	2.7808	14.7763	0.5099	73.7301	467500	11.3788	14.3686	22.0552	52.6603	52.7745	-0.0028	-0.0577	0.2375	3.5375	0.4177	0.6271
WP02-C2-S4	Breccia Cemen	132.2	1.7048	53.6738	0.3763	71.7988	467500	11.0386	11.1739	-21.9244	55.8098	54.8917	0.0054	0.1610	1.1258	2.0577	0.1386	0.0651
WP03-C3-S1	Igneous quartz	1546.4	2.6726	6.1142	0.0642	67.1388	467500	12.1273	2.4768	23.3350	7.1872	7.5905	-0.0035	0.0833	0.0374	0.5019	0.0758	0.0120
WP03-C3-S2	Igneous quartz	1546.4	0.6671	19.3730	0.0488	30.9644	467500	19.9027	2.3351	22.9347	3.9945	3.7155	0.0043	-0.0442	0.0883	0.6258	0.2491	0.3502
WP03-C3-S3	Igneous quartz	1546.4	4.7576	20.0959	0.1480	103.6295	467500	16.6096	4.7362	-38.7484	10.2717	8.6309	0.0141	-0.0024	0.0745	0.3130	0.2103	0.1888
WP03-C3-S4	Igneous quartz	1546.4	2.8655	10.5370	0.0806	82.0180	467500	20.0798	1.3528	29.4679	7.1410	6.6210	-0.0336	-0.0580	0.0902	0.4773	0.0508	0.0238
WP03-C3-S5	Igneous quartz	1546.4	2.5460	5.9483	0.0710	62.2635	467500	17.5323	1.2592	-38.7012	6.9168	7.2966	-0.0002	0.0083	0.0769	-0.3194	0.0008	0.0030
WP13-C1-S1	Igneous quartz	1553.6	4.3468	-0.3169	0.1042	47.5364	467500	20.9295	-0.5813	-18.3012	57.0961	56.9888	-0.0067	0.1287	0.0305	0.0782	0.0453	0.0899
WP13-C1-S2	Igneous quartz	1553.6	4.4180	6.3130	5.1336	127.8599	467500	20.9437	16.7344	121.9350	39.9641	41.8713	0.0961	0.0941	0.4031	13.0654	-0.0191	0.1964
WP13-C1-S3	Igneous quartz	1553.6	5.8140	-1.5812	0.0374	45.7100	467500	21.3856	0.0840	-50.7985	46.8298	47.3357	0.0091	0.0241	0.0340	-0.1078	-0.0480	0.0501
WP13-C1-S4	Igneous quartz	1553.6	4.5142	2.7619	0.2448	110.3730	467500	21.4067	17.4276	-55.6093	46.2038	46.1523	0.0098	0.0461	0.2636	5.5385	-0.0026	0.0121
WP22-C2-S1	Igneous quartz	2588.2	1.3889	-0.9048	0.0049	38.2289	467500	18.7177	0.1614	15.5126	1.9998	2.2049	0.0240	-0.1607	0.0901	-0.1145	-0.0313	-0.0892
WP22-C2-S2	Igneous quartz	2588.2	0.9747	-7.6154	0.0330	22.5518	467500	23.3278	-1.4832	-4.8097	1.4955	0.9437	0.0094	-0.2203	0.0609	2.3815	0.2394	0.0930
WP22-C2-S3	Igneous quartz	2588.2	1.8342	-5.3021	0.0027	25.4514	467500	17.7446	-0.1225	31.1852	1.0682	0.9079	-0.0128	0.0084	0.0374	2.6340	0.0571	0.0990
WP22-C2-S4	Igneous quartz	2588.2	2.1115	-4.3907	0.0041	40.9592	467500	16.4660	-0.4506	-14.2661	1.3858	1.4920	0.0077	0.1506	-0.0019	2.2194	0.0558	-0.0230
WP22-C2-S5	Igneous quartz	2588.2	0.8067	-0.9838	-0.0101	24.7336	467500	20.8950	-0.1386	13.0457	1.1360	1.5195	-0.0031	-0.0382	0.0917	7.6530	0.2090	0.1202
WP06-C1-S1	Igneous quartz	1429.0	2.2762	58.1517	0.5912	52.7902	467500	13.6120	13.5974	23.2821	37.7174	38.1368	0.0082	0.0753	0.5406	41.9217	0.6217	0.6599
WP06-C1-S2	Igneous quartz	1429.0	2.2047	28.3746	0.2279	44.5988	467500	12.8782	9.6984	27.0424	6.4278	5.0649	0.0073	-0.0401	0.0906	2.1053	0.6233	0.6880
WP06-C1-S3	Igneous quartz	1429.0	1.6881	5.5000	0.0786	23.3699	467500	11.0874	2.0834	28.8122	4.9928	4.5498	-0.0032	-0.0126	0.0147	-0.1204	0.1170	0.1455
WP06-C1-S4	Igneous quartz	1429.0	1.2492	11.1142	0.0371	20.5793	467500	12.5854	2.3148	-4.5329	5.1623	5.1087	0.0036	0.0254	0.0520	-0.5472	0.3147	0.4051
WP64-C4-S1	Igneous quartz	704.8	3.2319	0.4662	0.0872	50.3350	467500	28.9138	2.6416	-126.9638	14.8205	20.7657	0.0055	-0.0222	0.0784	12.6619	0.3806	0.2264
WP64-C4-S2	Igneous quartz	704.8	3.5704	3.9397	0.4618	61.0831	467500	17.6923	10.8398	44.4995	15.4562	15.6856	0.0016	0.0449	0.1852	1.0141	0.2916	0.3202
WP64-C4-S3	Igneous quartz	704.8	2.5598	3.2138	0.1684	49.3904	467500	19.8064	4.4207	-32.5150	14.1225	13.2167	-0.0006	0.0524	0.0758	8.5382	0.2142	0.2353
WP64-C4-S3	Igneous quartz	704.8	4.0183	-2.1091	0.2874	59.0114	467500	19.1968	1.4937	69.7917	13.2552	12.8618	-0.0048	-0.0235	0.0550	1.3831	0.0579	0.1572
WP52-C1-S1	Igneous quartz	785.5	0.8428	14.7410	0.1282	46.6599	467500	8.5478	5.0213	-44.5556	58.0675	58.5171	-0.0067	0.0568	0.0733	2.0061	0.4651	0.5891
WP52-C1-S2	Igneous quartz	785.5	1.1686	-1.2902	0.1775	73.8111	467500	13.6950	8.8559	24.0003	57.5048	60.1756	-0.0006	0.2696	0.3709	-0.1489	0.2279	0.1827
WP52-C1-S3	Igneous quartz	785.5	0.0536	9.8745	2.5145	61.2609	467500	30.5795	15.8417	12.8294	36.6180	37.2811	0.0451	-0.0616	0.2653	582.3826	5.3185	5.6901
WP52-C2-S1	Igneous quartz	785.5	0.3368	7.5361	0.0236	36.4894	467500	7.2470	2.3305	7.3302	6.1264	6.3104	0.0198	0.4872	0.0387	25.3805	0.0740	0.2015
WP52-C2-S2	Igneous quartz	785.5	0.4410	28.0084	0.0889	34.6000	467500	12.8387	4.1018	40.3785	7.3632	7.0582	0.0089	0.0242	0.0681	0.4044	0.1355	0.1601
WP52-C2-S3	Igneous quartz	785.5	0.9446	34.2484	0.8554	73.8889	467500	12.7578	7.9325	43.6466	8.8325	8.2638	-0.0208	0.2661	0.2317	8.0855	0.1178	0.1512
WP52-C2-S4	Igneous quartz	785.5	0.5794	24.2961	0.3844	55.1935	467500	10.7797	10.6618	-12.4487	7.7356	8.6331	0.0207	-0.0712	0.2135	3.8449	0.0998	0.2119
WP65-C1-S1	Igneous quartz	609.4	3.0265	0.3191	0.2604	32.7861	467500	7.8594	-0.4096	-44.6427	7.1509	8.9091	-0.0173	-0.0815	0.0626	3.0634	0.7057	0.6809
WP65-C1-S3	Igneous quartz	609.4	5.5457	-0.9173	0.1832	46.3475	467500	14.5102	0.7530	-1.4210	7.5626	8.0186	-0.0085	0.0540	0.0211	2.6922	0.0243	0.0260
WP65-C1-S4	Igneous quartz	609.4	4.1056	-0.7305	0.0698	36.0657	467500	10.8934	2.0691	-27.6616	8.2189	9.3212	0.0101	0.1086	-0.0142	4.8550	-0.0087	0.0780
WP23-C1-S1	Igneous quartz	1688.3	8.1242	0.7822	0.1482	52.8113	467500	16.5694	0.2949	3.4253	55.3356	55.9340	0.0027	0.0427	0.1004	0.2782	0.0529	0.0790
WP23-C1-S2	Igneous quartz	1688.3	8.4061	6.7311	0.3553	97.0008	467500	20.1119	12.9860	10.6138	81.7040	81.4327	0.1410	0.2777	0.2094	297.8386	0.2233	0.0775
WP23-C1-S3	Igneous quartz	1688.3	6.1709	2.7400	0.1110	51.2952	467500	14.4406	0.4373	-4.8251	39.6648	37.9745	0.2125	-0.1077	0.0766	6.6319	0.0961	0.3631
WP23-C1-S4	Igneous quartz	1688.3	7.7270	2.6699	0.3786	88.9013	467500	16.1379	6.5161	-33.7374	76.8804	77.0651	0.0337	0.0901	0.1625	31.7881	0.0815	0.1734
WP23-C2-S1	Igneous quartz	1688.3	8.1669	-1.0499	1.0026	85.2388	467500	12.9378	7.8763	-1.4295	49.1174	48.3913	0.0044	-0.0732	0.2174	1.5621	-0.0043	-0.0086
WP23-C2-S2	Igneous quartz	1688.3	8.4100	-2.3494	0.1773	70.0056	467500	10.7393	0.8722	44.8501	51.5062	54.2600	0.0070	-0.1304	0.1385	0.6058	0.0288	0.0080
WP23-C2-S3	Igneous quartz	1688.3	7.5747	0.4782	0.2219	81.4805	467500	11.7135	2.0785	-3.8278	60.3309	58.5071	-0.0016	0.0423	0.1582	1.2640	-0.0125	0.0726
WP23-C2-S4	Igneous quartz	1688.3	5.5054	0.6988	0.6217	76.0493	467500	14.5902	4.1139	81.2517	50.4809	50.0517	0.0114	0.0686	0.2236	1.0535	-0.0307	0.0805
WP07-C4-S1	Igneous quartz	1360.2	3.4029	4.3174	0.0133	56.1449	467500	24.1949	11.0204	-26.5461	32.1676	31.4928	-0.0141	-0.0586	0.2215	6.3154	0.0633	0.1540
WP07-C4-S2	Igneous quartz	1360.2	5.3353	15.7788	0.2722	60.9290	467500	15.1347	7.1541	77.0729	43.9661	45.2983	0.0058	-0.0032	0.0708	0.9842	0.0198	0.0060
WP07-C4-S3	Igneous quartz	1360.2	5.0449	2.8825	0.2164	52.3197	467500	18.1907	3.8552	18.0549	48.5470	49.7006	0.0044	-0.0520	0.0853	4.8283	0.1556	0.1787
WP07-C4-S4	Igneous quartz	1360.2	5.0723	1.4196	0.3159	53.5900	467500	16.0300	4.3104	-9.9026	45.4758	43.4147	0.0017	0.0790	0.1048	1.3976	0.0777	0.1121

* distance from center of deposit

** All elements in ppm except Au which is in ppb

Appendix 6: White Pine
quartz mineral chemistry by LA-ICP-MS

Quartz sample		Distance*	Zn66	Ge74	As75	Rb85	Sr88	Zr90	Ag107	Sb121	Cs133	Gd157	Hf178	Ta181	Au197**	Pb208	Bi209	U238
Sample	type	(m)																
WP46-C1-S1	Vein Quartz	372.6	-0.0481	1.1059	4.2962	0.0104	0.4879	0.0083	-0.0255	0.0947	0.0115	-0.0129	-0.0054	-0.0009	-0.0054	0.1456	-0.0055	0.0141
WP46-C1-S2	Vein Quartz	372.6	0.1742	0.8387	4.7901	0.0150	0.0842	0.0059	0.0000	-0.0170	0.0034	0.0059	0.0055	0.0001	0.0013	0.0108	-0.0021	0.0001
WP46-C1-S3	Vein Quartz	372.6	-0.0016	0.8248	3.8286	0.0298	0.0572	0.0027	-0.0098	0.0044	0.0074	0.0045	-0.0001	0.0000	-0.0034	0.0156	-0.0001	0.0004
WP46-C1-S4	Vein Quartz	372.6	-0.0265	1.0354	3.5851	0.0995	0.1524	-0.0067	0.0065	-0.0082	0.0053	0.0022	0.0048	0.0007	-0.0061	0.0918	0.0039	0.0051
WP46-C1-S5	Vein Quartz	372.6	0.2825	0.9334	3.7571	0.0523	0.1701	0.0184	0.0415	0.0236	0.0070	0.0151	0.0042	-0.0003	-0.0015	0.0313	0.0022	0.0069
WP46-C1-S6	Vein Quartz	372.6	0.0890	0.8666	3.9412	0.0157	0.0738	0.0075	-0.0009	-0.0042	0.0000	-0.0014	0.0014	-0.0015	-0.0090	0.0184	-0.0022	0.0007
WP46-C1-S7	Vein Quartz	372.6	0.1072	0.9241	3.7082	0.0366	0.2135	-0.0002	0.1769	0.1190	0.0069	0.0005	-0.0008	-0.0012	0.0098	0.7548	0.0086	0.0031
WP46-C1-S8	Vein Quartz	372.6	0.0183	0.7670	2.9844	0.0758	0.4334	0.0107	0.0457	0.0429	0.0066	-0.0091	-0.0044	0.0010	0.0152	0.1618	0.0071	0.0220
WP46-C1-S9	Vein Quartz	372.6	0.0973	0.9440	3.6527	0.0098	0.2100	0.0017	0.0587	0.0644	0.0107	-0.0022	-0.0022	0.0013	0.0051	0.1556	0.0059	0.0038
WP46-C1-S10	Vein Quartz	372.6	0.0215	0.8079	3.6800	0.0602	0.2357	-0.0019	0.0297	0.0072	0.0133	0.0042	0.0047	0.0007	0.0035	0.2414	0.0041	-0.0005
WP46-C1-S11	Vein Quartz	372.6	-0.0544	0.8486	4.1394	0.0106	0.0921	0.0018	0.0113	0.0212	0.0055	-0.0046	-0.0029	-0.0004	-0.0013	0.0650	0.0023	0.0017
WP46-C1-S12	Vein Quartz	372.6	0.0158	0.7932	4.1962	0.0042	0.0361	0.0030	-0.0048	-0.0094	0.0062	0.0010	0.0005	0.0002	-0.0118	-0.0018	0.0074	0.0041
WP46-C1-S13	Vein Quartz	372.6	0.0971	0.7712	3.8468	0.0040	0.0504	-0.0057	-0.0016	0.0009	0.0026	-0.0007	0.0033	-0.0009	-0.0045	0.0016	-0.0013	-0.0016
WP46-C1-S14	Vein Quartz	372.6	-0.0267	0.7750	3.6176	0.0237	0.1254	0.0024	-0.0144	0.0727	0.0023	-0.0142	-0.0028	-0.0010	0.0009	0.1379	0.0025	0.0072
WP46-C1-S15	Vein Quartz	372.6	0.0723	0.8055	4.9891	0.0052	0.0948	0.0009	0.0065	0.0010	0.0039	0.0047	0.0051	0.0003	-0.0013	0.0243	-0.0004	-0.0001
WP03-C1-S1	Vein Quartz	1546.4	-0.0300	2.8563	7.6945	0.0284	0.0625	0.0108	-0.0026	0.0082	0.0172	0.0014	0.0049	-0.0007	-0.0006	0.0189	0.0676	-0.0007
WP03-C1-S2	Vein Quartz	1546.4	0.0956	3.3270	6.5674	0.1672	0.1374	-0.0053	0.0062	0.0573	0.0436	0.0020	-0.0031	0.0019	0.0014	0.0607	0.0546	0.0073
WP03-C1-S3	Vein Quartz	1546.4	0.2697	3.0439	7.9568	0.0739	0.1693	0.0091	0.0048	0.0577	0.0328	0.0156	-0.0021	0.0025	0.0054	0.6947	0.7496	0.0039
WP03-C1-S4	Vein Quartz	1546.4	0.1394	2.9819	8.1668	0.0554	0.0963	0.0010	0.0067	0.0312	0.0167	-0.0044	0.0008	0.0002	0.0027	0.3129	0.2560	0.0063
WP03-C1-S5	Vein Quartz	1546.4	0.0707	2.5138	8.7187	0.0201	0.0721	0.0003	0.0002	0.0183	0.0170	-0.0066	-0.0008	0.0004	0.0076	0.1708	0.3257	0.0013
WP03-C2-S1	Vein Quartz	1546.4	0.0503	3.1908	7.9911	0.0280	0.0342	0.0001	0.0063	0.4563	0.0116	-0.0084	0.0017	0.0006	0.0007	0.0572	0.0850	0.0058
WP03-C2-S2	Vein Quartz	1546.4	0.0809	2.8841	8.1478	0.0064	0.0794	-0.0007	-0.0003	-0.0046	0.0074	-0.0056	0.0044	0.0005	0.0038	0.0265	0.0176	-0.0001
WP03-C2-S3	Vein Quartz	1546.4	-0.0221	2.9183	8.7434	0.0077	0.0077	0.0020	-0.0062	-0.0008	0.0081	-0.0063	0.0003	-0.0001	-0.0039	0.0431	0.0403	0.0006
WP03-C2-S4	Vein Quartz	1546.4	-0.0380	3.3413	8.6894	0.0131	0.0016	0.0019	0.0021	0.0134	0.0328	-0.0078	-0.0018	-0.0003	0.0009	0.1937	0.0854	0.0002
WP03-C2-S5	Vein Quartz	1546.4	0.0672	3.4022	6.9338	0.0071	0.0231	-0.0002	-0.0011	0.0277	0.0078	-0.0091	0.0003	0.0015	0.0113	0.0476	0.3004	0.0025
WP13-C3-S1	Vein Quartz	1553.6	-0.0270	1.0590	0.0611	-0.0051	0.0101	0.0024	0.0183	0.0220	0.0000	-0.0006	0.0001	-0.0003	0.0024	-0.0006	-0.0011	-0.0006
WP13-C3-S2	Vein Quartz	1553.6	0.0298	1.1248	0.0300	-0.0012	0.0074	-0.0033	-0.0026	0.0121	0.0000	0.0054	-0.0005	0.0003	-0.0018	-0.0028	0.0010	-0.0008
WP13-C3-S3	Vein Quartz	1553.6	-0.0924	1.0168	0.0570	0.0051	0.0137	-0.0079	0.0216	-0.0168	0.0023	-0.0021	0.0002	0.0010	-0.0013	0.0212	0.0012	0.0004
WP13-C3-S4	Vein Quartz	1553.6	0.0075	1.2318	0.0722	0.0365	0.0523	0.0010	0.0275	0.0392	0.0184	0.0008	-0.0006	-0.0001	0.0075	0.0150	0.0024	-0.0004
WP13-C5-S1	Vein Quartz	1553.6	0.0863	1.2021	0.0676	0.0281	0.0733	0.0019	-0.0044	-0.0240	0.0033	-0.0009	-0.0024	-0.0016	-0.0019	0.0498	0.0009	0.0014
WP13-C5-S2	Vein Quartz	1553.6	-0.0187	1.2537	-0.0071	0.0212	0.3221	0.0065	-0.0045	0.0672	0.0028	0.0064	0.0012	0.0014	0.0081	0.0001	0.0016	0.0023
WP13-C5-S3	Vein Quartz	1553.6	0.0777	1.2674	0.1123	0.0053	0.0524	0.0110	0.0066	-0.0030	0.0125	-0.0021	0.0021	-0.0017	0.0029	0.0295	0.0013	0.0019
WP13-C5-S4	Vein Quartz	1553.6	0.1165	1.2984	-0.0073	0.0082	0.0460	-0.0013	0.0038	0.0054	0.0026	0.0004	0.0018	0.0002	-0.0022	0.0159	0.0039	0.0009
WP22-C4-S1	Vein Quartz	2588.2	0.0301	1.2058	0.1169	-0.0030	0.0126	0.0005	0.0102	0.0096	0.0009	0.0068	-0.0012	-0.0013	0.0093	-0.0022	-0.0020	0.0020
WP22-C4-S2	Vein Quartz	2588.2	-0.0162	1.4757	0.1396	0.0073	0.0134	-0.0075	0.0067	0.0179	-0.0040	0.0007	0.0050	-0.0002	0.0036	0.0867	0.0037	-0.0005
WP22-C4-S3	Vein Quartz	2588.2	0.2390	1.4497	0.1244	0.0546	0.0500	-0.0050	-0.0031	0.0126	0.0145	0.0096	-0.0007	0.0004	-0.0010	0.1458	-0.0025	0.0005
WP22-C4-S4	Vein Quartz	2588.2	0.1600	1.6957	0.0791	0.0127	0.0292	-0.0023	0.0194	0.2036	0.0063	-0.0046	0.0015	-0.0001	-0.0021	0.1892	0.0039	0.0015
WP22-C4-S5	Vein Quartz	2588.2	0.1336	1.4454	0.2781	0.1000	0.1339	-0.0018	0.0149	0.1087	0.0196	-0.0056	0.0087	-0.0017	-0.0002	0.2487	-0.0002	0.0107
WP06-C2-S1	Vein Quartz	1429.0	0.0539	0.4279	-0.0039	0.0402	0.0870	-0.0032	0.0063	-0.0025	0.0160	0.0056	-0.0033	0.0005	0.0117	0.0249	0.0013	-0.0003
WP06-C2-S2	Vein Quartz	1429.0	0.0931	0.4585	0.0873	0.0237	0.1346	-0.0015	-0.0033	0.0143	0.0032	-0.0095	0.0033	-0.0002	0.0001	0.0230	-0.0005	-0.0004
WP06-C2-S3	Vein Quartz	1429.0	0.0888	0.4111	0.1055	0.0273	0.1040	0.0026	0.0229	0.0180	0.0069	0.0034	0.0023	0.0003	-0.0019	0.0500	0.0028	-0.0001
WP06-C2-S4	Vein Quartz	1429.0	0.0582	0.4674	0.0344	0.0226	0.0773	0.0016	-0.0100	-0.0076	0.0080	-0.0016	-0.0014	0.0018	0.0001	0.0135	0.0045	-0.0001
WP06-C3-S2	Vein Quartz	1429.0	0.2195	0.6024	0.2337	0.2470	0.8954	-0.0030	0.0131	-0.0230	0.1783	-0.0059	0.0025	0.0026	0.0190	0.0261	0.0020	0.0019
WP06-C3-S3	Vein Quartz	1429.0	0.1795	0.4264	0.1100	0.0415	0.0924	-0.0011	-0.0180	0.0149	0.0059	0.0085	0.0060	-0.0010	-0.0027	0.0649	0.0033	0.0101
WP06-C3-S4	Vein Quartz	1429.0	0.1015	0.5452	0.1184	0.0115	0.2350	0.0059	-0.0033	-0.0110	0.0042	0.0049	0.0018	0.0018	-0.0081	0.0706	-0.0018	0.0028
WP53-C1-S1	Vein Quartz	548.8	0.0121	1.0448	0.1797	0.0909	0.0252	0.0019	0.0073	0.0415	0.0408	-0.0138	-0.0032	0.0033	-0.0024	0.0092	-0.0025	0.0011
WP53-C1-S2	Vein Quartz	548.8	0.0754	0.9932	0.0677	0.2099	0.0710	0.0082	0.0168	0.0028	0.1028	-0.0030	-0.0053	-0.0015	0.0017	0.0083	0.0011	0.0036

* distance from center of deposit

** All elements in ppm except Au which is in ppb

Appendix 6: White Pine
quartz mineral chemistry by LA-ICP-MS

Quartz sample		Distance*	Zn66	Ge74	As75	Rb85	Sr88	Zr90	Ag107	Sb121	Cs133	Gd157	Hf178	Ta181	Au197**	Pb208	Bi209	U238
Sample	type	(m)																
WP53-C1-S3	Vein Quartz	548.8	0.0172	0.8972	0.1186	0.0574	0.0212	0.0063	-0.0117	0.0250	0.0101	0.0007	0.0017	-0.0003	0.0068	0.0067	0.0014	0.0004
WP53-C1-S4	Vein Quartz	548.8	-0.0262	0.9862	0.1485	0.0907	0.0275	0.0055	-0.0077	0.0396	0.0125	0.0069	0.0041	0.0001	0.0094	0.0055	0.0005	-0.0014
WP53-C1-S5	Vein Quartz	548.8	0.0975	1.0283	0.1986	0.0236	0.0283	0.0031	0.0187	-0.0091	0.0152	-0.0005	-0.0049	-0.0005	0.0099	0.0544	-0.0027	0.0021
WP53-C2-S1	Vein Quartz	548.8	0.2103	1.2004	0.2084	0.0319	0.1059	0.0076	0.0258	0.0119	0.0165	0.0034	-0.0023	0.0001	0.0033	0.8202	0.0278	0.1013
WP53-C2-S2	Vein Quartz	548.8	0.0019	1.2311	0.1548	0.0161	0.0617	0.0056	0.0066	0.0009	0.0237	-0.0017	-0.0044	0.0022	0.0012	0.0344	0.0041	0.0206
WP53-C2-S3	Vein Quartz	548.8	0.0347	1.4766	0.2266	0.2263	0.1294	0.0855	-0.0027	0.0010	0.0875	-0.0033	0.0104	0.0019	0.0028	0.0255	0.0043	0.0154
WP53-C2-S4	Vein Quartz	548.8	0.0039	1.0170	0.1215	0.0756	0.0225	0.0134	-0.0020	0.0254	0.0211	0.0062	0.0065	0.0002	0.0117	0.0228	0.0002	0.0059
WP53-C2-S5	Vein Quartz	548.8	-0.0453	1.0659	0.1910	0.0794	0.1119	0.0102	0.0394	0.0050	0.0271	-0.0009	-0.0023	0.0002	-0.0049	0.4856	0.0094	0.0445
WP05-C1-S1	Vein Quartz	1429.0	0.1135	0.3331	0.1382	0.0295	0.0830	-0.0013	-0.0330	0.0361	0.0049	0.0017	-0.0029	0.0007	-0.0067	0.0317	-0.0074	0.0044
WP05-C1-S2	Vein Quartz	1429.0	0.1417	0.5861	0.1803	0.0303	0.2536	0.0040	-0.0169	0.0388	0.0144	-0.0019	0.0016	-0.0012	-0.0046	0.0701	-0.0017	0.0022
WP05-C1-S3	Vein Quartz	1429.0	0.0907	0.5406	0.0118	0.0035	0.0476	-0.0019	-0.0357	-0.0068	0.0033	0.0034	0.0055	0.0007	0.0001	0.0005	0.0034	0.0007
WP05-C1-S4	Vein Quartz	1429.0	-0.0019	0.5433	0.1735	-0.0076	0.0305	0.0100	0.0003	-0.0010	0.0015	0.0035	0.0019	0.0019	0.0112	0.0031	-0.0040	-0.0025
WP05-C2-S1	Vein Quartz	1429.0	0.0123	0.7871	-0.0374	0.0237	0.0439	-0.0025	-0.0002	-0.0028	0.0052	-0.0094	-0.0031	0.0006	0.0071	0.0276	0.0023	-0.0004
WP05-C2-S2	Vein Quartz	1429.0	0.1006	1.7672	0.0684	0.0257	0.2532	0.0080	0.0500	0.0027	0.0032	-0.0156	-0.0017	0.0007	0.0287	0.0220	-0.0007	0.0013
WP05-C2-S3	Vein Quartz	1429.0	-0.1132	0.8762	0.1219	0.0124	0.0352	-0.0051	-0.0261	0.0115	0.0028	-0.0021	-0.0083	0.0019	0.0011	0.0194	-0.0015	-0.0006
WP05-C2-S4	Vein Quartz	1429.0	0.0724	0.8504	0.2007	0.0238	0.0290	0.0023	-0.0010	0.0049	0.0055	0.0045	-0.0003	-0.0009	-0.0021	0.0144	-0.0084	0.0004
WP05-C2-S5	Vein Quartz	1429.0	0.0383	0.5445	0.0621	0.0359	0.0659	0.0002	-0.0036	0.0139	0.0056	0.0203	-0.0046	-0.0022	0.0139	0.0090	0.0060	-0.0002
WP05-C3-S1	Vein Quartz	1429.0	0.0555	2.5214	0.3137	0.0710	0.3674	0.0000	0.0038	0.0658	0.0516	0.0055	0.0061	-0.0015	0.0134	0.0463	0.0225	-0.0007
WP05-C3-S2	Vein Quartz	1429.0	0.0419	2.5806	0.1048	0.0127	0.1036	0.0012	0.0068	0.1138	0.0036	0.0017	0.0037	-0.0022	-0.0039	0.0204	0.0070	-0.0010
WP05-C3-S3	Vein Quartz	1429.0	0.1248	1.5042	0.1734	0.0117	0.0485	0.0087	-0.0089	-0.0225	0.0125	-0.0090	-0.0027	-0.0018	0.0065	0.0196	-0.0021	0.0034
WP05-C3-S4	Vein Quartz	1429.0	0.0033	1.7332	0.1986	0.0499	0.1390	-0.0040	0.0077	0.0248	0.0150	-0.0020	0.0019	0.0005	-0.0016	0.0393	-0.0034	0.0001
WP64-C1-S1	Vein Quartz	704.8	0.0381	1.2681	0.0962	0.0134	0.0553	0.0005	0.6442	0.0372	0.0057	-0.0034	0.0005	0.0018	-0.0077	0.3162	0.0030	-0.0001
WP64-C1-S2	Vein Quartz	704.8	-0.0796	1.1286	0.1488	0.0290	0.0075	0.0003	-0.0066	0.0504	0.0031	0.0064	-0.0057	0.0003	0.0011	0.0172	-0.0027	0.0012
WP64-C1-S3	Vein Quartz	704.8	0.0761	1.3354	0.0115	0.0436	0.0259	-0.0041	0.0093	-0.0677	0.0214	-0.0092	0.0010	-0.0013	0.0108	0.0898	0.0045	0.0012
WP64-C1-S4	Vein Quartz	704.8	0.0172	1.2717	0.0856	0.1159	0.0308	-0.0023	0.0050	0.0384	0.0081	0.0051	0.0035	0.0006	-0.0041	0.0358	-0.0057	-0.0011
WP64-C2-S1	Vein Quartz	704.8	0.5620	1.5334	0.2715	0.3577	0.0723	-0.0017	-0.0094	0.0084	0.0181	0.0168	-0.0024	0.0003	0.0021	0.1850	0.0252	0.0080
WP64-C2-S2	Vein Quartz	704.8	0.2111	2.0400	0.3060	0.4464	0.0567	0.0053	0.0384	0.0583	0.0076	-0.0055	0.0035	0.0007	0.0067	0.0488	0.0028	0.0074
WP64-C2-S4	Vein Quartz	704.8	0.2390	1.9597	0.1296	0.2678	0.0570	-0.0049	0.0109	0.0828	0.0231	0.0036	0.0033	0.0017	0.0040	0.5791	0.0004	0.0005
WP64-C3-S1	Vein Quartz	704.8	-0.0630	1.0966	0.2761	0.0038	0.0029	0.0060	0.0135	-0.0121	0.0018	0.0004	-0.0053	0.0047	-0.0098	0.0087	0.0011	0.0011
WP64-C3-S2	Vein Quartz	704.8	0.0638	1.7742	0.0960	0.1552	0.0523	0.0072	0.0051	-0.0092	0.0390	-0.0079	0.0018	0.0014	0.0066	0.1024	-0.0019	0.0005
WP64-C3-S3	Vein Quartz	704.8	0.5021	1.3732	0.1565	0.0227	0.0475	-0.0026	0.0029	0.0428	0.0147	0.0200	-0.0037	-0.0002	-0.0037	0.5944	0.0256	0.0099
WP52-C3-S1	Vein Quartz	785.5	0.3560	0.4670	0.0313	0.0726	0.2622	0.0167	0.0150	0.0130	0.0137	-0.0226	0.0024	-0.0002	0.0082	0.0223	0.0036	0.0052
WP52-C3-S2	Vein Quartz	785.5	0.1769	0.5294	0.0746	0.0179	0.0934	-0.0046	0.0265	-0.0061	0.0062	-0.0059	-0.0030	-0.0001	0.0103	0.0092	0.0012	0.0001
WP52-C3-S3	Vein Quartz	785.5	0.0205	0.5017	0.1482	0.0211	0.4811	0.0088	0.0047	0.0467	0.0081	0.0039	0.0019	-0.0004	0.0028	0.1793	0.0080	-0.0016
WP52-C3-S4	Vein Quartz	785.5	0.1078	0.4812	0.0408	0.0279	0.1248	-0.0026	0.0120	-0.0008	0.0057	0.0048	0.0019	0.0013	-0.0052	0.0252	-0.0056	0.0025
WP65-C2-S3	Vein Quartz	609.4	0.0700	1.2731	0.0199	0.4167	0.3516	-0.0012	-0.0184	-0.0270	0.0099	-0.0086	0.0028	0.0039	-0.0034	0.0747	0.0040	-0.0003
WP65-C2-S4	Vein Quartz	609.4	0.0556	0.9937	-0.0523	0.0401	0.0561	-0.0022	-0.0044	0.0169	0.0123	-0.0079	-0.0001	0.0011	-0.0054	0.0035	0.0005	0.0019
WP65-C3-S1	Vein Quartz	609.4	0.1311	0.9605	0.0752	0.0351	0.1564	-0.0004	-0.0001	0.0008	0.0132	0.0068	0.0040	0.0001	-0.0014	0.0054	0.0008	0.0015
WP65-C3-S2	Vein Quartz	609.4	0.2615	0.9233	0.0565	0.0415	0.1194	0.0005	0.0068	0.4268	0.0089	-0.0023	0.0047	0.0003	0.0027	0.4222	0.0120	0.0002
WP65-C3-S3	Vein Quartz	609.4	0.1807	0.9655	-0.0252	0.0245	0.1313	-0.0012	-0.0149	-0.0110	0.0125	-0.0010	0.0042	0.0011	-0.0061	0.0157	0.0050	0.0023
WP65-C3-S4	Vein Quartz	609.4	0.1654	0.9164	0.0405	0.0956	0.2329	-0.0031	-0.0053	0.0053	0.0254	0.0019	0.0033	0.0003	0.0079	0.0047	-0.0012	0.0001
WP65-C4-S1	Vein Quartz	609.4	0.0938	0.8881	-0.0189	0.0206	0.1601	-0.0043	0.0088	0.0173	0.0089	0.0150	0.0060	0.0005	0.0024	0.0878	0.0063	0.0085
WP65-C4-S2	Vein Quartz	609.4	0.0089	0.9316	0.0021	0.0125	0.0173	0.0029	0.0108	-0.0039	0.0033	0.0040	0.0035	-0.0016	0.0076	-0.0048	-0.0020	0.0024
WP65-C4-S3	Vein Quartz	609.4	0.0359	0.9886	-0.0041	-0.0005	0.0189	-0.0039	0.0151	0.0053	0.0131	0.0028	0.0014	0.0002	-0.0025	0.0003	-0.0003	0.0016
WP65-C4-S4	Vein Quartz	609.4	0.1520	1.2251	-0.0072	0.0326	0.0546	-0.0030	0.0326	0.0533	0.0055	-0.0060	0.0055	-0.0007	-0.0067	0.4365	0.0153	0.0011
WP23-C5-S2	Vein Quartz	1688.3	0.4833	1.0675	1.5042	0.1899	0.2720	0.0056	-0.0126	0.0145	0.0316	-0.0007	-0.0013	0.0004	-0.0053	0.0462	0.0055	0.0004
WP07-C1-S3	Vein Quartz	1360.2	0.1823	0.9446	6.9261	0.0385	0.7287	0.1495	0.0437	0.1128	0.0173	-0.0220	0.0006	0.0022	0.0041	0.1543	0.0126	0.0077

* distance from center of deposit

** All elements in ppm except Au which is in ppb

Appendix 6: White Pine
quartz mineral chemistry by LA-ICP-MS

Quartz sample		Distance*	Zn66	Ge74	As75	Rb85	Sr88	Zr90	Ag107	Sb121	Cs133	Gd157	Hf178	Ta181	Au197**	Pb208	Bi209	U238
Sample	type	(m)																
WP07-C1-S4	Vein Quartz	1360.2	0.1036	1.0885	6.6033	0.0245	0.3292	0.1449	0.0075	0.0983	0.0049	-0.0046	0.0003	-0.0021	0.0026	0.1140	0.0138	0.0078
WP07-C2-S1	Vein Quartz	1360.2	0.0733	0.4246	9.0787	0.0254	0.0170	0.0048	0.0011	0.0113	0.0017	-0.0017	-0.0046	0.0001	-0.0003	0.0136	0.0005	-0.0012
WP07-C2-S2	Vein Quartz	1360.2	0.0535	0.4367	8.0818	0.0259	0.0116	0.0071	-0.0043	0.0284	0.0027	-0.0025	0.0018	0.0009	-0.0003	0.0018	0.0028	0.0088
WP07-C2-S3	Vein Quartz	1360.2	0.1309	0.4620	9.3265	0.1315	0.1449	0.0094	0.0501	0.0458	0.0435	-0.0048	0.0026	0.0019	-0.0056	0.0746	-0.0049	0.0072
WP07-C4-S1	Vein Quartz	1360.2	0.0079	0.3967	6.8910	0.0466	0.0065	0.0030	0.0005	0.0057	0.0072	0.0121	-0.0007	-0.0018	-0.0070	0.0157	-0.0002	-0.0020
WP07-C4-S2	Vein Quartz	1360.2	0.1117	0.5056	7.3281	0.0483	0.0089	0.0026	0.0008	0.0538	0.0101	-0.0038	-0.0024	-0.0004	0.0047	0.0074	0.0001	0.0001
WP07-C4-S3	Vein Quartz	1360.2	0.0336	0.3798	6.0110	0.0387	0.0144	0.0040	-0.0093	-0.0066	0.0009	-0.0080	0.0097	0.0017	0.0015	0.0191	-0.0023	0.0003
WP07-C4-S4	Vein Quartz	1360.2	0.0628	0.5162	7.1562	0.0344	0.0039	-0.0014	0.0060	0.0208	-0.0004	0.0033	-0.0002	-0.0011	-0.0042	0.0084	-0.0006	-0.0005
WP07-C1-S1	Vein Quartz	1360.2	0.2035	0.8788	6.6846	0.0148	1.2131	0.0703	0.0267	0.4806	0.0144	-0.0009	-0.0083	0.0013	0.0120	0.2399	2.3292	0.1224
WP07-C1-S3	Vein Quartz	1360.2	0.1823	0.9446	6.9261	0.0385	0.7287	0.1495	0.0437	0.1128	0.0173	-0.0220	0.0006	0.0022	0.0041	0.1543	0.0126	0.0077
WP07-C1-S4	Vein Quartz	1360.2	0.1820	1.1157	7.0510	0.0260	0.2748	0.1348	0.0099	0.1037	0.0046	-0.0073	0.0026	-0.0016	0.0042	0.1210	0.0186	0.0054
WP07-C2-S1	Vein Quartz	1360.2	0.0674	0.4089	9.6721	0.0306	0.0176	0.0063	0.0025	0.0135	-0.0005	0.0079	-0.0062	0.0006	0.0051	0.0084	0.0019	-0.0009
WP07-C2-S2	Vein Quartz	1360.2	-0.0067	0.3839	8.0667	0.0385	0.0142	0.0028	0.0013	0.0126	0.0046	-0.0083	-0.0018	-0.0002	-0.0049	0.0043	0.0021	0.0060
WP07-C2-S3	Vein Quartz	1360.2	0.0948	0.4313	9.7760	0.0476	0.0321	0.0154	-0.0032	0.0043	0.0220	0.0034	-0.0016	-0.0003	-0.0070	0.0147	-0.0025	0.0012
WP03-C1-S1	Vein Quartz	1546.4	-0.0450	0.9047	8.2500	0.0123	0.1650	-0.0017	0.0146	0.0154	0.0117	0.0317	-0.0013	0.0001	-0.0041	0.1280	0.0010	0.0068
WP03-C1-S2	Vein Quartz	1546.4	0.1093	0.5299	9.0647	0.0091	0.2452	-0.0006	-0.0080	0.0008	0.0111	0.0004	-0.0004	-0.0014	-0.0050	0.0044	0.0002	0.0004
WP03-C1-S3	Vein Quartz	1546.4	0.0856	0.5776	9.4503	0.0021	0.1764	-0.0013	0.0045	0.0133	0.0108	0.0048	0.0008	0.0007	0.0042	0.0035	0.0003	0.0001
WP03-C1-S4	Vein Quartz	1546.4	0.0506	0.4914	9.1728	0.0114	0.3171	-0.0006	0.0039	-0.0019	0.0111	-0.0045	0.0007	-0.0007	-0.0023	0.0151	-0.0006	0.0007
WP03-C2-S2	Vein Quartz	1546.4	0.2102	0.5173	7.4541	0.0171	0.1239	-0.0003	0.0009	0.0128	0.0059	0.0030	-0.0035	-0.0010	0.0097	0.0121	0.0018	-0.0002
WP03-C2-S3	Vein Quartz	1546.4	0.0198	0.4504	7.9610	0.0474	0.2283	-0.0003	0.0065	0.0161	0.0131	0.0010	-0.0024	0.0006	0.0021	0.0265	0.0003	0.0007
WP03-C2-S4	Vein Quartz	1546.4	0.0886	0.5036	8.7907	0.0115	0.1349	0.0054	-0.0011	0.0352	0.0152	-0.0007	0.0028	0.0001	-0.0042	0.0076	0.0031	0.0024
WP03-C3-S1	Vein Quartz	1546.4	0.0702	1.9958	11.9589	0.0181	0.0464	0.0039	-0.0058	0.0006	0.0077	0.0031	0.0017	-0.0002	-0.0077	-0.0022	0.0004	0.0007
WP03-C3-S2	Vein Quartz	1546.4	0.0811	1.7059	13.9429	0.0767	0.2029	0.0031	0.0193	0.0112	0.0239	0.0031	-0.0018	0.0007	0.0023	0.0327	0.0005	0.0001
WP03-C3-S3	Vein Quartz	1546.4	0.0445	1.7893	12.8330	0.0365	0.0477	-0.0005	-0.0191	-0.0030	0.0116	-0.0074	-0.0017	0.0005	0.0002	0.0081	0.0030	0.0011
WP03-C3-S4	Vein Quartz	1546.4	0.0263	1.8022	12.4682	0.0335	0.2555	0.0011	0.0035	-0.0024	0.0217	0.0017	-0.0005	0.0023	0.0004	0.0364	0.0024	0.0015
WP03-C4-S1	Vein Quartz	1546.4	0.0637	1.9487	13.1516	0.0474	0.1272	0.0030	0.0083	0.0093	0.0210	0.0152	-0.0025	-0.0002	0.0033	0.0532	0.0005	0.0003
WP03-C4-S2	Vein Quartz	1546.4	0.0100	1.4393	10.9930	0.0487	0.7207	0.0041	-0.0099	0.0232	0.0402	-0.0109	-0.0017	-0.0023	-0.0100	0.0400	0.0031	0.0016
WP03-C4-S3	Vein Quartz	1546.4	0.0603	1.9950	11.8602	0.0476	0.2072	0.0052	-0.0083	0.0140	0.0217	-0.0043	-0.0041	0.0013	-0.0088	0.0228	-0.0010	-0.0007
WP03-C4-S4	Vein Quartz	1546.4	0.0888	2.5033	10.7264	0.0232	0.0095	-0.0021	0.1813	-0.0102	0.0093	-0.0128	0.0045	-0.0010	-0.0111	0.0356	-0.0001	-0.0037
WP63-C1-S1	Breccia Cemen	0.0	0.0897	0.4159	0.0633	0.0590	0.0993	0.0035	0.0035	0.0302	0.0046	-0.0018	-0.0011	0.0020	-0.0012	0.0387	0.0000	-0.0023
WP63-C1-S2	Breccia Cemen	0.0	-0.0340	0.6155	0.1487	0.0515	0.1477	0.0045	-0.0090	-0.0069	0.0004	0.0056	-0.0023	-0.0011	-0.0083	0.0444	0.0016	0.0004
WP63-C1-S3	Breccia Cemen	0.0	-0.0244	0.4845	-0.0472	0.0530	0.0682	0.0040	0.0193	-0.0006	0.0016	0.0121	0.0048	0.0001	0.0036	0.0366	0.0016	-0.0013
WP63-C2-S1	Breccia Cemen	0.0	-0.0510	0.4606	0.0257	0.0506	0.0779	0.0051	-0.0008	0.0089	-0.0002	0.0008	0.0013	0.0004	0.0021	0.0294	0.0008	0.0000
WP63-C2-S2	Breccia Cemen	0.0	0.1889	0.5400	0.0295	0.0925	0.1292	0.0025	0.0198	0.0437	-0.0017	0.0111	0.0012	0.0014	-0.0030	0.0636	0.0043	0.0008
WP63-C2-S3	Breccia Cemen	0.0	0.0523	0.4440	0.0092	0.0593	0.1255	0.0026	0.0322	-0.0037	0.0057	0.0083	-0.0064	-0.0032	-0.0080	0.1556	-0.0060	0.0006
WP63-C3-S1	Breccia Cemen	0.0	0.4469	1.0941	-0.0566	0.1688	0.2057	-0.0008	0.1157	0.0045	0.0385	0.0163	0.0012	-0.0010	-0.0089	0.4697	0.0189	0.0020
WP02-C1-S1	Breccia Cemen	132.2	0.1764	1.5546	7.8596	0.0775	0.0170	-0.0028	-0.0027	0.0176	0.0021	0.0029	-0.0060	-0.0003	-0.0016	0.0274	-0.0001	-0.0004
WP02-C1-S2	Breccia Cemen	132.2	0.2046	1.5810	8.4454	0.5186	0.0925	0.0080	-0.0034	-0.0060	0.0519	0.0128	-0.0002	0.0006	-0.0033	0.0807	0.0023	0.0020
WP02-C1-S4	Breccia Cemen	132.2	-0.0341	1.5104	8.7945	0.0921	0.0732	0.0047	0.0064	0.0209	0.0033	0.0009	0.0004	-0.0008	0.0107	0.0389	-0.0013	-0.0004
WP02-C1-S5	Breccia Cemen	132.2	0.2644	1.5549	8.7210	0.0099	0.0307	0.0058	-0.0229	0.0188	-0.0016	-0.0144	0.0005	0.0005	-0.0010	0.1499	-0.0005	0.0008
WP02-C1-S6	Breccia Cemen	132.2	0.0837	1.7640	8.5670	0.0798	0.0510	0.0028	-0.0142	0.0137	0.0036	0.0010	0.0043	0.0000	-0.0010	0.2269	0.0013	-0.0011
WP02-C1-S7	Breccia Cemen	132.2	0.1578	1.3578	8.5554	0.0519	0.0770	0.0073	0.0092	0.0129	0.0054	0.0016	0.0006	0.0004	-0.0047	0.0737	0.0028	0.0007
WP02-C1-S9	Breccia Cemen	132.2	-0.0662	1.6947	8.2349	0.0491	0.0120	-0.0024	-0.0020	-0.0092	0.0031	-0.0093	0.0160	0.0015	0.0054	0.0075	0.0019	0.0017
WP02-C1-S10	Breccia Cemen	132.2	0.1843	1.7062	7.8654	0.0906	0.0336	0.0106	0.0021	-0.0092	0.0060	0.0113	-0.0002	0.0004	0.0038	0.0150	-0.0019	0.0009
WP02-C1-S11	Breccia Cemen	132.2	0.1173	1.5072	8.8277	0.0170	0.0782	-0.0071	0.0061	-0.0018	0.0018	-0.0022	0.0025	-0.0008	-0.0027	0.1409	0.0009	0.0031
WP02-C1-S12	Breccia Cemen	132.2	0.0340	1.6303	8.5158	0.0346	0.0582	0.0120	-0.0084	0.0079	-0.0071	0.0109	-0.0002	-0.0001	0.0075	0.0129	-0.0031	0.0023
WP02-C2-S1	Breccia Cemen	132.2	0.1447	0.4891	12.3342	0.1333	0.0165	0.0046	0.0017	0.0065	0.3755	-0.0141	0.0075	-0.0008	0.0057	0.0241	0.0013	0.0003

* distance from center of deposit

** All elements in ppm except Au which is in ppb

Appendix 6: White Pine
quartz mineral chemistry by LA-ICP-MS

Sample	Quartz sample type	Distance* (m)	Zn66	Ge74	As75	Rb85	Sr88	Zr90	Ag107	Sb121	Cs133	Gd157	Hf178	Ta181	Au197**	Pb208	Bi209	U238
WP02-C2-S2	Breccia Cemen	132.2	0.0929	0.5562	10.3063	0.0938	0.0495	0.0029	-0.0037	0.0093	0.0388	-0.0026	-0.0011	-0.0012	-0.0016	0.0184	-0.0002	0.0138
WP02-C2-S3	Breccia Cemen	132.2	0.0220	0.5599	10.4464	0.1522	0.0056	0.0073	-0.0071	-0.0013	0.2355	0.0116	0.0036	-0.0003	-0.0022	0.0178	0.0006	0.0020
WP02-C2-S4	Breccia Cemen	132.2	0.0249	0.5677	10.6182	0.1119	0.2631	0.0070	0.0117	-0.0009	0.1382	0.0153	-0.0057	0.0015	-0.0008	0.0370	-0.0026	-0.0012
WP03-C3-S1	Igneous quartz	1546.4	0.0130	2.8718	7.9098	0.0048	0.1803	0.0063	0.0001	0.0218	0.0095	0.0017	0.0011	0.0010	-0.0094	0.0073	0.0122	0.0037
WP03-C3-S2	Igneous quartz	1546.4	0.0032	2.6012	6.2991	0.0346	0.0475	-0.0005	0.0035	0.0134	0.0276	-0.0235	-0.0040	0.0018	-0.0083	-0.0008	0.0053	0.0002
WP03-C3-S3	Igneous quartz	1546.4	0.0723	3.2901	6.5885	0.0363	0.3454	0.0020	-0.0014	0.0306	0.0181	-0.0034	0.0035	-0.0008	0.0028	0.0122	0.0074	0.0075
WP03-C3-S4	Igneous quartz	1546.4	0.0167	2.8052	5.8861	0.0560	0.0851	-0.0004	-0.0077	0.0304	0.0225	-0.0028	-0.0028	0.0008	0.0050	0.1654	0.0752	0.0096
WP03-C3-S5	Igneous quartz	1546.4	0.0072	2.7650	6.7622	0.0046	0.0821	-0.0023	0.0104	0.0273	0.0091	-0.0063	-0.0031	-0.0005	-0.0022	0.3832	0.0679	0.0033
WP13-C1-S1	Igneous quartz	1553.6	-0.0630	0.4440	0.0283	0.0078	0.0192	-0.0004	0.0039	-0.0193	0.0012	0.0005	0.0056	-0.0014	0.0081	0.0374	-0.0037	0.0012
WP13-C1-S2	Igneous quartz	1553.6	0.1294	0.7826	-0.0514	0.1539	0.4224	0.0027	-0.0351	0.0349	0.0765	0.0059	0.0065	0.0003	-0.0088	0.1086	0.0090	0.0075
WP13-C1-S3	Igneous quartz	1553.6	-0.0518	0.4221	0.0456	-0.0214	0.0210	-0.0047	-0.0014	-0.0487	0.0034	-0.0021	-0.0027	0.0017	-0.0034	0.0059	0.0084	0.0011
WP13-C1-S4	Igneous quartz	1553.6	0.1046	0.9516	0.0261	0.1703	0.3740	0.0028	-0.0146	0.0365	0.0783	0.0050	0.0009	-0.0023	0.0075	0.0460	-0.0047	0.0011
WP22-C2-S1	Igneous quartz	2588.2	-0.0139	1.2145	0.0481	0.0214	0.0301	-0.0026	-0.0093	0.0115	0.0032	-0.0007	0.0029	0.0019	0.0047	0.0058	-0.0016	0.0004
WP22-C2-S2	Igneous quartz	2588.2	0.0945	1.1097	0.0507	0.0123	-0.0028	-0.0009	-0.0141	-0.0036	-0.0040	-0.0031	-0.0012	-0.0013	-0.0010	0.0153	-0.0004	-0.0004
WP22-C2-S3	Igneous quartz	2588.2	0.0256	1.6813	0.0999	0.0041	0.0036	0.0042	-0.0031	-0.0039	0.0002	-0.0041	0.0009	-0.0012	-0.0007	0.0042	-0.0017	0.0007
WP22-C2-S4	Igneous quartz	2588.2	0.0274	1.5865	-0.0155	-0.0027	0.0059	0.0000	0.0223	0.0022	0.0000	0.0000	0.0014	0.0000	-0.0103	0.0139	-0.0006	0.0015
WP22-C2-S5	Igneous quartz	2588.2	0.0028	1.5937	0.0692	0.0122	0.0200	-0.0009	0.0219	-0.0117	-0.0011	-0.0066	0.0079	0.0000	-0.0033	0.0884	0.0003	-0.0010
WP06-C1-S1	Igneous quartz	1429.0	0.2325	0.6457	0.1961	0.1714	0.2283	0.0185	-0.0025	-0.0010	0.0444	0.0043	0.0026	0.0002	0.0025	0.2585	0.0531	0.0606
WP06-C1-S2	Igneous quartz	1429.0	0.1090	2.4504	0.1593	0.0924	0.1030	0.0018	-0.0080	0.0305	0.0235	-0.0031	-0.0028	-0.0001	0.0012	0.0822	-0.0023	0.0000
WP06-C1-S3	Igneous quartz	1429.0	-0.0065	2.0460	0.1096	0.0226	0.0398	0.0084	-0.0049	0.0072	0.0049	-0.0003	-0.0049	-0.0009	0.0008	0.0043	0.0061	0.0016
WP06-C1-S4	Igneous quartz	1429.0	0.0595	2.0001	0.1762	0.0353	0.0683	-0.0002	0.0070	0.0032	0.0144	-0.0062	-0.0019	-0.0020	0.0005	0.0308	0.0046	0.0014
WP64-C4-S1	Igneous quartz	704.8	0.0033	1.2569	0.3434	0.0020	0.1009	0.0049	-0.0242	0.0260	0.0038	-0.0093	0.0009	0.0013	0.0062	68.7129	-0.0005	0.0005
WP64-C4-S2	Igneous quartz	704.8	0.0170	1.2287	0.1267	0.0494	0.0198	0.0008	-0.0243	-0.0010	0.0124	-0.0085	0.0004	0.0014	0.0048	0.0213	-0.0016	0.0004
WP64-C4-S3	Igneous quartz	704.8	0.0922	1.4038	0.0880	0.0107	0.1852	0.0053	0.0099	0.0104	0.0059	0.0073	0.0002	-0.0019	0.0034	22.6847	0.0029	0.0001
WP64-C4-S3	Igneous quartz	704.8	0.0361	1.0932	-0.0082	0.0072	0.0489	0.0035	0.0087	-0.0024	0.0004	0.0079	-0.0034	0.0013	0.0099	1.6364	0.0030	0.0004
WP52-C1-S1	Igneous quartz	785.5	0.1607	0.4634	0.0751	0.0090	0.2185	0.0018	0.0133	-0.0172	0.0192	-0.0127	-0.0009	-0.0008	0.0062	0.0786	0.0068	0.0001
WP52-C1-S2	Igneous quartz	785.5	0.0427	0.5427	0.1261	0.0697	0.1796	0.0048	-0.0036	-0.0041	0.0075	-0.0033	0.0013	0.0000	-0.0003	0.0524	-0.0041	0.0037
WP52-C1-S3	Igneous quartz	785.5	8.9576	0.7937	0.3381	0.1139	0.6416	0.0059	0.0251	0.0215	0.0470	-0.0134	0.0053	0.0012	0.0005	3.2924	0.3709	0.1523
WP52-C2-S1	Igneous quartz	785.5	-0.0435	1.6010	0.2094	0.0199	0.1042	-0.0041	-0.0207	-0.0228	0.0077	0.0051	-0.0004	-0.0012	-0.0022	0.0253	0.0123	0.0082
WP52-C2-S2	Igneous quartz	785.5	0.0487	1.3632	0.1022	0.0435	0.0950	0.0046	-0.0017	0.0108	0.0178	-0.0036	-0.0026	-0.0017	0.0039	-0.0002	-0.0020	0.0001
WP52-C2-S3	Igneous quartz	785.5	0.1901	1.9462	0.1084	0.0840	0.6079	0.0186	0.0089	0.0635	0.0143	0.0007	-0.0007	0.0000	-0.0171	0.0304	0.0004	0.0023
WP52-C2-S4	Igneous quartz	785.5	0.0426	1.3871	0.0625	0.0731	0.3991	-0.0017	-0.0138	0.0082	0.0452	-0.0024	0.0036	0.0011	-0.0030	0.0151	0.0016	0.0006
WP65-C1-S1	Igneous quartz	609.4	0.2360	0.9623	-0.1361	0.0058	0.0333	-0.0072	-0.0354	0.0282	-0.0005	0.0036	-0.0095	0.0001	-0.0018	0.0680	-0.0051	0.0007
WP65-C1-S3	Igneous quartz	609.4	0.1177	0.9374	0.0453	-0.0072	0.0089	-0.0030	0.0049	-0.0055	0.0001	0.0012	-0.0042	0.0021	-0.0093	-0.0003	0.0003	0.0008
WP65-C1-S4	Igneous quartz	609.4	0.0860	0.9167	0.0576	0.0018	0.0027	-0.0025	-0.0027	-0.0157	0.0058	0.0079	0.0011	-0.0012	-0.0010	-0.0025	0.0030	-0.0007
WP23-C1-S1	Igneous quartz	1688.3	0.0336	0.5868	4.2811	0.0031	0.0567	0.0011	-0.0053	0.0027	0.0080	-0.0045	0.0041	0.0007	0.0041	0.0218	0.0008	0.0000
WP23-C1-S2	Igneous quartz	1688.3	0.0606	0.6491	2.6431	0.0990	0.0879	-0.0008	-0.0032	-0.0006	0.0226	-0.0036	0.0147	-0.0023	-0.0059	0.0466	0.0008	0.0498
WP23-C1-S3	Igneous quartz	1688.3	0.1042	0.5857	2.6144	0.0012	0.0254	0.0028	-0.0118	-0.0027	0.0012	-0.0016	0.0002	0.0131	-0.0047	0.0134	0.0014	0.0024
WP23-C1-S4	Igneous quartz	1688.3	0.1593	0.6047	2.5523	0.0689	0.0859	0.0138	-0.0088	0.0234	0.0260	-0.0011	-0.0027	0.0025	-0.0026	0.1201	0.0043	0.0150
WP23-C2-S1	Igneous quartz	1688.3	0.0439	0.5922	2.3219	0.0679	0.0523	0.0064	0.0117	0.0037	0.0204	0.0047	0.0029	-0.0001	0.0060	0.0240	0.0027	0.0009
WP23-C2-S2	Igneous quartz	1688.3	0.0486	0.5307	2.2533	0.0323	0.0293	-0.0004	-0.0035	-0.0045	0.0081	-0.0063	0.0015	0.0005	0.0020	0.0108	0.0296	0.0007
WP23-C2-S3	Igneous quartz	1688.3	0.0129	0.5595	2.2946	0.0321	0.0709	0.0016	-0.0053	-0.0083	0.0387	0.0078	0.0038	0.0008	0.0000	0.0242	0.0016	0.0005
WP23-C2-S4	Igneous quartz	1688.3	0.1488	0.5417	1.6493	0.0369	0.0929	-0.0049	0.0133	0.0086	0.0237	0.0031	-0.0013	-0.0009	0.0116	0.0182	-0.0005	0.0010
WP07-C4-S1	Igneous quartz	1360.2	-0.0181	0.4176	7.7669	0.0780	0.0253	0.0069	0.0056	0.0096	0.0075	0.0068	-0.0039	-0.0012	-0.0046	0.0178	-0.0015	-0.0018
WP07-C4-S2	Igneous quartz	1360.2	0.1462	0.5253	7.3333	0.0592	0.0115	-0.0031	0.0005	0.2554	0.0225	-0.0098	-0.0004	0.0011	0.0069	-0.0025	0.0006	0.0002
WP07-C4-S3	Igneous quartz	1360.2	0.0201	0.4070	6.9260	0.0330	0.0100	0.0034	0.0016	0.0008	0.0017	-0.0092	0.0038	0.0007	0.0012	0.0149	-0.0014	-0.0003
WP07-C4-S4	Igneous quartz	1360.2	0.0671	0.5259	7.2857	0.0317	0.0058	-0.0020	0.0049	0.0266	-0.0001	0.0049	0.0003	-0.0013	-0.0052	0.0115	-0.0001	-0.0001

* distance from center of deposit

** All elements in ppm except Au which is in ppb

Appendix 6: White Pine
quartz mineral chemistry by LA-ICP-MS

Sample	Sample type	Distance*																
		(m)	Li7	Na23	Mg24	Al27	Si29	P31	K39	Ca43	Ti47	Ti49	V51	Cr53	Mn55	Fe57	Cu63	
WP46-C1-S1	Vein Quartz	372.6	3.115	2.060	0.5250	72.02	467500	18.56	1.684	-89.21	57.12	54.77	0.01701	0.1784	0.1415	3.254	0.08579	
WP46-C1-S2	Vein Quartz	372.6	4.892	-0.9230	0.1792	65.93	467500	17.33	0.9393	37.69	58.32	57.62	0.004538	0.1527	0.06294	1.672	0.06668	
WP46-C1-S3	Vein Quartz	372.6	2.202	0.3262	0.1708	49.71	467500	15.70	-0.04945	13.50	28.93	28.64	-0.0004721	-0.05786	0.06879	-0.1732	0.06125	
WP46-C1-S4	Vein Quartz	372.6	3.757	2.463	0.2400	92.61	467500	16.66	50.60	6.870	50.88	52.33	0.04853	0.1018	0.09457	0.6884	0.01006	
WP46-C1-S5	Vein Quartz	372.6	1.828	3.038	0.1551	53.15	467500	14.87	14.64	14.18	79.29	84.53	0.06009	0.1696	0.07049	1.212	0.01070	
WP46-C1-S6	Vein Quartz	372.6	6.170	0.2956	0.2602	89.52	467500	11.02	9.899	20.44	60.51	61.84	-0.001147	0.03993	0.1010	1.231	0.1556	
WP46-C1-S7	Vein Quartz	372.6	1.305	1.355	0.4967	54.13	467500	16.29	6.894	-29.62	42.63	44.90	-0.002974	-0.05536	0.1071	6.440	0.1176	
WP46-C1-S8	Vein Quartz	372.6	2.061	1.738	0.3583	61.67	467500	15.81	29.31	-5.956	72.85	71.59	0.06968	0.09950	0.07081	9.370	0.8023	
WP46-C1-S9	Vein Quartz	372.6	2.365	16.28	0.5572	63.14	467500	18.69	6.483	-22.64	52.20	52.55	0.01469	-0.08000	0.1083	10.22	0.1114	
WP46-C1-S10	Vein Quartz	372.6	2.456	5.787	0.2535	75.21	467500	15.17	20.10	6.556	54.40	54.97	0.01072	0.008719	0.1299	1.240	0.2646	
WP46-C1-S11	Vein Quartz	372.6	1.486	0.9336	0.4081	41.66	467500	19.12	3.398	49.50	33.99	34.23	0.01296	0.005721	0.04804	3.273	0.1604	
WP46-C1-S12	Vein Quartz	372.6	4.123	2.432	0.2358	66.01	467500	17.69	0.7698	1.136	47.50	47.30	-0.003084	0.05472	0.05590	-0.05088	0.05286	
WP46-C1-S13	Vein Quartz	372.6	4.070	1.525	0.2241	66.30	467500	12.54	-0.1867	13.68	37.74	39.38	0.007873	-0.1411	0.04720	0.1776	0.01212	
WP46-C1-S14	Vein Quartz	372.6	3.264	-2.232	0.4567	69.40	467500	18.61	6.730	65.23	42.18	42.98	0.01539	0.01263	0.07965	1.923	0.08608	
WP46-C1-S15	Vein Quartz	372.6	3.280	-0.8833	0.2192	67.84	467500	10.47	2.286	-1.828	44.20	45.26	-0.001742	0.1340	0.09433	0.6599	0.0006844	
WP03-C1-S1	Vein Quartz	1546.4	0.6944	34.89	0.01361	30.55	467500	10.70	5.108	30.37	4.976	3.503	-0.008543	0.002154	0.04588	0.2017	0.1735	
WP03-C1-S2	Vein Quartz	1546.4	5.777	23.52	0.1002	176.6	467500	15.91	22.63	0.7037	12.52	12.27	0.0005495	0.02868	0.3737	0.9958	0.7343	
WP03-C1-S3	Vein Quartz	1546.4	7.432	12.85	5.510	165.8	467500	16.42	10.99	-1.508	13.05	12.98	0.02159	-0.06005	0.4835	21.96	1.834	
WP03-C1-S4	Vein Quartz	1546.4	1.561	9.704	0.2662	57.78	467500	15.26	5.914	7.786	7.627	6.809	0.005359	0.05607	0.09426	6.601	0.3651	
WP03-C1-S5	Vein Quartz	1546.4	0.1652	11.92	0.1520	10.55	467500	15.67	3.124	23.47	1.410	1.299	0.01414	0.02003	0.04044	4.545	0.1579	
WP03-C2-S1	Vein Quartz	1546.4	4.060	4.992	-0.02095	101.0	467500	14.82	1.624	23.11	9.237	8.665	0.01189	0.05493	0.08423	2.200	0.02891	
WP03-C2-S2	Vein Quartz	1546.4	4.272	3.551	0.1344	76.24	467500	15.61	1.923	-12.70	7.806	8.716	0.006900	-0.08766	0.08689	0.1727	0.1908	
WP03-C2-S3	Vein Quartz	1546.4	1.429	6.347	0.02700	47.69	467500	13.09	1.661	70.76	5.950	6.492	-0.001375	-0.07709	-0.0007446	0.8498	0.002431	
WP03-C2-S4	Vein Quartz	1546.4	1.716	19.73	0.1335	61.27	467500	13.25	2.202	16.84	8.302	8.144	-0.009690	-0.09256	0.1199	1.548	0.1650	
WP03-C2-S5	Vein Quartz	1546.4	3.088	10.71	0.05669	81.49	467500	18.21	1.762	3.709	9.349	7.853	-0.006925	0.06270	0.1492	9.792	0.1313	
WP13-C3-S1	Vein Quartz	1553.6	5.097	-1.737	0.03440	53.01	467500	19.45	0.09246	74.26	35.48	37.01	-0.01213	0.1202	0.03730	-0.1924	0.03195	
WP13-C3-S2	Vein Quartz	1553.6	5.730	1.024	0.02898	57.12	467500	20.25	-0.4549	23.13	33.44	33.58	0.007780	0.03880	0.03509	-0.8015	-0.01002	
WP13-C3-S3	Vein Quartz	1553.6	4.318	-0.1257	0.06743	47.95	467500	23.14	-0.4864	-47.59	33.95	34.83	-0.01268	-0.0008132	0.03473	0.3324	-0.09059	
WP13-C3-S4	Vein Quartz	1553.6	5.048	6.963	0.1275	62.90	467500	18.96	2.019	-19.20	37.67	39.57	0.01291	0.04919	0.04477	0.5272	0.08202	
WP13-C5-S1	Vein Quartz	1553.6	4.017	2.096	0.4885	48.77	467500	18.71	5.119	-32.76	42.97	45.37	-0.01155	-0.05915	0.02677	0.4709	0.09146	
WP13-C5-S2	Vein Quartz	1553.6	4.603	4.432	0.2672	73.13	467500	17.17	3.531	-46.61	44.84	47.23	0.005388	-0.005312	-0.02644	1.017	0.05622	
WP13-C5-S3	Vein Quartz	1553.6	3.344	1.436	2.555	47.06	467500	21.28	1.035	28.72	45.76	46.30	-0.009031	-0.07420	0.06333	0.6801	0.07553	
WP13-C5-S4	Vein Quartz	1553.6	2.354	-2.805	0.3458	31.80	467500	18.76	0.8515	17.08	34.28	34.42	0.001724	-0.04116	0.02394	1.316	0.04134	
WP22-C4-S1	Vein Quartz	2588.2	1.860	-0.3018	0.02222	29.90	467500	19.64	-0.5035	43.76	1.018	0.8855	0.005246	-0.1119	0.02488	-1.830	0.007948	
WP22-C4-S2	Vein Quartz	2588.2	0.5366	0.2764	0.03097	19.04	467500	17.43	-0.7301	227.4	1.509	0.4858	0.002700	-0.07345	0.04858	5.066	0.06515	
WP22-C4-S3	Vein Quartz	2588.2	0.5548	15.65	0.03611	24.43	467500	18.84	5.349	35.16	1.336	1.128	0.005118	-0.04778	0.09125	7.648	0.3301	
WP22-C4-S4	Vein Quartz	2588.2	0.8813	-0.5892	0.05094	26.87	467500	16.68	0.3945	27.06	1.859	1.347	0.01430	-0.1994	0.02362	21.89	0.2960	
WP22-C4-S5	Vein Quartz	2588.2	0.6348	31.98	0.2016	31.34	467500	14.81	7.234	43.45	1.448	1.316	-0.0005951	0.01746	0.4451	22.21	0.7688	
WP06-C2-S1	Vein Quartz	1429.0	5.700	1.001	0.1680	67.96	467500	15.52	4.308	45.58	52.74	54.53	0.004509	-0.02811	0.09874	0.7276	0.02283	
WP06-C2-S2	Vein Quartz	1429.0	4.864	-2.477	0.07532	59.85	467500	13.64	3.190	11.00	48.70	48.00	0.005961	-0.04075	0.1144	0.9605	0.02357	
WP06-C2-S3	Vein Quartz	1429.0	5.152	-0.1475	0.1070	61.08	467500	12.12	5.534	-14.83	46.91	48.73	-0.00006058	0.06094	0.1073	-0.1165	0.01576	
WP06-C2-S4	Vein Quartz	1429.0	5.232	-3.317	0.09683	59.15	467500	11.96	3.846	-12.12	37.69	39.57	-0.001213	-0.01476	0.08377	0.5657	0.02031	
WP06-C3-S2	Vein Quartz	1429.0	2.377	115.4	0.4570	101.2	467500	17.17	19.16	111.9	25.77	26.62	0.04705	0.1013	0.4509	2.800	0.1104	

* distance from center of deposit

** All elements in ppm except Au which is in ppb

Appendix 6: White Pine
quartz mineral chemistry by LA-ICP-MS

Sample	Sample type	Distance*																
		(m)	Li7	Na23	Mg24	Al27	Si29	P31	K39	Ca43	Ti47	Ti49	V51	Cr53	Mn55	Fe57	Cu63	
WP06-C3-S3	Vein Quartz	1429.0	4.160	7.902	0.1424	66.07	467500	15.02	6.515	-37.50	47.34	48.90	0.01151	0.1437	0.1205	7.241	0.1898	
WP06-C3-S4	Vein Quartz	1429.0	3.201	-1.026	0.1547	40.96	467500	14.73	2.252	14.12	43.10	43.04	-0.01173	0.1131	0.07962	0.2779	-0.009502	
WP53-C1-S1	Vein Quartz	548.8	1.446	36.44	0.1465	69.12	467500	16.29	14.74	45.51	44.36	45.06	-0.003232	0.1542	0.1461	-0.4923	0.5633	
WP53-C1-S2	Vein Quartz	548.8	1.087	130.2	0.2918	79.48	467500	17.90	29.44	-5.182	43.87	42.97	0.005612	-0.05620	0.2335	1.968	0.1035	
WP53-C1-S3	Vein Quartz	548.8	3.313	1.526	0.1832	81.06	467500	19.00	8.306	-18.16	58.99	58.99	-0.0008343	0.05305	0.09485	0.4756	0.06311	
WP53-C1-S4	Vein Quartz	548.8	1.840	17.26	0.1469	75.50	467500	15.12	13.05	-21.37	58.91	58.15	-0.0002907	0.1106	0.1197	-0.03684	0.2786	
WP53-C1-S5	Vein Quartz	548.8	0.8511	14.36	0.1379	28.11	467500	17.10	1.536	-17.58	17.30	15.92	-0.002499	-0.009284	0.03658	0.3511	0.2335	
WP53-C2-S1	Vein Quartz	548.8	1.371	10.87	0.2559	47.20	467500	15.89	3.520	-6.236	41.37	40.02	0.01530	0.1553	1.811	22.64	1.587	
WP53-C2-S2	Vein Quartz	548.8	1.432	16.82	0.1861	39.19	467500	16.25	3.891	-32.59	39.07	37.35	-0.004527	0.005073	0.1194	2.341	0.08556	
WP53-C2-S3	Vein Quartz	548.8	0.6940	35.59	0.3602	116.4	467500	16.04	32.05	8.403	68.40	66.40	-0.005128	0.08007	0.2893	2.251	0.3183	
WP53-C2-S4	Vein Quartz	548.8	1.761	8.095	0.2666	66.02	467500	14.88	11.12	-30.43	51.96	52.38	0.002398	-0.1381	0.1608	1.364	0.07856	
WP53-C2-S5	Vein Quartz	548.8	0.7916	38.93	0.7956	65.73	467500	17.06	14.47	31.76	26.66	28.29	0.005615	-0.007097	1.426	7.029	1.892	
WP05-C1-S1	Vein Quartz	1429.0	3.300	-0.1922	0.06666	53.62	467500	13.72	1.205	21.18	51.40	52.90	0.0001884	-0.0007950	0.1239	2.821	0.01292	
WP05-C1-S2	Vein Quartz	1429.0	1.268	22.01	0.06363	34.38	467500	13.89	2.489	-40.01	42.61	41.96	0.003387	0.09307	0.009731	0.1487	1.176	
WP05-C1-S3	Vein Quartz	1429.0	2.022	1.577	0.2312	42.13	467500	15.37	2.608	26.59	47.82	50.34	-0.001397	-0.04722	0.06550	0.03966	0.07393	
WP05-C1-S4	Vein Quartz	1429.0	3.294	-0.6730	0.1648	46.82	467500	15.12	0.4434	-23.71	59.12	58.99	-0.01302	0.1381	0.07063	-0.3509	0.03968	
WP05-C2-S1	Vein Quartz	1429.0	1.033	0.7886	0.3402	26.75	467500	17.85	2.042	-17.39	38.19	36.30	0.01090	0.02770	0.07519	-0.04887	0.7079	
WP05-C2-S2	Vein Quartz	1429.0	0.8433	8.102	0.1222	27.68	467500	14.49	2.749	-46.92	16.91	18.20	-0.002389	-0.1702	0.1303	-0.04475	1.573	
WP05-C2-S3	Vein Quartz	1429.0	1.119	-0.4103	0.4570	25.45	467500	16.79	-0.1839	15.93	43.24	41.61	-0.001222	-0.1389	0.01227	0.4700	0.4159	
WP05-C2-S4	Vein Quartz	1429.0	2.286	-0.3917	0.3945	39.21	467500	16.30	1.496	28.08	36.12	35.61	0.001788	-0.08100	0.05185	0.7866	0.02728	
WP05-C2-S5	Vein Quartz	1429.0	2.007	0.2918	0.2861	42.41	467500	14.94	2.868	3.702	47.06	47.11	0.003253	0.08302	0.04013	0.7656	0.006932	
WP05-C3-S1	Vein Quartz	1429.0	1.963	78.58	0.3046	57.33	467500	13.05	7.414	10.95	1.477	1.324	-0.002934	-0.07741	0.09210	3.039	0.08720	
WP05-C3-S2	Vein Quartz	1429.0	4.822	3.399	0.04237	88.51	467500	14.48	7.568	-2.987	2.907	2.019	0.006992	-0.1343	0.08850	0.3029	0.3877	
WP05-C3-S3	Vein Quartz	1429.0	1.054	1.684	0.1265	31.52	467500	16.23	0.3270	23.09	0.8640	3.228	0.01895	-0.02123	0.2048	-1.380	0.06640	
WP05-C3-S4	Vein Quartz	1429.0	2.983	19.56	0.3854	68.35	467500	12.53	6.657	22.66	1.725	1.306	-0.005588	0.04184	0.09896	-0.4323	3.162	
WP64-C1-S1	Vein Quartz	704.8	1.399	5.115	0.3400	32.22	467500	21.33	1.153	30.43	1.223	0.8229	0.01044	0.04027	0.01395	7.266	0.2037	
WP64-C1-S2	Vein Quartz	704.8	3.018	2.773	0.4207	50.28	467500	23.54	5.559	3.012	1.988	1.325	-0.004857	0.08569	0.05427	6.918	0.2175	
WP64-C1-S3	Vein Quartz	704.8	3.067	9.199	0.3489	41.75	467500	19.64	5.213	-22.56	1.949	0.6303	0.004243	-0.2399	0.1155	8.368	0.3117	
WP64-C1-S4	Vein Quartz	704.8	5.310	0.5542	1.879	81.95	467500	19.02	22.18	16.89	2.642	1.890	0.02769	-0.08258	0.2167	3.359	0.07382	
WP64-C2-S1	Vein Quartz	704.8	3.894	18.42	5.830	145.4	467500	23.44	67.85	-89.56	2.982	2.059	0.1553	-0.1051	0.5388	34.10	3.425	
WP64-C2-S2	Vein Quartz	704.8	3.786	-2.402	8.468	163.7	467500	23.05	68.32	35.46	4.368	4.502	0.1715	-0.1277	0.5810	5.441	0.1442	
WP64-C2-S4	Vein Quartz	704.8	7.889	46.39	2.287	177.6	467500	20.43	49.45	10.61	2.695	2.232	0.03834	0.2008	0.7877	3.041	1.682	
WP64-C3-S1	Vein Quartz	704.8	1.692	-0.1181	-0.005337	17.37	467500	21.17	-0.2176	-14.31	4.286	3.130	0.006720	0.05555	0.03264	0.7621	0.1144	
WP64-C3-S2	Vein Quartz	704.8	5.617	32.62	1.770	121.2	467500	19.12	28.61	-49.55	1.949	1.861	0.02597	-0.1208	0.3133	34.47	6.929	
WP64-C3-S3	Vein Quartz	704.8	4.795	4.930	0.8909	73.73	467500	25.65	7.975	-65.22	1.974	1.380	0.01317	-0.2510	0.4423	114.4	5.069	
WP52-C3-S1	Vein Quartz	785.5	1.923	-3.821	0.2225	85.14	467500	14.86	14.29	1.874	57.97	58.73	-0.002183	0.05939	0.2045	1.276	0.0006282	
WP52-C3-S2	Vein Quartz	785.5	1.230	-0.2208	0.1568	49.59	467500	12.58	1.936	6.236	50.83	50.96	-0.003864	-0.03990	0.06888	0.5794	0.03709	
WP52-C3-S3	Vein Quartz	785.5	0.4682	23.16	0.09896	56.54	467500	14.97	1.908	40.60	67.93	69.07	0.02310	0.04302	0.09865	26.49	0.1993	
WP52-C3-S4	Vein Quartz	785.5	1.099	-2.245	0.1825	60.00	467500	11.52	6.467	33.05	75.44	71.16	-0.001408	-0.1112	0.1942	5.877	0.01080	
WP65-C2-S3	Vein Quartz	609.4	4.033	68.58	8.649	161.3	467500	15.30	91.10	82.60	9.808	10.72	0.06440	0.1068	0.08899	53.83	0.2698	
WP65-C2-S4	Vein Quartz	609.4	6.513	0.9475	0.8971	65.85	467500	13.52	3.808	38.21	10.82	11.36	0.004282	0.1396	0.06494	166.4	0.09695	
WP65-C3-S1	Vein Quartz	609.4	8.587	-5.008	0.3441	88.19	467500	11.77	2.902	16.64	38.79	37.05	-0.003493	0.05209	0.1149	1.128	-0.002299	
WP65-C3-S2	Vein Quartz	609.4	7.689	-2.344	0.5447	71.99	467500	13.23	1.493	18.75	32.78	32.87	0.004333	0.03678	0.1340	2.978	0.5019	

* distance from center of deposit

** All elements in ppm except Au which is in ppb

Appendix 6: White Pine
quartz mineral chemistry by LA-ICP-MS

Sample	Sample type	Distance*																
		(m)	Li7	Na23	Mg24	Al27	Si29	P31	K39	Ca43	Ti47	Ti49	V51	Cr53	Mn55	Fe57	Cu63	
WP65-C3-S3	Vein Quartz	609.4	7.823	2.255	0.3204	75.74	467500	14.42	0.9135	-4.555	33.66	35.11	0.008975	0.09385	0.08984	1.404	0.2222	
WP65-C3-S4	Vein Quartz	609.4	9.514	-2.035	0.2550	107.8	467500	13.32	31.56	25.62	34.20	34.99	-0.002821	-0.02371	0.1069	0.9806	0.004693	
WP65-C4-S1	Vein Quartz	609.4	5.495	-2.627	0.9078	58.06	467500	15.66	5.453	-6.433	34.94	34.96	-0.008542	0.1118	0.1837	1.974	0.7190	
WP65-C4-S2	Vein Quartz	609.4	5.410	-2.114	0.1675	50.81	467500	12.35	4.262	-22.04	33.23	34.24	0.007092	0.0005882	0.05433	0.9066	0.1347	
WP65-C4-S3	Vein Quartz	609.4	4.540	-1.929	0.08223	43.76	467500	15.57	-1.546	10.87	31.60	31.34	0.01865	-0.04968	0.03433	-0.06610	0.02107	
WP65-C4-S4	Vein Quartz	609.4	2.747	5.459	0.2945	38.08	467500	15.64	3.067	-98.10	28.43	26.15	0.06562	-0.005827	0.01184	12.06	0.4867	
WP23-C5-S2	Vein Quartz	1688.3	10.29	-1.545	0.9349	142.5	467500	13.16	22.91	51.23	17.63	16.97	0.008799	0.04834	0.2953	12.78	0.1376	
WP07-C1-S3	Vein Quartz	1360.2	2.076	13.86	1.230	58.12	467500	23.43	3.571	71.58	28.62	26.79	0.01965	-0.02284	0.1438	8.178	0.2898	
WP07-C1-S4	Vein Quartz	1360.2	1.245	4.745	0.2476	36.86	467500	24.11	1.944	10.64	25.76	27.21	0.004225	-0.1532	0.1097	10.73	0.3793	
WP07-C2-S1	Vein Quartz	1360.2	5.422	-0.8085	0.1480	60.60	467500	19.90	3.708	9.186	45.42	43.79	0.001749	0.1472	0.1284	0.3621	0.1455	
WP07-C2-S2	Vein Quartz	1360.2	5.418	-0.1710	0.2047	66.39	467500	19.53	6.640	-17.65	45.60	42.77	-0.0004029	-0.01686	0.08389	0.8538	0.002219	
WP07-C2-S3	Vein Quartz	1360.2	4.040	7.227	0.4896	84.16	467500	18.85	19.97	-63.29	56.38	54.14	0.004854	-0.1523	0.2782	2.032	0.3020	
WP07-C4-S1	Vein Quartz	1360.2	3.959	1.111	-0.03324	53.46	467500	24.99	6.314	-46.90	33.65	35.22	-0.01255	0.04598	0.1571	3.084	0.03083	
WP07-C4-S2	Vein Quartz	1360.2	4.989	6.338	0.1488	56.81	467500	17.24	5.251	26.28	42.37	42.39	0.01088	-0.02482	0.1004	2.143	0.1398	
WP07-C4-S3	Vein Quartz	1360.2	4.361	1.546	0.1097	49.45	467500	18.15	3.770	19.54	47.26	47.67	0.002908	-0.02295	0.09493	0.4794	0.1471	
WP07-C4-S4	Vein Quartz	1360.2	4.885	1.244	0.1393	52.20	467500	16.68	4.003	-8.277	42.79	42.26	0.003565	0.09693	0.1083	1.200	0.07494	
WP07-C1-S1	Vein Quartz	1360.2	2.607	54.68	0.6480	127.1	467500	125.1	6.562	58.51	36.05	36.25	0.01691	0.1469	0.1091	621.9	2.255	
WP07-C1-S3	Vein Quartz	1360.2	2.076	13.86	1.230	58.12	467500	23.43	3.571	71.58	28.62	26.79	0.01965	-0.02284	0.1438	8.178	0.2898	
WP07-C1-S4	Vein Quartz	1360.2	1.319	5.373	1.417	38.76	467500	23.58	2.210	11.51	29.47	25.57	0.005990	-0.09665	0.1197	55.84	1.408	
WP07-C2-S1	Vein Quartz	1360.2	5.610	-0.6459	0.1779	61.40	467500	19.91	4.438	7.790	44.21	43.97	0.01127	0.1838	0.1613	0.8100	0.1584	
WP07-C2-S2	Vein Quartz	1360.2	5.395	-0.3353	0.2430	67.84	467500	20.58	8.357	-18.77	45.56	44.61	0.007249	0.004460	0.06699	1.784	-0.004624	
WP07-C2-S3	Vein Quartz	1360.2	5.843	13.54	0.2166	63.95	467500	17.61	15.20	-6.498	63.85	61.50	0.003953	-0.04135	0.1340	2.329	0.1531	
WP03-C1-S1	Vein Quartz	1546.4	2.596	5.734	0.2171	28.76	467500	14.92	1.247	12.96	26.72	25.80	-0.02083	0.1429	0.1199	3.762	0.09855	
WP03-C1-S2	Vein Quartz	1546.4	6.160	3.506	0.04459	59.05	467500	14.83	2.879	-22.70	45.61	45.53	0.002492	-0.02244	0.1261	-0.1322	-0.02079	
WP03-C1-S3	Vein Quartz	1546.4	6.936	0.7479	0.05571	64.04	467500	11.51	1.535	86.29	48.01	47.57	-0.002273	-0.03463	0.05150	-0.5329	-0.06139	
WP03-C1-S4	Vein Quartz	1546.4	6.710	0.8256	0.07882	58.90	467500	8.930	2.529	0.4893	47.77	47.98	-0.01016	0.1418	0.04447	0.5569	-0.03774	
WP03-C2-S2	Vein Quartz	1546.4	5.713	0.7342	0.08858	53.67	467500	14.30	4.561	15.05	42.22	43.99	-0.01853	-0.01207	0.07737	0.5252	0.03432	
WP03-C2-S3	Vein Quartz	1546.4	7.881	9.613	0.06711	80.70	467500	12.48	12.28	27.44	63.24	62.69	-0.009802	-0.02203	0.09481	0.2299	0.003716	
WP03-C2-S4	Vein Quartz	1546.4	7.403	0.8722	0.04775	69.56	467500	13.38	1.443	25.89	44.96	43.80	-0.006654	-0.03503	0.06797	-0.3579	-0.004712	
WP03-C3-S1	Vein Quartz	1546.4	1.756	6.969	0.02192	24.29	467500	12.06	1.960	18.96	2.212	2.143	-0.009113	-0.2117	0.07315	0.5008	-0.004049	
WP03-C3-S2	Vein Quartz	1546.4	1.361	30.40	0.1524	24.23	467500	12.74	4.435	10.26	3.753	3.355	0.0001946	-0.08571	0.1461	0.9373	0.8075	
WP03-C3-S3	Vein Quartz	1546.4	1.253	13.37	0.05840	15.96	467500	11.95	3.461	-5.698	2.266	1.659	-0.009129	0.09251	0.003554	-0.002278	0.02643	
WP03-C3-S4	Vein Quartz	1546.4	0.9683	23.15	0.1449	20.63	467500	11.57	3.569	41.54	1.875	1.768	0.01237	0.05247	0.07200	1.533	0.9953	
WP03-C4-S1	Vein Quartz	1546.4	1.123	17.73	0.08497	22.45	467500	11.93	6.002	18.14	2.228	2.701	0.01724	-0.04874	0.03882	-0.2221	0.1693	
WP03-C4-S2	Vein Quartz	1546.4	1.008	58.26	0.4345	21.46	467500	13.15	4.690	54.13	1.226	1.536	-0.01147	-0.2251	0.09446	24.07	0.2991	
WP03-C4-S3	Vein Quartz	1546.4	2.149	21.80	0.07258	28.59	467500	13.15	1.785	-48.30	3.628	3.290	0.009065	0.02659	0.03888	10.26	0.1300	
WP03-C4-S4	Vein Quartz	1546.4	0.8230	5.787	0.01742	15.09	467500	13.69	1.060	82.85	1.848	1.960	0.01020	0.02353	0.06315	-0.06722	0.8516	
WP63-C1-S1	Breccia Cement	0.0	4.337	0.9527	0.2291	74.21	467500	14.11	10.92	-3.804	67.63	68.10	0.01324	0.009924	0.1836	1.158	0.06110	
WP63-C1-S2	Breccia Cement	0.0	5.013	-1.043	0.1972	76.71	467500	12.42	12.46	15.25	66.74	68.13	0.001999	0.03027	0.2094	-0.8536	0.05091	
WP63-C1-S3	Breccia Cement	0.0	3.747	2.546	0.1550	65.88	467500	12.62	8.416	6.108	56.79	51.40	-0.01440	0.1389	0.1193	-0.1910	0.08092	
WP63-C2-S1	Breccia Cement	0.0	6.033	1.188	0.1733	75.32	467500	12.97	9.116	-11.68	70.93	73.73	-0.005292	0.01256	0.2223	1.504	-0.05102	
WP63-C2-S2	Breccia Cement	0.0	5.979	1.524	0.3203	75.00	467500	12.72	20.63	-23.79	62.92	67.26	-0.0009943	0.05670	0.2114	1.784	-0.01452	
WP63-C2-S3	Breccia Cement	0.0	5.834	-1.473	0.2050	76.27	467500	10.11	10.71	19.76	58.37	61.08	-0.003579	-0.06875	0.1613	4.734	-0.05154	

* distance from center of deposit

** All elements in ppm except Au which is in ppb

Appendix 6: White Pine
quartz mineral chemistry by LA-ICP-MS

Sample	Sample type	Distance*															
		(m)	Li7	Na23	Mg24	Al27	Si29	P31	K39	Ca43	Ti47	Ti49	V51	Cr53	Mn55	Fe57	Cu63
WP63-C3-S1	Breccia Cement	0.0	2.686	83.99	3.295	115.5	467500	13.47	29.44	24.41	34.24	34.46	0.06401	-0.01634	0.2013	31.46	2.337
WP02-C1-S1	Breccia Cement	132.2	3.281	-0.09597	1.479	71.77	467500	13.72	14.74	-0.9718	16.10	16.78	0.02980	0.1049	0.1257	2.428	0.005790
WP02-C1-S2	Breccia Cement	132.2	3.469	29.81	5.992	202.0	467500	14.35	101.1	49.03	26.47	23.83	0.1701	-0.05689	0.1389	20.68	0.6558
WP02-C1-S4	Breccia Cement	132.2	3.169	-3.942	0.4843	49.27	467500	14.14	10.59	101.5	13.28	13.81	0.009941	0.02209	0.06353	4.050	0.1829
WP02-C1-S5	Breccia Cement	132.2	2.709	-5.341	0.1979	38.01	467500	16.17	-0.9855	59.63	13.86	13.98	0.03725	-0.07219	0.9819	4.953	0.1520
WP02-C1-S6	Breccia Cement	132.2	2.986	2.331	0.5026	52.03	467500	16.68	6.718	96.42	15.89	13.91	-0.002035	-0.2121	3.168	4.284	0.1425
WP02-C1-S7	Breccia Cement	132.2	3.287	0.4240	0.9283	78.87	467500	14.80	13.14	-27.42	16.90	16.19	0.0006277	-0.07854	0.6045	4.361	0.1819
WP02-C1-S9	Breccia Cement	132.2	3.960	-1.253	0.9019	56.64	467500	12.58	10.40	7.240	14.95	13.68	0.01092	0.01142	0.06789	3.914	0.07273
WP02-C1-S10	Breccia Cement	132.2	5.011	1.746	1.435	89.24	467500	12.62	19.24	-1.870	17.71	16.36	-0.007712	0.1605	0.09783	6.913	0.1431
WP02-C1-S11	Breccia Cement	132.2	2.449	-2.339	0.3197	39.80	467500	13.68	0.5056	-22.09	19.30	20.02	-0.007137	0.03224	0.2805	12.73	0.2570
WP02-C1-S12	Breccia Cement	132.2	2.825	-4.304	0.1468	42.82	467500	13.55	9.147	-25.36	14.13	15.40	-0.008711	-0.06008	0.08155	3.979	0.06027
WP02-C2-S1	Breccia Cement	132.2	3.000	7.817	0.5217	79.83	467500	13.28	14.61	-44.86	51.78	52.76	0.0003865	-0.04899	0.1853	2.071	0.04227
WP02-C2-S2	Breccia Cement	132.2	2.495	18.83	0.2212	75.88	467500	15.50	8.953	31.39	43.07	42.11	0.009867	-0.05270	0.3089	2.729	0.2595
WP02-C2-S3	Breccia Cement	132.2	2.781	14.78	0.5099	73.73	467500	11.38	14.37	22.06	52.66	52.77	-0.002766	-0.05773	0.2375	3.537	0.4177
WP02-C2-S4	Breccia Cement	132.2	1.705	53.67	0.3763	71.80	467500	11.04	11.17	-21.92	55.81	54.89	0.005393	0.1610	1.126	2.058	0.1386
WP03-C3-S1	Igneous quartz	1546.4	2.673	6.114	0.06420	67.14	467500	12.13	2.477	23.34	7.187	7.590	-0.003455	0.08326	0.03738	0.5019	0.07582
WP03-C3-S2	Igneous quartz	1546.4	0.6671	19.37	0.04883	30.96	467500	19.90	2.335	22.93	3.994	3.716	0.004309	-0.04416	0.08830	0.6258	0.2491
WP03-C3-S3	Igneous quartz	1546.4	4.758	20.10	0.1480	103.6	467500	16.61	4.736	-38.75	10.27	8.631	0.01408	-0.002356	0.07447	0.3130	0.2103
WP03-C3-S4	Igneous quartz	1546.4	2.865	10.54	0.08056	82.02	467500	20.08	1.353	29.47	7.141	6.621	-0.03360	-0.05799	0.09016	0.4773	0.05075
WP03-C3-S5	Igneous quartz	1546.4	2.546	5.948	0.07101	62.26	467500	17.53	1.259	-38.70	6.917	7.297	-0.0001873	0.008256	0.07689	-0.3194	0.0007714
WP13-C1-S1	Igneous quartz	1553.6	4.347	-0.3169	0.1042	47.54	467500	20.93	-0.5813	-18.30	57.10	56.99	-0.006671	0.1287	0.03050	0.07825	0.04532
WP13-C1-S2	Igneous quartz	1553.6	4.418	6.313	5.134	127.9	467500	20.94	16.73	121.9	39.96	41.87	0.09614	0.09407	0.4031	13.07	-0.01915
WP13-C1-S3	Igneous quartz	1553.6	5.814	-1.581	0.03740	45.71	467500	21.39	0.08405	-50.80	46.83	47.34	0.009149	0.02407	0.03400	-0.1078	-0.04800
WP13-C1-S4	Igneous quartz	1553.6	4.514	2.762	0.2448	110.4	467500	21.41	17.43	-55.61	46.20	46.15	0.009796	0.04611	0.2636	5.539	-0.002590
WP22-C2-S1	Igneous quartz	2588.2	1.389	-0.9048	0.004946	38.23	467500	18.72	0.1614	15.51	2.000	2.205	0.02398	-0.1607	0.09006	-0.1145	-0.03132
WP22-C2-S2	Igneous quartz	2588.2	0.9747	-7.615	0.03299	22.55	467500	23.33	-1.483	-4.810	1.496	0.9437	0.009373	-0.2203	0.06087	2.382	0.2394
WP22-C2-S3	Igneous quartz	2588.2	1.834	-5.302	0.002747	25.45	467500	17.74	-0.1225	31.19	1.068	0.9079	-0.01279	0.008366	0.03744	2.634	0.05710
WP22-C2-S4	Igneous quartz	2588.2	2.111	-4.391	0.004130	40.96	467500	16.47	-0.4506	-14.27	1.386	1.492	0.007679	0.1506	-0.001938	2.219	0.05577
WP22-C2-S5	Igneous quartz	2588.2	0.8067	-0.9838	-0.01007	24.73	467500	20.89	-0.1386	13.05	1.136	1.519	-0.003121	-0.03824	0.09174	7.653	0.2090
WP06-C1-S1	Igneous quartz	1429.0	2.276	58.15	0.5912	52.79	467500	13.61	13.60	23.28	37.72	38.14	0.008159	0.07529	0.5406	41.92	0.6217
WP06-C1-S2	Igneous quartz	1429.0	2.205	28.37	0.2279	44.60	467500	12.88	9.698	27.04	6.428	5.065	0.007332	-0.04013	0.09060	2.105	0.6233
WP06-C1-S3	Igneous quartz	1429.0	1.688	5.500	0.07861	23.37	467500	11.09	2.083	28.81	4.993	4.550	-0.003248	-0.01260	0.01470	-0.1204	0.1170
WP06-C1-S4	Igneous quartz	1429.0	1.249	11.11	0.03707	20.58	467500	12.59	2.315	-4.533	5.162	5.109	0.003645	0.02537	0.05198	-0.5472	0.3147
WP64-C4-S1	Igneous quartz	704.8	3.232	0.4662	0.08720	50.33	467500	28.91	2.642	-127.0	14.82	20.77	0.005521	-0.02218	0.07837	12.66	0.3806
WP64-C4-S2	Igneous quartz	704.8	3.570	3.940	0.4618	61.08	467500	17.69	10.84	44.50	15.46	15.69	0.001617	0.04490	0.1852	1.014	0.2916
WP64-C4-S3	Igneous quartz	704.8	2.560	3.214	0.1684	49.39	467500	19.81	4.421	-32.51	14.12	13.22	-0.0005815	0.05242	0.07581	8.538	0.2142
WP64-C4-S4	Igneous quartz	704.8	4.018	-2.109	0.2874	59.01	467500	19.20	1.494	69.79	13.26	12.86	-0.004800	-0.02353	0.05503	1.383	0.05789
WP52-C1-S1	Igneous quartz	785.5	0.8428	14.74	0.1282	46.66	467500	8.548	5.021	-44.56	58.07	58.52	-0.006721	0.05680	0.07330	2.006	0.4651
WP52-C1-S2	Igneous quartz	785.5	1.169	-1.290	0.1775	73.81	467500	13.69	8.856	24.00	57.50	60.18	-0.0005983	0.2696	0.3709	-0.1489	0.2279
WP52-C1-S3	Igneous quartz	785.5	0.05361	9.875	2.514	61.26	467500	30.58	15.84	12.83	36.62	37.28	0.04514	-0.06164	0.2653	582.4	5.318
WP52-C2-S1	Igneous quartz	785.5	0.3368	7.536	0.02363	36.49	467500	7.247	2.331	7.330	6.126	6.310	0.01985	0.4872	0.03872	25.38	0.07395
WP52-C2-S2	Igneous quartz	785.5	0.4410	28.01	0.08890	34.60	467500	12.84	4.102	40.38	7.363	7.058	0.008892	0.02417	0.06811	0.4044	0.1355
WP52-C2-S3	Igneous quartz	785.5	0.9446	34.25	0.8554	73.89	467500	12.76	7.933	43.65	8.832	8.264	-0.02078	0.2661	0.2317	8.085	0.1178

* distance from center of deposit

** All elements in ppm except Au which is in ppb

Appendix 6: White Pine
quartz mineral chemistry by LA-ICP-MS

Sample	Sample type	Distance*															
		(m)	Li7	Na23	Mg24	Al27	Si29	P31	K39	Ca43	Ti47	Ti49	V51	Cr53	Mn55	Fe57	Cu63
WP52-C2-S4	Igneous quartz	785.5	0.5794	24.30	0.3844	55.19	467500	10.78	10.66	-12.45	7.736	8.633	0.02067	-0.07117	0.2135	3.845	0.09985
WP65-C1-S1	Igneous quartz	609.4	3.026	0.3191	0.2604	32.79	467500	7.859	-0.4096	-44.64	7.151	8.909	-0.01734	-0.08152	0.06263	3.063	0.7057
WP65-C1-S3	Igneous quartz	609.4	5.546	-0.9173	0.1832	46.35	467500	14.51	0.7530	-1.421	7.563	8.019	-0.008546	0.05404	0.02113	2.692	0.02430
WP65-C1-S4	Igneous quartz	609.4	4.106	-0.7305	0.06978	36.07	467500	10.89	2.069	-27.66	8.219	9.321	0.01011	0.1086	-0.01422	4.855	-0.008715
WP23-C1-S1	Igneous quartz	1688.3	8.124	0.7822	0.1482	52.81	467500	16.57	0.2949	3.425	55.34	55.93	0.002733	0.04275	0.1004	0.2782	0.05292
WP23-C1-S2	Igneous quartz	1688.3	8.406	6.731	0.3553	97.00	467500	20.11	12.99	10.61	81.70	81.43	0.1410	0.2777	0.2094	297.8	0.2233
WP23-C1-S3	Igneous quartz	1688.3	6.171	2.740	0.1110	51.30	467500	14.44	0.4373	-4.825	39.66	37.97	0.2125	-0.1077	0.07657	6.632	0.09608
WP23-C1-S4	Igneous quartz	1688.3	7.727	2.670	0.3786	88.90	467500	16.14	6.516	-33.74	76.88	77.07	0.03369	0.09009	0.1625	31.79	0.08154
WP23-C2-S1	Igneous quartz	1688.3	8.167	-1.050	1.003	85.24	467500	12.94	7.876	-1.429	49.12	48.39	0.004367	-0.07316	0.2174	1.562	-0.004272
WP23-C2-S2	Igneous quartz	1688.3	8.410	-2.349	0.1773	70.01	467500	10.74	0.8722	44.85	51.51	54.26	0.006977	-0.1304	0.1385	0.6058	0.02875
WP23-C2-S3	Igneous quartz	1688.3	7.575	0.4782	0.2219	81.48	467500	11.71	2.078	-3.828	60.33	58.51	-0.001639	0.04227	0.1582	1.264	-0.01251
WP23-C2-S4	Igneous quartz	1688.3	5.505	0.6988	0.6217	76.05	467500	14.59	4.114	81.25	50.48	50.05	0.01139	0.06855	0.2236	1.054	-0.03070
WP07-C4-S1	Igneous quartz	1360.2	3.403	4.317	0.01328	56.14	467500	24.19	11.02	-26.55	32.17	31.49	-0.01411	-0.05856	0.2215	6.315	0.06329
WP07-C4-S2	Igneous quartz	1360.2	5.335	15.78	0.2722	60.93	467500	15.13	7.154	77.07	43.97	45.30	0.005759	-0.003221	0.07084	0.9842	0.01982
WP07-C4-S3	Igneous quartz	1360.2	5.045	2.883	0.2164	52.32	467500	18.19	3.855	18.05	48.55	49.70	0.004418	-0.05200	0.08531	4.828	0.1556
WP07-C4-S4	Igneous quartz	1360.2	5.072	1.420	0.3159	53.59	467500	16.03	4.310	-9.903	45.48	43.41	0.001710	0.07899	0.1048	1.398	0.07767

* distance from center of deposit

** All elements in ppm except Au which is in ppb

Appendix 6: White Pine
quartz mineral chemistry by LA-ICP-MS

Sample	Sample type	Distance* (m)	Cu65	Zn66	Ge74	As75	Rb85	Sr88	Zr90	Ag107	Sb121	Cs133	Gd157	Hf178
WP46-C1-S1	Vein Quartz	372.6	0.1271	-0.04806	1.106	4.296	0.01039	0.4879	0.008285	-0.02549	0.09471	0.01148	-0.01294	-0.005370
WP46-C1-S2	Vein Quartz	372.6	-0.01807	0.1742	0.8387	4.790	0.01499	0.08424	0.005913	0.000	-0.01702	0.003408	0.005940	0.005505
WP46-C1-S3	Vein Quartz	372.6	0.03144	-0.001554	0.8248	3.829	0.02982	0.05724	0.002747	-0.009809	0.004419	0.007407	0.004506	-0.00005791
WP46-C1-S4	Vein Quartz	372.6	0.02348	-0.02653	1.035	3.585	0.09949	0.1524	-0.006691	0.006451	-0.008158	0.005294	0.002156	0.004787
WP46-C1-S5	Vein Quartz	372.6	0.05479	0.2825	0.9334	3.757	0.05234	0.1701	0.01841	0.04154	0.02361	0.006987	0.01510	0.004215
WP46-C1-S6	Vein Quartz	372.6	0.1383	0.08904	0.8666	3.941	0.01567	0.07378	0.007533	-0.0009122	-0.004201	-0.00001637	-0.001365	0.001445
WP46-C1-S7	Vein Quartz	372.6	0.1795	0.1072	0.9241	3.708	0.03660	0.2135	-0.0002373	0.1769	0.1190	0.006855	0.0004674	-0.0008372
WP46-C1-S8	Vein Quartz	372.6	1.014	0.01827	0.7670	2.984	0.07582	0.4334	0.01069	0.04569	0.04291	0.006565	-0.009056	-0.004425
WP46-C1-S9	Vein Quartz	372.6	0.1409	0.09731	0.9440	3.653	0.009839	0.2100	0.001694	0.05868	0.06444	0.01068	-0.002163	-0.002235
WP46-C1-S10	Vein Quartz	372.6	0.1187	0.02152	0.8079	3.680	0.06020	0.2357	-0.001905	0.02970	0.007220	0.01332	0.004240	0.004722
WP46-C1-S11	Vein Quartz	372.6	0.2599	-0.05441	0.8486	4.139	0.01059	0.09214	0.001757	0.01129	0.02120	0.005516	-0.004555	-0.002889
WP46-C1-S12	Vein Quartz	372.6	-0.03459	0.01579	0.7932	4.196	0.004249	0.03613	0.002993	-0.004757	-0.009383	0.006180	0.001035	0.0005060
WP46-C1-S13	Vein Quartz	372.6	0.04601	0.09706	0.7712	3.847	0.003955	0.05037	-0.005688	-0.001584	0.0008892	0.002558	-0.0006608	0.003276
WP46-C1-S14	Vein Quartz	372.6	0.1911	-0.02673	0.7750	3.618	0.02370	0.1254	0.002358	-0.01444	0.07271	0.002291	-0.01421	-0.002842
WP46-C1-S15	Vein Quartz	372.6	-0.02674	0.07234	0.8055	4.989	0.005225	0.09482	0.0008979	0.006522	0.001040	0.003942	0.004692	0.005051
WP03-C1-S1	Vein Quartz	1546.4	0.07548	-0.03004	2.856	7.694	0.02844	0.06251	0.01075	-0.002639	0.008160	0.01723	0.001382	0.004866
WP03-C1-S2	Vein Quartz	1546.4	0.7336	0.09555	3.327	6.567	0.1672	0.1374	-0.005350	0.006236	0.05735	0.04355	0.002027	-0.003079
WP03-C1-S3	Vein Quartz	1546.4	1.844	0.2697	3.044	7.957	0.07390	0.1693	0.009061	0.004768	0.05767	0.03283	0.01559	-0.002096
WP03-C1-S4	Vein Quartz	1546.4	0.4366	0.1394	2.982	8.167	0.05541	0.09629	0.001028	0.006694	0.03119	0.01666	-0.004416	0.0007509
WP03-C1-S5	Vein Quartz	1546.4	0.1954	0.07066	2.514	8.719	0.02014	0.07208	0.0002731	0.0001622	0.01828	0.01701	-0.006620	-0.0008398
WP03-C2-S1	Vein Quartz	1546.4	-0.0001383	0.05031	3.191	7.991	0.02798	0.03420	0.0001173	0.006281	0.4563	0.01162	-0.008416	0.001682
WP03-C2-S2	Vein Quartz	1546.4	0.2416	0.08091	2.884	8.148	0.006372	0.07944	-0.0007008	-0.0003390	-0.004594	0.007385	-0.005641	0.004434
WP03-C2-S3	Vein Quartz	1546.4	0.05861	-0.02209	2.918	8.743	0.007728	0.007721	0.002034	-0.006197	-0.0007996	0.008079	-0.006328	0.0003036
WP03-C2-S4	Vein Quartz	1546.4	0.1472	-0.03798	3.341	8.689	0.01311	0.001633	0.001928	0.002054	0.01340	0.03278	-0.007842	-0.001840
WP03-C2-S5	Vein Quartz	1546.4	0.1119	0.06722	3.402	6.934	0.007082	0.02309	-0.0002044	-0.001067	0.02769	0.007829	-0.009092	0.0003297
WP13-C3-S1	Vein Quartz	1553.6	-0.01060	-0.02703	1.059	0.06114	-0.005072	0.01006	0.002428	0.01825	0.02205	0.000007255	-0.0006318	0.00008059
WP13-C3-S2	Vein Quartz	1553.6	0.08564	0.02983	1.125	0.03005	-0.001176	0.007447	-0.003260	-0.002556	0.01207	-0.00002910	0.005368	-0.0005494
WP13-C3-S3	Vein Quartz	1553.6	0.03245	-0.09242	1.017	0.05699	0.005091	0.01370	-0.007869	0.02160	-0.01676	0.002250	-0.002070	0.0001893
WP13-C3-S4	Vein Quartz	1553.6	0.02657	0.007466	1.232	0.07222	0.03648	0.05234	0.0009744	0.02753	0.03919	0.01839	0.0007690	-0.0005962
WP13-C5-S1	Vein Quartz	1553.6	1.045	0.08625	1.202	0.06758	0.02814	0.07328	0.001897	-0.004435	-0.02403	0.003306	-0.0008978	-0.002374
WP13-C5-S2	Vein Quartz	1553.6	0.02778	-0.01873	1.254	-0.007121	0.02121	0.3221	0.006529	-0.004499	0.06722	0.002803	0.006422	0.001152
WP13-C5-S3	Vein Quartz	1553.6	0.08183	0.07768	1.267	0.1123	0.005300	0.05235	0.01102	0.006582	-0.002994	0.01251	-0.002123	0.002056
WP13-C5-S4	Vein Quartz	1553.6	0.08425	0.1165	1.298	-0.007334	0.008191	0.04595	-0.001254	0.003764	0.005409	0.002565	0.0003832	0.001794
WP22-C4-S1	Vein Quartz	2588.2	-0.01616	0.03011	1.206	0.1169	-0.002997	0.01263	0.0005128	0.01017	0.009581	0.0008579	0.006825	-0.001220
WP22-C4-S2	Vein Quartz	2588.2	0.2622	-0.01616	1.476	0.1396	0.007285	0.01342	-0.007538	0.006689	0.01786	-0.003951	0.0006905	0.005039
WP22-C4-S3	Vein Quartz	2588.2	0.3468	0.2390	1.450	0.1244	0.05465	0.05004	-0.004954	-0.003115	0.01262	0.01450	0.009579	-0.0007086
WP22-C4-S4	Vein Quartz	2588.2	0.2778	0.1600	1.696	0.07907	0.01267	0.02918	-0.002300	0.01941	0.2036	0.006304	-0.004580	0.001500
WP22-C4-S5	Vein Quartz	2588.2	0.5572	0.1336	1.445	0.2781	0.09998	0.1339	-0.001791	0.01488	0.1087	0.01957	-0.005598	0.008740
WP06-C2-S1	Vein Quartz	1429.0	0.07516	0.05392	0.4279	-0.003908	0.04024	0.08695	-0.003219	0.006347	-0.002494	0.01600	0.005568	-0.003289
WP06-C2-S2	Vein Quartz	1429.0	0.006301	0.09307	0.4585	0.08732	0.02372	0.1346	-0.001518	-0.003251	0.01427	0.003174	-0.009489	0.003266
WP06-C2-S3	Vein Quartz	1429.0	0.01101	0.08880	0.4111	0.1055	0.02730	0.1040	0.002593	0.02286	0.01804	0.006892	0.003404	0.002269
WP06-C2-S4	Vein Quartz	1429.0	-0.05638	0.05816	0.4674	0.03445	0.02262	0.07726	0.001645	-0.01005	-0.007587	0.008048	-0.001614	-0.001365
WP06-C3-S2	Vein Quartz	1429.0	0.003387	0.2195	0.6024	0.2337	0.2470	0.8954	-0.002978	0.01309	-0.02298	0.1783	-0.005927	0.002534

* distance from center of deposit

** All elements in ppm except Au which is in ppb

Appendix 6: White Pine
quartz mineral chemistry by LA-ICP-MS

Sample	Sample type	Distance*												
		(m)	Cu65	Zn66	Ge74	As75	Rb85	Sr88	Zr90	Ag107	Sb121	Cs133	Gd157	Hf178
WP06-C3-S3	Vein Quartz	1429.0	0.1398	0.1795	0.4264	0.1100	0.04152	0.09236	-0.001074	-0.01799	0.01490	0.005929	0.008498	0.005974
WP06-C3-S4	Vein Quartz	1429.0	0.03484	0.1015	0.5452	0.1184	0.01147	0.2350	0.005893	-0.003310	-0.01105	0.004202	0.004933	0.001772
WP53-C1-S1	Vein Quartz	548.8	0.4905	0.01213	1.045	0.1797	0.09088	0.02523	0.001915	0.007343	0.04150	0.04085	-0.01379	-0.003220
WP53-C1-S2	Vein Quartz	548.8	0.06626	0.07539	0.9932	0.06774	0.2099	0.07103	0.008236	0.01684	0.002784	0.1028	-0.002953	-0.005334
WP53-C1-S3	Vein Quartz	548.8	0.08025	0.01718	0.8972	0.1186	0.05735	0.02115	0.006331	-0.01168	0.02499	0.01007	0.0006809	0.001744
WP53-C1-S4	Vein Quartz	548.8	0.1597	-0.02623	0.9862	0.1485	0.09069	0.02751	0.005485	-0.007659	0.03962	0.01251	0.006893	0.004063
WP53-C1-S5	Vein Quartz	548.8	0.2520	0.09751	1.028	0.1986	0.02362	0.02831	0.003073	0.01869	-0.009106	0.01523	-0.0004942	-0.004862
WP53-C2-S1	Vein Quartz	548.8	1.547	0.2103	1.200	0.2084	0.03188	0.1059	0.007642	0.02582	0.01194	0.01652	0.003443	-0.002319
WP53-C2-S2	Vein Quartz	548.8	0.1747	0.001910	1.231	0.1548	0.01610	0.06169	0.005599	0.006594	0.0009177	0.02367	-0.001739	-0.004377
WP53-C2-S3	Vein Quartz	548.8	0.3324	0.03475	1.477	0.2266	0.2263	0.1294	0.08548	-0.002700	0.0009875	0.08748	-0.003348	0.01038
WP53-C2-S4	Vein Quartz	548.8	0.04684	0.003903	1.017	0.1215	0.07561	0.02251	0.01341	-0.002033	0.02545	0.02108	0.006181	0.006523
WP53-C2-S5	Vein Quartz	548.8	2.137	-0.04533	1.066	0.1910	0.07945	0.1119	0.01021	0.03937	0.004988	0.02706	-0.0008722	-0.002264
WP05-C1-S1	Vein Quartz	1429.0	0.005914	0.1135	0.3331	0.1382	0.02947	0.08305	-0.001262	-0.03303	0.03608	0.004935	0.001708	-0.002896
WP05-C1-S2	Vein Quartz	1429.0	1.321	0.1417	0.5861	0.1803	0.03032	0.2536	0.003951	-0.01693	0.03880	0.01443	-0.001943	0.001603
WP05-C1-S3	Vein Quartz	1429.0	0.04438	0.09070	0.5406	0.01183	0.003486	0.04756	-0.001908	-0.03571	-0.006834	0.003297	0.003419	0.005477
WP05-C1-S4	Vein Quartz	1429.0	0.03931	-0.001937	0.5433	0.1735	-0.007587	0.03046	0.01001	0.0002871	-0.0009852	0.001534	0.003484	0.001866
WP05-C2-S1	Vein Quartz	1429.0	0.8559	0.01230	0.7871	-0.03741	0.02366	0.04393	-0.002506	-0.0002279	-0.002769	0.005160	-0.009414	-0.003064
WP05-C2-S2	Vein Quartz	1429.0	1.955	0.1006	1.767	0.06844	0.02570	0.2532	0.008020	0.05004	0.002668	0.003229	-0.01557	-0.001681
WP05-C2-S3	Vein Quartz	1429.0	0.5087	-0.1132	0.8762	0.1219	0.01243	0.03515	-0.005118	-0.02605	0.01148	0.002825	-0.002096	-0.008327
WP05-C2-S4	Vein Quartz	1429.0	0.05159	0.07240	0.8504	0.2007	0.02383	0.02896	0.002276	-0.001026	0.004937	0.005549	0.004538	-0.0002504
WP05-C2-S5	Vein Quartz	1429.0	0.03196	0.03828	0.5445	0.06215	0.03593	0.06586	0.0002362	-0.003568	0.01386	0.005597	0.02028	-0.004619
WP05-C3-S1	Vein Quartz	1429.0	0.1422	0.05546	2.521	0.3137	0.07097	0.3674	0.00002079	0.003775	0.06576	0.05156	0.005512	0.006053
WP05-C3-S2	Vein Quartz	1429.0	0.3686	0.04189	2.581	0.1048	0.01269	0.1036	0.001182	0.006842	0.1138	0.003601	0.001663	0.003715
WP05-C3-S3	Vein Quartz	1429.0	0.03219	0.1248	1.504	0.1734	0.01175	0.04851	0.008696	-0.008930	-0.02245	0.01253	-0.008986	-0.002716
WP05-C3-S4	Vein Quartz	1429.0	3.463	0.003285	1.733	0.1986	0.04992	0.1390	-0.004019	0.007678	0.02477	0.01501	-0.002016	0.001850
WP64-C1-S1	Vein Quartz	704.8	0.2310	0.03807	1.268	0.09618	0.01341	0.05525	0.0004991	0.6442	0.03718	0.005654	-0.003358	0.0004871
WP64-C1-S2	Vein Quartz	704.8	0.2021	-0.07964	1.129	0.1488	0.02896	0.007490	0.0002983	-0.006619	0.05043	0.003054	0.006359	-0.005730
WP64-C1-S3	Vein Quartz	704.8	0.3917	0.07612	1.335	0.01151	0.04355	0.02588	-0.004082	0.009274	-0.06772	0.02140	-0.009214	0.0009913
WP64-C1-S4	Vein Quartz	704.8	0.09447	0.01719	1.272	0.08563	0.1159	0.03085	-0.002263	0.004994	0.03837	0.008142	0.005138	0.003490
WP64-C2-S1	Vein Quartz	704.8	2.210	0.5620	1.533	0.2715	0.3577	0.07234	-0.001702	-0.009351	0.008370	0.01807	0.01676	-0.002397
WP64-C2-S2	Vein Quartz	704.8	0.09673	0.2111	2.040	0.3060	0.4464	0.05669	0.005284	0.03836	0.05831	0.007566	-0.005527	0.003504
WP64-C2-S4	Vein Quartz	704.8	1.504	0.2390	1.960	0.1296	0.2678	0.05700	-0.004901	0.01086	0.08280	0.02306	0.003623	0.003305
WP64-C3-S1	Vein Quartz	704.8	0.1037	-0.06299	1.097	0.2761	0.003796	0.002945	0.005979	0.01349	-0.01213	0.001844	0.0004274	-0.005262
WP64-C3-S2	Vein Quartz	704.8	7.903	0.06376	1.774	0.09598	0.1552	0.05226	0.007229	0.005088	-0.009170	0.03903	-0.007864	0.001821
WP64-C3-S3	Vein Quartz	704.8	5.316	0.5021	1.373	0.1565	0.02265	0.04745	-0.002562	0.002931	0.04277	0.01474	0.01997	-0.003704
WP52-C3-S1	Vein Quartz	785.5	-0.01774	0.3560	0.4670	0.03130	0.07263	0.2622	0.01670	0.01498	0.01302	0.01373	-0.02256	0.002401
WP52-C3-S2	Vein Quartz	785.5	0.004018	0.1769	0.5294	0.07463	0.01792	0.09341	-0.004603	0.02647	-0.006067	0.006171	-0.005857	-0.002954
WP52-C3-S3	Vein Quartz	785.5	0.1536	0.02047	0.5017	0.1482	0.02115	0.4811	0.008790	0.004704	0.04669	0.008138	0.003874	0.001896
WP52-C3-S4	Vein Quartz	785.5	0.03330	0.1078	0.4812	0.04076	0.02791	0.1248	-0.002625	0.01203	-0.0007518	0.005748	0.004793	0.001869
WP65-C2-S3	Vein Quartz	609.4	0.2434	0.07002	1.273	0.01985	0.4167	0.3516	-0.001164	-0.01841	-0.02703	0.009895	-0.008615	0.002762
WP65-C2-S4	Vein Quartz	609.4	0.06680	0.05557	0.9937	-0.05232	0.04010	0.05610	-0.002155	-0.004372	0.01694	0.01234	-0.007882	-0.0001377
WP65-C3-S1	Vein Quartz	609.4	0.03782	0.1311	0.9605	0.07515	0.03506	0.1564	-0.0004360	-0.00009849	0.0008147	0.01321	0.006796	0.004006
WP65-C3-S2	Vein Quartz	609.4	0.4782	0.2615	0.9233	0.05649	0.04151	0.1194	0.0005483	0.006762	0.4268	0.008931	-0.002268	0.004668

* distance from center of deposit

** All elements in ppm except Au which is in ppb

Appendix 6: White Pine
quartz mineral chemistry by LA-ICP-MS

Sample	Sample type	Distance*	Cu65	Zn66	Ge74	As75	Rb85	Sr88	Zr90	Ag107	Sb121	Cs133	Gd157	Hf178
		(m)												
WP65-C3-S3	Vein Quartz	609.4	0.1813	0.1807	0.9655	-0.02516	0.02453	0.1313	-0.001164	-0.01492	-0.01096	0.01250	-0.001037	0.004229
WP65-C3-S4	Vein Quartz	609.4	0.002883	0.1654	0.9164	0.04048	0.09561	0.2329	-0.003147	-0.005258	0.005290	0.02535	0.001883	0.003266
WP65-C4-S1	Vein Quartz	609.4	0.7385	0.09382	0.8881	-0.01892	0.02060	0.1601	-0.004268	0.008810	0.01726	0.008914	0.01497	0.005962
WP65-C4-S2	Vein Quartz	609.4	-0.01364	0.008949	0.9316	0.002119	0.01253	0.01726	0.002938	0.01084	-0.003896	0.003317	0.003986	0.003480
WP65-C4-S3	Vein Quartz	609.4	0.02145	0.03590	0.9886	-0.004067	-0.0005210	0.01893	-0.003937	0.01511	0.005253	0.01309	0.002767	0.001354
WP65-C4-S4	Vein Quartz	609.4	0.4456	0.1520	1.225	-0.007151	0.03260	0.05464	-0.002976	0.03262	0.05333	0.005454	-0.006031	0.005485
WP23-C5-S2	Vein Quartz	1688.3	0.1232	0.4833	1.067	1.504	0.1899	0.2720	0.005630	-0.01263	0.01450	0.03162	-0.0007460	-0.001283
WP07-C1-S3	Vein Quartz	1360.2	0.3742	0.1823	0.9446	6.926	0.03854	0.7287	0.1495	0.04371	0.1128	0.01733	-0.02199	0.0006399
WP07-C1-S4	Vein Quartz	1360.2	0.3981	0.1036	1.088	6.603	0.02448	0.3292	0.1449	0.007523	0.09828	0.004871	-0.004603	0.0003024
WP07-C2-S1	Vein Quartz	1360.2	0.1075	0.07328	0.4246	9.079	0.02538	0.01702	0.004787	0.001145	0.01131	0.001671	-0.001715	-0.004586
WP07-C2-S2	Vein Quartz	1360.2	-0.05718	0.05350	0.4367	8.082	0.02595	0.01164	0.007089	-0.004304	0.02842	0.002733	-0.002528	0.001756
WP07-C2-S3	Vein Quartz	1360.2	0.2391	0.1309	0.4620	9.326	0.1315	0.1449	0.009363	0.05015	0.04582	0.04351	-0.004832	0.002636
WP07-C4-S1	Vein Quartz	1360.2	0.08987	0.007902	0.3967	6.891	0.04664	0.006472	0.002997	0.0005413	0.005719	0.007249	0.01206	-0.0006820
WP07-C4-S2	Vein Quartz	1360.2	0.1136	0.1117	0.5056	7.328	0.04829	0.008882	0.002646	0.0007833	0.05383	0.01008	-0.003804	-0.002439
WP07-C4-S3	Vein Quartz	1360.2	0.1364	0.03360	0.3798	6.011	0.03872	0.01441	0.004018	-0.009282	-0.006608	0.0008633	-0.007981	0.009706
WP07-C4-S4	Vein Quartz	1360.2	0.1206	0.06280	0.5162	7.156	0.03441	0.003887	-0.001369	0.006012	0.02084	-0.0003851	0.003253	-0.0001840
WP07-C1-S1	Vein Quartz	1360.2	2.582	0.2035	0.8788	6.685	0.01478	1.213	0.07028	0.02675	0.4806	0.01439	-0.0008680	-0.008271
WP07-C1-S3	Vein Quartz	1360.2	0.3742	0.1823	0.9446	6.926	0.03854	0.7287	0.1495	0.04371	0.1128	0.01733	-0.02199	0.0006399
WP07-C1-S4	Vein Quartz	1360.2	1.333	0.1820	1.116	7.051	0.02604	0.2748	0.1348	0.009884	0.1037	0.004581	-0.007307	0.002618
WP07-C2-S1	Vein Quartz	1360.2	0.2392	0.06745	0.4089	9.672	0.03058	0.01760	0.006348	0.002534	0.01346	-0.0004745	0.007869	-0.006222
WP07-C2-S2	Vein Quartz	1360.2	-0.02994	-0.006685	0.3839	8.067	0.03852	0.01421	0.002781	0.001301	0.01257	0.004639	-0.008271	-0.001796
WP07-C2-S3	Vein Quartz	1360.2	0.08803	0.09477	0.4313	9.776	0.04757	0.03211	0.01540	-0.003200	0.004348	0.02196	0.003373	-0.001574
WP03-C1-S1	Vein Quartz	1546.4	0.2432	-0.04495	0.9047	8.250	0.01229	0.1650	-0.001695	0.01460	0.01542	0.01170	0.03173	-0.001269
WP03-C1-S2	Vein Quartz	1546.4	0.04153	0.1093	0.5299	9.065	0.009136	0.2452	-0.0005547	-0.008026	0.0008410	0.01108	0.0003606	-0.0004152
WP03-C1-S3	Vein Quartz	1546.4	-0.006208	0.08556	0.5776	9.450	0.002127	0.1764	-0.001342	0.004510	0.01328	0.01076	0.004765	0.0008487
WP03-C1-S4	Vein Quartz	1546.4	0.05527	0.05061	0.4914	9.173	0.01144	0.3171	-0.0006188	0.003879	-0.001904	0.01108	-0.004528	0.0007030
WP03-C2-S2	Vein Quartz	1546.4	0.01484	0.2102	0.5173	7.454	0.01709	0.1239	-0.0002797	0.0008916	0.01278	0.005900	0.002968	-0.003477
WP03-C2-S3	Vein Quartz	1546.4	0.02450	0.01982	0.4504	7.961	0.04741	0.2283	-0.0003270	0.006517	0.01613	0.01311	0.001021	-0.002449
WP03-C2-S4	Vein Quartz	1546.4	0.01441	0.08863	0.5036	8.791	0.01148	0.1349	0.005356	-0.001132	0.03521	0.01525	-0.0006646	0.002786
WP03-C3-S1	Vein Quartz	1546.4	0.009743	0.07024	1.996	11.96	0.01814	0.04642	0.003867	-0.005834	0.0005581	0.007735	0.003106	0.001660
WP03-C3-S2	Vein Quartz	1546.4	0.7613	0.08106	1.706	13.94	0.07672	0.2029	0.003146	0.01934	0.01123	0.02386	0.003087	-0.001821
WP03-C3-S3	Vein Quartz	1546.4	0.01260	0.04448	1.789	12.83	0.03655	0.04766	-0.0005440	-0.01907	-0.002958	0.01163	-0.007395	-0.001732
WP03-C3-S4	Vein Quartz	1546.4	1.181	0.02633	1.802	12.47	0.03348	0.2555	0.001085	0.003479	-0.002369	0.02169	0.001693	-0.0004810
WP03-C4-S1	Vein Quartz	1546.4	0.1112	0.06373	1.949	13.15	0.04742	0.1272	0.003046	0.008284	0.009337	0.02098	0.01520	-0.002544
WP03-C4-S2	Vein Quartz	1546.4	-0.02068	0.01003	1.439	10.99	0.04871	0.7207	0.004138	-0.009930	0.02317	0.04024	-0.01085	-0.001736
WP03-C4-S3	Vein Quartz	1546.4	0.02385	0.06025	1.995	11.86	0.04765	0.2072	0.005205	-0.008297	0.01398	0.02173	-0.004251	-0.004081
WP03-C4-S4	Vein Quartz	1546.4	1.100	0.08881	2.503	10.73	0.02321	0.009488	-0.002057	0.1813	-0.01017	0.009262	-0.01285	0.004471
WP63-C1-S1	Breccia Cement	0.0	0.02474	0.08967	0.4159	0.06334	0.05897	0.09933	0.003508	0.003453	0.03018	0.004608	-0.001837	-0.001083
WP63-C1-S2	Breccia Cement	0.0	-0.03161	-0.03403	0.6155	0.1487	0.05146	0.1477	0.004504	-0.009016	-0.006855	0.0003678	0.005626	-0.002285
WP63-C1-S3	Breccia Cement	0.0	0.09397	-0.02442	0.4845	-0.04724	0.05302	0.06821	0.004050	0.01926	-0.0005993	0.001633	0.01206	0.004828
WP63-C2-S1	Breccia Cement	0.0	0.02972	-0.05098	0.4606	0.02572	0.05059	0.07793	0.005112	-0.0007644	0.008903	-0.0001796	0.0007994	0.001253
WP63-C2-S2	Breccia Cement	0.0	0.06800	0.1889	0.5400	0.02954	0.09254	0.1292	0.002515	0.01978	0.04375	-0.001723	0.01113	0.001168
WP63-C2-S3	Breccia Cement	0.0	0.01697	0.05231	0.4440	0.009240	0.05933	0.1255	0.002612	0.03224	-0.003675	0.005738	0.008258	-0.006448

* distance from center of deposit

** All elements in ppm except Au which is in ppb

Appendix 6: White Pine
quartz mineral chemistry by LA-ICP-MS

Sample	Sample type	Distance*													
		(m)	Cu65	Zn66	Ge74	As75	Rb85	Sr88	Zr90	Ag107	Sb121	Cs133	Gd157	Hf178	
WP63-C3-S1	Breccia Cement	0.0	5.216	0.4469	1.094	-0.05658	0.1688	0.2057	-0.0007579	0.1157	0.004538	0.03851	0.01634	0.001223	
WP02-C1-S1	Breccia Cement	132.2	0.06555	0.1764	1.555	7.860	0.07754	0.01695	-0.002839	-0.002719	0.01758	0.002075	0.002887	-0.006010	
WP02-C1-S2	Breccia Cement	132.2	0.4548	0.2046	1.581	8.445	0.5186	0.09254	0.008014	-0.003377	-0.005950	0.05188	0.01280	-0.0002488	
WP02-C1-S4	Breccia Cement	132.2	0.1008	-0.03408	1.510	8.795	0.09207	0.07319	0.004652	0.006419	0.02087	0.003260	0.0008845	0.0004297	
WP02-C1-S5	Breccia Cement	132.2	0.1206	0.2644	1.555	8.721	0.009927	0.03067	0.005830	-0.02286	0.01885	-0.001633	-0.01439	0.0005139	
WP02-C1-S6	Breccia Cement	132.2	0.1060	0.08368	1.764	8.567	0.07983	0.05099	0.002789	-0.01419	0.01367	0.003602	0.001012	0.004326	
WP02-C1-S7	Breccia Cement	132.2	0.3209	0.1578	1.358	8.555	0.05191	0.07699	0.007326	0.009156	0.01292	0.005403	0.001649	0.0005827	
WP02-C1-S9	Breccia Cement	132.2	0.001313	-0.06618	1.695	8.235	0.04915	0.01203	-0.002368	-0.001986	-0.009192	0.003098	-0.009277	0.01603	
WP02-C1-S10	Breccia Cement	132.2	0.3560	0.1843	1.706	7.865	0.09058	0.03357	0.01061	0.002100	-0.009234	0.005975	0.01133	-0.0001765	
WP02-C1-S11	Breccia Cement	132.2	0.1720	0.1173	1.507	8.828	0.01697	0.07820	-0.007059	0.006094	-0.001829	0.001752	-0.002200	0.002516	
WP02-C1-S12	Breccia Cement	132.2	0.04470	0.03400	1.630	8.516	0.03462	0.05824	0.01201	-0.008444	0.007918	-0.007091	0.01086	-0.0002070	
WP02-C2-S1	Breccia Cement	132.2	0.05656	0.1447	0.4891	12.33	0.1333	0.01649	0.004647	0.001723	0.006461	0.3755	-0.01413	0.007485	
WP02-C2-S2	Breccia Cement	132.2	0.1367	0.09288	0.5562	10.31	0.09378	0.04947	0.002911	-0.003698	0.009334	0.03875	-0.002592	-0.001138	
WP02-C2-S3	Breccia Cement	132.2	0.6271	0.02197	0.5599	10.45	0.1522	0.005572	0.007303	-0.007107	-0.001336	0.2355	0.01164	0.003597	
WP02-C2-S4	Breccia Cement	132.2	0.06508	0.02488	0.5677	10.62	0.1119	0.2631	0.007017	0.01168	-0.0008766	0.1382	0.01530	-0.005723	
WP03-C3-S1	Igneous quartz	1546.4	0.01204	0.01301	2.872	7.910	0.004750	0.1803	0.006293	0.00008792	0.02182	0.009535	0.001703	0.001088	
WP03-C3-S2	Igneous quartz	1546.4	0.3502	0.003224	2.601	6.299	0.03464	0.04752	-0.0004511	0.003528	0.01344	0.02761	-0.02354	-0.004003	
WP03-C3-S3	Igneous quartz	1546.4	0.1888	0.07226	3.290	6.588	0.03627	0.3454	0.002010	-0.001416	0.03061	0.01811	-0.003448	0.003476	
WP03-C3-S4	Igneous quartz	1546.4	0.02382	0.01668	2.805	5.886	0.05597	0.08510	-0.0003685	-0.007681	0.03044	0.02254	-0.002835	-0.002777	
WP03-C3-S5	Igneous quartz	1546.4	0.002957	0.007195	2.765	6.762	0.004571	0.08211	-0.002301	0.01039	0.02727	0.009131	-0.006284	-0.003078	
WP13-C1-S1	Igneous quartz	1553.6	0.08989	-0.06305	0.4440	0.02832	0.007830	0.01917	-0.0003908	0.003857	-0.01935	0.001189	0.0005381	0.005602	
WP13-C1-S2	Igneous quartz	1553.6	0.1964	0.1294	0.7826	-0.05136	0.1539	0.4224	0.002677	-0.03513	0.03488	0.07653	0.005909	0.006485	
WP13-C1-S3	Igneous quartz	1553.6	0.05010	-0.05185	0.4221	0.04564	-0.02141	0.02101	-0.004660	-0.001382	-0.04871	0.003431	-0.002058	-0.002655	
WP13-C1-S4	Igneous quartz	1553.6	0.01215	0.1046	0.9516	0.02609	0.1703	0.3740	0.002784	-0.01458	0.03654	0.07834	0.005030	0.0008721	
WP22-C2-S1	Igneous quartz	2588.2	-0.08925	-0.01388	1.215	0.04813	0.02140	0.03009	-0.002620	-0.009264	0.01151	0.003154	-0.0006580	0.002914	
WP22-C2-S2	Igneous quartz	2588.2	0.09297	0.09454	1.110	0.05073	0.01226	-0.002767	-0.0008881	-0.01412	-0.003628	-0.004028	-0.003139	-0.001210	
WP22-C2-S3	Igneous quartz	2588.2	0.09899	0.02559	1.681	0.09993	0.004114	0.003585	0.004219	-0.003103	-0.003871	0.0002485	-0.004065	0.0009284	
WP22-C2-S4	Igneous quartz	2588.2	-0.02296	0.02738	1.586	-0.01548	-0.002706	0.005934	0.000	0.02235	0.002212	0.000	0.000	0.001392	
WP22-C2-S5	Igneous quartz	2588.2	0.1202	0.002789	1.594	0.06919	0.01223	0.01999	-0.0009348	0.02195	-0.01168	-0.001076	-0.006599	0.007911	
WP06-C1-S1	Igneous quartz	1429.0	0.6599	0.2325	0.6457	0.1961	0.1714	0.2283	0.01850	-0.002463	-0.001028	0.04439	0.004284	0.002618	
WP06-C1-S2	Igneous quartz	1429.0	0.6880	0.1090	2.450	0.1593	0.09241	0.1030	0.001841	-0.007995	0.03053	0.02351	-0.003066	-0.002754	
WP06-C1-S3	Igneous quartz	1429.0	0.1455	-0.006515	2.046	0.1096	0.02262	0.03978	0.008411	-0.004935	0.007151	0.004926	-0.0002986	-0.004859	
WP06-C1-S4	Igneous quartz	1429.0	0.4051	0.05947	2.000	0.1762	0.03526	0.06835	-0.0001686	0.006977	0.003182	0.01438	-0.006240	-0.001930	
WP64-C4-S1	Igneous quartz	704.8	0.2264	0.003279	1.257	0.3434	0.002002	0.1009	0.004874	-0.02423	0.02600	0.003822	-0.009324	0.0009480	
WP64-C4-S2	Igneous quartz	704.8	0.3202	0.01701	1.229	0.1267	0.04944	0.01977	0.0008190	-0.02425	-0.001028	0.01243	-0.008497	0.0004452	
WP64-C4-S3	Igneous quartz	704.8	0.2353	0.09219	1.404	0.08798	0.01068	0.1852	0.005251	0.009874	0.01035	0.005915	0.007306	0.0001708	
WP64-C4-S4	Igneous quartz	704.8	0.1572	0.03612	1.093	-0.008168	0.007157	0.04891	0.003476	0.008727	-0.002407	0.0004167	0.007894	-0.003401	
WP52-C1-S1	Igneous quartz	785.5	0.5891	0.1607	0.4634	0.07509	0.009034	0.2185	0.001847	0.01334	-0.01720	0.01921	-0.01270	-0.0009451	
WP52-C1-S2	Igneous quartz	785.5	0.1827	0.04272	0.5427	0.1261	0.06969	0.1796	0.004787	-0.003573	-0.004144	0.007487	-0.003288	0.001311	
WP52-C1-S3	Igneous quartz	785.5	5.690	8.958	0.7937	0.3381	0.1139	0.6416	0.005948	0.02513	0.02152	0.04696	-0.01341	0.005254	
WP52-C2-S1	Igneous quartz	785.5	0.2015	-0.04351	1.601	0.2094	0.01988	0.1042	-0.004070	-0.02073	-0.02283	0.007715	0.005089	-0.0003664	
WP52-C2-S2	Igneous quartz	785.5	0.1601	0.04867	1.363	0.1022	0.04352	0.09500	0.004650	-0.001676	0.01080	0.01783	-0.003583	-0.002593	
WP52-C2-S3	Igneous quartz	785.5	0.1512	0.1901	1.946	0.1084	0.08401	0.6079	0.01863	0.008861	0.06353	0.01433	0.0006705	-0.0006565	

* distance from center of deposit

** All elements in ppm except Au which is in ppb

Appendix 6: White Pine
quartz mineral chemistry by LA-ICP-MS

Sample	Sample type	Distance*												
		(m)	Cu65	Zn66	Ge74	As75	Rb85	Sr88	Zr90	Ag107	Sb121	Cs133	Gd157	Hf178
WP52-C2-S4	Igneous quartz	785.5	0.2119	0.04262	1.387	0.06245	0.07309	0.3991	-0.001656	-0.01383	0.008153	0.04522	-0.002430	0.003608
WP65-C1-S1	Igneous quartz	609.4	0.6809	0.2360	0.9623	-0.1361	0.005849	0.03327	-0.007162	-0.03542	0.02818	-0.0004551	0.003593	-0.009462
WP65-C1-S3	Igneous quartz	609.4	0.02599	0.1177	0.9374	0.04525	-0.007160	0.008897	-0.003010	0.004911	-0.005508	0.00005964	0.001178	-0.004229
WP65-C1-S4	Igneous quartz	609.4	0.07803	0.08603	0.9167	0.05763	0.001807	0.002720	-0.002525	-0.002741	-0.01566	0.005818	0.007905	0.001105
WP23-C1-S1	Igneous quartz	1688.3	0.07899	0.03361	0.5868	4.281	0.003057	0.05673	0.001105	-0.005289	0.002664	0.007980	-0.004457	0.004130
WP23-C1-S2	Igneous quartz	1688.3	0.07749	0.06063	0.6491	2.643	0.09902	0.08788	-0.0007529	-0.003191	-0.0005877	0.02257	-0.003563	0.01468
WP23-C1-S3	Igneous quartz	1688.3	0.3631	0.1042	0.5857	2.614	0.001198	0.02538	0.002844	-0.01179	-0.002730	0.001205	-0.001613	0.0002339
WP23-C1-S4	Igneous quartz	1688.3	0.1734	0.1593	0.6047	2.552	0.06890	0.08594	0.01378	-0.008767	0.02343	0.02605	-0.001094	-0.002694
WP23-C2-S1	Igneous quartz	1688.3	-0.008611	0.04392	0.5922	2.322	0.06787	0.05233	0.006431	0.01165	0.003738	0.02043	0.004721	0.002948
WP23-C2-S2	Igneous quartz	1688.3	0.007988	0.04862	0.5307	2.253	0.03226	0.02929	-0.0004111	-0.003471	-0.004534	0.008147	-0.006298	0.001470
WP23-C2-S3	Igneous quartz	1688.3	0.07260	0.01291	0.5595	2.295	0.03210	0.07086	0.001624	-0.005348	-0.008300	0.03873	0.007766	0.003822
WP23-C2-S4	Igneous quartz	1688.3	0.08047	0.1488	0.5417	1.649	0.03692	0.09290	-0.004879	0.01333	0.008592	0.02369	0.003064	-0.001292
WP07-C4-S1	Igneous quartz	1360.2	0.1540	-0.01814	0.4176	7.767	0.07798	0.02526	0.006947	0.005616	0.009612	0.007537	0.006823	-0.003899
WP07-C4-S2	Igneous quartz	1360.2	0.006044	0.1462	0.5253	7.333	0.05917	0.01152	-0.003142	0.0004734	0.2554	0.02250	-0.009827	-0.0004288
WP07-C4-S3	Igneous quartz	1360.2	0.1787	0.02012	0.4070	6.926	0.03299	0.009965	0.003398	0.001581	0.0007875	0.001671	-0.009218	0.003833
WP07-C4-S4	Igneous quartz	1360.2	0.1121	0.06710	0.5259	7.286	0.03170	0.005841	-0.002019	0.004865	0.02661	-0.00007698	0.004941	0.0002942

* distance from center of deposit

** All elements in ppm except Au which is in ppb

Appendix 6: White Pine
quartz mineral chemistry by LA-ICP-MS

Sample	Sample type	Distance*					
		(m)	Ta181	Au197**	Pb208	Bi209	U238
WP46-C1-S1	Vein Quartz	372.6	-0.0009304	-0.005385	0.1456	-0.005483	0.01406
WP46-C1-S2	Vein Quartz	372.6	0.0001356	0.001261	0.01078	-0.002078	0.0001440
WP46-C1-S3	Vein Quartz	372.6	-0.00003788	-0.003369	0.01559	-0.00007167	0.0003620
WP46-C1-S4	Vein Quartz	372.6	0.0006887	-0.006109	0.09182	0.003947	0.005084
WP46-C1-S5	Vein Quartz	372.6	-0.0003444	-0.001493	0.03130	0.002170	0.006944
WP46-C1-S6	Vein Quartz	372.6	-0.001550	-0.008972	0.01839	-0.002226	0.0006807
WP46-C1-S7	Vein Quartz	372.6	-0.001169	0.009775	0.7548	0.008598	0.003052
WP46-C1-S8	Vein Quartz	372.6	0.001030	0.01518	0.1618	0.007066	0.02202
WP46-C1-S9	Vein Quartz	372.6	0.001252	0.005081	0.1556	0.005901	0.003752
WP46-C1-S10	Vein Quartz	372.6	0.0006763	0.003455	0.2414	0.004110	-0.0004699
WP46-C1-S11	Vein Quartz	372.6	-0.0003770	-0.001271	0.06504	0.002312	0.001721
WP46-C1-S12	Vein Quartz	372.6	0.0002476	-0.01178	-0.001824	0.007406	0.004063
WP46-C1-S13	Vein Quartz	372.6	-0.0009028	-0.004490	0.001583	-0.001265	-0.001577
WP46-C1-S14	Vein Quartz	372.6	-0.001029	0.0008900	0.1379	0.002452	0.007190
WP46-C1-S15	Vein Quartz	372.6	0.0003195	-0.001303	0.02425	-0.0003778	-0.0001148
WP03-C1-S1	Vein Quartz	1546.4	-0.0007037	-0.0005692	0.01890	0.06756	-0.0006504
WP03-C1-S2	Vein Quartz	1546.4	0.001918	0.001391	0.06070	0.05457	0.007332
WP03-C1-S3	Vein Quartz	1546.4	0.002481	0.005407	0.6947	0.7496	0.003857
WP03-C1-S4	Vein Quartz	1546.4	0.0002192	0.002727	0.3129	0.2560	0.006283
WP03-C1-S5	Vein Quartz	1546.4	0.0004159	0.007644	0.1708	0.3257	0.001296
WP03-C2-S1	Vein Quartz	1546.4	0.0006139	0.0007139	0.05718	0.08496	0.005808
WP03-C2-S2	Vein Quartz	1546.4	0.0005299	0.003774	0.02645	0.01761	-0.0001074
WP03-C2-S3	Vein Quartz	1546.4	-0.0001380	-0.003905	0.04307	0.04034	0.0005613
WP03-C2-S4	Vein Quartz	1546.4	-0.0002986	0.0008863	0.1937	0.08542	0.0002171
WP03-C2-S5	Vein Quartz	1546.4	0.001498	0.01128	0.04765	0.3004	0.002480
WP13-C3-S1	Vein Quartz	1553.6	-0.0003314	0.002424	-0.0006005	-0.001091	-0.0005982
WP13-C3-S2	Vein Quartz	1553.6	0.0002585	-0.001846	-0.002802	0.001018	-0.0007701
WP13-C3-S3	Vein Quartz	1553.6	0.0009950	-0.001267	0.02124	0.001153	0.0004062
WP13-C3-S4	Vein Quartz	1553.6	-0.00007302	0.007489	0.01501	0.002350	-0.0004337
WP13-C5-S1	Vein Quartz	1553.6	-0.001640	-0.001949	0.04979	0.0009193	0.001351
WP13-C5-S2	Vein Quartz	1553.6	0.001363	0.008119	0.00008260	0.001582	0.002288
WP13-C5-S3	Vein Quartz	1553.6	-0.001680	0.002877	0.02948	0.001315	0.001869
WP13-C5-S4	Vein Quartz	1553.6	0.0002224	-0.002166	0.01592	0.003906	0.0009445
WP22-C4-S1	Vein Quartz	2588.2	-0.001327	0.009343	-0.002199	-0.002037	-0.002024
WP22-C4-S2	Vein Quartz	2588.2	-0.0001600	0.003599	0.08675	0.003745	-0.0004655
WP22-C4-S3	Vein Quartz	2588.2	0.0004227	-0.001046	0.1458	-0.002492	0.0005303
WP22-C4-S4	Vein Quartz	2588.2	-0.0001076	-0.002076	0.1892	0.003911	0.001459
WP22-C4-S5	Vein Quartz	2588.2	-0.001729	-0.0001898	0.2487	-0.0002235	0.01074
WP06-C2-S1	Vein Quartz	1429.0	0.0005123	0.01173	0.02492	0.001310	-0.0002560
WP06-C2-S2	Vein Quartz	1429.0	-0.0002348	0.0001498	0.02304	-0.0004923	-0.0004012
WP06-C2-S3	Vein Quartz	1429.0	0.0003050	-0.001946	0.05001	0.002813	-0.00009003
WP06-C2-S4	Vein Quartz	1429.0	0.001760	0.0001471	0.01347	0.004489	-0.0001182
WP06-C3-S2	Vein Quartz	1429.0	0.002562	0.01904	0.02612	0.001967	0.001893

* distance from center of deposit

** All elements in ppm except Au which is in ppb

Appendix 6: White Pine
quartz mineral chemistry by LA-ICP-MS

Sample	Sample type	Distance*					
		(m)	Ta181	Au197**	Pb208	Bi209	U238
WP06-C3-S3	Vein Quartz	1429.0	-0.001022	-0.002744	0.06486	0.003272	0.01008
WP06-C3-S4	Vein Quartz	1429.0	0.001790	-0.008074	0.07056	-0.001844	0.002785
WP53-C1-S1	Vein Quartz	548.8	0.003276	-0.002371	0.009224	-0.002462	0.001148
WP53-C1-S2	Vein Quartz	548.8	-0.001502	0.001657	0.008272	0.001084	0.003574
WP53-C1-S3	Vein Quartz	548.8	-0.0003212	0.006812	0.006698	0.001400	0.0004408
WP53-C1-S4	Vein Quartz	548.8	0.00005426	0.009405	0.005509	0.0004994	-0.001398
WP53-C1-S5	Vein Quartz	548.8	-0.0005284	0.009924	0.05438	-0.002679	0.002066
WP53-C2-S1	Vein Quartz	548.8	0.00009036	0.003260	0.8202	0.02776	0.1013
WP53-C2-S2	Vein Quartz	548.8	0.002157	0.001200	0.03442	0.004147	0.02057
WP53-C2-S3	Vein Quartz	548.8	0.001893	0.002815	0.02553	0.004308	0.01544
WP53-C2-S4	Vein Quartz	548.8	0.0001603	0.01171	0.02285	0.0002440	0.005920
WP53-C2-S5	Vein Quartz	548.8	0.0001892	-0.004890	0.4856	0.009366	0.04448
WP05-C1-S1	Vein Quartz	1429.0	0.0006867	-0.006652	0.03172	-0.007353	0.004359
WP05-C1-S2	Vein Quartz	1429.0	-0.001217	-0.004613	0.07014	-0.001671	0.002211
WP05-C1-S3	Vein Quartz	1429.0	0.0006716	0.0001179	0.0005480	0.003421	0.0007290
WP05-C1-S4	Vein Quartz	1429.0	0.001868	0.01121	0.003078	-0.003951	-0.002534
WP05-C2-S1	Vein Quartz	1429.0	0.0006339	0.007148	0.02763	0.002254	-0.0004256
WP05-C2-S2	Vein Quartz	1429.0	0.0006610	0.02871	0.02204	-0.0007127	0.001331
WP05-C2-S3	Vein Quartz	1429.0	0.001884	0.001134	0.01942	-0.001524	-0.0005606
WP05-C2-S4	Vein Quartz	1429.0	-0.0009232	-0.002150	0.01442	-0.008437	0.0003659
WP05-C2-S5	Vein Quartz	1429.0	-0.002159	0.01388	0.008952	0.005981	-0.0001998
WP05-C3-S1	Vein Quartz	1429.0	-0.001460	0.01344	0.04626	0.02246	-0.0006552
WP05-C3-S2	Vein Quartz	1429.0	-0.002206	-0.003872	0.02035	0.007003	-0.001027
WP05-C3-S3	Vein Quartz	1429.0	-0.001780	0.006549	0.01959	-0.002146	0.003436
WP05-C3-S4	Vein Quartz	1429.0	0.0005137	-0.001582	0.03934	-0.003351	0.0001067
WP64-C1-S1	Vein Quartz	704.8	0.001841	-0.007748	0.3162	0.003022	-0.0001484
WP64-C1-S2	Vein Quartz	704.8	0.0002913	0.001066	0.01722	-0.002744	0.001169
WP64-C1-S3	Vein Quartz	704.8	-0.001322	0.01083	0.08976	0.004521	0.001206
WP64-C1-S4	Vein Quartz	704.8	0.0005611	-0.004078	0.03577	-0.005687	-0.001132
WP64-C2-S1	Vein Quartz	704.8	0.0002693	0.002061	0.1850	0.02516	0.008008
WP64-C2-S2	Vein Quartz	704.8	0.0006974	0.006691	0.04885	0.002756	0.007436
WP64-C2-S4	Vein Quartz	704.8	0.001732	0.003967	0.5791	0.0003855	0.0005079
WP64-C3-S1	Vein Quartz	704.8	0.004658	-0.009812	0.008706	0.001052	0.001090
WP64-C3-S2	Vein Quartz	704.8	0.001407	0.006615	0.1024	-0.001897	0.0005050
WP64-C3-S3	Vein Quartz	704.8	-0.0001834	-0.003672	0.5944	0.02563	0.009936
WP52-C3-S1	Vein Quartz	785.5	-0.0002405	0.008230	0.02225	0.003643	0.005230
WP52-C3-S2	Vein Quartz	785.5	-0.0001088	0.01029	0.009238	0.001216	0.00006377
WP52-C3-S3	Vein Quartz	785.5	-0.0004397	0.002805	0.1793	0.008010	-0.001624
WP52-C3-S4	Vein Quartz	785.5	0.001336	-0.005228	0.02521	-0.005599	0.002453
WP65-C2-S3	Vein Quartz	609.4	0.003929	-0.003401	0.07472	0.004013	-0.0002672
WP65-C2-S4	Vein Quartz	609.4	0.001120	-0.005432	0.003528	0.0005148	0.001925
WP65-C3-S1	Vein Quartz	609.4	0.00009904	-0.001403	0.005427	0.0007688	0.001547
WP65-C3-S2	Vein Quartz	609.4	0.0003406	0.002733	0.4222	0.01195	0.0001760

* distance from center of deposit

** All elements in ppm except Au which is in ppb

Appendix 6: White Pine
quartz mineral chemistry by LA-ICP-MS

Sample	Sample type	Distance* (m)	Ta181	Au197**	Pb208	Bi209	U238
WP65-C3-S3	Vein Quartz	609.4	0.001122	-0.006128	0.01568	0.004950	0.002280
WP65-C3-S4	Vein Quartz	609.4	0.0003382	0.007887	0.004742	-0.001218	0.0001156
WP65-C4-S1	Vein Quartz	609.4	0.0005218	0.002407	0.08776	0.006346	0.008508
WP65-C4-S2	Vein Quartz	609.4	-0.001645	0.007578	-0.004833	-0.001970	0.002447
WP65-C4-S3	Vein Quartz	609.4	0.0002459	-0.002524	0.0002938	-0.0002857	0.001638
WP65-C4-S4	Vein Quartz	609.4	-0.0007337	-0.006672	0.4365	0.01532	0.001143
WP23-C5-S2	Vein Quartz	1688.3	0.0003574	-0.005308	0.04625	0.005467	0.0003784
WP07-C1-S3	Vein Quartz	1360.2	0.002225	0.004075	0.1543	0.01265	0.007668
WP07-C1-S4	Vein Quartz	1360.2	-0.002104	0.002603	0.1140	0.01380	0.007846
WP07-C2-S1	Vein Quartz	1360.2	0.00007068	-0.0002788	0.01364	0.0005212	-0.001173
WP07-C2-S2	Vein Quartz	1360.2	0.0009474	-0.0002992	0.001849	0.002842	0.008762
WP07-C2-S3	Vein Quartz	1360.2	0.001878	-0.005622	0.07460	-0.004899	0.007178
WP07-C4-S1	Vein Quartz	1360.2	-0.001769	-0.007015	0.01567	-0.0001634	-0.001959
WP07-C4-S2	Vein Quartz	1360.2	-0.0004411	0.004738	0.007356	0.0001181	0.0001327
WP07-C4-S3	Vein Quartz	1360.2	0.001721	0.001454	0.01911	-0.002301	0.0003244
WP07-C4-S4	Vein Quartz	1360.2	-0.001051	-0.004177	0.008362	-0.0006475	-0.0004695
WP07-C1-S1	Vein Quartz	1360.2	0.001347	0.01195	0.2399	2.329	0.1224
WP07-C1-S3	Vein Quartz	1360.2	0.002225	0.004075	0.1543	0.01265	0.007668
WP07-C1-S4	Vein Quartz	1360.2	-0.001566	0.004198	0.1210	0.01861	0.005424
WP07-C2-S1	Vein Quartz	1360.2	0.0006256	0.005116	0.008413	0.001913	-0.0009113
WP07-C2-S2	Vein Quartz	1360.2	-0.0002306	-0.004909	0.004338	0.002071	0.006023
WP07-C2-S3	Vein Quartz	1360.2	-0.0002781	-0.006960	0.01475	-0.002508	0.001180
WP03-C1-S1	Vein Quartz	1546.4	0.0001039	-0.004082	0.1280	0.001040	0.006774
WP03-C1-S2	Vein Quartz	1546.4	-0.001434	-0.005048	0.004386	0.0002481	0.0004047
WP03-C1-S3	Vein Quartz	1546.4	0.0006922	0.004238	0.003470	0.0002839	0.0001468
WP03-C1-S4	Vein Quartz	1546.4	-0.0006856	-0.002333	0.01508	-0.0006021	0.0006879
WP03-C2-S2	Vein Quartz	1546.4	-0.001022	0.009721	0.01213	0.001776	-0.0001917
WP03-C2-S3	Vein Quartz	1546.4	0.0006416	0.002105	0.02653	0.0003009	0.0006642
WP03-C2-S4	Vein Quartz	1546.4	0.00008246	-0.004210	0.007593	0.003052	0.002441
WP03-C3-S1	Vein Quartz	1546.4	-0.0002385	-0.007674	-0.002169	0.0004091	0.0007006
WP03-C3-S2	Vein Quartz	1546.4	0.0007133	0.002253	0.03274	0.0004677	0.0001211
WP03-C3-S3	Vein Quartz	1546.4	0.0004894	0.0002437	0.008132	0.003017	0.001123
WP03-C3-S4	Vein Quartz	1546.4	0.002330	0.0003571	0.03635	0.002417	0.001535
WP03-C4-S1	Vein Quartz	1546.4	-0.0001776	0.003277	0.05324	0.0005283	0.0003425
WP03-C4-S2	Vein Quartz	1546.4	-0.002274	-0.009977	0.03995	0.003096	0.001640
WP03-C4-S3	Vein Quartz	1546.4	0.001310	-0.008796	0.02279	-0.0009905	-0.0006580
WP03-C4-S4	Vein Quartz	1546.4	-0.001035	-0.01108	0.03564	-0.00006308	-0.003659
WP63-C1-S1	Breccia Cement	0.0	0.002039	-0.001198	0.03869	0.00001482	-0.002266
WP63-C1-S2	Breccia Cement	0.0	-0.001126	-0.008326	0.04445	0.001566	0.0003679
WP63-C1-S3	Breccia Cement	0.0	0.00005948	0.003620	0.03664	0.001641	-0.001276
WP63-C2-S1	Breccia Cement	0.0	0.0003974	0.002067	0.02937	0.0008456	0.00001631
WP63-C2-S2	Breccia Cement	0.0	0.001443	-0.002951	0.06356	0.004328	0.0008247
WP63-C2-S3	Breccia Cement	0.0	-0.003178	-0.007951	0.1556	-0.005953	0.0006373

* distance from center of deposit

** All elements in ppm except Au which is in ppb

Appendix 6: White Pine
quartz mineral chemistry by LA-ICP-MS

Sample	Sample type	Distance*					
		(m)	Ta181	Au197**	Pb208	Bi209	U238
WP63-C3-S1	Breccia Cement	0.0	-0.0009649	-0.008867	0.4697	0.01890	0.001994
WP02-C1-S1	Breccia Cement	132.2	-0.0002624	-0.001553	0.02735	-0.0001236	-0.0004111
WP02-C1-S2	Breccia Cement	132.2	0.0006244	-0.003274	0.08069	0.002251	0.002042
WP02-C1-S4	Breccia Cement	132.2	-0.0008160	0.01067	0.03887	-0.001273	-0.0003526
WP02-C1-S5	Breccia Cement	132.2	0.0005048	-0.001015	0.1499	-0.0005076	0.0007730
WP02-C1-S6	Breccia Cement	132.2	0.000	-0.0009717	0.2269	0.001295	-0.001143
WP02-C1-S7	Breccia Cement	132.2	0.0003816	-0.004732	0.07373	0.002759	0.0007219
WP02-C1-S9	Breccia Cement	132.2	0.001531	0.005427	0.007541	0.001925	0.001711
WP02-C1-S10	Breccia Cement	132.2	0.0004161	0.003843	0.01498	-0.001861	0.0009407
WP02-C1-S11	Breccia Cement	132.2	-0.0007620	-0.002669	0.1409	0.0009327	0.003094
WP02-C1-S12	Breccia Cement	132.2	-0.0001355	0.007465	0.01289	-0.003112	0.002297
WP02-C2-S1	Breccia Cement	132.2	-0.0008475	0.005654	0.02411	0.001322	0.0003075
WP02-C2-S2	Breccia Cement	132.2	-0.001191	-0.001611	0.01841	-0.0001926	0.01376
WP02-C2-S3	Breccia Cement	132.2	-0.0003463	-0.002209	0.01779	0.0006321	0.002022
WP02-C2-S4	Breccia Cement	132.2	0.001499	-0.0008106	0.03701	-0.002595	-0.001172
WP03-C3-S1	Igneous quartz	1546.4	0.0009586	-0.009434	0.007332	0.01215	0.003710
WP03-C3-S2	Igneous quartz	1546.4	0.001849	-0.008289	-0.0008197	0.005329	0.0001657
WP03-C3-S3	Igneous quartz	1546.4	-0.0007567	0.002814	0.01216	0.007351	0.007524
WP03-C3-S4	Igneous quartz	1546.4	0.0008036	0.004972	0.1654	0.07521	0.009606
WP03-C3-S5	Igneous quartz	1546.4	-0.0005080	-0.002182	0.3832	0.06789	0.003286
WP13-C1-S1	Igneous quartz	1553.6	-0.001407	0.008135	0.03737	-0.003728	0.001235
WP13-C1-S2	Igneous quartz	1553.6	0.0002951	-0.008796	0.1086	0.008980	0.007466
WP13-C1-S3	Igneous quartz	1553.6	0.001708	-0.003429	0.005867	0.008444	0.001103
WP13-C1-S4	Igneous quartz	1553.6	-0.002259	0.007502	0.04601	-0.004666	0.001075
WP22-C2-S1	Igneous quartz	2588.2	0.001931	0.004663	0.005847	-0.001617	0.0003777
WP22-C2-S2	Igneous quartz	2588.2	-0.001278	-0.0009913	0.01527	-0.0003505	-0.0004335
WP22-C2-S3	Igneous quartz	2588.2	-0.001199	-0.0006847	0.004187	-0.001740	0.0006652
WP22-C2-S4	Igneous quartz	2588.2	0.000	-0.01027	0.01392	-0.0006049	0.001495
WP22-C2-S5	Igneous quartz	2588.2	0.000	-0.003335	0.08840	0.0003070	-0.001012
WP06-C1-S1	Igneous quartz	1429.0	0.0002459	0.002535	0.2585	0.05312	0.06061
WP06-C1-S2	Igneous quartz	1429.0	-0.0001378	0.001191	0.08216	-0.002256	0.00001498
WP06-C1-S3	Igneous quartz	1429.0	-0.0009172	0.0008381	0.004256	0.006091	0.001594
WP06-C1-S4	Igneous quartz	1429.0	-0.002015	0.0004978	0.03082	0.004570	0.001370
WP64-C4-S1	Igneous quartz	704.8	0.001284	0.006236	68.71	-0.0004609	0.0004663
WP64-C4-S2	Igneous quartz	704.8	0.001369	0.004830	0.02131	-0.001600	0.0003761
WP64-C4-S3	Igneous quartz	704.8	-0.001887	0.003431	22.68	0.002933	0.0001258
WP64-C4-S3	Igneous quartz	704.8	0.001289	0.009937	1.636	0.002978	0.0004104
WP52-C1-S1	Igneous quartz	785.5	-0.0007846	0.006191	0.07858	0.006789	0.0001443
WP52-C1-S2	Igneous quartz	785.5	-0.00004933	-0.0002800	0.05239	-0.004066	0.003691
WP52-C1-S3	Igneous quartz	785.5	0.001190	0.0004905	3.292	0.3709	0.1523
WP52-C2-S1	Igneous quartz	785.5	-0.001183	-0.002184	0.02528	0.01226	0.008249
WP52-C2-S2	Igneous quartz	785.5	-0.001740	0.003887	-0.0002465	-0.002036	0.0001049
WP52-C2-S3	Igneous quartz	785.5	0.000	-0.01708	0.03040	0.0004257	0.002288

* distance from center of deposit

** All elements in ppm except Au which is in ppb

Appendix 6: White Pine
quartz mineral chemistry by LA-ICP-MS

Sample	Sample type	Distance*					
		(m)	Ta181	Au197**	Pb208	Bi209	U238
WP52-C2-S4	Igneous quartz	785.5	0.001087	-0.003019	0.01506	0.001592	0.0005632
WP65-C1-S1	Igneous quartz	609.4	0.00005519	-0.001849	0.06795	-0.005061	0.0006921
WP65-C1-S3	Igneous quartz	609.4	0.002127	-0.009317	-0.0003135	0.0003200	0.0007971
WP65-C1-S4	Igneous quartz	609.4	-0.001229	-0.001014	-0.002463	0.002981	-0.0007109
WP23-C1-S1	Igneous quartz	1688.3	0.0006615	0.004102	0.02182	0.0007536	0.000
WP23-C1-S2	Igneous quartz	1688.3	-0.002349	-0.005936	0.04662	0.0007888	0.04979
WP23-C1-S3	Igneous quartz	1688.3	0.01311	-0.004674	0.01342	0.001353	0.002413
WP23-C1-S4	Igneous quartz	1688.3	0.002537	-0.002584	0.1201	0.004332	0.01501
WP23-C2-S1	Igneous quartz	1688.3	-0.0001427	0.006002	0.02396	0.002732	0.0008626
WP23-C2-S2	Igneous quartz	1688.3	0.0004776	0.002019	0.01082	0.02961	0.0007433
WP23-C2-S3	Igneous quartz	1688.3	0.0008311	0.00004452	0.02416	0.001564	0.0004567
WP23-C2-S4	Igneous quartz	1688.3	-0.0008627	0.01155	0.01822	-0.0005202	0.0009751
WP07-C4-S1	Igneous quartz	1360.2	-0.001164	-0.004615	0.01784	-0.001495	-0.001829
WP07-C4-S2	Igneous quartz	1360.2	0.001089	0.006899	-0.002508	0.0006281	0.0002053
WP07-C4-S3	Igneous quartz	1360.2	0.0006706	0.001244	0.01490	-0.001435	-0.0003145
WP07-C4-S4	Igneous quartz	1360.2	-0.001298	-0.005161	0.01152	-0.0001118	-0.00007402

* distance from center of deposit

** All elements in ppm except Au which is in ppb

Appendix 7: Buckingham
quartz mineral chemistry by LA-ICP-MS

Sample	Sample type	Distance*															
		(m)	Li7	Na23	Mg24	Al27	Si29	P31	K39	Ca43	Ti47	Ti49	V51	Cr53	Mn55	Fe57	Cu63
BK01-C1-S1	Vein quartz	591.4	13.62	46.67	1.425	242.1	467500	9.400	183.8	-1.396	76.90	77.96	0.02171	-0.06289	0.2331	3.728	1.389
BK01-C1-S2	Vein quartz	591.4	12.43	3.600	0.3311	91.72	467500	8.238	6.166	-7.422	59.92	60.90	0.002231	0.1113	0.1663	1.177	0.08988
BK01-C1-S3	Vein quartz	591.4	11.97	4.145	0.7121	111.1	467500	9.915	17.23	22.08	70.93	68.19	-0.02046	-0.1136	0.1323	3.363	0.4365
BK01-C2-S1	Vein quartz	591.4	6.007	8.517	0.09547	54.28	467500	14.32	4.935	-4.151	11.28	10.68	-0.01389	-0.06474	0.07478	0.8268	-0.03612
BK01-C2-S2	Vein quartz	591.4	4.211	7.872	0.05959	37.36	467500	11.22	3.298	-47.56	10.12	10.89	-0.01411	-0.02554	0.09310	-0.5999	0.04343
BK01-C2-S3	Vein quartz	591.4	13.29	6.749	0.4901	138.3	467500	9.479	17.35	41.02	22.98	23.09	-0.007577	0.08689	0.1964	0.7022	0.07164
BK01-C2-S4	Vein quartz	591.4	4.424	4.737	0.06580	35.59	467500	8.207	1.119	35.78	11.22	10.63	0.003473	-0.1779	0.07940	-0.2935	0.07361
BK01-C3-S1	Vein quartz	591.4	9.646	18.82	0.2670	78.07	467500	6.409	13.89	-23.46	26.60	26.01	-0.01718	0.1093	0.1091	0.3107	-0.03829
BK01-C3-S2	Vein quartz	591.4	6.334	16.64	0.1111	66.35	467500	10.32	30.58	58.04	16.30	15.36	0.01243	-0.07255	0.1583	-0.2957	0.08756
BK01-C3-S3	Vein quartz	591.4	2.835	19.19	0.3679	59.08	467500	7.983	6.478	57.05	15.05	16.09	-0.01095	0.2361	0.3337	1.430	0.06191
BK01-C5-S1	Vein quartz	591.4	3.994	-1.833	0.8429	55.30	467500	11.60	0.3431	-7.095	20.96	20.26	0.7390	0.4208	0.7717	199.9	0.9629
BK01-C5-S4	Vein quartz	591.4	7.017	1.350	0.3174	69.31	467500	14.31	6.101	29.69	21.38	20.18	0.1182	-0.03884	0.07920	25.96	0.3171
BK021-C3-S1	Vein quartz	517.7	6.388	26.49	5.991	1445	467500	17.21	231.9	39.44	1.644	3.318	0.008803	-0.04224	4.825	21.22	0.05739
BK021-C3-S2	Vein quartz	517.7	2.422	7.368	6.611	472.7	467500	18.53	155.8	-14.83	1.921	2.128	0.005779	0.3363	2.155	20.45	0.08239
BK021-C3-S4	Vein quartz	517.7	5.310	27.98	14.88	1496	467500	15.47	648.0	72.44	50.60	49.09	0.2654	0.1872	5.733	46.80	0.1445
BK021-C4-S1	Vein quartz	517.7	5.015	32.76	1.556	1600	467500	16.83	270.5	0.7658	1.208	0.5784	-0.007987	0.1536	4.509	11.24	0.8124
BK021-C4-S3	Vein quartz	517.7	3.558	18.45	17.83	1220	467500	14.66	518.4	-1.645	5.571	6.195	0.1415	-0.03776	3.515	56.21	0.006051
BK021-C4-S4	Vein quartz	517.7	3.417	24.99	18.00	1473	467500	12.69	484.5	37.58	2.248	2.553	0.05035	0.2242	4.023	42.86	0.2180
BK021-C4-S5	Vein quartz	517.7	5.184	4.357	2.826	313.8	467500	15.08	101.3	-4.691	0.9547	0.4967	0.02908	0.08524	1.124	9.440	0.005509
BK03-C1-S2	Vein quartz	337.4	4.934	-5.488	0.5232	54.65	467500	10.64	4.547	36.24	51.10	52.07	0.005257	0.09903	0.1821	1.155	0.1257
BK03-C4-S1	Vein quartz	337.4	5.817	20.88	3.390	163.6	467500	10.79	58.91	3.332	31.12	30.93	0.2295	-0.05066	3.129	28.13	0.5772
BK03-C4-S2	Vein quartz	337.4	3.662	-4.823	1.697	84.05	467500	15.32	12.81	63.30	17.32	19.34	0.1353	0.4626	0.02421	1.419	0.2003
BK03-C4-S3	Vein quartz	337.4	4.935	7.401	1.531	97.81	467500	8.041	21.93	-21.51	21.68	21.23	0.1096	0.05032	0.9668	6.428	2.271
BK06-C1-S1	Vein quartz	940.0	6.748	8.661	0.05456	41.43	467500	14.20	2.254	-17.67	12.51	10.59	-0.02223	0.03509	0.5122	1.060	-0.02072
BK06-C1-S2	Vein quartz	940.0	9.839	-6.336	0.09555	56.49	467500	14.31	8.611	41.34	28.85	28.27	0.01171	0.1045	0.06016	0.3503	-0.03243
BK06-C1-S3	Vein quartz	940.0	10.68	1.520	0.07335	83.20	467500	12.07	102.4	36.79	24.35	24.15	0.01842	-0.1088	0.01878	1.890	0.08312
BK06-C1-S4	Vein quartz	940.0	9.335	8.252	0.2190	63.83	467500	13.17	25.16	-13.88	24.13	24.17	0.08351	0.3041	0.02028	22.08	0.2794
BK06-C2-S1	Vein quartz	940.0	9.414	-3.522	0.05716	50.23	467500	11.25	0.5816	5.640	27.65	28.89	-0.02606	0.1110	0.02931	0.7159	0.1005
BK06-C2-S2	Vein quartz	940.0	10.62	-0.5281	0.1405	60.34	467500	12.30	8.454	40.40	31.38	34.99	0.1425	-0.02716	0.06363	50.41	0.2045
BK06-C2-S4	Vein quartz	940.0	11.60	-1.311	0.1434	61.90	467500	13.91	0.2614	23.28	31.45	31.63	0.01728	-0.1153	0.07405	11.71	0.2224
BK06-C2-S5	Vein quartz	940.0	11.59	1.305	0.1212	61.28	467500	8.913	4.113	1.154	29.79	30.99	0.008357	0.06463	0.08650	8.909	0.8805
BK06-C3-S1	Vein quartz	940.0	9.094	4.779	0.2366	52.09	467500	10.66	1.818	41.95	30.34	31.00	-0.007501	-0.1587	0.07337	0.6742	2.796
BK06-C3-S2	Vein quartz	940.0	5.981	17.37	0.1488	38.80	467500	12.77	5.956	5.089	29.47	28.25	0.04875	0.1920	0.09573	34.49	0.3453
BK06-C3-S3	Vein quartz	940.0	12.57	-4.706	0.1507	70.85	467500	13.31	5.548	18.78	37.85	37.41	0.09626	-0.1225	0.06002	26.93	0.2065
BK09-C1-S1	Vein quartz	1043.0	7.117	20.96	0.08894	71.42	467500	10.06	9.959	4.501	28.47	27.02	0.003728	0.1228	0.1405	0.1354	0.1278
BK09-C1-S2	Vein quartz	1043.0	4.305	20.87	0.9009	103.8	467500	11.75	24.35	72.75	40.97	42.81	0.01550	0.08268	0.4458	1.751	0.2119
BK09-C1-S3	Vein quartz	1043.0	5.996	45.28	0.2828	83.88	467500	16.04	42.38	-49.42	38.41	37.78	0.009137	-0.02684	0.8676	127.6	1.680
BK09-C1-S4	Vein quartz	1043.0	3.523	36.08	0.2050	75.62	467500	18.28	70.09	-15.21	40.39	42.04	0.0005146	0.1374	0.7462	33.39	1.382
BK09-C2-S1	Vein quartz	1043.0	12.20	21.75	0.1803	114.7	467500	8.944	10.80	16.09	33.69	34.18	-0.008481	-0.1858	0.2863	0.5666	0.3111
BK09-C2-S2	Vein quartz	1043.0	6.078	48.92	0.2721	82.35	467500	14.37	21.14	103.2	42.77	42.91	-0.004742	0.01804	1.739	0.2289	0.2904
BK09-C2-S4	Vein quartz	1043.0	5.378	16.41	0.2751	76.35	467500	15.31	10.55	-27.27	38.75	37.41	0.007756	-0.01919	0.2113	0.4942	1.802
BK09-C3-S2	Vein quartz	1043.0	6.940	7.497	1.916	328.3	467500	10.55	100.8	61.67	143.8	138.1	0.01697	-0.01229	1.286	6.232	0.07714
BK09-C3-S3	Vein quartz	1043.0	5.106	9.130	0.04968	60.85	467500	17.25	5.918	2.181	18.19	17.17	0.02250	-0.04687	0.4096	-0.008485	0.03672

* distance from center of deposit

** All elements in ppm except Au which is in ppb

Appendix 7: Buckingham
quartz mineral chemistry by LA-ICP-MS

Sample	Sample type	Distance*															
		(m)	Li7	Na23	Mg24	Al27	Si29	P31	K39	Ca43	Ti47	Ti49	V51	Cr53	Mn55	Fe57	Cu63
BK09-C3-S4	Vein quartz	1043.0	6.550	-3.363	0.1499	82.13	467500	17.64	4.144	-1.955	48.81	46.14	0.001498	-0.06624	0.1016	-0.2731	-0.02120
BK09-C4-S1	Vein quartz	1043.0	6.069	14.94	0.5414	121.8	467500	14.13	25.18	37.14	75.24	71.97	0.006102	-0.04030	0.9278	1.336	0.1718
BK09-C4-S2	Vein quartz	1043.0	4.663	26.72	0.6577	66.42	467500	9.370	15.39	-25.68	22.55	28.91	-0.01251	0.004768	1.113	1.071	0.4456
BK09-C4-S3	Vein quartz	1043.0	6.931	18.34	2.208	252.2	467500	12.11	93.42	39.78	95.57	99.88	0.04548	0.01847	1.067	4.532	0.9913
BK09-C4-S4	Vein quartz	1043.0	4.483	15.24	2.457	86.13	467500	14.26	32.25	22.88	22.58	22.02	0.07667	-0.1530	0.4608	2.191	0.6819
BK100-C1-S2	Vein quartz	1443.7	11.35	2.689	0.2744	88.73	467500	14.70	3.294	-24.68	59.32	53.68	0.02070	0.1201	0.1713	4.979	3.111
BK100-C1-S3	Vein quartz	1443.7	11.87	20.08	1.094	85.65	467500	14.59	8.895	-17.58	27.39	27.03	0.0001280	-0.007567	0.2726	1.558	0.3681
BK100-C1-S4	Vein quartz	1443.7	13.49	17.26	0.4695	114.1	467500	15.65	13.69	47.58	65.92	63.83	0.008145	-0.007911	0.2728	1.137	0.2802
BK100-C4-S1	Vein quartz	1443.7	14.22	9.142	0.8006	185.0	467500	13.18	28.84	39.04	81.45	82.78	-0.01463	0.1254	0.7854	1.572	0.07779
BK100-C4-S2	Vein quartz	1443.7	12.90	15.27	0.6946	159.8	467500	15.05	30.94	-18.79	79.49	78.88	0.002038	-0.05842	0.4557	1.301	0.09082
BK100-C4-S3	Vein quartz	1443.7	10.58	7.883	0.9582	139.7	467500	19.59	23.02	-5.402	80.97	80.21	0.01685	-0.1378	0.2489	1.628	0.9435
BK100-C4-S4	Vein quartz	1443.7	13.47	11.97	0.8368	199.3	467500	11.29	46.70	31.97	90.43	86.04	0.01238	-0.01858	0.7470	1.520	0.4844
BK101-C2-S1	Vein quartz	1061.5	5.858	28.62	1.056	103.2	467500	18.67	16.33	-1.278	19.52	20.38	0.002083	-0.05376	0.2959	2.136	0.7270
BK101-C2-S2	Vein quartz	1061.5	3.885	0.6761	0.2774	47.43	467500	19.26	4.274	-25.75	12.94	12.02	-0.009626	0.02618	0.1226	32.33	0.2094
BK101-C2-S3	Vein quartz	1061.5	4.941	23.44	0.6850	106.2	467500	18.25	44.43	-30.10	26.92	26.43	-0.00007096	0.07926	0.3331	1.832	0.7219
BK101-C3-S1	Vein quartz	1061.5	5.680	3.453	0.2800	60.00	467500	17.31	1.886	11.51	33.16	33.26	0.006113	0.03975	0.01812	-0.2351	-0.03186
BK101-C3-S1	Vein quartz	1061.5	5.060	4.221	0.3092	63.50	467500	18.10	1.991	0.1291	17.03	18.33	0.0004280	0.03692	0.1448	6.891	0.1578
BK101-C3-S2	Vein quartz	1061.5	6.812	4.207	0.2957	65.33	467500	16.28	3.326	20.87	54.72	45.14	0.01404	0.003027	0.08188	0.01565	0.1159
BK101-C3-S3	Vein quartz	1061.5	8.773	1.708	0.5386	90.82	467500	12.35	2.854	20.64	54.76	56.31	0.004220	0.01274	0.2145	10.87	0.3150
BK101-C3-S4	Vein quartz	1061.5	11.62	0.5001	0.9318	124.5	467500	17.29	6.930	17.38	46.89	46.98	0.001284	0.05041	0.1120	11.99	0.3978
BK101-C3-S5	Vein quartz	1061.5	7.520	2.660	0.4292	74.34	467500	17.26	6.745	7.036	36.86	36.80	0.05014	-0.03081	0.01912	40.86	1.065
BK101-C5-S1	Vein quartz	1061.5	5.032	0.5070	0.2572	74.69	467500	17.07	5.108	45.29	11.72	11.74	-0.003556	0.001179	0.05755	0.3090	0.02310
BK101-C5-S1	Vein quartz	1061.5	13.34	-0.8067	1.058	217.4	467500	14.84	6.845	-29.91	14.56	12.66	0.02260	0.2939	0.1622	32.60	0.4113
BK102-C1-S1	Vein quartz	890.8	10.05	2.555	0.3682	137.0	467500	16.54	9.054	31.35	9.536	9.250	0.002350	-0.2445	0.1454	0.9920	0.05111
BK102-C1-S2	Vein quartz	890.8	2.519	-3.426	0.1952	31.08	467500	10.69	-0.2201	1.243	4.800	4.594	-0.005997	0.2021	0.07389	37.79	0.3244
BK102-C1-S3	Vein quartz	890.8	3.557	-4.758	0.09695	37.64	467500	14.00	-0.5849	15.89	6.064	5.792	0.001833	-0.06363	0.01394	17.01	0.2488
BK102-C1-S4	Vein quartz	890.8	4.209	20.46	1.921	97.89	467500	9.426	32.16	72.12	25.40	24.58	0.03512	0.2449	1.203	11.33	-0.03284
BK102-C2-S1	Vein quartz	890.8	10.78	-1.285	1.286	251.4	467500	12.01	1.348	-2.406	12.72	12.68	0.006853	-0.1833	0.1407	11.16	0.1687
BK102-C2-S2	Vein quartz	890.8	7.475	9.703	1.599	174.6	467500	8.181	18.54	23.32	13.13	11.28	-0.004983	-0.09272	0.4672	30.92	1.856
BK102-C2-S3	Vein quartz	890.8	2.857	11.52	1.958	57.17	467500	11.16	14.41	-7.406	14.13	13.84	0.04028	0.1203	1.285	7.138	0.2591
BK102-C2-S5	Vein quartz	890.8	4.694	-4.557	0.4526	67.84	467500	13.97	3.436	-21.47	6.958	6.859	-0.004055	0.02623	0.05500	8.906	0.1621
BK106-C2-S1	Vein quartz	466.2	3.410	3.399	4.983	311.2	467500	12.51	20.65	103.1	25.04	20.15	0.04911	0.2640	0.4929	24.94	0.5390
BK106-C2-S2	Vein quartz	466.2	8.035	10.90	2.344	156.3	467500	10.97	21.86	58.36	43.95	47.52	0.01622	-0.07817	0.3290	2.984	0.2734
BK106-C2-S3	Vein quartz	466.2	7.026	28.80	0.9929	81.39	467500	14.84	18.88	68.71	36.07	33.22	-0.005992	0.02961	0.3803	1.584	0.9912
BK106-C3-S1	Vein quartz	466.2	15.42	12.60	1.072	214.2	467500	11.67	15.22	8.815	6.813	7.124	-0.007627	-0.05451	0.2602	0.8165	0.3771
BK106-C3-S2	Vein quartz	466.2	6.880	2.731	14.19	1720	467500	16.84	43.27	62.67	38.05	35.50	0.06779	0.1697	0.3130	187.6	2.607
BK12-C2-S1	Vein quartz	1475.3	3.822	-0.1389	-0.03659	31.94	467500	18.32	-0.5102	-16.67	2.603	-0.1385	-0.009019	-0.01718	0.02394	0.1493	0.01560
BK12-C2-S3	Vein quartz	1475.3	28.01	19.79	0.5073	292.7	467500	16.60	10.84	37.48	0.1464	0.01274	0.02473	-0.1495	3.882	3.367	0.03348
BK12-C4-S1	Vein quartz	1475.3	33.19	1.202	1.042	316.2	467500	17.67	2.089	-12.60	0.6333	0.4491	0.006573	-0.1931	0.1095	1.717	0.06765
BK12-C4-S3	Vein quartz	1475.3	71.48	40.28	1.479	1051	467500	17.84	37.23	49.05	0.9760	0.4226	0.05708	0.1404	0.1665	2.733	-0.03777
BK12-C6-S2	Vein quartz	1475.3	84.38	42.28	0.1736	1317	467500	19.50	7.171	2.505	0.5111	0.7232	0.01202	0.08360	0.7562	2.567	0.02815
BK13-C3-S2	Vein quartz	1381.0	47.90	37.71	0.1508	828.4	467500	17.29	61.28	12.65	0.4111	0.4933	-0.001185	0.1075	0.03204	-0.1561	-0.06173
BK13-C3-S3	Vein quartz	1381.0	42.21	31.53	1.839	938.5	467500	20.92	106.5	0.9178	0.9136	0.9684	0.008080	0.1749	0.1699	4.847	-0.0007741

* distance from center of deposit

** All elements in ppm except Au which is in ppb

Appendix 7: Buckingham
quartz mineral chemistry by LA-ICP-MS

Sample	Sample type	Distance*															
		(m)	Li7	Na23	Mg24	Al27	Si29	P31	K39	Ca43	Ti47	Ti49	V51	Cr53	Mn55	Fe57	Cu63
BK13-C3-S4	Vein quartz	1381.0	39.31	34.50	1.059	623.1	467500	21.01	50.55	23.91	0.6128	0.6291	0.1423	0.09171	1.904	148.7	0.3620
BK13-C4-S1	Vein quartz	1381.0	15.70	20.25	0.1184	188.0	467500	17.64	14.67	-6.622	0.8935	0.5144	0.008048	-0.08738	0.1130	0.1841	0.07020
BK13-C4-S2	Vein quartz	1381.0	56.11	53.18	0.1899	884.3	467500	19.18	59.52	48.33	0.9559	1.434	0.004765	-0.1091	0.1285	10.18	0.007775
BK13-C4-S3	Vein quartz	1381.0	46.21	36.84	0.5630	720.4	467500	18.99	64.04	10.79	0.6710	0.3964	0.02569	-0.04921	0.1473	32.19	0.05044
BK13-C4-S4	Vein quartz	1381.0	28.70	46.96	1.040	580.0	467500	16.83	97.72	21.04	0.4333	0.08184	0.01552	0.04782	0.2436	25.54	0.08701
BK15-C1-S1	Vein quartz	981.5	8.696	11.54	0.08729	99.66	467500	20.48	15.17	8.252	16.08	16.24	-0.001176	-0.03627	0.2042	0.7397	0.02086
BK15-C2-S1	Vein quartz	981.5	12.18	0.7085	0.1106	101.1	467500	20.49	-0.9581	-38.28	1.157	1.088	0.01244	0.09285	0.06706	16.04	0.1276
BK15-C2-S2	Vein quartz	981.5	9.669	2.754	0.1937	88.34	467500	23.46	1.484	58.55	1.403	2.010	0.01777	-0.04859	0.1124	30.73	0.1568
BK15-C2-S2	Vein quartz	981.5	4.142	44.24	0.1160	49.25	467500	23.94	16.78	23.59	0.9435	0.4984	-0.01052	-0.07171	0.1017	1.760	0.02111
BK15-C2-S3	Vein quartz	981.5	9.761	4.025	0.1790	121.9	467500	19.65	5.198	17.45	1.492	1.402	0.02922	-0.02906	0.1731	45.97	0.2495
BK15-C2-S3	Vein quartz	981.5	30.58	9.488	-0.004430	288.9	467500	19.53	8.342	36.01	2.159	2.031	-0.003089	0.01600	0.04005	0.5448	-0.01678
BK15-C2-S4	Vein quartz	981.5	12.10	8.871	1.413	124.4	467500	25.21	7.085	-33.40	1.802	1.454	0.2254	0.02514	0.3884	171.8	0.4600
BK15-C2-S4	Vein quartz	981.5	31.07	16.29	0.01041	288.0	467500	18.10	11.51	-34.98	1.944	1.573	0.00008350	0.03001	0.05021	-0.3238	0.02430
BK17-C1-S1	Vein quartz	770.8	2.883	13.82	0.7952	80.63	467500	18.17	9.191	87.89	1.045	0.9666	-0.005055	0.09551	0.6004	0.8015	0.3077
BK17-C1-S2	Vein quartz	770.8	3.605	13.24	6.101	95.35	467500	12.26	11.47	119.8	1.734	1.345	0.01620	-0.1313	1.172	2.531	0.9047
BK17-C1-S3	Vein quartz	770.8	5.312	2.346	6.647	116.2	467500	10.41	10.75	78.71	1.764	1.928	0.006273	-0.2634	0.8128	-0.5404	0.2330
BK17-C3-S1	Vein quartz	770.8	1.453	1.810	0.06044	19.43	467500	14.72	2.938	-3.353	0.1419	0.2099	-0.009186	-0.01013	0.08966	0.1874	-0.05764
BK17-C3-S2	Vein quartz	770.8	10.06	10.64	0.2229	249.0	467500	14.10	29.89	-31.02	2.891	2.530	0.02753	-0.06011	0.3032	5.716	0.1725
BK17-C3-S3	Vein quartz	770.8	3.043	4.808	0.6387	54.80	467500	12.71	4.448	-43.20	1.539	1.202	0.004913	0.1475	0.1750	7.267	0.3912
BK17-C3-S4	Vein quartz	770.8	1.244	-0.7358	4.272	46.66	467500	15.03	6.520	15.27	1.350	0.9538	0.007876	0.1255	0.1677	7.186	0.2642
BK18-C2-S2	Vein quartz	608.8	9.784	101.4	10.45	1533	467500	8.108	394.5	67.87	0.8563	0.9805	0.1272	-0.03289	2.081	20.58	2.177
BK18-C2-S4	Vein quartz	608.8	11.78	47.94	8.247	678.1	467500	12.95	139.6	-12.05	0.1560	0.09092	0.1015	0.01206	3.376	25.89	0.7382
BK18-C5-S1	Vein quartz	608.8	11.86	38.02	6.332	855.6	467500	9.069	87.28	60.52	0.8952	1.097	0.6275	0.08850	2.293	20.98	0.3351
BK18-C5-S2	Vein quartz	608.8	9.541	25.57	4.079	659.6	467500	10.23	116.8	51.98	0.4501	0.4750	1.032	0.2115	1.270	17.31	0.01570
BK18-C5-S3	Vein quartz	608.8	9.459	57.81	1.131	840.4	467500	13.41	156.7	116.3	0.5122	0.3242	0.2212	0.1170	1.518	5.708	0.4965
BK18-C5-S4	Vein quartz	608.8	8.580	22.09	2.359	446.4	467500	11.32	28.08	91.73	0.4213	0.05046	0.01471	0.07328	0.4702	6.160	0.07470
BK20-C3-S1	Vein quartz	640.5	3.212	8.400	0.2358	36.56	467500	11.65	3.152	24.84	0.3085	-0.07270	0.0003366	-0.03666	0.06531	15.98	0.04758
BK20-C3-S2	Vein quartz	640.5	2.608	26.45	0.06783	35.03	467500	16.11	10.31	36.11	0.1050	0.1662	0.0002603	-0.2123	0.06087	1.182	0.06507
BK20-C3-S3	Vein quartz	640.5	3.422	6.552	5.940	124.0	467500	8.822	36.63	24.34	1.535	0.3606	0.1328	-0.1131	0.1650	19.61	0.1892
BK20-C3-S4	Vein quartz	640.5	6.727	23.15	0.1068	76.30	467500	12.88	4.963	5.780	0.3904	0.07651	0.01133	-0.06777	0.05903	1.606	0.01387
BK20-C4-S2	Vein quartz	640.5	18.49	9.735	0.1496	219.4	467500	14.73	13.56	-19.85	0.4990	0.03909	0.006732	-0.06348	0.1778	9.688	0.0009006
BK28-C1-S1	Vein quartz	778.0	2.875	21.67	0.4277	27.28	467500	14.38	3.250	52.32	6.179	7.373	-0.01512	0.07937	0.4102	1.443	2.097
BK28-C1-S2	Vein quartz	778.0	10.24	1.904	0.1518	57.65	467500	10.56	2.271	-2.484	16.77	16.29	0.001723	-0.05199	0.1043	0.5717	0.2420
BK28-C2-S3	Vein quartz	778.0	2.391	3.653	0.1242	28.77	467500	16.81	6.369	4.496	1.399	0.4020	0.01500	0.03221	0.1870	1.400	0.04107
BK28-C2-S4	Vein quartz	778.0	4.527	1.689	0.04417	45.45	467500	18.77	21.77	17.09	1.382	1.486	-0.006537	-0.1068	0.03798	0.6237	0.01212
BK28-C3-S3	Vein quartz	778.0	7.455	27.27	1.063	48.32	467500	18.12	12.84	42.33	16.57	15.36	0.05988	-0.03522	0.1234	103.9	2.439
BK28-C3-S4	Vein quartz	778.0	8.504	18.09	0.5908	64.36	467500	14.12	7.952	104.3	16.21	15.99	0.004426	0.1171	0.4613	13.73	0.9582
BK44-C1-S1	Vein quartz	1600.4	7.048	-5.380	0.2329	58.99	467500	14.81	0.5433	-34.95	37.81	38.43	0.009996	-0.05562	0.06491	-0.1252	0.2553
BK44-C1-S4	Vein quartz	1600.4	6.599	-1.479	0.1318	63.53	467500	14.41	17.18	17.62	28.66	29.10	-0.01103	0.1243	0.08418	-0.4224	0.9477
BK44-C3-S1	Vein quartz	1600.4	9.356	3.611	0.1453	78.35	467500	18.12	5.555	154.1	32.65	33.30	0.04057	0.1221	0.5538	7.907	1.170
BK44-C3-S2	Vein quartz	1600.4	7.493	24.43	0.1823	81.37	467500	14.72	19.97	88.42	17.44	17.66	-0.004787	-0.1522	1.113	2.068	1.760
BK44-C3-S3	Vein quartz	1600.4	8.419	19.71	0.2197	80.06	467500	11.18	31.15	46.03	30.73	27.94	0.009665	0.1088	0.3440	2.368	1.478
BK44-C3-S4	Vein quartz	1600.4	7.057	15.18	0.2812	77.91	467500	11.52	14.17	75.52	38.66	40.10	-0.01153	-0.1749	0.6677	1.546	1.887

* distance from center of deposit

** All elements in ppm except Au which is in ppb

Appendix 7: Buckingham
quartz mineral chemistry by LA-ICP-MS

Sample	Sample type	Distance*	Li7	Na23	Mg24	Al27	Si29	P31	K39	Ca43	Ti47	Ti49	V51	Cr53	Mn55	Fe57	Cu63
		(m)															
BK46-C1-S1	Vein quartz	1774.0	19.70	33.57	0.02224	188.9	467500	7.843	12.58	5.632	0.3518	0.2418	0.00002988	-0.005383	0.04045	0.6993	-0.03802
BK46-C1-S2	Vein quartz	1774.0	12.54	54.66	0.2409	116.7	467500	7.413	18.66	9.033	0.2510	0.09532	-0.001692	-0.09798	0.1476	0.8163	0.004974
BK46-C1-S3	Vein quartz	1774.0	31.32	58.72	0.07625	346.6	467500	8.813	35.94	-2.634	0.3911	0.1384	-0.003573	-0.09500	0.09240	-0.4046	-0.01383
BK46-C1-S4	Vein quartz	1774.0	4.665	22.08	0.1104	41.54	467500	8.997	7.469	4.115	0.3343	0.09989	-0.008333	0.009413	0.02867	4.689	0.04133
BK46-C2-S1	Vein quartz	1774.0	31.51	14.63	0.3261	299.0	467500	12.17	11.05	-18.74	0.3506	0.3455	0.009596	0.1794	0.08943	9.340	0.1051
BK46-C2-S2	Vein quartz	1774.0	4.812	0.7753	0.1034	37.57	467500	9.931	1.526	3.408	0.1625	0.1269	-0.008497	0.1584	0.02590	2.719	0.04094
BK46-C2-S3	Vein quartz	1774.0	44.45	124.6	0.3543	583.6	467500	8.977	87.34	-26.67	0.4671	0.5499	0.01616	0.07756	0.1293	0.1028	-0.01427
BK46-C2-S4	Vein quartz	1774.0	24.41	88.46	0.09583	266.3	467500	12.16	39.17	-9.314	0.2550	-0.04109	0.003069	-0.09788	0.07515	-0.4390	-0.002625
BK46-C3-S1	Vein quartz	1774.0	11.51	3.151	0.3801	132.2	467500	9.855	2.376	173.1	0.4637	0.08224	-0.01581	-0.01577	0.08136	1.842	-0.03771
BK46-C3-S1	Vein quartz	1774.0	11.19	-0.6746	1.064	154.5	467500	14.30	3.664	275.1	0.3521	0.2368	-0.001550	-0.2509	0.1206	0.7746	0.001132
BK46-C3-S1	Vein quartz	1774.0	47.43	15.67	1.277	552.6	467500	11.34	16.09	359.7	0.5453	0.5680	0.006281	0.05827	0.09177	0.7964	0.005747
BK46-C3-S1	Vein quartz	1774.0	25.23	3.690	0.008606	272.9	467500	9.725	8.772	98.86	0.3540	0.2955	0.006234	-0.05674	-0.01508	-0.4026	-0.02195
BK46-C4-S1	Vein quartz	1774.0	28.86	13.31	8.895	580.5	467500	12.70	56.58	189.8	0.5829	0.4405	0.04951	-0.1426	0.6562	69.24	0.2733
BK46-C4-S1	Vein quartz	1774.0	39.21	19.63	5.018	561.8	467500	11.13	32.10	47.75	0.2408	0.4078	0.004636	0.04969	0.4757	6.185	0.08806
BK50-C1-S1	Vein quartz	3090.9	6.019	8.271	0.6694	63.56	467500	19.66	4.744	-16.28	47.85	48.92	0.01420	-0.2012	1.076	10.33	0.2903
BK50-C1-S2	Vein quartz	3090.9	6.817	23.75	1.115	76.86	467500	19.09	10.64	16.82	113.3	116.8	0.3615	0.1720	3.294	111.2	0.6075
BK50-C1-S3	Vein quartz	3090.9	7.244	-1.546	24.65	108.0	467500	20.50	17.83	123.6	60.20	66.70	0.8557	0.8934	0.7426	217.9	0.4417
BK50-C1-S4	Vein quartz	3090.9	5.925	60.50	34.70	326.3	467500	23.42	72.54	141.6	49.68	50.57	11.76	0.3036	47.14	3258	22.82
BK50-C3-S1	Vein quartz	3090.9	6.909	8.470	18.34	169.1	467500	20.12	23.92	74.11	44.92	43.61	0.6917	0.3743	2.523	234.7	4.725
BK50-C3-S2	Vein quartz	3090.9	8.939	14.42	2.880	162.3	467500	19.57	24.60	24.35	64.42	60.33	0.06526	-0.2175	0.2558	22.66	0.2371
BK50-C3-S3	Vein quartz	3090.9	6.106	-1.970	1.314	86.22	467500	15.73	5.439	-21.50	56.47	55.02	0.04677	-0.01746	0.2284	17.04	0.4211
BK50-C3-S4	Vein quartz	3090.9	6.913	-2.939	1.325	99.98	467500	20.32	12.91	-9.653	40.06	41.87	0.06688	0.01580	0.2765	6.779	0.1558
BK59-C1-S1	Vein quartz	2339.0	5.555	-1.785	0.3235	93.20	467500	11.39	7.074	5.482	8.914	10.15	0.01059	-0.07579	0.06414	16.00	0.4495
BK59-C1-S2	Vein quartz	2339.0	2.836	-2.033	0.1349	50.38	467500	11.47	2.002	32.52	7.000	8.341	-0.009242	0.06015	0.2654	21.72	0.5962
BK59-C1-S3	Vein quartz	2339.0	4.255	1.674	1.319	166.1	467500	12.75	94.53	-16.67	140.8	136.1	0.04022	0.1010	0.3639	27.10	0.008772
BK59-C1-S4	Vein quartz	2339.0	6.215	-3.045	1.074	140.1	467500	11.15	24.36	-1.595	14.79	15.18	-0.01082	0.1843	0.1019	15.23	0.2031
BK59-C2-S1	Vein quartz	2339.0	2.690	-3.767	0.1028	39.68	467500	13.78	1.774	38.99	5.802	5.956	0.02767	-0.1892	0.1516	0.5297	0.04942
BK59-C2-S2	Vein quartz	2339.0	1.512	-1.741	0.3176	46.36	467500	12.43	3.804	-37.20	5.125	5.348	0.02418	0.02111	0.03889	22.31	0.6668
BK59-C2-S4	Vein quartz	2339.0	4.137	8.641	0.5076	104.3	467500	13.12	21.57	64.36	11.68	11.49	-0.008306	0.06158	0.5623	13.43	0.4774
BK61-C1-S1	Vein quartz	2030.1	0.6363	31.42	0.04800	29.12	467500	15.26	8.752	-26.57	1.096	0.9328	0.002014	-0.1230	0.4905	1.694	0.4417
BK61-C1-S1	Vein quartz	2030.1	3.895	18.74	0.6127	67.57	467500	10.15	15.45	80.59	17.81	17.81	-0.002589	-0.1561	0.3798	4.494	0.1355
BK61-C1-S2	Vein quartz	2030.1	3.427	44.84	0.8875	138.5	467500	21.30	50.52	55.40	16.19	19.28	0.03313	-0.2111	0.4377	0.03970	0.09351
BK61-C1-S3	Vein quartz	2030.1	4.911	47.69	0.3840	92.24	467500	11.98	27.08	48.70	18.57	17.99	0.02700	-0.3102	2.062	3.220	0.4549
BK61-C2-S1	Vein quartz	2030.1	8.629	28.86	0.7220	145.9	467500	18.34	35.49	50.47	61.81	60.61	0.0004643	0.4621	0.6571	1.868	0.3310
BK61-C2-S2	Vein quartz	2030.1	5.280	23.15	0.6304	90.94	467500	13.61	18.60	-21.96	46.50	42.67	0.01512	-0.04777	0.2234	2.056	0.6154
BK61-C2-S3	Vein quartz	2030.1	8.444	9.284	0.9286	141.8	467500	14.36	25.15	38.92	73.17	70.61	0.01931	0.09168	0.4105	3.196	0.2632
BK61-C2-S4	Vein quartz	2030.1	6.722	6.776	0.7914	132.2	467500	14.43	28.32	-33.61	61.46	64.15	0.004648	0.05277	0.2943	5.967	0.3857
BK63-C1-S1	Vein quartz	1817.2	4.840	17.84	0.1134	51.35	467500	21.36	7.183	31.68	14.58	15.02	0.01216	0.05126	0.06086	0.2739	0.4087
BK63-C1-S1	Vein quartz	1818.6	4.111	25.30	0.1519	69.63	467500	18.42	20.35	22.34	30.20	27.33	0.02291	0.01238	1.939	2.338	1.720
BK63-C1-S2	Vein quartz	1817.2	6.051	14.96	0.1111	66.33	467500	24.70	5.953	20.82	32.54	32.39	0.009722	0.008051	0.08768	1.027	1.185
BK63-C1-S2	Vein quartz	1818.6	5.353	13.66	0.3226	66.89	467500	21.83	8.452	15.13	31.43	34.67	0.01254	0.05175	0.02971	-0.2260	0.6904
BK63-C1-S3	Vein quartz	1817.2	3.153	1.863	-0.01468	30.17	467500	23.12	0.2265	5.829	13.71	13.27	0.001378	0.1298	0.002097	-0.6023	0.07235
BK63-C1-S3	Vein quartz	1818.6	5.533	3.456	0.04378	50.20	467500	23.19	1.372	-6.520	25.23	25.90	0.001946	0.05791	-0.004879	0.9008	0.1450

* distance from center of deposit

** All elements in ppm except Au which is in ppb

Appendix 7: Buckingham
quartz mineral chemistry by LA-ICP-MS

Sample	Sample type	Distance*															
		(m)	Li7	Na23	Mg24	Al27	Si29	P31	K39	Ca43	Ti47	Ti49	V51	Cr53	Mn55	Fe57	Cu63
BK63-C1-S4	Vein quartz	1817.2	6.016	23.17	0.1575	64.14	467500	20.55	13.58	16.50	19.85	17.62	0.01143	0.1210	0.1545	2.088	0.8971
BK63-C1-S4	Vein quartz	1818.6	5.539	36.31	0.4786	207.5	467500	21.39	77.22	57.49	25.03	27.23	0.01662	0.06454	1.095	43.21	39.90
BK63-C2-S1	Vein quartz	1817.2	4.257	10.74	0.04297	37.53	467500	21.71	5.475	23.72	14.52	14.91	0.005620	0.05851	0.03214	1.370	0.2013
BK63-C2-S1	Vein quartz	1818.6	3.742	8.254	0.05115	35.47	467500	22.51	5.011	17.81	11.80	11.25	0.008030	0.02071	0.1194	3.514	6.790
BK63-C2-S2	Vein quartz	1818.6	4.829	22.43	0.2473	101.1	467500	22.03	72.42	3.907	29.81	30.06	0.01379	-0.04761	0.1628	35.16	35.33
BK63-C2-S3	Vein quartz	1817.2	5.130	15.83	0.5550	59.78	467500	22.49	9.297	14.82	31.69	32.37	0.008416	-0.04302	0.1328	0.8043	0.4557
BK63-C2-S3	Vein quartz	1818.6	8.504	16.21	0.4319	102.2	467500	24.15	21.39	42.22	36.00	36.31	0.009230	0.05254	0.1465	1.306	2.642
BK63-C2-S4	Vein quartz	1818.6	6.588	22.36	4.934	275.4	467500	23.56	193.2	27.13	69.52	71.50	1.416	0.3516	0.1473	57.92	21.32
BK63-C3-S1	Vein quartz	1817.2	5.864	2.356	0.4143	56.14	467500	19.76	1.667	-6.757	26.30	26.57	0.002181	0.04101	-0.02271	0.9960	-0.03278
BK63-C3-S1	Vein quartz	1818.6	5.864	2.356	0.4143	56.14	467500	19.76	1.667	-6.757	26.30	26.57	0.002181	0.04101	-0.02271	0.9960	-0.03278
BK63-C3-S2	Vein quartz	1817.2	4.142	28.25	0.1255	41.89	467500	19.28	13.64	-6.105	9.078	9.578	-0.004200	0.09044	0.04454	4.296	0.6093
BK63-C3-S2	Vein quartz	1818.6	4.165	19.12	37.07	377.5	467500	186.0	11.27	269.5	40.60	41.37	14.71	12.31	0.7662	1472	357.6
BK63-C3-S3	Vein quartz	1817.2	3.170	-0.6686	0.1525	30.69	467500	18.57	0.01747	36.40	7.591	8.311	0.05582	0.01398	-0.01504	6.465	1.473
BK63-C3-S3	Vein quartz	1818.6	4.214	0.8053	1.044	40.80	467500	25.68	0.8069	15.93	14.98	18.91	0.3349	0.4175	0.06682	34.85	8.427
BK63-C3-S4	Vein quartz	1817.2	6.810	4.409	0.1666	65.86	467500	27.23	3.743	8.469	28.14	29.91	0.01387	-0.03970	0.04647	0.3569	0.5603
BK63-C3-S4	Vein quartz	1818.6	6.785	7.785	0.2170	68.15	467500	25.56	5.170	29.77	29.70	31.39	0.02439	-0.02012	0.02785	-0.8310	0.7658
BK63-C4-S1	Vein quartz	1818.6	6.338	56.11	15.43	172.1	467500	20.54	21.04	41.55	10.75	10.18	0.09711	0.1466	1.314	23.81	28.26
BK63-C4-S2	Vein quartz	1818.6	5.747	27.22	0.5736	55.94	467500	19.93	14.48	-17.61	7.971	10.46	0.006310	0.05230	0.7250	35.31	36.70
BK63-C5-S1	Vein quartz	1818.6	6.193	10.78	11.46	171.5	467500	21.40	18.56	25.37	89.18	90.99	0.03710	0.08820	0.2226	12.53	5.179
BK63-C5-S2	Vein quartz	1818.6	8.253	27.73	2.654	120.5	467500	21.06	14.77	23.48	94.64	96.21	0.004063	0.07449	0.3512	5.243	0.4487
BK63-C5-S3	Vein quartz	1818.6	8.571	23.66	4.176	107.6	467500	19.65	20.97	31.43	86.95	88.31	0.009832	-0.04312	1.445	10.46	0.1369
BK025-C1-S1	Breccia Ceme	0.0	0.1474	-1.168	0.1246	1.386	467500	17.14	0.3798	-16.24	0.4553	0.08961	0.006990	0.000	0.03257	-1.013	-0.04946
BK025-C1-S4	Breccia Ceme	0.0	99.77	21.57	0.3798	1618	467500	18.47	53.27	-3.466	0.3132	0.1219	0.01198	-0.08314	0.008605	0.1165	-0.001324
BK025-C2-S1	Breccia Ceme	0.0	0.1260	-1.019	0.08216	2.431	467500	19.91	0.1708	-12.12	0.2374	0.1925	0.007042	0.05720	0.04597	0.07938	0.01189
BK025-C2-S3	Breccia Ceme	0.0	492.5	64.03	0.3313	3073	467500	16.45	32.32	21.50	2.098	1.992	0.0007402	-0.006621	0.1191	-0.3561	-0.01955
BK025-C2-S4	Breccia Ceme	0.0	450.2	4.010	0.2401	2824	467500	15.64	5.455	11.66	1.967	1.853	0.0009854	0.03218	0.06061	0.5409	0.01540
BK025-C3-S1	Breccia Ceme	0.0	1.657	-0.5555	0.001008	11.84	467500	18.37	4.110	4.054	0.1486	-0.1493	0.001502	-0.02838	-0.004840	0.6920	-0.02558
BK025-C3-S2	Breccia Ceme	0.0	1.242	-0.5488	0.01275	7.415	467500	12.60	2.878	85.41	0.1777	0.02593	0.01097	0.01424	0.02012	0.05630	-0.03156
BK025-C3-S3	Breccia Ceme	0.0	0.9006	-3.058	0.01291	9.512	467500	25.41	1.578	-38.26	0.3314	-0.1803	-0.004609	-0.05553	0.03902	-0.2938	0.03477
BK025-C3-S4	Breccia Ceme	0.0	0.2257	-3.287	0.09564	4.118	467500	15.24	0.8384	47.03	0.3412	0.04143	-0.01709	-0.03612	-0.03248	1.501	-0.01913
BK025-C4-S2	Breccia Ceme	0.0	36.98	13.05	0.03040	431.7	467500	18.89	46.44	-7.950	0.2495	0.007164	0.002552	0.06458	0.02881	0.8054	0.06658
BK025-C4-S2	Breccia Ceme	0.0	558.1	1.027	0.07068	3784	467500	17.88	3.660	-6.878	0.8651	0.3914	0.002780	-0.01214	0.02826	0.3609	-0.003763
BK025-C4-S2	Breccia Ceme	0.0	562.6	10.78	-0.0009721	3754	467500	20.07	11.84	-40.05	2.577	1.903	-0.006367	0.02782	0.01573	-0.6576	0.03381
BK104-C1-S1	Breccia Ceme	361.5	3.216	7.874	299.1	868.6	467500	13.78	307.2	256.8	3.045	3.142	2.139	0.2268	14.43	137.5	3.671
BK104-C1-S2	Breccia Ceme	361.5	4.576	10.84	305.8	1074	467500	15.83	325.7	364.8	24.21	25.51	1.991	0.3712	18.09	160.9	1.651
BK104-C1-S3	Breccia Ceme	361.5	5.969	-1.800	1.515	201.9	467500	13.31	4.315	5.056	0.6749	0.3560	0.03062	0.1693	0.3127	2.717	-0.007421
BK104-C1-S4	Breccia Ceme	361.5	2.581	5.837	277.1	674.5	467500	16.24	262.1	313.5	4.834	7.047	1.818	0.3764	13.71	142.0	8.227
BK104-C1-S5	Breccia Ceme	361.5	5.732	2.303	32.29	349.7	467500	13.10	53.09	105.7	0.9080	0.9019	0.1865	-0.04281	2.192	434.3	0.9515
BK104-C2-S1	Breccia Ceme	361.5	6.732	7.081	293.2	1681	467500	22.02	522.0	593.4	3.862	3.701	5.514	0.8174	16.26	153.9	0.5531
BK104-C2-S2	Breccia Ceme	361.5	5.776	8.985	273.9	1929	467500	40.35	420.7	671.7	5.078	5.526	8.827	1.589	18.44	129.2	1.039
BK104-C2-S3	Breccia Ceme	361.5	1.285	8.869	20.35	323.1	467500	17.38	107.0	209.8	3.297	3.220	0.6905	0.06852	7.355	14.20	1.013
BK104-C2-S4	Breccia Ceme	361.5	6.258	15.10	56.53	924.3	467500	13.52	406.3	-41.45	49.13	45.50	3.472	0.4800	5.630	41.80	0.6281
BK104-C2-S5	Breccia Ceme	361.5	7.198	13.17	216.4	1274	467500	19.79	464.6	316.3	79.71	80.40	6.540	0.7707	13.53	122.1	1.172

* distance from center of deposit

** All elements in ppm except Au which is in ppb

Appendix 7: Buckingham
quartz mineral chemistry by LA-ICP-MS

Sample	Sample type	Distance*															
		(m)	Li7	Na23	Mg24	Al27	Si29	P31	K39	Ca43	Ti47	Ti49	V51	Cr53	Mn55	Fe57	Cu63
BK104-C3-S1	Breccia Cemei	361.5	4.122	13.25	22.07	568.7	467500	13.42	84.46	250.3	1.820	2.629	0.04208	-0.08587	2.806	9.826	1.072
BK104-C3-S2	Breccia Cemei	361.5	5.391	15.24	124.3	1158	467500	14.10	219.0	539.2	8.412	8.639	2.477	0.1132	14.57	55.35	2.403
BK104-C3-S5	Breccia Cemei	361.5	1.542	10.37	11.00	134.8	467500	17.46	28.97	-46.26	19.97	21.93	0.07368	0.2275	4.906	22.10	0.1058
BK50-C2-S1	Igneous	3090.9	8.585	28.22	0.6829	168.0	467500	18.63	39.01	19.00	73.54	70.08	0.01128	0.05071	0.1990	0.7114	-0.05548
BK50-C2-S2	Igneous	3090.9	7.556	56.99	1.060	114.5	467500	18.43	17.01	71.66	38.88	38.14	0.01824	0.2000	2.620	8.449	0.5295
BK50-C2-S3	Igneous	3090.9	7.258	3.503	0.6080	86.31	467500	21.22	4.668	-30.10	59.61	63.41	0.04259	-0.03742	0.5651	5.539	-0.009853
BK50-C2-S4	Igneous	3090.9	7.466	-0.1485	1.079	95.89	467500	16.82	2.527	60.79	68.04	61.90	0.005352	0.02799	0.09790	3.739	0.1732
BK50-C2-S5	Igneous	3090.9	7.270	10.80	2.666	137.9	467500	14.90	23.32	-5.053	69.79	69.18	0.02433	0.1237	0.3020	4.048	0.03751
BK100-C3-S1	Igneous	1443.7	8.712	26.00	1.270	65.11	467500	13.44	11.50	14.02	18.29	18.10	-0.004424	0.03224	0.1562	0.4993	0.4900
BK100-C3-S2	Igneous	1443.7	11.34	-2.219	0.4761	77.58	467500	12.00	0.1782	-12.63	24.93	24.57	0.005125	-0.09035	0.03673	0.5578	0.1391
BK100-C3-S4	Igneous	1443.7	14.25	-1.396	0.9379	101.6	467500	15.16	1.859	-18.34	77.20	72.49	0.09187	0.09551	0.08155	28.44	0.3901
BK101-C1-S1	Igneous	1061.5	7.649	26.25	1.456	104.9	467500	18.34	30.53	29.64	40.05	38.73	0.003805	0.1426	0.08122	1.382	0.4028
BK101-C1-S2	Igneous	1061.5	8.267	1.117	0.4877	97.95	467500	20.03	3.951	34.61	36.36	35.13	-0.009850	0.000	0.1622	1.138	0.3770
BK101-C1-S3	Igneous	1061.5	8.570	0.2789	0.4644	90.66	467500	20.72	2.289	11.93	55.15	56.17	0.002666	-0.005484	0.07526	1.459	-0.01176
BK101-C1-S4	Igneous	1061.5	9.876	1.323	0.6935	111.1	467500	16.43	2.673	-7.213	51.62	53.32	0.005909	-0.04651	0.05280	0.8084	-0.02103
BK101-C1-S5	Igneous	1061.5	11.41	1.588	0.9191	118.4	467500	16.51	6.394	-5.899	60.04	58.59	-0.006124	0.1569	0.1772	0.3879	0.2758
BK44-C2-S1	Sedimentary	1600.4	8.322	9.983	0.4053	68.54	467500	18.05	3.157	9.569	40.83	38.49	0.02021	0.05160	0.1568	1.259	0.9803
BK44-C2-S2	Sedimentary	1600.4	7.441	-6.135	0.2109	68.65	467500	18.22	3.441	-1.280	48.59	52.57	-0.01246	-0.1806	0.09731	2.201	5.253
BK44-C2-S4	Sedimentary	1600.4	9.319	2.043	1.063	81.24	467500	16.40	8.025	-27.61	55.40	54.29	0.03523	0.06140	0.08992	-0.4643	1.159
BK44-C4-S1	Sedimentary	1600.4	7.809	5.139	0.2326	64.10	467500	14.65	1.255	-14.48	49.84	51.44	0.01580	0.1327	0.1201	1.312	0.4960
BK44-C4-S2	Sedimentary	1600.4	7.888	-5.787	0.4170	70.69	467500	13.38	2.386	144.9	45.09	50.98	0.006798	0.09263	-0.03655	2.156	-0.07849
BK44-C4-S3	Sedimentary	1600.4	6.844	6.433	0.6705	59.99	467500	15.01	4.537	-45.38	47.46	45.82	0.01705	0.1225	0.1666	1.703	1.140
BK44-C4-S4	Sedimentary	1600.4	6.269	1.806	0.2913	54.55	467500	14.36	3.997	10.70	43.98	40.69	0.05047	-0.08284	0.08652	16.26	0.9335
BK17-C2-S1	Sedimentary	770.8	0.8985	3.185	2.108	200.3	467500	14.06	95.23	28.66	68.35	67.73	0.0003837	0.05873	0.2491	12.45	-0.003795
BK17-C2-S2	Sedimentary	770.8	1.235	10.24	1.348	151.8	467500	11.23	68.53	-27.03	60.42	58.71	-0.001097	0.1654	0.3512	8.660	0.01692
BK17-C2-S3	Sedimentary	770.8	1.094	12.64	1.917	166.0	467500	13.47	76.79	36.04	59.32	59.33	-0.006571	-0.08013	0.6122	11.18	0.03829
BK17-C4-S2	Sedimentary	770.8	1.708	3.727	1.382	64.24	467500	13.90	24.37	-9.629	38.00	37.39	0.01482	0.1103	0.4944	13.54	0.03530
BK17-C4-S3	Sedimentary	770.8	0.8891	-3.442	1.781	35.12	467500	14.88	13.76	-21.93	20.63	22.73	-0.003342	0.1627	0.3296	6.153	0.09411
BK12-C1-S1	Sedimentary	1475.3	4.096	22.75	1.223	125.3	467500	16.27	22.81	2.123	51.07	50.43	-0.001789	0.04508	0.3616	2.742	0.06212
BK12-C1-S2	Sedimentary	1475.3	4.755	52.98	1.664	199.0	467500	16.33	51.49	108.6	54.95	54.68	-0.006313	0.03427	0.9350	9.322	0.3619
BK12-C1-S3	Sedimentary	1475.3	5.737	26.43	21.97	438.1	467500	19.87	168.7	258.3	62.05	61.49	0.4016	0.3487	1.645	145.3	0.7037
BK12-C3-S1	Sedimentary	1475.3	9.810	-2.582	0.3546	83.74	467500	14.16	0.6097	6.132	45.67	45.44	0.003769	0.08336	0.1413	8.048	0.06908
BK12-C3-S2	Sedimentary	1475.3	11.07	-0.6094	0.2493	105.8	467500	17.08	4.434	12.75	34.93	37.12	0.01191	-0.003699	0.2774	3.336	0.02024
BK12-C3-S3	Sedimentary	1475.3	8.289	9.272	0.3197	86.37	467500	14.62	6.928	3.666	16.22	15.89	0.0006596	0.01130	0.1389	-0.2455	0.06940
BK13-C1-S1	Sedimentary	1381.0	9.958	38.08	1.105	199.7	467500	20.07	32.53	11.62	38.11	39.23	0.003695	0.02977	1.567	15.19	-0.03671
BK13-C1-S2	Sedimentary	1381.0	8.966	24.05	1.047	200.0	467500	14.45	32.95	54.54	43.59	43.18	0.01068	-0.03814	1.847	19.54	0.03438
BK13-C1-S3	Sedimentary	1381.0	7.774	30.89	1.411	154.8	467500	17.74	24.06	40.98	40.21	41.62	0.01272	-0.004049	1.967	13.13	-0.008117
BK13-C6-S1	Sedimentary	1381.0	50.84	79.88	0.3212	917.6	467500	18.78	90.15	-2.141	1.113	0.7740	0.0009092	-0.06926	0.09236	-1.249	-0.06380
BK13-C6-S1	Sedimentary	1381.0	43.19	80.16	1.073	1082	467500	18.34	194.2	24.36	1.415	0.9856	-0.01234	0.05210	0.06402	1.524	-0.1184
BK13-C6-S1	Sedimentary	1381.0	45.09	65.73	1.832	875.2	467500	19.03	126.1	33.85	1.492	0.9705	0.01380	0.2872	0.2099	7.432	0.03753
BK61-C3-S1	Sedimentary	2030.1	9.918	25.68	4.383	204.3	467500	17.07	25.97	65.92	91.10	83.89	0.01383	0.01253	0.5110	12.67	0.0009866
BK61-C3-S2	Sedimentary	2030.1	9.571	12.14	2.428	186.4	467500	17.33	30.02	53.91	78.46	76.27	-0.0005191	0.2199	0.3404	11.46	-0.02499
BK15-C1-S2	Sedimentary	981.5	7.201	4.133	0.02640	81.76	467500	18.18	9.979	-14.08	32.92	32.43	-0.002596	-0.1298	0.09997	0.1164	0.001899

* distance from center of deposit

** All elements in ppm except Au which is in ppb

Appendix 7: Buckingham
quartz mineral chemistry by LA-ICP-MS

Sample	Sample type	Distance*															
		(m)	Li7	Na23	Mg24	Al27	Si29	P31	K39	Ca43	Ti47	Ti49	V51	Cr53	Mn55	Fe57	Cu63
BK15-C1-S3	Sedimentary	981.5	9.773	6.272	0.2224	93.50	467500	17.32	9.759	13.18	115.7	120.7	0.004353	0.07397	0.2233	7.120	0.02339
BK15-C1-S4	Sedimentary	981.5	10.63	13.11	0.6491	101.8	467500	17.08	13.22	23.57	118.6	122.7	0.03586	-0.06752	0.5289	15.90	0.009425
BK15-C5-S1	Sedimentary	981.5	0.01935	-2.127	-0.0009828	2.574	467500	20.40	-0.4564	-0.3869	0.09974	0.006264	-0.004053	-0.09703	0.01360	-0.1172	0.0003009
BK15-C5-S2	Sedimentary	981.5	3.621	-3.641	0.05286	30.43	467500	18.71	-0.1159	14.72	0.3449	-0.07610	0.005662	-0.003820	0.002876	-0.7653	-0.003923
BK15-C5-S3	Sedimentary	981.5	3.618	4.762	0.4121	47.43	467500	19.92	7.693	59.25	53.89	54.53	0.000	0.1062	0.1295	1.091	0.007952
BK15-C5-S4	Sedimentary	981.5	4.439	6.207	0.09340	63.11	467500	18.61	11.42	6.156	53.84	55.40	-0.001458	0.08843	0.3423	0.5301	-0.006061
BK03-C3-S1	Sedimentary	337.4	4.705	-3.991	0.1918	48.08	467500	11.05	0.5402	-0.4822	29.02	28.23	-0.01454	0.07795	0.01150	1.778	0.003935
BK03-C3-S2	Sedimentary	337.4	5.667	-9.942	4.276	103.9	467500	13.35	34.52	81.19	32.63	34.84	0.1181	-0.1438	0.08614	5.495	-0.03968
BK59-C3-S1	Sedimentary	2339.0	5.674	0.2680	0.1625	76.30	467500	11.48	4.565	2.307	8.983	8.374	-0.006825	0.1331	0.7396	2.287	0.08331
BK59-C3-S2	Sedimentary	2339.0	11.78	32.09	0.5306	265.0	467500	12.89	39.23	-5.326	18.92	18.41	-0.006983	0.2002	2.594	23.92	0.2802
BK59-C3-S3	Sedimentary	2339.0	1.157	6.310	0.1188	18.72	467500	8.405	3.266	44.00	12.93	12.92	0.01024	0.1329	1.263	9.448	1.309
BK59-C3-S4	Sedimentary	2339.0	3.013	0.5564	1.684	109.6	467500	11.23	32.97	-42.09	23.88	24.09	-0.008039	0.01576	0.1009	5.237	0.07415
BK59-C4-S1	Sedimentary	2339.0	3.078	-0.4011	1.473	88.01	467500	15.96	17.52	-27.49	51.38	49.89	0.002332	-0.1072	0.1661	6.631	0.06163
BK59-C4-S2	Sedimentary	2339.0	3.504	56.90	2.160	90.91	467500	14.67	56.99	53.61	48.27	53.97	0.001474	-0.1034	6.378	42.79	0.03388
BK59-C4-S3	Sedimentary	2339.0	2.921	2.216	7.964	249.5	467500	13.14	133.2	21.81	76.09	75.00	0.1940	0.3008	0.6031	26.41	0.02613
BK102-C3-S1	Sedimentary	890.8	3.777	16.49	1.268	81.15	467500	14.02	28.06	21.39	31.99	32.57	0.01151	-0.02355	1.068	11.49	-0.02608
BK102-C3-S2	Sedimentary	890.8	3.491	11.59	0.3415	45.26	467500	13.35	9.131	-19.56	25.54	24.59	0.007427	0.09437	1.362	7.296	0.1410
BK102-C3-S3	Sedimentary	890.8	3.845	40.56	1.304	87.35	467500	11.39	51.69	-5.435	54.54	55.72	0.02037	0.08213	4.731	34.70	0.3116
BK102-C3-S4	Sedimentary	890.8	2.920	7.083	0.3002	36.92	467500	11.22	7.901	11.42	10.47	10.71	-0.009279	0.1671	0.8911	6.499	0.03680
BK106-C1-S1	Sedimentary	466.2	3.014	2.273	2.470	69.20	467500	16.42	9.618	109.8	16.38	15.09	-0.006323	-0.1152	1.384	12.11	0.2012
BK106-C1-S2	Sedimentary	466.2	2.841	2.626	2.877	139.7	467500	10.67	13.75	-6.161	13.99	12.40	0.03543	0.2856	0.3530	24.49	0.2883
BK106-C1-S3	Sedimentary	466.2	3.103	3.937	6.166	161.6	467500	6.834	15.49	-44.20	14.87	16.14	0.009588	-0.03196	1.432	39.86	1.369
BK106-C4-S2	Sedimentary	466.2	7.597	-1.954	0.5751	75.85	467500	11.22	7.736	-22.43	35.98	35.54	-0.0006786	-0.04927	0.09588	0.2169	0.06706
BK106-C4-S3	Sedimentary	466.2	6.760	31.18	1.356	107.9	467500	12.09	19.06	43.72	30.04	30.56	-0.02796	-0.01605	0.1574	5.445	0.06884
BK106-C4-S4	Sedimentary	466.2	1.422	51.14	0.3452	17.17	467500	12.92	34.45	70.82	7.636	8.580	0.01279	-0.02247	0.3376	1.565	1.132
BK106-C4-S5	Sedimentary	466.2	0.9569	52.33	0.7464	34.47	467500	10.83	12.42	13.04	19.27	22.19	-0.005204	0.07449	0.2878	4.143	0.1463
BK106-C5-S1	Sedimentary	466.2	4.671	8.822	0.6022	118.2	467500	12.18	31.99	-28.65	37.83	38.70	0.004927	-0.09174	0.6413	7.397	0.08456
BK106-C5-S2	Sedimentary	466.2	5.117	-0.2535	0.6123	110.3	467500	11.55	13.18	30.78	36.47	39.35	0.006988	0.07215	0.1405	2.259	-0.02779
BK106-C5-S3	Sedimentary	466.2	5.004	-0.3814	0.6694	94.21	467500	5.258	12.49	41.41	39.22	40.64	-0.008134	-0.1864	0.3296	2.764	0.01029
BK18-C1-S1	Sedimentary	608.8	2.103	22.41	0.6757	198.1	467500	12.23	84.81	37.32	50.87	48.74	0.001249	0.1495	0.3604	7.765	0.06206
BK18-C1-S2	Sedimentary	608.8	0.9804	9.544	0.3066	111.6	467500	11.44	44.74	52.24	49.78	52.93	0.001689	0.003389	0.5590	10.14	0.2603
BK18-C1-S3	Sedimentary	608.8	0.9741	11.16	0.5238	71.60	467500	10.47	26.29	-46.26	38.59	39.02	0.08981	-0.1407	0.4065	6.407	0.9545
BK18-C3-S1	Sedimentary	608.8	2.112	-1.444	0.6654	32.22	467500	10.87	-0.1268	0.9420	30.45	31.94	-0.001812	0.1372	0.02786	0.3302	-0.01255
BK18-C3-S2	Sedimentary	608.8	3.282	-3.100	0.2846	45.92	467500	12.22	1.163	17.79	31.51	30.49	0.007593	-0.1576	0.07016	-0.3258	0.04334
BK18-C3-S3	Sedimentary	608.8	1.871	-2.500	0.07967	27.73	467500	12.06	1.562	30.11	26.83	25.69	0.005609	0.04836	0.07701	1.147	-0.04079
BK20-C1-S2	Sedimentary	640.5	0.8910	-2.047	0.9656	27.36	467500	12.05	7.215	-31.36	56.89	57.96	-0.001324	-0.1010	0.05400	5.577	-0.005998
BK20-C1-S3	Sedimentary	640.5	0.4176	-3.813	19.80	47.15	467500	16.78	8.151	98.46	56.60	53.16	0.05551	0.2061	0.4824	112.2	0.1170
BK20-C1-S4	Sedimentary	640.5	-0.01950	-1.333	3.295	22.52	467500	12.11	3.581	-61.04	46.26	42.47	-0.003153	0.01386	0.1849	42.46	0.09494
BK20-C2-S1	Sedimentary	640.5	5.825	-1.107	0.02717	72.57	467500	14.57	7.333	-10.62	33.45	32.46	-0.008166	-0.1231	0.07308	1.978	0.02529
BK20-C2-S2	Sedimentary	640.5	5.176	-0.6465	0.1973	101.7	467500	17.62	13.63	-16.56	30.18	28.74	0.04216	-0.05338	0.1358	25.78	0.03826
BK20-C2-S3	Sedimentary	640.5	5.284	8.126	0.1524	98.50	467500	13.65	8.540	43.57	33.65	32.99	0.005121	0.03904	0.5129	14.48	0.1175
BK20-C2-S4	Sedimentary	640.5	4.789	31.44	10.90	151.5	467500	12.54	12.17	55.49	41.78	39.33	0.05500	0.2579	1.193	103.2	0.08446
BK021-C1-S1	Sedimentary	517.7	0.8231	28.53	0.7017	124.6	467500	15.06	51.08	5.445	21.13	18.40	-0.004718	0.01267	7.404	14.31	0.006202

* distance from center of deposit

** All elements in ppm except Au which is in ppb

Appendix 7: Buckingham
quartz mineral chemistry by LA-ICP-MS

Sample	Sample type	Distance* (m)	Li7	Na23	Mg24	Al27	Si29	P31	K39	Ca43	Ti47	Ti49	V51	Cr53	Mn55	Fe57	Cu63
BK021-C1-S2	Sedimentary	517.7	6.810	28.59	131.2	2517	467500	142.1	1291	41.31	256.1	254.9	2.723	1.753	5.668	642.0	2.076
BK021-C2-S1	Sedimentary	517.7	3.357	10.08	0.8833	126.3	467500	16.49	33.30	30.13	54.19	56.25	0.004879	0.01918	2.211	5.893	-0.05640
BK021-C2-S2	Sedimentary	517.7	1.952	2.465	1.448	64.89	467500	16.15	27.66	2.850	31.65	35.30	0.007242	0.09805	0.9868	5.485	0.1738
BK021-C2-S3	Sedimentary	517.7	0.6212	7.825	1.230	53.00	467500	14.28	17.58	4.349	13.55	12.72	0.007119	-0.08239	1.805	4.928	0.1223
BK021-C2-S4	Sedimentary	517.7	0.8156	4.007	0.6140	76.29	467500	13.97	27.00	-17.49	55.46	53.63	-0.01554	0.1256	1.523	8.561	0.03010
BK63-C4-S1	Sedimentary	1817.2	5.974	57.60	0.2691	79.34	467500	21.38	19.78	35.03	10.87	9.250	0.008581	0.3036	0.6569	1.933	0.2230
BK63-C4-S2	Sedimentary	1817.2	4.367	20.07	1.966	53.64	467500	23.76	6.390	8.727	11.00	11.28	0.004991	0.04627	0.4017	2.262	2.503
BK63-C5-S1	Sedimentary	1817.2	6.970	5.141	1.113	74.77	467500	20.74	3.928	-6.436	83.35	83.60	0.008080	-0.02242	0.09725	3.231	0.2360
BK63-C5-S2	Sedimentary	1817.2	8.418	26.62	2.321	122.3	467500	21.10	12.94	16.80	95.71	99.00	0.004458	0.06823	0.3462	4.672	0.3707
BK63-C5-S3	Sedimentary	1817.2	9.001	23.13	4.275	103.2	467500	19.41	20.89	16.41	95.30	92.21	0.009169	-0.01047	1.946	11.23	0.2695

* distance from center of deposit

** All elements in ppm except Au which is in ppb

Appendix 7: Buckingham
quartz mineral chemistry by LA-ICP-MS

Sample	Sample type	Distance*												
		(m)	Cu65	Zn66	Ge74	As75	Rb85	Sr88	Zr90	Ag107	Sb121	Cs133	Gd157	Hf178
BK01-C1-S1	Vein quartz	591.4	1.629	0.2496	1.144	0.09001	0.6173	0.6021	0.007791	-0.008761	0.009550	0.1034	0.002200	-0.002477
BK01-C1-S2	Vein quartz	591.4	0.1567	0.08009	0.9644	0.01398	0.04242	0.04994	0.005776	-0.009036	0.007599	0.03660	0.01402	0.007470
BK01-C1-S3	Vein quartz	591.4	0.2415	0.1139	1.103	-0.07488	0.07149	0.03908	-0.005587	0.009350	0.03100	0.02357	0.009549	0.003842
BK01-C2-S1	Vein quartz	591.4	-0.08215	-0.01022	2.802	0.04604	0.03497	0.07186	0.003896	0.005894	0.003697	0.06522	0.01149	-0.005732
BK01-C2-S2	Vein quartz	591.4	0.08979	-0.03592	1.985	-0.03475	0.03320	0.1476	0.007185	0.009444	0.01458	0.04052	-0.01568	0.0006403
BK01-C2-S3	Vein quartz	591.4	-0.008771	0.03138	3.154	0.1158	0.1052	0.1343	0.01799	0.01204	0.02017	0.05154	-0.002145	0.0004665
BK01-C2-S4	Vein quartz	591.4	0.1857	-0.01828	2.792	0.1182	0.01304	0.02580	-0.005311	-0.01573	0.008789	0.02364	-0.008698	-0.002403
BK01-C3-S1	Vein quartz	591.4	0.07843	0.006077	2.407	0.1833	0.1259	0.06987	0.001616	-0.01092	0.04394	0.08780	0.002294	0.0005546
BK01-C3-S2	Vein quartz	591.4	0.01915	-0.08551	2.216	0.05017	0.1813	0.05887	-0.002422	-0.01198	0.03878	0.1467	-0.008915	-0.001702
BK01-C3-S3	Vein quartz	591.4	0.001644	0.1844	1.987	-0.1450	0.1409	0.2766	-0.01165	0.01680	0.01345	0.1221	0.01210	0.009128
BK01-C5-S1	Vein quartz	591.4	1.544	0.2045	1.979	0.2425	-0.001550	0.04188	0.02042	0.01154	0.09854	0.004645	0.01255	-0.006801
BK01-C5-S4	Vein quartz	591.4	0.3472	-0.001639	2.154	0.01982	0.03229	0.02241	-0.001222	0.004994	-0.004368	0.005694	-0.006831	0.002895
BK021-C3-S1	Vein quartz	517.7	0.03619	0.2286	4.753	1.901	0.7885	0.6954	0.01719	-0.006929	1.913	0.04625	-0.0002583	-0.0007697
BK021-C3-S2	Vein quartz	517.7	0.01460	4.648	2.036	1.597	0.6819	0.3201	0.01229	0.4492	1.356	0.03150	0.006946	-0.001231
BK021-C3-S4	Vein quartz	517.7	0.05758	0.3549	3.080	1.658	2.724	0.7852	1.686	0.01895	0.6717	0.05569	-0.005790	0.04030
BK021-C4-S1	Vein quartz	517.7	0.7785	0.1402	3.766	1.767	0.6614	1.039	0.007719	-0.005289	0.1621	0.06283	0.003868	-0.0005637
BK021-C4-S3	Vein quartz	517.7	0.08845	0.5695	3.146	1.749	2.149	0.6154	0.06212	0.005063	2.559	0.1099	0.007747	0.004916
BK021-C4-S4	Vein quartz	517.7	0.2532	0.3651	3.645	1.615	1.961	0.7782	0.05665	0.009169	2.944	0.1301	0.0006010	0.003628
BK021-C4-S5	Vein quartz	517.7	0.02237	0.1394	1.370	1.675	0.4113	0.1249	-0.002140	-0.004040	0.4393	0.01619	0.008513	0.002474
BK03-C1-S2	Vein quartz	337.4	0.1041	0.1480	0.9992	0.06729	0.05632	0.003054	0.009748	0.01880	0.05496	0.007848	0.002052	0.001151
BK03-C4-S1	Vein quartz	337.4	0.4361	1.367	0.9347	0.3463	0.4610	0.1778	0.02812	-0.02481	0.3093	0.1090	0.005717	-0.005958
BK03-C4-S2	Vein quartz	337.4	0.2848	0.06373	0.7427	0.07048	0.1004	0.01879	0.0002101	0.04454	0.1654	0.01466	0.003773	0.00008665
BK03-C4-S3	Vein quartz	337.4	2.162	0.6616	0.7533	0.5281	0.1856	0.05677	0.03430	0.5165	0.04737	0.03576	0.006113	0.0001967
BK06-C1-S1	Vein quartz	940.0	0.01224	0.4375	2.563	10.14	0.04999	0.07555	-0.005311	-0.004488	0.1303	0.04503	-0.006986	0.005311
BK06-C1-S2	Vein quartz	940.0	-0.04753	0.1134	2.013	9.008	1.231	0.02066	0.003655	-0.002330	0.003896	-0.001175	0.004259	-0.002698
BK06-C1-S3	Vein quartz	940.0	0.09112	0.04168	2.453	9.849	0.2676	0.05103	-0.003237	0.002602	0.05150	0.004152	-0.005057	-0.008498
BK06-C1-S4	Vein quartz	940.0	0.2961	0.1412	2.157	10.10	0.1684	0.03691	0.01037	0.01137	0.02752	0.1057	-0.009326	0.001650
BK06-C2-S1	Vein quartz	940.0	0.1198	0.1884	1.892	9.652	-0.002841	0.01492	-0.001605	0.02092	-0.001217	0.02435	-0.007525	0.0009463
BK06-C2-S2	Vein quartz	940.0	0.2927	0.002186	2.148	9.741	0.03065	0.02607	0.002310	-0.0003875	0.01089	0.007214	-0.004511	-0.002166
BK06-C2-S4	Vein quartz	940.0	0.2500	-0.006360	2.050	7.526	0.02035	0.02747	-0.007186	0.01831	0.01541	0.007250	0.003063	-0.0001401
BK06-C2-S5	Vein quartz	940.0	0.6369	0.1139	2.001	7.462	0.03017	0.1141	0.006111	0.07259	0.02884	0.009133	-0.006805	0.001147
BK06-C3-S1	Vein quartz	940.0	2.991	0.01362	2.095	9.454	0.02670	0.03089	-0.001330	0.09301	0.07414	0.02693	-0.004402	-0.002232
BK06-C3-S2	Vein quartz	940.0	0.3235	0.1951	2.176	7.767	0.07082	0.07807	0.002456	-0.003499	0.03825	0.1139	-0.004667	-0.001121
BK06-C3-S3	Vein quartz	940.0	0.08831	0.2073	2.193	8.679	0.01527	0.02955	0.000	-0.01005	0.01371	0.003924	-0.005187	0.006228
BK09-C1-S1	Vein quartz	1043.0	0.1143	0.01769	1.257	4.894	0.07752	0.1419	-0.002216	0.01029	0.06717	0.09913	0.001254	-0.0001014
BK09-C1-S2	Vein quartz	1043.0	0.1361	0.06268	0.8024	4.102	0.2077	0.2026	0.002169	0.2282	0.5420	0.1414	0.006664	0.006184
BK09-C1-S3	Vein quartz	1043.0	1.982	1.998	1.135	3.773	0.2398	0.2943	0.0001995	0.04366	0.1028	0.2047	0.001493	0.008068
BK09-C1-S4	Vein quartz	1043.0	1.297	0.1341	0.9717	3.754	0.4071	0.4311	0.009655	0.02441	0.1822	0.2307	0.006372	-0.0001472
BK09-C2-S1	Vein quartz	1043.0	0.1759	0.05054	1.565	3.574	0.1258	0.02270	-0.009159	0.02258	0.4278	0.1382	0.0002965	0.0002877
BK09-C2-S2	Vein quartz	1043.0	0.3195	0.8549	1.362	3.613	0.2664	0.2771	0.0002016	-0.002387	0.1891	0.1928	0.01561	0.001619
BK09-C2-S4	Vein quartz	1043.0	2.074	-0.03232	1.275	3.932	0.1098	0.1640	-0.005008	0.05083	0.6440	0.1124	-0.005729	0.0005560
BK09-C3-S2	Vein quartz	1043.0	0.06555	0.1296	0.9986	3.093	1.295	0.7723	0.007165	0.01167	0.02946	0.4752	-0.005036	0.005363
BK09-C3-S3	Vein quartz	1043.0	0.08288	-0.02634	1.221	3.829	0.09189	0.1012	0.003156	0.008911	0.1288	0.08136	-0.002113	0.002095

* distance from center of deposit

** All elements in ppm except Au which is in ppb

Appendix 7: Buckingham
quartz mineral chemistry by LA-ICP-MS

Sample	Sample type	Distance*												
		(m)	Cu65	Zn66	Ge74	As75	Rb85	Sr88	Zr90	Ag107	Sb121	Cs133	Gd157	Hf178
BK09-C3-S4	Vein quartz	1043.0	0.07444	0.1022	0.9556	2.920	0.03536	0.03991	-0.003207	-0.006462	0.03060	0.008806	-0.005197	-0.002553
BK09-C4-S1	Vein quartz	1043.0	0.3838	0.03399	1.391	3.917	0.2497	0.3082	0.01205	0.01685	0.003565	0.2023	-0.002410	0.001170
BK09-C4-S2	Vein quartz	1043.0	0.4618	0.1716	1.623	4.020	0.2312	0.1186	0.003923	0.07886	0.3520	0.2062	0.004564	-0.006924
BK09-C4-S3	Vein quartz	1043.0	0.7362	-0.003465	1.321	4.045	1.050	0.4838	-0.003871	0.002062	0.1421	0.2934	-0.003096	0.004151
BK09-C4-S4	Vein quartz	1043.0	0.8828	0.01515	1.642	4.153	0.3975	0.08855	0.001008	0.04150	0.1799	0.1452	-0.006009	0.002419
BK100-C1-S2	Vein quartz	1443.7	3.432	0.05142	1.382	3.685	0.01537	0.04770	0.006250	0.01648	0.01741	0.009455	-0.001401	0.003235
BK100-C1-S3	Vein quartz	1443.7	0.9599	0.2157	1.130	3.526	0.07343	0.2107	0.006108	0.01603	0.01255	0.1049	-0.002207	-0.00005261
BK100-C1-S4	Vein quartz	1443.7	0.2721	-0.005043	1.610	3.369	0.1131	0.07875	-0.0007089	-0.0004556	0.01494	0.1093	0.006641	-0.001975
BK100-C4-S1	Vein quartz	1443.7	0.02913	0.005278	1.530	3.332	0.3557	0.2482	0.001129	0.01318	0.02498	0.1486	0.002639	0.001369
BK100-C4-S2	Vein quartz	1443.7	0.1241	0.06866	1.609	2.870	0.3259	0.1290	0.004179	-0.003393	0.01678	0.1680	0.006041	-0.001486
BK100-C4-S3	Vein quartz	1443.7	1.169	0.1007	1.171	2.838	0.1677	0.1890	0.03431	-0.01595	-0.01168	0.1146	-0.005527	0.004807
BK100-C4-S4	Vein quartz	1443.7	0.6493	0.08675	1.350	3.777	0.4205	0.2408	0.002409	-0.01987	0.01722	0.1601	0.007418	0.0002961
BK101-C2-S1	Vein quartz	1061.5	0.5831	0.3996	2.253	3.786	0.1988	0.2970	0.0006431	0.009751	0.2614	0.1777	0.01412	-0.0006759
BK101-C2-S2	Vein quartz	1061.5	0.5275	0.09462	2.359	4.160	0.02835	0.03075	-0.004610	0.009164	0.08185	0.03504	-0.008255	0.001135
BK101-C2-S3	Vein quartz	1061.5	0.7877	0.02090	2.015	3.848	0.2443	0.07469	0.01112	0.007130	0.04855	0.1139	-0.01163	-0.0005297
BK101-C3-S1	Vein quartz	1061.5	0.02694	-0.03319	1.279	4.597	0.02433	0.04303	-0.0009900	0.01021	0.001323	0.03071	0.0005994	-0.001967
BK101-C3-S1	Vein quartz	1061.5	0.1577	0.09798	1.907	4.213	0.04530	0.05634	0.0006403	0.01612	0.05194	0.02943	0.003274	0.001498
BK101-C3-S2	Vein quartz	1061.5	0.1409	0.04372	1.063	4.509	0.03635	0.09114	0.0001304	-0.009580	0.01305	0.05159	-0.006171	-0.002518
BK101-C3-S3	Vein quartz	1061.5	0.5204	0.02435	2.354	4.113	0.01972	0.01333	-0.004110	0.003531	0.09247	0.04552	-0.002637	-0.001680
BK101-C3-S4	Vein quartz	1061.5	0.3906	0.1212	2.421	4.361	0.03631	0.03735	-0.004330	0.02649	0.03991	0.02730	-0.003782	0.004732
BK101-C3-S5	Vein quartz	1061.5	1.061	0.04519	1.247	4.500	0.03664	0.1028	-0.001445	0.1068	0.02394	0.03896	-0.005184	-0.002593
BK101-C5-S1	Vein quartz	1061.5	0.05118	0.02463	2.303	5.045	0.03016	0.03308	-0.003124	-0.01526	0.09377	0.02861	-0.006013	-0.003444
BK101-C5-S1	Vein quartz	1061.5	0.6584	-0.09365	3.244	5.918	0.04386	0.06475	-0.003795	0.03227	0.4974	0.02327	-0.007710	-0.001445
BK102-C1-S1	Vein quartz	890.8	-0.02244	0.01601	2.651	0.1354	0.07233	0.06195	-0.003981	-0.02932	0.01741	0.04016	-0.001004	0.003365
BK102-C1-S2	Vein quartz	890.8	0.4319	0.02372	2.290	0.2186	-0.002156	0.01063	0.002621	-0.01119	0.05332	0.001682	-0.01218	-0.001967
BK102-C1-S3	Vein quartz	890.8	0.3490	-0.009884	2.883	0.09950	0.005912	0.01259	-0.002141	0.003404	0.06600	0.01849	0.001980	-0.005617
BK102-C1-S4	Vein quartz	890.8	0.03838	0.1428	1.629	0.1994	0.2630	0.06142	0.0006031	0.01528	0.3680	0.06059	0.006404	-0.006487
BK102-C2-S1	Vein quartz	890.8	0.3420	0.1030	2.949	0.1280	0.02667	0.1003	-0.006344	0.005175	0.2441	0.01296	-0.007729	-0.003472
BK102-C2-S2	Vein quartz	890.8	1.838	0.2689	2.778	0.08811	0.1631	0.08864	0.007439	-0.01291	0.1146	0.05749	-0.0006620	-0.0004988
BK102-C2-S3	Vein quartz	890.8	0.06713	0.3428	0.8065	0.1552	0.1854	0.04794	-0.006172	0.000	0.8378	0.1025	-0.01857	-0.0007099
BK102-C2-S5	Vein quartz	890.8	0.3696	0.1291	2.671	0.03900	0.02515	0.006674	0.0005841	-0.0006855	0.2594	0.008768	-0.003396	-0.0005756
BK106-C2-S1	Vein quartz	466.2	0.9411	0.1059	1.015	0.1105	0.1223	0.6625	0.01780	-0.01158	0.1788	0.01738	0.01256	-0.005370
BK106-C2-S2	Vein quartz	466.2	0.4444	1.305	1.001	0.07950	0.1353	0.1473	0.001597	0.004500	-0.02025	0.01830	-0.01371	-0.002086
BK106-C2-S3	Vein quartz	466.2	0.8499	0.2517	0.9369	0.1174	0.05407	0.4595	0.01726	0.009468	-0.008205	0.03606	-0.01224	0.002240
BK106-C3-S1	Vein quartz	466.2	0.4515	0.01261	1.447	0.3532	0.08721	0.2159	0.004388	0.01660	0.1339	0.05705	0.01354	-0.002161
BK106-C3-S2	Vein quartz	466.2	2.530	0.8241	0.8886	0.07330	0.2320	0.7710	0.009410	-0.007942	0.02686	0.03474	-0.006252	0.004058
BK12-C2-S1	Vein quartz	1475.3	0.03590	0.07273	0.4806	0.1681	0.001092	0.005440	-0.002078	0.01070	0.02274	0.0008188	0.005583	-0.003568
BK12-C2-S3	Vein quartz	1475.3	0.02119	-0.003904	1.501	0.09195	0.003628	0.5407	-0.007393	0.0007121	0.008893	-0.0008099	-0.01212	-0.003214
BK12-C4-S1	Vein quartz	1475.3	-0.01722	0.01253	1.913	0.02759	0.02276	0.08868	0.002891	-0.01627	0.05022	0.003430	-0.001943	0.0005319
BK12-C4-S3	Vein quartz	1475.3	0.1094	-0.004118	3.492	0.05452	0.05274	0.8978	0.004253	-0.02172	0.1150	0.007610	-0.0005468	0.001834
BK12-C6-S2	Vein quartz	1475.3	0.1930	0.06524	2.884	0.07300	0.01799	0.08620	0.01175	0.002939	0.07401	0.001145	0.004219	0.0006520
BK13-C3-S2	Vein quartz	1381.0	-0.01014	-0.01897	2.715	0.02652	0.06416	0.8800	-0.0005762	0.0002127	0.08017	0.01294	0.01270	-0.001043
BK13-C3-S3	Vein quartz	1381.0	0.01747	0.01473	3.347	-0.02912	0.3585	1.921	0.0007482	0.08580	0.1810	0.08215	-0.002731	0.003887

* distance from center of deposit

** All elements in ppm except Au which is in ppb

Appendix 7: Buckingham
quartz mineral chemistry by LA-ICP-MS

Sample	Sample type	Distance*												
		(m)	Cu65	Zn66	Ge74	As75	Rb85	Sr88	Zr90	Ag107	Sb121	Cs133	Gd157	Hf178
BK13-C3-S4	Vein quartz	1381.0	0.3159	0.5688	2.880	0.3385	0.1935	1.383	0.07386	-0.01735	0.06926	0.01686	0.01540	-0.002770
BK13-C4-S1	Vein quartz	1381.0	0.04354	-0.06459	1.151	0.07991	0.06658	0.6156	0.0006454	0.008629	0.01894	0.002909	0.001110	0.004293
BK13-C4-S2	Vein quartz	1381.0	0.07041	-0.04526	3.398	0.3272	0.06715	1.100	0.0001899	-0.002030	0.05677	0.005461	0.004145	-0.002067
BK13-C4-S3	Vein quartz	1381.0	0.02952	0.1201	2.713	0.1141	0.1231	1.072	0.01708	0.03162	0.07654	0.002199	0.002830	0.002052
BK13-C4-S4	Vein quartz	1381.0	0.1680	0.1041	1.923	0.1099	0.2643	1.496	0.007203	0.02140	0.08664	0.02650	-0.002589	-0.001046
BK15-C1-S1	Vein quartz	981.5	0.05487	0.1176	1.303	0.3396	0.08174	0.4422	0.0005148	-0.004499	0.05681	0.03856	0.005388	0.003169
BK15-C2-S1	Vein quartz	981.5	0.06991	0.07013	2.453	0.9072	-0.00007072	0.002560	-0.003597	0.04745	0.2392	0.002202	-0.01499	0.004093
BK15-C2-S2	Vein quartz	981.5	0.09560	0.3698	3.414	3.743	0.001557	0.01839	0.001851	0.02805	0.3412	0.005492	0.002249	-0.003165
BK15-C2-S2	Vein quartz	981.5	0.01744	0.05582	2.750	0.07669	0.08331	0.4735	0.0006537	-0.03312	0.1857	0.06855	0.008891	-0.002027
BK15-C2-S3	Vein quartz	981.5	0.3054	0.4339	3.084	2.852	0.01471	0.06411	-0.0003294	0.05985	0.5327	0.008372	-0.0004798	-0.0001174
BK15-C2-S3	Vein quartz	981.5	0.03408	-0.1208	5.752	0.1810	0.02398	0.07423	0.0002729	0.007586	0.7116	0.02813	0.003394	0.0007885
BK15-C2-S4	Vein quartz	981.5	0.3668	0.1161	2.893	4.860	0.03257	0.1355	0.01457	0.02958	0.9442	0.04960	-0.006168	-0.006032
BK15-C2-S4	Vein quartz	981.5	-0.1085	0.04142	3.949	0.1912	0.008933	0.1260	0.004268	-0.01237	0.5577	0.04408	0.005591	-0.002990
BK17-C1-S1	Vein quartz	770.8	0.2565	1.521	1.065	0.2751	0.05385	0.1814	-0.003136	0.2544	1.074	0.03404	-0.007212	0.0007845
BK17-C1-S2	Vein quartz	770.8	1.033	1.796	1.069	0.3509	0.07374	1.044	0.0005982	0.3156	1.369	0.03644	-0.009349	-0.001031
BK17-C1-S3	Vein quartz	770.8	0.4145	0.1532	1.186	0.02045	0.03058	0.2456	0.004302	-0.009951	0.6758	0.02692	0.006426	0.001505
BK17-C3-S1	Vein quartz	770.8	0.07730	-0.07208	0.2944	0.07352	0.01531	0.08261	0.002974	-0.02163	0.02640	0.01060	0.01016	-0.0005912
BK17-C3-S2	Vein quartz	770.8	0.1652	0.2214	1.905	0.2011	0.04849	0.2421	0.005101	0.01221	0.6891	0.007214	0.009531	0.0003571
BK17-C3-S3	Vein quartz	770.8	0.3521	0.09420	0.9109	0.1010	0.008667	0.01106	0.002342	0.006321	0.1784	0.005830	-0.0005248	0.001666
BK17-C3-S4	Vein quartz	770.8	0.1110	0.1440	0.8873	-0.02193	0.01210	0.2013	0.03125	0.03714	0.3127	0.003553	0.007218	-0.001382
BK18-C2-S2	Vein quartz	608.8	2.132	0.004654	2.978	6.203	0.6111	2.672	-0.003108	0.1384	0.09986	0.03728	0.005750	0.0003687
BK18-C2-S4	Vein quartz	608.8	0.8597	0.1206	1.631	1.054	0.4245	1.803	-0.009214	0.02960	0.04496	0.05171	-0.005308	0.002961
BK18-C5-S1	Vein quartz	608.8	0.4144	0.1361	1.829	0.6912	0.3233	3.368	0.002195	0.01934	0.02153	0.06825	-0.009675	0.0009155
BK18-C5-S2	Vein quartz	608.8	0.1872	-0.007832	1.790	0.04440	0.2634	0.8523	-0.001569	0.005845	0.01218	0.03762	-0.01133	-0.002765
BK18-C5-S3	Vein quartz	608.8	0.6547	0.2058	2.340	0.6793	0.2800	2.102	-0.01158	0.001547	0.04475	0.02537	0.01472	-0.001140
BK18-C5-S4	Vein quartz	608.8	0.1120	0.08055	1.080	0.3336	0.06344	0.9437	-0.003356	0.003315	-0.0009629	0.02151	-0.007884	0.006787
BK20-C3-S1	Vein quartz	640.5	0.02444	0.008369	0.4876	2.714	0.02964	0.2691	-0.004316	-0.0004082	0.02604	0.02816	0.01029	-0.001453
BK20-C3-S2	Vein quartz	640.5	0.04568	0.05035	0.5866	1.815	0.03243	0.4607	0.003930	-0.01564	0.02984	0.03504	0.01028	0.001346
BK20-C3-S3	Vein quartz	640.5	0.05099	0.005089	0.2559	2.182	0.2975	0.2071	-0.0008192	0.008382	0.05125	0.03555	0.002396	-0.01034
BK20-C3-S4	Vein quartz	640.5	0.009197	0.1029	0.7169	2.081	0.04229	0.2973	0.005305	0.007360	0.008139	0.03455	0.001699	0.001394
BK20-C4-S2	Vein quartz	640.5	0.02860	0.1006	1.536	1.916	0.03649	0.2829	0.004371	0.01123	0.03465	0.02082	-0.001022	-0.0002474
BK28-C1-S1	Vein quartz	778.0	2.300	0.4372	1.914	0.9776	0.06095	0.03822	-0.001433	0.05157	0.1281	0.03661	0.01409	0.005140
BK28-C1-S2	Vein quartz	778.0	0.2421	-0.03954	2.570	0.004836	-0.003590	0.02508	-0.005807	0.002725	-0.003627	0.01302	0.004337	-0.006240
BK28-C2-S3	Vein quartz	778.0	-0.03130	0.01033	2.332	0.02153	0.09226	0.1204	0.0006340	0.003595	0.06441	0.02827	-0.01437	-0.001974
BK28-C2-S4	Vein quartz	778.0	-0.04498	0.03076	3.413	0.006795	0.1146	0.02398	-0.01114	-0.03445	0.1148	0.01424	0.007111	-0.006033
BK28-C3-S3	Vein quartz	778.0	2.590	0.5039	2.496	0.7292	0.01385	0.03628	-0.004232	0.01696	0.04551	0.009408	0.01779	-0.001391
BK28-C3-S4	Vein quartz	778.0	1.191	0.7320	2.175	0.2697	0.04972	0.2020	-0.006452	-0.005994	0.03574	0.05797	0.003298	0.0005381
BK44-C1-S1	Vein quartz	1600.4	0.2596	0.02714	1.231	0.1217	0.002876	0.01526	0.003395	0.02514	0.008436	0.001367	0.006495	0.002410
BK44-C1-S4	Vein quartz	1600.4	1.097	-0.04370	1.350	-0.08070	0.06051	0.05483	0.01260	-0.01000	0.01777	0.002637	0.002759	-0.006651
BK44-C3-S1	Vein quartz	1600.4	0.9343	0.1389	1.426	0.2389	0.02848	0.01071	-0.007037	-0.01149	-0.03612	0.02081	0.002660	0.007304
BK44-C3-S2	Vein quartz	1600.4	1.493	-0.01258	1.466	-0.02955	0.06197	0.05123	0.004022	0.02421	0.02674	0.06702	-0.005608	0.00007149
BK44-C3-S3	Vein quartz	1600.4	1.894	-0.03236	1.412	0.1177	0.1924	0.1120	-0.004418	-0.01094	0.06102	0.07060	-0.01206	0.001491
BK44-C3-S4	Vein quartz	1600.4	1.296	-0.01308	1.210	0.005873	0.1279	0.05463	0.01018	-0.01431	0.03702	0.08115	0.005235	-0.0002959

* distance from center of deposit

** All elements in ppm except Au which is in ppb

Appendix 7: Buckingham
quartz mineral chemistry by LA-ICP-MS

Sample	Sample type	Distance*												
		(m)	Cu65	Zn66	Ge74	As75	Rb85	Sr88	Zr90	Ag107	Sb121	Cs133	Gd157	Hf178
BK46-C1-S1	Vein quartz	1774.0	0.1202	0.01639	1.821	-0.03046	0.03154	0.6419	0.001304	-0.02174	0.01874	0.01312	0.0006212	0.0004008
BK46-C1-S2	Vein quartz	1774.0	-0.05380	0.006357	1.032	0.02587	0.03802	1.846	-0.004612	-0.01087	0.02393	0.01734	0.003521	-0.003740
BK46-C1-S3	Vein quartz	1774.0	-0.06206	0.01446	1.860	0.08691	0.05165	0.8945	0.005119	-0.006994	-0.002401	0.03419	0.001801	-0.003117
BK46-C1-S4	Vein quartz	1774.0	-0.01014	0.01544	0.6902	0.06324	0.02367	0.6300	-0.001106	0.004252	0.01082	0.006626	0.003994	0.001397
BK46-C2-S1	Vein quartz	1774.0	0.07449	0.01970	1.602	-0.04101	0.02419	0.2975	0.0002241	0.007455	0.05561	0.01056	0.001694	-0.005997
BK46-C2-S2	Vein quartz	1774.0	-0.008008	0.002347	0.5449	0.003402	0.009615	0.1756	-0.001686	-0.007266	-0.005164	0.001638	0.0005304	0.003605
BK46-C2-S3	Vein quartz	1774.0	-0.05834	0.02020	1.911	-0.02356	0.1130	2.074	0.004881	-0.007236	0.02357	0.04764	0.004656	-0.003245
BK46-C2-S4	Vein quartz	1774.0	0.02577	0.01207	0.9112	0.02657	0.06658	2.422	0.0008912	-0.02098	-0.001886	0.02650	0.007147	-0.004780
BK46-C3-S1	Vein quartz	1774.0	0.1251	-0.1273	1.359	-0.003358	0.006515	0.2120	-0.01198	-0.0008000	0.02584	0.006582	-0.02064	-0.003347
BK46-C3-S1	Vein quartz	1774.0	0.008235	0.02670	1.536	0.1064	0.03440	0.2780	-0.001960	0.02117	0.02395	0.006463	-0.004101	0.005873
BK46-C3-S1	Vein quartz	1774.0	0.1625	-0.005013	2.643	-0.01034	0.05473	0.9625	-0.002084	-0.01567	-0.02979	0.008266	-0.01319	-0.001964
BK46-C3-S1	Vein quartz	1774.0	-0.06349	-0.007751	1.803	0.008616	0.02990	0.1918	-0.0002206	0.04465	0.01721	0.004931	-0.005708	0.0007421
BK46-C4-S1	Vein quartz	1774.0	0.1692	0.09606	2.910	0.1265	0.2686	1.949	0.02110	0.04083	0.04774	0.1517	0.007611	0.007029
BK46-C4-S1	Vein quartz	1774.0	0.2623	0.08099	3.062	0.1243	0.1328	1.704	0.04450	0.007672	-0.01221	0.01845	-0.001006	-0.003443
BK50-C1-S1	Vein quartz	3090.9	0.1333	0.1977	1.143	0.1455	0.02852	0.05452	0.01057	-0.03511	0.008084	0.01223	-0.006078	-0.004857
BK50-C1-S2	Vein quartz	3090.9	0.7391	0.8193	1.069	0.1580	0.09857	0.09428	0.06563	0.03118	0.009892	0.03153	0.002848	-0.0005364
BK50-C1-S3	Vein quartz	3090.9	0.2560	0.1301	1.189	0.1174	0.01910	0.1733	0.03736	0.0004590	0.008668	0.003343	-0.005683	0.0008175
BK50-C1-S4	Vein quartz	3090.9	23.99	6.029	1.180	11.39	0.4532	1.697	0.2935	0.07174	0.2584	0.08511	0.09141	0.008187
BK50-C3-S1	Vein quartz	3090.9	5.462	1.321	1.476	2.839	0.1518	0.4026	0.06292	0.07875	0.05669	0.04434	0.02242	0.001600
BK50-C3-S2	Vein quartz	3090.9	0.3518	0.2155	0.7263	0.2826	0.1403	0.07512	0.008724	0.007209	-0.01074	0.005732	-0.002494	-0.002451
BK50-C3-S3	Vein quartz	3090.9	0.3173	0.03128	1.463	0.08663	0.03379	0.02827	0.003272	0.02813	0.03638	0.003741	0.01461	-0.003219
BK50-C3-S4	Vein quartz	3090.9	0.1278	0.2609	1.182	0.09531	0.07368	0.01218	-0.002851	0.01512	-0.03200	0.004061	-0.004718	0.009691
BK59-C1-S1	Vein quartz	2339.0	0.4235	0.01206	2.751	0.7344	0.06348	0.01790	0.001231	-0.006473	0.03281	0.01495	-0.005926	-0.002172
BK59-C1-S2	Vein quartz	2339.0	0.4911	0.07362	2.717	1.944	0.02912	0.003586	-0.0002201	0.005926	0.05439	0.005605	-0.01523	-0.001573
BK59-C1-S3	Vein quartz	2339.0	0.1776	0.2818	0.7582	0.6331	0.3306	0.1838	0.05847	-0.002302	0.01412	0.02628	0.03481	0.006481
BK59-C1-S4	Vein quartz	2339.0	0.1472	0.06516	3.227	0.2656	0.1068	0.05389	0.01734	0.01630	0.01498	0.02522	0.005361	0.006427
BK59-C2-S1	Vein quartz	2339.0	0.1851	0.05297	2.459	0.4531	-0.003304	0.01425	0.005204	0.01361	-0.005212	0.003597	-0.004385	0.00003938
BK59-C2-S2	Vein quartz	2339.0	0.5815	-0.02932	2.227	1.609	0.03886	0.02328	0.01400	0.01214	0.05328	0.03431	0.001928	-0.0005499
BK59-C2-S4	Vein quartz	2339.0	0.5757	0.2452	3.124	0.6926	0.09011	0.05018	-0.006033	-0.001065	0.03480	0.02259	0.0007178	-0.0002215
BK61-C1-S1	Vein quartz	2030.1	0.3531	0.05744	1.723	0.2267	0.07252	0.03593	-0.003110	0.03452	0.01217	0.03344	0.01201	0.0001207
BK61-C1-S1	Vein quartz	2030.1	0.1353	0.2070	2.189	0.08075	0.1135	0.1204	0.003398	0.03470	0.01930	0.1060	0.01038	0.003720
BK61-C1-S2	Vein quartz	2030.1	0.1200	0.08812	2.582	0.1252	0.5833	0.1367	-0.0002061	0.02539	0.04556	0.2374	-0.001977	0.0004651
BK61-C1-S3	Vein quartz	2030.1	0.6036	1.041	2.219	0.03234	0.3552	0.1976	-0.003975	0.02115	0.02763	0.1895	0.01134	-0.002988
BK61-C2-S1	Vein quartz	2030.1	0.3937	0.2809	2.032	0.1302	0.2937	0.2413	0.001161	0.01573	-0.01275	0.1774	-0.008470	0.003112
BK61-C2-S2	Vein quartz	2030.1	0.6927	0.4849	2.054	0.1053	0.1509	0.1617	-0.003344	-0.003091	0.01205	0.1070	-0.01237	-0.004791
BK61-C2-S3	Vein quartz	2030.1	0.3145	-0.08793	1.915	0.1024	0.2435	0.2296	0.003753	0.01840	0.01054	0.1216	-0.0005657	0.002705
BK61-C2-S4	Vein quartz	2030.1	0.4531	0.07132	2.089	0.04033	0.2468	0.1710	0.006556	-0.00009884	0.02135	0.1016	-0.001161	-0.001338
BK63-C1-S1	Vein quartz	1817.2	0.3945	0.2237	1.127	3.739	0.06943	0.06483	-0.001994	-0.0003125	0.01167	0.06798	-0.003468	0.001187
BK63-C1-S1	Vein quartz	1818.6	1.489	0.1017	1.179	3.593	0.1223	0.1016	0.08850	0.01197	0.02799	0.1169	-0.01795	0.01558
BK63-C1-S2	Vein quartz	1817.2	1.376	0.008888	1.277	3.146	0.06697	0.09228	0.005994	0.008459	-0.0005211	0.05128	-0.004986	0.001149
BK63-C1-S2	Vein quartz	1818.6	0.8753	-0.09027	1.238	2.600	0.1114	0.2756	-0.0003010	-0.006246	-0.01878	0.07159	-0.008586	-0.001361
BK63-C1-S3	Vein quartz	1817.2	0.04212	-0.004177	1.251	3.006	0.01301	0.01027	-0.004633	0.009239	0.002764	0.004235	0.01298	-0.002243
BK63-C1-S3	Vein quartz	1818.6	0.1156	0.03765	1.048	2.711	0.02405	0.006999	0.01774	0.007372	-0.01222	-0.001396	0.006665	-0.006858

* distance from center of deposit

** All elements in ppm except Au which is in ppb

Appendix 7: Buckingham
quartz mineral chemistry by LA-ICP-MS

Sample	Sample type	Distance*												
		(m)	Cu65	Zn66	Ge74	As75	Rb85	Sr88	Zr90	Ag107	Sb121	Cs133	Gd157	Hf178
BK63-C1-S4	Vein quartz	1817.2	0.8351	0.2937	1.115	3.101	0.08944	0.03030	0.003002	-0.003224	0.01646	0.09876	-0.01781	0.004921
BK63-C1-S4	Vein quartz	1818.6	42.01	0.09664	1.547	2.241	0.7303	0.3592	0.03497	0.09834	0.1253	0.2303	-0.01550	0.0009979
BK63-C2-S1	Vein quartz	1817.2	0.2289	0.01574	1.182	2.903	0.03299	0.01343	0.0005482	0.01853	0.006222	0.04709	-0.006592	-0.005081
BK63-C2-S1	Vein quartz	1818.6	7.131	0.5843	1.291	2.689	0.03070	0.02163	0.003243	0.02068	0.01378	0.03414	-0.004692	-0.004720
BK63-C2-S2	Vein quartz	1818.6	54.59	0.2758	1.159	2.185	0.3607	0.2024	0.5795	0.1668	0.07304	0.07497	0.007229	0.02564
BK63-C2-S3	Vein quartz	1817.2	0.3995	0.1340	0.9877	2.029	0.08352	0.07350	-0.004123	0.03977	0.01626	0.08539	0.001159	-0.0001475
BK63-C2-S3	Vein quartz	1818.6	2.922	0.1116	1.243	2.374	0.1527	0.08295	0.001044	0.03079	0.01561	0.07746	-0.002971	0.002522
BK63-C2-S4	Vein quartz	1818.6	22.17	0.5359	1.228	2.904	0.9281	0.4778	0.2309	0.2012	0.3707	0.09776	0.3875	0.01094
BK63-C3-S1	Vein quartz	1817.2	0.01645	0.003026	2.083	2.495	0.01430	0.04686	0.006154	-0.007434	0.004068	0.01222	-0.002931	-0.0007789
BK63-C3-S1	Vein quartz	1818.6	0.01645	0.003026	2.083	2.495	0.01430	0.04686	0.006154	-0.007434	0.004068	0.01222	-0.002931	-0.0007789
BK63-C3-S2	Vein quartz	1817.2	0.5213	0.05800	2.760	2.469	0.07505	0.06344	-0.001049	0.02492	0.01417	0.1181	-0.0002708	0.002575
BK63-C3-S2	Vein quartz	1818.6	378.4	5.327	2.521	29.25	0.07723	2.047	0.1546	1.325	3.811	0.08784	0.8807	0.004964
BK63-C3-S3	Vein quartz	1817.2	1.871	0.06666	2.626	2.204	0.006910	0.004348	0.008843	0.01145	0.03522	-0.0003003	0.02032	0.006209
BK63-C3-S3	Vein quartz	1818.6	9.110	0.1927	2.548	3.090	0.008817	0.04643	0.01041	0.03922	0.09176	0.0007544	0.02473	0.005786
BK63-C3-S4	Vein quartz	1817.2	0.7451	0.05968	2.251	1.676	0.02886	0.01443	0.004829	0.03798	0.02705	0.02173	0.02742	0.001293
BK63-C3-S4	Vein quartz	1818.6	0.8006	0.06734	2.475	1.364	0.03863	0.01494	0.01370	0.04524	0.0009205	0.02902	0.03463	0.0008448
BK63-C4-S1	Vein quartz	1818.6	30.80	0.4531	0.4622	2.113	0.1886	0.4221	0.01711	0.01271	0.1851	0.08946	0.07457	-0.003786
BK63-C4-S2	Vein quartz	1818.6	40.02	4.145	0.7857	3.081	0.1708	0.1021	-0.0002124	0.3664	0.08320	0.1065	0.01887	-0.002045
BK63-C5-S1	Vein quartz	1818.6	5.989	0.5759	0.4863	2.135	0.2373	0.2374	0.01239	0.1129	0.08622	0.1507	0.003036	0.001467
BK63-C5-S2	Vein quartz	1818.6	0.4724	0.08961	0.4457	2.049	0.1356	0.2005	0.003639	0.02064	0.00003394	0.04324	0.002291	0.004396
BK63-C5-S3	Vein quartz	1818.6	0.07876	0.4708	0.4599	2.191	0.2123	0.1982	0.002833	0.2205	0.01867	0.08445	-0.001376	-0.001829
BK025-C1-S1	Breccia Ceme	0.0	0.04434	-0.07881	0.6703	18.29	0.0006242	0.006300	0.0005113	0.008997	1.084	0.007678	0.0004772	-0.004843
BK025-C1-S4	Breccia Ceme	0.0	-0.0001444	0.02056	1.319	12.80	0.2657	0.7761	0.006170	-0.01006	9.931	0.1909	0.001392	0.0007054
BK025-C2-S1	Breccia Ceme	0.0	-0.009778	0.02717	0.4742	15.52	0.007794	0.003452	0.007954	0.002386	0.9308	0.007842	-0.004888	0.004617
BK025-C2-S3	Breccia Ceme	0.0	-0.03961	0.08306	1.409	16.07	0.1781	2.225	-0.002822	-0.007635	30.31	0.3593	-0.005203	0.006455
BK025-C2-S4	Breccia Ceme	0.0	-0.02379	0.02575	2.295	17.03	0.05938	0.2347	-0.0001072	-0.007110	10.58	0.07833	0.005523	0.008681
BK025-C3-S1	Breccia Ceme	0.0	-0.02128	-0.03777	1.415	16.37	0.02692	0.00008210	-0.001585	-0.001656	1.778	0.006315	0.0005707	0.001414
BK025-C3-S2	Breccia Ceme	0.0	-0.05754	0.04348	0.6416	15.97	0.005620	-0.003629	0.004910	-0.002934	1.094	0.004637	-0.02015	0.01137
BK025-C3-S3	Breccia Ceme	0.0	-0.006792	0.02291	0.7366	15.79	0.03710	0.0006273	0.001189	0.003087	1.275	0.005870	0.001581	-0.004492
BK025-C3-S4	Breccia Ceme	0.0	0.03590	-0.09341	0.7432	15.75	0.01360	0.002143	-0.01174	0.002240	2.175	0.01520	0.004266	-0.002411
BK025-C4-S2	Breccia Ceme	0.0	0.01889	-0.07945	0.9442	15.14	0.1952	0.1731	-0.002505	-0.006501	7.745	0.08346	0.006263	-0.001591
BK025-C4-S2	Breccia Ceme	0.0	-0.005683	0.01510	5.545	14.32	0.02591	0.01954	-0.003063	-0.001559	12.03	0.007267	0.009063	0.002259
BK025-C4-S2	Breccia Ceme	0.0	0.001446	-0.007092	1.506	14.79	0.04758	0.5288	-0.0008245	-0.002139	27.90	0.008250	0.006981	0.005030
BK104-C1-S1	Breccia Ceme	361.5	3.921	9.108	1.290	35.13	2.450	0.8552	0.4208	0.1790	1.491	0.1986	0.002308	0.0004158
BK104-C1-S2	Breccia Ceme	361.5	1.784	5.399	1.280	42.39	2.313	1.393	0.1429	0.1056	0.8968	0.2906	0.04978	0.003337
BK104-C1-S3	Breccia Ceme	361.5	-0.02336	3.382	1.923	31.86	0.08175	0.5386	-0.01056	0.01372	4.757	0.09217	-0.005505	-0.002644
BK104-C1-S4	Breccia Ceme	361.5	8.328	8.307	0.9427	37.15	2.063	0.9633	0.2150	0.1425	12.10	0.2060	0.04027	-0.001172
BK104-C1-S5	Breccia Ceme	361.5	0.7228	12.30	1.951	48.54	0.4423	0.6981	0.01365	0.1128	13.77	0.2157	0.005905	-0.002619
BK104-C2-S1	Breccia Ceme	361.5	0.3975	27.03	1.355	45.45	3.563	1.008	0.2462	0.003618	9.607	0.3180	0.03122	0.03116
BK104-C2-S2	Breccia Ceme	361.5	0.7959	16.23	1.350	37.78	2.849	1.164	2.753	0.01666	3.461	0.3098	0.02862	0.04039
BK104-C2-S3	Breccia Ceme	361.5	0.8474	6.248	0.8861	40.95	0.5543	0.5679	0.01504	0.008161	0.7615	0.1135	-0.004708	0.002488
BK104-C2-S4	Breccia Ceme	361.5	0.4057	0.9290	0.9492	32.05	1.807	0.2529	0.3088	-0.008548	0.6896	0.1798	0.008543	0.03136
BK104-C2-S5	Breccia Ceme	361.5	1.086	14.22	1.341	47.73	3.112	1.133	0.3473	0.04193	6.600	0.3728	0.01008	0.007852

* distance from center of deposit

** All elements in ppm except Au which is in ppb

Appendix 7: Buckingham
quartz mineral chemistry by LA-ICP-MS

Sample	Sample type	Distance*												
		(m)	Cu65	Zn66	Ge74	As75	Rb85	Sr88	Zr90	Ag107	Sb121	Cs133	Gd157	Hf178
BK104-C3-S1	Breccia Cemei	361.5	1.434	1.594	1.800	28.43	0.7022	1.962	0.02228	0.05502	0.9595	0.5595	-0.008980	0.0007615
BK104-C3-S2	Breccia Cemei	361.5	2.484	3.561	1.576	25.76	1.818	1.101	0.2830	0.1013	0.7070	0.2892	0.01372	0.009318
BK104-C3-S5	Breccia Cemei	361.5	0.09874	0.5994	0.9431	69.14	0.2565	0.2157	0.007055	-0.009289	2.621	0.05573	0.01611	0.007744
BK50-C2-S1	Igneous	3090.9	0.06415	0.2188	0.8291	0.1414	0.07365	0.3292	0.6076	0.01195	0.02351	-0.0007402	-0.002795	0.02106
BK50-C2-S2	Igneous	3090.9	0.6098	1.347	0.8446	0.02203	0.09615	0.1547	0.009091	0.07368	-0.01395	0.02770	-0.006210	-0.001051
BK50-C2-S3	Igneous	3090.9	0.003089	0.1924	1.170	0.08660	0.02442	0.07086	0.04083	0.01909	0.02278	0.009583	0.004166	0.004180
BK50-C2-S4	Igneous	3090.9	0.2081	-0.1214	1.252	0.09241	-0.003185	0.01667	-0.001290	-0.009447	0.004773	0.001481	0.003390	0.004767
BK50-C2-S5	Igneous	3090.9	-0.02706	0.03585	1.630	-0.002244	0.2028	0.08462	0.001517	0.002090	0.01278	0.007759	-0.001492	-0.002219
BK100-C3-S1	Igneous	1443.7	0.4984	-0.07512	0.8351	4.165	0.08049	0.1262	-0.001623	0.02216	0.004383	0.08351	-0.007426	-0.001227
BK100-C3-S2	Igneous	1443.7	0.1327	0.04015	0.8485	3.255	0.01220	0.01262	-0.002023	-0.02194	-0.01012	0.001111	0.006948	0.003389
BK100-C3-S4	Igneous	1443.7	0.4165	0.1204	0.9741	2.822	0.02867	0.01590	0.005942	0.001829	-0.005779	0.01474	0.007457	0.003604
BK101-C1-S1	Igneous	1061.5	0.5401	0.05782	2.192	3.745	0.1527	0.2862	0.002614	-0.007100	0.1313	0.1404	-0.005361	0.003733
BK101-C1-S2	Igneous	1061.5	0.3781	0.01002	2.470	4.442	0.01359	0.02402	-0.002048	-0.01906	-0.001842	0.02682	0.01092	0.005852
BK101-C1-S3	Igneous	1061.5	0.07466	0.06688	2.543	4.881	0.007583	0.01367	0.002253	0.005931	0.008508	0.006036	-0.006027	-0.002509
BK101-C1-S4	Igneous	1061.5	0.03874	0.08473	2.370	4.155	0.007509	0.03326	0.0001581	0.1483	0.06784	0.01118	0.002744	-0.001911
BK101-C1-S5	Igneous	1061.5	0.2351	0.1783	1.951	5.089	0.04224	0.02240	-0.002354	0.006078	0.01067	0.01370	-0.002410	0.002198
BK44-C2-S1	Sedimentary	1600.4	0.8788	0.04534	1.181	0.04685	0.02517	0.1178	0.0001751	-0.01973	-0.001036	0.03448	0.002718	0.003793
BK44-C2-S2	Sedimentary	1600.4	4.974	0.01343	1.022	0.06631	0.02627	0.01092	-0.006314	0.01309	-0.003861	0.009204	0.000	-0.001543
BK44-C2-S4	Sedimentary	1600.4	1.169	0.02111	1.195	0.2229	0.06738	0.01902	0.005470	-0.004226	0.05518	0.02145	0.0004380	0.001655
BK44-C4-S1	Sedimentary	1600.4	0.4929	0.03208	1.029	0.09836	0.01107	0.007650	0.001237	0.02606	0.03570	0.01104	-0.002841	-0.001869
BK44-C4-S2	Sedimentary	1600.4	-0.05655	-0.07833	0.8693	-0.02321	0.01236	0.1273	-0.0004709	-0.01165	0.4385	0.008305	-0.003384	-0.001592
BK44-C4-S3	Sedimentary	1600.4	1.292	0.1090	1.085	0.06349	0.04088	0.1440	0.009873	-0.01199	0.2141	0.04534	-0.0009289	0.005010
BK44-C4-S4	Sedimentary	1600.4	1.035	0.2140	1.243	0.08188	0.02695	0.1022	0.03902	-0.01006	0.5342	0.01906	0.003199	0.004134
BK17-C2-S1	Sedimentary	770.8	0.06180	0.2206	0.8377	0.1780	0.2982	0.2556	0.005830	-0.005309	0.01327	0.04513	-0.001060	-0.001078
BK17-C2-S2	Sedimentary	770.8	-0.07945	0.1624	1.027	-0.02247	0.2550	0.3470	-0.002319	-0.004585	-0.00002704	0.04006	0.0001738	0.003806
BK17-C2-S3	Sedimentary	770.8	0.02989	0.1106	0.9956	0.06620	0.2706	0.3774	0.001959	0.02743	0.1372	0.02431	0.01020	0.001911
BK17-C4-S2	Sedimentary	770.8	-0.04462	0.1372	0.9104	0.1374	0.2040	0.2009	0.009421	0.005816	0.07584	0.01760	-0.005355	0.001916
BK17-C4-S3	Sedimentary	770.8	-0.1051	0.1739	0.8565	0.1565	0.1858	0.04038	0.004522	0.02771	0.04601	0.001732	-0.001849	0.000
BK12-C1-S1	Sedimentary	1475.3	-0.01031	0.2638	0.8082	0.01249	0.05374	0.6853	-0.004443	-0.03258	-0.01934	0.02208	0.0009547	-0.002745
BK12-C1-S2	Sedimentary	1475.3	0.2469	0.2010	0.9102	0.04977	0.08149	1.331	0.006110	0.007307	-0.01036	0.01800	-0.01182	0.002842
BK12-C1-S3	Sedimentary	1475.3	0.8083	0.3885	1.007	0.08791	0.5411	1.367	0.4564	0.02501	-0.02157	0.09520	-0.004204	0.02216
BK12-C3-S1	Sedimentary	1475.3	0.1516	0.1080	0.7739	0.02117	0.009547	0.04051	0.008859	-0.006182	0.009586	0.006550	0.001777	-0.0003301
BK12-C3-S2	Sedimentary	1475.3	0.04638	0.04351	0.8093	0.1364	0.04591	0.07634	0.04353	0.01913	0.01112	0.08952	-0.004856	0.001677
BK12-C3-S3	Sedimentary	1475.3	-0.08034	-0.06575	1.008	0.03012	0.03010	0.1061	0.003095	0.01969	0.01918	0.02985	0.002023	0.001260
BK13-C1-S1	Sedimentary	1381.0	0.03201	0.2835	1.157	-0.07345	0.07230	1.084	-0.0002986	0.01201	0.03134	0.03480	0.001375	-0.002121
BK13-C1-S2	Sedimentary	1381.0	-0.005268	0.06156	1.054	0.1063	0.09947	0.4636	-0.001139	-0.004978	0.007691	0.1015	-0.0005984	0.002937
BK13-C1-S3	Sedimentary	1381.0	-0.03182	0.6552	1.112	-0.01869	0.06850	0.9753	0.004302	-0.009603	-0.02266	0.005296	0.001902	-0.008882
BK13-C6-S1	Sedimentary	1381.0	-0.02280	-0.08860	3.174	0.1208	0.07483	1.615	-0.001971	0.008169	0.1257	0.01236	-0.005160	0.002236
BK13-C6-S1	Sedimentary	1381.0	-0.02106	0.003995	3.818	0.1315	0.2252	2.442	0.01072	-0.001272	0.2178	0.01731	-0.005582	-0.003948
BK13-C6-S1	Sedimentary	1381.0	-0.1308	-0.04380	3.539	0.02012	0.1993	2.259	-0.002694	-0.02128	0.1462	0.01444	-0.002308	-0.006693
BK61-C3-S1	Sedimentary	2030.1	0.03381	0.4520	0.8438	0.2045	0.2504	0.1741	0.001261	0.008090	0.01308	0.03505	-0.0005480	-0.006011
BK61-C3-S2	Sedimentary	2030.1	-0.02495	0.2210	0.8706	0.8216	0.3224	0.1139	0.005360	0.008911	-0.001554	0.04322	0.000	0.001246
BK15-C1-S2	Sedimentary	981.5	0.007675	-0.01692	0.8835	0.1127	0.02103	0.3086	-0.001406	0.004507	0.02505	0.08040	-0.006193	-0.002470

* distance from center of deposit

** All elements in ppm except Au which is in ppb

Appendix 7: Buckingham
quartz mineral chemistry by LA-ICP-MS

Sample	Sample type	Distance*												
		(m)	Cu65	Zn66	Ge74	As75	Rb85	Sr88	Zr90	Ag107	Sb121	Cs133	Gd157	Hf178
BK15-C1-S3	Sedimentary	981.5	0.01636	0.2881	0.8913	0.04236	0.03230	0.3366	0.03846	-0.01557	0.01366	0.03280	0.006131	0.003151
BK15-C1-S4	Sedimentary	981.5	0.1001	0.7669	0.8498	0.07150	0.09157	0.4487	0.02568	-0.007818	-0.004151	0.06912	-0.001377	-0.0007742
BK15-C5-S1	Sedimentary	981.5	0.03100	-0.04977	0.4495	0.09557	0.00009199	0.004062	-0.0009333	0.02364	-0.03186	0.0006839	0.00007664	-0.005498
BK15-C5-S2	Sedimentary	981.5	0.02543	-0.1044	0.6575	0.07167	0.008430	0.09224	0.002553	0.00008860	0.07944	0.006260	0.01195	0.001154
BK15-C5-S3	Sedimentary	981.5	0.003681	0.09024	0.7732	0.08585	0.03131	0.1688	-0.001196	0.0009217	-0.01771	0.0006571	-0.006465	0.001261
BK15-C5-S4	Sedimentary	981.5	0.05750	0.5947	0.8122	0.1074	0.05189	0.3252	-0.0009260	0.01106	0.01925	0.007535	-0.002639	0.0003385
BK03-C3-S1	Sedimentary	337.4	0.05046	0.1331	1.229	0.05823	-0.004834	0.004840	-0.001577	0.02045	-0.003376	-0.002373	0.01669	-0.007669
BK03-C3-S2	Sedimentary	337.4	-0.04774	0.1265	1.282	0.01805	0.2773	0.009670	0.006604	-0.01875	0.03402	0.006413	-0.007431	-0.01130
BK59-C3-S1	Sedimentary	2339.0	-0.08996	0.4487	3.168	0.6926	0.02114	0.03763	0.002218	-0.007859	0.1459	0.006305	-0.003363	0.001763
BK59-C3-S2	Sedimentary	2339.0	0.5757	1.236	3.599	0.3526	0.1967	0.2223	-0.008939	0.01093	0.1059	0.03175	0.001490	-0.001926
BK59-C3-S3	Sedimentary	2339.0	1.600	1.163	0.4853	0.4231	0.08313	0.05224	-0.0004057	-0.01614	0.03002	0.02726	-0.007226	-0.003503
BK59-C3-S4	Sedimentary	2339.0	-0.03745	0.07053	1.222	0.1254	0.1633	0.06660	-0.0005403	0.02751	-0.01631	-0.001198	0.003844	-0.002654
BK59-C4-S1	Sedimentary	2339.0	-0.03413	0.4455	0.9457	0.1802	0.09658	0.02952	0.001027	-0.02885	0.01288	0.01202	0.01211	0.004869
BK59-C4-S2	Sedimentary	2339.0	0.03165	0.4092	0.8610	0.1876	0.4205	0.2262	0.001906	0.01506	0.008970	0.1317	0.0004115	0.002593
BK59-C4-S3	Sedimentary	2339.0	0.03829	0.6943	1.071	0.1706	0.7302	0.04988	0.02123	-0.009183	-0.006153	0.02504	0.005647	-0.001369
BK102-C3-S1	Sedimentary	890.8	0.04539	0.08382	0.6043	0.01616	0.2313	0.03745	-0.0003324	0.005418	0.04137	0.07014	-0.004020	0.004014
BK102-C3-S2	Sedimentary	890.8	-0.04831	0.1522	0.8220	0.09072	0.1186	0.03640	0.002569	-0.01250	0.02239	0.04811	-0.002856	-0.001679
BK102-C3-S3	Sedimentary	890.8	0.4125	0.1048	0.7401	0.1384	0.3813	0.2152	0.01616	0.01718	2.579	0.1563	0.003147	-0.002857
BK102-C3-S4	Sedimentary	890.8	0.02334	0.06373	0.6032	0.01738	0.08412	0.03680	0.09121	-0.007826	0.3218	0.02942	-0.005150	0.01043
BK106-C1-S1	Sedimentary	466.2	0.2853	0.2523	0.9092	0.08283	0.02323	0.4232	0.007464	0.02822	-0.05281	0.001052	0.002041	-0.003783
BK106-C1-S2	Sedimentary	466.2	0.1393	0.3479	1.045	-0.04552	0.03769	0.1095	-0.006884	0.005340	-0.02080	0.009933	0.005756	0.004505
BK106-C1-S3	Sedimentary	466.2	1.427	0.6354	0.7883	0.2120	0.05502	0.09942	-0.001564	0.001137	0.02560	0.01003	0.02713	0.001006
BK106-C4-S2	Sedimentary	466.2	0.08513	-0.05082	0.8898	0.08495	0.03658	0.01269	0.007258	0.01276	-0.01314	0.0004584	0.007054	-0.001014
BK106-C4-S3	Sedimentary	466.2	0.2836	-0.04099	0.8975	0.1089	0.1201	0.4295	0.02200	-0.007745	0.008354	0.03456	-0.004199	-0.003317
BK106-C4-S4	Sedimentary	466.2	1.094	0.1870	0.4518	0.1315	0.1635	0.7935	0.009969	0.06781	0.04007	0.05382	-0.008410	-0.001046
BK106-C4-S5	Sedimentary	466.2	0.3070	0.2305	0.4477	0.1938	0.1707	0.4914	0.004809	-0.01313	-0.02316	0.04911	-0.008783	-0.0009915
BK106-C5-S1	Sedimentary	466.2	0.02468	1.216	1.873	0.1075	0.09312	0.09115	-0.0003445	-0.01021	-0.002643	0.05248	0.01198	0.0003046
BK106-C5-S2	Sedimentary	466.2	0.1338	0.3688	1.744	0.06309	0.04622	0.03225	0.008463	0.006316	0.008657	0.01804	0.003293	0.005620
BK106-C5-S3	Sedimentary	466.2	0.005617	0.2350	1.772	0.1245	0.04561	0.04555	0.0006274	-0.01663	-0.001190	0.01874	-0.01253	-0.007001
BK18-C1-S1	Sedimentary	608.8	0.02511	0.1020	1.264	0.1933	0.4306	0.7523	0.03744	0.01764	0.03633	0.09018	-0.005084	0.001007
BK18-C1-S2	Sedimentary	608.8	0.1541	0.2152	1.203	0.2954	0.2470	0.1091	0.02735	0.007688	0.009200	0.01605	-0.009812	-0.0007954
BK18-C1-S3	Sedimentary	608.8	1.106	0.1134	1.292	0.6813	0.1694	0.1554	0.01252	0.01583	0.08202	0.01148	0.004049	0.006345
BK18-C3-S1	Sedimentary	608.8	-0.03887	-0.05330	0.4377	0.07383	0.01155	0.01706	0.009310	-0.01274	-0.02736	0.0004240	0.01649	-0.004772
BK18-C3-S2	Sedimentary	608.8	0.01228	0.08736	0.6017	0.1350	0.003263	0.04179	-0.006599	-0.01593	0.0002616	-0.0006934	-0.006778	0.002577
BK18-C3-S3	Sedimentary	608.8	-0.02065	0.07577	0.4848	0.04193	0.006133	0.1103	-0.007491	-0.004112	0.01794	0.002157	-0.007521	-0.0004865
BK20-C1-S2	Sedimentary	640.5	0.03145	0.01949	0.5300	5.013	0.02589	0.07437	0.005204	-0.001353	0.01783	0.0002752	0.004782	0.0002949
BK20-C1-S3	Sedimentary	640.5	0.08408	0.8155	0.5044	3.031	0.06741	0.03594	0.008570	0.002113	0.005491	0.005986	-0.0002893	0.004004
BK20-C1-S4	Sedimentary	640.5	-0.04687	-0.09768	0.4274	2.137	0.04197	0.02663	0.001442	-0.001024	0.004604	0.003091	-0.01176	-0.001733
BK20-C2-S1	Sedimentary	640.5	-0.02721	-0.009509	0.8407	3.774	0.05177	0.04511	-0.001494	0.004703	0.01609	0.01177	0.0001994	0.008808
BK20-C2-S2	Sedimentary	640.5	0.1647	0.07858	0.8684	2.384	0.1550	0.04742	0.01573	-0.01190	0.04703	0.03015	0.007290	0.001789
BK20-C2-S3	Sedimentary	640.5	0.04583	0.1397	0.7508	2.083	0.2144	0.1077	0.006343	0.002689	0.01780	0.08599	0.01518	0.006582
BK20-C2-S4	Sedimentary	640.5	0.09195	0.1556	1.008	1.908	0.2845	0.2506	0.01332	0.001789	0.05189	0.09959	-0.0006262	-0.002733
BK021-C1-S1	Sedimentary	517.7	0.02253	1.255	0.9221	2.877	0.3499	0.2963	0.009499	0.01453	0.01128	0.08066	0.003057	0.0002033

* distance from center of deposit

** All elements in ppm except Au which is in ppb

Appendix 7: Buckingham
quartz mineral chemistry by LA-ICP-MS

Sample	Sample type	Distance* (m)	Cu65	Zn66	Ge74	As75	Rb85	Sr88	Zr90	Ag107	Sb121	Cs133	Gd157	Hf178
BK021-C1-S2	Sedimentary	517.7	2.279	0.9152	1.683	3.135	9.988	2.217	8.014	0.1048	2.089	0.2904	3.071	0.2711
BK021-C2-S1	Sedimentary	517.7	0.02845	0.2026	0.8062	2.329	0.1533	0.06891	-0.001090	-0.001093	0.03724	0.01719	-0.004049	0.005365
BK021-C2-S2	Sedimentary	517.7	0.1940	0.07539	0.7318	2.160	0.1177	0.03192	0.02586	0.01297	0.2194	0.01676	0.001548	0.01047
BK021-C2-S3	Sedimentary	517.7	0.1466	0.2283	0.6092	2.046	0.1067	0.06267	0.07409	0.004368	0.09226	0.01966	-0.001992	0.003757
BK021-C2-S4	Sedimentary	517.7	0.02055	0.1810	0.6849	1.706	0.1776	0.07124	0.02010	0.01978	0.1597	0.01681	0.04304	0.004403
BK63-C4-S1	Sedimentary	1817.2	0.1451	0.1082	0.4628	2.135	0.1758	0.1930	0.01023	0.004334	0.03475	0.06715	0.01063	-0.005238
BK63-C4-S2	Sedimentary	1817.2	2.551	0.05574	0.4843	2.080	0.07287	0.3258	0.009793	0.05741	0.04762	0.08077	0.03082	0.004777
BK63-C5-S1	Sedimentary	1817.2	0.4004	0.1025	0.4629	2.294	0.03100	0.07084	0.004640	0.008984	0.1189	0.03291	0.006511	-0.003451
BK63-C5-S2	Sedimentary	1817.2	0.3819	0.06796	0.4721	1.848	0.1138	0.1921	-0.0002321	0.01989	-0.001536	0.03711	0.004604	0.001340
BK63-C5-S3	Sedimentary	1817.2	0.2635	0.4210	0.4572	2.202	0.2066	0.1700	0.003836	0.1249	0.01300	0.07466	0.005008	-0.002729

* distance from center of deposit

** All elements in ppm except Au which is in ppb

Appendix 7: Buckingham
quartz mineral chemistry by LA-ICP-MS

Sample	Sample type	Distance*					
		(m)	Ta181	Au197**	Pb208	Bi209	U238
BK01-C1-S1	Vein quartz	591.4	-0.0001554	-0.008313	0.04842	-0.01712	0.004397
BK01-C1-S2	Vein quartz	591.4	0.00006814	-0.006950	0.07252	0.001768	0.0009711
BK01-C1-S3	Vein quartz	591.4	-0.0001771	0.003961	0.005604	-0.0002333	0.001011
BK01-C2-S1	Vein quartz	591.4	-0.0004216	-0.01062	0.003166	-0.004754	0.0001445
BK01-C2-S2	Vein quartz	591.4	-0.0005761	-0.005341	0.004578	-0.004084	-0.001031
BK01-C2-S3	Vein quartz	591.4	-0.002022	-0.006826	0.02464	-0.002496	-0.002191
BK01-C2-S4	Vein quartz	591.4	-0.0002196	-0.0009819	0.01635	-0.001361	-0.0006638
BK01-C3-S1	Vein quartz	591.4	0.001012	-0.007120	0.01210	-0.004814	0.001092
BK01-C3-S2	Vein quartz	591.4	0.002576	0.002837	0.01028	-0.0001970	0.001330
BK01-C3-S3	Vein quartz	591.4	-0.0005391	-0.001032	0.03363	-0.001320	0.004155
BK01-C5-S1	Vein quartz	591.4	0.0003196	0.006427	0.02939	0.0006851	0.02570
BK01-C5-S4	Vein quartz	591.4	-0.001972	0.004253	0.01214	0.001256	-0.0002935
BK021-C3-S1	Vein quartz	517.7	-0.0006649	-0.005518	0.2430	0.001381	0.02560
BK021-C3-S2	Vein quartz	517.7	-0.001197	-0.008949	0.1786	0.005404	0.009979
BK021-C3-S4	Vein quartz	517.7	0.01797	-0.001937	0.3902	0.004651	0.06931
BK021-C4-S1	Vein quartz	517.7	0.001571	0.004367	0.1593	0.002463	-0.0001936
BK021-C4-S3	Vein quartz	517.7	0.0006578	-0.001163	0.2828	0.003092	0.001989
BK021-C4-S4	Vein quartz	517.7	-0.0002556	0.0004032	0.2675	0.006618	0.004460
BK021-C4-S5	Vein quartz	517.7	-0.0003097	0.002180	0.06285	-0.00005214	0.001745
BK03-C1-S2	Vein quartz	337.4	-0.001264	0.005965	0.009588	0.004186	0.01593
BK03-C4-S1	Vein quartz	337.4	0.0004436	-0.009044	0.5527	0.006013	0.01401
BK03-C4-S2	Vein quartz	337.4	-0.002696	0.01239	0.01206	-0.003957	0.007872
BK03-C4-S3	Vein quartz	337.4	0.001367	-0.01335	0.1838	0.01174	0.009217
BK06-C1-S1	Vein quartz	940.0	0.0005261	-0.008049	0.3470	-0.0003143	-0.001137
BK06-C1-S2	Vein quartz	940.0	-0.0003276	0.003447	0.001451	0.006529	0.002420
BK06-C1-S3	Vein quartz	940.0	0.002305	0.008397	0.01041	0.0008934	0.0009057
BK06-C1-S4	Vein quartz	940.0	0.0005143	0.0002265	0.01155	0.00009633	0.002104
BK06-C2-S1	Vein quartz	940.0	-0.001971	-0.01390	0.04677	0.0007735	0.001138
BK06-C2-S2	Vein quartz	940.0	0.0004254	-0.009377	0.05379	0.001239	0.01190
BK06-C2-S4	Vein quartz	940.0	-0.001284	-0.001214	0.01763	-0.0009157	0.002114
BK06-C2-S5	Vein quartz	940.0	0.001107	0.001656	0.04274	0.001007	-0.0007388
BK06-C3-S1	Vein quartz	940.0	-0.0007111	0.005177	0.04298	0.0005277	0.002749
BK06-C3-S2	Vein quartz	940.0	-0.0003667	0.0006271	0.03002	0.0009892	0.006792
BK06-C3-S3	Vein quartz	940.0	0.0002038	-0.001801	0.01948	0.001780	0.002957
BK09-C1-S1	Vein quartz	1043.0	0.00006640	0.005964	0.02761	0.001663	0.0007646
BK09-C1-S2	Vein quartz	1043.0	0.0005524	-0.0005908	0.09638	-0.0004036	0.0001927
BK09-C1-S3	Vein quartz	1043.0	-0.0007962	-0.009062	0.7651	0.02572	0.002624
BK09-C1-S4	Vein quartz	1043.0	0.001639	-0.001032	2.096	0.004047	0.001059
BK09-C2-S1	Vein quartz	1043.0	-0.0007773	0.005901	0.03064	-0.0002214	0.000
BK09-C2-S2	Vein quartz	1043.0	-0.0006158	0.007768	0.4701	0.003473	0.002344
BK09-C2-S4	Vein quartz	1043.0	0.000	-0.004683	0.02702	0.0004566	-0.0001905
BK09-C3-S2	Vein quartz	1043.0	-0.001145	0.002050	0.09141	0.004977	0.002744
BK09-C3-S3	Vein quartz	1043.0	0.0002336	-0.007768	0.03155	0.001740	-0.0003511

* distance from center of deposit

** All elements in ppm except Au which is in ppb

Appendix 7: Buckingham
quartz mineral chemistry by LA-ICP-MS

Sample	Sample type	Distance*					
		(m)	Ta181	Au197**	Pb208	Bi209	U238
BK09-C3-S4	Vein quartz	1043.0	0.0007756	0.003243	0.1030	-0.001036	0.001211
BK09-C4-S1	Vein quartz	1043.0	0.0007663	-0.005757	0.06205	0.0002404	0.01222
BK09-C4-S2	Vein quartz	1043.0	-0.001814	0.02142	0.1604	0.01127	0.003982
BK09-C4-S3	Vein quartz	1043.0	0.0004219	-0.002014	0.09987	0.002735	0.001886
BK09-C4-S4	Vein quartz	1043.0	0.002423	-0.008712	0.07854	0.002076	0.001023
BK100-C1-S2	Vein quartz	1443.7	-0.0006154	-0.001313	0.007437	0.002582	-0.001555
BK100-C1-S3	Vein quartz	1443.7	-0.0004171	-0.0001453	0.07966	0.001166	0.001644
BK100-C1-S4	Vein quartz	1443.7	-0.0005023	0.003507	0.01757	0.0005920	0.002097
BK100-C4-S1	Vein quartz	1443.7	0.0003159	-0.001325	0.03618	0.0007162	0.001743
BK100-C4-S2	Vein quartz	1443.7	-0.00007571	0.002989	0.02542	0.002650	-0.001353
BK100-C4-S3	Vein quartz	1443.7	-0.0009682	-0.001866	0.02554	-0.003794	0.007073
BK100-C4-S4	Vein quartz	1443.7	-0.0004619	-0.002381	0.05100	-0.00004772	0.002792
BK101-C2-S1	Vein quartz	1061.5	-0.002020	0.007543	0.03995	0.0008409	0.002470
BK101-C2-S2	Vein quartz	1061.5	-0.0008663	-0.009166	0.01769	0.006710	-0.001000
BK101-C2-S3	Vein quartz	1061.5	-0.001014	0.002089	0.04419	0.00004242	0.0002213
BK101-C3-S1	Vein quartz	1061.5	-0.0004967	-0.002471	0.008378	-0.0005228	-0.001039
BK101-C3-S1	Vein quartz	1061.5	-0.0003049	0.006502	0.02103	0.004024	-0.0001808
BK101-C3-S2	Vein quartz	1061.5	0.0008538	0.0007788	0.07869	0.002839	-0.002267
BK101-C3-S3	Vein quartz	1061.5	0.0004670	-0.0006535	0.03801	0.002592	-0.0001250
BK101-C3-S4	Vein quartz	1061.5	-0.0009205	0.000	0.01864	-0.0003784	0.003609
BK101-C3-S5	Vein quartz	1061.5	-0.0008758	0.009712	0.01850	0.002865	0.01267
BK101-C5-S1	Vein quartz	1061.5	-0.0006054	0.0007556	0.0004550	-0.001201	0.001180
BK101-C5-S1	Vein quartz	1061.5	-0.001067	-0.006236	0.03844	0.01045	0.001275
BK102-C1-S1	Vein quartz	890.8	-0.0004196	0.006483	-0.001645	-0.009074	0.002598
BK102-C1-S2	Vein quartz	890.8	-0.0009309	-0.01110	0.03065	-0.003444	0.000
BK102-C1-S3	Vein quartz	890.8	-0.001563	-0.0003983	0.006409	0.001403	-0.002432
BK102-C1-S4	Vein quartz	890.8	-0.001112	0.005248	0.1153	0.001041	-0.001219
BK102-C2-S1	Vein quartz	890.8	0.0005146	0.001484	0.02900	-0.005052	0.0002820
BK102-C2-S2	Vein quartz	890.8	0.002740	-0.006524	0.09849	0.001727	0.001630
BK102-C2-S3	Vein quartz	890.8	-0.0008556	0.02854	0.1664	0.001421	0.005456
BK102-C2-S5	Vein quartz	890.8	-0.0004054	-0.002389	0.01994	0.002644	0.002104
BK106-C2-S1	Vein quartz	466.2	-0.0001267	0.02370	0.05128	0.003158	0.005206
BK106-C2-S2	Vein quartz	466.2	0.0009256	0.009762	0.03128	0.002473	0.003812
BK106-C2-S3	Vein quartz	466.2	-0.002440	0.005016	0.04834	-0.001735	-0.001310
BK106-C3-S1	Vein quartz	466.2	-0.001190	-0.002135	0.05571	-0.004682	-0.003343
BK106-C3-S2	Vein quartz	466.2	0.0003127	0.001546	0.04233	0.01679	0.02546
BK12-C2-S1	Vein quartz	1475.3	-0.0005357	0.006400	0.004220	0.004003	0.0005320
BK12-C2-S3	Vein quartz	1475.3	-0.0001019	0.02902	0.04764	-0.00004430	0.0009264
BK12-C4-S1	Vein quartz	1475.3	-0.0008703	-0.002673	0.004426	0.002441	-0.002322
BK12-C4-S3	Vein quartz	1475.3	-0.002400	-0.003763	0.02528	-0.006672	-0.0009015
BK12-C6-S2	Vein quartz	1475.3	0.0006608	-0.002061	0.01037	0.002308	-0.001528
BK13-C3-S2	Vein quartz	1381.0	0.0006616	-0.001121	0.008817	-0.0009844	-0.001256
BK13-C3-S3	Vein quartz	1381.0	-0.0006042	0.0006331	0.01512	-0.001610	-0.0008957

* distance from center of deposit

** All elements in ppm except Au which is in ppb

Appendix 7: Buckingham
quartz mineral chemistry by LA-ICP-MS

Sample	Sample type	Distance*					
		(m)	Ta181	Au197**	Pb208	Bi209	U238
BK13-C3-S4	Vein quartz	1381.0	0.0007668	0.001417	0.1729	-0.001880	0.01099
BK13-C4-S1	Vein quartz	1381.0	-0.001407	0.003794	0.01079	0.003217	0.0005844
BK13-C4-S2	Vein quartz	1381.0	-0.0009055	-0.003796	0.004046	0.001426	0.0001146
BK13-C4-S3	Vein quartz	1381.0	0.0008464	0.003875	0.01449	0.0007926	0.0009085
BK13-C4-S4	Vein quartz	1381.0	-0.0005820	-0.0004499	0.02742	0.002513	0.0007727
BK15-C1-S1	Vein quartz	981.5	0.005338	-0.005982	0.03147	0.002436	-0.001769
BK15-C2-S1	Vein quartz	981.5	0.002145	0.008538	-0.009166	0.005658	0.003508
BK15-C2-S2	Vein quartz	981.5	-0.00004467	0.004297	0.01105	0.009759	0.002725
BK15-C2-S2	Vein quartz	981.5	-0.001503	0.006463	0.01244	-0.006768	-0.0004768
BK15-C2-S3	Vein quartz	981.5	0.0002571	0.01461	0.01355	0.007124	0.008764
BK15-C2-S3	Vein quartz	981.5	0.0002818	-0.0008044	0.01144	-0.001061	0.0005178
BK15-C2-S4	Vein quartz	981.5	0.0004349	-0.002190	0.02833	0.02933	0.008989
BK15-C2-S4	Vein quartz	981.5	-0.001011	-0.008482	-0.006505	-0.0009493	0.0009975
BK17-C1-S1	Vein quartz	770.8	-0.0002261	0.004633	0.04860	0.003910	-0.001318
BK17-C1-S2	Vein quartz	770.8	0.003313	0.01507	0.1465	0.007432	0.003861
BK17-C1-S3	Vein quartz	770.8	0.001960	0.002786	0.08104	-0.001098	0.003649
BK17-C3-S1	Vein quartz	770.8	-0.001647	-0.006451	0.02100	0.003666	-0.0006287
BK17-C3-S2	Vein quartz	770.8	-0.0008459	0.002678	0.06613	0.001160	0.0005809
BK17-C3-S3	Vein quartz	770.8	0.0003156	0.005044	0.01549	0.005894	0.002625
BK17-C3-S4	Vein quartz	770.8	0.005962	0.009492	1.400	0.008530	0.003095
BK18-C2-S2	Vein quartz	608.8	0.0001216	0.001089	0.1023	0.0009594	0.0004597
BK18-C2-S4	Vein quartz	608.8	0.002144	0.01106	0.2314	0.006294	0.0002481
BK18-C5-S1	Vein quartz	608.8	0.0006857	-0.005525	0.2041	-0.004873	0.002221
BK18-C5-S2	Vein quartz	608.8	0.002374	0.002146	0.1419	0.004419	0.000
BK18-C5-S3	Vein quartz	608.8	0.0006538	-0.008467	0.2076	0.007655	0.001232
BK18-C5-S4	Vein quartz	608.8	0.002326	-0.01121	0.08641	0.002041	0.0008048
BK20-C3-S1	Vein quartz	640.5	0.001123	-0.0004727	0.04196	0.001262	0.0005283
BK20-C3-S2	Vein quartz	640.5	0.00008143	0.003058	0.007894	0.001340	0.002549
BK20-C3-S3	Vein quartz	640.5	0.001725	-0.002503	0.02713	-0.002539	0.0008997
BK20-C3-S4	Vein quartz	640.5	0.0007522	0.01097	0.02976	0.001973	0.001592
BK20-C4-S2	Vein quartz	640.5	-0.0001214	-0.002201	0.03810	0.001276	0.0003693
BK28-C1-S1	Vein quartz	778.0	0.001648	-0.003902	0.3517	-0.0007267	0.001473
BK28-C1-S2	Vein quartz	778.0	-0.0003059	0.01001	0.0009945	0.001096	0.002792
BK28-C2-S3	Vein quartz	778.0	0.0007420	-0.003501	0.0006170	-0.002156	-0.0002602
BK28-C2-S4	Vein quartz	778.0	-0.001488	-0.004697	0.006811	-0.007625	0.001044
BK28-C3-S3	Vein quartz	778.0	-0.001550	-0.004154	0.05917	0.003506	0.01237
BK28-C3-S4	Vein quartz	778.0	0.001399	-0.005609	0.2830	-0.0001651	0.002519
BK44-C1-S1	Vein quartz	1600.4	-0.0006925	0.0004296	0.001961	-0.003805	0.0003050
BK44-C1-S4	Vein quartz	1600.4	-0.003817	0.006340	0.009019	-0.001887	0.003130
BK44-C3-S1	Vein quartz	1600.4	0.001462	0.001405	0.05072	-0.001286	-0.0006832
BK44-C3-S2	Vein quartz	1600.4	0.0004698	0.002217	0.01510	-0.002854	-0.001914
BK44-C3-S3	Vein quartz	1600.4	-0.0002144	-0.005532	0.04386	0.004780	-0.0003777
BK44-C3-S4	Vein quartz	1600.4	0.001167	0.001242	0.02373	-0.004940	0.001739

* distance from center of deposit

** All elements in ppm except Au which is in ppb

Appendix 7: Buckingham
quartz mineral chemistry by LA-ICP-MS

Sample	Sample type	Distance*					
		(m)	Ta181	Au197**	Pb208	Bi209	U238
BK46-C1-S1	Vein quartz	1774.0	-0.001647	0.01605	-0.004900	-0.005478	-0.0004518
BK46-C1-S2	Vein quartz	1774.0	-0.0002916	0.01055	0.003016	-0.008908	-0.0008266
BK46-C1-S3	Vein quartz	1774.0	-0.0001122	0.003125	0.003115	0.002482	-0.0007713
BK46-C1-S4	Vein quartz	1774.0	-0.0005367	0.002236	0.005470	-0.001753	0.0007215
BK46-C2-S1	Vein quartz	1774.0	0.001933	0.006816	0.009172	-0.003253	0.0005885
BK46-C2-S2	Vein quartz	1774.0	0.0005009	-0.001897	0.005738	-0.001080	-0.001014
BK46-C2-S3	Vein quartz	1774.0	-0.001255	0.008564	0.004797	-0.0002893	0.0003585
BK46-C2-S4	Vein quartz	1774.0	0.0006859	-0.01015	0.005881	0.0008496	0.0002427
BK46-C3-S1	Vein quartz	1774.0	-0.001111	-0.005308	-0.0007490	0.003320	0.001070
BK46-C3-S1	Vein quartz	1774.0	-0.0006625	0.007901	0.02475	0.01125	-0.0008411
BK46-C3-S1	Vein quartz	1774.0	-0.001169	0.002687	0.01317	-0.002913	-0.002194
BK46-C3-S1	Vein quartz	1774.0	-0.0003079	-0.01803	-0.001546	0.001089	0.0002657
BK46-C4-S1	Vein quartz	1774.0	0.00008806	-0.002084	0.07371	0.003944	0.0009024
BK46-C4-S1	Vein quartz	1774.0	-0.0001634	0.01087	0.1157	0.004927	0.003347
BK50-C1-S1	Vein quartz	3090.9	0.001277	0.01739	0.2319	-0.003439	0.0007050
BK50-C1-S2	Vein quartz	3090.9	0.0006731	-0.001327	0.7373	-0.002887	0.01597
BK50-C1-S3	Vein quartz	3090.9	0.0002686	-0.002732	0.02666	0.0002337	0.01313
BK50-C1-S4	Vein quartz	3090.9	0.001002	-0.0004599	8.942	0.04482	0.2640
BK50-C3-S1	Vein quartz	3090.9	0.003526	0.002622	1.210	0.03016	0.01986
BK50-C3-S2	Vein quartz	3090.9	-0.001177	-0.003600	0.09608	-0.002176	0.0008182
BK50-C3-S3	Vein quartz	3090.9	0.001575	0.006883	0.3373	-0.0008947	-0.0008741
BK50-C3-S4	Vein quartz	3090.9	0.001113	0.001853	0.1075	-0.004840	0.0004647
BK59-C1-S1	Vein quartz	2339.0	0.002685	0.01395	0.01203	-0.01248	-0.001930
BK59-C1-S2	Vein quartz	2339.0	-0.0009846	0.008197	0.02807	0.002863	-0.00005261
BK59-C1-S3	Vein quartz	2339.0	0.001120	0.01043	0.06918	0.0005135	0.004171
BK59-C1-S4	Vein quartz	2339.0	0.002513	-0.003070	0.03778	-0.006393	-0.0008823
BK59-C2-S1	Vein quartz	2339.0	-0.0009958	0.008081	0.02871	-0.0002202	0.002224
BK59-C2-S2	Vein quartz	2339.0	-0.0009752	0.01032	0.01895	0.001194	0.001731
BK59-C2-S4	Vein quartz	2339.0	-0.0001455	-0.007320	0.1213	0.003482	-0.0006831
BK61-C1-S1	Vein quartz	2030.1	0.0003487	-0.002068	0.1422	0.002771	0.001771
BK61-C1-S1	Vein quartz	2030.1	-0.0003816	-0.002404	0.05282	0.004650	0.002828
BK61-C1-S2	Vein quartz	2030.1	0.003308	0.002748	0.04995	-0.003909	0.0004435
BK61-C1-S3	Vein quartz	2030.1	-0.001962	0.01009	0.3270	0.001763	0.003931
BK61-C2-S1	Vein quartz	2030.1	-0.0007358	-0.0003680	0.05791	-0.001191	-0.00004450
BK61-C2-S2	Vein quartz	2030.1	0.001461	0.007250	0.07042	0.001438	0.0006931
BK61-C2-S3	Vein quartz	2030.1	-0.0005315	0.007832	0.01719	-0.0005784	0.0006576
BK61-C2-S4	Vein quartz	2030.1	0.0001704	-0.007710	0.03270	0.0007361	0.0006146
BK63-C1-S1	Vein quartz	1817.2	0.00007094	0.005522	0.02027	0.0002374	0.0008390
BK63-C1-S1	Vein quartz	1818.6	-0.0005096	-0.0003457	0.007353	-0.002773	0.004584
BK63-C1-S2	Vein quartz	1817.2	0.002254	0.001346	0.003658	-0.001041	0.001647
BK63-C1-S2	Vein quartz	1818.6	0.003998	-0.0003606	0.02807	0.0006085	0.001718
BK63-C1-S3	Vein quartz	1817.2	-0.0006071	0.004678	0.004495	-0.002681	-0.0002088
BK63-C1-S3	Vein quartz	1818.6	-0.001528	-0.0002523	0.002908	-0.002685	-0.0004084

* distance from center of deposit

** All elements in ppm except Au which is in ppb

Appendix 7: Buckingham
quartz mineral chemistry by LA-ICP-MS

Sample	Sample type	Distance*					
		(m)	Ta181	Au197**	Pb208	Bi209	U238
BK63-C1-S4	Vein quartz	1817.2	0.002421	0.003971	0.01488	0.002556	0.00006297
BK63-C1-S4	Vein quartz	1818.6	-0.0004960	-0.0006752	0.3168	0.005831	0.004721
BK63-C2-S1	Vein quartz	1817.2	-0.0003837	0.002799	0.003789	0.001005	-0.001189
BK63-C2-S1	Vein quartz	1818.6	-0.0003027	0.006067	0.1858	0.008915	-0.001259
BK63-C2-S2	Vein quartz	1818.6	-0.0005709	0.001666	0.05837	0.03436	0.05777
BK63-C2-S3	Vein quartz	1817.2	-0.0003324	0.01084	0.06261	0.003245	0.0008894
BK63-C2-S3	Vein quartz	1818.6	-0.001461	0.008169	0.06288	0.002377	0.000
BK63-C2-S4	Vein quartz	1818.6	0.001351	0.002955	0.1501	0.01338	0.1490
BK63-C3-S1	Vein quartz	1817.2	0.002242	-0.0008717	0.006218	0.001902	0.001435
BK63-C3-S1	Vein quartz	1818.6	0.002242	-0.0008717	0.006218	0.001902	0.001435
BK63-C3-S2	Vein quartz	1817.2	0.0002667	-0.001265	0.04378	0.003059	0.004377
BK63-C3-S2	Vein quartz	1818.6	0.001367	0.0004607	0.6435	0.02457	0.1707
BK63-C3-S3	Vein quartz	1817.2	-0.0008272	0.0008296	-0.001186	0.0001631	-0.001412
BK63-C3-S3	Vein quartz	1818.6	-0.0002194	0.001919	0.1288	0.0002681	0.001452
BK63-C3-S4	Vein quartz	1817.2	0.003335	0.01184	0.01139	0.0007136	0.0008735
BK63-C3-S4	Vein quartz	1818.6	0.003507	0.01325	0.01081	-0.0008325	-0.001577
BK63-C4-S1	Vein quartz	1818.6	0.00007877	0.001841	0.05288	-0.001349	0.01338
BK63-C4-S2	Vein quartz	1818.6	0.0007257	0.006945	1.055	0.05328	0.001747
BK63-C5-S1	Vein quartz	1818.6	0.001120	0.007273	0.05969	0.006295	0.006220
BK63-C5-S2	Vein quartz	1818.6	0.0004117	-0.002396	0.06207	0.003433	0.002736
BK63-C5-S3	Vein quartz	1818.6	-0.001207	-0.003735	0.1426	0.001817	0.002595
BK025-C1-S1	Breccia Ceme	0.0	-0.00007891	-0.003097	0.02105	0.002256	0.001577
BK025-C1-S4	Breccia Ceme	0.0	-0.001132	0.0005281	0.007421	-0.003847	0.0005460
BK025-C2-S1	Breccia Ceme	0.0	0.001205	-0.001041	0.01449	-0.001431	-0.001425
BK025-C2-S3	Breccia Ceme	0.0	-0.0001861	-0.0004872	-0.0007940	0.0008328	0.001290
BK025-C2-S4	Breccia Ceme	0.0	-0.001332	-0.004175	0.007199	0.001511	-0.001448
BK025-C3-S1	Breccia Ceme	0.0	-0.001803	0.003896	0.002260	-0.0001107	-0.0001239
BK025-C3-S2	Breccia Ceme	0.0	-0.0005030	0.007491	0.01820	0.002238	-0.001462
BK025-C3-S3	Breccia Ceme	0.0	-0.001364	-0.006069	0.006285	-0.0008053	-0.001995
BK025-C3-S4	Breccia Ceme	0.0	-0.002086	-0.0007625	0.06947	0.004674	0.002194
BK025-C4-S2	Breccia Ceme	0.0	-0.0002996	0.002066	0.01440	0.0003460	0.001871
BK025-C4-S2	Breccia Ceme	0.0	0.0003225	-0.007079	0.005210	0.001132	-0.002781
BK025-C4-S2	Breccia Ceme	0.0	-0.0003271	0.001361	-0.002082	0.001520	0.00008930
BK104-C1-S1	Breccia Ceme	361.5	-0.0001058	0.001072	0.3134	0.01769	0.02727
BK104-C1-S2	Breccia Ceme	361.5	0.01066	-0.001533	0.2398	0.01030	0.05999
BK104-C1-S3	Breccia Ceme	361.5	-0.002035	0.003047	0.3062	0.008282	-0.001345
BK104-C1-S4	Breccia Ceme	361.5	-0.001151	0.0002836	0.6600	0.02607	0.02340
BK104-C1-S5	Breccia Ceme	361.5	-0.001428	0.006020	1.032	0.005163	0.004442
BK104-C2-S1	Breccia Ceme	361.5	0.004043	0.003376	1.211	0.009823	0.1411
BK104-C2-S2	Breccia Ceme	361.5	0.0003865	-0.004371	0.1583	0.003286	0.2681
BK104-C2-S3	Breccia Ceme	361.5	0.0005919	-0.009864	0.2530	-0.0001845	0.006829
BK104-C2-S4	Breccia Ceme	361.5	-0.0001033	-0.0004591	0.4846	0.006437	0.02785
BK104-C2-S5	Breccia Ceme	361.5	0.02502	0.004617	3.750	0.004836	0.1002

* distance from center of deposit

** All elements in ppm except Au which is in ppb

Appendix 7: Buckingham
quartz mineral chemistry by LA-ICP-MS

Sample	Sample type	Distance*					
		(m)	Ta181	Au197**	Pb208	Bi209	U238
BK104-C3-S1	Breccia Cemei	361.5	0.0003320	-0.009234	0.4625	0.004139	0.005855
BK104-C3-S2	Breccia Cemei	361.5	-0.0005641	0.006844	1.039	0.01485	0.008812
BK104-C3-S5	Breccia Cemei	361.5	0.0003130	-0.0003804	0.4992	0.009075	0.003778
BK50-C2-S1	Igneous	3090.9	0.002358	-0.01344	0.02356	0.0009848	0.09944
BK50-C2-S2	Igneous	3090.9	-0.0003451	0.003387	0.9542	0.002139	0.008261
BK50-C2-S3	Igneous	3090.9	0.001022	-0.0009981	0.05855	0.002428	-0.002214
BK50-C2-S4	Igneous	3090.9	-0.001031	0.004580	0.01286	0.007961	-0.002072
BK50-C2-S5	Igneous	3090.9	-0.0005908	0.006467	0.02031	0.0004437	0.001779
BK100-C3-S1	Igneous	1443.7	0.0003600	-0.003234	0.03641	-0.00002344	-0.0007911
BK100-C3-S2	Igneous	1443.7	-0.00009159	0.004690	0.001199	-0.001587	0.002836
BK100-C3-S4	Igneous	1443.7	-0.0008571	0.001592	0.02021	0.001423	0.003284
BK101-C1-S1	Igneous	1061.5	-0.001174	-0.0005772	0.006726	0.0004077	0.0006631
BK101-C1-S2	Igneous	1061.5	0.001455	0.006330	0.008253	0.002164	-0.0001602
BK101-C1-S3	Igneous	1061.5	0.00004936	-0.008033	0.007970	0.0001220	0.00007984
BK101-C1-S4	Igneous	1061.5	0.001113	-0.001565	0.003061	-0.0009013	0.001007
BK101-C1-S5	Igneous	1061.5	-0.0008560	-0.003733	0.006899	-0.002026	0.001881
BK44-C2-S1	Sedimentary	1600.4	0.0008859	-0.005283	0.02573	-0.003098	0.0004746
BK44-C2-S2	Sedimentary	1600.4	-0.00002532	-0.004761	-0.004629	-0.0008313	-0.001628
BK44-C2-S4	Sedimentary	1600.4	0.0002490	-0.001264	0.004885	0.0006858	0.0003882
BK44-C4-S1	Sedimentary	1600.4	-0.001085	0.006943	0.02870	0.004252	0.001260
BK44-C4-S2	Sedimentary	1600.4	0.0009352	-0.003088	0.003829	-0.007552	0.002448
BK44-C4-S3	Sedimentary	1600.4	-0.0004312	-0.001902	0.02873	0.004667	0.001968
BK44-C4-S4	Sedimentary	1600.4	0.003340	0.007921	0.03838	-0.001812	0.01301
BK17-C2-S1	Sedimentary	770.8	-0.0001637	-0.008181	0.1047	0.006068	0.001478
BK17-C2-S2	Sedimentary	770.8	-0.0005472	-0.006888	0.1291	0.002048	0.0005069
BK17-C2-S3	Sedimentary	770.8	0.0006306	0.0007768	0.1239	-0.003175	0.00002666
BK17-C4-S2	Sedimentary	770.8	-0.0004508	-0.002872	0.03368	0.0005464	0.0007214
BK17-C4-S3	Sedimentary	770.8	0.01172	-0.01137	0.01953	0.003149	0.002929
BK12-C1-S1	Sedimentary	1475.3	-0.001400	-0.0004376	0.009861	-0.002349	0.002571
BK12-C1-S2	Sedimentary	1475.3	0.001157	-0.005040	0.02837	0.01153	0.003271
BK12-C1-S3	Sedimentary	1475.3	0.001815	0.001446	0.03790	0.0006461	0.01642
BK12-C3-S1	Sedimentary	1475.3	-0.0001650	-0.0004739	0.1304	0.007608	0.0003351
BK12-C3-S2	Sedimentary	1475.3	-0.0005713	0.008622	0.02207	0.001294	0.001014
BK12-C3-S3	Sedimentary	1475.3	-0.0009200	0.001113	-0.001442	-0.0003311	0.002662
BK13-C1-S1	Sedimentary	1381.0	0.00006806	-0.001345	0.007430	-0.002524	0.001179
BK13-C1-S2	Sedimentary	1381.0	0.001273	-0.0008149	0.01448	0.0001414	0.005169
BK13-C1-S3	Sedimentary	1381.0	0.002501	-0.002398	0.01265	-0.001240	-0.0003176
BK13-C6-S1	Sedimentary	1381.0	-0.002003	0.007439	0.003583	-0.002212	-0.0001248
BK13-C6-S1	Sedimentary	1381.0	-0.0009069	-0.004015	-0.002127	0.006545	-0.0009549
BK13-C6-S1	Sedimentary	1381.0	0.0004100	-0.007034	0.005739	-0.002488	0.001716
BK61-C3-S1	Sedimentary	2030.1	0.000	-0.002159	0.06031	0.0007095	0.001442
BK61-C3-S2	Sedimentary	2030.1	-0.0004547	0.005936	0.01142	-0.004213	0.001904
BK15-C1-S2	Sedimentary	981.5	-0.001949	0.003576	0.009210	0.001908	-0.0008814

* distance from center of deposit

** All elements in ppm except Au which is in ppb

Appendix 7: Buckingham
quartz mineral chemistry by LA-ICP-MS

Sample	Sample type	Distance*					
		(m)	Ta181	Au197**	Pb208	Bi209	U238
BK15-C1-S3	Sedimentary	981.5	0.004379	0.001988	0.1026	0.006448	0.001131
BK15-C1-S4	Sedimentary	981.5	0.001079	0.003299	0.1807	-0.001885	-0.0007062
BK15-C5-S1	Sedimentary	981.5	0.0009457	0.002767	-0.007300	-0.001389	-0.001161
BK15-C5-S2	Sedimentary	981.5	-0.00005904	-0.004984	-0.01224	-0.002230	0.0004211
BK15-C5-S3	Sedimentary	981.5	-0.001430	0.006692	0.08066	0.0006142	0.0008435
BK15-C5-S4	Sedimentary	981.5	-0.001865	-0.0001800	0.2612	0.003886	-0.0007159
BK03-C3-S1	Sedimentary	337.4	-0.001720	-0.0002130	0.007405	0.001349	0.0006515
BK03-C3-S2	Sedimentary	337.4	-0.001297	0.01253	0.002684	-0.003904	0.002639
BK59-C3-S1	Sedimentary	2339.0	0.00005789	0.0002564	0.2640	-0.002689	0.01303
BK59-C3-S2	Sedimentary	2339.0	-0.0001977	-0.003503	0.7425	0.04460	0.001300
BK59-C3-S3	Sedimentary	2339.0	0.001856	0.007726	0.3496	-0.0004370	0.002033
BK59-C3-S4	Sedimentary	2339.0	0.001011	0.004477	0.01960	-0.001577	-0.001433
BK59-C4-S1	Sedimentary	2339.0	0.001411	-0.01833	0.003137	0.004675	0.006133
BK59-C4-S2	Sedimentary	2339.0	-0.0009391	-0.0006768	0.2562	0.0008566	0.0005743
BK59-C4-S3	Sedimentary	2339.0	-0.0004496	0.009951	0.02997	-0.004114	0.004434
BK102-C3-S1	Sedimentary	890.8	0.00009896	0.001866	0.09205	-0.0004904	0.001063
BK102-C3-S2	Sedimentary	890.8	0.001169	0.007175	0.1068	0.0003387	0.001388
BK102-C3-S3	Sedimentary	890.8	0.00005693	0.0006288	0.4556	0.003695	0.009342
BK102-C3-S4	Sedimentary	890.8	0.0007965	0.002389	0.07117	-0.001432	0.001307
BK106-C1-S1	Sedimentary	466.2	-0.001129	-0.01829	0.02530	0.004230	0.004360
BK106-C1-S2	Sedimentary	466.2	0.0004549	-0.01095	0.02967	0.005694	0.005097
BK106-C1-S3	Sedimentary	466.2	-0.002537	-0.006101	0.03141	-0.003565	0.002906
BK106-C4-S2	Sedimentary	466.2	-0.0008188	-0.001669	0.007597	0.007182	-0.001368
BK106-C4-S3	Sedimentary	466.2	0.001408	0.001403	0.02479	0.01484	0.005874
BK106-C4-S4	Sedimentary	466.2	-0.0009863	0.001327	0.03073	0.004922	0.001705
BK106-C4-S5	Sedimentary	466.2	0.01006	0.008804	0.05275	-0.001397	0.0009725
BK106-C5-S1	Sedimentary	466.2	-0.002413	-0.007151	0.1130	-0.003460	-0.0006301
BK106-C5-S2	Sedimentary	466.2	0.0009737	0.006391	0.03032	0.003183	-0.0003382
BK106-C5-S3	Sedimentary	466.2	-0.001985	0.01948	0.04917	-0.0001798	0.00001849
BK18-C1-S1	Sedimentary	608.8	0.006391	-0.0009095	0.06137	-0.008553	0.01205
BK18-C1-S2	Sedimentary	608.8	0.003823	0.002687	0.1874	0.009238	0.01439
BK18-C1-S3	Sedimentary	608.8	-0.001617	0.001065	0.07417	0.004533	0.0008220
BK18-C3-S1	Sedimentary	608.8	0.0007320	-0.01681	0.02274	-0.0007786	0.001514
BK18-C3-S2	Sedimentary	608.8	0.000	0.003042	0.01035	0.003725	-0.0009784
BK18-C3-S3	Sedimentary	608.8	0.0008730	-0.009173	0.02620	0.003482	0.001501
BK20-C1-S2	Sedimentary	640.5	0.0002884	-0.003948	0.06114	0.003617	0.0009780
BK20-C1-S3	Sedimentary	640.5	-0.001855	-0.002150	0.07210	0.001596	0.0004301
BK20-C1-S4	Sedimentary	640.5	0.002594	0.01462	0.01057	-0.001283	-0.0001041
BK20-C2-S1	Sedimentary	640.5	0.002473	0.005345	0.04630	-0.002923	0.005151
BK20-C2-S2	Sedimentary	640.5	0.00006040	-0.0008591	0.05106	0.005040	0.004817
BK20-C2-S3	Sedimentary	640.5	0.0001894	0.0008082	0.06220	0.007136	0.001758
BK20-C2-S4	Sedimentary	640.5	0.0008429	-0.01143	0.1038	0.002842	0.009414
BK021-C1-S1	Sedimentary	517.7	-0.0007235	-0.002163	2.202	0.001251	-0.0008023

* distance from center of deposit

** All elements in ppm except Au which is in ppb

Appendix 7: Buckingham
quartz mineral chemistry by LA-ICP-MS

Sample	Sample type	Distance* (m)	Ta181	Au197**	Pb208	Bi209	U238
BK021-C1-S2	Sedimentary	517.7	0.04186	-0.006407	4.305	0.4206	0.3793
BK021-C2-S1	Sedimentary	517.7	-0.001322	-0.001238	0.1397	0.002557	0.01388
BK021-C2-S2	Sedimentary	517.7	-0.001188	0.007037	0.2600	0.004185	0.003018
BK021-C2-S3	Sedimentary	517.7	0.0003258	0.006786	0.2157	0.003576	0.0007934
BK021-C2-S4	Sedimentary	517.7	-0.002037	0.008444	0.3897	-0.0005014	0.003456
BK63-C4-S1	Sedimentary	1817.2	0.0002291	0.002453	0.03238	-0.001191	-0.00009476
BK63-C4-S2	Sedimentary	1817.2	0.001141	0.001327	0.06346	0.006073	0.001259
BK63-C5-S1	Sedimentary	1817.2	-0.0001529	0.005624	0.006244	-0.00005346	0.001591
BK63-C5-S2	Sedimentary	1817.2	0.001045	-0.001408	0.05619	0.003575	0.001830
BK63-C5-S3	Sedimentary	1817.2	-0.0009031	0.00001731	0.1853	0.002435	0.002840

* distance from center of deposit

** All elements in ppm except Au which is in ppb

Appendix 8: White Pine
pyrite mineral chemistry by LA-ICP-MS

Sample	Distance* (m)	Mg24	Al27	S34	K39	Ca43	Ti49	Cr53	Mn55	Fe57	Co59	Ni60	Cu65	Zn66	As75	Se77
ESWP001-C1-S1	161.31	-0.1065	-0.3812	5.177E+05	0.2002	-38.01	0.2551	-0.1611	-0.04506	4.650E+05	103.6	33.99	0.1547	0.02632	0.08523	6.077
ESWP001-C1-S2	161.31	61.00	49.78	4.311E+05	13.58	76.04	0.4770	0.1107	27.28	4.650E+05	115.1	71.59	97.81	290.1	0.7864	8.179
ESWP001-C1-S3	161.31	0.7009	0.4089	5.263E+05	-0.9047	2.418	0.3918	-0.1493	-0.02857	4.650E+05	57.00	21.18	0.8629	0.1689	0.1214	7.793
ESWP001-C1-S4	161.31	-0.08039	-0.5594	5.075E+05	-1.787	-41.21	0.7905	-0.2359	0.01382	4.650E+05	55.19	29.13	1.661	0.07142	0.07919	9.517
ESWP001-C1-S5	161.31	-0.3792	-0.2813	5.141E+05	-1.428	35.59	0.4819	-0.5812	0.06210	4.650E+05	326.5	14.98	0.1579	0.1655	0.4307	6.016
ESWP001-C1-S6	161.31	0.5838	4.610	5.752E+05	-0.4790	610.7	7905	4.768	0.8840	4.650E+05	79.11	24.14	10.76	0.4971	1.210	9.503
ESWP001-C1-S7	161.31	320.7	2701	4.954E+05	1721	4.568	33.13	0.1254	28.33	4.650E+05	73.58	139.4	110.1	98.05	1.099	11.65
ESWP001-C2-S10	161.31	-0.01870	0.6424	4.939E+05	-0.7836	3.152	0.4118	-0.2975	-0.06917	4.650E+05	102.3	30.23	0.1158	0.1874	-0.5781	7.569
ESWP001-C2-S11	161.31	-0.1100	0.1517	4.925E+05	-0.01944	-55.39	0.2042	0.3972	0.06260	4.650E+05	98.89	14.56	0.2255	0.4144	0.05421	6.273
ESWP001-C2-S12	161.31	-0.03195	42.72	5.155E+05	5.947	48.99	0.6141	-0.02375	0.1168	4.650E+05	59.40	17.63	1.195	1.158	-0.1828	8.983
ESWP001-C2-S13	161.31	0.8707	8.230	5.074E+05	0.8125	7.432	0.5455	-0.3898	0.1517	4.650E+05	91.24	23.80	1.444	0.5636	-0.2179	8.476
ESWP001-C2-S14	161.31	-0.3802	0.7049	5.165E+05	0.1036	-69.72	0.4216	0.1743	0.006155	4.650E+05	9.975	149.6	0.6571	0.2377	1.134	8.541
ESWP001-C2-S8	161.31	-0.8204	0.8675	5.275E+05	0.2667	-24.20	0.3534	-0.03945	0.005503	4.650E+05	68.85	9.565	0.2214	0.08617	0.5832	9.829
ESWP001-C2-S9	161.31	-0.1491	0.3817	4.901E+05	-2.207	-15.42	0.5459	-0.03408	-0.07905	4.650E+05	79.70	24.45	0.3487	0.1196	0.3354	7.690
ESWP001-C2-S1	132.23	0.02109	-0.1053	5.567E+05	-0.3277	8.749	0.8766	-0.01598	0.05479	4.650E+05	25.75	7.747	1.396	0.2534	0.2927	16.94
ESWP002-C1-S10	132.23	0.1224	-0.06902	4.886E+05	-0.4142	1.694	0.6132	-0.1244	-0.07352	4.650E+05	8.521	2.196	3.266	0.2086	0.6904	27.12
ESWP002-C1-S11	132.23	0.06869	0.2541	4.653E+05	-0.3029	-28.17	0.3557	0.3372	-0.02404	4.650E+05	4.501	2.505	0.5170	0.2972	0.2048	6.019
ESWP002-C1-S12	132.23	0.06842	0.02178	4.956E+05	-0.2297	9.096	0.5781	-0.3450	-0.09753	4.650E+05	1.907	0.8953	0.2256	0.2739	0.4297	6.181
ESWP002-C1-S13	132.23	0.03008	0.05785	4.897E+05	-1.901	24.34	0.7015	-0.09282	-0.05946	4.650E+05	50.57	20.14	0.9260	0.2601	-0.2690	12.27
ESWP002-C1-S14	132.23	0.2932	-0.01800	4.826E+05	-0.5390	-43.75	0.4474	-0.1005	-0.01892	4.650E+05	15.21	3.979	0.2672	0.2627	0.2329	7.678
ESWP002-C1-S15	132.23	0.08564	-0.06956	4.826E+05	-2.206	9.899	0.5563	-0.04709	0.03350	4.650E+05	39.25	17.55	1.236	0.2545	0.2432	12.64
ESWP002-C1-S3	132.23	-0.03500	-0.1422	5.630E+05	-1.352	25.39	0.8377	0.2987	0.0005810	4.650E+05	0.4476	1.107	2.079	0.1314	-0.2812	24.19
ESWP002-C1-S4	132.23	0.2880	0.07560	5.246E+05	-0.03653	-31.31	0.5784	0.1794	-0.02086	4.650E+05	9.217	9.316	0.3644	0.03994	0.1868	6.901
ESWP002-C1-S5	132.23	-0.04783	0.2084	5.236E+05	-0.3630	13.66	0.8112	0.08853	-0.02522	4.650E+05	9.020	5.480	0.2074	0.3163	0.6055	5.426
ESWP002-C1-S6	132.23	-0.07307	0.2336	5.111E+05	-0.5477	16.56	0.7937	0.05339	-0.05641	4.650E+05	17.63	12.61	0.3500	0.1941	0.7392	6.284
ESWP002-C1-S7	132.23	0.03730	0.2846	4.910E+05	0.2258	26.77	0.5957	0.3759	0.05547	4.650E+05	17.75	17.14	0.2973	0.2578	-0.1203	8.010
ESWP002-C1-S8	132.23	0.1580	0.07611	4.964E+05	-1.021	-11.48	0.9541	0.09044	0.05903	4.650E+05	17.09	3.854	0.3097	0.1029	-0.5845	8.178
ESWP002-C1-S9	132.23	-0.06829	0.02814	4.935E+05	-0.9317	10.06	0.7971	0.1041	0.03824	4.650E+05	10.09	3.017	0.2672	0.2742	0.2364	7.402
ESWP006-C1-S1	1429.02	0.1375	224.1	5.210E+05	4.026	39.72	0.1205	-0.1721	0.09880	4.650E+05	6.963	6.779	0.9209	0.2913	0.6381	15.54
ESWP006-C1-S2	1429.02	0.01721	0.3685	5.047E+05	-1.490	-49.20	0.6590	0.1609	0.01803	4.650E+05	20.67	6.822	0.3094	0.2721	0.8688	9.484
ESWP006-C1-S3	1429.02	-0.04609	0.1736	4.782E+05	-0.8081	-10.29	-0.06627	0.1869	0.008921	4.650E+05	58.07	13.38	0.5102	0.09710	0.4794	9.342
ESWP006-C1-S4	1429.02	-0.1840	0.5572	5.100E+05	-1.278	12.73	0.4754	0.04707	0.05997	4.650E+05	193.4	9.550	0.5938	0.1153	0.1252	23.81
ESWP006-C1-S5	1429.02	-0.6419	0.1220	4.777E+05	-3.149	24.03	0.6415	-0.1186	-0.04201	4.650E+05	36.10	21.06	0.4708	0.2057	0.1563	21.25
ESWP006-C1-S6	1429.02	1.076	-0.2998	5.390E+05	-4.283	-62.97	0.6249	0.1392	0.1657	4.650E+05	68.45	84.71	2.642	0.9599	1.333	27.66
ESWP006-C2-S10	1429.02	0.7872	0.08835	5.043E+05	-0.2496	51.94	0.4771	-0.2812	0.006111	4.650E+05	50.34	20.31	0.6694	0.1012	0.7361	24.62
ESWP006-C2-S11	1429.02	-0.09534	-0.5083	5.130E+05	-1.351	6.788	0.3676	0.04275	-0.05573	4.650E+05	29.23	17.86	1.276	1.198	0.8135	24.71
ESWP006-C2-S12	1429.02	-0.2261	-0.3603	4.955E+05	0.3401	27.94	0.5061	0.4810	0.04634	4.650E+05	133.8	19.31	26.26	6.701	0.9115	25.08
ESWP006-C2-S13	1429.02	-0.2753	-0.1559	4.802E+05	-0.1150	15.11	0.5466	0.01524	-0.01436	4.650E+05	296.8	7.009	0.3550	0.2173	0.4397	24.77
ESWP006-C2-S14	1429.02	0.3324	-0.8123	4.772E+05	-1.003	-19.58	0.6074	0.1183	-0.09043	4.650E+05	31.92	11.01	1.164	0.3260	0.5268	9.467
ESWP006-C2-S15	1429.02	-0.1318	-0.3006	4.832E+05	0.4651	8.129	0.3113	-0.1940	-0.002145	4.650E+05	64.70	27.99	0.2016	0.04073	0.4966	10.13
ESWP006-C2-S7	1429.02	0.1870	-0.3010	4.891E+05	-0.8992	-25.77	0.2908	0.4351	0.07190	4.650E+05	50.25	12.97	0.2834	0.1827	0.2591	6.548
ESWP006-C2-S8	1429.02	-0.03699	-0.6714	5.004E+05	1.706	38.02	0.5829	-0.1204	0.05109	4.650E+05	144.8	18.37	0.3978	0.2457	0.1135	9.270
ESWP006-C2-S9	1429.02	-0.008487	-0.6296	4.813E+05	1.025	-2.970	0.6170	-0.08903	-0.08030	4.650E+05	362.2	44.06	0.5979	0.3510	0.9276	30.69

* distance from center of deposit

** All elements in ppm except Au which is in ppb

Appendix 8: White Pine
pyrite mineral chemistry by LA-ICP-MS

Sample	Distance* (m)	Mg24	Al27	S34	K39	Ca43	Ti49	Cr53	Mn55	Fe57	Co59	Ni60	Cu65	Zn66	As75	Se77
ESWP007-C1-S2	1360.22	-0.1431	4.570	5.614E+05	-1.324	-1.254	0.9244	-0.09354	-0.1190	4.650E+05	56.84	19.94	0.2318	0.1379	-0.9674	4.568
ESWP007-C1-S3	1360.22	-0.008828	0.1991	5.096E+05	-0.3126	-2.219	0.3639	0.3632	-0.004539	4.650E+05	113.2	149.9	0.2442	0.1064	0.2078	3.871
ESWP007-C1-S4	1360.22	0.1526	-0.1772	5.017E+05	-0.7029	-9.389	0.5033	0.01657	-0.006648	4.650E+05	66.46	41.49	0.1073	0.3316	0.5817	8.590
ESWP007-C1-S5	1360.22	0.08042	-0.05065	4.907E+05	-2.307	13.29	0.5665	-0.1342	0.07576	4.650E+05	59.59	31.62	0.1220	0.1483	0.6696	8.363
ESWP007-C2-S6	1360.22	0.1894	0.3864	5.132E+05	-0.1573	15.02	0.3938	-0.1059	-0.007807	4.650E+05	328.6	79.58	0.2273	0.1478	0.4544	4.282
ESWP007-C2-S8	1360.22	-0.03779	0.1913	5.658E+05	-0.5202	-11.99	1.589	-0.03281	5.738	4.650E+05	162.1	61.28	0.1813	0.1306	0.7136	5.652
ESWP007-C2-S9	1360.22	0.2332	2.389	4.971E+05	-0.9850	-0.7745	2.071	-0.3444	2.889	4.650E+05	33.66	46.69	0.3044	0.2831	0.7176	8.055
ESWP007-C3-S11	1360.22	0.003311	-0.2700	5.146E+05	0.3525	-2.496	0.4528	0.1004	-0.02749	4.650E+05	2.595	7.845	0.07132	0.3154	0.05428	4.665
ESWP007-C3-S12	1360.22	-0.02785	-0.1781	4.931E+05	-1.496	-24.31	0.4564	0.1693	-0.02521	4.650E+05	32.56	31.11	0.09704	0.1471	-0.1216	4.351
ESWP018-C1-S3	513.17	-0.09580	0.5406	4.874E+05	-0.3488	-2.403	0.5978	0.1567	0.04299	4.650E+05	161.3	32.00	0.09613	0.09306	0.5718	5.513
ESWP018-C1-S4	513.17	3.177	1.169	5.033E+05	-1.613	17.89	1.234	-0.1389	0.1339	4.650E+05	35.31	36.80	0.1226	0.1138	0.4306	5.821
ESWP018-C1-S5	513.17	0.1065	0.2771	4.677E+05	-1.052	-4.803	0.5340	-0.4522	0.03305	4.650E+05	47.69	30.05	0.1443	0.2465	0.5287	3.248
ESWP018-C1-S6	513.17	0.3032	0.3704	4.564E+05	-0.3037	-31.01	0.3368	-0.2566	-0.03726	4.650E+05	87.54	28.13	0.05461	0.2771	0.8964	4.104
ESWP018-C1-S7	513.17	10.70	11.52	4.642E+05	17.62	30.85	2.685	-0.00002355	1.431	4.650E+05	79.62	29.73	0.06821	0.9910	1.205	3.341
ESWP018-C1-S8	513.17	0.3174	0.06760	4.734E+05	1.963	-7.736	0.9832	0.1043	0.01637	4.650E+05	113.4	21.98	-0.01088	0.05794	0.7922	3.887
ESWP018-C2-S11	513.17	0.9922	-0.5006	4.536E+05	-2.523	55.04	0.9281	0.2917	0.08466	4.650E+05	20.60	34.62	0.4804	5.393	0.4574	4.371
ESWP018-C2-S12	513.17	0.07371	0.7369	5.116E+05	-2.235	-33.74	0.8295	0.3894	-0.1448	4.650E+05	6.612	25.07	0.06257	0.2994	0.6595	5.968
ESWP018-C2-S13	513.17	0.7803	0.3007	4.645E+05	-0.5304	16.44	0.6055	0.1358	0.03244	4.650E+05	403.8	94.58	0.2622	1.508	1.162	4.660
ESWP018-C2-S14	513.17	1.135	0.4921	4.779E+05	-0.03024	14.57	0.8885	0.2871	0.1330	4.650E+05	50.14	89.67	0.1540	1.223	0.5845	3.754
ESWP058-C1-S1	1709.21	0.2390	-0.02536	5.145E+05	-0.3265	-49.51	0.2624	0.1747	0.04103	4.650E+05	322.7	95.33	0.4065	0.2483	0.1055	8.511
ESWP058-C1-S2	1709.21	0.3353	0.2976	5.242E+05	0.8609	-15.37	0.4836	0.04164	0.05799	4.650E+05	139.5	84.95	32.96	0.2276	-0.2925	4.785
ESWP058-C1-S3	1709.21	-0.3974	1.393	5.259E+05	0.5471	-3.444	0.9086	0.09414	0.02017	4.650E+05	68.09	40.08	16.17	0.2069	0.4896	4.551
ESWP058-C1-S4	1709.21	-0.03195	4.071	5.087E+05	-0.9363	32.87	0.4968	-0.003398	0.04677	4.650E+05	149.8	43.68	1.099	0.04452	-0.2063	10.37
ESWP058-C1-S5	1709.21	25.30	1138	5.429E+05	483.9	74.64	5.046	0.1581	-0.01500	4.650E+05	19.61	12.87	6.265	0.2654	-0.4735	6.331
ESWP058-C1-S6	1709.21	0.4358	-0.05783	5.049E+05	-0.8920	42.00	0.4503	0.1228	-0.04501	4.650E+05	46.00	36.58	14.31	0.1886	0.4741	7.473
ESWP058-C2-S10	1709.21	0.5819	-0.6706	5.084E+05	-1.361	35.32	0.5475	0.1825	-0.08890	4.650E+05	145.8	77.28	0.07487	0.1645	0.5513	9.342
ESWP058-C2-S7	1709.21	0.1288	-0.4733	5.121E+05	0.4369	-34.78	0.2094	0.1013	-0.06456	4.650E+05	60.94	25.28	7.946	0.2753	0.4813	7.088
ESWP058-C2-S8	1709.21	5.686	35.07	4.804E+05	16.11	23.87	81.67	0.3767	0.03496	4.650E+05	114.9	38.83	0.6277	0.3267	0.3313	9.456
ESWP058-C2-S9	1709.21	0.005105	0.1775	4.563E+05	-2.346	-1.580	0.4940	-0.3485	-0.1072	4.650E+05	90.11	25.75	1.045	0.06793	0.5424	9.460
ESWP058-C3-S11	1709.21	0.4662	6.651	5.036E+05	1.366	-9.190	5.013	0.6073	-0.04335	4.650E+05	239.1	75.34	0.6861	0.2368	0.6443	7.701
ESWP058-C3-S12	1709.21	7.289	369.8	5.780E+05	40.68	-24.10	23.76	0.8147	0.4458	4.650E+05	162.3	92.81	26.70	2.335	1.046	7.229
ESWP058-C3-S13	1709.21	-0.05502	1.935	5.194E+05	-2.032	-20.80	2.835	0.02112	-0.006003	4.650E+05	58.30	24.31	4.740	0.1042	-0.1876	12.35
ESWP058-C3-S14	1709.21	100.9	1626	5.777E+05	509.1	160.4	187.1	11.46	11.32	4.650E+05	106.2	42.91	86.44	13.91	1.784	12.07
ESWP065-C1-S1	609.43	-0.1390	-0.2855	5.417E+05	-0.2946	-1.776	0.4954	-0.1142	0.006808	4.650E+05	0.3049	229.8	0.2943	0.1251	0.6341	49.68
ESWP065-C1-S10	609.43	-0.2229	-0.5763	4.996E+05	-1.134	-36.31	0.5194	-0.2147	-0.02155	4.650E+05	1042	4.470	0.1690	0.2916	0.09894	15.66
ESWP065-C1-S2	609.43	-0.1624	-0.3301	5.248E+05	-0.3662	38.28	0.6395	0.2323	-0.01628	4.650E+05	3.282	239.5	0.6725	0.4165	0.5985	24.56
ESWP065-C1-S3	609.43	0.1025	-0.5747	5.225E+05	-1.809	-8.848	0.4906	0.04430	0.07601	4.650E+05	1.344	10.82	0.2046	0.1314	0.6319	25.28
ESWP065-C1-S5	609.43	0.7447	1.770	5.713E+05	-1.166	19.99	1.712	-0.5416	-0.1444	4.650E+05	0.3640	17.67	4.154	4.023	0.2608	28.95
ESWP065-C1-S6	609.43	0.07462	-0.3400	5.122E+05	-0.5887	29.57	0.2353	0.2393	0.05914	4.650E+05	4.480	5.768	0.1723	0.1746	0.7302	26.85
ESWP065-C1-S7	609.43	-0.08807	-0.01374	4.974E+05	1.063	2.506	0.6504	0.02350	-0.07646	4.650E+05	90.20	3.524	0.1055	0.1142	0.01281	15.81
ESWP065-C1-S8	609.43	-0.02308	0.04085	5.124E+05	1.201	-24.97	0.5177	0.3740	-0.04725	4.650E+05	4610	4.031	0.3420	0.1726	0.8063	17.26
ESWP065-C1-S9	609.43	0.05080	-0.7495	4.969E+05	2.150	-3.436	0.4341	0.02399	-0.08355	4.650E+05	27.88	4.291	-0.002772	0.2181	0.1056	17.43
WPO3-C1-S1	1546.40	0.1838	0.1049	5.369E+05	0.7282	10.67	0.2630	-0.05638	-0.005833	4.650E+05	56.20	13.01	0.4954	0.2510	0.9761	12.67

* distance from center of deposit

** All elements in ppm except Au which is in ppb

Appendix 8: White Pine
pyrite mineral chemistry by LA-ICP-MS

Sample	Distance* (m)	Mg24	Al27	S34	K39	Ca43	Ti49	Cr53	Mn55	Fe57	Co59	Ni60	Cu65	Zn66	As75	Se77
WP03-C1-S2	1546.40	0.7525	0.2951	5.312E+05	-2.282	56.75	0.5575	-0.1220	-0.005896	4.650E+05	26.41	6.224	0.6559	0.2171	0.7565	8.223
WP03-C1-S3	1546.40	0.6901	-0.2570	5.367E+05	-0.005429	3.150	0.3596	0.2655	0.04446	4.650E+05	106.2	20.59	0.2927	0.3258	1.206	12.43
WP03-C1-S4	1546.40	-0.7595	-0.1394	5.001E+05	2.219	-21.66	0.5687	0.02434	0.04376	4.650E+05	60.88	20.08	0.6185	0.1154	0.3223	6.671
WP03-C1-S5	1546.40	0.6505	0.6394	5.059E+05	-0.3871	-21.25	0.5873	0.2292	-0.02102	4.650E+05	17.53	2.540	0.4130	0.1947	2.097	21.04
WP03-C1-S6	1546.40	0.3504	-0.4131	5.109E+05	0.6956	22.16	1.526	0.2012	-0.05708	4.650E+05	33.63	7.449	0.7069	0.2025	1.106	8.004
WP03-C1-S7	1546.40	0.1093	1.699	5.053E+05	20.79	0.3253	0.3697	0.1834	0.02298	4.650E+05	41.88	6.771	0.6487	0.2636	1.777	10.86
WP03-C1-S8	1546.40	-0.2181	3.238	5.356E+05	0.2724	-34.49	0.5952	0.01517	-0.02672	4.650E+05	46.45	11.04	0.6053	0.2823	0.5678	3.793
WP06-C1-S1	1429.02	0.2535	0.06646	5.326E+05	0.8160	15.63	0.2546	-0.2044	0.08485	4.650E+05	17.04	262.8	-0.02634	-0.1045	0.6051	28.75
WP06-C1-S2	1429.02	0.1633	0.05023	5.304E+05	794.6	44.43	0.7579	0.3045	2.689	4.650E+05	13.13	445.9	6558	125.7	0.7895	37.12
WP06-C1-S3	1429.02	-0.2088	-0.04658	5.222E+05	0.7345	17.92	0.5922	0.3237	0.03443	4.650E+05	8.192	397.5	0.02520	0.5595	0.7547	40.87
WP06-C1-S4	1429.02	0.2383	-0.04917	5.153E+05	-1.136	-29.13	0.9719	-0.3509	-0.1886	4.650E+05	39.46	804.7	0.04780	0.1509	0.8304	40.27
WP06-C1-S5	1429.02	-0.2627	-0.3331	5.346E+05	2.914	25.40	0.2550	0.2735	0.03726	4.650E+05	878.6	262.1	0.2292	0.1205	2.362	26.54
WP06-C2-S10	1429.02	0.1922	-0.6660	5.219E+05	-1.554	-6.572	1.186	0.4044	0.1433	4.650E+05	82.97	235.2	-0.003099	0.1685	0.7333	35.51
WP06-C2-S6	1429.02	-0.3256	0.04290	5.302E+05	0.2965	85.19	0.8581	0.2988	0.01116	4.650E+05	579.5	68.57	0.1297	0.2252	0.8895	7.825
WP06-C2-S7	1429.02	0.04108	-0.07404	5.343E+05	0.1796	-37.90	0.1945	0.3742	-0.08057	4.650E+05	216.3	149.8	0.1270	0.2440	0.9872	24.12
WP06-C2-S8	1429.02	0.02320	0.3704	5.249E+05	-3.097	23.28	0.9266	-0.2223	-0.06564	4.650E+05	62.47	103.6	0.1268	0.2257	0.8971	31.07
WP06-C2-S9	1429.02	0.1941	0.3346	5.112E+05	-0.4437	-36.13	0.9971	-0.3550	-0.06415	4.650E+05	62.22	85.32	0.1835	0.1028	0.8064	29.36
WP06-C3-S11	1429.02	0.07738	0.3539	5.373E+05	0.5953	22.62	1.131	0.2357	-0.06463	4.650E+05	70.20	370.5	0.1199	-0.004155	0.1941	41.94
WP06-C3-S12	1429.02	-0.06928	0.2777	5.104E+05	-1.522	-1.885	0.2108	-0.1868	0.01413	4.650E+05	67.47	122.7	-0.1204	0.1758	0.4723	26.34
WP06-C3-S13	1429.02	-0.2737	0.09547	5.426E+05	0.3763	54.65	0.6351	0.7956	0.01905	4.650E+05	36.14	146.4	0.3152	0.1455	0.7838	26.27
WP06-C3-S14	1429.02	-0.4820	-0.2283	5.163E+05	1.525	32.75	0.8252	0.1291	-0.1128	4.650E+05	36.54	132.8	0.1044	0.2168	0.5035	38.13
WP06-C3-S15	1429.02	-0.3098	0.1805	5.258E+05	0.8484	-22.03	0.8218	0.2786	-0.01315	4.650E+05	25.70	256.0	-0.06384	0.2654	0.06878	33.69
WP17-C1-S1	712.89	0.04365	-0.3714	5.088E+05	0.1648	-5.583	1.119	-0.02062	0.09868	4.650E+05	63.11	103.7	0.3148	0.2306	2.150	7.832
WP17-C1-S2	712.89	6.119	-0.07953	5.171E+05	0.5079	22.85	0.5169	0.2901	0.1459	4.650E+05	290.1	79.37	0.01302	0.2456	0.8340	4.795
WP17-C1-S3	712.89	0.05639	-0.002341	5.228E+05	-1.302	-18.80	0.9850	-0.2835	0.04972	4.650E+05	29.57	35.56	0.06201	0.1342	1.127	6.146
WP17-C1-S4	712.89	-0.09092	0.5088	5.136E+05	0.4916	7.897	0.7739	0.4296	0.07704	4.650E+05	71.49	101.3	0.06752	0.8162	1.678	5.434
WP17-C1-S5	712.89	2.205	0.08359	5.249E+05	0.3656	57.54	1.359	0.07906	0.2864	4.650E+05	309.5	174.8	0.1620	1.233	1.636	7.142
WP17-C1-S6	712.89	0.05358	-0.3621	5.142E+05	0.003522	-23.19	1.536	0.5999	0.4421	4.650E+05	25.04	83.01	0.6575	0.9471	1.702	6.661
WP17-C1-S7	712.89	0.08350	0.1278	5.081E+05	-1.210	4.872	0.8047	0.3675	0.1377	4.650E+05	32.82	68.87	0.06804	0.1359	1.962	7.035
WP17-C2-S10	712.89	108.2	0.08710	5.036E+05	0.4044	39.27	0.6407	0.2523	0.1609	4.650E+05	206.9	87.18	1.023	0.4756	1.226	6.635
WP17-C2-S11	712.89	106.9	1.555	4.793E+05	0.4751	197.4	0.5395	0.1392	13.61	4.650E+05	93.43	66.84	31.23	2.844	1.284	6.238
WP17-C2-S12	712.89	0.000	-0.2168	4.864E+05	-1.053	-32.26	0.4174	0.1202	-0.02006	4.650E+05	176.6	292.3	0.08851	0.1306	1.850	8.469
WP17-C2-S13	712.89	0.05695	-0.05757	5.027E+05	0.8967	-13.08	0.4748	0.1682	0.04766	4.650E+05	218.5	168.4	0.07121	0.07303	1.776	7.763
WP17-C2-S14	712.89	-0.09065	0.2857	5.172E+05	-1.675	47.55	0.8771	0.2100	-0.03724	4.650E+05	95.65	191.1	2.312	0.1785	1.683	7.527
WP17-C2-S15	712.89	0.2720	0.5498	5.155E+05	-1.193	13.19	0.4577	-0.1611	0.03671	4.650E+05	141.6	186.1	0.2710	0.1433	3.243	12.88
WP17-C2-S8	712.89	-0.01717	-0.3097	5.018E+05	-0.1781	8.993	0.6653	-0.2626	0.01652	4.650E+05	27.78	34.15	0.4123	0.1937	0.8500	8.038
WP17-C2-S9	712.89	0.6256	0.8319	5.332E+05	-1.312	17.76	0.7650	0.3606	0.1353	4.650E+05	22.48	30.58	0.08942	0.1647	1.626	5.351
WP20-C1-S1	1110.01	0.002101	0.2133	5.364E+05	-1.562	-7.143	0.8113	-0.06743	0.01216	4.650E+05	130.4	331.9	0.1707	0.2239	0.9748	22.22
WP20-C1-S10	1110.01	0.02099	-0.06099	5.441E+05	-1.681	-6.629	0.2592	0.02491	-0.06043	4.650E+05	69.10	59.12	0.1044	0.2354	1.463	26.80
WP20-C1-S11	1110.01	0.1554	0.1171	5.308E+05	-1.309	-15.00	0.6154	0.1564	-0.002775	4.650E+05	122.2	77.25	0.05749	0.2250	0.4659	22.98
WP20-C1-S12	1110.01	0.06373	-0.4458	5.179E+05	-0.1687	27.39	0.6797	0.3206	0.1051	4.650E+05	98.89	356.2	0.2648	0.1413	0.7385	26.05
WP20-C1-S13	1110.01	0.2257	0.1934	5.072E+05	-2.620	19.18	0.8133	-0.1564	-0.04460	4.650E+05	51.58	48.44	0.06100	0.1691	0.4023	19.07
WP20-C1-S14	1110.01	-0.1294	-0.1550	5.178E+05	-1.722	-17.46	0.7450	0.2044	-0.1644	4.650E+05	158.8	128.0	0.09242	0.1554	0.6700	22.90

* distance from center of deposit

** All elements in ppm except Au which is in ppb

Appendix 8: White Pine
pyrite mineral chemistry by LA-ICP-MS

Sample	Distance* (m)	Mg24	Al27	S34	K39	Ca43	Ti49	Cr53	Mn55	Fe57	Co59	Ni60	Cu65	Zn66	As75	Se77
WP20-C1-S15	1110.01	0.1681	0.1362	5.281E+05	0.8184	-76.63	0.9408	0.06023	-0.1218	4.650E+05	100.1	62.03	0.2019	0.2831	0.7533	21.28
WP20-C1-S2	1110.01	0.01889	0.05099	5.415E+05	-1.007	6.942	1.018	0.2787	0.1197	4.650E+05	125.2	195.3	0.1486	0.2092	1.055	23.56
WP20-C1-S3	1110.01	0.1178	0.2128	5.315E+05	-1.390	-47.51	1.137	-0.2550	-0.01962	4.650E+05	95.27	154.9	0.2505	0.01236	0.4698	24.53
WP20-C1-S4	1110.01	0.1267	0.2530	5.397E+05	0.3701	-52.29	0.6474	0.04715	-0.03379	4.650E+05	68.23	46.26	0.1126	0.1061	0.2641	14.70
WP20-C1-S5	1110.01	0.06613	-0.3395	5.507E+05	0.04405	37.64	0.2794	-0.1778	-0.1693	4.650E+05	81.26	51.86	-0.1701	-0.002357	0.9698	17.96
WP20-C1-S6	1110.01	-0.1186	0.1896	5.444E+05	0.1084	31.20	0.7934	-0.2665	-0.02060	4.650E+05	52.59	59.44	0.1442	0.1371	0.9293	24.32
WP20-C1-S7	1110.01	-0.001709	-0.03276	5.349E+05	2.275	-51.64	0.4098	0.09654	0.09873	4.650E+05	208.5	560.0	0.3566	-0.1810	0.4574	17.54
WP20-C1-S8	1110.01	0.06200	-0.1420	5.476E+05	-0.1043	-48.89	0.4113	-0.02721	-0.04170	4.650E+05	147.1	69.04	-0.05186	0.08556	1.010	24.15
WP20-C1-S9	1110.01	-0.06536	0.2286	5.350E+05	-0.8216	-15.67	1.023	0.1691	-0.02005	4.650E+05	83.78	15.37	0.2289	0.05412	0.4358	15.89
WP23-C1-S1	1688.35	2.250	-0.2760	5.243E+05	-1.443	-45.84	0.7619	0.1179	0.01787	4.650E+05	22.92	3.350	0.3875	0.09045	0.3273	8.770
WP23-C1-S2	1688.35	0.2774	1.172	5.265E+05	0.4446	13.38	0.7298	0.1650	-0.02665	4.650E+05	24.30	6.366	0.4028	1.613	0.2909	8.382
WP23-C1-S3	1688.35	0.1037	0.3351	5.290E+05	-1.424	5.131	0.5770	0.1076	-0.005841	4.650E+05	13.66	3.497	0.3922	0.1014	0.5219	8.886
WP23-C1-S4	1688.35	0.04893	0.1513	5.204E+05	-1.053	-8.005	0.6149	-0.05814	-0.03565	4.650E+05	22.70	6.957	0.3425	0.1939	0.2433	9.658
WP23-C2-S5	1688.35	0.04372	0.01934	5.017E+05	1.071	17.57	0.6355	-0.07363	0.04031	4.650E+05	50.83	7.581	0.2495	0.2424	0.1641	8.210
WP23-C2-S6	1688.35	17.54	0.2400	5.077E+05	2.363	9.170	0.7390	0.07030	-0.005344	4.650E+05	27.99	6.972	0.4128	0.7936	0.1289	8.306
WP23-C2-S7	1688.35	-0.1202	0.4673	5.050E+05	0.4456	-32.24	0.9531	-0.03517	-0.03519	4.650E+05	40.85	25.34	1.204	0.1296	0.1903	9.556
WP23-C2-S8	1688.35	0.5727	-0.06795	5.159E+05	-0.3854	5.161	0.5821	-0.2820	-0.03178	4.650E+05	19.48	3.952	0.2198	0.5589	0.3875	9.373
WP23-C3-S10	1688.35	-0.5124	0.04788	5.057E+05	-1.202	-3.619	0.7899	0.1493	0.03748	4.650E+05	27.54	11.64	0.7378	0.2352	0.09693	8.711
WP23-C3-S11	1688.35	0.03985	-0.2845	4.989E+05	-1.920	1.734	0.2865	-0.08288	0.003604	4.650E+05	37.82	13.23	0.3958	0.1475	0.1923	8.590
WP23-C3-S12	1688.35	0.06497	0.1336	5.162E+05	-0.7635	24.75	0.4804	-0.1256	0.03450	4.650E+05	31.84	17.65	0.8704	0.6547	0.3914	7.799
WP23-C3-S13	1688.35	0.004506	0.06001	5.132E+05	-0.6533	55.04	0.6459	-0.08575	0.03994	4.650E+05	38.64	18.78	0.6585	0.3963	0.1509	7.841
WP23-C3-S9	1688.35	0.3462	-0.04945	5.206E+05	-1.631	-1.838	0.9518	0.01998	0.001965	4.650E+05	10.66	2.384	0.1324	0.1851	0.8046	5.291
WP26-C1-S1	1314.77	0.8395	0.9527	5.360E+05	1.202	-11.45	0.1982	-0.1556	-0.08496	4.650E+05	36.98	24.12	1.470	0.05738	0.3721	7.731
WP26-C1-S2	1314.77	0.1149	-0.4761	5.303E+05	-0.5429	23.38	0.6241	-0.05425	0.03263	4.650E+05	32.04	10.44	1.465	0.2028	-0.1262	8.741
WP26-C1-S3	1314.77	0.01817	0.7864	5.219E+05	0.1137	27.60	0.6948	0.1292	-0.08552	4.650E+05	116.2	36.61	1.659	0.1471	0.3091	7.446
WP26-C1-S4	1314.77	0.2245	0.1528	5.275E+05	-3.286	-6.304	0.2598	-0.1483	-0.002254	4.650E+05	14.90	5.126	0.5355	0.1786	-0.07366	7.901
WP26-C1-S5	1314.77	-0.5525	-0.3120	4.985E+05	-0.4125	17.23	0.2693	0.1160	-0.01538	4.650E+05	9.304	4.231	0.5879	1.162	0.1423	8.330
WP26-C1-S6	1314.77	0.5255	0.3473	5.424E+05	-2.659	-85.65	0.7433	-0.003525	0.008719	4.650E+05	20.99	15.35	1.860	0.1400	0.04194	8.073
WP26-C2-S10	1314.77	-0.1873	0.6645	5.018E+05	0.7697	-16.85	0.4030	-0.2135	-0.007469	4.650E+05	20.01	12.25	1.081	0.2544	0.3751	8.007
WP26-C2-S11	1314.77	-0.3542	3.112	5.233E+05	1.887	-3.040	0.7282	0.05346	-0.01989	4.650E+05	41.52	22.56	5.127	0.6494	0.4826	8.263
WP26-C2-S12	1314.77	0.1978	2.204	5.245E+05	0.3856	-27.69	0.5057	0.2605	-0.04504	4.650E+05	15.13	11.18	1.593	0.2484	0.2937	6.143
WP26-C2-S13	1314.77	0.1093	0.4214	5.263E+05	0.8719	4.508	0.7990	-0.06797	0.03833	4.650E+05	19.42	14.27	1.752	0.2205	0.06723	6.867
WP26-C2-S14	1314.77	0.4722	-0.6302	5.221E+05	-2.964	-44.04	0.7924	0.2415	-0.04038	4.650E+05	7.342	3.580	0.3222	0.2608	0.1115	7.633
WP26-C2-S15	1314.77	-0.02753	-0.3233	5.219E+05	2.260	-1.746	0.3218	-0.004045	0.01506	4.650E+05	18.65	14.30	2.530	0.09522	0.2194	7.428
WP26-C2-S8	1314.77	-0.02825	0.3398	5.416E+05	-1.285	4.804	0.4572	-0.1127	0.005493	4.650E+05	84.47	33.62	0.8920	0.2229	0.3078	8.061
WP26-C2-S9	1314.77	0.1583	-1.270	5.387E+05	-0.6993	-34.82	0.2954	-0.2957	-0.03702	4.650E+05	13.69	9.356	1.391	0.07810	0.3021	8.548
WP27-C1-S1	1182.57	0.03308	0.4752	5.409E+05	1.941	48.15	0.6880	0.5616	0.02555	4.650E+05	26.70	21.42	0.1369	0.2360	0.4494	10.60
WP27-C1-S2	1182.57	0.1882	0.06378	5.180E+05	-0.3985	29.46	0.4648	-0.04491	0.04118	4.650E+05	141.6	25.58	0.1094	-0.001566	0.2385	7.580
WP27-C1-S3	1182.57	0.1486	-0.006429	5.056E+05	-0.1661	-17.77	0.5052	-0.07358	0.05189	4.650E+05	37.80	10.59	3.365	0.4065	0.4100	14.03
WP27-C1-S4	1182.57	-0.03418	0.5401	4.908E+05	7.660	-48.83	1.008	-0.1224	0.02746	4.650E+05	87.37	27.37	0.7266	0.2094	0.6892	10.85
WP27-C2-S5	1182.57	-0.01567	0.04963	4.970E+05	0.6889	58.12	1.193	0.5655	-0.006592	4.650E+05	81.21	23.66	0.4256	4.104	0.3813	7.866
WP27-C2-S6	1182.57	0.9989	0.4648	4.932E+05	0.7753	21.95	0.6255	-0.09134	0.07715	4.650E+05	82.78	20.55	0.2002	0.1213	0.4493	7.199
WP27-C2-S7	1182.57	0.2997	-0.5224	5.249E+05	3.073	15.05	3.225	0.3064	0.007826	4.650E+05	123.1	22.48	0.2410	0.2641	0.4191	8.084

* distance from center of deposit

** All elements in ppm except Au which is in ppb

Appendix 8: White Pine
pyrite mineral chemistry by LA-ICP-MS

Sample	Distance* (m)	Mg24	Al27	S34	K39	Ca43	Ti49	Cr53	Mn55	Fe57	Co59	Ni60	Cu65	Zn66	As75	Se77
WP27-C2-S8	1182.57	-0.01017	1.282	4.923E+05	-0.3907	-47.13	0.5035	0.2209	-0.03558	4.650E+05	46.92	13.95	0.5301	0.08300	0.1500	9.769
WP27-C3-S10	1182.57	0.1050	0.02283	5.071E+05	-0.7719	21.33	0.5714	-0.1150	-0.06061	4.650E+05	16.64	3.975	0.3804	0.1600	0.2784	8.542
WP27-C3-S11	1182.57	-0.02035	0.2222	5.224E+05	1.890	-72.82	0.4764	-0.01692	0.03415	4.650E+05	35.00	6.274	0.3374	0.1860	0.2764	10.33
WP28-C1-S1	1183.91	-0.1576	0.1840	5.206E+05	-0.1415	15.60	0.7251	0.1128	0.02835	4.650E+05	78.77	71.58	0.5175	0.1732	0.2780	11.45
WP28-C1-S2	1183.91	0.8487	6.706	5.055E+05	571.3	-0.0001742	0.8987	-0.3561	-0.0009286	4.650E+05	55.91	30.96	13.46	0.7361	0.5711	16.07
WP28-C1-S3	1183.91	-0.01924	0.1928	4.841E+05	-1.123	-21.57	0.4473	-0.3498	0.03019	4.650E+05	213.7	86.77	0.4022	0.1366	0.1788	12.06
WP28-C1-S5	1183.91	0.05336	-0.2097	5.257E+05	0.6496	-25.13	0.8316	-0.3561	0.02671	4.650E+05	32.26	14.57	0.08855	0.3499	0.7281	11.63
WP28-C1-S6	1183.91	-0.1732	0.3033	5.161E+05	-0.6651	-28.04	0.8328	-0.1715	0.005172	4.650E+05	71.05	9.917	0.2212	0.2510	0.7740	16.71
WP28-C1-S7	1183.91	0.4756	0.7912	4.956E+05	-0.9279	-8.985	0.6967	-0.03411	-0.01435	4.650E+05	71.08	10.59	0.8495	0.08244	0.4944	17.51
WP28-C2-S10	1183.91	-0.1457	0.05746	5.321E+05	0.6669	10.82	0.6147	-0.06402	-0.02521	4.650E+05	118.0	66.12	1.028	0.04148	0.2634	20.58
WP28-C2-S11	1183.91	-0.1523	0.1661	5.198E+05	-2.785	-3.770	0.3769	-0.1749	0.01796	4.650E+05	5.200	20.95	1.107	0.1714	0.5385	28.86
WP28-C2-S12	1183.91	-0.3642	0.2818	4.923E+05	0.5093	13.77	0.8793	0.2656	0.03259	4.650E+05	4.542	29.93	1.147	0.1491	0.4955	28.75
WP28-C2-S13	1183.91	0.1352	0.04103	5.152E+05	-0.2861	11.29	0.5579	0.05284	0.01737	4.650E+05	4.375	28.42	0.7760	0.2206	0.6581	32.08
WP28-C2-S14	1183.91	-0.1611	0.4071	5.053E+05	0.5420	-9.798	0.4722	-0.1242	-0.04764	4.650E+05	5.230	42.06	1.199	0.1759	0.3538	30.13
WP28-C2-S8	1183.91	-0.4730	0.04850	5.110E+05	0.3661	-3.037	0.6041	-0.4029	0.08382	4.650E+05	99.47	21.26	0.9729	0.1997	0.3369	9.882
WP28-C2-S9	1183.91	-0.4346	-0.5514	4.739E+05	1.417	43.32	0.6878	0.02330	0.0003166	4.650E+05	142.4	17.42	0.8594	0.1604	0.1738	6.943
WP30-C1-S1	2282.00	0.5019	-0.09922	5.123E+05	-0.1944	14.45	0.2759	0.02592	-0.02542	4.650E+05	92.46	36.99	0.1057	0.1106	0.3500	3.631
WP30-C1-S2	2282.00	0.08140	0.04272	5.267E+05	0.06385	-9.661	0.4409	-0.2507	-0.04395	4.650E+05	24.58	10.75	0.8989	0.1938	1.733	7.246
WP30-C1-S3	2282.00	-0.05079	0.02835	5.155E+05	0.7170	-9.686	0.4080	0.1264	0.06246	4.650E+05	217.9	36.34	0.3082	0.1664	0.08273	6.342
WP30-C1-S4	2282.00	0.04183	0.09541	4.909E+05	0.01644	-55.99	0.3585	0.2433	0.001464	4.650E+05	347.8	25.60	0.6751	0.04721	0.8392	19.58
WP30-C1-S5	2282.00	0.1421	-0.6188	5.216E+05	0.1432	30.88	0.5730	0.1719	-0.009225	4.650E+05	49.02	10.54	0.4106	0.1339	1.353	9.334
WP30-C2-S10	2282.00	0.08414	1.840	5.199E+05	-1.331	-30.85	0.4255	0.05731	-0.01795	4.650E+05	60.14	14.59	0.2029	2.000	1.559	9.240
WP30-C2-S7	2282.00	0.2006	-0.3330	5.344E+05	-0.4519	-1.571	0.4254	-0.2049	-0.01892	4.650E+05	275.9	20.20	0.1726	0.2612	0.9328	4.220
WP30-C2-S8	2282.00	0.2370	-0.1227	5.227E+05	-0.3305	-21.65	0.5110	-0.001455	-0.004270	4.650E+05	41.43	14.65	0.2304	0.1540	0.9525	5.967
WP30-C2-S9	2282.00	0.4000	0.7593	5.090E+05	1.794	-1.242	0.2964	0.1983	0.03367	4.650E+05	61.99	21.66	0.3312	0.2170	0.7270	4.889
WP30-C3-S12	2282.00	0.1709	-0.1627	4.991E+05	-0.5596	6.836	0.2985	-0.3816	0.06369	4.650E+05	82.41	12.73	0.5084	0.2168	1.030	8.598
WP30-C3-S13	2282.00	-0.1999	0.6511	4.873E+05	-0.4046	0.8993	0.6313	0.2646	0.04278	4.650E+05	70.79	33.46	0.4444	0.1473	0.3665	27.32
WP30-C3-S14	2282.00	9.241	1.147	5.109E+05	0.3440	24.39	0.5896	0.06892	0.4989	4.650E+05	1084	9.358	1.088	0.1862	0.5391	24.24
WP30-C3-S15	2282.00	7.644	0.4147	4.907E+05	0.2195	35.14	0.5943	-0.1043	0.1504	4.650E+05	31.80	30.33	0.5638	0.3645	0.7178	27.41
WP33-C1-S1	2078.05	0.4781	-0.1940	5.524E+05	1.022	14.07	0.4007	-0.05216	0.006116	4.650E+05	282.8	20.60	0.1375	0.2434	0.2691	4.469
WP33-C1-S10	2078.05	-0.09177	0.2818	5.231E+05	-0.3767	1.745	0.7226	0.2543	-0.06184	4.650E+05	169.2	35.96	0.1118	0.06862	1.018	5.449
WP33-C1-S11	2078.05	0.4309	0.1622	4.811E+05	-1.476	-32.50	0.2805	0.04187	0.03837	4.650E+05	181.2	38.01	0.08548	0.09807	0.5686	5.985
WP33-C1-S12	2078.05	-0.05869	0.3147	4.988E+05	-1.860	30.03	6.818	-0.2501	0.008426	4.650E+05	522.7	57.14	0.2382	0.2697	0.4357	7.005
WP33-C1-S2	2078.05	0.06594	0.2511	5.370E+05	-0.1009	-15.53	0.8100	0.1155	-0.002657	4.650E+05	125.2	27.95	0.2209	0.4585	0.1468	5.200
WP33-C1-S3	2078.05	0.1335	0.2523	5.369E+05	-0.5276	5.169	0.3823	-0.2405	-0.01756	4.650E+05	170.3	31.19	0.2675	0.1281	0.3728	4.953
WP33-C1-S4	2078.05	-0.2330	0.3153	5.108E+05	0.7646	5.253	0.6971	-0.1872	0.01328	4.650E+05	12.81	5.127	0.3327	0.2334	0.4109	5.716
WP33-C1-S5	2078.05	0.2439	0.2967	5.104E+05	0.8037	2.909	0.4944	-0.1172	-0.03667	4.650E+05	41.65	9.767	0.01562	0.2361	0.4198	6.952
WP33-C1-S7	2078.05	-0.2229	0.4151	5.208E+05	1.115	10.00	0.4778	0.3959	0.01015	4.650E+05	46.58	42.32	0.1804	0.1694	0.7534	9.710
WP33-C1-S8	2078.05	-0.1524	-0.4306	5.287E+05	-0.5929	-11.81	0.7112	-0.3394	-0.07141	4.650E+05	185.4	32.04	0.09451	0.07246	0.5004	5.056
WP33-C1-S9	2078.05	0.1980	0.1084	5.162E+05	-1.013	12.25	0.6574	-0.2375	0.09404	4.650E+05	110.1	27.59	0.1417	0.9269	0.9696	7.629
WP36-C1-S1	1404.01	0.06298	-0.1480	5.144E+05	-0.5052	-10.88	0.5074	0.1908	-0.04636	4.650E+05	198.0	131.3	0.1458	0.05989	0.4439	3.049
WP36-C1-S2	1404.01	-0.1232	-0.1541	5.029E+05	-0.5647	-17.59	0.9318	-0.3819	-0.002865	4.650E+05	110.4	65.06	0.1769	0.1498	0.2821	4.282
WP36-C1-S3	1404.01	-0.1119	0.09606	5.121E+05	-0.5003	-25.42	0.4566	-0.1830	0.03987	4.650E+05	78.35	53.16	0.09500	0.2080	0.3238	3.794

* distance from center of deposit

** All elements in ppm except Au which is in ppb

Appendix 8: White Pine
pyrite mineral chemistry by LA-ICP-MS

Sample	Distance* (m)	Mg24	Al27	S34	K39	Ca43	Ti49	Cr53	Mn55	Fe57	Co59	Ni60	Cu65	Zn66	As75	Se77
WP36-C1-S4	1404.01	0.04726	1.563	5.317E+05	0.2338	3.884	1.187	0.08085	0.06951	4.650E+05	48.76	24.12	0.4263	0.2452	0.4225	5.077
WP36-C1-S5	1404.01	-0.04647	-0.2363	5.167E+05	1.102	23.52	0.7482	0.08568	-0.01746	4.650E+05	72.99	42.61	0.3612	0.3398	0.2026	3.025
WP36-C1-S6	1404.01	-0.1347	-0.07055	5.053E+05	-2.434	0.2405	0.8730	-0.01429	0.09981	4.650E+05	241.5	68.31	1.196	0.04595	0.5288	4.439
WP36-C2-S10	1404.01	0.9306	836.9	2.704E+05	13.45	-19.07	0.6554	0.2167	0.5370	4.650E+05	4.250	3.378	30.99	6.254	1.423	5.777
WP36-C2-S11	1404.01	3.209	1389	2.247E+05	75.14	42.00	0.9938	0.5431	1.351	4.650E+05	45.36	17.13	26.02	6.870	1.060	2.330
WP36-C2-S12	1404.01	0.2560	3.412	5.144E+05	-0.6208	7.289	0.7706	-0.1143	0.04088	4.650E+05	28.34	12.38	0.4620	0.2187	0.04483	4.112
WP36-C2-S7	1404.01	0.0006485	-0.3086	5.212E+05	-3.058	11.09	1.051	0.2835	-0.05867	4.650E+05	27.28	23.59	0.1879	0.2492	-0.005361	3.289
WP36-C2-S8	1404.01	-0.1662	0.1594	4.969E+05	0.3314	9.359	0.6290	-0.09974	-0.07668	4.650E+05	47.72	32.09	0.1881	0.1431	0.4714	6.362
WP36-C2-S9	1404.01	0.3094	0.3497	4.840E+05	-0.2779	-15.09	0.7918	-0.1177	-0.01816	4.650E+05	61.12	27.34	0.1705	0.2547	0.3446	5.033
WP40-C1-S1	1139.14	-0.2379	-0.06536	5.132E+05	0.6540	9.996	0.6685	-0.1496	-0.03138	4.650E+05	4.503	26.62	0.2392	0.04248	0.4360	3.042
WP40-C1-S10	1139.14	0.3485	0.4614	4.981E+05	-0.4930	-17.40	0.2505	0.3738	-0.03129	4.650E+05	73.57	41.96	0.003162	0.2268	2.276	26.63
WP40-C1-S11	1139.14	0.02525	0.5563	5.090E+05	-0.6031	-33.20	0.8098	0.2160	0.07462	4.650E+05	102.7	69.76	0.3490	0.1723	2.277	16.64
WP40-C1-S12	1139.14	0.1056	-0.5780	5.063E+05	-0.07260	-17.53	0.4789	0.1934	0.01050	4.650E+05	1.957	2.252	0.1159	0.3083	0.9982	3.280
WP40-C1-S13	1139.14	0.5418	-0.5961	5.088E+05	2.840	-20.96	0.5703	0.06531	-0.04076	4.650E+05	3.282	4.942	0.8368	0.04255	2.039	3.116
WP40-C1-S14	1139.14	0.1235	1.221	5.107E+05	2.241	11.82	0.06698	0.2731	-0.03993	4.650E+05	60.09	52.65	0.05873	0.2699	1.112	6.010
WP40-C1-S15	1139.14	-0.4593	-0.5850	5.017E+05	1.006	-5.093	0.3128	0.2282	-0.06538	4.650E+05	2.706	11.20	0.2744	0.1783	1.079	3.084
WP40-C1-S2	1139.14	0.1836	0.3145	5.336E+05	0.4304	20.53	0.6434	0.1734	-0.03017	4.650E+05	9.742	5.866	0.07620	0.3844	1.598	3.135
WP40-C1-S3	1139.14	0.7312	0.2625	5.284E+05	2.227	29.32	0.6896	-0.2280	-0.04841	4.650E+05	92.14	99.03	0.3485	0.1542	5.343	11.60
WP40-C1-S4	1139.14	0.06979	-0.2800	5.325E+05	1.413	14.35	0.3921	0.2711	-0.04502	4.650E+05	97.90	110.5	-0.008774	0.1466	0.3406	3.557
WP40-C1-S5	1139.14	0.6631	-1.057	4.999E+05	3.370	82.66	0.6843	0.07805	0.004267	4.650E+05	83.85	40.97	0.3132	0.1577	2.415	14.55
WP40-C1-S6	1139.14	-0.06313	1.376	4.978E+05	-3.183	-13.31	0.6829	-0.1069	-0.01973	4.650E+05	17.93	10.26	0.1395	0.1923	2.741	38.66
WP40-C1-S7	1139.14	0.3388	-0.1200	5.065E+05	1.342	26.72	0.3956	0.07044	0.02402	4.650E+05	39.35	35.63	0.6673	0.4632	4.555	12.58
WP40-C1-S8	1139.14	-0.09591	0.09363	5.104E+05	-1.528	-12.37	0.4505	0.2949	0.03245	4.650E+05	68.92	54.87	0.5654	0.2146	4.872	12.81
WP40-C1-S9	1139.14	0.4854	-0.08946	5.197E+05	0.8685	9.761	0.3110	-0.2221	0.01136	4.650E+05	15.88	6.439	0.2833	0.1697	2.597	37.70
WP44-C1-S2	622.10	-0.05943	-0.2340	5.310E+05	1.637	-23.07	1.066	0.09146	-0.02774	4.650E+05	14.77	6.143	0.4080	0.1425	0.5098	5.378
WP44-C1-S3	622.10	0.2078	-0.2018	5.449E+05	0.2063	15.69	0.4192	-0.1164	0.07239	4.650E+05	82.59	97.32	0.1179	0.1413	0.3871	12.46
WP44-C1-S4	622.10	-0.4398	0.2345	5.346E+05	-0.6932	-6.367	0.3528	0.5720	0.01333	4.650E+05	22.77	20.27	0.1306	0.2201	0.1582	8.751
WP44-C1-S5	622.10	0.4890	0.3215	5.298E+05	0.3845	32.27	0.5213	-0.1207	-0.06621	4.650E+05	186.4	29.10	0.1518	0.4206	0.4796	9.197
WP44-C2-S6	622.10	0.4419	-1.112	5.382E+05	0.6785	22.12	0.4883	0.1507	0.002905	4.650E+05	130.3	33.69	0.09443	0.1755	0.2351	8.343
WP44-C2-S7	622.10	-0.9175	-0.06895	5.009E+05	-1.152	-0.0003195	0.7546	-0.07009	-0.02920	4.650E+05	153.2	50.69	0.3154	-0.09656	0.4197	6.449
WP44-C3-S13	622.10	-0.2401	0.4303	5.295E+05	-0.4956	-116.6	0.5189	0.1781	0.02446	4.650E+05	92.80	39.40	0.1170	0.2520	0.2150	8.094
WP44-C3-S14	622.10	-0.3412	1.841	5.220E+05	0.1316	8.211	0.4835	0.2941	-0.03143	4.650E+05	90.55	26.57	0.2030	0.1217	0.3801	5.774
WP44-C3-S15	622.10	-0.2935	1.621	5.337E+05	-2.062	-20.54	0.1506	-0.2094	-0.01358	4.650E+05	111.4	111.1	0.1670	0.2528	0.3412	8.932
WP52-C1-S1	785.45	1.030	-0.3725	5.054E+05	6.158	-65.35	0.02505	1.242	0.0005249	4.650E+05	22.68	22.00	1.590	0.2947	-0.1270	8.189
WP52-C1-S2	785.45	-0.8514	-0.007327	5.192E+05	-1.432	-18.32	0.8078	-0.1191	0.04853	4.650E+05	13.92	12.67	1.364	0.2307	0.1390	8.739
WP52-C1-S3	785.45	0.3983	0.5911	5.005E+05	-1.557	-10.34	0.8137	-0.02149	-0.06424	4.650E+05	32.61	22.80	1.651	0.1823	0.08528	7.335
WP52-C1-S4	785.45	0.1458	-0.08228	4.959E+05	-0.5797	27.90	0.2846	-0.01306	0.03969	4.650E+05	26.08	21.33	1.426	0.02761	0.2286	7.838
WP52-C1-S5	785.45	0.4758	-0.5070	5.090E+05	18.98	5.209	0.5833	-0.1481	0.09701	4.650E+05	21.15	12.92	1.102	0.1664	0.08258	7.613
WP52-C2-S10	785.45	0.5284	-0.4806	5.214E+05	7.671	-83.93	0.3180	0.07931	0.07016	4.650E+05	120.4	46.83	0.4924	0.2603	0.3533	7.035
WP52-C2-S6	785.45	0.02786	0.4643	5.198E+05	2.242	-36.56	0.1095	0.2599	0.07024	4.650E+05	14.66	14.82	0.8668	0.2696	0.1453	8.879
WP52-C2-S7	785.45	-0.4456	0.2665	4.967E+05	-0.4221	19.98	0.4524	-0.09636	0.008167	4.650E+05	18.84	28.30	1.716	0.1947	0.03317	8.053
WP52-C2-S8	785.45	-0.04506	0.2590	5.217E+05	1.233	-20.99	0.5685	0.2443	-0.01196	4.650E+05	11.78	19.99	1.770	0.4041	0.4085	11.99
WP52-C2-S9	785.45	-0.6420	0.07101	5.048E+05	2.291	-31.52	0.5269	0.03979	-0.02386	4.650E+05	13.53	10.72	0.1630	0.1037	0.4035	6.778

* distance from center of deposit

** All elements in ppm except Au which is in ppb

Appendix 8: White Pine
pyrite mineral chemistry by LA-ICP-MS

Sample	Distance* (m)	Mg24	Al27	S34	K39	Ca43	Ti49	Cr53	Mn55	Fe57	Co59	Ni60	Cu65	Zn66	As75	Se77
WP52-C3-S11	785.45	0.01339	0.8154	5.342E+05	0.8005	-23.19	0.1025	0.07928	-0.03529	4.650E+05	7.904	10.35	0.3132	0.2244	0.2536	7.277
WP52-C3-S12	785.45	1.126	-0.1070	5.958E+05	-1.715	3.567	0.6721	0.04103	-0.05871	4.650E+05	13.87	13.27	0.5078	1.795	0.2237	12.22
WP52-C3-S13	785.45	1.165	0.5474	5.235E+05	-0.1553	-9.565	0.4900	0.3248	0.04968	4.650E+05	28.95	32.20	0.6736	0.1780	0.2776	7.296
WP52-C3-S14	785.45	0.3153	-0.8812	5.262E+05	1.446	-40.02	0.4565	0.01003	-0.03251	4.650E+05	12.73	15.98	0.6408	0.2635	0.2560	6.726
WP52-C3-S15	785.45	0.008840	0.7749	5.225E+05	1.270	26.05	0.2556	-0.2222	-0.01090	4.650E+05	10.58	12.01	0.7556	0.2696	0.2801	8.539
WP54-C1-S1	432.59	0.5943	0.6236	5.244E+05	-0.5432	98.50	0.1303	0.4879	-0.03539	4.650E+05	225.4	19.23	0.9037	0.5663	0.1214	12.48
WP54-C1-S2	432.59	0.2345	-1.431	5.455E+05	-2.924	55.36	0.3584	-0.1316	0.002973	4.650E+05	91.66	29.18	1.539	0.1978	-0.06472	15.63
WP54-C1-S3	432.59	0.1570	0.1874	5.056E+05	-0.3942	-31.01	0.9182	0.4674	0.02554	4.650E+05	42.73	18.01	1.209	0.1892	0.001405	12.84
WP54-C1-S4	432.59	0.3142	-0.3634	5.200E+05	-2.673	41.53	0.2697	0.3637	-0.06669	4.650E+05	95.71	49.68	1.661	0.2002	0.1004	14.00
WP54-C1-S5	432.59	-0.007643	-0.2356	5.074E+05	1.254	-7.027	0.5831	0.1864	-0.06351	4.650E+05	109.8	18.01	1.139	0.2731	0.2352	13.70
WP54-C1-S6	432.59	0.3854	0.4571	4.963E+05	3.564	4.405	1.028	0.3220	-0.01911	4.650E+05	335.1	30.45	0.6619	0.1385	0.1830	11.65
WP54-C2-S10	432.59	-0.09821	-0.2585	5.160E+05	0.2678	-5.913	0.5554	-0.05424	-0.08967	4.650E+05	213.9	78.91	1.221	0.08451	0.1659	10.91
WP54-C2-S11	432.59	0.3242	0.7940	5.121E+05	-0.5821	1.650	0.3197	-0.2731	-0.008947	4.650E+05	175.5	49.34	0.5674	0.1142	0.1627	8.918
WP54-C2-S12	432.59	-0.007828	0.3821	5.034E+05	-2.221	-6.827	0.7366	0.1351	0.01189	4.650E+05	198.7	71.16	0.6275	0.09752	0.1573	10.64
WP54-C2-S13	432.59	-0.1271	2.042	4.973E+05	1.435	-2.503	1.178	-0.5205	0.5337	4.650E+05	175.6	60.44	1.324	0.1607	-0.2787	7.371
WP54-C2-S14	432.59	0.4847	0.1913	5.242E+05	-0.6960	-3.151	0.7979	0.1924	0.07654	4.650E+05	193.6	72.56	0.9641	0.09600	-0.01120	7.952
WP54-C2-S15	432.59	-0.3102	-0.5701	5.208E+05	-2.615	60.97	0.3875	0.3348	0.06467	4.650E+05	80.03	42.62	2.015	0.2515	0.1546	10.19
WP54-C2-S8	432.59	1.311	-0.4428	4.999E+05	-2.533	1.104	0.3908	0.4240	0.07556	4.650E+05	55.77	36.61	0.6576	0.1177	-0.003433	10.04
WP54-C2-S9	432.59	0.04006	-0.2011	5.273E+05	0.1116	24.58	0.5503	0.3193	-0.01645	4.650E+05	158.1	37.40	0.7097	0.2821	0.1794	7.791
WP63-C1-S1	0.00	0.1502	0.2258	5.167E+05	0.3954	-11.97	0.6258	0.2704	-0.01815	4.650E+05	23.85	14.83	1.589	1.031	0.8427	13.95
WP63-C1-S10	0.00	1.938	-0.2299	5.196E+05	-1.624	26.07	0.4468	-0.1394	0.02616	4.650E+05	7.178	8.774	3.202	0.1637	0.07208	23.54
WP63-C1-S11	0.00	-0.05692	-0.1682	5.019E+05	-0.6106	-13.83	0.8540	0.4564	-0.03124	4.650E+05	3.830	3.405	0.5689	0.1792	0.4832	12.87
WP63-C1-S12	0.00	0.08488	-0.07356	5.069E+05	-1.633	-23.29	0.7021	0.3456	-0.04998	4.650E+05	7.600	5.681	0.8089	0.2080	0.1025	13.77
WP63-C1-S13	0.00	-0.06373	0.8180	5.082E+05	0.1287	-1.547	0.5417	0.1690	-0.04435	4.650E+05	17.44	12.91	1.892	0.4804	0.3562	15.50
WP63-C1-S14	0.00	-0.09554	0.1063	5.073E+05	-1.854	8.777	0.6041	-0.2952	0.04776	4.650E+05	4.559	5.318	0.8612	2.122	0.2919	13.70
WP63-C1-S2	0.00	0.04420	-0.6246	5.249E+05	0.8060	43.25	0.8183	-0.002038	-0.01268	4.650E+05	3.321	3.411	2.744	0.9268	0.04503	21.99
WP63-C1-S3	0.00	-0.1077	0.2225	5.369E+05	-0.1822	59.69	0.3319	0.4483	-0.05986	4.650E+05	9.164	6.446	2.235	0.1288	-0.06796	24.57
WP63-C1-S4	0.00	0.07082	0.1475	5.339E+05	0.3176	26.49	0.6427	0.2295	-0.04946	4.650E+05	13.50	3.438	0.4273	-0.01684	0.1631	10.58
WP63-C1-S5	0.00	61.85	584.1	6.671E+05	358.8	-16.67	13.04	0.4063	0.9888	4.650E+05	3.936	1.931	34.14	5.385	40.95	44.10
WP63-C1-S6	0.00	0.1718	0.04993	5.113E+05	1.034	25.56	0.5472	0.4477	-0.008671	4.650E+05	4.639	2.438	0.8436	0.1202	0.1094	17.55
WP63-C1-S7	0.00	-0.02360	0.07608	5.044E+05	0.4814	-8.955	0.5105	-0.2580	-0.04332	4.650E+05	15.00	11.23	1.476	0.4407	0.1058	18.36
WP63-C1-S8	0.00	-0.1969	-0.2382	5.233E+05	-0.5644	17.13	0.9639	-0.1542	0.07203	4.650E+05	5.855	2.484	0.6372	0.6164	-0.1037	12.66
WP63-C1-S9	0.00	-0.1864	-0.1975	5.179E+05	-0.7757	0.4056	0.5514	0.2830	-0.007222	4.650E+05	19.75	10.22	1.500	0.1467	0.4063	14.03

* distance from center of deposit

** All elements in ppm except Au which is in ppb

Appendix 8: White Pine
pyrite mineral chemistry by LA-ICP-MS

Sample	Distance* (m)	Zr90	Mo95	Ag107	Cd111	Sn118	Sb121	Te125	Ba137	Gd157	Hf178	Ta181	W182	Pt195
ESWP001-C1-S1	161.31	0.0001163	0.01931	-0.005841	0.008212	0.08625	0.02631	0.09706	0.01253	0.0004278	-0.003976	-0.0002033	0.0002927	-0.00004139
ESWP001-C1-S2	161.31	0.009403	5.713	4.166	14.83	0.09727	0.06453	0.1710	13.01	0.3307	0.0008590	0.0003108	0.9233	0.0002580
ESWP001-C1-S3	161.31	0.001116	-0.001944	0.0007614	0.03519	0.1182	-0.01429	0.09895	0.0009500	0.0004243	-0.0005453	0.0002624	0.001127	0.001771
ESWP001-C1-S4	161.31	0.01275	-0.02371	-0.007617	0.02013	0.1145	-0.01193	0.02362	0.01055	0.003531	0.0008500	0.0005351	0.001246	-0.0004575
ESWP001-C1-S5	161.31	0.003976	0.01759	-0.005405	-0.02334	0.1160	0.02094	0.1439	-0.009540	-0.0008452	0.002511	-0.0001537	0.002725	0.003844
ESWP001-C1-S6	161.31	995.5	0.03937	0.1020	0.04728	8.705	0.1026	0.2175	0.008319	3.263	28.34	24.41	125.3	0.004701
ESWP001-C1-S7	161.31	0.002914	0.2741	0.8813	3.852	0.1670	0.02946	1.491	78.78	0.04447	-0.0006472	-0.0001732	0.2192	-0.0001034
ESWP001-C2-S10	161.31	0.003100	0.001633	-0.004434	-0.003194	0.09973	0.02396	0.1173	0.01333	-0.002359	0.0007543	0.0005254	-0.001227	0.002874
ESWP001-C2-S11	161.31	0.002666	-0.02533	0.02456	-0.03746	0.09100	-0.009959	0.2605	0.03496	-0.008585	0.005738	-0.001640	0.007922	-0.0001478
ESWP001-C2-S12	161.31	0.001221	0.03708	0.01316	0.04465	0.1182	0.01970	0.05730	0.01974	0.009093	-0.001997	0.001524	0.003624	-0.001607
ESWP001-C2-S13	161.31	69.71	-0.003741	0.02613	0.01638	0.1220	0.02595	0.2336	0.0003373	0.02765	1.442	-0.0001817	0.002627	-0.004827
ESWP001-C2-S14	161.31	7807	-0.01463	0.1491	0.01866	0.1227	-0.007000	1.174	0.0006834	0.7670	159.0	0.006071	0.02752	0.01767
ESWP001-C2-S8	161.31	-0.001592	-0.009308	-0.006374	-0.02473	0.1008	-0.01223	0.1602	-0.01018	0.0007101	-0.007597	-0.0009369	0.006692	0.004571
ESWP001-C2-S9	161.31	0.006366	-0.008603	0.007508	0.04440	0.08824	-0.006834	0.06643	-0.004381	0.000	0.002650	-0.0004174	0.000	0.003404
ESWP001-C2-S1	132.23	0.003209	0.006573	-0.01296	-0.05456	0.09928	0.02500	0.6760	0.005156	0.01683	-0.002813	0.0001079	-0.0009840	0.007770
ESWP002-C1-S10	132.23	0.001519	-0.01784	0.003464	-0.0009842	0.08007	-0.002196	3.954	0.007105	-0.006872	0.002246	0.00005880	0.004184	-0.0009197
ESWP002-C1-S11	132.23	0.004418	0.7798	0.01812	-0.002286	0.1014	-0.005443	0.1154	-0.007155	0.008901	0.0009490	-0.0004116	-0.001540	0.00002654
ESWP002-C1-S12	132.23	0.006115	0.009076	0.008191	-0.02273	0.1008	0.03096	0.05512	0.007286	-0.005255	0.002912	-0.00007700	-0.005795	-0.002409
ESWP002-C1-S13	132.23	0.0003930	0.006121	0.01062	-0.04894	0.08783	0.01180	0.1515	0.3957	0.009249	0.002201	0.001104	0.001833	0.002022
ESWP002-C1-S14	132.23	0.0008681	-0.01965	0.007888	-0.01068	0.09560	0.03287	0.04888	0.002860	-0.006469	0.0009005	0.00002925	0.0006746	-0.004967
ESWP002-C1-S15	132.23	0.004514	0.01861	0.01745	-0.03842	0.06686	0.04092	0.04575	0.01546	0.001849	0.0002669	0.0009127	-0.001474	-0.0008638
ESWP002-C1-S3	132.23	0.002399	0.1708	0.01013	-0.07778	0.07255	0.01140	1.568	0.003282	-0.0005218	-0.01692	-0.002011	0.009278	0.003590
ESWP002-C1-S4	132.23	0.001632	0.00006158	0.01436	0.02028	0.07990	-0.04824	0.06442	-0.001421	0.009467	0.006042	-0.001188	-0.004346	-0.003139
ESWP002-C1-S5	132.23	-0.0006636	0.005153	0.0007315	0.002396	0.1060	-0.004718	0.03165	0.0009071	-0.01444	-0.004677	-0.001037	-0.009318	-0.002835
ESWP002-C1-S6	132.23	0.003183	0.01053	0.007852	0.004226	0.06749	0.02304	0.07185	0.01633	-0.004114	-0.007472	0.0003846	0.003743	0.002726
ESWP002-C1-S7	132.23	0.003873	-0.001168	0.03106	0.007823	0.08963	0.01845	0.1448	0.8416	0.001503	0.0004835	0.001437	0.002634	0.005114
ESWP002-C1-S8	132.23	0.003963	-0.01137	-0.002083	-0.009644	0.09148	0.02285	0.07390	0.009899	0.003346	0.003872	-0.001699	-0.01292	0.006450
ESWP002-C1-S9	132.23	0.003297	0.006658	0.01090	0.01969	0.08033	0.06784	0.1631	0.06032	0.004909	-0.001819	0.0008122	-0.0009214	0.002189
ESWP006-C1-S1	1429.02	-0.0006637	-0.007007	0.04129	0.02202	0.1165	0.03924	0.3379	0.08073	0.0004331	0.0002957	0.0005097	-0.002525	-0.003854
ESWP006-C1-S2	1429.02	0.001027	0.01051	0.002252	-0.01816	0.1090	0.03161	0.1334	-0.008800	-0.01257	-0.0003657	0.0007574	0.0004135	0.0008720
ESWP006-C1-S3	1429.02	-0.0006971	0.004072	0.05424	-0.01299	0.08530	0.005503	0.2909	-0.005007	0.001181	0.002247	0.0009424	0.006369	0.003558
ESWP006-C1-S4	1429.02	-0.004299	0.0006724	0.005269	0.02877	0.1076	-0.002005	0.09701	0.003267	-0.002998	0.0001023	-0.0003987	0.002853	0.0008918
ESWP006-C1-S5	1429.02	-0.004553	-0.008374	0.09355	-0.006064	0.07135	0.004943	-0.06678	0.02610	-0.008411	-0.0008924	-0.0008057	0.0003945	0.003980
ESWP006-C1-S6	1429.02	0.004628	0.01700	0.1173	-0.02808	0.1329	0.06234	0.6518	1.772	0.000	-0.002534	-0.001521	0.009393	0.001289
ESWP006-C2-S10	1429.02	-0.0004653	0.007570	0.09290	-0.03561	0.1196	0.04748	0.1591	-0.02240	0.005621	0.0003190	0.0008048	0.003663	0.0008521
ESWP006-C2-S11	1429.02	-0.001509	0.004535	0.02558	-0.05333	0.1141	0.04016	0.6572	-0.01640	0.003460	-0.005770	-0.0002153	0.008232	0.0008842
ESWP006-C2-S12	1429.02	-0.003482	0.005959	0.06307	0.06799	0.1290	0.03281	0.5931	-0.002309	-0.002863	-0.002107	0.0002877	-0.001433	-0.005956
ESWP006-C2-S13	1429.02	-0.001676	0.007696	-0.0006377	0.01977	0.1030	0.05928	0.4972	0.005644	0.007110	0.003226	-0.0002209	-0.005213	0.002362
ESWP006-C2-S14	1429.02	0.005976	0.01132	0.03371	-0.03471	0.07836	0.003718	0.1164	0.01367	0.005748	-0.001340	-0.0006499	0.001178	0.008514
ESWP006-C2-S15	1429.02	-0.004394	0.01673	-0.001745	0.04522	0.1007	0.04041	0.07861	-0.01000	0.006074	-0.002093	0.002393	0.0001118	-0.002236
ESWP006-C2-S7	1429.02	0.003734	-0.007444	0.05968	0.01338	0.1229	-0.0005329	0.1816	0.002921	-0.001274	-0.003610	0.0007421	-0.005918	0.001817
ESWP006-C2-S8	1429.02	0.005016	-0.0008562	0.006973	-0.008198	0.1050	-0.03009	0.1299	0.0007050	-0.006278	0.003387	-0.001125	0.004318	-0.001673
ESWP006-C2-S9	1429.02	0.003222	-0.005578	0.0002894	0.01897	0.1107	0.02539	0.8998	-0.001661	0.0002379	-0.0006123	-0.002182	-0.001366	0.0007984

* distance from center of deposit

** All elements in ppm except Au which is in ppb

Appendix 8: White Pine
pyrite mineral chemistry by LA-ICP-MS

Sample	Distance* (m)	Zr90	Mo95	Ag107	Cd111	Sn118	Sb121	Te125	Ba137	Gd157	Hf178	Ta181	W182	Pt195
ESWP007-C1-S2	1360.22	0.01296	-0.005360	-0.01757	0.02279	0.1088	0.03422	0.1475	0.02341	0.02548	-0.001656	-0.001562	0.01768	-0.01425
ESWP007-C1-S3	1360.22	0.0007926	-0.003640	0.01349	0.01242	0.09356	0.02072	-0.0007412	-0.01496	0.006637	0.001534	-0.0005320	-0.009988	-0.0008712
ESWP007-C1-S4	1360.22	-0.001324	0.006194	-0.005198	0.01917	0.06544	0.06519	1.116	-0.003859	-0.005202	-0.001022	0.0005202	0.001471	-0.002822
ESWP007-C1-S5	1360.22	-0.0003406	0.005359	0.01204	0.04223	0.06386	0.01642	0.03703	0.004712	0.009607	-0.00003858	-0.001798	-0.003817	0.001617
ESWP007-C2-S6	1360.22	-0.001572	0.01655	0.1820	-0.03818	0.07623	-0.01131	0.07302	0.4074	0.004043	-0.003640	-0.001125	0.008427	-0.005344
ESWP007-C2-S8	1360.22	0.003011	0.01248	0.01034	0.04592	0.07126	-0.003384	0.01335	0.01754	0.002440	0.001125	-0.001508	-0.005460	-0.002209
ESWP007-C2-S9	1360.22	0.001096	0.007300	0.003767	0.003499	0.06776	0.06335	0.1611	0.01762	-0.001474	-0.0006797	0.0002989	-0.004324	-0.007491
ESWP007-C3-S11	1360.22	-0.001294	-0.004598	0.009012	0.01162	0.07339	0.02073	0.09270	-0.01563	0.004740	-0.001746	0.00008271	-0.006225	-0.0004717
ESWP007-C3-S12	1360.22	-0.0004533	-0.0006575	0.01163	-0.01678	0.06547	-0.02809	-0.03738	0.005183	-0.005248	-0.002998	0.0009287	-0.002839	0.001270
ESWP018-C1-S3	513.17	0.006367	0.01346	0.03791	-0.04201	0.08617	0.02477	0.05346	-0.002200	0.01089	0.003347	0.001058	0.01531	-0.004049
ESWP018-C1-S4	513.17	0.003070	0.01131	0.005742	0.01596	0.1299	-0.05263	0.1504	0.04109	-0.0002707	0.004239	0.0004334	-0.004880	0.005746
ESWP018-C1-S5	513.17	0.0009506	0.005530	0.0002451	0.04447	0.1146	0.002303	0.05014	0.02034	0.0006370	0.001596	0.0002677	0.01147	-0.001266
ESWP018-C1-S6	513.17	0.004272	0.002171	-0.0001651	-0.002751	0.1086	0.02513	0.08672	0.01399	0.001731	0.003614	-0.0001936	0.0005530	0.002012
ESWP018-C1-S7	513.17	0.002945	0.007956	0.01554	0.000	0.08230	-0.006408	0.2013	0.1313	-0.02272	0.000	0.0004128	0.01048	-0.005452
ESWP018-C1-S8	513.17	-0.002638	0.001000	-0.007067	-0.05253	0.09225	0.01561	0.05687	0.01077	-0.007619	-0.004668	0.001786	0.003819	0.0008782
ESWP018-C2-S11	513.17	0.001842	0.5300	0.2065	0.07628	0.06303	0.08256	0.05185	0.1225	-0.005427	-0.001245	0.0005117	0.03607	-0.002070
ESWP018-C2-S12	513.17	-0.007482	0.05591	0.01140	0.04969	0.1188	0.01287	0.3814	0.01408	-0.004013	-0.003380	-0.001619	0.004125	0.004268
ESWP018-C2-S13	513.17	0.001675	0.3202	0.02927	0.02594	0.08321	0.05862	0.1560	0.1392	-0.0008320	0.002007	0.0003427	0.007884	-0.005447
ESWP018-C2-S14	513.17	0.003408	0.5131	0.1631	-0.004736	0.08319	0.02603	0.1419	0.1845	-0.002697	-0.001602	-0.0001158	0.02247	-0.0002167
ESWP058-C1-S1	1709.21	-0.004127	0.01114	0.002011	0.003883	0.09118	0.07241	-0.03017	-0.001999	0.007647	-0.002354	-0.0001922	-0.003023	-0.002759
ESWP058-C1-S2	1709.21	-0.003764	-0.005118	0.007924	0.02152	0.1004	0.004060	0.05005	0.0006172	-0.001369	-0.001968	0.0005140	0.001753	0.002586
ESWP058-C1-S3	1709.21	-0.0006312	-0.0007428	-0.0008379	0.03118	0.1066	0.004866	0.04282	0.000	-0.001391	0.002918	0.00006024	0.005305	-0.001268
ESWP058-C1-S4	1709.21	0.005010	0.01544	0.1409	0.02092	0.08886	0.01468	0.02220	0.01440	0.0003991	0.00009099	0.0008833	-0.0009582	0.001036
ESWP058-C1-S5	1709.21	0.02069	-0.005912	0.002404	0.03388	0.2001	0.009608	0.05885	6.828	0.005959	-0.003424	0.001420	0.5250	0.002786
ESWP058-C1-S6	1709.21	-0.001183	0.005410	0.002490	0.03203	0.1095	0.05590	0.04393	-0.001825	0.001643	-0.006246	-0.001535	0.0005960	0.0007303
ESWP058-C2-S10	1709.21	0.006627	-0.007477	0.01008	-0.02469	0.1005	0.004071	-0.002209	-0.001966	0.001771	-0.0003849	0.0008316	-0.001706	0.004848
ESWP058-C2-S7	1709.21	0.001827	-0.002237	-0.003435	-0.007174	0.09180	0.04004	0.09351	0.008041	-0.006169	0.001556	0.00009643	-0.004130	-0.006987
ESWP058-C2-S8	1709.21	0.08406	-0.004385	0.004865	0.006152	0.1483	0.03540	0.08307	0.4794	0.003740	0.001348	0.01824	1.930	-0.0008181
ESWP058-C2-S9	1709.21	0.002895	0.007012	-0.006739	0.005621	0.06109	0.03042	0.03109	-0.008438	0.01464	-0.0004560	0.001329	0.0007414	-0.002815
ESWP058-C3-S11	1709.21	0.007856	0.1624	0.1268	-0.01930	0.09917	0.01179	0.01576	0.003839	-0.00006390	0.001335	0.0004046	0.1123	-0.0001382
ESWP058-C3-S12	1709.21	0.04882	15.68	3.633	0.06258	0.2290	0.3240	0.4489	5.598	0.1449	0.001613	0.0008112	0.1652	0.002986
ESWP058-C3-S13	1709.21	0.007772	0.07863	0.4375	-0.007869	0.1326	0.04910	2.549	0.01993	0.004845	0.002198	-0.0001212	0.07979	-0.0001425
ESWP058-C3-S14	1709.21	3.536	40.35	6.462	0.04535	2.656	0.7717	2.399	12.59	0.1733	0.06608	0.06278	4.374	0.0003246
ESWP065-C1-S1	609.43	0.004722	0.01407	0.01609	-0.04808	0.09209	0.04457	0.03696	-0.003860	-0.009303	0.001799	-0.001379	0.001128	0.0002470
ESWP065-C1-S10	609.43	0.002834	0.009275	-0.005414	-0.02388	0.1055	0.006092	0.08937	-0.006614	0.002007	-0.005264	-0.0008603	0.003543	0.004984
ESWP065-C1-S2	609.43	-0.002381	0.007036	0.01075	0.01603	0.1025	-0.01974	0.04490	-0.005731	0.00008484	-0.0002716	0.001411	-0.006883	-0.009049
ESWP065-C1-S3	609.43	0.0008670	0.01275	0.008776	0.05111	0.1263	0.01777	0.03480	0.008693	0.01158	-0.001612	0.001584	-0.003112	-0.0001366
ESWP065-C1-S5	609.43	0.000	-0.008634	0.001521	0.1410	0.1278	0.05887	-0.05066	-0.006220	-0.004142	-0.01137	-0.0009462	0.01374	0.005231
ESWP065-C1-S6	609.43	-0.005308	0.002915	-0.0002138	0.01828	0.1197	0.04914	0.1181	0.0007152	0.003889	-0.003014	-0.0006890	-0.004672	-0.001943
ESWP065-C1-S7	609.43	0.0003630	0.005730	0.004397	-0.06425	0.09109	0.04648	-0.1077	0.008215	0.002203	0.0001042	-0.0006264	0.001243	-0.0009176
ESWP065-C1-S8	609.43	-0.001432	-0.01473	0.0008307	0.002693	0.1020	0.008417	-0.02118	-0.01346	-0.001019	-0.001999	0.00006321	-0.008479	0.005286
ESWP065-C1-S9	609.43	-0.002330	0.004095	-0.008516	-0.03538	0.09520	-0.006309	-0.03122	0.005662	0.001999	-0.0004926	-0.0008901	0.003742	-0.003350
WP03-C1-S1	1546.40	0.0003324	0.02655	0.006328	-0.003285	0.4149	0.04124	2.582	0.1758	-0.004448	0.0008362	0.001190	0.008852	-0.0001030

* distance from center of deposit

** All elements in ppm except Au which is in ppb

Appendix 8: White Pine
pyrite mineral chemistry by LA-ICP-MS

Sample	Distance* (m)	Zr90	Mo95	Ag107	Cd111	Sn118	Sb121	Te125	Ba137	Gd157	Hf178	Ta181	W182	Pt195
WP03-C1-S2	1546.40	-0.001153	0.002032	0.007418	-0.01430	0.4662	0.02834	3.337	0.3318	0.001715	0.0003734	-0.0003222	0.01531	-0.001286
WP03-C1-S3	1546.40	0.0002378	-0.001649	0.001995	-0.03295	0.4628	0.02833	1.530	0.1410	0.005663	-0.0003780	0.0003206	-0.0001829	-0.0005950
WP03-C1-S4	1546.40	0.001739	0.01251	-0.001270	-0.005527	0.3646	0.01186	1.295	0.01025	-0.002335	-0.002420	0.0004366	-0.0009749	0.004635
WP03-C1-S5	1546.40	-0.001910	-0.001095	0.004629	-0.01695	0.4226	0.03198	1.023	0.01663	-0.0002749	-0.0002499	0.001809	-0.001760	0.003939
WP03-C1-S6	1546.40	-0.00009375	-0.0001773	0.001226	-0.008332	0.4107	0.01062	0.1050	0.01976	-0.005572	0.001185	0.0007883	0.006529	0.001483
WP03-C1-S7	1546.40	0.01150	-0.006145	0.1119	0.02003	0.4071	-0.009763	0.2383	0.3279	-0.002682	-0.001218	0.001728	0.005745	0.001651
WP03-C1-S8	1546.40	0.002823	0.007835	0.02097	0.02197	0.4516	0.05728	0.3469	0.04321	0.002611	0.002397	0.0003812	-0.0001127	-0.0008758
WP06-C1-S1	1429.02	-0.004296	0.008244	0.01484	-0.01795	0.03546	0.0006630	0.4020	0.02307	-0.01424	-0.0008741	-0.002005	0.001174	-0.006543
WP06-C1-S2	1429.02	0.002499	0.005610	18.69	0.8842	0.07505	0.01821	2.188	0.3291	0.004000	0.008642	-0.002822	-0.01494	-0.009178
WP06-C1-S3	1429.02	0.003471	0.01275	0.001331	0.01893	0.002632	0.02280	0.2478	-0.007858	0.01209	-0.003841	0.003663	-0.01971	-0.002771
WP06-C1-S4	1429.02	-0.004206	-0.003158	-0.005183	0.05161	0.05373	-0.01661	0.1090	-0.002751	-0.01577	0.001583	0.0005675	-0.01148	-0.002904
WP06-C1-S5	1429.02	0.0004214	-0.001862	-0.001061	0.02822	0.02996	0.002972	0.7811	0.01137	0.03260	-0.002560	0.0005347	-0.003620	-0.0003234
WP06-C2-S10	1429.02	-0.005646	-0.01032	-0.006514	-0.0007252	0.04047	-0.002357	0.2745	-0.03930	-0.02023	0.002941	0.001604	0.003895	0.002102
WP06-C2-S6	1429.02	-0.007598	0.01372	-0.001283	0.05646	0.06018	0.004484	0.1745	0.02913	-0.008880	0.009198	0.002055	0.005743	0.01260
WP06-C2-S7	1429.02	-0.002867	-0.02405	0.001616	-0.01033	0.06951	-0.01470	0.2617	0.02427	0.007325	0.007882	0.001571	0.004919	0.01699
WP06-C2-S8	1429.02	0.01161	-0.003358	-0.02521	-0.005098	0.03899	0.0003115	0.4072	-0.01189	0.0008347	-0.01048	0.0006614	0.008567	0.0001665
WP06-C2-S9	1429.02	-0.001370	-0.01743	-0.007620	-0.03311	0.04925	0.01554	1.092	0.06096	-0.003767	-0.006586	0.001039	-0.01044	-0.004945
WP06-C3-S11	1429.02	0.01039	0.008960	-0.01034	-0.003026	0.04430	-0.01138	0.09398	-0.003690	-0.002891	0.0005998	-0.004416	0.002872	-0.005124
WP06-C3-S12	1429.02	0.007341	0.004019	-0.006294	0.06679	0.02981	-0.001855	0.07878	-0.002951	-0.006981	0.006333	0.001294	0.006025	-0.003156
WP06-C3-S13	1429.02	0.002102	0.004828	-0.0006708	-0.1257	0.04245	-0.01666	0.07847	-0.008547	0.01677	0.003402	-0.003853	-0.02465	-0.005375
WP06-C3-S14	1429.02	0.008214	-0.01206	0.003020	0.01356	0.02448	-0.02001	0.07893	-0.02935	0.04120	-0.002322	0.001050	0.01579	0.0001698
WP06-C3-S15	1429.02	-0.001232	-0.01575	-0.02023	-0.04347	0.02774	-0.01537	0.2364	0.03570	-0.02074	-0.008227	-0.005590	-0.001926	0.01237
WP17-C1-S1	712.89	0.002254	0.008624	0.01568	0.02453	0.1411	0.4659	0.7896	0.007615	0.005159	-0.002099	0.0004587	-0.002180	-0.005359
WP17-C1-S2	712.89	0.0002233	-0.02527	0.01190	-0.05917	0.1466	0.4571	0.4900	21.29	0.0004606	0.003329	0.00006734	-0.004092	0.002803
WP17-C1-S3	712.89	0.01260	0.00005160	0.009134	-0.02498	0.1759	0.4103	0.1140	-0.008050	0.009505	0.006343	-0.001439	-0.003124	-0.0009468
WP17-C1-S4	712.89	0.0004322	0.008337	-0.003192	0.01139	0.1950	0.4850	0.1325	0.002851	0.008972	-0.007650	-0.0006188	-0.007127	-0.002737
WP17-C1-S5	712.89	0.3637	0.01357	0.006118	-0.02823	0.1677	0.3953	0.02331	15.13	-0.002530	0.007133	0.0003489	-0.001932	0.002187
WP17-C1-S6	712.89	0.007116	0.01712	0.01149	-0.001022	0.1872	0.4023	0.1035	0.01344	0.0004615	0.0004215	-0.001128	0.005254	0.001677
WP17-C1-S7	712.89	-0.002930	0.007567	0.006614	0.03595	0.1942	0.6008	0.02859	-0.01191	-0.01116	-0.0006059	0.001088	-0.006122	-0.001851
WP17-C2-S10	712.89	-0.001087	0.3728	0.2723	0.07797	0.1756	0.2138	0.06116	68.55	-0.001111	-0.003761	-0.0003557	0.005824	-0.003528
WP17-C2-S11	712.89	-0.003955	1.226	0.4260	0.4230	0.1587	0.2579	0.09721	284.3	-0.003848	0.0008494	-0.0007553	0.01459	-0.00009820
WP17-C2-S12	712.89	-0.002622	-0.01253	-0.003938	0.000	0.1353	0.2584	0.1008	-0.007953	0.008027	0.000	-0.001577	-0.001290	0.000
WP17-C2-S13	712.89	0.7014	0.005247	0.005402	-0.03157	0.1465	0.2905	0.01103	-0.008778	0.008485	0.06843	-0.0004352	0.004004	0.002459
WP17-C2-S14	712.89	0.2715	0.01584	0.0008319	0.04220	0.1936	0.3636	0.06955	0.0009454	0.0006354	0.008838	-0.0003542	-0.007017	-0.003829
WP17-C2-S15	712.89	0.4785	-0.01075	0.05059	0.008869	0.1716	0.2543	1.453	0.02025	0.001645	-0.004030	0.0001214	0.009093	0.003700
WP17-C2-S8	712.89	0.006024	0.008313	-0.003839	0.03034	0.1415	0.3448	0.2047	0.006366	0.006441	0.004363	0.0006307	-0.002119	0.001263
WP17-C2-S9	712.89	0.001568	0.01088	0.002086	-0.03894	0.1466	0.3277	1.278	-0.003208	0.002023	-0.003282	-0.0003487	0.001848	0.005673
WP20-C1-S1	1110.01	0.006879	0.02428	0.002960	0.04446	0.05321	-0.007938	-0.05407	0.01681	0.001427	0.003244	0.003766	-0.004145	0.005400
WP20-C1-S10	1110.01	-0.004993	-0.01307	-0.005099	0.04010	0.06291	0.007158	0.1012	-0.03407	0.001126	0.005911	-0.001390	-0.006930	0.006514
WP20-C1-S11	1110.01	0.002810	0.005069	0.01169	0.04653	0.02469	-0.0006513	-0.04794	0.02201	0.006355	-0.002115	-0.0002017	-0.02053	0.001116
WP20-C1-S12	1110.01	-0.001009	0.003577	0.001884	0.05749	0.03583	0.009798	0.3615	-0.01817	-0.007109	-0.003323	-0.0009597	-0.005058	0.004552
WP20-C1-S13	1110.01	-0.002171	0.01436	0.006718	0.04650	0.03354	0.01655	-0.1227	-0.02594	0.01613	-0.009068	-0.0006487	-0.0001133	-0.003679
WP20-C1-S14	1110.01	0.001780	0.02228	-0.005672	0.04038	0.02321	-0.002992	0.08706	0.01309	0.004274	-0.007013	0.0001098	0.005321	0.001211

* distance from center of deposit

** All elements in ppm except Au which is in ppb

Appendix 8: White Pine
pyrite mineral chemistry by LA-ICP-MS

Sample	Distance* (m)	Zr90	Mo95	Ag107	Cd111	Sn118	Sb121	Te125	Ba137	Gd157	Hf178	Ta181	W182	Pt195
WP20-C1-S15	1110.01	0.001620	0.009135	-0.004920	0.02808	0.02132	-0.01032	0.07346	-0.01105	0.003217	-0.002137	-0.005098	0.01688	0.004055
WP20-C1-S2	1110.01	0.008295	-0.008609	-0.02453	-0.02259	0.01331	-0.006214	0.03108	-0.01070	-0.009583	0.004560	-0.001390	-0.01662	0.008047
WP20-C1-S3	1110.01	0.008252	0.01222	0.002806	-0.02065	0.06860	0.01110	0.07582	0.02035	-0.002022	-0.004469	0.001343	-0.001806	0.005684
WP20-C1-S4	1110.01	-0.002211	-0.02562	0.002178	-0.1038	0.05149	0.006729	0.08190	0.01353	0.001091	0.001821	-0.003503	0.001245	-0.004330
WP20-C1-S5	1110.01	0.001582	0.01995	0.003735	-0.02240	0.02585	-0.01266	-0.02672	0.01796	-0.004555	0.002022	-0.003075	-0.004632	0.0009270
WP20-C1-S6	1110.01	0.001735	0.02152	0.0007463	0.009925	0.02241	0.01254	0.008222	-0.01079	-0.01728	0.002946	-0.003325	-0.005543	-0.004507
WP20-C1-S7	1110.01	0.006839	-0.02226	-0.01909	-0.03245	0.02479	0.004856	0.1271	-0.01791	0.01344	-0.004216	-0.0005972	-0.007463	0.004905
WP20-C1-S8	1110.01	-0.001008	-0.01087	0.002848	0.02490	0.03478	0.005123	-0.03543	0.02042	-0.02183	-0.001732	-0.002510	-0.002789	0.008713
WP20-C1-S9	1110.01	0.005582	0.001375	-0.01481	0.02547	0.04272	-0.002160	0.09662	-0.01505	-0.002071	-0.007016	0.002214	0.002786	-0.003244
WP23-C1-S1	1688.35	0.0008037	0.01916	0.1895	0.02478	0.1324	0.4239	0.09587	0.01442	-0.006968	-0.003733	0.001520	0.003134	0.001142
WP23-C1-S2	1688.35	-0.0006112	-0.005800	0.01015	0.02821	0.1677	0.3157	0.08130	-0.01684	-0.001245	-0.005224	-0.0004181	0.003625	0.003205
WP23-C1-S3	1688.35	0.001869	0.005202	0.006406	-0.006051	0.1833	0.3688	0.06078	-0.01544	0.01388	-0.004834	-0.0005884	0.004876	-0.008573
WP23-C1-S4	1688.35	0.001107	0.007812	0.003296	-0.001687	0.1451	0.3269	0.09864	0.0003449	-0.009996	0.003308	0.00006901	0.003680	0.003390
WP23-C2-S5	1688.35	-0.001590	0.001274	0.06509	-0.06852	0.1926	0.2655	0.1048	-0.009227	0.0008990	0.006599	0.0006118	0.004109	-0.008050
WP23-C2-S6	1688.35	-0.0006908	0.004219	0.01799	-0.006459	0.1927	0.2752	-0.02515	0.2491	-0.01162	-0.005098	-0.001336	0.01758	-0.003103
WP23-C2-S7	1688.35	-0.001448	0.001961	0.002036	0.06809	0.1931	0.2741	0.1433	-0.02260	0.001033	0.001872	-0.0008694	-0.004483	-0.002931
WP23-C2-S8	1688.35	-0.0007724	0.004521	0.002348	-0.02511	0.2195	0.2888	0.02142	-0.008554	-0.01114	0.0009364	0.0005672	0.002127	0.0004095
WP23-C3-S10	1688.35	0.003152	0.009879	-0.003262	-0.06023	0.1808	0.3001	0.02908	-0.007360	0.008449	-0.004239	-0.00005463	-0.001999	0.002432
WP23-C3-S11	1688.35	0.002914	0.005950	0.0003369	-0.0001107	0.2159	0.3293	0.01538	-0.009805	-0.004059	0.0006607	-0.001421	-0.0009163	0.0002133
WP23-C3-S12	1688.35	0.0002354	-0.01186	-0.003927	-0.02567	0.2010	0.2588	0.1441	0.003035	-0.001101	-0.0006161	0.0004096	-0.001621	0.003211
WP23-C3-S13	1688.35	0.002791	0.006052	0.003146	-0.01107	0.2034	0.3363	0.04202	0.005643	-0.004888	-0.001322	-0.001190	0.0004575	0.001739
WP23-C3-S9	1688.35	0.002954	-0.003535	-0.01134	0.009613	0.1761	0.3524	0.09304	-0.003667	-0.004942	-0.0001691	-0.0005510	0.0009162	0.001679
WP26-C1-S1	1314.77	0.005155	0.0008459	-0.002712	-0.003314	0.2487	0.02630	0.08118	-0.01334	0.0004270	-0.0004568	-0.0006312	-0.002064	0.001763
WP26-C1-S2	1314.77	0.000	0.003896	0.009573	0.03400	0.2629	0.02381	0.01601	0.005276	-0.007244	0.0002473	0.0004214	-0.001006	-0.003167
WP26-C1-S3	1314.77	0.001747	-0.01355	-0.003309	0.02914	0.2669	0.05735	0.04873	-0.006456	-0.004337	-0.002088	0.0007370	0.0004191	0.0001861
WP26-C1-S4	1314.77	0.0009966	-0.0005789	-0.005414	0.002401	0.2432	0.03875	0.02317	0.0006513	-0.004594	-0.006318	-0.001357	-0.003522	-0.003513
WP26-C1-S5	1314.77	-0.001489	-0.001928	0.02636	0.009773	0.2259	0.03455	0.03542	0.02482	-0.0001618	0.005526	0.0005497	-0.002735	0.001534
WP26-C1-S6	1314.77	-0.001178	-0.003002	0.0007093	-0.01229	0.2895	0.004359	0.1389	0.01200	-0.003693	0.0006668	-0.0003305	0.01593	0.001031
WP26-C2-S10	1314.77	-0.002114	0.001962	0.01073	0.002711	0.2925	0.01301	0.07980	0.002201	0.003729	0.001483	0.00007264	0.001187	0.0005723
WP26-C2-S11	1314.77	-0.002013	0.01107	0.2127	-0.01752	0.3489	0.04004	0.5241	0.01744	-0.008990	-0.002953	0.0003002	0.007235	-0.005210
WP26-C2-S12	1314.77	0.005527	-0.002297	-0.01597	0.01535	0.2882	0.02170	0.01646	-0.005646	0.003640	-0.001157	0.001008	0.03533	-0.002168
WP26-C2-S13	1314.77	0.004693	-0.0008065	-0.002732	0.02511	0.3223	0.02654	0.1994	-0.004051	-0.004629	0.001649	-0.0004333	-0.003539	0.006618
WP26-C2-S14	1314.77	0.0001166	-0.005438	0.008614	0.02517	0.3308	0.01911	0.02604	0.01327	-0.006110	0.0001012	0.0007486	-0.004572	0.004466
WP26-C2-S15	1314.77	0.006354	-0.0008209	-0.002928	0.04390	0.3166	-0.009022	0.08623	-0.01180	0.003436	-0.002737	0.0005394	0.002913	-0.007219
WP26-C2-S8	1314.77	0.002826	0.008411	0.001529	0.02405	0.2568	-0.004364	0.04964	-0.008759	-0.002794	0.002325	-0.0001193	0.001241	0.0005951
WP26-C2-S9	1314.77	0.002846	0.0004301	-0.003745	-0.006141	0.2935	0.02967	0.03139	0.007401	0.0002160	0.002376	-0.0009137	0.001806	0.0009189
WP27-C1-S1	1182.57	-0.002797	0.01281	-0.005020	-0.001076	0.2134	0.2727	-0.03051	-0.005104	-0.006495	-0.002194	0.0005169	-0.0006146	0.004966
WP27-C1-S2	1182.57	0.001962	-0.008926	0.005824	-0.001090	0.2310	0.2822	0.1617	0.01373	0.006040	-0.001259	0.0008532	0.002945	-0.001171
WP27-C1-S3	1182.57	0.004828	-0.01519	0.1706	0.007019	0.2683	0.3672	0.1335	0.007833	-0.009794	0.008921	-0.0007910	-0.003507	0.002535
WP27-C1-S4	1182.57	0.006520	0.009697	0.4336	0.001540	0.2092	0.2549	0.2187	0.1650	0.01365	-0.005756	0.0005019	0.01466	0.006565
WP27-C2-S5	1182.57	0.0001031	0.005917	0.3173	0.004615	0.2168	0.1932	0.1669	0.02147	-0.004337	0.008741	-0.0001291	-0.005994	0.0006098
WP27-C2-S6	1182.57	-0.005055	0.01510	-0.006549	-0.02703	0.1804	0.2228	0.01200	0.02371	-0.006814	-0.004590	0.002365	0.01237	0.007086
WP27-C2-S7	1182.57	0.004377	0.1999	0.004647	0.04794	0.2943	0.1890	0.2456	0.006646	0.008748	0.01191	0.0007387	0.004510	-0.0007675

* distance from center of deposit

** All elements in ppm except Au which is in ppb

Appendix 8: White Pine
pyrite mineral chemistry by LA-ICP-MS

Sample	Distance* (m)	Zr90	Mo95	Ag107	Cd111	Sn118	Sb121	Te125	Ba137	Gd157	Hf178	Ta181	W182	Pt195
WP27-C2-S8	1182.57	0.01104	-0.002079	0.001360	-0.003720	0.2217	0.1547	0.1181	0.01879	0.001006	-0.0005473	0.001236	0.004958	-0.006182
WP27-C3-S10	1182.57	0.003807	0.009033	0.04469	0.0006636	0.2287	0.1503	-0.02322	0.01003	-0.005380	0.006982	0.0001617	0.001889	-0.0009971
WP27-C3-S11	1182.57	0.001125	-0.0001630	0.01742	-0.02406	0.2473	0.1442	0.008577	-0.002567	0.003958	0.001268	-0.0002148	-0.002116	0.001801
WP28-C1-S1	1183.91	0.001169	-0.011116	-0.002904	0.007266	0.1897	0.3938	0.2198	0.05850	0.004197	-0.0004069	-0.0004069	0.007563	0.002131
WP28-C1-S2	1183.91	-0.001512	-0.005852	0.2287	0.008508	0.1664	0.4194	0.1911	4.031	0.003030	-0.002776	-0.0008976	-0.001492	-0.001975
WP28-C1-S3	1183.91	-0.007793	0.01266	0.007130	-0.01227	0.1681	0.2931	-0.01214	-0.009262	0.01627	0.000	-0.002777	0.002460	-0.001873
WP28-C1-S5	1183.91	0.0001250	-0.0004028	0.005010	0.007493	0.1724	0.3334	0.1731	0.006822	0.005788	0.002878	-0.0007056	-0.001273	-0.0008734
WP28-C1-S6	1183.91	0.000	0.001673	0.0005047	0.008684	0.1484	0.4132	0.05856	-0.004790	0.01110	-0.001482	0.0006798	0.01383	-0.001976
WP28-C1-S7	1183.91	-0.0009903	0.05654	0.01286	0.01334	0.1547	0.2464	0.04218	-0.01299	0.005917	-0.007126	-0.001295	0.0008192	-0.004739
WP28-C2-S10	1183.91	-0.0007106	-0.0008870	-0.004753	0.01218	0.1717	0.3233	0.1581	-0.004622	0.0005084	0.0002320	0.0009319	-0.003289	-0.003125
WP28-C2-S11	1183.91	-0.0007075	0.01846	-0.0003414	0.01678	0.2095	0.2602	-0.03101	0.006099	0.004140	-0.002967	-0.001522	-0.0003274	-0.007266
WP28-C2-S12	1183.91	-0.001063	-0.001171	0.08234	0.01361	0.2063	0.2954	0.06261	-0.009094	-0.006176	0.003661	-0.002439	-0.002538	-0.0006748
WP28-C2-S13	1183.91	0.002700	-0.005246	-0.009312	0.01587	0.1903	0.2936	0.04405	0.009460	0.003354	-0.0007005	-0.001123	0.0001349	0.004624
WP28-C2-S14	1183.91	0.003446	-0.001587	0.01022	-0.02737	0.1656	0.2802	0.03511	-0.01437	-0.009978	0.0008811	0.0003119	-0.001006	0.003872
WP28-C2-S8	1183.91	-0.003183	0.02187	0.5653	0.003677	0.1790	0.3904	0.09064	0.1257	-0.006435	0.003545	0.003366	0.004424	-0.004451
WP28-C2-S9	1183.91	0.002636	-0.006857	0.01859	0.01831	0.1648	0.3468	-0.01795	0.01899	-0.01032	-0.004290	-0.002759	0.0006203	0.003911
WP30-C1-S1	2282.00	-0.001842	0.002041	-0.003973	0.03503	0.1809	0.1647	0.1653	0.002770	0.002156	0.002396	0.0003163	0.001937	0.0001121
WP30-C1-S2	2282.00	0.002889	-0.007305	0.01124	0.007578	0.1679	0.1265	0.4631	-0.004748	-0.007721	0.001061	-0.0003971	0.01041	0.001020
WP30-C1-S3	2282.00	0.001905	0.006293	-0.0001998	-0.03643	0.1903	0.1656	0.07238	-0.01543	-0.001151	0.001850	0.0003858	-0.005314	0.005038
WP30-C1-S4	2282.00	0.000	-0.02093	-0.001650	0.03724	0.1537	0.2006	1.274	0.001833	-0.002924	0.006501	-0.0008579	-0.005642	-0.006407
WP30-C1-S5	2282.00	-0.0002379	-0.007802	-0.005594	0.03178	0.1630	0.1623	0.2394	0.006679	-0.0004724	0.003307	-0.0006931	-0.001367	0.001370
WP30-C2-S10	2282.00	0.002134	-0.007650	-0.004870	0.01435	0.1958	0.3262	0.2036	0.003725	-0.006406	0.0001190	0.001461	-0.003670	0.01020
WP30-C2-S7	2282.00	0.001288	-0.01497	0.005625	0.01247	0.2266	0.2223	0.03621	0.003804	0.008118	0.0002428	-0.0008157	0.006381	-0.006181
WP30-C2-S8	2282.00	0.004273	0.002693	0.001537	0.05587	0.2053	0.1967	0.1374	-0.002656	0.0002682	-0.001516	-0.0005640	-0.003188	-0.001575
WP30-C2-S9	2282.00	-0.001692	0.01347	0.04728	-0.04909	0.2077	0.1657	0.4000	2.109	-0.001249	-0.003083	-0.0003385	0.004677	0.003720
WP30-C3-S12	2282.00	0.006298	-0.001695	-0.007998	-0.01073	0.2208	0.1511	0.2070	0.01723	0.006433	0.006715	0.001077	-0.001902	0.0002136
WP30-C3-S13	2282.00	0.002399	-0.008372	0.0001031	-0.007892	0.1745	0.1204	0.1820	-0.04151	-0.009341	0.00009497	0.001188	0.01009	-0.004791
WP30-C3-S14	2282.00	-0.0005548	0.005544	2.230	0.01049	0.2006	0.1679	0.4172	0.3207	0.002288	0.001046	-0.0004631	0.002961	0.002097
WP30-C3-S15	2282.00	0.002802	-0.007037	0.6486	0.03512	0.2286	0.1049	0.07712	0.08207	0.007592	0.0009208	0.001865	0.001081	0.004246
WP33-C1-S1	2078.05	0.003518	0.002558	0.006535	-0.002963	0.1687	0.2217	0.2950	0.004004	0.007657	-0.002026	0.002121	-0.005937	-0.0009425
WP33-C1-S10	2078.05	-0.007771	0.003966	-0.006187	-0.03144	0.2033	0.2139	0.1747	-0.009908	-0.001150	0.0002243	0.0005832	-0.002614	-0.003479
WP33-C1-S11	2078.05	-0.002873	0.003840	0.001834	-0.009017	0.1581	0.1781	-0.02428	-0.004230	0.01120	-0.005304	-0.0008441	-0.002937	0.0002093
WP33-C1-S12	2078.05	-0.001427	-0.01052	0.005403	-0.01486	0.1631	0.2331	1.556	0.01961	-0.002676	-0.002731	-0.001351	0.01932	-0.002068
WP33-C1-S2	2078.05	0.005416	0.009060	-0.006297	0.01127	0.2167	0.2104	0.06888	0.005744	0.006010	-0.003645	-0.0004651	-0.007826	-0.008134
WP33-C1-S3	2078.05	-0.003282	-0.005574	0.006054	-0.03487	0.2031	0.2319	0.06276	0.003419	0.003953	-0.001028	0.0005735	-0.002482	0.004636
WP33-C1-S4	2078.05	0.002445	0.006974	0.001277	0.01345	0.1729	0.1837	0.1106	0.01544	0.004984	-0.0002765	-0.0001322	-0.0008617	-0.003940
WP33-C1-S5	2078.05	-0.002392	0.0006765	-0.009277	-0.04581	0.1795	0.2103	0.1100	-0.01074	0.003111	0.0007076	0.0003308	-0.001223	0.0008469
WP33-C1-S7	2078.05	-0.001676	-0.007159	-0.01406	0.01236	0.1794	0.1612	0.1919	-0.004274	-0.004759	0.003537	0.00006898	-0.0004102	-0.008673
WP33-C1-S8	2078.05	0.002812	0.07176	0.006347	0.04867	0.2130	0.1972	1.003	0.005164	0.001183	0.002601	-0.0003000	0.00009253	-0.002381
WP33-C1-S9	2078.05	-0.005018	-0.01075	0.04925	-0.006721	0.1847	0.1908	0.1588	0.008823	-0.001133	0.002761	0.0003751	0.009705	-0.001520
WP36-C1-S1	1404.01	0.003436	0.01031	0.06711	0.01078	0.1244	0.6542	0.2351	0.01070	-0.009337	0.001682	0.001909	-0.0005359	0.001876
WP36-C1-S2	1404.01	0.001786	0.01482	0.06398	0.02806	0.1244	0.5078	0.5812	0.0004924	-0.006217	-0.0007067	0.001111	0.001086	-0.003872
WP36-C1-S3	1404.01	0.000	-0.009695	0.009954	0.008669	0.1243	0.4102	0.8711	0.008747	-0.004410	-0.001667	0.001139	0.002797	-0.003798

* distance from center of deposit

** All elements in ppm except Au which is in ppb

Appendix 8: White Pine
pyrite mineral chemistry by LA-ICP-MS

Sample	Distance* (m)	Zr90	Mo95	Ag107	Cd111	Sn118	Sb121	Te125	Ba137	Gd157	Hf178	Ta181	W182	Pt195
WP36-C1-S4	1404.01	0.002709	-0.006369	0.4825	0.01075	0.1226	0.5792	2.582	0.01636	0.001095	0.001755	-0.0003972	0.005893	0.006578
WP36-C1-S5	1404.01	0.0002883	0.007036	0.01020	0.01111	0.1847	0.6172	0.08644	0.01630	-0.003922	-0.003704	-0.0002449	0.01293	0.004144
WP36-C1-S6	1404.01	0.001729	-0.002545	0.06250	-0.01023	0.1335	0.6874	0.05603	0.01070	0.003616	-0.0009008	0.001066	-0.002824	-0.002990
WP36-C2-S10	1404.01	0.3023	0.009347	25.87	0.006962	0.1869	0.2298	2.058	2.463	0.01364	0.009778	0.0008351	0.003968	0.0003878
WP36-C2-S11	1404.01	0.7625	0.1552	43.63	0.04040	0.3112	0.4628	0.2645	414.0	0.03221	0.02418	0.001049	0.01832	-0.001932
WP36-C2-S12	1404.01	0.005632	-0.01249	0.3020	-0.03996	0.1574	0.4481	0.9841	0.2094	-0.008019	0.0007853	0.0003956	0.006080	-0.003822
WP36-C2-S7	1404.01	0.001350	0.01748	-0.004193	0.008667	0.1953	0.7338	0.08980	-0.003336	0.004190	0.005360	-0.001008	-0.002139	0.004895
WP36-C2-S8	1404.01	0.0007393	0.006760	0.0007832	-0.04026	0.1671	0.5528	0.5035	-0.001388	-0.005569	0.003559	-0.001411	0.006982	-0.0002457
WP36-C2-S9	1404.01	-0.001175	0.02633	0.01040	-0.03788	0.1423	0.4062	0.3478	-0.003290	-0.004899	-0.002154	0.0004251	-0.01296	-0.006088
WP40-C1-S1	1139.14	0.0001213	0.01004	0.001554	0.03059	0.2799	0.009682	0.1577	0.002617	-0.006360	0.003295	0.0003229	-0.003826	0.001853
WP40-C1-S10	1139.14	0.001934	-0.005139	0.02013	0.03551	0.2758	-0.01639	2.098	0.0006635	0.003645	-0.003474	0.001495	0.004281	0.004232
WP40-C1-S11	1139.14	0.002867	0.008848	0.1327	-0.02018	0.3069	0.02099	1.512	-0.004126	0.002175	0.0003062	-0.0001858	0.005162	0.005775
WP40-C1-S12	1139.14	0.008733	-0.01139	0.006225	0.01234	0.3015	0.01531	2.108	0.0003493	-0.006263	0.001030	0.0008557	-0.002180	0.003415
WP40-C1-S13	1139.14	-0.001738	0.004188	0.006781	0.02733	0.2689	0.01802	5.659	-0.001667	0.008595	0.001950	-0.0003268	-0.009087	0.0002447
WP40-C1-S14	1139.14	0.006788	-0.0007544	0.004187	-0.04236	0.3131	0.04979	0.1880	-0.006879	0.01276	-0.001532	0.0006945	0.0008595	0.003866
WP40-C1-S15	1139.14	0.008369	-0.001085	-0.008604	0.03581	0.3107	0.02544	2.495	0.01300	0.005470	-0.002069	-0.0001551	-0.001264	0.004652
WP40-C1-S2	1139.14	-0.005226	0.002536	0.001005	0.02115	0.2873	0.02027	1.321	-0.006648	0.003849	0.003378	0.001085	0.0003429	0.004822
WP40-C1-S3	1139.14	-0.0008154	0.009196	0.008309	0.002627	0.2695	0.01378	9.389	-0.004928	-0.006173	-0.002900	-0.0004488	-0.007829	0.001870
WP40-C1-S4	1139.14	0.001060	-0.008029	-0.006779	-0.02760	0.2730	0.007558	0.1844	-0.001947	-0.006632	0.0002096	0.0007739	-0.0006369	-0.004899
WP40-C1-S5	1139.14	0.006927	0.007670	0.004146	0.05527	0.2609	0.04915	1.169	0.005017	0.006341	0.00009366	0.000	-0.001139	0.006533
WP40-C1-S6	1139.14	0.002487	0.02390	0.006061	-0.003009	0.2522	0.04615	5.123	0.1405	-0.003758	-0.001543	-0.0009399	0.003599	0.001732
WP40-C1-S7	1139.14	0.002737	0.02406	0.04976	-0.007560	0.2307	0.005243	45.70	0.01509	0.000	-0.002508	0.0002796	-0.003250	-0.001152
WP40-C1-S8	1139.14	0.0003183	0.002082	0.008167	-0.01628	0.2274	0.04177	53.04	0.01711	-0.0008510	0.000	0.001341	0.005194	0.001016
WP40-C1-S9	1139.14	0.005574	0.02405	0.1312	-0.02175	0.2759	0.01555	5.795	-0.001246	0.003504	0.001589	0.0006101	0.002042	0.003314
WP44-C1-S2	622.10	0.004348	-0.009078	-0.009482	-0.004738	0.3125	0.05839	0.4827	0.007458	-0.0002682	-0.002001	-0.0002100	0.002162	0.0009697
WP44-C1-S3	622.10	0.002700	0.006251	0.007059	-0.02128	0.2792	0.04440	0.2400	-0.01389	0.003851	0.005442	-0.002303	0.0003223	-0.0009102
WP44-C1-S4	622.10	0.001783	-0.005676	0.006049	0.006554	0.3302	0.03925	0.04631	0.01289	0.01034	0.0001004	-0.0006775	0.005001	-0.001093
WP44-C1-S5	622.10	0.002917	0.009174	0.01292	-0.006995	0.2737	0.02724	0.003814	0.01765	0.0002209	-0.001343	-0.0009278	0.002670	-0.0004730
WP44-C2-S6	622.10	-0.0004791	-0.009796	0.001303	0.04121	0.3570	0.06288	0.06231	-0.01181	-0.002722	-0.0004134	-0.0001328	-0.001315	0.0004627
WP44-C2-S7	622.10	-0.001639	0.006234	0.006777	-0.03472	0.2560	-0.008603	0.7084	0.01847	0.006208	-0.002827	0.000	-0.007499	-0.003613
WP44-C3-S13	622.10	0.005725	0.002472	-0.001866	0.05598	0.3174	0.02748	0.07547	-0.002289	-0.006624	0.001713	-0.0004152	-0.0005205	0.005755
WP44-C3-S14	622.10	-0.003301	-0.02783	-0.008028	-0.03477	0.3339	0.01739	0.2584	-0.01861	0.01324	0.0001291	-0.0004352	0.001786	-0.001558
WP44-C3-S15	622.10	0.003685	-0.006096	-0.0007740	0.03011	0.3421	0.01311	0.1635	0.01694	-0.004561	-0.005822	-0.001648	-0.001981	-0.0006121
WP52-C1-S1	785.45	0.003607	0.01769	0.09810	-0.02334	0.2832	0.02675	-0.04293	0.09159	-0.005581	-0.003795	0.0009841	-0.001584	-0.002964
WP52-C1-S2	785.45	-0.003628	0.001594	-0.004410	-0.001688	0.4055	0.02427	0.1918	0.003229	-0.004002	0.003794	-0.00008834	-0.0001188	-0.001081
WP52-C1-S3	785.45	0.01523	0.009661	0.01025	0.01818	0.3731	0.003396	0.09273	0.004892	0.000	-0.004183	0.0004715	0.001616	-0.004543
WP52-C1-S4	785.45	0.02002	0.01286	0.01201	0.06179	0.3826	-0.001877	0.05142	0.01850	0.003255	-0.004062	0.000	-0.001326	-0.004442
WP52-C1-S5	785.45	-0.001532	0.009483	0.02941	0.02043	0.3629	0.05282	0.007947	0.2847	-0.01432	-0.001300	-0.0004176	0.0003996	-0.004328
WP52-C2-S10	785.45	-0.0005308	0.009700	0.03400	0.009997	0.4714	0.04248	0.03989	0.03395	-0.004944	0.001399	0.0009633	-0.003153	-0.002668
WP52-C2-S6	785.45	0.007501	0.001073	-0.0008907	-0.01350	0.3439	0.02883	0.07834	0.0007918	0.000	0.0007259	-0.001300	0.006167	-0.001136
WP52-C2-S7	785.45	0.003453	0.01193	0.01405	0.05536	0.3468	0.01641	0.06102	-0.002991	0.003403	-0.001218	-0.0001957	-0.0009805	-0.0004929
WP52-C2-S8	785.45	0.006613	0.001965	0.006821	-0.002286	0.4204	0.02456	0.1196	0.0006720	0.002181	-0.002836	0.00003294	-0.001869	0.001755
WP52-C2-S9	785.45	0.0005634	0.0005551	0.01540	0.009918	0.3789	0.02063	0.08890	0.01368	-0.0009949	-0.0006784	0.0007428	-0.0009687	0.0006127

* distance from center of deposit

** All elements in ppm except Au which is in ppb

Appendix 8: White Pine
pyrite mineral chemistry by LA-ICP-MS

Sample	Distance* (m)	Zr90	Mo95	Ag107	Cd111	Sn118	Sb121	Te125	Ba137	Gd157	Hf178	Ta181	W182	Pt195
WP52-C3-S11	785.45	0.005323	0.007947	0.01434	0.01471	0.4527	0.01889	0.1059	0.01288	0.0006894	-0.006233	-0.0002771	0.002931	-0.001733
WP52-C3-S12	785.45	-0.0006235	0.01379	0.002524	0.004387	0.6138	0.01666	0.04206	-0.001735	-0.003915	-0.001782	0.0008058	0.004013	0.004837
WP52-C3-S13	785.45	-0.0006868	-0.005829	0.002439	0.01118	0.4205	0.02052	0.1350	-0.005738	-0.0007183	0.0008358	-0.0008290	0.001084	-0.003843
WP52-C3-S14	785.45	0.0002381	-0.005675	0.004926	0.01517	0.4487	0.01188	0.1435	0.0006633	-0.004424	0.0009738	0.0002805	0.001966	-0.0006219
WP52-C3-S15	785.45	0.001987	0.001128	0.0009495	0.01548	0.4383	0.03678	-0.03198	0.005539	0.0002259	0.0003088	0.001014	-0.007732	-0.001612
WP54-C1-S1	432.59	0.0008023	0.0001869	0.00009777	-0.01127	0.3056	0.05165	0.1330	-0.006164	0.0003723	-0.001273	0.0002182	0.02433	-0.002105
WP54-C1-S2	432.59	0.003531	0.002863	-0.004341	0.02589	0.4505	0.03459	0.09078	-0.0003217	-0.007197	-0.001786	-0.0005741	-0.0002069	0.001735
WP54-C1-S3	432.59	0.004685	-0.001896	0.004571	0.009384	0.3481	0.02304	-0.06929	-0.004339	-0.002884	0.003297	0.0002841	-0.004642	0.001085
WP54-C1-S4	432.59	-0.004214	0.002376	0.008497	0.02463	0.4375	0.01954	0.1282	0.04346	0.006798	-0.002121	0.0002813	-0.003681	0.002937
WP54-C1-S5	432.59	0.001223	-0.01562	0.008213	-0.01789	0.3769	0.01323	0.1136	-0.004254	-0.009042	-0.003992	-0.0004142	0.002065	-0.002919
WP54-C1-S6	432.59	0.009911	-0.005990	-0.003307	0.005841	0.3928	0.04006	0.1743	0.1896	0.002634	-0.003911	-0.0004610	0.0007751	0.0004091
WP54-C2-S10	432.59	0.004743	-0.009527	-0.005971	-0.03524	0.3857	0.03047	0.07358	-0.007274	-0.004843	-0.001084	-0.0009335	0.0003342	0.0003855
WP54-C2-S11	432.59	0.001084	0.006959	0.0003240	0.02140	0.3617	0.03303	-0.02321	-0.009018	0.004603	0.001174	0.0003366	-0.001789	0.004742
WP54-C2-S12	432.59	0.005615	0.001493	-0.005168	0.005665	0.3596	0.01820	-0.03064	0.09350	0.002334	-0.0001294	-0.0008909	0.002116	-0.0002895
WP54-C2-S13	432.59	-0.0004563	0.007044	0.2180	0.04663	0.3284	0.04267	-0.008181	2.793	-0.008686	0.0009288	0.001146	0.008549	0.0006978
WP54-C2-S14	432.59	0.001048	-0.01109	0.004660	0.04853	0.4023	0.006189	0.08025	0.7468	-0.001054	-0.0004789	-0.0004403	-0.0003996	-0.0006475
WP54-C2-S15	432.59	0.001491	0.01902	-0.002298	-0.006913	0.4300	0.03739	0.03282	0.3482	-0.006184	0.001711	-0.0006285	-0.006183	0.002738
WP54-C2-S8	432.59	-0.003142	-0.004100	0.002017	0.02833	0.3745	0.01577	0.08917	-0.004826	-0.003499	-0.0002610	-0.00004197	0.001995	-0.002306
WP54-C2-S9	432.59	0.001053	-0.004332	0.01220	-0.003542	0.4151	0.02604	0.07443	0.0006802	-0.004528	0.002472	-0.001899	-0.002078	-0.003932
WP63-C1-S1	0.00	0.007495	13.72	0.6704	0.01110	0.1913	0.4214	0.1234	0.02802	0.002129	-0.001812	0.0002823	0.01577	0.001851
WP63-C1-S10	0.00	-0.002688	-0.02110	0.04514	0.03091	0.1946	0.2793	0.08167	0.008831	0.003760	-0.001872	-0.002167	-0.0009419	-0.002928
WP63-C1-S11	0.00	0.002392	0.004089	0.004082	-0.005117	0.1864	0.2984	0.03379	0.01029	0.003561	0.0003464	-0.001480	0.003482	-0.0005177
WP63-C1-S12	0.00	0.002158	-0.007085	0.01249	0.2135	0.1624	0.3444	0.09245	0.0007120	-0.004775	-0.002915	0.001893	-0.003776	-0.005949
WP63-C1-S13	0.00	-0.003276	-0.0009357	0.1494	-0.02579	0.1640	0.2739	0.1302	-0.009911	0.003143	-0.0002057	-0.001512	-0.0004395	0.003376
WP63-C1-S14	0.00	0.002901	0.06503	0.6903	-0.007147	0.1862	0.9709	0.06271	-0.01256	-0.002779	-0.003857	-0.0001690	0.007604	0.006125
WP63-C1-S2	0.00	0.005422	0.01643	0.01313	-0.03463	0.1620	0.3151	-0.005523	-0.004941	0.005049	0.003919	-0.0001323	0.0001025	-0.001631
WP63-C1-S3	0.00	0.0002786	0.007916	0.01257	-0.02682	0.2045	0.2320	0.04311	-0.02072	0.006779	-0.003512	0.00008355	0.01168	-0.002423
WP63-C1-S4	0.00	-0.001429	0.002818	0.03455	0.001950	0.1696	0.3086	0.1333	0.0003504	0.01802	0.007521	-0.001158	-0.003476	-0.002711
WP63-C1-S5	0.00	0.3771	184.5	29.01	0.1467	0.3527	21.09	2.913	3.404	0.08807	0.02014	0.003554	0.2710	0.007049
WP63-C1-S6	0.00	0.006392	-0.002095	0.01413	-0.006802	0.1715	0.3144	0.08352	0.01697	0.0002371	-0.001554	-0.0007011	-0.001196	-0.003834
WP63-C1-S7	0.00	0.001125	0.02593	0.04166	-0.01685	0.1587	0.4821	0.09057	0.005396	-0.001101	0.001980	0.001105	0.0002689	0.003948
WP63-C1-S8	0.00	0.006000	-0.006225	0.003909	0.003858	0.2298	0.3600	0.02138	0.008599	-0.008592	-0.001504	-0.0006478	0.007999	0.006426
WP63-C1-S9	0.00	0.001043	0.002466	0.1337	0.04841	0.1821	0.2592	0.09704	0.02791	0.01546	0.0003352	-0.001203	-0.002704	0.002886

* distance from center of deposit

** All elements in ppm except Au which is in ppb

Appendix 8: White Pine
pyrite mineral chemistry by LA-ICP-MS

Sample	Distance* (m)	Au197**	Tl205	Pb208	Bi209	U238
ESWP001-C1-S1	161.31	-0.00007220	-0.00009591	0.005119	0.04513	0.001241
ESWP001-C1-S2	161.31	0.001184	0.003496	74.49	0.2346	1.350
ESWP001-C1-S3	161.31	-0.002185	-0.0002404	0.01632	0.07530	-0.0003167
ESWP001-C1-S4	161.31	0.00001485	-0.001119	0.01481	0.04756	-0.00002688
ESWP001-C1-S5	161.31	-0.001449	0.001096	0.009963	0.02062	-0.0003095
ESWP001-C1-S6	161.31	0.004898	0.0009026	1.401	4.313	4.882
ESWP001-C1-S7	161.31	0.0006134	0.06895	9.252	5.072	0.06385
ESWP001-C2-S10	161.31	0.0008881	0.0007589	0.01180	0.01632	0.00009764
ESWP001-C2-S11	161.31	-0.0003628	-0.0006315	0.1276	0.04453	-0.0001254
ESWP001-C2-S12	161.31	-0.002624	-0.002363	0.4011	0.3692	0.007925
ESWP001-C2-S13	161.31	0.0003416	-0.0002259	0.3037	1.757	0.04439
ESWP001-C2-S14	161.31	0.004972	0.0007073	0.8354	1.405	3.245
ESWP001-C2-S8	161.31	0.001017	-0.0008933	0.01285	0.007218	-0.0002000
ESWP001-C2-S9	161.31	0.002481	-0.001484	0.02855	0.02225	0.0006521
ESWP002-C1-S1	132.23	-0.003792	-0.0001722	0.02439	0.01853	-0.0009539
ESWP002-C1-S10	132.23	0.003255	-0.001036	0.009593	0.01332	-0.0001211
ESWP002-C1-S11	132.23	0.01273	0.002560	0.02180	0.01346	0.001202
ESWP002-C1-S12	132.23	-0.002271	0.0008945	0.005145	0.003812	-0.0003016
ESWP002-C1-S13	132.23	-0.0006609	0.002615	0.04062	0.003370	-0.0005629
ESWP002-C1-S14	132.23	-0.001784	-0.002647	0.005084	0.003651	0.0005977
ESWP002-C1-S15	132.23	0.00008947	-0.0003029	0.007166	0.002297	-0.001036
ESWP002-C1-S3	132.23	0.005687	0.0002159	0.03361	0.01454	0.004164
ESWP002-C1-S4	132.23	-0.001320	-0.0001457	0.009305	0.009259	-0.0002430
ESWP002-C1-S5	132.23	-0.001588	-0.001115	0.01050	0.005868	0.0006466
ESWP002-C1-S6	132.23	0.0001832	0.002563	0.009537	0.006645	-0.001228
ESWP002-C1-S7	132.23	0.002139	-0.001028	0.005660	0.002609	0.00008593
ESWP002-C1-S8	132.23	0.0007396	0.0003600	0.006110	0.0004026	-0.0004993
ESWP002-C1-S9	132.23	0.002655	0.001731	0.004925	0.003874	-0.0008865
ESWP006-C1-S1	1429.02	-0.0005488	0.0009436	0.1921	2.040	-0.0004196
ESWP006-C1-S2	1429.02	-0.0003836	-0.0001520	0.008496	0.02556	0.0002094
ESWP006-C1-S3	1429.02	0.001794	0.001371	0.3917	2.453	0.006201
ESWP006-C1-S4	1429.02	0.001620	0.0001713	0.008498	0.008194	0.0009600
ESWP006-C1-S5	1429.02	-0.0006375	0.0001521	0.02556	0.002671	0.0005489
ESWP006-C1-S6	1429.02	0.005465	-0.003176	0.8007	0.4657	0.02429
ESWP006-C2-S10	1429.02	-0.003824	-0.002145	0.01762	0.02207	0.0006447
ESWP006-C2-S11	1429.02	-0.0003321	-0.001764	0.08352	1.557	0.001089
ESWP006-C2-S12	1429.02	-0.003662	0.002558	0.02408	0.06130	0.001619
ESWP006-C2-S13	1429.02	0.004729	-0.0008600	0.005011	0.008598	-0.00006371
ESWP006-C2-S14	1429.02	-0.001484	0.001029	0.3113	2.023	-0.0002871
ESWP006-C2-S15	1429.02	-0.0007650	0.002876	0.003388	0.009216	0.0002971
ESWP006-C2-S7	1429.02	0.00001555	-0.0002425	0.04105	0.02329	0.00008456
ESWP006-C2-S8	1429.02	0.001614	-0.0009114	0.09744	0.2311	-0.001976
ESWP006-C2-S9	1429.02	0.003101	-0.001624	0.006100	0.005112	-0.001328

* distance from center of deposit

** All elements in ppm except Au which is in ppb

Appendix 8: White Pine
pyrite mineral chemistry by LA-ICP-MS

Sample	Distance* (m)	Au197**	Tl205	Pb208	Bi209	U238
ESWP007-C1-S2	1360.22	0.002174	0.005883	0.02632	0.08713	0.0003208
ESWP007-C1-S3	1360.22	0.001909	-0.0004677	0.003796	0.002331	0.0002550
ESWP007-C1-S4	1360.22	-0.0001352	-0.0008918	0.002723	0.008456	-0.0006977
ESWP007-C1-S5	1360.22	-0.005440	-0.001679	0.005096	0.01748	-0.0002808
ESWP007-C2-S6	1360.22	0.002054	-0.0008049	0.007318	0.004679	0.0007074
ESWP007-C2-S8	1360.22	-0.001887	0.001051	-0.001509	0.01841	-0.001186
ESWP007-C2-S9	1360.22	0.0001604	0.002332	0.01205	0.03335	0.0006243
ESWP007-C3-S11	1360.22	-0.003152	0.0009675	0.003421	0.01077	0.0006855
ESWP007-C3-S12	1360.22	0.0006759	-0.001075	0.004413	0.01483	0.000005041
ESWP018-C1-S3	513.17	-0.001546	0.0009658	0.01708	0.004464	-0.00003226
ESWP018-C1-S4	513.17	0.0004101	-0.0008030	0.03892	0.008942	0.0009502
ESWP018-C1-S5	513.17	0.001114	-0.001047	0.01184	0.008930	0.002755
ESWP018-C1-S6	513.17	0.0005797	0.002207	0.002569	0.01017	-0.0008460
ESWP018-C1-S7	513.17	0.001563	0.004322	0.1833	0.1667	0.001576
ESWP018-C1-S8	513.17	0.003276	0.001014	0.01051	0.01008	-0.0005181
ESWP018-C2-S11	513.17	-0.004979	0.001308	0.1382	0.001533	0.05488
ESWP018-C2-S12	513.17	0.001493	0.001126	0.1452	0.2274	0.0006356
ESWP018-C2-S13	513.17	-0.001791	0.001098	0.05873	0.005994	0.01611
ESWP018-C2-S14	513.17	-0.004068	-0.0007470	0.2052	0.02248	0.02029
ESWP058-C1-S1	1709.21	-0.0007405	-0.001510	0.002384	0.007781	-0.0001084
ESWP058-C1-S2	1709.21	-0.0008853	-0.001228	0.005452	0.01493	0.003649
ESWP058-C1-S3	1709.21	-0.0008249	-0.001462	0.007545	0.006972	-0.0002873
ESWP058-C1-S4	1709.21	0.002530	0.0002480	0.005398	0.008219	0.03895
ESWP058-C1-S5	1709.21	0.002800	0.01548	0.03677	0.07665	0.001434
ESWP058-C1-S6	1709.21	0.002791	-0.0004229	0.0005123	0.003322	-0.00004359
ESWP058-C2-S10	1709.21	0.0005402	-0.0008081	0.006280	0.009330	-0.001053
ESWP058-C2-S7	1709.21	0.002090	-0.00008258	0.004005	0.01003	0.001093
ESWP058-C2-S8	1709.21	-0.004430	-0.001583	0.02073	0.03506	0.01254
ESWP058-C2-S9	1709.21	0.0008136	0.001389	0.00005976	0.008824	0.0004118
ESWP058-C3-S11	1709.21	0.001052	-0.005260	0.04707	0.06873	0.08093
ESWP058-C3-S12	1709.21	0.001976	0.001962	111.3	3.869	5.684
ESWP058-C3-S13	1709.21	0.03326	0.0004534	1.991	6.224	0.05822
ESWP058-C3-S14	1709.21	0.007657	0.02946	12.34	18.40	14.41
ESWP065-C1-S1	609.43	0.0002375	-0.00005631	0.02037	0.004693	0.001824
ESWP065-C1-S10	609.43	-0.00002774	0.0008277	0.006503	0.003283	-0.0003397
ESWP065-C1-S2	609.43	0.0008310	-0.002331	0.01022	0.001358	0.0006642
ESWP065-C1-S3	609.43	0.006492	-0.001267	-0.004165	-0.0005353	0.00007802
ESWP065-C1-S5	609.43	-0.0005382	-0.002546	0.002099	0.03091	0.001046
ESWP065-C1-S6	609.43	0.001347	-0.0003177	0.004719	0.003610	0.00009208
ESWP065-C1-S7	609.43	0.003377	-0.00008521	0.004585	0.003479	-0.0007868
ESWP065-C1-S8	609.43	-0.003479	-0.001409	0.001689	0.0008619	-0.00002813
ESWP065-C1-S9	609.43	-0.003875	-0.0003162	0.001251	0.002009	-0.001104
WPO3-C1-S1	1546.40	-0.001076	0.001275	0.02423	0.1259	0.0003155

* distance from center of deposit

** All elements in ppm except Au which is in ppb

Appendix 8: White Pine
pyrite mineral chemistry by LA-ICP-MS

Sample	Distance* (m)	Au197**	Tl205	Pb208	Bi209	U238
WP03-C1-S2	1546.40	0.001954	-0.001067	0.03941	0.07657	0.001086
WP03-C1-S3	1546.40	0.0007672	-0.0006829	0.02077	0.07799	0.001633
WP03-C1-S4	1546.40	0.0007169	0.0002635	0.03539	0.1473	-0.0001291
WP03-C1-S5	1546.40	-0.001584	0.00007025	0.01439	0.05754	-0.00006296
WP03-C1-S6	1546.40	0.004406	-0.0003653	0.01871	0.04623	0.002475
WP03-C1-S7	1546.40	0.007719	0.002259	0.04259	0.02564	0.0004918
WP03-C1-S8	1546.40	0.004806	0.0008857	0.3128	0.1471	0.004024
WP06-C1-S1	1429.02	0.007321	-0.0003270	0.007036	-0.001758	0.001569
WP06-C1-S2	1429.02	0.02603	0.007932	5.277	11.01	-0.001572
WP06-C1-S3	1429.02	-0.0008953	0.001362	0.008015	0.005804	0.002483
WP06-C1-S4	1429.02	-0.003202	0.0009086	-0.003893	0.003932	0.001330
WP06-C1-S5	1429.02	0.004428	-0.003404	0.01921	0.002360	0.002059
WP06-C2-S10	1429.02	-0.01718	-0.004084	0.005938	0.002078	-0.001196
WP06-C2-S6	1429.02	-0.002542	-0.005818	0.01032	0.007237	0.001885
WP06-C2-S7	1429.02	-0.002117	-0.001868	0.002361	0.005101	0.003849
WP06-C2-S8	1429.02	0.003814	0.006678	0.01042	0.009737	0.0008545
WP06-C2-S9	1429.02	0.001919	0.0008529	0.001064	0.005347	0.0001835
WP06-C3-S11	1429.02	0.02029	0.001984	0.005246	0.0006122	0.002142
WP06-C3-S12	1429.02	0.01715	-0.0008055	0.02619	0.002097	0.0004615
WP06-C3-S13	1429.02	-0.003283	0.001780	0.02129	0.02210	-0.002424
WP06-C3-S14	1429.02	-0.01682	-0.0004066	0.002087	0.002544	-0.002500
WP06-C3-S15	1429.02	-0.005162	0.001666	0.0006235	0.0005035	-0.001370
WP17-C1-S1	712.89	0.007364	-0.001156	0.03353	0.3227	-0.0003539
WP17-C1-S2	712.89	-0.004467	0.0004934	0.02239	0.06991	0.0004365
WP17-C1-S3	712.89	0.004735	-0.003833	-0.0009885	0.07460	0.001169
WP17-C1-S4	712.89	0.3245	0.0005986	0.006506	0.04989	0.0009006
WP17-C1-S5	712.89	-0.001472	-0.0007670	0.01086	0.1272	0.001239
WP17-C1-S6	712.89	-0.002054	-0.00003915	0.03034	0.2154	-0.0002335
WP17-C1-S7	712.89	-0.005834	0.004374	-0.0005275	0.04556	-0.0005892
WP17-C2-S10	712.89	0.001205	-0.0009871	0.2463	1.617	0.02766
WP17-C2-S11	712.89	-0.0007417	0.0007117	0.2153	0.06377	0.02422
WP17-C2-S12	712.89	-0.003848	-0.0007334	0.002883	0.02865	0.0006240
WP17-C2-S13	712.89	0.005029	-0.0004693	-0.0006155	0.02129	0.002380
WP17-C2-S14	712.89	0.002485	0.0001588	-0.0006526	0.06791	0.0006967
WP17-C2-S15	712.89	0.008648	0.0005640	0.2202	1.486	0.0007782
WP17-C2-S8	712.89	0.005667	-0.001708	-0.0007423	0.03323	-0.0001253
WP17-C2-S9	712.89	-0.001768	0.0004882	0.002520	0.06980	0.0007054
WP20-C1-S1	1110.01	0.003603	-0.004791	0.01593	-0.0008205	-0.001589
WP20-C1-S10	1110.01	-0.008012	-0.0007531	0.01923	0.007988	0.001043
WP20-C1-S11	1110.01	-0.008262	0.002854	-0.001711	0.006696	0.00006651
WP20-C1-S12	1110.01	0.005365	-0.001755	0.01406	0.001137	0.0002206
WP20-C1-S13	1110.01	-0.01259	0.004324	0.008525	0.004465	-0.0004617
WP20-C1-S14	1110.01	-0.007349	-0.002578	0.007281	0.006987	-0.0007265

* distance from center of deposit

** All elements in ppm except Au which is in ppb

Appendix 8: White Pine
pyrite mineral chemistry by LA-ICP-MS

Sample	Distance* (m)	Au197**	Tl205	Pb208	Bi209	U238
WP20-C1-S15	1110.01	-0.004812	0.002551	0.01997	0.005201	0.001737
WP20-C1-S2	1110.01	0.004916	-0.003337	0.02975	-0.003051	0.0004467
WP20-C1-S3	1110.01	0.01274	0.002670	0.008903	0.003072	-0.0001224
WP20-C1-S4	1110.01	0.003084	0.0006605	0.01245	-0.003051	-0.0001818
WP20-C1-S5	1110.01	-0.006473	-0.003587	0.009514	-0.002222	0.0006498
WP20-C1-S6	1110.01	-0.003764	-0.001879	0.03639	0.0009609	0.05520
WP20-C1-S7	1110.01	0.006403	0.00006151	0.004339	-0.0007175	0.003399
WP20-C1-S8	1110.01	0.0004145	-0.003488	0.01125	0.006057	0.001298
WP20-C1-S9	1110.01	0.002166	0.0001017	-0.005170	0.003998	-0.001436
WP23-C1-S1	1688.35	-0.0001785	0.001443	0.01337	0.05881	-0.001469
WP23-C1-S2	1688.35	-0.0003469	0.001674	0.05645	0.04632	0.00007738
WP23-C1-S3	1688.35	-0.001001	0.002680	0.01032	0.05071	0.002764
WP23-C1-S4	1688.35	0.005240	0.001648	0.01305	0.03616	0.001083
WP23-C2-S5	1688.35	-0.0008214	0.001372	0.01604	0.04194	-0.001185
WP23-C2-S6	1688.35	0.0007235	-0.0009376	0.02479	0.03430	-0.0007885
WP23-C2-S7	1688.35	-0.002206	-0.0005609	0.01412	0.03996	-0.0002140
WP23-C2-S8	1688.35	0.003189	0.0004358	0.01934	0.03470	-0.0002357
WP23-C3-S10	1688.35	-0.002952	0.004987	0.01502	0.03198	-0.0005081
WP23-C3-S11	1688.35	0.0007511	0.001715	0.007734	0.03104	0.001667
WP23-C3-S12	1688.35	-0.001072	0.001354	0.003918	0.02079	0.001208
WP23-C3-S13	1688.35	0.004191	-0.001777	0.005668	0.05242	-0.0005082
WP23-C3-S9	1688.35	0.002984	-0.002424	0.01468	0.04003	0.00002127
WP26-C1-S1	1314.77	0.002601	-0.003721	0.01175	0.01429	-0.00009576
WP26-C1-S2	1314.77	0.006273	0.002254	0.004405	0.02284	-0.00006698
WP26-C1-S3	1314.77	-0.003034	-0.0001581	0.01269	0.0006616	0.00006843
WP26-C1-S4	1314.77	-0.004810	0.00003383	0.007078	0.006573	-0.0004077
WP26-C1-S5	1314.77	0.003207	0.002364	0.06835	0.01253	0.00005726
WP26-C1-S6	1314.77	0.001467	-0.003136	-0.0004854	0.02759	-0.0004129
WP26-C2-S10	1314.77	0.001638	-0.002090	0.02155	0.001875	0.001163
WP26-C2-S11	1314.77	0.002250	0.001606	1.391	2.548	0.0008190
WP26-C2-S12	1314.77	0.001555	-0.0005669	0.01148	0.008457	-0.0004795
WP26-C2-S13	1314.77	0.003040	0.002414	0.005504	0.01478	-0.0006675
WP26-C2-S14	1314.77	-0.0007793	-0.0003586	0.01085	0.008765	-0.0007989
WP26-C2-S15	1314.77	0.006825	0.001090	0.003329	0.004764	-0.0003123
WP26-C2-S8	1314.77	0.003760	0.001757	0.01849	0.02359	0.0003566
WP26-C2-S9	1314.77	-0.001922	0.001326	0.01515	0.02357	0.001682
WP27-C1-S1	1182.57	-0.001917	-0.001443	0.05783	0.1595	-0.0008594
WP27-C1-S2	1182.57	0.002122	0.002507	0.06610	0.05588	0.0003761
WP27-C1-S3	1182.57	-0.003305	0.002280	0.01547	0.05476	0.0007409
WP27-C1-S4	1182.57	-0.001592	-0.0009570	0.1075	0.02907	0.00008671
WP27-C2-S5	1182.57	-0.001552	0.0008579	0.09074	0.04027	0.0004555
WP27-C2-S6	1182.57	-0.004541	0.0003255	0.02741	0.03262	0.001200
WP27-C2-S7	1182.57	0.0005717	0.006029	0.009511	0.03039	-0.0002256

* distance from center of deposit

** All elements in ppm except Au which is in ppb

Appendix 8: White Pine
pyrite mineral chemistry by LA-ICP-MS

Sample	Distance* (m)	Au197**	Tl205	Pb208	Bi209	U238
WP27-C2-S8	1182.57	-0.001069	0.002451	0.02462	0.01672	0.01723
WP27-C3-S10	1182.57	-0.001098	-0.0008349	0.002492	0.01044	0.0009939
WP27-C3-S11	1182.57	0.006235	-0.0001745	0.02147	0.01695	-0.0009952
WP28-C1-S1	1183.91	0.001754	0.002713	0.01705	0.04537	-0.0002772
WP28-C1-S2	1183.91	-0.002237	0.01693	1.486	0.05149	0.007853
WP28-C1-S3	1183.91	0.006070	0.004547	0.04941	0.04227	-0.0008811
WP28-C1-S5	1183.91	-0.001263	-0.004750	0.03132	0.03069	-0.0008725
WP28-C1-S6	1183.91	0.001706	0.001770	0.005445	0.03734	0.0002930
WP28-C1-S7	1183.91	0.004565	0.002462	0.08299	0.03673	0.001326
WP28-C2-S10	1183.91	0.001196	0.001927	0.01493	0.04700	0.0002428
WP28-C2-S11	1183.91	0.006258	0.001743	0.02049	0.07370	0.0007889
WP28-C2-S12	1183.91	-0.0003181	0.001469	0.07240	0.04794	0.0006735
WP28-C2-S13	1183.91	-0.006162	-0.001505	0.01281	0.03809	-0.0002099
WP28-C2-S14	1183.91	0.002757	-0.004499	0.007707	0.03366	0.0004810
WP28-C2-S8	1183.91	-0.001380	-0.0007083	0.07453	0.09615	-0.0002147
WP28-C2-S9	1183.91	0.0002088	-0.0003041	0.03016	0.04565	-0.001489
WP30-C1-S1	2282.00	0.003227	-0.0007860	0.004397	0.02106	0.0003212
WP30-C1-S2	2282.00	-0.002354	0.0001952	0.01716	0.1012	-0.0001482
WP30-C1-S3	2282.00	-0.004157	-0.001782	0.07722	0.1665	-0.0005752
WP30-C1-S4	2282.00	-0.001720	0.002034	0.02613	0.02888	0.001455
WP30-C1-S5	2282.00	0.001623	0.001556	0.01034	0.04014	0.0003604
WP30-C2-S10	2282.00	0.001094	0.0003036	0.01204	0.03371	-0.0007146
WP30-C2-S7	2282.00	0.004565	-0.002465	0.002277	0.01989	-0.0001444
WP30-C2-S8	2282.00	-0.005965	0.002245	0.01173	0.05419	-0.0007580
WP30-C2-S9	2282.00	-0.0006530	-0.00006198	0.01490	0.03143	0.001694
WP30-C3-S12	2282.00	0.001280	-0.0009154	0.004563	0.02814	0.0009564
WP30-C3-S13	2282.00	0.001874	0.001196	0.01337	0.02124	0.0002623
WP30-C3-S14	2282.00	0.004750	0.0001927	0.3117	0.01705	0.004420
WP30-C3-S15	2282.00	-0.003215	-0.0004604	1.557	0.1951	0.002803
WP33-C1-S1	2078.05	0.006532	-0.0004123	0.02641	0.02604	-0.0001107
WP33-C1-S10	2078.05	-0.003630	-0.001311	0.01259	0.01718	-0.0004348
WP33-C1-S11	2078.05	0.005582	0.001409	0.03088	0.05719	-0.0005944
WP33-C1-S12	2078.05	0.002158	0.0001608	0.1623	0.06189	-0.0001347
WP33-C1-S2	2078.05	-0.0001151	0.002466	0.01247	0.02607	0.0009324
WP33-C1-S3	2078.05	0.0002458	0.00009279	0.005538	0.02225	0.0002467
WP33-C1-S4	2078.05	0.002513	0.000006925	0.09288	0.01926	0.00007253
WP33-C1-S5	2078.05	-0.002638	0.0004096	0.006447	0.02398	-0.0006185
WP33-C1-S7	2078.05	0.0003292	-0.002258	0.009537	0.04183	-0.0004198
WP33-C1-S8	2078.05	0.004258	0.002413	0.02332	0.03300	-0.0009847
WP33-C1-S9	2078.05	-0.001752	0.0007922	0.02005	0.02522	-0.0005488
WP36-C1-S1	1404.01	0.004744	0.0003505	0.01453	0.07196	0.0007916
WP36-C1-S2	1404.01	0.0005903	0.002783	0.01113	0.06983	-0.00004619
WP36-C1-S3	1404.01	-0.003206	-0.002970	0.009425	0.04203	0.0005983

* distance from center of deposit

** All elements in ppm except Au which is in ppb

Appendix 8: White Pine
pyrite mineral chemistry by LA-ICP-MS

Sample	Distance* (m)	Au197**	Tl205	Pb208	Bi209	U238
WP36-C1-S4	1404.01	0.0001367	-0.0006470	0.02476	0.08221	-0.0006901
WP36-C1-S5	1404.01	-0.00002592	-0.005091	0.007352	0.07097	0.001309
WP36-C1-S6	1404.01	-0.003281	-0.003554	0.01520	0.05658	0.0007134
WP36-C2-S10	1404.01	0.0006834	0.001040	1.647	0.08172	0.1885
WP36-C2-S11	1404.01	0.004850	0.002742	2.207	1.251	0.3339
WP36-C2-S12	1404.01	0.004337	0.001266	0.02262	0.03469	0.001732
WP36-C2-S7	1404.01	0.0001923	-0.0002309	0.01241	0.07314	0.00008370
WP36-C2-S8	1404.01	0.003069	0.001792	0.01273	0.06241	0.001539
WP36-C2-S9	1404.01	0.0001882	0.002178	0.03356	0.1382	-0.0009553
WP40-C1-S1	1139.14	-0.0005859	0.0002242	0.004079	0.01056	-0.0003315
WP40-C1-S10	1139.14	0.001656	0.0004114	0.05390	0.02748	-0.0003038
WP40-C1-S11	1139.14	0.006583	-0.0001960	0.3125	0.1248	0.0005728
WP40-C1-S12	1139.14	0.003436	0.001409	0.004112	0.008932	0.001107
WP40-C1-S13	1139.14	-0.006271	-0.0004300	0.01665	0.01442	-0.0001765
WP40-C1-S14	1139.14	0.005614	-0.0005938	0.02366	0.01536	0.0002270
WP40-C1-S15	1139.14	0.003727	-0.002871	0.001603	0.01247	-0.00006310
WP40-C1-S2	1139.14	0.002095	0.0007986	0.01251	0.009480	-0.002098
WP40-C1-S3	1139.14	-0.0006263	0.0004001	0.03961	0.09074	0.0004565
WP40-C1-S4	1139.14	0.009705	0.001116	0.02387	0.009567	-0.0003332
WP40-C1-S5	1139.14	-0.0001551	0.0005187	0.01072	0.01115	0.001024
WP40-C1-S6	1139.14	0.001403	0.001598	0.06044	0.008803	0.0001512
WP40-C1-S7	1139.14	-0.004722	0.002125	0.2852	0.06157	-0.0005195
WP40-C1-S8	1139.14	-0.004070	0.0007111	0.02465	0.001695	0.0002652
WP40-C1-S9	1139.14	0.004441	0.0003907	0.4249	0.1804	0.001608
WP44-C1-S2	622.10	0.002968	0.001613	0.01901	0.05733	-0.0002884
WP44-C1-S3	622.10	-0.001476	0.0009312	0.01668	0.005500	0.0005740
WP44-C1-S4	622.10	0.009805	-0.0007512	0.008068	0.02090	0.0007146
WP44-C1-S5	622.10	0.001795	0.0005431	0.02491	0.1971	-0.0004347
WP44-C2-S6	622.10	0.006663	0.001760	0.007372	0.03524	0.0006516
WP44-C2-S7	622.10	0.007077	-0.001403	0.1142	0.2145	0.0004753
WP44-C3-S13	622.10	0.0004309	0.002018	0.02200	0.03033	-0.0005347
WP44-C3-S14	622.10	0.006142	-0.001237	0.03072	0.3209	0.00004341
WP44-C3-S15	622.10	-0.003421	0.001773	0.02571	0.009637	-0.0001969
WP52-C1-S1	785.45	0.003599	0.001535	0.4214	0.04274	0.001997
WP52-C1-S2	785.45	0.002152	0.0001564	0.1055	0.02629	-0.001367
WP52-C1-S3	785.45	0.003129	0.00005642	0.09520	0.7764	0.0007193
WP52-C1-S4	785.45	0.002719	0.002284	0.01669	0.02341	0.0004898
WP52-C1-S5	785.45	0.004675	-0.0005972	0.2940	0.05525	0.0007697
WP52-C2-S10	785.45	0.005567	0.001951	0.09779	0.006769	-0.0001078
WP52-C2-S6	785.45	0.004921	-0.00009769	0.01789	-0.002217	0.0004644
WP52-C2-S7	785.45	-0.0001112	-0.002199	0.03637	0.009334	-0.00002331
WP52-C2-S8	785.45	-0.002056	0.001514	0.07398	0.01299	-0.0002892
WP52-C2-S9	785.45	0.007966	0.002904	0.05935	0.01627	0.0006921

* distance from center of deposit

** All elements in ppm except Au which is in ppb

Appendix 8: White Pine
pyrite mineral chemistry by LA-ICP-MS

Sample	Distance* (m)	Au197**	Tl205	Pb208	Bi209	U238
WP52-C3-S11	785.45	0.001531	0.001169	0.006183	0.01379	0.0002082
WP52-C3-S12	785.45	0.01546	-0.002351	0.001157	0.01468	-0.0004711
WP52-C3-S13	785.45	-0.002786	0.002529	0.0001834	0.01052	0.0007784
WP52-C3-S14	785.45	-0.0007784	0.0002044	0.007205	0.01483	0.0004016
WP52-C3-S15	785.45	0.001489	-0.001807	0.01032	0.001491	0.0003134
WP54-C1-S1	432.59	0.008780	0.0007316	-0.00002837	0.01488	0.0003379
WP54-C1-S2	432.59	0.002123	0.003847	0.003506	0.003875	0.0001185
WP54-C1-S3	432.59	0.001761	0.0001892	0.009341	0.009756	0.0004755
WP54-C1-S4	432.59	0.001552	-0.0005538	0.008099	0.02053	-0.00001116
WP54-C1-S5	432.59	-0.002356	-0.0007145	0.01286	0.02491	-0.0005528
WP54-C1-S6	432.59	-0.005120	0.001524	0.003266	0.02416	-0.0002506
WP54-C2-S10	432.59	0.002871	0.0002300	0.001401	0.01040	-0.0004458
WP54-C2-S11	432.59	0.00008290	0.002806	0.007679	0.01183	-0.0006887
WP54-C2-S12	432.59	0.001191	0.0007745	0.006507	0.009776	0.0002870
WP54-C2-S13	432.59	0.001801	0.004119	0.006926	-0.0008978	0.00008965
WP54-C2-S14	432.59	0.001768	0.0006422	0.03314	0.009539	-0.00004527
WP54-C2-S15	432.59	-0.002098	0.0004035	0.007755	0.01215	-0.0008614
WP54-C2-S8	432.59	0.001136	-0.0008633	0.007855	0.01943	-0.001544
WP54-C2-S9	432.59	0.0005725	0.0001685	0.07185	0.2677	0.0006710
WP63-C1-S1	0.00	0.003503	-0.0005775	5.023	63.78	0.2171
WP63-C1-S10	0.00	0.005881	-0.00005622	0.07615	0.06881	0.05395
WP63-C1-S11	0.00	-0.002320	0.001882	0.02765	0.1605	-0.001778
WP63-C1-S12	0.00	-0.003589	0.003554	0.06891	0.09522	0.00009258
WP63-C1-S13	0.00	-0.003577	0.001384	0.02000	0.1255	-0.0005851
WP63-C1-S14	0.00	-0.001159	-0.004192	0.3191	1.784	0.003449
WP63-C1-S2	0.00	0.008563	-0.003634	0.2578	0.2734	-0.0003794
WP63-C1-S3	0.00	0.006245	0.001896	0.1080	0.2486	0.0003681
WP63-C1-S4	0.00	-0.002321	-0.001436	1.346	7.060	0.002029
WP63-C1-S5	0.00	0.03164	0.01551	424.0	4795	0.3567
WP63-C1-S6	0.00	0.002624	0.0003874	0.2006	0.2129	-0.0001165
WP63-C1-S7	0.00	0.003913	-0.0008731	0.2517	1.017	-0.001587
WP63-C1-S8	0.00	-0.008816	-0.001264	0.03182	0.08324	-0.001176
WP63-C1-S9	0.00	-0.001812	-0.001512	0.02929	0.1138	-0.0002461

* distance from center of deposit

** All elements in ppm except Au which is in ppb

Appendix 9: Buckingham
pyrite mineral chemistry by LA-ICP-MS

Sample	Sample type	Distance*															
		(m)	Mg24	Al27	S34	K39	Ca43	Ti49	Cr53	Mn55	Fe57	Co59	Ni60	Cu65	Zn66	As75	Se77
BK025-C1-S1	Arsenian pyrite	0.0	101.1	1325	3.999E+05	672.4	12.87	76.81	2.984	14.23	4.650E+05	15.31	44.65	201.3	1052	215400	13.39
BK025-C1-S2	Arsenian pyrite	0.0	118.0	1413	3.936E+05	823.4	-0.05988	204.1	4.329	11.53	4.650E+05	5.296	16.59	96.71	558.4	252900	14.86
BK025-C1-S3	Arsenian pyrite	0.0	245.1	2725	3.634E+05	1527	27.01	192.1	5.834	96.33	4.650E+05	3.302	6.858	2227	8090	209000	16.35
BK025-C1-S4	Arsenian pyrite	0.0	102.1	83.44	5.076E+05	10.73	32.61	54.88	0.4239	77.42	4.650E+05	74.72	37.61	26.26	2390	7712	3.495
BK025-C1-S5	Arsenian pyrite	0.0	182.8	2158	4.317E+05	1213	82.65	185.7	4.326	7.739	4.650E+05	3.391	5.706	9.986	53.76	233000	17.12
BK025-C1-S6	Arsenian pyrite	0.0	62.69	575.6	3.712E+05	334.7	33.33	272.4	3.588	4.580	4.650E+05	126.7	154.6	7.877	6.311	209500	16.98
BK025-C1-S7	Arsenian pyrite	0.0	47.23	365.0	3.894E+05	227.2	140.8	280.0	4.115	33.27	4.650E+05	2041	824.8	2053	60.86	223200	19.35
BK025-C1-S8	Arsenian pyrite	0.0	0.5524	9.179	3.548E+05	8.640	-0.6513	16.39	0.1714	0.3435	4.650E+05	1.163	5.279	5.641	10.78	199900	13.69
BK025-C1-S9	Arsenian pyrite	0.0	19.80	290.1	3.823E+05	118.2	-18.13	14.77	1.271	3.262	4.650E+05	7.299	12.42	565.1	209.5	216300	17.07
BK025-C1-S10	Arsenian pyrite	0.0	3.512	85.25	3.641E+05	25.03	15.97	72.62	0.4404	4.347	4.650E+05	5.619	12.48	1218	159.0	219900	17.55
BK025-C1-S11	Arsenian pyrite	0.0	27.09	400.3	3.655E+05	188.6	43.99	82.53	1.154	4.385	4.650E+05	3.996	6.427	1002	205.5	192400	14.36
BK025-C1-S12	Arsenian pyrite	0.0	164.2	2049	3.841E+05	1151	20.18	588.7	5.474	21.23	4.650E+05	3.545	7.566	11620	844.9	242600	25.06
BK025-C1-S13	Arsenian pyrite	0.0	18.20	185.6	3.712E+05	93.05	-12.19	11.79	0.5480	3.067	4.650E+05	1.512	3.027	502.3	127.7	221500	16.96
BK025-C1-S14	Arsenian pyrite	0.0	30.21	400.2	3.681E+05	195.7	33.50	177.0	1.762	7.409	4.650E+05	4.079	5.471	2091	300.9	210600	18.49
BK025-C1-S15	Arsenian pyrite	0.0	267.6	3029	3.684E+05	1900	3016	3623	11.23	19.16	4.650E+05	518.9	78.51	29.91	142.2	189500	12.11
BK104-C1-S1	Arsenian pyrite	361.5	221.5	1444	6.582E+05	608.2	-38.07	7.850	1.018	5.987	4.650E+05	2.746	82.43	266.6	2134	6564	50.52
BK104-C1-S2	Arsenian pyrite	361.5	86.81	539.7	5.135E+05	218.6	-2.189	4.308	0.9989	2.786	4.650E+05	7.042	32.21	265.6	75.06	188500	29.39
BK104-C1-S3	Arsenian pyrite	361.5	59.24	736.0	5.663E+05	269.4	-15.70	2.866	0.06941	1.042	4.650E+05	3.070	10.09	27.93	137.8	5248	10.52
BK104-C1-S4	Arsenian pyrite	361.5	129.1	1065	5.821E+05	340.7	14.66	6.134	0.4054	7.070	4.650E+05	3.412	22.28	170.3	1532	6536	14.13
BK104-C1-S5	Arsenian pyrite	361.5	2.922	12.54	5.308E+05	6.866	-35.44	2.645	-0.01249	2.222	4.650E+05	0.8280	8.371	103.1	957.4	5716	13.31
BK104-C1-S6	Arsenian pyrite	361.5	0.6084	4.478	4.990E+05	0.08196	-19.88	0.4670	-0.03155	0.07614	4.650E+05	0.2632	0.2019	31.42	9.825	4244	10.54
BK104-C1-S7	Arsenian pyrite	361.5	4.164	4.191	5.109E+05	3.553	37.90	0.8199	-0.02438	0.9491	4.650E+05	4.257	17.87	41.50	16.04	4543	5.923
BK104-C1-S10	Arsenian pyrite	361.5	225.3	345.4	5.633E+05	64.45	442.9	1.612	1.435	49.38	4.650E+05	7.163	40.39	73.48	136.0	14470	12.46
BK104-C1-S11	Arsenian pyrite	361.5	213.2	1493	5.449E+05	594.2	-43.95	7.874	1.340	8.674	4.650E+05	3.256	18.89	52.37	435.6	2585	6.779
BK104-C1-S12	Arsenian pyrite	361.5	757.7	12880	8.654E+05	4409	1076	40.38	4.382	62.68	4.650E+05	1.152	18.46	230.9	1510	4730	14.33
BK104-C1-S13	Arsenian pyrite	361.5	5.717	3.882	5.262E+05	4.461	33.41	4.311	0.4111	2.034	4.650E+05	22.73	4.069	19.06	0.6216	1035	18.89
BK104-C1-S14	Arsenian pyrite	361.5	125.4	103.2	5.036E+05	73.40	39.74	1.240	0.2324	7.350	4.650E+05	37.08	1.617	61.86	14.60	676.2	20.76
BK102-C1-S2	Pyrite	890.8	-0.8330	-0.07926	5.255E+05	2.602	29.78	0.4990	0.4694	0.002790	4.650E+05	440.8	45.46	0.3401	0.1577	1.328	38.62
BK102-C1-S3	Pyrite	890.8	-0.5410	0.1350	5.187E+05	1.465	42.56	0.6457	-0.02997	0.07356	4.650E+05	161.9	24.32	0.4372	0.3524	2.300	48.10
BK102-C1-S4	Pyrite	890.8	0.1020	-0.2518	5.339E+05	0.4577	20.50	0.01207	0.4068	-0.09788	4.650E+05	407.6	66.61	0.4475	0.2445	1.547	46.51
BK102-C1-S5	Pyrite	890.8	0.7975	1.517	5.193E+05	-0.5956	31.84	0.3018	-0.1023	-0.03016	4.650E+05	210.4	112.3	0.9367	0.2466	0.5778	30.78
BK102-C1-S6	Pyrite	890.8	-0.5825	-0.2048	5.112E+05	0.3886	36.28	0.6613	0.6619	-0.01374	4.650E+05	226.5	112.8	0.7858	0.01805	0.8316	29.40
BK102-C1-S7	Pyrite	890.8	0.5734	-0.2030	5.215E+05	-0.5397	-54.67	0.4178	0.5308	-0.05038	4.650E+05	278.5	83.27	0.1909	0.2650	0.6823	26.31
BK102-C1-S8	Pyrite	890.8	-0.1906	0.05357	5.217E+05	-2.781	18.36	0.8618	0.3233	0.07916	4.650E+05	1210	135.7	0.3196	0.1943	1.725	31.44
BK102-C1-S10	Pyrite	890.8	-0.6590	-0.3862	5.273E+05	0.9062	-43.02	0.4857	0.08562	-0.04910	4.650E+05	703.6	74.38	0.3344	0.2153	2.182	44.19
BK102-C1-S11	Pyrite	890.8	0.1765	-0.08595	5.167E+05	-0.2299	2.460	0.8393	-0.2820	-0.003720	4.650E+05	550.7	55.51	0.1213	0.1523	2.497	42.01
BK102-C1-S12	Pyrite	890.8	-0.06804	-0.4909	5.077E+05	0.1219	10.39	0.4215	0.03944	-0.05611	4.650E+05	208.1	67.16	0.3707	0.2882	1.764	29.83
BK102-C1-S13	Pyrite	890.8	0.4558	-0.2150	4.950E+05	-2.476	-44.76	0.5406	0.02781	-0.007882	4.650E+05	399.6	51.79	0.4316	0.1556	1.637	31.98
BK102-C1-S14	Pyrite	890.8	0.2294	-0.7305	5.302E+05	0.9538	-8.285	0.5247	0.1323	-0.03018	4.650E+05	398.5	52.96	0.3018	0.1292	2.177	42.88
BK102-C1-S15	Pyrite	890.8	0.2552	0.9750	5.173E+05	2.831	-4.264	0.3051	-0.2109	0.1291	4.650E+05	316.0	37.89	2.501	0.3635	1.799	38.76
BK59-C1-S1	Pyrite	2339.0	-0.09695	0.2765	5.177E+05	1.067	-12.48	0.5972	0.1348	0.01327	4.650E+05	1.380	220.5	0.4954	0.2004	6.370	71.84
BK59-C1-S2	Pyrite	2339.0	0.5401	0.08271	5.060E+05	-2.726	62.00	0.07218	-0.3146	0.001737	4.650E+05	2.838	211.4	0.4767	0.02966	1.092	54.33
BK59-C1-S3	Pyrite	2339.0	0.4316	1.851	5.656E+05	-3.696	9.666	0.4205	-0.4450	-0.06404	4.650E+05	3.187	644.2	0.6644	0.3120	1.565	62.30

* distance from center of deposit

** All elements in ppm except Au which is in ppb

Appendix 9: Buckingham
pyrite mineral chemistry by LA-ICP-MS

Sample	Sample type	Distance*															
		(m)	Mg24	Al27	S34	K39	Ca43	Ti49	Cr53	Mn55	Fe57	Co59	Ni60	Cu65	Zn66	As75	Se77
BK59-C1-S4	Pyrite	2339.0	0.9769	-1.190	4.804E+05	-2.005	4.555	1.198	-0.07928	-0.002194	4.650E+05	5.378	515.0	0.5007	0.2234	1.612	55.38
BK59-C1-S5	Pyrite	2339.0	1.725	12.31	5.018E+05	13.10	-0.6302	6.072	0.03256	0.09964	4.650E+05	3.582	247.1	2.125	0.4037	6.081	73.44
BK59-C1-S6	Pyrite	2339.0	-0.03433	1.277	4.988E+05	-3.920	108.2	0.2712	-0.04004	-0.03329	4.650E+05	150.5	186.0	0.1801	0.3547	4.100	49.22
BK59-C1-S7	Pyrite	2339.0	0.7914	3.030	4.858E+05	1.681	-32.66	0.7234	0.1532	-0.01029	4.650E+05	66.24	89.65	1.340	0.3054	2.249	56.11
BK59-C1-S8	Pyrite	2339.0	0.07189	-0.4182	4.844E+05	-4.750	26.10	1.527	0.3060	0.03475	4.650E+05	147.3	321.0	0.4854	0.002347	1.274	43.25
BK59-C1-S9	Pyrite	2339.0	-0.2781	1.784	4.865E+05	-4.250	14.48	0.3236	0.1035	0.02725	4.650E+05	117.6	161.2	0.1440	0.2851	2.109	63.45
BK59-C1-S10	Pyrite	2339.0	1.000	3.052	5.136E+05	1.818	33.22	0.3286	-0.06139	-0.01237	4.650E+05	92.46	125.9	0.2470	0.07215	2.009	61.39
BK59-C1-S12	Pyrite	2339.0	-0.1959	-0.07543	4.914E+05	7.677	7.959	0.6377	0.09695	0.8640	4.650E+05	117.0	156.3	1.500	1.300	37.85	57.35
BK59-C1-S13	Pyrite	2339.0	0.5370	3.137	4.791E+05	-1.817	-51.42	0.1127	-0.008946	-0.06078	4.650E+05	76.16	105.1	0.1890	0.1762	2.074	57.41
BK59-C1-S15	Pyrite	2339.0	0.5251	-0.5407	5.207E+05	-5.742	15.69	0.3868	-0.04679	0.01355	4.650E+05	163.1	239.2	0.1775	0.02295	1.771	64.09
BK28-C1-S1	Pyrite	778.0	0.3667	-0.1420	5.191E+05	5.503	17.88	0.4137	0.005655	0.09995	4.650E+05	25.45	307.8	0.07816	0.1358	403.2	29.99
BK28-C1-S2	Pyrite	778.0	0.4890	0.9686	4.887E+05	0.9782	-19.75	-0.05715	-0.1013	0.09010	4.650E+05	17.32	690.4	-0.01282	-0.08103	1002	33.84
BK28-C1-S7	Pyrite	778.0	-0.2758	0.5057	5.000E+05	2.252	35.11	0.9304	0.2830	0.1071	4.650E+05	13.86	128.4	9.542	0.3174	519.9	31.05
BK28-C1-S11	Pyrite	778.0	0.5927	1.394	5.336E+05	-2.458	-27.05	0.5117	0.4174	-0.06250	4.650E+05	829.9	53.62	3.362	0.4425	74.31	10.20

* distance from center of deposit

** All elements in ppm except Au which is in ppb

Appendix 9: Buckingham
pyrite mineral chemistry by LA-ICP-MS

Sample	Sample type	Distance*													
		(m)	Zr90	Mo95	Ag107	Cd111	Sn118	Sb121	Te125	Ba137	Gd157	Hf178	Ta181	W182	
BK025-C1-S1	Arsenian pyrite	0.0	40.58	0.5280	8.657	25.81	15.17	1406	13.28	2.929	0.06653	0.9995	0.03015	2.083	
BK025-C1-S2	Arsenian pyrite	0.0	36.54	0.3684	12.51	13.89	25.70	1445	15.27	3.070	0.03373	0.9318	0.05937	6.107	
BK025-C1-S3	Arsenian pyrite	0.0	981.6	0.6110	20.33	99.20	137.5	2762	16.65	10.16	16.30	20.48	0.05181	4.691	
BK025-C1-S4	Arsenian pyrite	0.0	9.932	0.01878	3.647	28.20	8.129	10.11	0.1352	0.04216	0.02375	0.2250	0.008505	0.5684	
BK025-C1-S5	Arsenian pyrite	0.0	5.533	0.04650	3.986	3.833	9.647	428.5	7.430	7.853	0.03359	0.1375	0.03944	0.9076	
BK025-C1-S6	Arsenian pyrite	0.0	12.16	0.06376	1.384	1.037	1.939	400.3	24.11	1.773	0.03246	0.3490	0.06347	3.157	
BK025-C1-S7	Arsenian pyrite	0.0	4.472	0.02074	189.8	2.310	37.17	570.3	9.062	0.9034	0.01721	0.1086	0.06880	1.744	
BK025-C1-S8	Arsenian pyrite	0.0	0.6369	0.05163	2.597	1.439	0.9092	619.3	12.61	0.1923	0.008736	0.006306	0.0002128	0.1770	
BK025-C1-S9	Arsenian pyrite	0.0	8.799	0.1812	14.65	2.522	2.462	725.8	12.15	0.8142	0.01351	0.2828	0.001875	0.1792	
BK025-C1-S10	Arsenian pyrite	0.0	60.51	0.1886	16.59	2.236	1.632	742.3	15.18	0.1685	0.01253	1.870	0.02092	1.201	
BK025-C1-S11	Arsenian pyrite	0.0	20.38	0.2990	12.88	2.831	3.339	913.8	11.74	1.163	0.001576	0.5832	0.03411	1.369	
BK025-C1-S12	Arsenian pyrite	0.0	37.37	0.4680	47.49	13.62	32.78	1996	24.67	5.526	0.09070	0.9046	0.1515	11.50	
BK025-C1-S13	Arsenian pyrite	0.0	1.488	0.1853	11.88	1.488	2.922	807.1	20.56	0.5812	0.007866	0.04899	0.002427	0.06211	
BK025-C1-S14	Arsenian pyrite	0.0	146.4	0.2729	34.83	3.942	3.039	984.8	24.13	1.133	0.1207	4.180	0.1241	2.183	
BK025-C1-S15	Arsenian pyrite	0.0	111.1	0.08653	14.11	1.356	17.09	510.4	4.494	11.49	5.168	3.539	0.4717	3.735	
BK104-C1-S1	Arsenian pyrite	361.5	1.349	0.8846	91.32	28.49	24.54	12850	2.862	11.05	0.01018	0.04489	0.009900	0.05259	
BK104-C1-S2	Arsenian pyrite	361.5	0.3312	4.118	121.0	2.900	29.19	2489	40.45	3.936	0.009428	0.008801	0.0008160	0.03949	
BK104-C1-S3	Arsenian pyrite	361.5	0.2593	1.144	7.798	2.515	1.937	52.86	0.4158	12.79	0.01234	0.005253	0.001338	0.02714	
BK104-C1-S4	Arsenian pyrite	361.5	0.1714	0.5034	198.2	18.72	3.610	826.2	0.5252	4.885	0.004502	0.006735	0.002981	0.02267	
BK104-C1-S5	Arsenian pyrite	361.5	0.006771	0.04679	88.04	11.93	4.556	284.4	0.5760	0.1848	0.008449	-0.002849	0.0004431	-0.004754	
BK104-C1-S6	Arsenian pyrite	361.5	-0.001312	0.008983	1.468	0.1241	0.09781	6.674	0.5098	0.03357	0.0007008	-0.0001955	-0.0001655	-0.002446	
BK104-C1-S7	Arsenian pyrite	361.5	0.01524	0.05130	16.73	0.3150	2.716	59.39	0.3662	0.1354	0.02016	0.006059	0.0002915	-0.006508	
BK104-C1-S10	Arsenian pyrite	361.5	0.1723	0.7104	69.77	2.030	0.8905	513.9	4.395	3.582	0.02077	0.002786	0.006550	0.9913	
BK104-C1-S11	Arsenian pyrite	361.5	0.1455	0.7287	50.39	5.140	2.055	289.2	0.3403	6.933	-0.0009521	0.003806	0.005641	0.06457	
BK104-C1-S12	Arsenian pyrite	361.5	5.328	3.539	300.3	28.11	12.79	4705	-0.8322	512.0	0.1330	0.09913	0.01196	0.3715	
BK104-C1-S13	Arsenian pyrite	361.5	0.2634	0.1958	6.812	0.02329	0.2330	72.44	0.05747	0.03776	0.004394	0.002764	0.001237	0.1142	
BK104-C1-S14	Arsenian pyrite	361.5	1.577	0.03652	17.82	1.876	0.5749	257.9	0.1929	0.6629	0.01832	0.04363	0.002784	0.01831	
BK102-C1-S2	Pyrite	890.8	0.001913	0.005877	0.03911	0.02229	0.3937	0.01511	0.02517	0.01916	-0.003331	0.003329	0.0002600	0.0003361	
BK102-C1-S3	Pyrite	890.8	0.002832	0.002475	0.1080	-0.01988	0.3760	0.02154	0.1649	0.005890	-0.003058	0.001591	0.0003234	-0.0005159	
BK102-C1-S4	Pyrite	890.8	0.006639	-0.004352	0.01622	0.008332	0.3937	0.01065	0.2907	-0.006534	-0.0009681	0.0002432	0.00007842	-0.0006738	
BK102-C1-S5	Pyrite	890.8	0.004791	0.009503	0.03334	0.01675	0.3845	0.02307	0.07473	0.0003452	0.003805	-0.0005968	0.001369	-0.002020	
BK102-C1-S6	Pyrite	890.8	0.0001275	0.004407	0.01902	0.02651	0.3768	0.03917	0.06212	-0.002348	-0.001585	0.0008236	-0.0001615	0.004616	
BK102-C1-S7	Pyrite	890.8	0.001082	-0.0008630	0.03761	-0.03991	0.3607	0.01307	0.1544	-0.01219	-0.002871	0.0001052	-0.0001920	0.003436	
BK102-C1-S8	Pyrite	890.8	0.004835	0.009475	0.02304	0.01500	0.3724	0.01327	0.03806	0.009607	0.006483	-0.003406	-0.001046	-0.002068	
BK102-C1-S10	Pyrite	890.8	-0.001084	0.005383	0.06546	-0.01958	0.3993	0.005931	0.1211	-0.006629	-0.004473	-0.004688	-0.001300	0.001383	
BK102-C1-S11	Pyrite	890.8	0.004171	0.004177	0.03255	-0.02131	0.3607	0.02537	0.06510	0.01625	-0.004768	-0.0006098	-0.0007273	-0.004699	
BK102-C1-S12	Pyrite	890.8	-0.001417	0.01909	0.05137	-0.02989	0.3823	0.03846	0.03073	0.09253	0.002099	0.0007000	-0.0001921	0.004408	
BK102-C1-S13	Pyrite	890.8	-0.001405	0.001160	0.07348	0.01201	0.3156	0.1969	0.04700	0.005592	-0.003199	-0.0006659	-0.0008450	-0.0007093	
BK102-C1-S14	Pyrite	890.8	0.004409	-0.005913	0.04584	0.01518	0.3833	0.01297	0.2596	-0.01434	-0.004419	0.005817	-0.0001213	-0.002811	
BK102-C1-S15	Pyrite	890.8	0.003103	0.002969	0.1957	0.001283	0.3469	0.05781	0.1171	-0.007224	-0.001547	-0.001395	-0.0004821	-0.0004085	
BK59-C1-S1	Pyrite	2339.0	0.0008185	0.006970	0.01661	-0.03620	0.3185	0.2819	0.09077	0.002292	-0.004244	-0.001313	-0.0001985	0.02460	
BK59-C1-S2	Pyrite	2339.0	0.001936	-0.009512	0.0002968	0.004879	0.3279	0.02937	0.1172	0.006718	0.002618	-0.001259	-0.002039	0.009409	
BK59-C1-S3	Pyrite	2339.0	-0.001851	0.01309	-0.007802	-0.02044	0.5991	0.04456	0.2049	0.02384	-0.003488	0.005532	-0.001126	0.000	

* distance from center of deposit

** All elements in ppm except Au which is in ppb

Appendix 9: Buckingham
pyrite mineral chemistry by LA-ICP-MS

Sample	Sample type	Distance*												
		(m)	Zr90	Mo95	Ag107	Cd111	Sn118	Sb121	Te125	Ba137	Gd157	Hf178	Ta181	W182
BK59-C1-S4	Pyrite	2339.0	-0.001474	0.001985	-0.007369	-0.03094	0.3565	0.05444	-0.03567	-0.008253	-0.002777	-0.007543	-0.0004070	-0.008161
BK59-C1-S5	Pyrite	2339.0	0.01283	0.009385	0.01454	-0.003246	0.5381	0.1961	0.2439	0.09136	-0.008930	0.004727	0.002753	0.01386
BK59-C1-S6	Pyrite	2339.0	-0.003093	-0.005881	0.01355	0.01379	0.4097	0.06751	0.1615	-0.009933	-0.005824	0.000	-0.0004261	-0.0004177
BK59-C1-S7	Pyrite	2339.0	0.0006346	0.01215	0.008047	-0.002408	0.3898	0.1222	0.08984	-0.005653	-0.002932	0.002258	-0.0004287	0.004862
BK59-C1-S8	Pyrite	2339.0	0.002591	-0.0008463	0.0001761	0.01116	0.3730	0.01596	0.09744	0.01151	0.000	-0.002582	0.000	0.009471
BK59-C1-S9	Pyrite	2339.0	0.002006	-0.01664	0.02987	-0.003208	0.3716	0.07625	0.2276	-0.008641	0.007550	-0.003931	0.001950	0.008301
BK59-C1-S10	Pyrite	2339.0	0.002185	0.02007	-0.007856	-0.008716	0.4950	0.01886	0.04479	0.03011	0.0004742	0.001747	0.0003343	0.003095
BK59-C1-S12	Pyrite	2339.0	-0.0005196	-0.002583	4.175	0.02608	0.3846	0.5660	1.628	0.08185	-0.001395	0.003080	-0.0008737	0.004837
BK59-C1-S13	Pyrite	2339.0	-0.0004478	0.005150	0.001627	0.01097	0.2942	0.1782	0.02091	-0.005482	-0.005681	-0.001657	0.0001683	-0.0004043
BK59-C1-S15	Pyrite	2339.0	0.005498	-0.01861	0.006494	0.01563	0.4028	0.005173	0.1445	-0.009057	0.01179	-0.001219	0.0007342	-0.003610
BK28-C1-S1	Pyrite	778.0	-0.002326	0.004455	0.02237	-0.006251	0.3748	0.01745	-0.03624	-0.01777	0.02088	-0.006812	-0.0003293	-0.004188
BK28-C1-S2	Pyrite	778.0	0.006258	-0.01272	-0.005665	-0.02246	0.3036	0.03087	-0.007556	-0.008342	0.000	-0.001145	-0.0004068	0.005754
BK28-C1-S7	Pyrite	778.0	0.004843	1.201	0.08995	-0.03921	0.3046	0.02522	-0.1142	0.1110	-0.002585	-0.001282	0.0004891	0.004472
BK28-C1-S11	Pyrite	778.0	0.002671	2.330	0.2388	0.06663	0.4312	0.01167	0.09909	0.2225	0.007039	0.0002445	-0.0007895	0.005774

* distance from center of deposit

** All elements in ppm except Au which is in ppb

Appendix 9: Buckingham
pyrite mineral chemistry by LA-ICP-MS

Sample	Sample type	Distance*						
		(m)	Pt195	Au197**	Tl205	Pb208	Bi209	U238
BK025-C1-S1	Arsenian pyrite	0.0	-0.0002380	32.36	0.2214	279.7	0.04268	2.046
BK025-C1-S2	Arsenian pyrite	0.0	0.003352	38.00	0.4088	175.7	0.1268	0.7395
BK025-C1-S3	Arsenian pyrite	0.0	0.002669	36.19	1.841	383.7	0.1467	2.789
BK025-C1-S4	Arsenian pyrite	0.0	-0.0004278	16.13	0.02171	24.36	0.3024	0.1198
BK025-C1-S5	Arsenian pyrite	0.0	-0.002242	26.26	0.1537	64.55	0.04871	0.2236
BK025-C1-S6	Arsenian pyrite	0.0	0.001315	46.68	0.04513	11.40	0.01138	0.3637
BK025-C1-S7	Arsenian pyrite	0.0	-0.002936	139.1	0.09991	54.93	0.03642	0.09170
BK025-C1-S8	Arsenian pyrite	0.0	-0.002742	17.83	0.03833	33.33	0.02174	0.05613
BK025-C1-S9	Arsenian pyrite	0.0	-0.006273	52.76	0.2128	40.70	0.1504	0.1659
BK025-C1-S10	Arsenian pyrite	0.0	0.001678	40.19	0.2440	42.20	0.1874	0.4730
BK025-C1-S11	Arsenian pyrite	0.0	-0.002361	43.51	0.3044	51.16	0.1738	0.3446
BK025-C1-S12	Arsenian pyrite	0.0	-0.003727	48.54	1.094	91.98	0.3286	3.217
BK025-C1-S13	Arsenian pyrite	0.0	-0.003963	39.94	0.2120	34.01	0.1862	0.05130
BK025-C1-S14	Arsenian pyrite	0.0	-0.0004409	44.08	0.5535	195.3	0.5220	2.645
BK025-C1-S15	Arsenian pyrite	0.0	0.005536	30.94	0.2320	26.49	0.6682	2.149
BK104-C1-S1	Arsenian pyrite	361.5	0.0007509	5.836	5.309	17980	47.61	0.06849
BK104-C1-S2	Arsenian pyrite	361.5	-0.001116	29.55	5.813	4522	4.533	0.01106
BK104-C1-S3	Arsenian pyrite	361.5	0.001690	4.616	0.1452	56.77	0.1986	0.01869
BK104-C1-S4	Arsenian pyrite	361.5	0.0001005	10.65	7.295	439.6	0.6013	0.02190
BK104-C1-S5	Arsenian pyrite	361.5	-0.004129	13.09	4.064	495.4	1.114	-0.00002480
BK104-C1-S6	Arsenian pyrite	361.5	-0.003745	9.044	0.04272	7.535	0.01813	0.0006906
BK104-C1-S7	Arsenian pyrite	361.5	0.0009623	3.154	0.3058	97.26	0.4944	0.003360
BK104-C1-S10	Arsenian pyrite	361.5	-0.0006373	11.46	38.79	149.6	0.3310	0.02110
BK104-C1-S11	Arsenian pyrite	361.5	0.004582	2.089	4.142	152.0	0.2833	0.01205
BK104-C1-S12	Arsenian pyrite	361.5	0.02412	1.207	7.238	5991	7.735	0.4150
BK104-C1-S13	Arsenian pyrite	361.5	-0.001804	0.5998	0.06203	112.2	0.2426	0.006644
BK104-C1-S14	Arsenian pyrite	361.5	-0.007113	0.6432	0.6129	256.0	0.5269	0.09051
BK102-C1-S2	Pyrite	890.8	-0.00004620	0.001251	0.001971	0.01267	0.01118	0.0008346
BK102-C1-S3	Pyrite	890.8	0.0008623	0.003560	-0.0006456	0.008753	0.01711	0.0002973
BK102-C1-S4	Pyrite	890.8	0.001051	-0.006493	-0.003780	0.007793	0.03257	-0.001061
BK102-C1-S5	Pyrite	890.8	-0.001102	0.002550	-0.0003938	0.005896	0.01108	0.0002204
BK102-C1-S6	Pyrite	890.8	0.003974	0.0006489	-0.0003963	0.004073	0.01297	0.0001893
BK102-C1-S7	Pyrite	890.8	-0.001622	0.005822	-0.0004649	0.003882	0.008402	0.0004516
BK102-C1-S8	Pyrite	890.8	-0.003376	0.0001643	0.001887	0.03406	0.03560	0.0003784
BK102-C1-S10	Pyrite	890.8	-0.002370	-0.004734	-0.001468	0.01648	0.02500	-0.00008730
BK102-C1-S11	Pyrite	890.8	0.0001395	0.002706	0.0003900	0.03094	0.006300	0.003883
BK102-C1-S12	Pyrite	890.8	0.001358	0.00007051	0.001206	0.006644	0.01392	0.0004280
BK102-C1-S13	Pyrite	890.8	-0.0004297	-0.0006903	0.002489	0.1056	0.1826	0.0006895
BK102-C1-S14	Pyrite	890.8	-0.001214	0.003168	-0.001784	-0.0008518	0.009401	0.0005506
BK102-C1-S15	Pyrite	890.8	-0.001593	0.004549	0.001043	0.02259	0.01755	0.008699
BK59-C1-S1	Pyrite	2339.0	0.003418	0.008091	0.0008796	0.7612	0.008396	-0.00008850
BK59-C1-S2	Pyrite	2339.0	0.004069	-0.001973	0.0006949	0.02734	0.005206	-0.0004358
BK59-C1-S3	Pyrite	2339.0	0.002895	-0.005263	-0.003437	0.009136	0.01838	-0.0002390

* distance from center of deposit

** All elements in ppm except Au which is in ppb

Appendix 9: Buckingham
pyrite mineral chemistry by LA-ICP-MS

Sample	Sample type	Distance*						
		(m)	Pt195	Au197**	Tl205	Pb208	Bi209	U238
BK59-C1-S4	Pyrite	2339.0	-0.001141	-0.004581	0.004779	0.01285	0.03378	-0.0002730
BK59-C1-S5	Pyrite	2339.0	0.001329	0.003640	-0.0003006	0.06612	0.04984	0.001381
BK59-C1-S6	Pyrite	2339.0	-0.001456	0.006788	-0.003823	0.001279	0.3131	-0.0009463
BK59-C1-S7	Pyrite	2339.0	0.002859	-0.00004438	0.002497	0.1308	0.08004	-0.001173
BK59-C1-S8	Pyrite	2339.0	-0.004722	0.0007223	-0.001536	0.6144	0.01412	-0.0007097
BK59-C1-S9	Pyrite	2339.0	-0.00009049	0.004384	-0.001476	0.01967	0.03695	-0.0003713
BK59-C1-S10	Pyrite	2339.0	-0.002372	-0.00001617	-0.002806	0.01274	0.01049	-0.001240
BK59-C1-S12	Pyrite	2339.0	-0.003425	0.04138	0.01018	132.5	20.60	0.0004383
BK59-C1-S13	Pyrite	2339.0	-0.004853	0.0009370	0.001812	0.1373	0.2633	-0.0004869
BK59-C1-S15	Pyrite	2339.0	0.002819	-0.002185	0.001344	0.02087	0.03716	0.0004086
BK28-C1-S1	Pyrite	778.0	-0.005583	-0.0001820	0.004545	0.03091	0.008317	0.001140
BK28-C1-S2	Pyrite	778.0	0.001084	-0.002041	-0.002364	0.07991	0.0007412	0.0002644
BK28-C1-S7	Pyrite	778.0	-0.002521	0.003905	0.0001001	0.01360	0.0005225	0.005809
BK28-C1-S11	Pyrite	778.0	0.04310	0.002309	-0.0005787	0.01273	0.02867	0.01049

* distance from center of deposit

** All elements in ppm except Au which is in ppb